DOT/FAA/AR-00/26

Office of Aviation Research
Washington, D.C. 20591

Verification of the Combined Load Compression (CLC) Test Method

August 2000

Final Report

U.S. Department of Transportation
Federal Aviation Administration

NOTICE

This report is available at the Federal Aviation Administration William J. Hughes Technical Center's Full-Text Technical Reports page: actlibrary.tc.faa.gov in Adobe Acrobat portable document format (PDF).

Technical Report Documentation Page

1. Report No.	2. Government Accession No.	3. Recipient's Catalog No.
DOT/FAA/AR-00/26		

4. Title and Subtitle	5. Report Date
VERIFICATION OF THE COMBINED LOAD COMPRESSION (CLC) TEST METHOD	August 2000
	6. Performing Organization Code

7. Author(s)	8. Performing Organization Report No.
Peter M. Wegner and Donald F. Adams	

9. Performing Organization Name and Address	10. Work Unit No. (TRAIS)
Dept. of Mechanical Engineering University of Wyoming Box 3295, University Station Laramie, WY 82071	11. Contract or Grant No. Grant 94-G-009

12. Sponsoring Agency Name and Address	13. Type of Report and Period Covered
U.S. Department of Transportation Federal Aviation Administration Office of Aviation Research Washington, DC 20591	Final Report
	14. Sponsoring Agency Code ACE-111

15. Supplementary Notes

The FAA William J. Hughes Technical Center COTR was Donald W. Oplinger.

16. Abstract

The determination of lamina compressive strength and modulus using the Combined Loading Compression (CLC) test method developed by the University of Wyoming was investigated. In this test method an untabbed, $[90/0]_{ns}$ cross-ply test coupon is tested in uniaxial compression using the CLC test fixture. The longitudinal modulus and strength of the 0°-plies are determined by applying a back-out factor, calculated using classical lamination theory, to the measured longitudinal laminate modulus and strength.

A parametric study revealed that specimen quality, load train alignment, and fixture dimensional tolerances have a large impact on the measured compressive properties. Thus, a significant amount of time was dedicated to developing specimen fabrication and testing procedures to minimize variations in the measured compressive properties. A comparative study of the CLC and Illinois Institute of Technology Research Institute (IITRI) test fixtures showed that results obtained with the CLC test fixture are statistically similar to those obtained from the IITRI test fixture. However, the CLC test fixture is easier to use, less expensive to fabricate, and much less massive than the IITRI test fixture.

In a second portion of the comparative study, the 0°-ply compressive strength obtained using $[90/0]_{ns}$ cross-ply test specimens was compared to the 0°-ply compressive strength obtained using quasi-isotropic test specimens. This revealed that the 0°-ply compressive strength was independent of the laminate orientation. This "backed out" 0°-ply compressive strength is then by definition the "design value" for the strength of the unidirectional composite material in compression.

17. Key Words	18. Distribution Statement
Compression, Composites, Testing method, Testing fixtures	This document is available to the public through the National Technical Information Service (NTIS) Springfield, Virginia 22161.

19. Security Classif. (of this report)	20. Security Classif. (of this page)	21. No. of Pages	22. Price
Unclassified	Unclassified	261	

PREFACE

This study is the Ph.D. dissertation research of the first author, Peter M. Wegner. Dr. Donald F. Adams served as his dissertation advisor.

Mr. Wegner was funded by the United States Air Force (USAF) Palace Knights Program. Financial support for the overall project was provided by the Federal Aviation Administration (FAA), William J. Hughes Technical Center, Atlantic City International Airport, New Jersey, under FAA Grant No. 94-G-009. The FAA Technical Monitor was Donald W. Oplinger. Dr. Adams was the principal investigator of this grant.

All work was conducted within the Composite Materials Research Group (CMRG) at the University of Wyoming. Both the financial and technical support of the FAA is gratefully acknowledged, as is the technical assistance of the various members of the CMRG and the members of Mr. Wegner's graduate committee. The donation of materials for use in this study as arranged by Mr. Jerry Sundsrud of the 3M Company and by Mr. Jack Esposito of Boeing Space Systems Division is sincerely appreciated.

TABLE OF CONTENTS

LIST OF FIGURES

LIST OF TABLES

EXECUTIVE SUMMARY

A review of the current compression testing literature reveals that presently there is a great deal of confusion in the composites industry surrounding the measurement of the compressive properties of fibrous composite materials. Different compression test methods often do not produce comparable compressive properties, and values generated by different testing laboratories using the same test method often disagree. These problems with current compression testing methods led the authors to design and evaluate the Combined Loading Compression (CLC) Test Method developed at the University of Wyoming. In this test method, the 0°-ply compressive strength of a fibrous composite material is obtained by testing an untabbed, $[90/0]_{ns}$ cross-ply specimen in the CLC test fixture.

A parametric study revealed that specimen quality, load train alignment, and fixture dimensional tolerances all have a large effect on the measured compressive properties. Thus, a significant portion of the present study was dedicated to developing specimen fabrication and testing procedures that will minimize variations in the measured compressive properties due to these parameters.

A comparative study of the CLC and ASTM D 3410 (1995) Method B which uses the wedge loading arrangement developed at the Illinois Institute of Technology Research Institute (IITRI) was conducted. Results of the study suggested that the CLC test fixture is preferable to the IITRI test fixture from a practical standpoint. Although the compressive properties measured using these two fixtures are statistically similar, the CLC test fixture is easier to use, less expensive to fabricate, and less massive than the IITRI test fixture, making it easier to install and, as a result, less likely to induce testing errors. Furthermore, because of its simpler design, the CLC test fixture is considerably less prone to machining errors.

In a second portion of the comparative study, the 0°-ply compressive strength obtained from $[90/0]_{ns}$ cross-ply test specimens was compared to the 0°-ply compressive strength obtained with quasi-isotropic test specimens. The 0°-ply compressive strength for each material was "backed out" from the measured laminate compressive strength using classical lamination theory. This comparison revealed that the 0°-ply compressive strength was independent of the laminate orientation. This "backed out" 0°-ply compressive strength is then by definition the "design strength" of the composite material in compression.

The present study showed that valid "design values" for the compressive strength of laminated fibrous composite materials can be obtained by testing cross-ply laminates in the CLC test fixture.

There are many benefits that result from this test method. First, the CLC test fixture is smaller and less massive than the IITRI test fixture. This is an important factor when testing at conditions other than ambient as the time required to come to thermal equilibrium is proportional to the mass of the test fixture. Second, the CLC test fixture has relatively few moving parts and most of the surfaces of the fixture are at right angles to each other. For this reason the CLC test fixture is less expensive to fabricate than the IITRI test fixture. Third, the CLC test fixture is easier to use than the IITRI test fixture, because the specimen/wedge grip assembly often gets

wedged into the cavities of the IITRI test fixture housings. This problem does not occur with the CLC test fixture.

There are also benefits to using a test specimen fabricated from a cross-ply laminate. Because the axial strength of the cross-ply laminate is lower then the axial strength of a unidirectional composite having the same number of plies, the cross-ply specimen can be tested without end tabs. This significantly reduces the time and expense involved in specimen fabrication.

1. INTRODUCTION.

1.1 BACKGROUND.

Fiber-reinforced composite materials have been used in such diverse applications as automobiles, aircraft, spacecraft, off-shore structures, sporting goods, civil infrastructure, electronics, and marine vehicles (Agarwal and Broutman, 1990). For high performance applications these materials are typically formed by imbedding unidirectional carbon or glass fibers in a polymer matrix material. These unidirectional composites thus have different stiffnesses and strengths in the longitudinal direction than in the transverse directions. This "orthotropic" nature of fiber-reinforced composites can be used to advantage by concentrating fibers in the directions of the applied loads. By laying up these unidirectional laminae in different directions, a "tailored" material can be developed that offers the optimum stiffness, strength, and weight for a given structure. Thus, unidirectional laminae are the building blocks for complex composite structures.

An infinite variety of laminates can be constructed from these unidirectional laminae by using various lay-up angles and fiber and matrix materials. But the designer must know the stiffness and strength of the laminate in any given direction. Since it is not practical to test each laminate combination in the laboratory, a method was developed by which the properties of the laminate in any given direction can be determined if the properties of the unidirectional laminae are known. This method is referred to as Linear Lamination Theory or Classical Lamination Theory (Agarwal and Broutman, 1990; Jones, 1975; Gibson, 1994).

In Linear Lamination Theory, independent coordinate axes are assigned to each unidirectional lamina and to the complete laminate. A 1-2-3 coordinate system is assigned to the principal material directions of each unidirectional lamina and the x-y-z coordinate system to the laminate. The 1-direction corresponds to the direction along the fiber axis, the 2-direction is transverse to the fiber axis in the plane of the lamina, and the 3-direction is perpendicular to the plane of the lamina. The x-y-z coordinate system is aligned with the geometry of the structure. To use Linear Lamination Theory, the stiffness (modulus) in the 1-direction (E_{11}), in the 2-direction (E_{22}), and the shear modulus (G_{12}) must be known. One of the Poisson's ratios, ν_{12} or ν_{21}, must also be known. Similarly, the tensile and compressive strengths, σ^t_{11}, σ^t_{22}, σ^c_{11}, σ^c_{22}, and the in-plane shear strength, τ_{12}, must be input. The Linear Lamination Theory assumes plane stress conditions hold, so values for E_{33}, G_{13}, and G_{23} as well as σ^t_{33}, σ^c_{33}, τ_{23}, and τ_{13} are not needed.

One of the most difficult of these properties to measure is the longitudinal compressive strength, σ^c_{11}, usually termed the 0°-ply axial compressive strength. An American Society for Testing and Materials (ASTM) round-robin comparison showed that even standardized compression test methods can yield significantly different results when the tests are conducted on identical materials by separate laboratories (Adsit, 1983). Variation in test specimen fabrication, test fixture alignment, and testing procedures between the participating laboratories had a tremendous influence on the measured compressive stiffness and strength. As another example of the difficulty and confusion surrounding compression test methods, representatives from five companies experienced with composite materials recently compared measured strengths of various carbon fiber composite materials. The compressive strengths for identical materials measured in the separate labs varied by as much as 20% (MIL-HDBK-17, 1996).

These wide variations in the measured compressive properties of composite materials cause great concern for engineers designing compressive-loaded composite structures. To counteract this variability, designers are forced to apply larger factors of safety. This results in a structure that is heavier than necessary. Therefore, the development of an easy to use, accurate, and reliable compression test method for composite materials is very important to structural designers as well as certifying agencies, testing laboratories, and material suppliers.

1.2 SCOPE OF THE PRESENT STUDY.

The objective of this study was to develop an improved compression test method. This test method should be accurate, precise, and easy to use. It should not rely on expensive or unwieldy test fixtures. The test method should also accurately evaluate the compressive "design strength" of a fibrous composite material. Some researchers have been able to obtain very high 0°-ply compressive strengths by sandwiching a few 0° plies between many off-axis plies (Adams and Welsh, 1997). This restricts buckling of the 0° plies; however, this forces a compressive failure mode that typically does not occur in an actual composite structure. Thus, using these abnormally high compressive strengths to design a composite structure will result in a non-conservative design. The compression test method should produce the compressive strength of the composite material that is achieved in an actual structural component.

A combination of experimental and analytical techniques were used to verify a compression test method that meets these requirements. The remainder of this report documents this research. First, a review of compression testing research is presented in section 2. This section also contains a discussion of existing test methods and test fixtures. Section 3 presents the process used to fabricate the compression test specimens used in this study. The experimental and analytical techniques used to develop an optimum compression test method and test fixture are covered in section 4. Section 5 contains a summary, as well as a discussion of possible future work.

2. THE COMBINED LOAD COMPRESSION (CLC) TEST METHOD.

2.1 STATE OF THE ART OF CURRENTLY USED COMPRESSION TEST METHODS.

Compression test methods can be separated into three main categories depending on the method used to impart the compressive load to the test coupon. These categories are shear-loaded, end-loaded, and sandwich-beam test methods. The most commonly used example of a shear-loaded compression test method is ASTM D 3410 (ASTM D 3410, 1995). This method includes the Celanese compression test fixture and the Illinois Institute of Technology Research Institute (IITRI) test fixture.

SRM1-88, a test method endorsed by Suppliers of Advanced Composite Materials Association (SACMA), relies on a modified ASTM D 695 test fixture (SACMA, 1988). This test fixture end loads the compression test coupon.

Another well known test method, ASTM D 5467-93, which has been in use since the mid-1960s, uses a honeycomb sandwich-beam loaded in four-point flexure to stabilize the compression face sheet which constitutes the specimen (ASTM D 5467, 1993).

These test methods and test fixtures represent the most commonly used approaches to compression testing of unidirectional composite materials in current use, and their advantages and disadvantages will be discussed in this section. As will be seen, none of them meets all of the requirements stated in section 1.2.

2.1.1 The Celanese Compression Test Fixture.

The Celanese compression test fixture, shown in figure 1, was developed by I.K. Park of the Celanese Corporation and was one of the first shear-loading compression test methods (Park, 1971). Studies have shown that the Celanese test fixture is capable of producing compressive data comparable to that of the IITRI test fixture (Adsit, 1983; Adams and Odom, 1991) discussed below. However, the Celanese test fixture is difficult to use (Adams and Odom, 1991; Chaterjee, et al., 1993). For example, specimen thickness must be within a very close tolerance (±0.002″) to ensure proper mating of the grip/collet faces (ASTM D 3410, 1995). If this thickness is not maintained, then line contact rather than the desired surface contact develops between the grip/collet surfaces. Problems encountered in meeting the severe specimen dimension tolerance requirements of the Celanese test fixture often cause test data obtained from it to be questioned or even discarded.

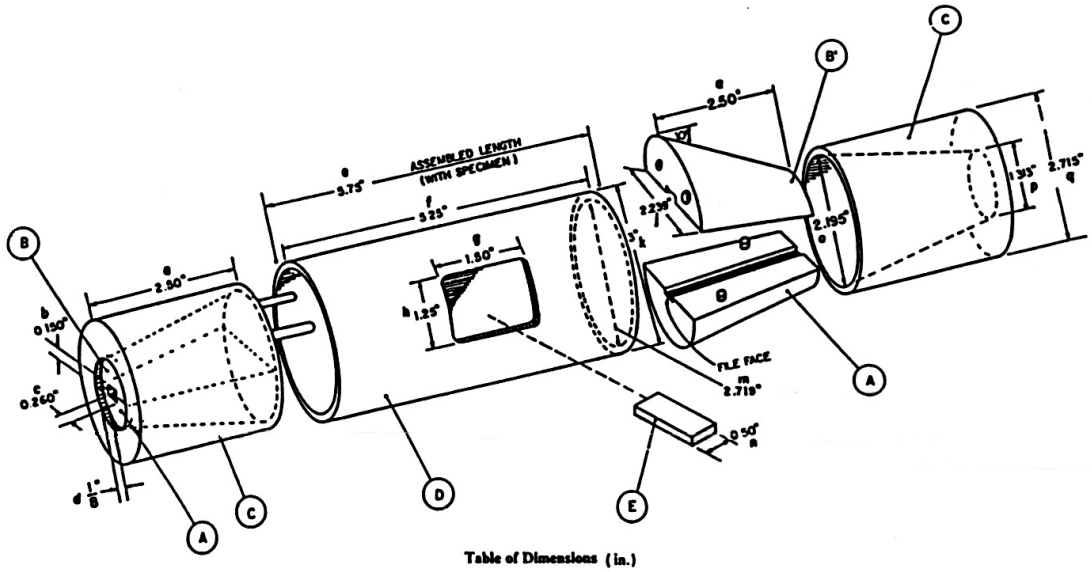

Dimension		Dimension	
a	2.500	j	2.239
b	0.150	k	3.000
c	0.260	m	2.719
d	0.125	n	0.500
e	5.75	o	2.195
f	5.25	p	1.313
g	1.50	q	2.715
h	1.25		

FIGURE 1. CELANESE COMPRESSION TEST FIXTURE (ASTM D 3410, 1987)

2.1.2 The IITRI Test Fixture.

To address problems with the Celanese test fixture, Hofer and Rao (1977) of IITRI developed what has come to be known as the IITRI test fixture. The conical wedge grips of the Celanese

test fixture were replaced with flat wedge grips and the alignment sleeve was replaced with a linear bearing/post assembly (see figures 2 and 3). The IITRI test fixture was standardized by ASTM in 1987 as Method B of ASTM D 3410.

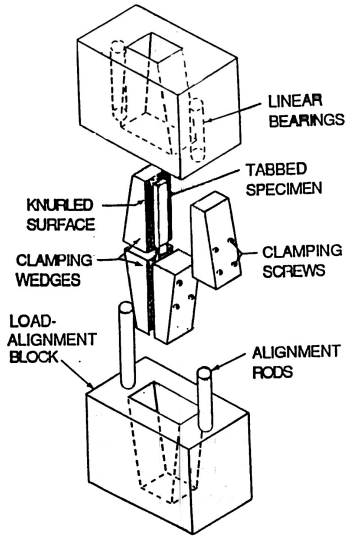

FIGURE 2. SCHEMATIC OF IITRI COMPRESSION TEST FIXTURE
(ASTM D 3410, 1995)

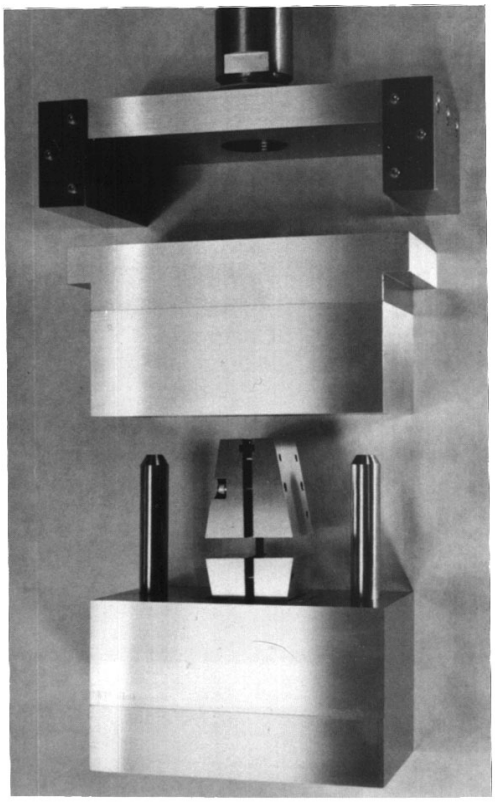

FIGURE 3. PHOTOGRAPH OF AN IITRI COMPRESSION TEST FIXTURE
(Wyoming Test Fixtures)

The data obtained from the IITRI test can be of very high quality, so that test results from it may be considered a standard of comparison. However, the IITRI test fixture is very massive and costly to fabricate, which constitutes its major disadvantages.

In regard to test fixture fabrication cost, there are two primary operations that make fabricating an IITRI test fixture difficult and costly. First, machining the large cavity in the upper and lower test fixture housing blocks is time consuming and difficult to do with a close tolerance on the finished dimensions. The second difficult operation is fabricating the wedge grips and wedge grip inserts with the required 10° angle on the loading faces. Each of these operations takes a highly skilled and experienced machinist to carry out. Even then, a great deal of care must be used to maintain the close tolerance required on the dimensions of these loading surfaces. (See discussion in section 5.2.4 regarding the effects of machining tolerances on both the IITRI and the Combined Loading Compression (CLC) test methods.)

Regarding the massiveness of the IITRI apparatus, the test fixture commonly weighs more than 40 kg (90 lbs), (Chaterjee, et al., 1993). Although the upper half of the test fixture is typically attached to the crosshead of the testing machine so that only the lower half must regularly be handled during testing, this half of the test fixture still weighs over 16 kg (35 lbs). The large mass of the test fixture also makes compression testing at nonambient temperatures more difficult because of the long soak time required to allow the compression test fixture and test specimen to come to an equilibrium state.

2.1.3 The Modified D 695 Test Fixture.

In 1988, the SACMA adapted a version of ASTM D 695 previously modified by Boeing (Boeing, 1988) as their recommended compression test method. The test fixture is used with two I-shaped lateral supports and four bolts which lightly clamp the supports to the faces of the compression coupon, as shown figure 4. This assembly is then end loaded between flat and parallel platens. The modified D 695 method, when used properly, yields compressive test data comparable to the IITRI and Celanese test methods (Adams and Lewis, 1991; Westberg and Abdallah, 1987).

However, the main disadvantage of this test fixture is that separate specimens must be used to measure the compressive strength and the compressive modulus of the material, since the distance between tabs of the strength coupon is only 4.76 mm (0.188″) there is not enough room to install a strain gage accordingly, a second (modulus) coupon is required. The need for two specimens makes this procedure time consuming and inefficient. Also, a complete stress-strain curve to failure is not obtained.

As with other compression test methods, tabs must be used on the strength coupon to keep the specimen from end crushing. Although finite element analysis (FEA) models have shown that stress concentrations due to end-loaded tabs are lower than those associated with shear-loaded tabs (Westberg and Abdallah, 1987; Xie and Adams, 1993), it still takes more time to prepare tabbed coupons than untabbed ones.

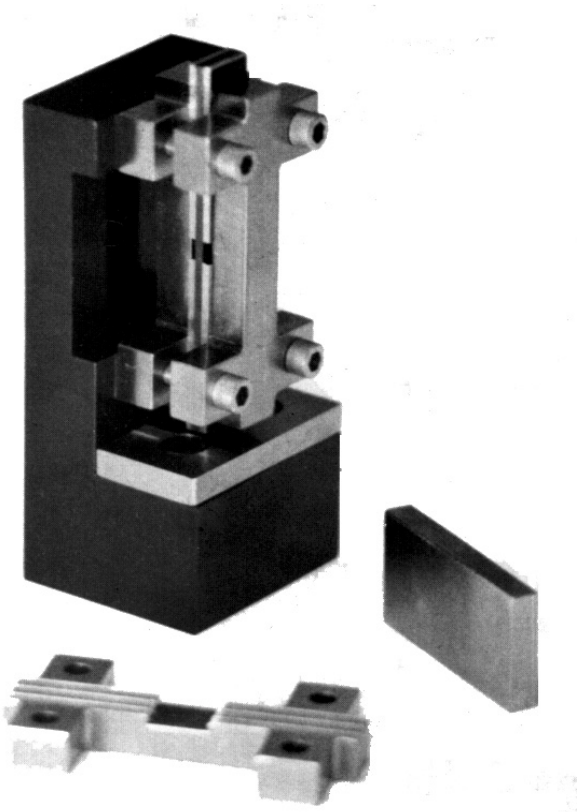

FIGURE 4. PHOTOGRAPH OF A MODIFIED D 695 TEST FIXTURE, SHOWN WITH ADDITIONAL LATERAL SUPPORT FOR MODULUS MEASUREMENT (Wyoming Test Fixtures, Inc., 1996)

Perhaps the most notable problem with the modified D 695 test fixture is that it allows for a redundant load path. Welsh and Adams (1997) showed that in the modified D 695 test fixture, part of the compressive load can be carried by the test fixture and not the coupon. The mechanism for this is the frictional force between the coupon and the lateral supports. Although this frictional force is typically small, its presence still raises doubts about the reliability of the modified D 695 test fixture.

Thus, a number of factors make the modified D 695 test fixture an undesirable choice for generating composite material compression data. These include the need for separate test coupons for strength and modulus measurements, the inability to obtain a complete stress-strain curve to failure, the necessity of bonding tabs to the strength coupons, and the presence of an alternate loading path.

2.1.4 The Sandwich-Beam Compression Test Method.

General Dynamics Corporation is credited with developing the sandwich-beam compression test (Shockey and Waddoups, 1966). This test method was originally included as Method C of ASTM D 3410; however, in 1993, this test method was made a separate standard which is now known as ASTM D 5467-93 (ASTM D 5467, 1993). This test method requires a honeycomb

core sandwich-beam having a width of 25.4 mm (1.0″) and a load span length of 508 mm (20.0″) of which the compressive face sheet made of a selected composite, which is stabilized by the honeycomb core, constitutes the specimen, while a metal strip (preferably titanium) is used for the tension face sheet, as shown in figure 5. The beam is loaded in four-point flexure, placing the upper face sheet in compression.

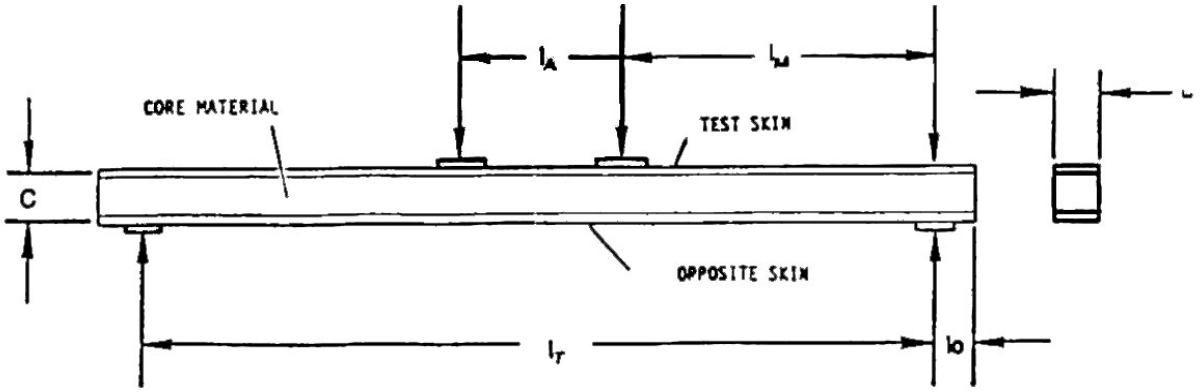

Dimensions	mm	in.
w	25.4	1.0
lo	25.4	1.0
l_T	508.0	20.0
l_M	203.2	8.0
l_A	101.6	4.0
C	38.1	1.5

FIGURE 5. TEST CONFIGURATION OF THE SANDWICH-BEAM COMPRESSION TEST METHOD (ASTM D 5467, 1993)

The sandwich beam tends to produce high test numbers which may not be representative of structural laminates because the restraint provided by the core may eliminate microbuckling failures that would be expected in structural laminates. However, the most significant problem with the sandwich-beam compression test is that it is very difficult to prepare acceptable specimens. The quality of the face sheets, the care used to bond the honeycomb core, and the rigidity of the honeycomb core all significantly affect the test results. Often the core material fails in shear or the face sheets debond from the core before the compressive failure stress in the test face sheet is reached. Shuart (1981) tested $[0]_8$ face sheets made of HTS1/PMR-15 carbon/polyimide composite at three temperatures: room temperature, -157°C (-250°F), and 316°C (600°F). None of the 12 specimens tested achieved a valid compression failure in the top face sheet. They all failed due to core crushing under the load points or by debonding of the core from the compression face sheets.

2.1.5 Innovative Compression Test Methods.

Aside from the standardized test methods, there are a number of test methods that have recently received a great deal of attention. These include novel coupons for use in existing test fixtures

such as the minisandwich compression coupon (Crasto and Kim, 1991), the thickness-tapered compression coupon (Adams and Finley, 1996), and the angle-ply compression coupon (Anquez, 1994) discussed below under the topic of testing of multidirectional laminates. New fixtures that show significant promise have also been developed.

2.1.6 Assessment of State-of-the-Art Test Methods.

A discussion of the most popular of the standardized compression test methods and recently developed compression test methods has been presented here to indicate the wide variety of compression test methods available and to indicate the types of problems encountered with them. A number of aspects of compression testing are worthy of summarizing.

First, it is important to note the state of confusion regarding the current status of compression testing in the composites community, and the wide range of conflicting results for identical materials that are being published (Rawlinson, 1991).

A second point to note is the nearly exclusive use of unidirectional laminates for strength determination in the standardized compression test methods. Compression testing a high modulus unidirectional composite laminate is often the most difficult challenge for a compression test method. This is due to the high ratio of axial compressive strength to shear strength of the composite material which tends to result in premature failure that may be related to failure modes which are not characteristic of laminates located in an actual structure and which are therefore nonrepresentative. One alternative which is discussed in the next section is the testing of angle- or cross-ply composite laminates and the subsequent determination of the effective 0°-ply strengths by the use of classical lamination theory. Note that ASTM standardized compression test methods, ASTM D 3410 and ASTM D 5467, are, in fact, applicable to coupons fabricated from multidirectional laminates, although these standards provide no method for determining the 0°-ply strengths from these types of laminates.

Another very important point is that for compressive strength data to be of use to the structural designer, the 0°-ply compressive strength measured must correspond to the actual behavior of that material when it is in the structure being designed. Until recently, the goal of compression test method developers was to obtain the highest possible 0°-ply compressive strength. The problem with this approach is that the failure modes usually achieved in structural laminates may not be present in tests of these “special” laboratory coupons.

Finally, although it was not explicitly discussed in the previous sections, it should be noted that the measurement of axial compressive strength is very sensitive to many factors outside the realm of the particular test method used. These include the quality and condition of the fixture, sensitivity of the test machine, operator skill, quality of the material, and the care used in coupon fabrication. Many standards do address the required dimensions and tolerance of the test fixtures and the test coupons. However, there are no standards for other aspects, such as panel fabrication, tabbing procedures, coupon machining, and data acquisition and reduction. It is important that any test method adopted for standardization by the composites community should be fairly robust against these outside factors. An inexperienced laboratory should be able to generate acceptable compressive strength data with a reasonable amount of care.

The results presented in Welsh and Adams (1997) indicated that the CLC test fixture discussed below, in combination with the use of cross-ply and angle-ply laminates such as those discussed in the next section for obtaining 0°-ply compressive strengths, gave a method which appeared to overcome the problems described above which are encountered with the most commonly used test methods for compression properties of composite laminates. The remainder of the report will address the development of the CLC specimen and will describe the results of a program that was conducted to examine in detail the specific issues needing to be considered to insure that the CLC test method is capable of providing high-quality test results as well as the practical advantages of low fabrication cost and ease of use which make it particularly attractive to the testing community.

2.2 COMPRESSION TESTING USING MULTIDIRECTIONAL LAMINATES.

In the early 1990s the concept of inferring properties of unidirectional laminates from tests on multidirectional laminates was introduced in discussions of the semiannual meetings of the MIL-HDBK-17 Coordination Group. Following up on this idea, as part of the present effort Adams, et al. (Adams and Welsh, 1997) conducted a study of compression strength of various multidirectional laminates using the CLC test. These tests used a calibration factor that has become commonly referred to as a "back-out factor," which is based on a calculation that assumes classical lamination theory for determining 0°-ply compressive strength from tests on multidirectional laminates. The laminates they termed "special laminates" were suggested by results reported in the literature (Anguez, 1994 as well as Whitney, et al., 1991 and Whitney, et al., 1992) and were specifically selected to constrain the 0° fibers from microbuckling. The results obtained from these laminates indicated an increasing compressive strength for an increasing back-out factor, an increasing back-out factor correlating with a decreasing laminate axial modulus corresponding to decreasing fractions of 0° fibers (see figure 6). However, for the wide range of "general" laminates tested (including $[0/90]_{ns}$ cross-ply and quasi-isotropic), the "backed out" 0°-ply strength remained essentially independent of laminate configuration. In fact, this backed out strength was consistent with results from previous tests of thickness-tapered and minisandwich unidirectional composite specimens.

Along with the development of the CLC specimen, the results shown in figure 6 represent a major breakthrough in the methodology of compression testing of composite materials by throwing light on the difference between compression failure in "structural" laminates containing primarily 0, 45, and 90° reinforcements of the fiber directions normally encountered in practical structures, as opposed to the special laminates which were designed specifically to eliminate fiber microbuckling, an important failure mode characteristic of the structural laminates. Laminates in which fiber microbuckling is not present are not representative of the type of failure expected to occur in most practical structures, and the unusually high test results obtained from such laminates should not be expected in practical structures unless such laminates have been specifically designed to incorporate nonstandard selections of fiber directions. On the other hand, test results represented by the horizontal part of figure 6 provide an upper bound on strength measurements that one should expect in compression tests and in actual structures so that striving to obtain the unusually high values reported for the special laminates corresponding to the sloping part at the left of figure 6 is inappropriate.

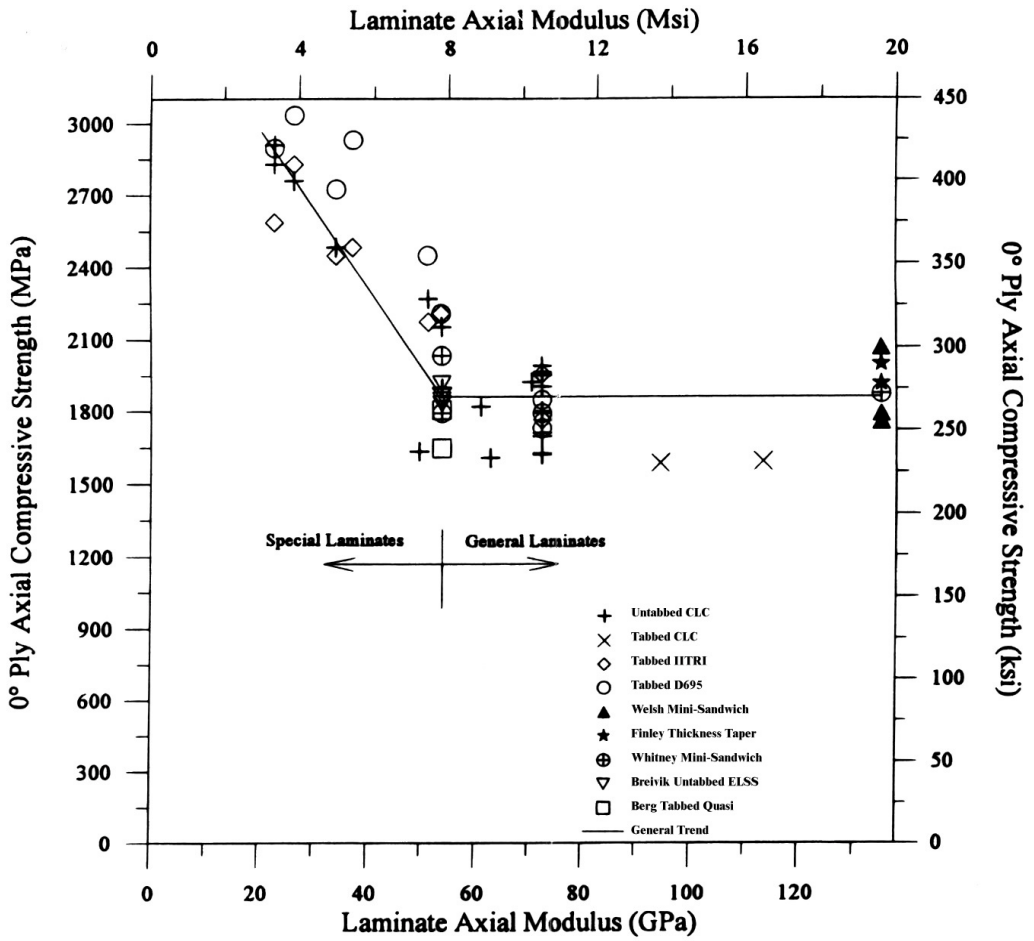

FIGURE 6. BACKED OUT 0°-PLY COMPRESSIVE STRENGTH VERSUS LAMINATE AXIAL MODULUS FOR VARIOUS HERCULES AS4/3501-6 CARBON/EPOXY LAMINATES (Adams and Welsh, 1997)

In addition to studies of the special laminates, Adams and Welsh (1997) compared experimental results for AS4/3501-6 data found in the literature (Adams and Finley, 1996; Welsh and Adams, 1995; Welsh and Adams, 1996; Whitney, et al., 1992; Berg and Adams, 1988; Breivik, et al., 1992) to their results. Again, the axial compressive stress at failure in the 0° plies of any general laminate of this material was essentially constant. By definition, this backed out strength is then the 0°-ply compressive strength "design" value for this material.

Adams and Welsh (1995) determined that the simplest and most reliable composite compression test is obtained from using a $[90/0]_{ns}$ untabbed, straight-sided coupon in the CLC test fixture. The 0°-ply compressive strength is then backed out using classical lamination theory. They were able to show that (1) the axial compressive strengths determined in this manner are representative of those occurring in the 0° plies of any general laminate, (2) low coefficients of variation can routinely be obtained, and (3) the test coupons are easier to fabricate as tabs are not required. Furthermore, the CLC test fixture is less massive and much less complex than the IITRI test fixture, making it easier to use and more economical to fabricate.

A subtle but important feature of this test method is that the specimens are fabricated such that 90° plies are placed on the outside of the test specimen. This protects the primary load bearing 0° plies from any detrimental effects of the thermal-sprayed gripping surfaces of the CLC test fixture (Welsh and Adams, 1997).

2.3 DEVELOPMENT OF THE CLC TEST FIXTURE.

In 1995 Adams and Welsh proposed that, by using a test fixture that would simultaneously shear and end load the specimen, it might be possible to test cross-ply laminates using untabbed coupons. The combined loading test fixture they used was a modified version of the End-Load Side-Support (ELSS) test fixture. This earlier test fixture had been used as a purely end-loaded test fixture since the late 1970s to compression test low strength composites (Irion and Adams, 1981). Finley and Adams (1995) also used the ELSS test fixture to successfully test thickness-tapered, unidirectional composite coupons. By using high bolt torques, i.e., 16.95 to 28.25 N·m (150 to 250 in-lb), on the eight ¼-28 UNF socket head cap screws, they were able to achieve a combined shear and end loading. However, this high clamping force causes unfavorable stress concentrations to develop. Welsh and Adams added a high coefficient of friction thermal-sprayed surface to the previously smooth specimen-contact surfaces of the ELSS test fixture so that the same level of shear loading could be developed with much less clamping force; bolt torques in the range of only 2.26 to 3.39 N·m (20 to 30 in-lb) were typically adequate. This modified ELSS test fixture is now called the Wyoming Combined Loading Compression (CLC) test fixture (see figures 7 and 8). Using this test fixture, Adams and Welsh (1997) tested the untabbed AS4/3501-6 carbon/epoxy laminates listed in table 1. In addition, an attempt was made to test untabbed unidirectional specimens in the CLC test fixture. However, these tests were not successful as the specimens all failed by end crushing if the clamping force was too low, and failure occurred prematurely outside the gage section if the clamping force was increased sufficiently to avoid end crushing.

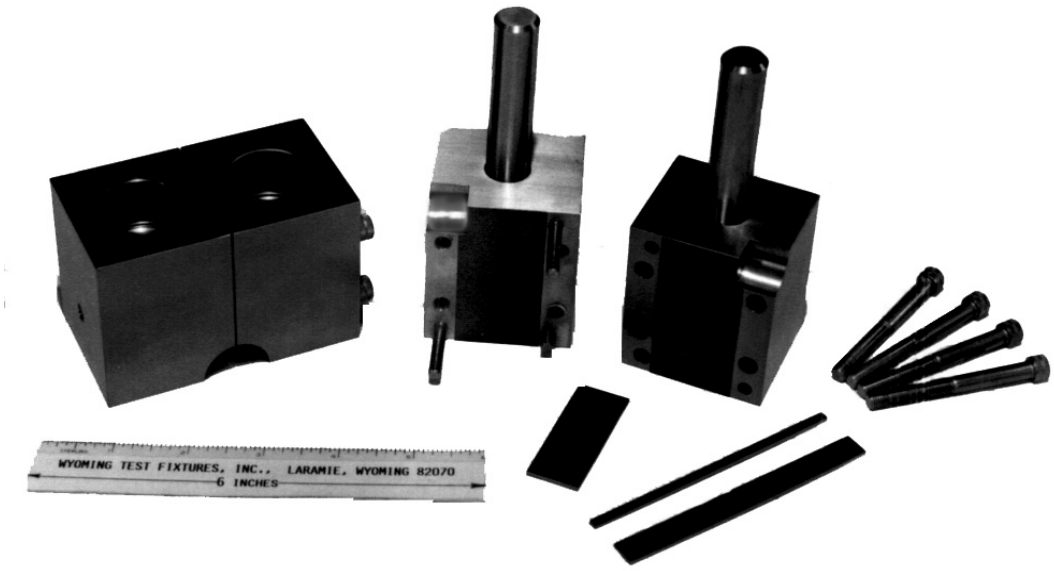

FIGURE 7. PHOTOGRAPH OF WYOMING COMBINED LOADING COMPRESSION TEST FIXTURE (Wyoming Test Fixtures, Inc., 1996)

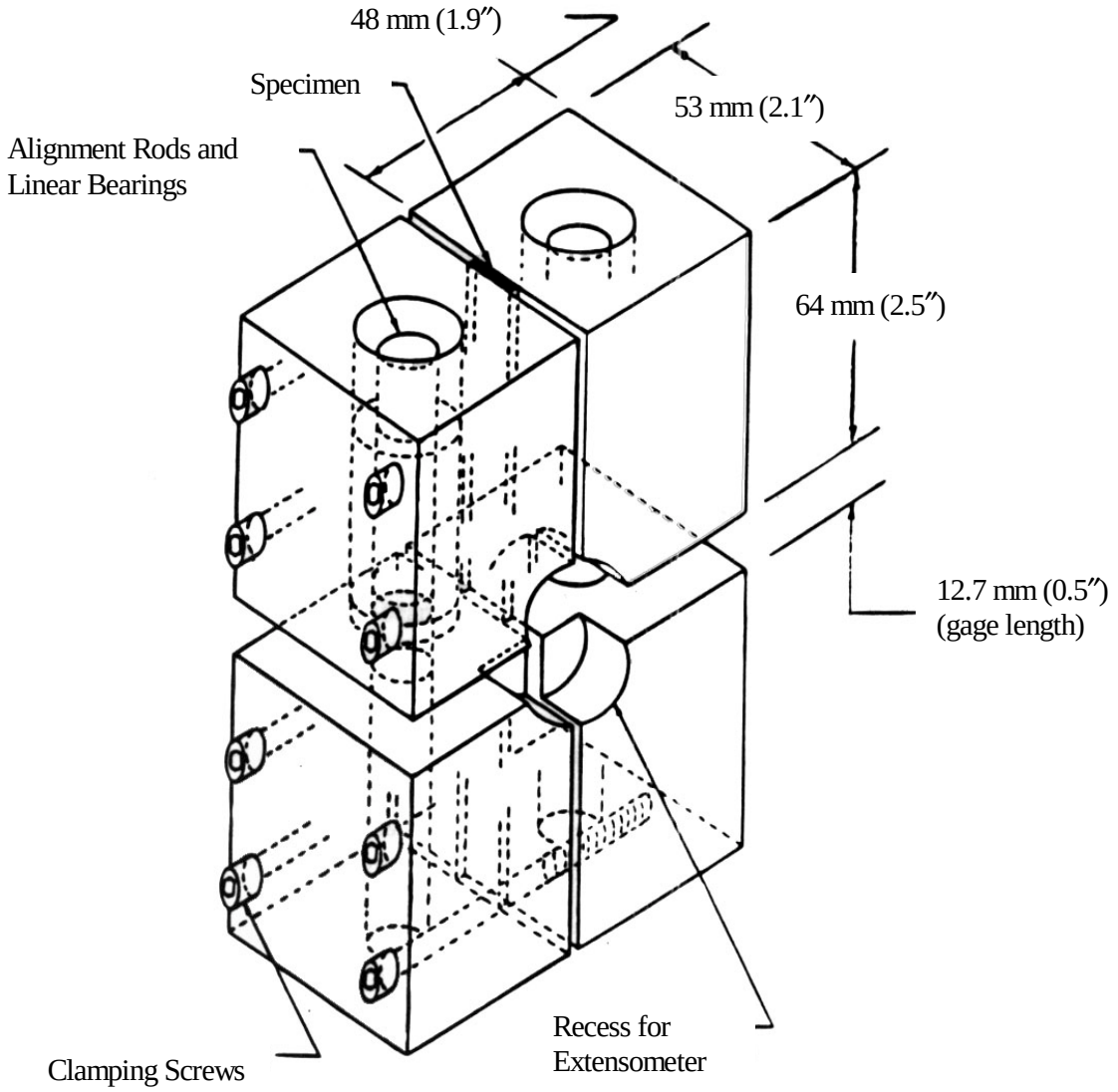

FIGURE 8. SKETCH OF WYOMING COMBINED LOADING COMPRESSION TEST FIXTURE (Adams and Welsh, 1997)

The specimens usually tested in the CLC test fixture are identical in size to the standard IITRI test coupon, but without end tabs. That is, the test specimen is 140 mm (5.5″) in length and 12.7 mm (0.5″) wide, with an unsupported gage section of 12.7 mm (0.50″). However, the standard CLC test fixture can accommodate specimens up to 30 mm (1.2″) wide, and of any reasonable thickness, e.g., up to 25 mm (1.0″) or more, although specimens in the range of 2 to 3 mm (0.080″ to 0.120″) thick are more commonly used.

In 1997, it was shown (Welsh and Adams, 1997b) that 0°-ply compressive strengths obtained by testing cross-ply and angle-ply laminates in the CLC test fixture exhibited less variation than did the results of similar tests conducted in the commonly used IITRI and modified D 695 test fixtures.

TABLE 1. BACKED OUT UNIDIRECTIONAL PLY COMPRESSIVE STRENGTHS OF VARIOUS AS4/3501-6 CARBON/EPOXY LAMINATES TESTED USING THE WYOMING CLC TEST FIXTURE
(Adams and Welsh, 1995)

Configuration	Bolt Torque		Strength		Linear Back-Out Factor
	[N-m]	[in-lb]	[MPa]	[ksi]	
Special Laminates					
$[90_4/0/90_4]_s$	11.3	0-100	2909	422	5.893
$[90_4/0/90_4]_s$	1.7	15	2827	410	5.893
$[(\pm60)_2/0/(\pm60)_2]_s$	1.7	15	2758	400	5.087
$[90_4/0_2/90_4]_s$	2.8	25	2482	360	3.957
$[90_2/0_2/90_4]_s$	5.7	50	2268	329	2.651
General Laminates					
$[(\pm30)_2/0_3/(90)_2]_s$	1.7	15	1027	149[1]	1.672
$[(\pm45/0_2)_2/90]_s$	4.5	40	1924	279	1.792
$[\pm45/0/90]_{2s}$	2.8	25	2151	312	2.517
$[(\pm45)_2/0_3/\pm45]_s$	2.3	20	1820	264	2.200
$[(\pm45)_2/0_3/90_2]_s$	2.3	20	1607	233	2.154
$[(\pm45)_2/90/0]_{2s}$	2.8	25	1896	275	2.517
$[(\pm45)_2/90_3/0_2]_s$	2.3	20	1634	237	2.730
Cross-Ply					
$[90/0]_{3s}$	1.7	15	1427	207[2]	1.877
$[90/0]_{3s}$	1.7	15	1731	251[2]	1.877
$[90/0]_{3s}$	2.8	25	1965	285	1.877
$[90/0]_{5s}$	4.0	35	1993	289	1.877
$[0/90]_{3s}$	2.3	20	1620	235	1.877
$[0/90]_{3s}$	2.8	25	1696	246	1.877
$[0/90]_{3s}$	4.6-13.6	41-120	1627	236[3]	1.877
$[0/90]_{5s}$	3.4	30	1710	248	1.877

[1] Possible edge delamination
[2] Buckled, not valid data
[3] Strength decreased with increasing bolt torque

Adams and Welsh (Adams and Welsh, 1997) also showed that specifically testing cross-ply laminates in the CLC test fixture resulted in "design values" of 0°-ply compressive strength with low variance, as opposed to values obtained from the special laminates discussed earlier. The advantages of the CLC test method relative to others are that tabbed coupons are not required, the fixture is small and relatively inexpensive to fabricate, and the combined loading induced by the CLC test fixture results in a smaller stress concentration in the specimen gage section than in pure shear-loading test fixtures. However, the number of laminates and composite material types tested were not sufficient to prove that the CLC method is applicable to the more general variety of composite materials and types of laminates that usually are encountered. In addition, the results obtained to show that the measured values obtained from the CLC test correspond to the compressive strength that a practical structure will achieve in service were only preliminary.

There also remained a number of other questions surrounding the use of the CLC test fixture. For example, what is the optimum clamping force in the test fixture? How does the amount of bending in a compression test affect the measured 0°-ply compressive strength? What factors influence the amount of bending in a compression test? What method should be used to back out the 0°-ply compressive strength from laminate data, and how is this method affected by material nonlinearities?

These issues were highlighted in discussions held at several meetings of the MIL-HDBK-17 Guidelines and Test Methods committees, and were identified as requiring investigation before the CLC test method could be generally accepted by the composites community. The remainder of this report discusses the research conducted to address these issues, thus documenting the verification of an efficient, precise, and accurate compression test method for fibrous composite materials.

2.4 SUMMARY OF COMPRESSION TEST METHODS.

This discussion of standardized compression test methods and recently developed compression test methods has been presented to indicate the wide variety of compression test methods and the problems associated with each method. In this discussion, a number of aspects of compression testing were discussed that are worthy of summarizing. First, it is important to note the state of confusion regarding compression testing in the composites community at the present time, and the wide range of conflicting results for identical materials that are being published (Rawlinson, 1991).

A second point to note is the nearly exclusive use of unidirectional laminates for strength determination in the standardized compression test methods. Compression testing of a high modulus unidirectional composite laminate is often the most difficult challenge for a compression test method. This is due to the high ratio of axial compressive strength to shear strength of the composite material. One alternative is to test angle- or cross-ply composite laminates and back-out the 0°-ply strengths based on lamination theory. The ASTM standardized compression test methods, ASTM D 34 10 and ASTM D 5467, are also applicable to coupons fabricated from multidirectional laminates, however, there is no method presented in these standards to determine the 0°-ply strengths from these types of laminates.

Another very important point is that for compressive strength data to be of use to the structural designer, the 0°-ply compressive strength measured must correspond to the actual behavior of that material when it is in the structure being designed. Until recently, the goal of compression test method developers was to obtain the highest possible 0°-ply compressive strength. The problem with these values is that the failure modes achieved in tests of these “special” laboratory coupons usually cannot be achieved in structural laminates.

Finally, although it was not explicitly discussed in the previous sections, it should be noted that the measurement of axial compressive strength is very sensitive to many factors outside the realm of the particular test method used. These include the quality and condition of the fixture, sensitivity of the test machine, operator skill, quality of the material, and the care used in coupon fabrication. Many standards do address the required dimensions and tolerance of the test fixtures

and the test coupons. However, there are no standards for other aspects, such as panel fabrication, tabbing procedures, coupon machining, and data acquisition and reduction. It is important that any test method adopted for standardization by the composites community should be fairly robust against these outside factors. An inexperienced laboratory should be able to generate acceptable compressive strength data with a reasonable amount of care. Welsh and Adams (1997) showed that 0°-ply compressive strengths obtained by testing cross-ply and angle-ply laminates in the CLC test fixture had less variation than did similar tests conducted in the IITRI and modified D 695 test fixtures.

At this point, a very attractive test method had been proposed. Adams and Welsh (1997) showed that testing cross-ply laminates in the CLC test fixture resulted in acceptable 0°-ply compressive strengths with a small amount of variance. The advantages of this test method are that tabbed coupons are not required, the CLC test fixture is small and relatively inexpensive to fabricate, and the combined loading in the CLC test fixture should result in a smaller stress concentration in the specimen gage section compared to pure shear-loading test fixtures. However, thorough testing of various laminates and materials had not been conducted to prove that this method works for a variety of materials and laminates. In addition, it had not been shown that this design value corresponds to the compressive strength that a "typical" structural component will achieve in service. There remained a number of other questions also surrounding the use of the CLC test fixture. For example, what is the optimum clamping force in the test fixture? How does the amount of bending in a compression test affect the measured 0°-ply compressive strength. What factors influence the amount of bending in a compression test? What method should be used to back out the 0°-ply compressive strength from laminate data, and how is this method affected by material nonlinearity?

The remainder of this report will discuss the research conducted to answer these questions. This report will also document the verification of an efficient, precise, and accurate compression test method for fibrous composite materials.

3. SPECIMEN FABRICATION.

3.1 INTRODUCTION.

The quality of the test specimens is very important in compression testing of fibrous composite materials (Chaterjee, et al., 1993). For the purposes of this discussion, a test specimen of high quality is one which has uniform and consistent material properties throughout and less than 1% voids and by volume impurities. In addition, the specimen should have a smooth or finely textured surface finish, and it should be uniform in geometry with dimensional variations of less than 2% (ASTM D 5687, 1995). This means that for a 2.54-mm (0.100″) -thick specimen the front and back surfaces of the specimen should be flat and parallel to within 0.051 mm (0.002″) over the length of the specimen. The width of the specimen should measure 12.7 ± 0.254 mm (0.5″ ± 0.01″). The top and bottom surfaces of the specimen should be flat to within ±0.0127 mm (±0.0005″) from one corner of the surface to the extreme opposite corner. This is a tighter tolerance than given in ASTM D 5687-95, but for specimens end loaded in the CLC test fixture it is important that the ends be as nearly flat as possible. The geometry of a typical compression

test specimen is shown in figure 9. A discussion of the effects of specimen thickness variation on the percent bending in a compression test is included in section 5.1.1.

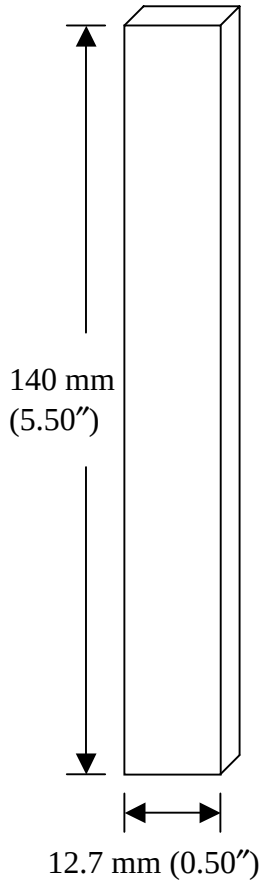

FIGURE 9. TYPICAL GEOMETRY OF CLC AND IITRI TEST SPECIMENS

Therefore, by definition, a set of high-quality test specimens have consistent material properties throughout and are of consistent dimensions and surface finish. Conversely, a set of poor-quality test specimens is a group of specimens that have a large number of voids (i.e., greater than 1% by volume), areas of delamination, inconsistent material properties between specimens or within the same specimen, rough or uneven surface finish, or dimensional variations of more than 2%.

A nearly infinite number of factors can cause these variations in specimen material properties and geometry, so it is nearly impossible to individually discuss each cause. However, these factors can be grouped into three categories, depending on how they are introduced into the finished product: (1) by defects in the starting materials, (2) by improper laminate fabrication, and (3) by poor specimen machining. Defects generated at each step build on the previous one, so variations accumulate very quickly in the finished specimen. In order to reduce variability in the specimens caused by defects in the starting materials, commercially produced unidirectional prepreg tapes were used to fabricate all of the specimens used in the present research. To maintain this quality, the material should be purchased to an appropriate specification. These

tapes were of high quality and consistency and were the most defect-free starting materials available.

The remainder of section 3 will be devoted to a discussion of the fabrication procedures used in this study to minimize the other two types of errors. Section 3.2 will cover general laminate fabrication procedures. The material systems, and their associated cure cycles, will be discussed in section 3.3. Section 3.4 will cover the measurement of fiber and void volume in a composite laminate. Finally, section 3.5 will cover the machining of compression test specimens from 305- × 305-mm (12″ × 12″) composite plates.

3.2 LAMINATE FABRICATION.

Materials and laminate lay-ups which were investigated are described in section 3.3 below. Laminates included those fabricated at Wyoming as well as laminates which were provided by Boeing (see section 3.3.4). For the most part, the Wyoming fabricated laminates were in a 0/90 degree configuration, as described in section 3.5, although 3M's S2/SP381 glass/epoxy laminates were made in both 0/90 and 0/+45/-45/90 quasi-isotropic lay-ups; these are identified along with the Boeing laminates in appendix D.

Many of the processes described in this section, and many suggestions to improve test specimen quality, were obtained from ASTM D 5687-95.

3.2.1 Prepreg Cutting Jig.

As mentioned above, commercially produced unidirectional prepreg tape was used to fabricate all of the laminates used in this study. The prepregs used were supplied on 305-mm (12″) -wide rolls. The prepreg was cut into 305- × 305-mm (12″ × 12″) sheets to lay up the laminates used in this research. For $[90/0]_{ns}$ cross-ply plates, the entire 305-mm (12″) -square sheets of prepreg were used since the fibers were aligned with the edges of the sheets. However, for panels with 45° plies, the 305-mm (12″) -square sheets were trimmed to 216-mm (8.50″) -square sheets to orient the fibers at 45° to the edges of the sheets.

An aluminum jig, shown in figure 10, was used to cut the 305-mm (12″) -square sheets from the roll of prepreg. The jig ensured that each ply of the laminate would have cleanly cut, straight and perpendicular edges. In addition, the cutting jig was used as an aid during laminate stacking to maintain even edges and parallel fiber alignment.

To cut 305-mm (12″) -square sheets of prepreg from the roll, the prepreg was first removed from the storage freezer and allowed to warm to room temperature in a sealed bag. This helps prevent moisture from condensing on the prepreg. The prepreg was then unrolled on a cutting surface that had been thoroughly cleaned with acetone. The prepreg was inserted between the straight edges of the cutting jig and pushed flush against the edges of the cutting jig. A razor blade was drawn through the special slot in the cutting jig to cut precisely 305 mm (12″) of tape from the roll. This approach ensured that the fiber alignment was maintained with the edges of the cut sheet, the edges were each at right angles to each other, and the sheets were each cut to the same dimensions.

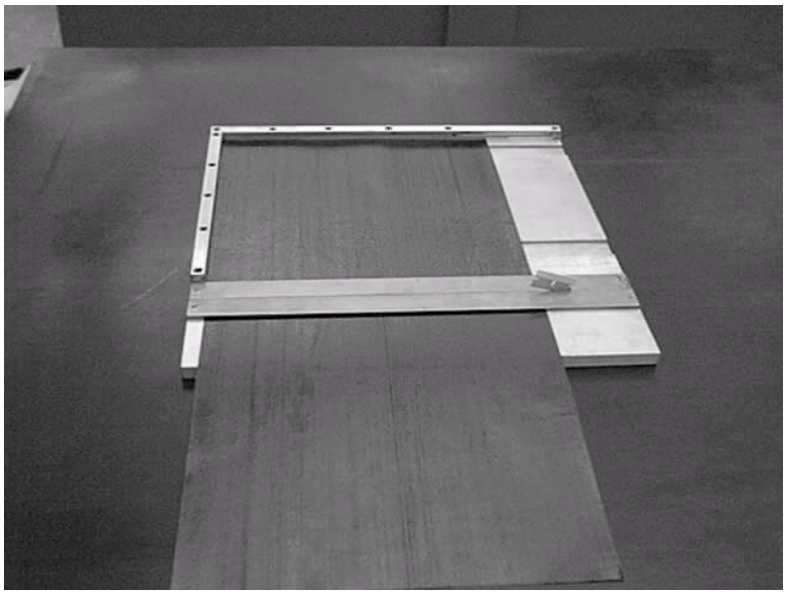

FIGURE 10. PREPREG CUTTING JIG

3.2.2 Laminate Lay-Up Procedure.

The laminates used in this study were formed by laying individual plies of unidirectional prepreg tape one on top of the other in the desired orientations. The prepreg cutting jig, shown in figure 10, was used to maintain edge alignment and consistency. The first ply of prepreg was taped paper side down to the prepreg cutting jig using double-sided carpet tape. The edges of the prepreg sheet were butted securely against the edges of the prepreg cutting jig. The next ply of prepreg was placed face down, with the paper backing up, on top of the first sheet with the fibers oriented in the desired direction. An iron warmed to approximately 110°C (230°F) was used to press the top ply onto the bottom one. This also helped to warm the paper backing for easier removal and to press out air pockets between the prepreg plies. The paper backing was then removed and kept on hand so that the number of plies in the laminate could be rechecked when the lay-up procedure was finished. Each successive lamina was pressed onto the laminate stack using this procedure

When the laminate stack was completed, the number of plies in the laminate were rechecked by counting the number of backing papers collected. Next, a small strip of aluminum foil, approximately 6.35×76.2 mm ($0.25'' \times 3.00''$), was cut and pressed onto one of the edges of the laminate stack that was in contact with the edge of the prepreg cutting jig to serve as a reference edge for machining operations on the finished plate. A ball point pen was used to write the panel number, panel material, panel lay-up, and orientation of the 0° plies on this aluminum tag.

The laminate was then weighed using an Ohaus Inc. triple-beam balance with a 2610 ± 0.1 gram capacity. This precured weight was recorded for each laminate. The laminate was then prepared for the curing process by following the steps outlined in the next section.

3.2.3 Bagging Procedure.

All of the laminates used in this study were cured under the action of both pressure and vacuum. The pressure was used to help consolidate the laminate during the curing cycle, and the vacuum was used to help eliminate voids and trapped gases from the cured laminate. A vacuum bag was placed around the laminate during the curing process so that the external pressure and internal vacuum could be simultaneously applied. In addition, a precision ground steel caul plate, 12.7 mm (0.5″) thick, was placed on each side of the laminate during the cure process to ensure that the cured laminate had flat surfaces and a uniform thickness throughout. Two different vacuum bagging procedures were used, depending on whether or not excess resin had to be bled off of the laminate during the cure cycle.

3.2.3.1 Resin Bleed Vacuum Bag System.

The first type of vacuum bagging procedure is referred to as a bleed system since resin is allowed to escape from the laminate into special bleeder cloths during the cure cycle. To produce a bleed vacuum bag system, the following procedure was used. First, the steel caul plates were cleaned with acetone and allowed to air dry. They were then generously coated with a high temperature release agent such as Zyvax Multi-Shield Release Coating (available from TMI, Inc.) and allowed to dry.

A 305-mm (12″) -square aluminum template was then used to cut two 305-mm (12″) -square sheets of each of the following materials: (1) Mylar film, 0.005″; (2) Northern 200TFNP Teflon-coated, porous glass scrim fabric; and (3) Richmond Aircraft Products No. RC-3000-10-A bleeder cloth. These bagging materials are available from a number of industrial suppliers including Airtech International, Inc. When a 216-mm (8.50″) -square laminate was being fabricated to provide for ±45° lay-ups (figure 11), a smaller 216-mm (8.50″) -square aluminum template was used in place of the 12″ square plate used for 0/90 degree laminates. In addition, the following materials were cut from their respective rolls: one 330- × 330-mm (13″ × 13″) sheet of Airtech N7 breather cloth, one 457- × 457-mm (18″ × 18″) sheet of Wrightlon 8400 Nylon vacuum bagging material, and one 381- × 381-mm (15″ × 15″) sheet of Airtech A4000R red stretch film.

Once these materials had been prepared, the vacuum bag stack was assembled. First, the lower caul plate was placed flush against the inside edges of the prepreg cutting jig. The jig was used during the bagging procedure to maintain alignment of the caul plates, the uncured laminate, and the bagging materials. Then the 381- × 381-mm (15″ × 15″) sheet of red stretch film was centered over the lower caul plate, leaving roughly 38 mm (1.5″) of film overlapping each side of the caul plate. Next, one layer of Mylar film was placed on top of the stretch film. This was followed by one sheet of bleeder cloth, one sheet of 200TFNP porous fabric, and then the uncured laminate. The stack was completed by covering the uncured laminate with one sheet of 200TFNP porous fabric, one sheet of bleeder cloth, one sheet of Mylar film, and finally the top caul plate.

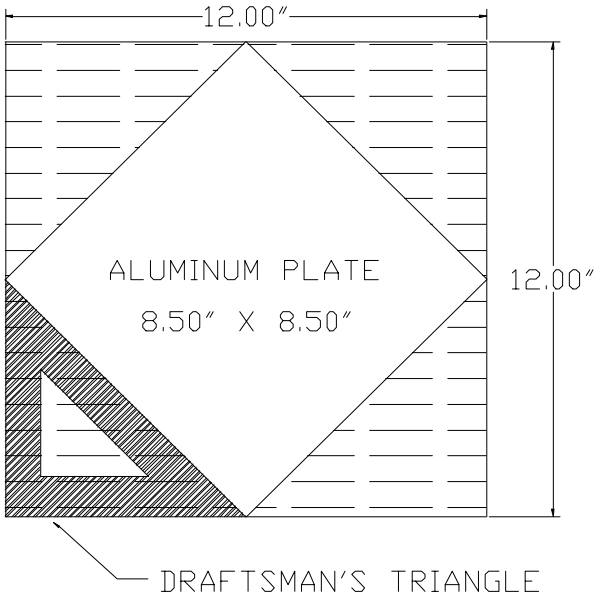

FIGURE 11. CUTTING ±45° LAMINA FROM 305- × 305-mm (12″ × 12″) UNIDIRECTIONAL PREPREG SHEETS

Four strings of glass fiber tow, approximately 304 mm (12″) long, were placed along the edges of the uncured laminate such that they extended beyond the edges of the laminate stack by roughly 51 mm (2″). Then the overlapping pieces of red stretch film were pulled over and taped to the top of the upper caul plate.

The uncured laminate was wrapped inside the red stretch film along with the other bagging materials and the top caul plate. The exposed ends of the glass fiber tows were brought to the top of the caul plate. These glass strings serve as vacuum paths for gases to escape from the panel during the curing process. A schematic of the stack of materials and a photograph of the final stack are shown in figure 12.

3.2.3.2 No-Bleed Vacuum Bag System.

The other type of vacuum bag system used does not allow any resin to escape from the laminate during the curing cycle. This system is referred to as a no-bleed vacuum bag system. A no-bleed vacuum bag is fabricated in nearly the same manner as the bleed vacuum bag system. The difference is that the two sheets of Northern 200TFNP Teflon-coated porous glass scrim fabric are replaced with an otherwise identical Northern 200TFNP Teflon-coated nonporous fabric. In addition, the two sheets of Richmond Aircraft Products No. RC-3000-10-A bleeder cloth are left out of the laminate stack. The remainder of the vacuum bag procedure is carried out in exactly the same way as previously described.

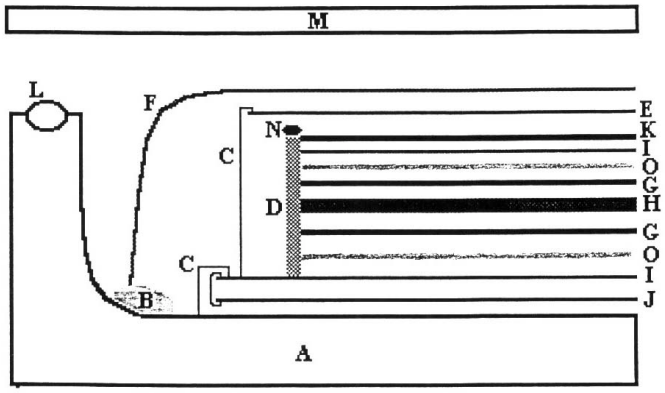

A. Press-clave (bottom plate)
B. Vacuum bag sealant (tacky tape)
C. High-temperature tape
D. Cork/rubber dam
E. Breather
F. Vacuum bag
G. Teflon-coated glass scrim (porous)
H. Prepreg stack
I. Mylar
J. Bottom caul plate (aluminum)
K. Top caul plate (steel)
L. Silicone O-ring
M. Press-clave (top plate)
N. Glass tow to vacuum port
O. Bleeder material

(a) Stacking Orientation of Bagging Films

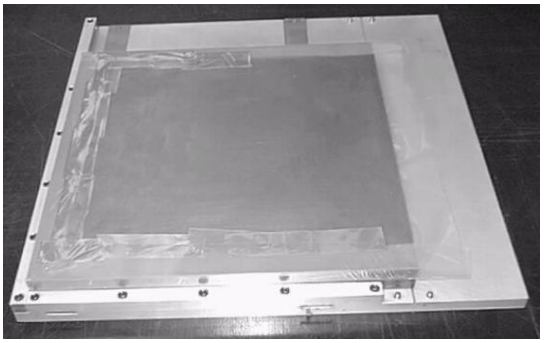

(b) Wrapping Stretch Film Around Laminate and Top Caul Plate

FIGURE 12. VACUUM BAGGING PROCEDURE

3.2.4 Press-Clave.

The stack containing the caul plates, bagging materials, and uncured laminate was placed in the bottom of the press-clave shown in figure 13. The press-clave used by the Composite Materials Research Group (CMRG) at the University of Wyoming contains two ports. One is used to apply external pressure to the uncured laminate, while the second one is used to draw a vacuum on the vacuum bag. The CMRG press-clave includes a Type J thermocouple to monitor the laminate temperature during the cure cycle. The vacuum is supplied by an external vacuum pump and the pressure is supplied by an external air compressor. Heat is supplied to the press-clave by a hot-press. This hot-press is also used to seal the halves of the press-clave together. Section 3.2.5 describes the hot-press used by the CMRG.

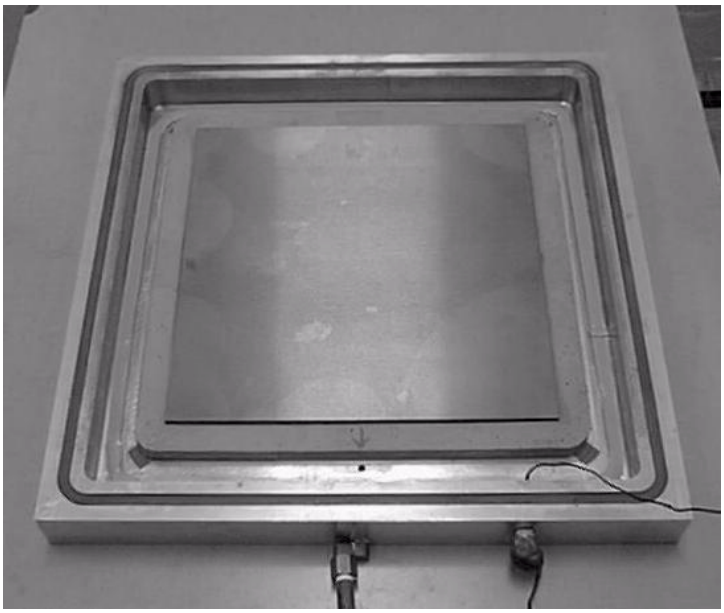

FIGURE 13. PRESS-CLAVE WITH SILICONE RUBBER DAM AROUND THE UNCURED PLATE

A silicone rubber dam 25 mm (1″) wide by 19 mm (0.75″) thick was placed around the perimeter of the bottom caul plate and the uncured laminate. This silicone rubber dam helped prevent resin from flowing out the edges of the uncured laminate during the cure cycle. In addition, the thermal expansion of the silicone rubber dam helped compact the edges of the laminate during the curing process. The laminate stack was covered with the 330- × 330-mm (13″ × 13″) sheet of Airtech N7 breather cloth so that the sharp edges of the top caul plate were covered by the breather cloth. A vacuum path was created between the laminate stack and the vacuum port in the bottom of the press-clave by running a 25-mm (1″) -wide by 127-mm (5″) -long strip of breather cloth from the vacuum hole in the bottom of the press-clave to the breather cloth on top of the laminate stack.

A bead of vacuum bag sealant tape, such as Airtech GS-213, was then placed on the inside surface of the press-clave around the perimeter of the laminate stack (Airtech International, Inc.). A space of about 25 mm (1″) was left between the edges of the bottom caul plate and the sealant tape. The protective paper covering was left on the top of the sealant tape during this step. Next, a row of vacuum bag sealant tape was placed around the perimeter of the 457- × 457-mm (18″ × 18″) sheet of vacuum bag film. Again, a space of about 25 mm (1″) was left between the outside edge of the bagging film and the sealant tape, and the protective paper covering was left in place on the sealant tape. Then, the vacuum bag film was placed over the top of the laminate stack so that the sealant tape on the vacuum bag film matched up with the sealant tape on the press-clave. Starting at one corner, the protective paper was simultaneously removed from the sealant tape on the press-clave and the tape on the vacuum bag film and the two beads of sealant tape were pressed together at this corner. Then working from the corner, the protective paper was removed from the sealant tape and the two beads of sealant tape were meshed together until the vacuum bag film was sealed over the top of the laminate stack. Excess vacuum bag film was taken up by pinching the excess film over on itself at the location of the sealant tape so that a double bead of

sealant tape was between the excess vacuum bag film. This created a tight seal of the vacuum bag over the laminate stack and allowed for flexing of the vacuum bag during the laminate cure cycle.

When this process was completed the vacuum pump was attached to the vacuum port of the press-clave. Air holes in the sealant tape were sealed by pressing the two beads of sealant tape together onto the bottom of the press-clave. The vacuum pump was operated until a vacuum of 75 kPa (22 inches of Hg) had been pulled on the vacuum bag. Then the vacuum pump was shut off. If the vacuum did not drop by more than 1.5 kPa (0.5 inch of Hg) in any 30 second period, the vacuum bag was judged acceptable for the cure cycle. If the vacuum bag leaked more than this amount, then the sealant tape around the perimeter was pushed harder against the base of the press-clave until the leaks in the vacuum bag were stopped.

Finally, the press-clave lid was placed on the base of the press-clave. The press-clave was then set into the hot-press and the pressure and vacuum lines were connected.

3.2.5 Hot-Press.

A Wabash Metal Products Company, Inc. hydraulic hot-press was used. The press has a 445-kN (50-ton) capacity, with 200-watt heaters in the upper and lower platens. There are separate temperature controllers for the upper and lower heaters. The lid of the press-clave was sealed to the base of the hot-press using a contact pressure of 688 kPa (100 psi). Figure 14 shows the press-clave in the Wabash hot-press.

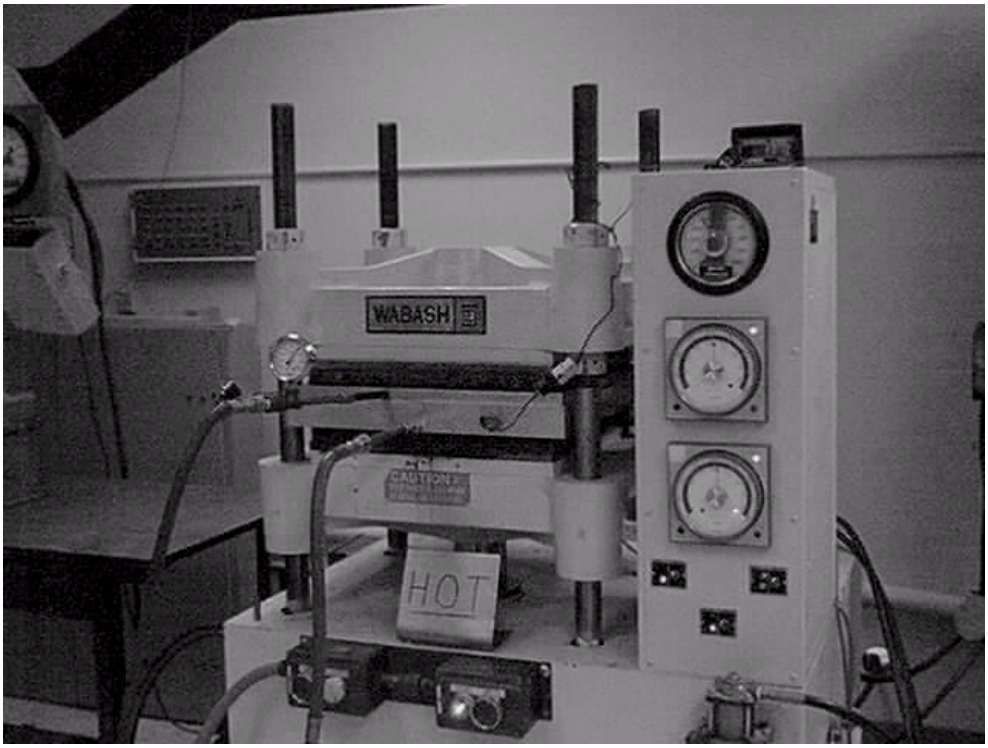

FIGURE 14. PRESS-CLAVE IN WABASH HOT-PRESS

3.3 MATERIAL SYSTEMS.

The material systems used to fabricate the specimens used in this study are described in this section. Commercially produced, unidirectional fibers preimpregnated with resin epoxy (prepreg) in 305-mm (12″) -wide rolls were used to fabricate all of the test specimens. This material form was selected so that uniform and consistent starting materials would be used in all of the laminates.

Additional materials were supplied by Boeing Space Systems Division; however, these materials were supplied as fully cured 305- × 38-mm (12″ × 1.50″) test blanks. Therefore, the fabrication procedures and cure cycles for these materials are not discussed in this report. However, the mechanical properties of these materials are given in section 3.3.4.

3.3.1 AS4/3501-6 Carbon/Epoxy.

Hercules AS4/3501-6 carbon/epoxy prepreg was the first material selected for this study because it is widely used in the composites industry and is one of the material systems most commonly found in the published compression testing literature (e.g., Adams and Lewis, 1991; Crasto and Kim, 1991). In addition, researchers in the CMRG have used this material system for many studies (e.g., Adams and Welsh, 1997; Adams and Finley, 1997). Therefore, the optimum fabrication techniques and the properties of this material are well defined.

The linear elastic lamina properties of this material are listed in table 2. These data were compiled from material characterization tests conducted at the CMRG (CMRG, 1992) to determine the values shown in the table 2.

TABLE 2. LINEAR ELASTIC PROPERTIES OF AS4/3501-6 CARBON/EPOXY UNIDIRECTIONAL COMPOSITE MATERIAL

Material Property	GPa	Msi
E_{11}	135	19.6
E_{22}	9.0	1.3
G_{12}	6.9	1.0
ν_{12}	0.28	0.28

AS4/3501-6 carbon/epoxy is a 177°C (350°F) cure system. The cure cycle shown in figure 15, as recommended by Hercules, Inc. (Hercules, 1991), was used for this material system. After the laminates had been cured, the panels were postcured at 177°C (350°F) for 4 hours ± 10 minutes.

The AS4/3501-6 carbon/epoxy prepreg used in this study had a fiber aerial weight of 150 g/m^2 and a resin content of 37% by weight. The target fiber content by volume for the test coupons used in this research was 62%. Therefore, it was required to bleed a small amount of resin from the system during the cure cycle. After some experimentation, it was determined that one bleeder ply placed on top of the laminate and a nonporous peel ply on the bottom of the laminate during the cure cycle resulted in the correct amount of resin bleed-off to reach the desired fiber volume percentage.

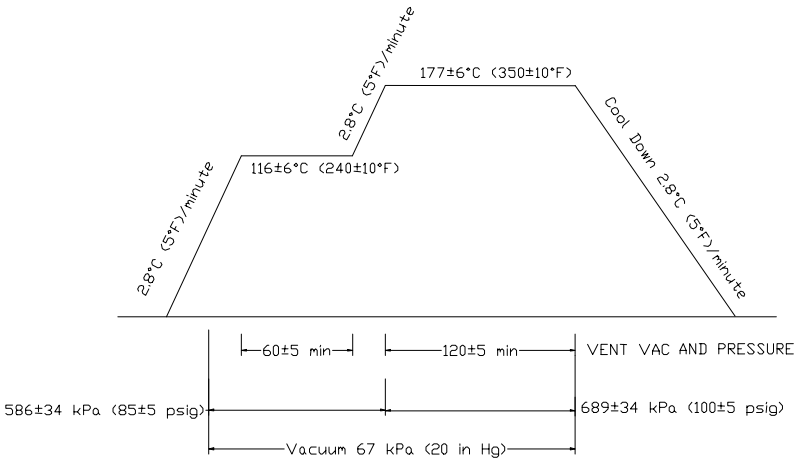

FIGURE 15. HERCULES RECOMMENDED CURE CYCLE FOR AS4/3501-6 CARBON/EPOXY PREPREG

3.3.2 S2/301-NCT Glass/Epoxy.

Newport, Inc. S2/301-NCT glass/epoxy prepreg was used to fabricate a number of compression test specimens. The material had a high resin content in its uncured form. The fiber content by volume, according to the suppliers data sheet, was approximately 44.7%, although the target fiber content by volume was 62%. Therefore, the prepreg was cured using a bleed system with two layers of bleeder cloth on each side of the laminate to bleed a large amount of resin from the laminate during the cure process. The resulting average fiber content by volume in the cured S2/301-NCT laminates was 57%. It may not be possible to raise the fiber volume content much more than this amount because it appeared that the second layer of bleeder cloth was not fully saturated with resin after the cure cycle was completed. This means that the epoxy was cross linking, or setting up and not allowing any additional resin to flow into the bleeder cloths.

The 301-NCT epoxy is a 120°C (250°F) curing system. The supplier's recommended cure cycle shown in figure 16 was used. The linear elastic properties of this material are shown in table 3.

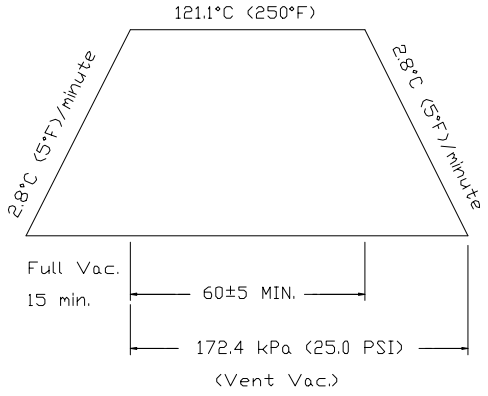

FIGURE 16. NEWPORT'S RECOMMENDED CURE CYCLE FOR S2/301-NCT GLASS/EPOXY PREPREG

TABLE 3. LINEAR ELASTIC MATERIAL PROPERTIES OF S2/301-NCT GLASS/EPOXY

Material Property	GPa	Msi
E_{11}	51.0	7.4
E_{22}	20.1	3.0
G_{12}	6.9	1.0
ν_{12}	0.28	0.28

3.3.3 S2/SP381 Glass/Epoxy.

3M Corporation, Inc. donated S2/SP381 glass/epoxy prepreg for use in this study. The material also had a high resin content, approximately 50% resin by volume. It was decided that the resin content would not be changed by the use of a bleed vacuum bag system since 3M has quoted material properties in MIL-HDBK-17 (1997) at 50% fiber volume. This allowed for a direct comparison of values obtained by the CMRG with those values published in MIL-HDBK-17.

The SP381 epoxy is also a 120°C (250°F) curing system. The cure cycle shown in figure 17, as recommended by 3M (3M, 1997), was used. The material property data shown in table 4 were obtained from the Proceedings of the MIL-HDBK-7 Polymer Matrix Composites Coordination Group, Spring 1997 Meeting in Tucson, Arizona (MIL-HDBK-17, 1997).

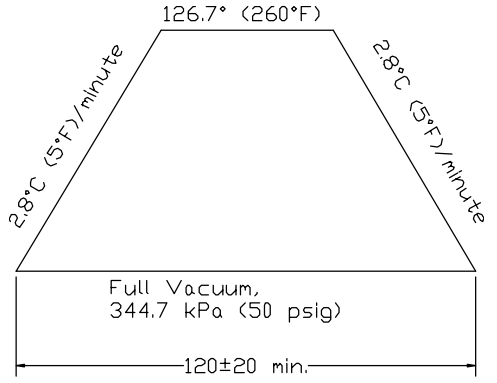

FIGURE 17. CURE CYCLE FOR S2/SP381 GLASS/EPOXY

TABLE 4. LINEAR ELASTIC MATERIAL PROPERTIES OF S2/SP381 GLASS/EPOXY

Material Property	GPa	Msi
E_{11}	51.8	7.5
E_{22}	22.1	3.2
G_{12}	6.9	1.0
ν_{12}	0.28	0.28

3.3.4 Boeing-Supplied Materials.

Boeing Space Systems Division provided the following materials for additional comparative testing: T50/2134A carbon/epoxy, T300/3034 carbon/epoxy, T800/2302-19 carbon/epoxy, and P75s/2034 carbon/epoxy. Two different laminates of each material were provided, a $[45/0/-45/90]_{2s}$ quasi-isotropic laminate and a $[90/0]_{4s}$ cross-ply laminate. The laminates were supplied in the form of fully cured test blanks, approximately 305 mm (12″) long by 38 mm (1.5″) wide. The 0° fiber direction was oriented along the length of the blanks. Compression test specimens were machined from these laminates as described in Section 3.5.2 Specimen Cutting and Grinding.

The linear elastic material properties listed in table 5 were supplied by the Boeing Space Systems Division (Boeing, 1997).

TABLE 5. MECHANICAL PROPERTIES OF BOEING-SUPPLIED MATERIALS

Material Property	T50/2134A		T300/3034		T800/2302-19		P75s/2034	
	GPa	Msi	GPa	Msi	GPa	Msi	GPa	Msi
E_{11}	211	30.6	118	17.1	139	20.1	227	32.9
E_{22}	7.93	1.15	8.96	1.30	8.00	1.16	6.41	0.93
G_{12}	5.52	0.80	4.55	0.66	4.00	0.58	3.24	0.47
ν_{12}	0.35		0.34		0.40		0.24	

3.4 FIBER AND VOID VOLUME MEASUREMENTS.

Two separate fiber and void volume measurement techniques were used for the glass fiber composite materials and the carbon fiber composite laminates fabricated in the course of this research. The fiber and void content of the materials supplied by Boeing Space Systems Division were not measured in this study. Both techniques followed the recommendations of ASTM D 3171-76 (1992) and ASTM D 792-66 (1991) in which fiber and void volume measurements are performed using a matrix digestion procedure. The initial steps in both methods are the same; the only difference in the two techniques is the method used to remove the matrix material from the fibers. The matrix material in the glass fiber composite materials was removed using a burn-off oven. The matrix material in the carbon fiber composite materials was removed using a nitric acid digestion process. These two processes are described in the following sections.

First, three small samples roughly 38 × 6.4 mm (1.5″ × 0.25″) with the thickness of the laminate were cut from each composite laminate. The samples were cut along the 0° direction of the fibers at a distance of about 12.7 mm (0.50″) from each edge of the laminate. The three specimens were marked as Nos. 1, 2, and 3 and the location of each specimen from the cut laminate was recorded. The edges of each cut specimen were polished using 320 grit emery paper immersed in tap water. This process removed any fiber splinters from the edges of the specimen which could hold air bubbles during the submerged weighing process described next.

The fiber and void volume specimens were individually weighed using a calibrated Mettler, Inc. Model HL32 balance. The balance has a resolution of 0.0001 gram. Next, the submerged

weights of the specimens were obtained by individually placing the specimens in a wire basket that was suspended from a hook on the balance. The wire basket containing the specimen was lowered into a beaker of distilled water, and the basket was gently tapped to remove any air bubbles from the specimen and the basket. Then the weight of the specimen was recorded, the weight of the empty basket submerged in the water having been previously zeroed out. The water temperature was measured using a mercury thermometer with a resolution of 0.5°C. The water density was calculated based upon the water temperature and this value was recorded.

3.4.1 Nitric Acid Digestion Method.

The carbon fiber specimens were then placed in individual 100-ml glass beakers marked Nos. 1, 2, and 3. These beakers were filled with 60 ml of 70% nitric acid, covered with a watch glass, and placed on a hot plate heated to approximately 120°C (250°F). The specimens remained in the beakers on the hot plate for roughly 1 hour after the nitric acid began to boil, or until, based on a visual inspection, no epoxy matrix material remained, bonding the individual fibers together. When this point had been reached, the beakers were removed from the hot plate and allowed to cool. The nitric acid was carefully drained off so that all fibers remained in the beaker. The nitric acid was poured into a waste container for disposal. The beakers containing the carbon fibers were then refilled with 100 ml of distilled water. The fibers were gently swirled in the beakers using a glass stirring rod to clean the acid and epoxy matrix residue from the fibers. Next, the distilled water was carefully drained off and disposed of. This process was repeated two more times, followed by a final rinse using 95% ethyl alcohol. The beakers were then placed in a drying oven at 49°C (120°F) for a minimum of 8 hours to thoroughly dry the fibers. The beakers were then placed in a sealed desiccator and allowed to cool to room temperature. The beakers were then removed from the desiccator and the fibers in the individual beakers were weighed using the Mettler balance. This weight was recorded for each specimen.

The dry weight of each fiber and void volume specimen, the submerged weight of each specimen, the weight of the fibers alone, and the densities of the fiber and matrix materials were used to calculate the fiber and void volume percentages of each specimen as described in ASTM D 3171-76 (1992) and ASTM D 792-66 (1992).

3.4.2 Burn-Off Oven Digestion Method.

The fiber and void volume specimens from the glass fiber composite laminates were prepared as described in the previous subsection and the dry weight and submerged weights were obtained in the same manner. After the submerged weight of the specimens was recorded, the specimens were placed in Coors No. 002 ceramic crucibles, marked Nos. 1, 2, and 3. The crucibles were then placed in a Hoskins Electric Furnace, Model No. FD202C, at a temperature of 538°C (1000°F) for 2 hours or until the epoxy matrix had been completely removed from the glass fibers. The crucibles were then placed in a sealed desiccator and allowed to cool to room temperature. The weights of the fibers from each individual specimen were then obtained using the Mettler balance. The fiber and void volume percentages were then calculated as specified in ASTM D 3171-76 (1992) and ASTM D 792-66 (1992).

3.4.3 Panel Identification and Fiber Volume Content.

A name was given to each panel to specify the panel fabricator, the panel material, the order of the panel fabrication, and the panel lay-up. This nomenclature is described below.

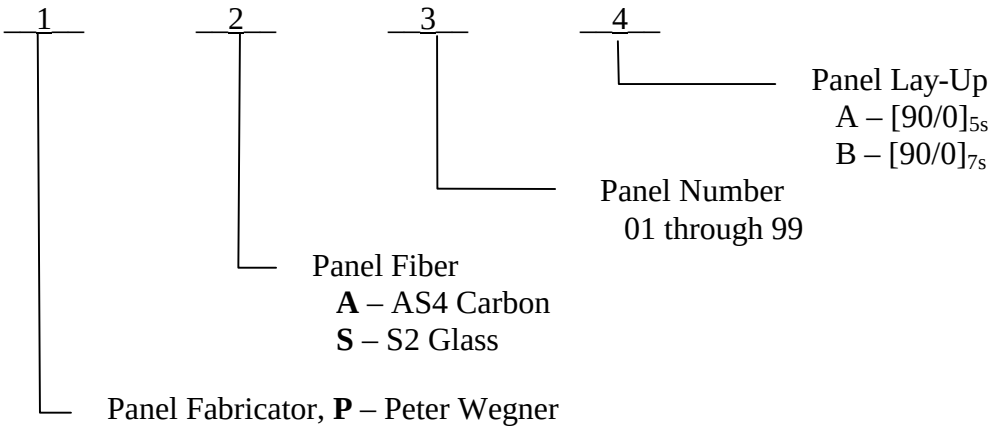

For example, Panel PA01A was fabricated by Peter Wegner, it contains AS4 carbon fiber, it was the first panel made in this group, and the panel lay-up was $[90/0]_{5s}$.

The fiber volume and void volume contents for the panels fabricated in the present study are listed in table 6.

TABLE 6. MEASURED FIBER VOLUME CONTENT OF PANELS FABRICATED FOR THE PRESENT STUDY

Panel No.	Material	Lay-Up	Fiber Volume [percent]	Void Volume [percent]	Comments
PA01A	AS4/3501-6	$[90/0]_{5s}$	n/a	n/a	Panel discarded, bad finish
PA02A	AS4/3501-6	$[90/0]_{5s}$	64.7	0.1	
PA03A	AS4/3501-6	$[90/0]_{5s}$	68.6	0.1	
PA04A	AS4/3501-6	$[90/0]_{5s}$	62.2	0.1	
PA05A	AS4/3501-6	$[90/0]_{5s}$	63.4	0.1	
PA06A	AS4/3501-6	$[90/0]_{5s}$	n/a	n/a	Lost vacuum, discarded
PA07A	AS4/3501-6	$[90/0]_{5s}$	62.8	0.1	
PA08A	AS4/3501-6	$[90/0]_{5s}$	62.2	0.1	
PA01B	AS4/3501-6	$[90/0]_{7s}$	60.1	0.1	
PS01A	S2/301-NCT	$[90/0]_{5s}$	44.6	0.1	Discarded, low fiber content
PS02A	S2/301-NCT	$[90/0]_{5s}$	47.8	0.2	Discarded, low fiber content
PS03A	S2/301-NCT	$[90/0]_{5s}$	51.7	0.2	Discarded, low fiber content
PS04A	S2/301-NCT	$[90/0]_{5s}$	56.1	0.3	
PS01B	S2/SP381	$[90/0]_{7s}$	49.2	0.5	Fiber content agreed with 3M data

n/a – not available

3.5 SPECIMEN FABRICATION.

Two different procedures were used to fabricate tabbed and untabbed specimens. To fabricate tabbed specimens, the 305-mm (12″) -square laminate panels were cut into smaller subpanels. The required tabbing material was then bonded to these subpanels and the individual specimens were machined from these subpanels. To fabricate untabbed test specimens, the 305-mm (12″) -square laminate panels were cut into strips 13.2 mm (0.520″) wide with the 0° direction running the length of the strip. These strips were then cut to the required lengths for the individual compression test specimens. These procedures are described in detail in the following paragraphs.

3.5.1 Specimen Tabbing Procedure.

Regal Plastics, Inc. balanced-weave E-glass fabric/epoxy G-10 composite material, 1.59 mm (0.0625″) thick, was used as the tabbing material in this study. The procedures used to fabricate tabbed specimens are discussed in this section. These procedures follow the recommendations found in the "Tabbing Guide for Composite Specimens," a report prepared for the Federal Aviation Administration by the CMRG (CMRG, 1996).

The 305-mm (12″) -square laminate panels were cut into subpanels approximately 85.3 mm (3.36″) wide by 150 mm (5.90″) long. The subpanels were cut so that the 0° direction was oriented parallel to the long side of the subpanel. Six finished test specimens could be fabricated from one of these subpanels. The finished test specimens were 12.7 mm (0.500″) wide and 140 mm (5.50″) long; it was necessary to leave 1.52 mm (0.060″) between each specimen to allow for the width of the cutting blade and for the final grinding operation. In addition, a strip of material 0.508 mm (0.020″) wide was left on the top and bottom of the subpanel to allow for final end grinding of the specimens.

The laminates were cut using a Brown and Sharpe Mfg. Co. Model 2L surface grinding machine. A 152-mm (6.0″) -diameter by 1.02-mm (0.040″) -thick abrasive cutting wheel was mounted to the surface grinding machine. The surface grinding machine has a horizontal table with a motorized carriage that moves the table back and forth beneath the rotating abrasive cutting wheel. The location of the abrasive cutting wheel over the horizontal table is precisely controlled by a gear-driven wheel with a 0.025-mm (0.001″) vernier scale that moves the table in and out beneath the rotating wheel. A second wheel with a similar 0.025-mm (0.001″) vernier scale moves the wheel up and down over the translating horizontal table to control the height of the wheel over the horizontal table. Two small nozzles spray water onto each side of the abrasive cutting wheel. This serves to cool the blade and to control dust generated during the cutting operation. This machine allows for very precise cuts to be made on the laminate panels.

The laminate panels were taped to a sacrificial piece of plexiglass using double-sided carpet tape. This plexiglass/laminate stack was then fixed with double-sided carpet tape to a steel plate roughly 305 mm (12″) square by 6.4 mm (0.25″) thick. The horizontal table of the surface grinding machine has a magnetic base that locks the steel plate securely against the surface of the table. This set-up holds the laminate tightly in place during the cutting operation.

Careful attention was paid to maintaining alignment of the 0° direction in the laminate panel and the subpanels during the cutting operation. The reference edge of the panel that was marked during the fabrication process (refer to section 3.3.2) was aligned with the direction of travel of the grinding machine's horizontal table with the aid of a machinist's dial indicator. The dial indicator was attached by a magnetic base to a stationary part of the grinding machine. The laminate, taped to the plexiglass/steel plate holder, was placed on the horizontal table and the dial indicator was set against the reference edge of the laminate. The horizontal table was then moved back and forth manually as adjustments were made to the location of the laminate on the table so that the dial indicator did not move as the laminate moved past it. This ensured that any cuts on the laminate were parallel to the reference edge, and therefore the 0° direction, of the laminate.

When the cutting operation was completed, all of the subpanels were wet sanded very lightly with Micro-Measurements Group Conditioner A and 3M Company 320 grit wet-or-dry sandpaper. Following this, the subpanels were measured at eight locations to determine the thickness variation of each subpanel. Acetone was then used to clean the subpanels to prepare for the tabbing procedure.

The G-10 material was supplied in 1.22-m (4-ft.) -square sheets so it was necessary to first cut four smaller pieces, 85.3 × 68.6 mm (3.36″ × 2.70″), from the larger sheet, using a DoAll Company, Inc. band saw. These four tab pieces were then lightly grit blasted using a Trinco Tool Co. Model 48/BP2 dry-grit blasting machine. This grit-blasting machine has an 8.26-mm (0.325″) -diameter nozzle; a pressure of 345 kPa (50 psig) was used with 300 grit sand. The tab pieces were cleaned with water, followed by acetone, and then allowed to air dry.

Two 12.7-mm (0.500″) -wide machinist's parallels were cleaned with acetone and coated with Zyvax Multi-Shield release coating. These parallels were used as spacers to keep the tabs from moving during the bonding operation and to maintain the required 12.7-mm (0.500″) gage section on the test specimens. One side of each spacer was covered with double-sided carpet tape with the protective paper covering left on one side of the tape.

With gloved hands, the 12.7-mm (0.500″) gage section was marked on each side of the subpanel using a machinist's scale and a pencil. Then the remaining protective paper was removed from the double-sided carpet tape on one of the spacers and the spacer was pressed onto the subpanel so that the edges of the spacer lined up with the gage section of the subpanel. This process was repeated on the other side of the subpanel using the second spacer. Then one of the four tab pieces was laid, grit-blasted side down, onto the subpanel so that it butted against the spacer bar. This tab was then attached to the spacer using a strip of masking tape. This process, as shown in figure 18, was repeated for all four tab pieces.

Next, the entire assembly of subpanel, tabs, and spacers was wrapped with masking tape. This ensured that excess adhesive did not get on the outside of the tabs, as excess adhesive can cause an uneven clamping force on the specimen when it is loaded in the test fixture. Then, using a razor blade, the tape on the edges of the subpanel was slit lengthwise to create a hinged tab, as shown in figure 19.

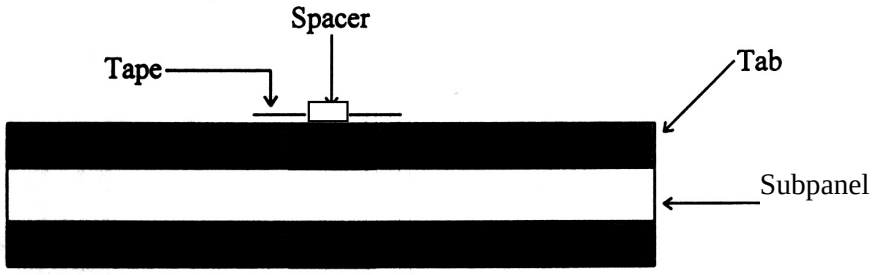

FIGURE 18. ASSEMBLY OF TAB PIECES, SPACERS, AND SUBPANEL (CMRG, 1996)

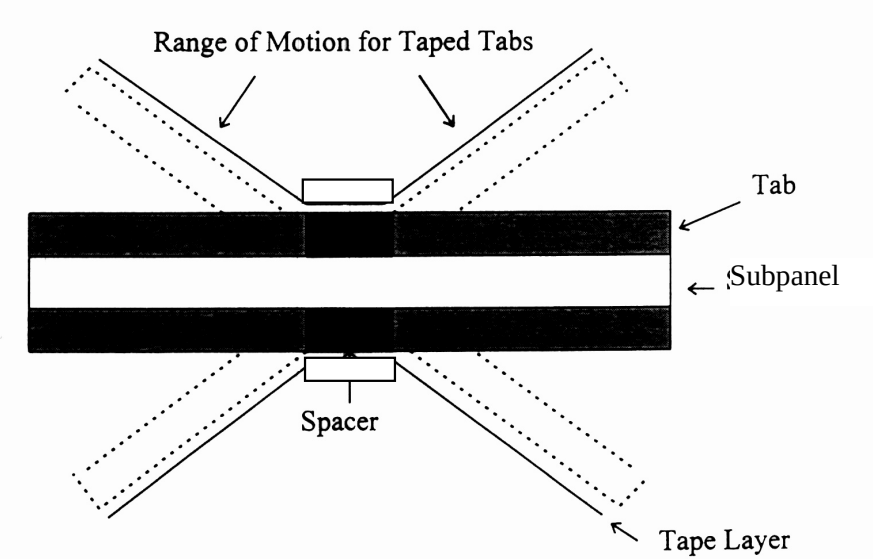

FIGURE 19. HINGED TABS ON SUBPANEL (CMRG, 1996)

3M Corporation AF163-2 film adhesive was used to bond the tabs to the subpanel. The adhesive was removed from the storage freezer and allowed to warm to room temperature in the sealed storage bag. Then square pieces of adhesive were cut to fit precisely under the tab pieces. The plastic backing material was peeled from the adhesive and the adhesive was pressed onto the subpanel. The hinged tab was then pressed down on top of the adhesive and the subpanel. This process was repeated for all four tab pieces. A piece of masking tape was placed across the edges of the subpanel to keep the tabs down.

The subpanel was then wrapped in Northern 200TFNP Teflon-coated, porous glass scrim fabric. This stack was wrapped in a piece of breather cloth and placed in a vacuum bag. A vacuum port was installed in the side of the vacuum bag. The vacuum bag and subpanel assembly was then placed in a Blue M Electric Company Model OV-490A-2 vacuum oven for 1 hour at 127°C (260°F) with a vacuum pressure of approximately 62 kPa (9 psig). Following this, the subpanel was allowed to cool to room temperature before it was removed from the oven and the vacuum bag.

3.5.2 Specimen Cutting and Grinding.

The next step in the fabrication process is the same for tabbed and untabbed specimens. The panels, or subpanels, were cut into 13.2-mm (0.52″) -wide strips using the same procedure that was used for cutting subpanels from the 305-mm (12″) -square laminate panels, as described in the previous section. These strips were then cut to the required lengths using a Craftsman 10″ Radial Arm Circular Saw with a 25-cm (10″) -diameter diamond cutoff blade installed. The specimens were cut approximately 141 mm (5.54″) in length so that the specimens could be precision ground to the final dimensions of 12.7 mm (0.500″) wide by 139.7 mm (5.500″) long.

The specimens were ground to the final dimensions using a Brown and Sharpe Model No. 5 surface grinding machine with a 19-mm (0.75″) -wide by 25-cm (10″) -diameter, 60 grit, aluminum oxide grinding wheel installed. This machine is very similar in operation to the Model 2L surface grinding machine previously described. However, in the final grinding operation, the specimens were clamped to the magnetic base of the horizontal table using precisely machined steel blocks. This technique produced specimens in which the dimensions were no more than ±0.025 mm (±0.001″) from the final dimensions listed above.

3.5.3 Specimen Inspection.

Each specimen was inspected following the final grinding operation. First, a visual inspection was conducted to locate any obvious imperfections in any of the specimens. The width, thickness, and length of each specimen was measured and recorded using a dial caliper with a resolution of 0.025 mm (0.001″). If any of these dimensions varied by more than ±0.025 mm (±0.001″) for a given specimen, then that specimen was discarded from the sample.

3.5.4 Strain Gage Instrumentation.

Single-element, foil-resistance strain gages were used to measure the strain during specimen testing. The strain gages were bonded back to back in the gage section of the test specimen so that the percent bending during the test could be determined. In addition, strain gages were used to determine the compressive modulus and the strain to failure. All of the gages used in this study were Measurements Group Type EA-06-125EP-350 strain gages (Measurements Group, Inc). These gages were bonded to the specimens using the procedures specified in Measurements Group Instruction Bulletin B-127-13 (1979). Measurements Group M-Bond 200 cyanoacrylate adhesive was used to bond the gages to the test specimens. All lead wires were soldered to the strain gages using Measurements Group 361A-20R solder. The gages used in this study were calibrated to a read a maximum strain of 0.0301 mm/mm (0.0301 in/in).

4. TESTING MACHINE SETUP AND TEST PROCEDURES.

The compression test specimens were tested using both the CLC and the IITRI test fixtures. The IITRI test fixture is considered to be the best of the test fixtures currently in common use and served as a standard of comparison for results obtained from the CLC test fixture. This section discusses the setup of the testing machine, the installation of the test fixtures in the testing machine, and the test procedures used to test specimens in each test fixture.

4.1 TESTING MACHINE.

All compression tests were conducted at room temperature and ambient humidity using either an Instron Model 1321 universal servo-hydraulic testing machine or an Instron Model 1334 universal servo-hydraulic testing machine. The Instron Model 1321 universal testing machine has an axial load capacity, compressive or tensile, of 90 kN (20,000 lbf) with an axial stroke range of 10 cm (4″). This machine also has a torque capacity of 1100 N-m (10,000 in-lbf) with a rotation range of ±40°. However, the torque capability was not needed in the present study. The Instron Model 1334 universal testing machine has a load capacity of 450 kN (100,000 lbf) and an axial stroke range of 15 cm (6″).

Most of the compression specimens were instrumented with two strain gages applied back to back in the gage section of the specimen, as discussed in section 3.5.4. Using the strain from two back-to-back gages, the percentage of strain due to bending was calculated at any point in the test using the following equation, from ASTM D 3410 (1995).

$$\%Bending = \frac{|\varepsilon_1 - \varepsilon_2|}{\varepsilon_1 + \varepsilon_2} \cdot 100 \qquad (1)$$

A few tests were conducted without strain gages, since in a few cases the gage section was reduced to a length that was not suitable for installing a strain gage, and in another group of specimens, the specimen strain during the tests was of no interest. The strain gages were connected to a Wheatstone quarter-bridge circuit to convert the change in resistance exhibited by the strain gages during the test to a change in voltage. This voltage was amplified using Micro Measurements Model 2310 Signal Conditioning Amplifiers. An excitation voltage of 1.4 volts and a gain of 600 to 800 was used to achieve the proper signal conditioning. The voltage signals from the amplifiers were connected to an A/D board in a digital computer, as described below.

A Compaq Pentium II computer, connected to the test machine with an MTS Model 322-79 Test Star controller, was used to control the testing machine and to take data during the test. MTS 790.00 Test Star software, version 4.0c, was used to configure the operation of the test machine. Using this software the load range was set to 90 kN (20,000 lbf), the stroke range was set to 25 mm (1″), and the strain gages were calibrated to measure a maximum strain of 0.0301.

The test parameters were programmed using MTS 790.90 Test Works software, Version 3.6a. This software controls the operation of the testing machine, records data, and calculates the results of the test. A loading rate of 1.27 mm/min (0.05 in/min), as specified in ASTM D 3410 (1995), was used. The following data was recorded: (1) test time in seconds, (2) applied load, (3) crosshead displacement, and (4) strain data from both back-to-back strain gages. In addition to recording these raw data, the software calculated the following values: (1) the applied stress throughout the test, based on the user-input specimen cross-sectional area; (2) the percent bending, based on equation 1 (ASTM D 3410 1995); and (3) the compressive modulus of the material, based on the slope of the stress-strain curve between 1000 and 3000 με, as recommended in ASTM D 3410 (1995).

4.2 CLC TEST METHOD.

This subsection describes the procedures used to conduct compression tests using the CLC test fixture.

4.2.1 Installation of Load Platens in Testing Machine.

The alignment of the loading surfaces is very critical in a compression test. Therefore, special loading platens and connecting hardware were fabricated to ensure that the loading surfaces were flat and parallel to each other. The parts are shown in figure 20. The upper loading platen connects to the testing machine load cell via a precision ground adapter ring. This ring has four counter-sunk holes that accept ½″-12 UNC socket-head cap head screws. These cap head screws thread into four matching threaded holes on the perimeter of the load cell. The hole in the center of the ring has a 2.00″-12 UNC thread. The upper loading platen is screwed into this hole after the adapter ring is attached to the load cell. The lower platen is a precision-fabricated fixed loading platen obtained from Wyoming Test Fixtures, Inc. This loading platen has a 1.50″-12 UNC threaded center-mounting hole. The lower ram of the universal testing machine has a 2.25″-12 UNC threaded male stud. An adapter was fabricated to connect the threaded stud on the lower ram to the lower load platen. To ensure that the loading surfaces of the upper platen and lower platen were parallel to the each other, each loading surface on the upper and lower adapters were surface ground to a tolerance of ±0.0127 mm (±0.0005″).

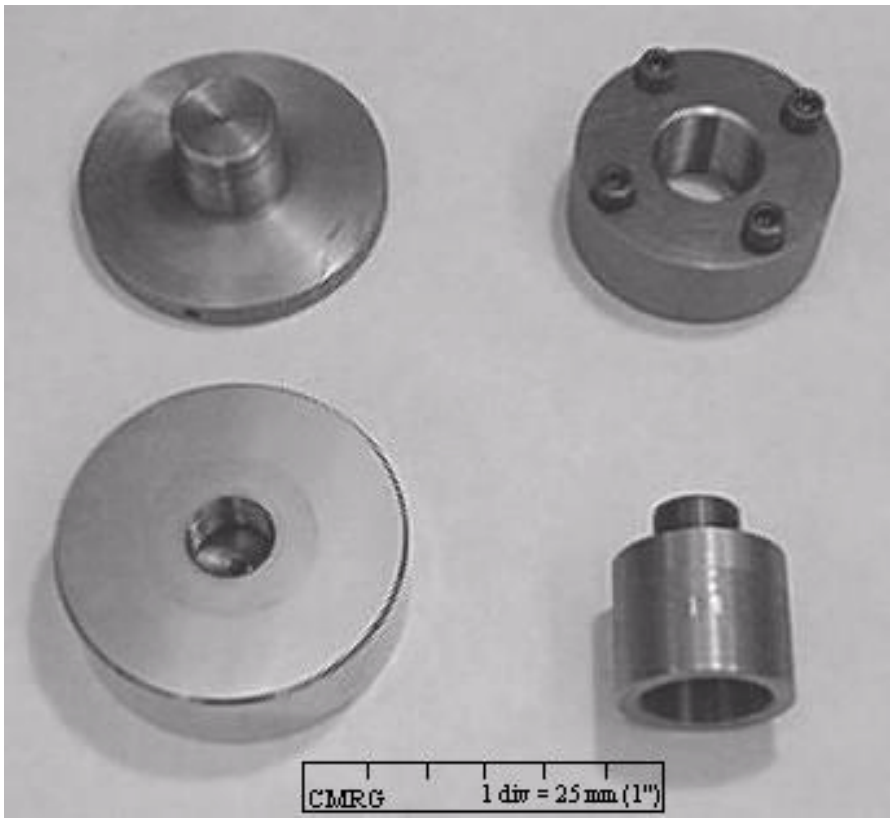

FIGURE 20. LOADING PLATENS AND ADAPTER RING

After the parts were installed in the testing machine, a dial indicator was used to measure the distance between the two loading platens. It showed that the loading platens were flat and parallel to each other to within ±0.0127 mm (±0.0005″) over the 150-mm (6″) -diameter surface of the platens. The alignment of the test fixture was also checked with a precision ground steel specimen fitted with back-to-back strain gages. The specimen was installed in the CLC test fixture and the percent bending of the specimen was measured. At a load of 560 kN (5000 lbf) there was less than 3% percent bending at this load level, which indicated that the loading surfaces were adequately aligned.

4.2.2 Installation of Specimen in CLC Test Fixture.

After installation of the platens, the next step in the testing procedure was to install the specimen in the test fixture. It is very important that the test specimen when installed in the test fixture, have the proper ratio of shear loading to end loading. The top and bottom of the test specimen must be flush with the top and bottom surfaces of the CLC test fixture. In addition, the loading surfaces should be free from particles, oil, or fine dust. Large particles were removed from the linear bearings and compressed air was used to blow the accumulated dust from these parts. Next, the thermal-sprayed surfaces of the CLC test fixture were scrubbed with a stiff wire brush to remove any imbedded particles from previous tests. This was followed by cleaning with a soft nylon bristle brush wetted with acetone. This removed fine dust and oil from the thermal-sprayed surface that could cause the specimen to slip in the test fixture. This cleaning procedure was carried out before each individual specimen test. Next, the test fixture clamping bolts were wiped clean with a soft rag. The bolts were then lubricated with Panef Manufacturing Company, Inc.'s Lub-a-Spray dry powdered graphite and reinserted in the test fixture. A great deal of care was taken to insure that the test fixture was clean and the test fixture bolts were well lubricated before any tests were conducted.

The bottom half of the CLC test fixture was then placed on a clean DoAll, Inc. Model No. 1387-5 marble surface plate. This surface plate is approximately 60 x 90 cm (24″x36″) and is guaranteed flat to within 0.0025 mm (±0.0001″) over the surface of the plate. A 9.8-mm (0.39″) -wide steel spacer was placed against the special alignment pins of the CLC test fixture. The test specimen was then inserted between the blocks of the lower half of the test fixture with the edge of the specimen against the edge of the steel spacer bar and the end pressed firmly onto the surface plate. The clamping bolts in the lower half of the test fixture were then finger tightened. A diagonal tightening pattern was used to insure that the test fixture clamped evenly across the surface of the test specimen.

The upper half of the CLC test fixture was then gently placed over the top of the lower half. The linear bearings were used to align the upper half of the test fixture with the lower half so that the test specimen would fit into the gap in the upper half of the test fixture. The clamping bolts in the upper half of the test fixture were finger tightened, using a diagonal pattern, enough so that the specimen would not slide in the test fixture. The test fixture was then gently turned over so that the upper half of the CLC test fixture was against the marble surface plate. The upper test fixture bolts, now on the bottom next to the surface plate, were gently loosened to allow the test specimen to slide down into the test fixture so that the end of the test specimen was pressed against the marble surface plate. The test fixture bolts were again finger tightened and the test

fixture was turned upright. This procedure aligned the ends of the test specimen with the top and bottom loading surfaces of the CLC test fixture.

The test fixture bolts were tightened to a torque of 2.8 to 3.4 N-m (25 to 30 in-lbf) using a Proto #6106 Torque Screwdriver. The bolts were tightened to this level in increments of 0.7 N-m (6 in-lbf); using a diagonal tightening pattern so the test fixture surfaces would be uniformly clamped against the surface of the test specimen.

The specimen was then inspected to make sure that both ends of the test specimen were precisely even with the top and bottom surfaces of the CLC test fixture. If the test fixture rocked even slightly on the marble surface plate, this indicated that the specimen was protruding out of the test fixture. Conversely, if a finger rubbed across the top and bottom surfaces of the CLC test fixture detected even the slightest drop, this indicated that the specimen was below the surface of the CLC test fixture. In either case, the test specimen was carefully removed from the test fixture and the installation process repeated until neither of these errors were detected. Once the test specimen was properly installed in the test fixture, the aluminum spacer bar was removed from the test fixture and the test begun.

4.2.3 Test Procedure.

The first step in the test procedure was to place the CLC test fixture between hardened steel blocks placed on the load platens of the universal testing machine and to connect the strain gage wires to the bridge circuits, as shown in figure 21. The strain gage wires were connected to the Wheatstone quarter-bridge circuits, described in section 4.1, using specially designed boxes with quick release connectors. The amplifiers were then adjusted so there was zero output voltage across the strain gage circuits. It was estimated from previous tests, and existing data, that the maximum strain in the compression tests would be less than 0.03 in./in. To calibrate the strain gage circuitry for this strain, a shunt resistor was placed in parallel across the arm of the Wheatstone bridge containing the strain gage. The required shunt resistance was calculated using equation 2. In this equation, N = 1 for quarter-bridge circuits, GF is the gage factor (GF = 2.075 for the gages used in this study), ε is the maximum strain (0.0301 mm/mm for this study), and R_g is the unstrained resistance of the strain gage (R_g = 350 Ω for these gages).

$$R_s = \left[\frac{1}{N \cdot GF \cdot \varepsilon} - 1 \right] \cdot R_g \qquad (2)$$

Using this equation, it was determined that a 5.26 kΩ resistor should be used. This simulates the change in resistance that would be observed in the strain gage if it were placed in a strain field where the strain was 0.03 in./in. along the measurement axis of the gage. Since this represents the maximum strain the gages were calibrated to read, the amplifier gain was adjusted so the output voltage was 10.00 volts when the shunt resistor was placed in parallel with the strain gage. Typically, an excitation voltage of 1.4 volts was used with a gain of 600 to 800 to achieve this output voltage.

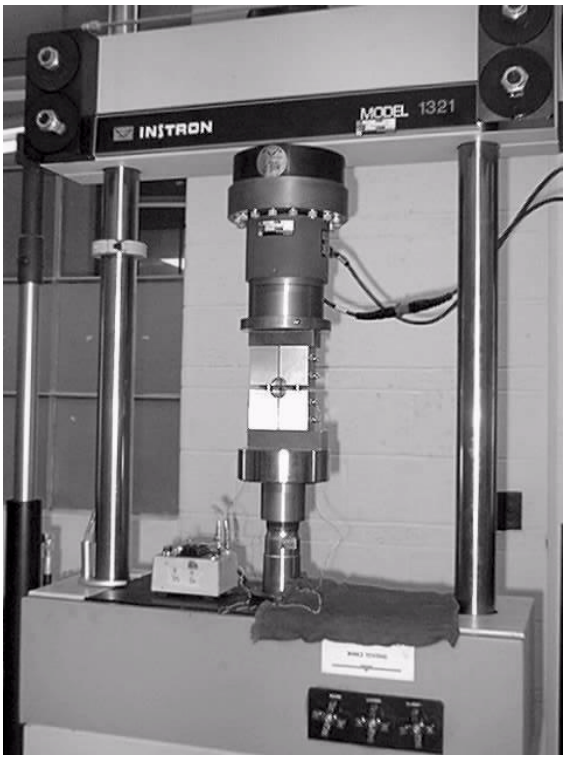

FIGURE 21. CLC TEST FIXTURE INSTALLED IN THE UNIVERSAL TESTING MACHINE

After the strain gages were properly connected and calibrated, the upper load platen was carefully moved down onto the top of the CLC test fixture and locked in place. Then the lower ram of the universal testing machine was slowly raised until a load of approximately 89 N (20 lbf) was applied to the test specimen. The specimen was then loaded in displacement control at the rate of 1.27 mm/min (0.05 in/min), as recommended by ASTM D 3410-95. The test program stops the lower ram when it senses failure of the test specimen, as defined by a drop in the applied load of more than 30%.

The failed test specimen was then carefully removed from the test fixture. The collected data were inspected and saved. These data included the test time, the crosshead displacement, the applied load, and the stress and strain in the specimen. The test program also automatically calculated the compressive modulus of the material, the percent bending at failure, and the maximum stress in the specimen. The failure mode was also recorded manually using the code designated in ASTM D 3410 (1995). The test fixture was then cleaned and prepared for the next specimen test. The load platens were also carefully cleaned of any specimen fragments and particles. The procedures described in this section were repeated for each compression test conducted in the CLC test fixture.

4.3 IITRI TEST METHOD.

This section describes the procedure used to conduct compression tests using the IITRI test fixture.

4.3.1 Installation of the IITRI Test Fixture in the Test Machine.

Typically, the bottom half of the IITRI test fixture is placed on a flat loading platen mounted to the lower ram of the universal testing machine. The upper half of the test fixture is mounted to the load cell of the universal testing machine using the C-shaped mounting bracket shown in figure 3. This C-shaped mounting bracket has a 41.28-mm (1.625″) threaded hole in the center for attaching the mounting bracket to the load cell. Therefore, an adapter was used to connect the C-bracket to the 50.8-mm (2.00″) threaded hole in the load cell. Originally, a cylindrical steel bar, approximately 130 mm (5″) long with the required threaded ends, was used to connect the C-bracket to the load cell. However, with this arrangement there was too much movement of the upper C-bracket. The C-bracket could be tilted by more than 0.203 mm (0.008″) simply by pushing or pulling on one end of it by hand. Thus, any eccentricity in the load train or in the specimen/fixture assembly could cause the C-bracket to be pushed out of alignment. This could induce unwanted bending in the specimen during the compression test.

For this reason, the C-shaped mounting bracket was not used in this study. The IITRI test fixture was simply loaded between the same two load platens as were used for the CLC test fixture, as described in section 4.2.1. To do this, the lower half of the IITRI test fixture was placed on the lower load platen. Then the specimen/wedge grip assembly was placed in the cavity of the lower half of the test fixture. Finally, the upper half of the IITRI test fixture was carefully placed over the top of the specimen/wedge grip assembly using the linear bearings for alignment. The upper platen was then brought down on top of the assembled IITRI test fixture and the specimen test was conducted. This arrangement was very convenient since specimens could be alternately tested in the IITRI test fixture and in the CLC test fixture without changing any hardware on the universal testing machine. However, one slight alteration was required when testing specimens in the IITRI test fixture. The weight of the upper half of the IITRI test fixture must be accounted for since it is not connected to the crosshead of the testing machine. This is easily accomplished by adjusting the zero on the testing machine load channel so that at the beginning of the test, before any load is applied by the testing machine, a preload of approximately 144 kN (32 lbf) is recorded by the computer software.

4.3.2 Installation of the Test Specimen in the IITRI Test Fixture.

A special aluminum alignment jig, shown in figure 22, was used to install the test specimen in the IITRI wedge grips. This jig is machined with the same 10° angle as the wedge spacers of the IITRI test fixture so that the gripping surfaces of the wedge grips would rest horizontally on the alignment jig. First, the wedge grips were cleaned as described in section 4.2.2. Then, the two left halves of the wedge grips were placed on the alignment jig. A 13-mm (0.50″) -wide steel spacer was placed against the special alignment pins of the wedge grips and the test specimen was placed on the horizontal gripping surfaces of the wedges so that it was flush against the spacer. Next, the two right halves of the wedge grips were placed over the top of the two left halves. The four ¼″-28 UNF socket-head cap head screws (two in each pair of wedge grips) were screwed into the wedge grips and tightened to a torque of 2.8 N-m (25 in-lbf) using increments of 0.68 N-m (6.0 in-lbf). A diagonal tightening pattern was used as described in section 4.2.2 for the CLC test fixture.

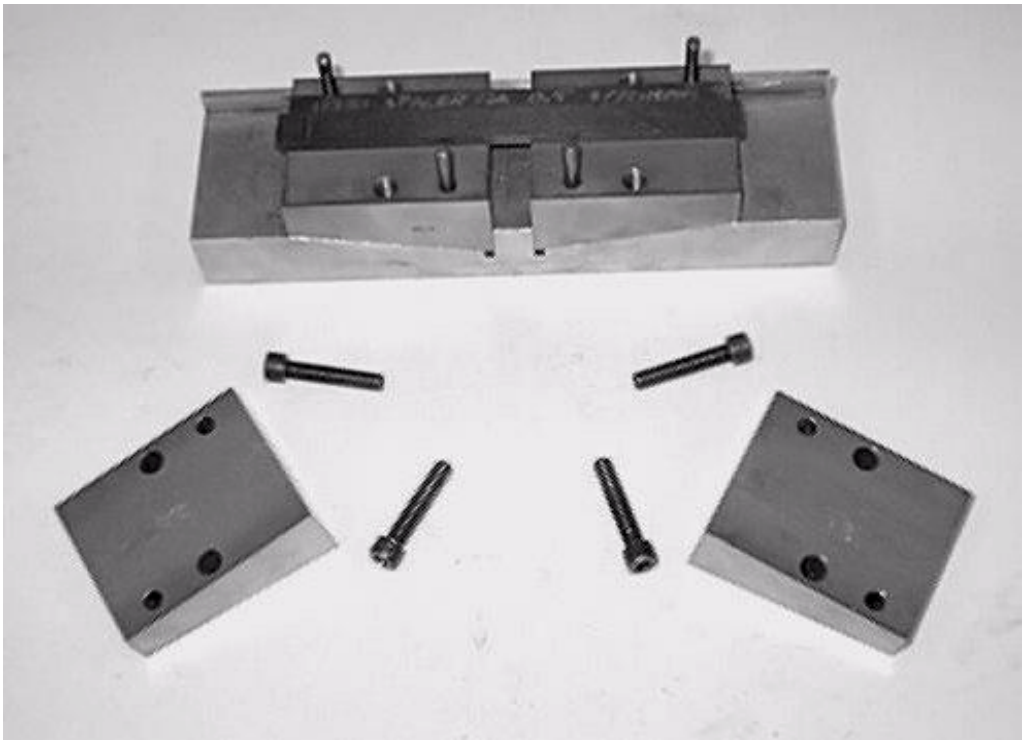

FIGURE 22. IITRI TEST SPECIMEN ALIGNMENT JIG

4.3.3 Test Procedure.

After the specimen was clamped between the wedge grips, the steel spacer was removed from the wedge grips. The outer surfaces of the wedge grips were then lightly lubricated with Panef Manufacturing Company, Inc.'s Lub-a-Spray dry powdered graphite. Next, the specimen/wedge grips assembly was placed in the lower cavity of the IITRI test fixture. The lower half of the IITRI test fixture, containing the specimen/wedge grip assembly, was placed on the lower load platen of the universal testing machine and the upper half of the IITRI test fixture was carefully lowered by hand onto the lower half as shown in figure 23. The crosshead of the universal testing machine was slowly moved down until the upper load platen was approximately 6.4 mm (0.25″) above the surface of the IITRI test fixture. The strain gage wires were connected to the bridge circuits, and the gages were calibrated as described in section 4.2.3. The lower ram of the universal testing machine was then moved up to apply a preload of 89 N (20 lbf) on the test specimen. The remainder of the compression test was conducted exactly as previously described for the CLC test fixture. The same calculations were made and the same type of data were saved.

When the test was completed, the specimen was removed from the wedge grips, the failure mode was recorded, and the wedge grips were cleaned in preparation for the next specimen test. At failure, the Poisson-induced stresses through the thickness of the specimen often cause the IITRI grips to be wedged tightly into the test fixture cavity. Special holes are machined into the top and bottom of the IITRI housings so that a brass punch can be used to gently push the failed specimen/wedge grip assembly from the test fixture housing. This is one additional problem that is often encountered when using the IITRI test fixture.

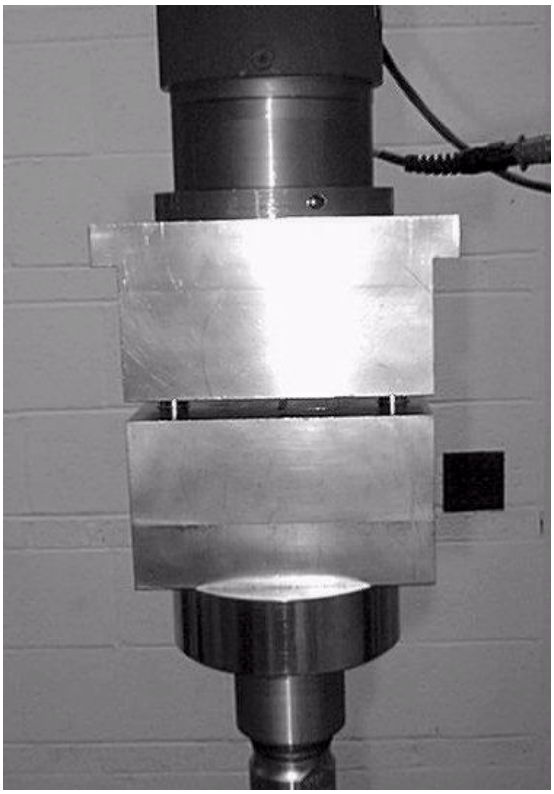

FIGURE 23. IITRI TEST FIXTURE INSTALLED IN THE UNIVERSAL TESTING MACHINE

4.4 DETERMINATION OF 0°-PLY COMPRESSIVE STRENGTH.

All of the compression tests in this study were conducted using cross-ply or angle-ply test specimens. It was, therefore, necessary to calculate the 0°-ply compressive strength from the measured laminate ultimate compressive strength (UCS). Camponeschi and Hoyns (1991) used linear lamination theory to develop a back-out factor that could be used to calculate that value. Using their procedure, the 0°-ply strength is calculated as:

$$\sigma_{11}^{0} = BF\,\frac{P_{ult}^{c}}{A} \tag{3}$$

where

BF = Back-out factor
P_{ult}^{c} = Ultimate load applied to the specimen
A = Cross-sectional area of the test specimen

However, their back-out factor derivation is limited to $[90/0]_{ns}$ laminates. The derivation in appendix A of this report extends this back-out factor calculation to any symmetric laminate containing 0° plies resulting in a back-out factor given by

$$BF = \left[Q_{11}^{0} \frac{A_{22}A_{66} - A_{26}^2}{d} + Q_{12}^{0} \frac{A_{16}A_{26} - A_{12}A_{66}}{d} \right] \cdot T \tag{4}$$

where

$$d = A_{11}A_{22}A_{66} - A_{11}A_{26}^2 - A_{12}^2A_{66} + 2A_{12}A_{16}A_{26} - A_{16}^2A_{22} \tag{5}$$

and

Q_{ij}^{0} = ij^{th} entry in the 0° lamina plane stress stiffness matrix
A_{ij} = ij^{th} entry in the laminate extensional stiffness matrix
T = Total laminate thickness

The 0°-ply strength is then calculated as shown in equation 3.

The back-out factor calculation given by equations 4 and 5 was programmed using Matlab Version 5.2.1 (see appendix A for the listing). The program prompts the user for the lamina properties E_{11}, E_{22}, G_{12}, and ν_{12} as well as the thickness of each lamina, t, and the laminate stacking sequence. The program then computes and prints out the back-out factor of the laminate. The program is written to handle any type of symmetric laminate, including laminates having plies of more than one material and sandwich laminates having a core of a different kind of material.

All of the back-out factor calculations used in this study were based on the linear elastic properties of the lamina. Welsh and Adams (1995) showed that this procedure was acceptable for cross-ply laminates made of laminae having a ratio of axial stiffness, E_{11}, to transverse stiffness, E_{22}, greater than about five. The reason for this limitation is that E_{11} is very linear, E_{22} is nearly linear, and thus ν_{12} is also nearly linear. For composites for which the ratio of E_{11} to E_{22} is greater than five, E_{11} has a much greater effect on the back-out factor calculation, so the slight nonlinear behavior of E_{22} is dominated by the linear behavior of E_{11}. However, for composites with a ratio of E_{11} to E_{22} less than five, the nonlinear behavior of E_{22} has a greater effect on the back-out factor calculations. Most of the cross-ply laminates tested in this study, excluding the S2-glass fiber/epoxy composites, had a ratio of E_{11} to E_{22} greater than five. The S2-glass fiber/epoxy specimens had a ratio of E_{11} to E_{22} of approximately 2.5. An analysis of the effect of the nonlinear behavior of E_{22} on the back-out factor for S2/SP381 glass/epoxy revealed that if the value of E_{22} at failure was 20% less than the initial elastic value, the back-out factor changed by less than 5% when compared to the back-out factor based on the linear elastic properties. Therefore, the back-out factor calculation for these materials was based on the linear elastic properties also.

The back-out factors for cross-ply laminates are independent of the shear modulus, G_{12}, which is very nonlinear. Therefore, as previously discussed, the back-out factor calculations for most cross-ply laminates can be based on the linear elastic properties of the lamina. On the other hand, the back-out factors for angle-ply composites are much more sensitive to the lamina shear modulus. Since G_{12} is very nonlinear, the back-out factors for angle-ply laminates are very

sensitive to material nonlinearity. The calculation of back-out factors based on the nonlinear material properties is really no different than it is for linear material properties. Instead of using the initial lamina stiffnesses (E_{11}, E_{22}, ν_{12}, and G_{12}), the lamina properties at failure are used. This means that for angle-ply laminates, the strains in the principal material directions for the angle plies at failure, must be calculated. Once these principal strains are determined, the lamina stiffnesses for the angle plies can be determined. However, this requires complete lamina stress versus strain curves to failure. Unfortunately, such data are not commonly available, i.e., the nonlinear properties of the lamina are often not known. This was most apparent for the materials supplied by Boeing Space Systems Division. These materials were supplied in the form of fully cured test blanks, and the stiffness properties of the lamina at the failure strains of the laminates were not given. Since unidirectional materials were not provided, the required properties could not be characterized by the CMRG. Consequently, it was not possible to calculate back-out factors based on the lamina properties at failure.

4.5 STATISTICAL ANALYSIS PROCEDURES.

In the present study, five replicates were usually used for each test configuration. This represents a small sample from a statistical viewpoint; most of the statistical analysis procedures would be more sensitive if larger sample sizes were used. However, five replicates is the standard sample size used in the composites industry when evaluating test methods with the main objective being to determine the mean value.

4.5.1 Descriptive Statistics.

The first step in analyzing the data generated in this study was to describe each set of experiments. The sample mean, $\bar{x}$, and the coefficient of variation, C_v, were used to describe the central tendency and the dispersion of the data. The sample mean is calculated using equation 6.

$$\bar{x} = \sum_{i=1}^{n} \frac{x_i}{n} \tag{6}$$

where n = number of replicates in the group. The coefficient of variation is calculated using equation 7.

$$C_v = \frac{S_x}{\bar{x}} \cdot 100 \tag{7}$$

where S_x is the sample standard deviation, given by

$$S_x = \frac{\sqrt{\sum_{i=1}^{n} \left(x_i - \bar{x}\right)^2}}{n-1} \tag{8}$$

A more detailed discussion of these equations can be found in Applied Statistics and Probability for Engineers, by Montgomery and Runger (1994).

4.5.2 Comparative Statistics.

The next type of statistical analysis procedure used in this study is often called comparative statistics or hypothesis testing (Montgomery and Runger, 1994). The experiments conducted can be organized into three groups, depending how many factors were studied and how many levels each factor had. A different hypothesis testing procedure was used for each of these three groups. SigmaStat Software Version 1.03 from Jandel Scientific Corporation, Inc. was used to make all of the necessary statistical calculations in this research. The procedures described below were taken from Montgomery and Runger (1994).

4.5.2.1 Experiments With a Single Factor Having Two Levels.

The simplest group of experiments in this study were experiments that had only one factor and only two levels of the factor. An example of this type of experiment is the comparing of measured 0°-ply compressive strengths of $[90/0]_{5s}$ specimens in the two different test fixtures, viz., the IITRI and CLC test fixtures. In these experiments the specimens were all cut from the same panels, the specimens were all tested by the same person, the tests were all conducted on the same day, the results were all measured with the same testing machine, and the test specimen selection was completely randomized. Therefore, the only influence on the measured compressive strengths was assumed to be the test fixtures.

The null hypothesis in this type of experiment is that the mean values of the two populations are equal. The alternative hypothesis is simply that the mean values of the two populations are not equal. It was assumed that the two populations were described by the Normal, or Gaussian Distribution. Thus, the hypothesis was tested using a two-sided t-test with a 95% confidence level. This means that the probability of a random variation being mistaken for a real difference is only 5%. Comparisons at the 99% confidence level reduce this probability to 1%; however, in such a strong test, real differences can often be attributed to random error.

4.5.2.2 Experiments With a Single Factor Having Multiple Levels.

The next type of experiment conducted in this study was an experiment with a single factor that had more than two levels. An example of this type of experiment was testing specimens with six different gage lengths in the CLC test fixture. In this experiment a completely randomized experimental design was used and the specimens were cut from the same panel and tested on the same test machine by the same person using the same test fixture so the effects of extraneous variables would be blocked out. Therefore, it was assumed that the only influence on the measured 0°-ply compressive strength was the change in specimen gage length.

The different gage lengths are the "treatments," and the null hypothesis is that the treatment effects are all zero. The alternative hypothesis in this case is that at least one of the treatment effects is nonzero. It was assumed that all N observations in the experiment were taken from a normal distribution with a mean, μ, and variance, σ^2. Therefore, the test of the hypothesis is based on a comparison of two independent estimates of the population variance. This type of test is referred to as a One-way ANalysis Of VAriance (ANOVA). The test statistic is the ratio of the treatment mean square to the error mean square of the data. This ratio has an F-distribution with *a-1* and *a(n-1)* degrees of freedom, where *a* is the number of treatments in the

experiment, and *n* is the number of replicates, or observations, in each treatment. If the null hypothesis is false, this ratio is greater than the population variance, so the null hypothesis is rejected if the ratio calculated is greater than the value of the F-distribution with *a-1* and *a(n-1)* degrees of freedom.

The ANOVA procedure can only determine if a statistically significant difference exists between treatments, it cannot determine which treatment or treatments are different than the others. A multiple comparison method, such as Duncan's Multiple Range Test, must be used to make this determination. The statistical analysis software used in this study, SigmaStat from Jandel Scientific, Inc., used the Student-Newman-Keuls Method to detect differences in the treatments.

4.5.2.3 Experiments With Multiple Factors Each Having Two Levels.

The last type of experiment conducted in this study is often called a "2^k Factorial Design." In this type of experiment there are multiple factors being investigated; however, each factor has only two levels, a high and a low level. An example of this type of experiment is testing specimens made of two different materials (e.g., AS4/3501-6 carbon/epoxy and T300/3034 carbon/epoxy) with two different laminate orientations (e.g., $[90/0]_{ns}$ cross-ply and $[45/0/-45/90]_{2s}$ angle-ply) in two compression test fixtures (the IITRI test fixture and the CLC test fixture). The factors in this experiment are the material, the laminate orientation, and the test fixture. Each factor has two levels. For example, in the case of the test fixture factor, these two levels are the IITRI test fixture and the CLC test fixture.

The null hypothesis in this type of experiment is that the treatment effects are all zero and the interactions of the treatment effects are all zero. The two-way analysis of variance procedure is used to test these hypotheses by comparing the actual variance in the data to the expected variance assuming the population is normally distributed. An ANOVA procedure is the only method available to test for interaction affects in a factorial experiment.

The first estimate of variance is the ratio of the first treatment mean square (Treatment *A*) to the error mean square of the treatment. This ratio has an F-distribution with *1* and $2^k(n-1)$ degrees of freedom, where *n* is the number of replicates for each treatment level. If the null hypothesis is false, this ratio is greater than the population variance, so the null hypothesis is rejected if the ratio calculated is greater than the value of the F-distribution with *1* and $2^k(n-1)$ degrees of freedom. The calculation is repeated for the next treatment mean, Treatment *B*, and for the interaction effects. The interaction effects also have *1* and $2^k(n-1)$ degrees of freedom. If any ratio of treatment mean square to error mean square is greater than the F-distribution with *1* and $2^k(n-1)$ degrees of freedom, then the null hypothesis must be rejected and a multiple-comparison method must be used to determine which effect, or effects, are statistically different than the others. The two-way ANOVA calculations were also carried out using SigmaStat software from Jandel Scientific, Inc.

5. EXPERIMENTAL RESEARCH.

The first step in the verification of the Wyoming CLC test fixture as an accurate and efficient compression test method was to develop an understanding of the parameters that affect the compression test. It is important to understand what factors influence the measured compressive

properties and how slight changes in these factors affect the measured properties. From this understanding, a set of guidelines can be developed that specify the test specimen dimensions, specimen fabrication procedures, test fixture dimensions, machining tolerances, and test procedures.

To start this parametric evaluation of the CLC test fixture, a list of factors that could influence the compression tests conducted in the CLC test fixture was developed. These factors fall into the following categories: (1) test specimen parameters and (2) test fixture parameters. The specific factors in each of these categories are shown in table 7.

TABLE 7. PARAMETERS THAT INFLUENCE THE RESULTS OF THE CLC TEST METHOD

Test Specimen Parameters	Test Fixture Parameters
1. Specimen thickness	1. Cleanliness of grip surfaces
2. Variation in specimen thickness	2. Dimensional tolerances
3. Laminate lay-up	3. Load platen alignment
4. Specimen surface finish	4. Use of spherical seat platen
5. Specimen gage length	5. Radius of fixture corners at gage section
	6. Fixture clamping force

Using this list of parameters, a series of experiments were conducted to determine how these factors influenced the CLC compression test method. These investigations are described here in the chronological order in which they were performed, to best convey the problems encountered in compression testing.

The studies described here were conducted using two different CLC test fixtures. The first (original) test fixture, CLC-OR, was fabricated from an existing ELSS Compression test fixture (Irion and Adams, 1981). Preliminary investigations, discussed in sections 5.1 and 5.2, revealed that this test fixture had a systematic error, and compressive strengths measured in this test fixture were statistically lower than comparable values obtained in the IITRI test fixture. A second fixture, CLC-15, was purchased from Wyoming Test Fixtures, Inc. This test fixture was fabricated to very precise dimensional tolerances and was made of 17-4PH stainless steel. The compressive strengths obtained with the CLC-15 test fixture were statistically equivalent, but slightly higher than comparable values obtained in the IITRI test fixture. These results are discussed fully in the following sections. Throughout the remainder of section 5, the CLC-OR test fixture and the CLC-15 test fixture will always be differentiated.

AS4/3501-6 carbon/epoxy $[90/0]_{5s}$ cross-ply specimens were cut from Panel PA02A to conduct preliminary tests of the CLC test method. This panel had a fiber content of 64.7% by volume. The specimens tested in this preliminary study had an average bending at failure of 12.0%, with

bending ranging from 1.93% to 25.4% at failure. Due to the large variability in the specimen bending at failure, the first task undertaken in this study was to determine the cause of bending in the CLC compression test.

5.1 CLC COMPRESSION TEST METHOD PARAMETRIC STUDY.

ASTM D 3410 (1995) states that, "In order for the elastic property test results to be considered valid, percent bending in the specimen shall be less than 10%…. The same requirement shall be met at the failure strain for the strength and strain-to-failure data to be considered valid."

The percent bending in the specimen is calculated using equation 2 in ASTM D 3410 (1995). This equation is derived based on the condition shown in figure 24. The average compressive stress in the specimen due to the applied load, P, is given by

$$\sigma_x^c = E_x \frac{\varepsilon_1 + \varepsilon_2}{2} \tag{9}$$

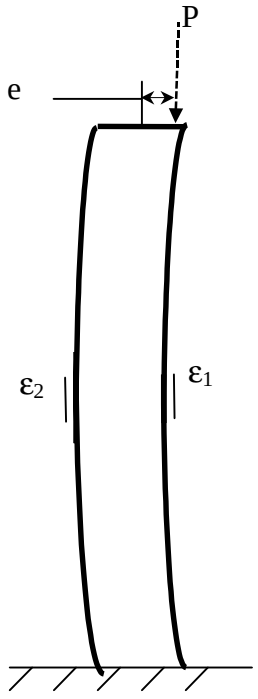

FIGURE 24. SPECIMEN BENDING DUE TO ECCENTRIC LOADING

The compressive stress due to bending at Location 1 is given as

$$\sigma_{x1}^b = E_x \varepsilon_1 - E_x \frac{\varepsilon_1 + \varepsilon_2}{2} = E_x \frac{\varepsilon_1 - \varepsilon_2}{2} \tag{10}$$

Thus, the percent of the total compressive stress that is due to bending at Location 1 is expressed as

$$\sigma_{x1}^{b} = \frac{E_x \dfrac{\varepsilon_1 - \varepsilon_2}{2}}{E_x \dfrac{\varepsilon_1 + \varepsilon_2}{2}} \times 100 = \frac{\varepsilon_1 - \varepsilon_2}{\varepsilon_1 + \varepsilon_2} \times 100 \tag{11}$$

This is the percent bending in the specimen referred to in ASTM D 3410 (1995) and is essentially equation 2 in that document. However, the equation is as follows:

$$B_y = \frac{|\varepsilon_1 - \varepsilon_2|}{|\varepsilon_1 + \varepsilon_2|} \times 100 \leq 10\% \tag{12}$$

therefore percent bending uses absolute value signs which is the form given in equation 2 of ASTM D 3410 (1995). The present authors prefer equation 11, since the sign of the percent bending indicates which direction the specimen bent during the test. This information reveals whether or not a systematic problem exists with the test fixture or the test setup. The percent bending in the test, as calculated using equation 12, can be determined by using back-to-back strain gages bonded to the specimen gage section.

ASTM D 3410 (1995) states that bending moments induced by specimen and fixture tolerances cause beam-column effects during the compression test, implying that this results in bending in the specimen. ASTM D 3410 (1995) further states that the specimen thickness variation should be less than ±4%. A careful examination of the failed specimens from Panel PA02A ($[90/0]5_s$) revealed that the specimens varied in thickness from end to end by as much as 0.254 mm (0.010″). The average thickness variation in the specimens was 0.178 mm (0.007″). These 20-ply specimens tested had an average thickness of 2.67 mm (0.105″) so that, according to the ASTM D 3410 standard, the allowable specimen thickness variation was limited to 0.203 mm (0.008″).

To examine the effects of thickness variation on the amount of bending in the CLC test fixture, a set of 6061-T6 aluminum test specimens were fabricated. Aluminum specimens were used because these specimens could be machined to very precise tolerances using common metal fabricating tools, and the isotropic nature of the aluminum prevented any problems with grinding away a portion of the specimen, such as would be encountered with a cross-ply composite specimen. The specimens were first ground to a nominal thickness of 0.254 mm (0.100″) using a precision surface grinder. Then, two specimens with each of the following thickness tapers were fabricated: (1) no taper, (2) 0.025-mm (0.001″) taper, (3) 0.051-mm (0.002″) taper, (4) 0.102-mm (0.004″) taper, and (5) 0.127-mm (0.005″) taper. Back-to-back strain gages were bonded to the specimens to measure the bending during the specimen test. The specimens were installed in the CLC-OR test fixture (original) so that the thin end of the specimen was at the top of the test fixture. A compressive load was applied to the specimen until the average compressive stress in the specimen was 210 GPa (30 ksi). The stress calculation was based on the average area of the

specimen gage section; three separate measurements of the specimen's gage section dimensions were averaged together to determine this quantity. When the load was increased beyond this level, the specimens began to exhibit buckling behavior. A plot of the percent bending, at this load level, versus the amount of taper in the specimen, is shown in figure 25. This plot indicates that, in general, the percent bending increased with the amount of specimen thickness taper. This was apparent even for a thickness taper of 0.051 mm (0.002″) which is a variation only of ±1%, much less than the ±4% limit given in ASTM D 3410 (1995). This result prompted the authors to investigate methods to control the thickness variation in the test specimens.

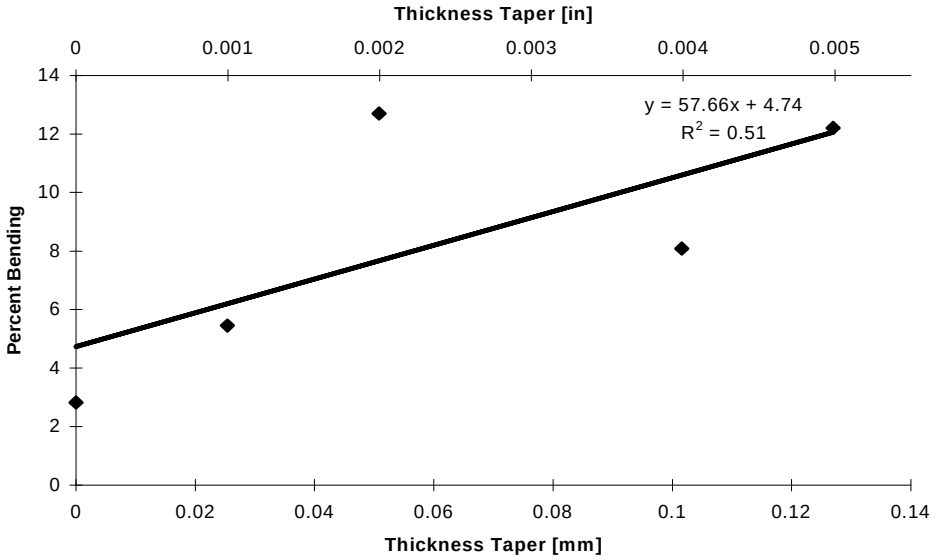

FIGURE 25. EFFECT OF THICKNESS TAPER ON SPECIMEN BENDING FOR 6061-T6 ALUMINUM SPECIMENS TESTED IN THE CLC-OR TEST FIXTURE

Another interesting observation from figure 25 is that at zero thickness taper there is still roughly 3% bending in the aluminum specimens. One explanation for this behavior is that the loading platens could have been slightly out of alignment. At this point in the research it had not been determined what alignment precision must be used in the loading platens to keep the percent bending below 10%; therefore, the loading platens were flat and parallel to within ±0.025 mm (±0.001″). In later research, as discussed in section 5.1.4, the loading platens were aligned to within ±0.0127 mm (±0.0005″). Another explanation for this behavior is that the test fixture used in this study, CLC-OR, was shown in later research (see section 5.2.4) to suffer from the effects of compounding dimensional tolerances. It is possible that this also induced a small amount of bending in the test specimen. Unfortunately, this characteristic had not been discovered at this point in the research program.

5.1.1 Specimen Fabrication Study.

The thickness profile of the AS4/3501-6, $[90/0]_{5s}$ cross-ply composite plate was measured using an Ultra Digit Mark IV digital micrometer from Sylvac Systems Corp. This micrometer can

measure parts up to 25 mm (1.0″) thick with an accuracy of 0.001 mm (0.00005″). The micrometer was used with 3.18-mm (0.125″) -diameter probes with hemispherical ends.

Using this instrument, it was determined that, on average, the plate was 0.305 mm (0.012″) thinner at the edges than it was at the center. After reviewing the fabrication guidelines given in ASTM D 5687/D 5687M (1995), it was postulated that this thickness variation could be caused by three factors. First, the caul plates used may not have met the flatness requirement given in ASTM D 5687 (1995) of no more than 0.05-mm deviation in any one meter square (or 0.002″ in any 12″ square). Second, the caul plates may not have been stiff enough to resist the external applied pressure of 689 kPa (100 psi) during the cure process. Third, too much resin could have flowed from the edges of the panel during the cure process so the panel is thinned out on the edges.

The caul plates were inspected using a dial indicator resting on a marble surface plate. The dial indicator showed that the caul plates were not flat; one was 0.203 mm (0.008″) higher on one corner, and the other was 0.254 mm (0.010″) higher on one corner. These caul plates were 9.53 mm (0.375″) thick. In order to correct this problem, two new caul plates were purchased. The new caul plates were also 305 × 305 mm (12″ × 12″), with a thickness of 12.7 mm (0.500″). These caul plates were precision ground so that the upper and lower surfaces were guaranteed to be flat and parallel to within 0.0127 mm (0.0005″) over the entire surface, which they were.

Next, the third factor was addressed. A cork dam was originally used to control resin bleed out the sides of the plate during the cure process, as shown in figure 12(a). This cork dam was fabricated by bonding together strips of adhesive-backed cork material that were 3.18 mm (0.125″) thick by 6.35 mm (0.25″) wide, to form a dam 6.35 mm (0.25″) wide by 15.9 mm (0.625″) high. It was observed that this cork dam was being compressed a great deal by the externally applied pressure during the plate curing process and that some layers of the material were sliding off of one another. It appeared that the cork dam was allowing too much resin to escape from the edges of the plate, as excess resin was found around the outside edges of the caul plates and in the top bleeder cloth after completion of the cure process. To solve this problem, an silicone rubber dam was cast to replace the cork dam. The silicone rubber dam was like a picture frame placed around the perimeter of the uncured plate before the curing process was initiated. The rubber dam was 19 mm (0.75″) high, with an inside opening of 305 × 305 mm (12″ × 12″). This one-piece dam prevented resin from escaping from the edges of the plate during the curing process. The silicone rubber used has a coefficient of thermal expansion nearly ten times that of aluminum. Therefore, the silicone rubber dam exhibits the added benefit that as the plate is heated during the cure process, the dam expands and compresses the edges of the composite plate.

The results of using the new caul plates and the silicone rubber dam in the laminate fabrication procedure were very positive. The variation in the thickness of the cured composite plate dropped to an average of 0.076 mm (0.003″). The largest thickness variation in the plates fabricated using this new procedure was 0.102 mm (0.004″). In addition, the edges of the composite plates were much smoother and better formed than they had been with the cork dam. All of the 140-mm (5.50″) -long specimens fabricated from these plates had a maximum

thickness variation of less than 0.051 mm (0.002″) from end to end, compared to the 0.203-mm (0.008″) variation in previous specimens. The remainder of the composite plates fabricated in this study were fabricated using this improved procedure. The result of fabricating better quality laminates was apparent in the reduced bending at failure in the specimens and in the smaller variability between the measured compressive properties.

5.1.2 Effect of Spherical Seat Platen on Bending in the CLC Test Fixture.

A number of specimens were left over from Panel PA02A used in the preliminary study. These specimens were used to investigate the effect of a spherical seat platen, also known as a swivel base, on bending in the CLC-OR test fixture. A 152-mm (6.0″) -diameter, high-quality spherical seat platen was obtained from Wyoming Test Fixtures, Inc. This spherical seat platen was used as the bottom load platen on the test machine. The average bending at failure in the five specimens tested with the spherical seat platen was 11.1%. The average bending at failure in the six specimens tested with a fixed base was 12.6%. A two-sided t-test at the 95% confidence level revealed that there was not a statistically significant difference between the two groups of test data. Therefore, it appears that the use of a spherical seat platen does not increase or decrease the amount of bending in the CLC test fixture. However, the specimens tested in this study had an average thickness variation of 0.152 mm (0.006″), so any change due to the swivel base could have been obscured by the effect of thickness variation in the specimens.

ASTM D 3410/3410M-95 recommends that the use of both a spherical seat platen and rigid platens be considered for compression testing polymer matrix composite materials in the IITRI test fixture. However, the present authors prefer to use rigid-loading platens that have been carefully aligned to prevent eccentric loading of the test specimen. The loading platens were routinely aligned to within ±0.0127 mm (±0.0005″), as discussed in section 5.1.3. This configuration consistently resulted in compression tests in which the specimen bending at failure was less than 10%; furthermore, the results presented in the previous paragraph do not indicate a strong benefit of using a spherical seat platen.

5.1.3 Effect of Strain Gage Misalignment on the Measured Bending.

Properly bonding strain gages onto the 12.7-mm (0.500″) -wide by 12.7-mm (0.500″) -long gage section of the test specimen takes a good deal of skill and patience. The strain gages were aligned with the aid of grid lines marked on the specimen with a soft No. 2 pencil and a machinist's scale. Even with this aid, it is still very easy to make alignment errors. The worst possible condition occurs when the strain gage on one side of the specimen is perfectly aligned with the longitudinal axis of the test specimen and the second strain gage on the other side of the specimen is misaligned. In this case, the first strain gage measures the true strain of the gage section, but the second strain gage measures a reduced strain. This difference in the strain gage readings gives the appearance of specimen bending when in fact the specimen may not be bending at all.

A 5° misalignment as shown in figure 26, is about the largest error that can be made before the error becomes visually very obvious. If the strain gages on both sides of the specimen were misaligned by 5°, there would be no contribution to the calculated specimen bending, since both

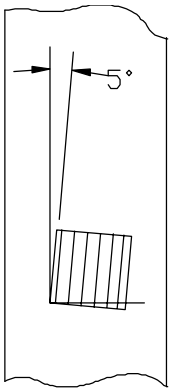

FIGURE 26. STRAIN GAGE BONDED TO SPECIMEN WITH 5° MISALIGNMENT

gages would be measuring the same component of the longitudinal strain.[1] Thus, a misalignment of 5° represents the worst case of gage misalignment. The effect of this error can be calculated using the following equations. The error in the measured strain is given as

$$\%error = \left(\frac{\varepsilon^{actual} - \varepsilon^{measured}}{\varepsilon^{actual}}\right) \times 100 = \left(\frac{\varepsilon^{actual} - \varepsilon^{actual}\cos(5°)}{\varepsilon^{actual}}\right) \times 100 \tag{13}$$

For a 5° error in strain gage alignment, the error in the measured strain is only 0.4%. The apparent bending in the specimen due to this gage alignment error is given as

$$B_y = \left(\frac{\left|\varepsilon^{actual} - (0.996\varepsilon^{actual}\right|}{\left|\varepsilon^{actual} + (0.996\varepsilon^{actual}\right|}\right) \times 100 = (0.2\% \tag{14}$$

Even if the error in the strain gage alignment was 10°, the apparent bending in the specimen due to the gage misalignment would still only be 0.8%. This analysis shows that typical errors in strain gage alignment do not have a significant effect on the measured bending in the test specimen.

5.1.4 Effect of Fixture Dimensional Tolerances on Specimen Bending.

The dimensions of the CLC-OR test fixture were checked on a Brown and Sharpe Manufacturing Co. MicroVal Digital Coordinate Measuring Machine (CMM). This machine has an accuracy of 0.0025 mm (0.0001″). First, the CLC-OR test fixture was disassembled and the loading surfaces were inspected. The loading surfaces were measured on a 12.7-mm (0.50″) grid using the CMM. This inspection revealed that the loading surfaces were flat and parallel to within 0.025 mm (0.001″) across the entire area. However, it was difficult to accurately measure the thermal-sprayed surface. A gross estimate of the flatness of the thermal-sprayed surfaces was obtained

[1] However, there would be an error in the measured compressive modulus of the specimen, since both strain gages would be measuring a reduced strain.

by taking the average of four measurements on a 6.35-mm (0.25″) grid. This estimate did not reveal any inconsistency in the thermal-sprayed surface.[2]

An aluminum test specimen, precision ground flat to within 0.013 mm (0.0005″), was placed in the CLC-OR test fixture. The test fixture bolts were then torqued to 1.1 N-m (10 in-lbf). As before, the CMM did not reveal any problems with the dimensions of the assembled CLC-OR test fixture. Next, the test fixture bolts were torqued to 3.4 N-m (30 in-lbf). When the test fixture bolts were torqued to this level, a slight rocking of the test fixture on the marble table of the CMM was apparent. The CLC-OR test fixture was then pushed across the marble surface plate in a figure-8 pattern to polish the bottom surface of the test fixture. This action revealed a high spot on the test fixture, near the region of the test fixture that contacts the specimen. This area is shown in figure 27. The test fixture was turned over and the process repeated, revealing a similar high spot on the top loading surface of the CLC-OR test fixture. These high spots were probably due to the very high stress concentrations present in these regions during failure of the specimen. The CLC-OR test fixture was made of AISI C1018 low-carbon steel, which apparently is not strong enough to resist the high stresses created when a specimen fails. Consequently, over time the material in this region was being plastically deformed.

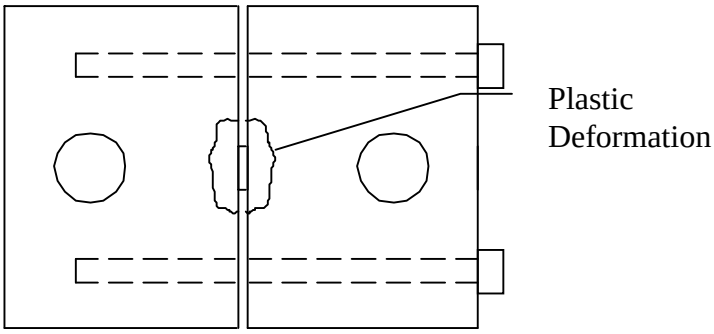

FIGURE 27. PLASTIC DEFORMATION OF CLC TEST FIXTURE (TOP VIEW)

The high spots on the CLC-OR test fixture were removed by lapping the test fixture on a granite surface plate using 240 grit wet/dry emery cloth. This process was continued until the test fixture did not rock on the marble surface plate. The test fixture was then lapped again on the marble surface plate using 320 grit wet/dry emery cloth to remove the fine scratches from the loading surfaces.

Next, a set of five AS4/3501-6 carbon/epoxy $[90/0]_{5s}$ cross-ply test specimens were machined from Panel PA04A, which was fabricated using the improved process described in section 5.1.1. These specimens had a thickness variation of less than 0.051 mm (0.002″) from one end of the specimen to the other. The specimens were tested in the CLC-OR test fixture between fixed loading platens that were parallel to within 0.025 mm (0.001″). This load plate alignment was determined by moving a dial indicator, mounted on a portable base, between the load platens. The dial indicator used had a resolution of 0.0025 mm (0.0001″).

[2] However, it was later determined that the CLC-OR test fixture suffers from the effects of compounding dimensional tolerances. This is discussed in detail in section 5.2.4.

Back-to-back strain gages were used to measure the bending in the specimen during each test. The average bending at failure for the specimens was 6.3%, and only one specimen had more than 10% bending at failure, viz., 10.08%. This set of specimens had the least amount of bending of any set that had been tested to this point. This reduction in bending was undoubtedly due to the close attention paid to specimen fabrication, fixture tolerances, and load platen alignment. Since the amount of bending at failure in the specimens was now under control, the compressive strengths obtained using the CLC-OR test fixture could be compared to the compressive strengths obtained using the IITRI test fixture.

5.2 INITIAL COMPARATIVE STUDY OF CLC AND IITRI TEST FIXTURES.

A comparative study of the CLC-OR and IITRI test fixtures was conducted using two materials, AS4/3501-6 carbon/epoxy and S2/301-NCT glass/epoxy (the original CLC test fixture, CLC-OR, was used in this study). These materials were supplied in the form of 305-mm (12″) -wide prepreg tape. This tape was used to fabricate $[90/0]_{5s}$ cross-ply laminates using the improved fabrication procedures described in section 5.1.1. The AS4/3501-6 carbon/epoxy panel, Number PA05A, had a 63.4% fiber volume content, and the S2/301-NCT glass/epoxy panel, Number PS04A, had a 56.1% fiber volume content. The fiber content of the glass/epoxy panel was lower than desired; however, the prepreg had a fiber volume content of only 43% and it was not practical to bleed any more resin from the panel during the curing cycle, as discussed in section 3.3.2. The end-to-end thickness variation of all the specimens tested was less than 0.051 mm (0.002″).

The results of these tests are shown in table 8. Plots of stress versus strain and percent bending versus average strain for all of the specimens tested in this study can be found in appendix B.

All of the S2/301-NCT glass/epoxy specimens with a 12.7-mm (0.50″) gage length showed signs of gross buckling. The Euler buckling equation, given in ASTM D 3410 (1995) and repeated in section 5.4 as equation 31, indicated that the minimum thickness of the glass/epoxy specimens necessary to resist gross bucking was 2.21 mm (0.087″). The average specimen thickness tested was 2.26 mm (0.089″), so it is not surprising that these specimens showed signs of buckling. All of the tabbed S2/301-NCT glass/epoxy and the tabbed IITRI specimens also exhibited signs of gross buckling. These specimens exhibited more than the ASTM D 3410 (1995) allowed limit of 10% bending at failure, and they also had a reduced 0°-ply compressive strength. The gage lengths of three of the untabbed IITRI specimens and three of the CLC specimens were then reduced to 10.2 mm (0.40″). This appeared to prevent gross buckling of the specimens. These reduced gage length specimens all exhibited less than 10% bending at failure; the specimens tested in the CLC test fixture had the lowest average percent bending at failure, viz., 5.8%.

A two-sided t-test at the 95% confidence level on the means of the 0°-ply compressive strengths of the glass/epoxy specimens measured in the CLC-OR test fixture versus the IITRI test fixture revealed a statistically significant difference in the two test fixtures. The untabbed 10.2-mm (0.40″) gage length specimens tested in the CLC-OR test fixture had a lower average compressive strength than the untabbed 10.2-mm (0.40″) gage length specimens tested in the IITRI test fixture. Similar results were found for the AS4/3501-6 carbon/epoxy specimens. The tabbed AS4/3501-6 carbon/epoxy specimens with a 12.7-mm (0.50″) gage length tested in

TABLE 8. TEST RESULTS FROM $[90/0]_{5s}$ SPECIMENS

AS4/3501-6 Carbon/Epoxy								
	E^c_x			σ^c_{11}			% Bending	
	[GPa]	[Msi]	CV	[MPa]	[ksi]	CV	Mean	CV
CLC-OR, untabbed								
12.7-mm (0.50″) gage length	74.4	10.8	1.2	1891	274	4.0	4.1	86
IITRI, untabbed								
12.7-mm (0.50″) gage length	73.7	10.7	7.8	2035	295	3.2	32.2	31
10.7-mm (0.42″) gage length	70.3	10.2	2.2	2020	293	1.9	5.9	45
IITRI, tabbed								
12.7-mm (0.50″) gage length	68.9	10.0	1.1	1920	279	5.0	28.0	36

S2/301-NCT Glass/Epoxy								
	E^c_x			σ^c_{11}			% Bending	
	[GPa]	[Msi]	CV	[MPa]	[ksi]	CV	Mean	CV
CLC-OR, untabbed								
12.7-mm (0.50″) gage length	35.1	5.1	8.9	1019	148	6.2	18.9	5.6
10.2-mm (0.40″) gage length	33.8	4.9	4.0	1053	153	4.8	5.8	41
IITRI, untabbed								
12.7-mm (0.50″) gage length	33.8	4.9	7.4	932	135	5.3	42.7	21
10.2-mm (0.40″) gage length	33.1	4.8	4.1	1125	163	7.4	8.4	40
IITRI, tabbed								
12.7-mm (0.50″) gage length	39.3	5.7	13.6	933	135	8.5	42.4	62

the IITRI test fixture all exhibited more than 10% bending at failure; the average bending at failure for these specimens was 28%. The untabbed specimens with a 12.7-mm (0.50″) gage length tested in the IITRI test fixture had an average bending at failure of 32.2%. The gage lengths of the tabbed specimens could not be shortened since the tabbing material had already been bonded to the specimens. However, the gage lengths of the remaining untabbed IITRI specimens were shortened to 10.7 mm (0.42″). This was slightly different from the 10.2-mm (0.40″) gage length of the specimens tested in the CLC-OR test fixture, because the spacers used to install the specimens in the IITRI test fixture resulted in a slightly longer gage length. This small difference in specimen gage length did not have a large effect on the measured compressive properties. A discussion of the effect of specimen gage length on the measured 0°-ply compressive strength is contained in section 5.4. The average bending at failure for these shorter specimens tested in the IITRI test fixture was only 5.9%. It was interesting to discover that there was not a statistically significant difference between the 0°-ply compressive strengths of these two groups of untabbed IITRI specimens, even though the average bending at failure of the first group was over 32%.

In contrast, all of the AS4/3501-6 carbon/epoxy specimens tested in the CLC-OR test fixture exhibited less than 10% bending at failure even though they had the standard 12.7-mm (0.50″) gage length. There was much less of a problem with specimen bending in the CLC-OR test fixture as compared with the IITRI test fixture. This is probably because the pairs of wedge grips in the IITRI test fixture can move relative to each another, and thus it is possible to shear load one side of the specimen more than the other side. This problem does not exist in the CLC-OR test fixture since the fixture blocks are bolted together and uniformly loaded by the platens.

The 0°-ply compressive strengths for the untabbed AS4/3501-6 carbon/epoxy specimens tested in the IITRI test fixture that had less than 10% bending at failure were compared to the strengths of the AS4/3501-6 carbon/epoxy specimens tested in the CLC-OR test fixture. In other words, the results from the acceptable compression tests, defined by the bending limit given in ASTM D 3410 (1995), were compared against each other. A two-sided t-test at the 95% confidence level was used to test for equivalence of these two test methods. As for the S2/S01-NCT glass/epoxy specimens, this test revealed that for the specimens which were free of buckling there was a statistically significant difference between the two test fixtures. The average 0°-ply compressive strength measured in the IITRI test fixture was about 7% higher than the comparable value obtained using the CLC-OR test fixture. One obvious difference between the two sets of test data generated for the AS4/3501-6 carbon/epoxy specimens was the difference in specimen gage length between the specimens tested in the IITRI and CLC-OR test fixtures. At this point in the investigation it was suspected that the difference in the two test fixtures could be due to the different specimen gage lengths tested.

5.2.1 Specimen Thickness Study.

In order to eliminate any difference that may be caused by the specimen gage length, an AS4/3501-6 carbon/epoxy $[90/0]_{7s}$ cross-ply panel was fabricated. This new panel, Number PA01B, had a 60.1% fiber volume content. It had an average thickness of 3.94 mm (0.155″) compared with the 2.59 mm (0.102″) thickness of Panel PA05A. By increasing the thickness of the panel, the critical buckling load of the specimens machined from this panel was increased. The critical Euler buckling thickness for these specimens was 2.06 mm (0.081″), but the average thickness of the specimens tested was 3.53 mm (0.139″), so buckling was not a problem in these specimens. Standard specimens with a gage length of 12.7 mm (0.50″) were machined from this thicker panel. Only, untabbed specimens were tested in both the IITRI and CLC-OR test fixtures.

The results of these tests are shown in table 9. These results were normalized to a fiber volume content of 63.4% so that the results could be compared directly to the results from Panel PA05A shown in table 8. Stress versus strain and percent bending versus average strain for all of the specimens tested are given in appendix B.

There was no systematic problem with excessive bending or buckling in these tests. Only one specimen tested had more than 10% bending at failure; Specimen AU704, tested in the IITRI test fixture, exhibited 13.1% bending at failure. The average bending at failure was 6.7% for specimens tested in the CLC-OR test fixture, and 5.9% for specimens tested in the IITRI test

TABLE 9. TEST RESULTS FOR UNTABBED, AS4/3501-6 CARBON/EPOXY $[90/0]_{7s}$ SPECIMENS TESTED WITH A 12.7-mm (0.50″) GAGE LENGTH IN THE IITRI AND CLC-OR TEST FIXTURES

(Results Normalized to V_f = 63.4%)

	E^c_x			σ^c_{11}			Mean %
Fixture Type	[GPa]	[Msi]	CV	[MPa]	[ksi]	CV	Bending
CLC-OR	70.3	10.2	4.1	1780	258	6.5	6.7
IITRI	68.9	10.0	2.5	1941	282	2.4	5.9

fixture. The achievement of such small amounts of bending can be attributed to the increase in specimen thickness, and to the careful attention given to fabrication of the test specimens, load platen alignment, and test procedures.

As in the previous series of tests, a two-sided t-test at the 95% confidence level revealed that there was a statistically significant difference between the average 0°-ply compressive strengths measured by the two test fixtures. The strength measured in the IITRI test fixture was 7% higher than the corresponding value measured in the CLC-OR test fixture. However, there was not a statistically significant difference between the 0°-ply compressive strengths of the $[90/0]_{7s}$ and $[90/0]_{5s}$ laminates. This indicates that neither the specimen gage length nor the specimen thickness influenced the measured 0°-ply compressive strength.

The influence of specimen thickness on the measured 0°-ply compressive strength has been studied by other researchers as well. Xie and Adams (1994) used a nonlinear finite element procedure to analyze tabbed compression-loaded unidirectional fiber-reinforced composite specimens having three different thicknesses. The specimens modeled had thicknesses of 2 mm (0.08″), 6 mm (0.24″), and 10 mm (0.39″). They found that the thicker specimens exhibited more severe stress concentrations in the gage section, even far away from the wedge grips. However, experimental data found in the literature as well as those generated in the present study indicate that the 0°-ply compressive strength is not affected by the specimen thickness.

It is interesting to note that Xie and Adams (1994) also modeled two methods of transferring the compression load into the specimen gage section, viz., end loading and shear loading. The shear-loading method was found to produce a more severe stress concentration than the end-loading method. This result was confirmed by Welsh and Adams (1997b) by comparing the ultimate compressive strengths of AS4/3501-6 carbon/epoxy unidirectional composites obtained using the IITRI test fixture with values measured in the Modified D 695 test fixture, an end-loading fixture (see section 2.1.3). The average strengths measured in the Modified D 695 test fixture were 5.5% higher than the corresponding strengths measured in the IITRI test fixture.

Another study of the effect of specimen thickness on the measured compressive strength was conducted by Camponeschi (1990), who tested AS4/3501-6 carbon/epoxy and S2/3501-6 glass/epoxy unidirectional composite specimens, with thicknesses of 6.35 mm (0.250″), 12.7 mm (0.500″), and 25.4 mm (1.00″), using a specially designed end-loading compression fixture.

Camponeschi found that even for these very thick specimens the compressive strength was independent of the laminate thickness when the fixture-induced waviness in the specimen outer fibers was accounted for.

Adams and Welsh (1997) tested specimens with four different laminate thicknesses in the Wyoming CLC-OR test fixture. The specimens they tested were fabricated from AS4/3501-6 carbon/epoxy $[90/0]_{ns}$ cross-ply laminates, where n = 3, 4, 5, and 6. They found that the backed out 0°-ply strength was independent of the laminate thickness.

Adams and Finley (1996) tested thickness-tapered unidirectional AS4/3501-6 carbon/epoxy specimens in the ELSS test fixture (see section 2.2.5) using specimens of 12 different geometries. They varied the gage section thickness of the test specimens as well as the shape of the thickness taper. They found that the compressive strength was highly dependent on the geometry of the specimen. The highest compressive strength was measured in a specimen with a thickness of 2.54 mm (0.100″). However, the differences in the measured compressive strength could have been due to the higher bolt torque used on the 1.78-mm (0.070″) and 1.02-mm (0.040″) -thick specimens compared to the 2.54-mm (0.100″) -thick specimens. A discussion of the effect of bolt torque on the measured compressive strength will be discussed in section 5.2.3. It is unclear from the study by Adams and Finley (1996) whether or not specimen thickness really affected the measured compressive strength; however, based on the other data discussed in this section, it is doubtful that it did.

The conclusion of the present limited test matrix, in conjunction with the evidence present in the literature, is that the 0°-ply compressive strength is not dependent on the thickness of the specimen tested. The limit of this independence is that the ratio of the specimen thickness to the specimen gage length must be such that gross (Euler) buckling does not occur. The effects of specimen gage length and Euler buckling on the 0°-ply compressive strength are discussed further in section 5.4.

5.2.2 Effect of the CLC Test Fixture Corner Radius on 0°-Ply Compressive Strengths.

The results of the previous comparative studies were presented at the MIL-HDBK-17 Test Methods Subcommittee Meeting in October 1997. It was suggested by some of the attendees that the low 0°-ply compressive strengths measured in the CLC-OR test fixture could be caused by a severe stress concentration at the ends of the specimen gage length. It was suggested that a small radius be machined on the corner of the test fixture blocks where the blocks form the specimen gage section. To investigate the effect of this fixture radius on the measured 0°-ply compressive strength, a small experiment was conducted.

First, a new $[90/0]_{5s}$ cross-ply AS4/3501-6 carbon/epoxy panel was fabricated. This panel, Number PA07A, had a fiber volume content of 62.8%. This panel was very uniform in thickness, 2.79 ± 0.025 mm (0.110″ ± 0.001″), over the entire 305- x 305-mm (12″x12″) area of the panel. Specimens with a gage length of 12.7 mm (0.500″) were machined from this panel. In order to measure the baseline strength for these specimens, a set of three specimens were tested in the CLC-OR test fixture using the original sharp-cornered configuration. These specimens were not instrumented with strain gages, since excessive bending had not been a

problem in the CLC-OR test fixture and only strength variations were of interest in this experiment. The average 0°-ply compressive strength for these three specimens was 1806 MPa (262 ksi), with a coefficient of variation (CV) of 2.9%.

Next, a 0.76-mm (0.030″) radius was ground into the CLC-OR test fixture using an abrasive grinding wheel and a radius gage. Five specimens were tested with this configuration. The average measured 0°-ply compressive strength for these specimens was 1861 MPa (270 ksi) with a CV of 4.5%. Following these tests, a 1.52-mm (0.060″) radius was machined into the same CLC-OR test fixture. The average 0°-ply compressive strength for the four specimens tested in this configuration was 1827 MPa (265 ksi) with a CV of only 0.72%. For comparison purposes, a set of five specimens was then tested in the IITRI test fixture. The average 0°-ply compressive strength for these specimens was 1936 MPa (281 ksi) with a CV of 2.7%.

A comparison, using a one-way ANOVA at the 95% confidence level, of the average 0°-ply compressive strengths obtained using the three different CLC configurations and the IITRI test fixture indicated that there was not a statistically significant difference between each of the CLC-OR test configurations. However, the specimens tested in the IITRI test fixture still exhibited a higher average 0°-ply compression. There continued to be a statistically significant difference between the compressive strengths obtained using the CLC-OR and the IITRI test fixtures. Adding a radius to the corner of the CLC-OR test fixture negligibly increased the average 0°-ply compressive strength of the specimens tested. Therefore, it was concluded that the sharp corners on the CLC-OR test fixture blocks were not the cause of the different 0°-ply compressive strengths measured in the two test fixtures. The fact that the IITRI wedge grips also have a sharp corner at the specimen gage length ends offers further evidence in support of this conclusion.

5.2.3 Effect of Clamping Force on 0°-Ply Compressive Strength.

There was no immediate explanation for the difference in the 0°-ply compressive strength measured in the IITRI and CLC test fixtures. One possible cause that was considered was the difference in clamping force between the two test fixtures. The clamping force in the CLC test fixture is provided by the eight ¼-28 UNF socket-head cap screws that clamp the pairs of fixture blocks together. This clamping force controls the ratio of shear loading to end loading. At one extreme, if there is no torque on the bolts, then all of the specimen loading will be due to end loading. At the other extreme, it is possible to load the specimen using pure shear loading, by applying a high torque to the test fixture bolts while leaving a space between the ends of the specimen and the test fixture loading surfaces.

This loading method was tried using a set of five $[90/0]_5$ cross-ply AS4/3501-6 carbon/epoxy specimens. A gap of 2.5 mm (0.10″) was left between the end of the test specimen and the loading surfaces of the CLC-OR test fixture. Because of this gap there was no end loading of the test specimen. A torque of 12.4 N-m (110 in-lbf) was required to keep the specimens from slipping in the CLC-OR test fixture. The average strength measured was 1578 GPa (229 ksi). This was significantly lower than the previous average strength measured in the CLC-OR test fixture of 1827 GPa (265 ksi). As discussed in the next section, it is probable that the high

clamping force in these tests caused a severe stress concentration in the specimen gage section and led to the reduced strength measurements.

5.2.3.1 Optimum Clamping Force in the CLC Test Fixture.

The first objective was to determine the optimum clamping force in the CLC test fixture. To find this value, a series of tests were conducted in the CLC-OR test fixture using bolt torques ranging from finger tight to 22.6 N-m (200 in-lbf). Specimens for this study were from Panel PA07A, a $[90/0]_{5s}$ cross-ply panel fabricated from AS4/3501-6 carbon/epoxy prepreg. The results of these tests are plotted in figure 28.

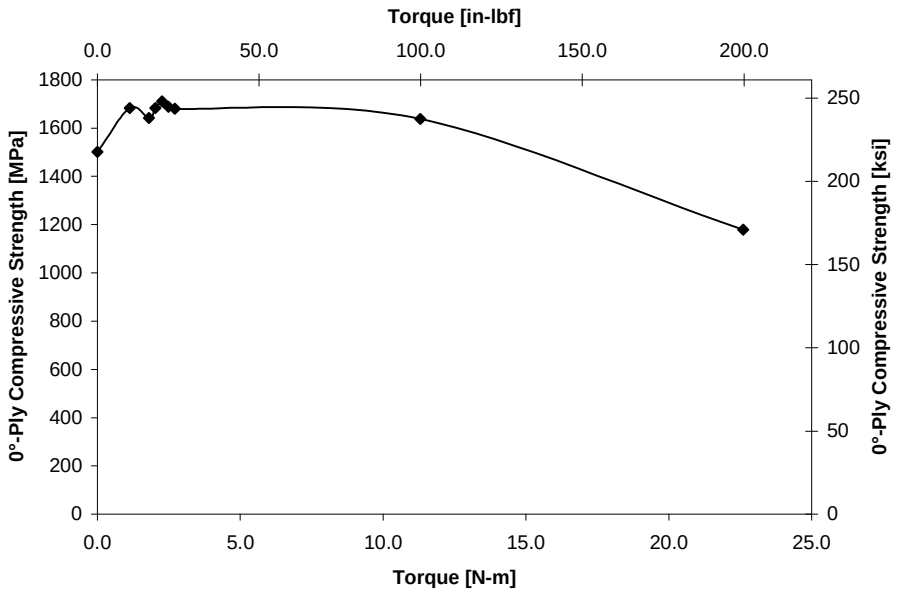

FIGURE 28. INFLUENCE OF CLC TEST FIXTURE BOLT TORQUE ON MEASURED 0°-PLY COMPRESSIVE STRENGTH

The specimens tested with the lowest bolt torques, finger-tight and 1.1 N-m (10 in-lbf), end crushed before the stress level in the gage section could reach the ultimate 0°-ply compressive strength. It was apparent from these tests that to prevent end crushing of the specimen, enough bolt torque must be applied so that some of the loading is applied through shear loading. Two specimens were tested at each of the following torque levels: finger-tight, 1.1 N-m (10 in-lbf), 1.8 N-m (16 in-lbf), 2.0 N-m (18 in-lbf), 2.3 N-m (20 in-lbf), 2.5 N-m (22 in-lbf), 2.7 N-m (24 in-lbf), 11 N-m (100 in-lbf), and 23 N-m (200 in-lbf). A two-sided t-test at the 95% confidence level showed that there was not a significant difference between the measured 0°-ply compressive strengths for the tests conducted with torque levels ranging from 1.1 N-m (10 in-lbf) to 2.7 N-m (24 in-lbf). When the test fixture bolts were torqued to 11 N-m (100 in-lbf), the average strength dropped only slightly, to 1626 MPa (236 ksi) from 1688 MPa (245 ksi). However, the measured 0°-ply compressive strength decreased significantly when the fixture bolts were torqued to 23 N-m (200 in-lbf), to 1178 MPa (171 ksi). This is similar to the result found by Haeberle (1991). It is suspected that the reduction in compressive strength is due to

two factors. First, with a high bolt torque more of the compressive load is applied by shear loading, and it has been shown by Xie and Adams (1994) that higher stress concentrations are present in the gage section for pure shear-loaded test specimens. Secondly, it was shown by Camponeschi (1991) that large clamping forces cause through-the-thickness distortion of the 0°-ply fibers. This leads to premature local microbuckling and then to premature failure of the specimen.

The conclusion of the present study is that the CLC test fixture is not highly sensitive to the fixture bolt torque used, as long as the bolt torque is large enough to prevent end crushing of the specimen but not so high that it causes a severe stress concentration at the ends of the specimen gage section, or distortion of the test specimen. The highest compressive strength measured in this phase of the study, 1763 MPa (256 ksi), was achieved with a bolt torque of 2.3 N-m (20 in-lbf), so this bolt torque was used for the remainder of the CLC tests in this study.

5.2.3.2 Analysis of Clamping Forces Generated in the IITRI and CLC Test Fixtures.

An analytical and experimental investigation was used to quantify the difference in clamping forces generated in the IITRI and CLC test fixtures. A simple mechanics of materials analysis can be used to calculate the clamping forces generated in the two test fixtures.

The torque applied to the test fixture bolts can be related to the force in the bolt using the following equation (Shigley and Mischke, 1983):

$$T = \left(f_{zI} d_m / 2 \right) \times \left[\left(l_t + \pi \mu_t d_m \sec(\alpha_t) \right) / \left(\pi d_m - \mu_t l_t \sec(\alpha_t) \right) \right] \tag{15}$$

where:

T = Torque [in-lbf]
f_{zI} = Bolt force [lbf]
d_m = Mean thread diameter (0.232″ for ¼-28 UNF (Shigley and Mischke, 1983))
μ_t = Dynamic coefficient of friction (0.15 from Shigley and Mischke, 1983)
l_t = Thread length (0.0357″ for ¼-28 UNF)
α_t = Thread angle divided by 2 (30° for ¼-28 UNF)

Substituting these values in equation 15 yields:

$$\begin{aligned} f_{zI} &= \left\{ 1514 \cdot T_{(SI\ units)} \right. \\ &= \left\{ 38.47 \cdot T_{(English\ units)} \right. \end{aligned} \tag{16}$$

The CLC test fixture has four ¼-28 UNF bolts on each half of the fixture, so the total clamping force at each end of the fixture is four times the value given by equation 16. Thus, the total clamping force in the CLC test fixture for a bolt torque of 2.3 N-m (20 in-lbf) is 13.7 kN (3078 lbf). However, the value assumed for the coefficient of friction has a very large influence on the calculated bolt force. The sliding coefficient of friction for steel on steel ranges from 0.06, if the surfaces are lubricated with graphite, to 0.39 for grease-free surfaces in air

(Marks Handbook, 1967). Substituting these values into equation 15, the calculated clamping force ranges from 30.9 kN (6946 lbf) to 7.32 kN (1646 lbf), respectively.

Since this range of values is so broad, and determining the exact coefficient of friction in the bolt threads is so difficult, the clamping force in the CLC-OR test fixture was measured experimentally. Two strain-gaged washers were fabricated from 6061-T6 aluminum tubing. The tubing had an I.D. of 6.60 mm (0.260″) and a wall thickness of 3.05 mm (0.120″). The tubing was cut into two 19 mm (0.75″) lengths on a lathe to insure that the ends of the tubing were flat and parallel. Then, a Micro-Measurements, Inc, EA-06-125EP-350 strain gage was bonded to each of the pieces of tubing so that the gage was aligned with the longitudinal axis of the tubing. These strain-gaged washers were then placed in line with the test fixture bolts, as shown in figure 29.

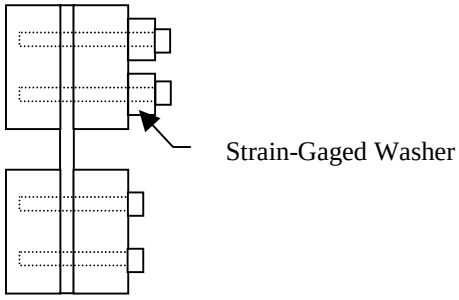

FIGURE 29. INSTALLATION OF STRAIN-GAGED WASHERS ON CLC TEST FIXTURE

The force in the bolt could be determined by a simple calculation, since the force in the strain-gaged washer is equal to the force in the bolt. Assuming a uniaxial stress state in the washer, the force in the bolt is given by

$$F = EA\varepsilon \tag{17}$$

where

F = Force in the bolt
E = Modulus of elasticity of aluminum
A = Cross-sectional area of the washer
ε = Measured strain in the washer

Test specimens were fabricated from Panel PA08A, a $[90/0]_{5s}$ cross-ply panel fabricated from AS4/3501-6 carbon/epoxy prepreg. This panel had a fiber content of 62.2% by volume. A specimen was installed in the CLC-OR test fixture and the fixture bolts were torqued to 2.5 N-m (22 in-lbf). Using the strain measured in the strain-gaged washers in conjunction with equation 17, it was determined that the average maximum force in each bolt was 3.82 kN (858 lbf). Consequently, the total clamping force at each end of the CLC-OR test fixture due to the four test fixture bolts was approximately 15.3 kN (3430 lbf). It will be noted that this value is close

to the value calculated assuming a dynamic coefficient of friction in the threads of 0.15 as suggested by Shigley and Mischke (1983).

An additional benefit of this experiment was that the Poisson-induced compressive stresses could also be determined using these strain-gaged washers. The strain level in the washers at the beginning of the test was used to calculate the initial force in the fixture bolts. The final strain level measured in the washers, just before the specimen failure, gives the final force in the bolts. The difference in these two values is the force induced by Poisson's expansion of the test specimen. Using this procedure, the average Poisson-induced force was found to be 654 kN (147 lbf) in each of the strain gaged washers. Thus, the total through-the-thickness compressive force on the test specimen for the four test fixture bolts was approximately 2620 N (588 lbf). The size of the test specimen area that was clamped between the test fixture blocks was 12.8 by 63.5 mm (0.5″ by 2.5″), so the average Poisson-induced compressive stress in the test specimen was 3.24 MPa (0.47 ksi). This is negligible compared with the average ultimate compressive stress in the gage section of 989 MPa (144 ksi). That is, Poisson-induced stresses in the CLC test fixture are not expected to have a strong influence on the measured 0°-ply compressive strength. Therefore, this factor was eliminated as a possible explanation for the difference in the 0°-ply compressive strengths measured in the CLC-OR and IITRI test fixtures.

The clamping force in the IITRI test fixture consist of two components; the clamping due to the two ¼-28 UNF bolts in the wedge grips, and the clamping due to the action of the wedge grips during the test. As for the CLC test fixture, the clamping force due to the wedge grip bolts can be calculated using equation 15. The clamping force due the action of the wedge grips can be determined from a Mechanics of Materials analysis; the derivations for these equations can be found in appendix B. This clamping force is given by

$$f_{zII} = \left(\tfrac{1}{2}\sigma \cdot A\right)\frac{1}{\tan(\tan^{-1}\mu + \phi)} \tag{18}$$

where

μ = Static coefficient of friction between wedge grip and mating wedge block (equal to 0.58 per Xie and Adams, 1994)
ϕ = Taper angle of wedge grips (10°) expressed in radians
σ = Stress applied to specimen [psi]
A = Cross-sectional area of specimen [in^2]

However, as the clamping force f_{zII} is applied, the specimen is compressed slightly. This allows the bolts to contract and the clamping force in the bolts, f_{zI}, is reduced. As long as the bolts are not torqued an excessive amount, at some point during the test the bolts will no longer be clamping the specimen and all of the clamping force will be due to the action of the wedge grips. At this point, the clamping force on the test specimen is given by equation 18. However, if the bolts are torqued too tightly, then the two clamping forces will combine together and the total clamping force on the specimen will be more than is necessary to prevent the specimen from

slipping in the wedge grips. This results in a larger stress concentration in the gage section of the specimen and could lead to premature failure of the test specimen.

The maximum amount of bolt torque that can be applied to the IITRI test fixture bolts in order to ensure that the force in the bolts goes to zero during the test can be calculated. Let Point 1 be the initial, unloaded state of the bolt, Point 2 the preloaded state of the bolt at the start of the compression test before any load is applied to the test specimen, and Point 3 the state of the bolt during the compression test. The force in the bolt at Point 2 is given by equation 15. As a clamping force, given by equation 19, is applied to the wedge grip, the specimen is compressed a small amount through-the-thickness and the tension in the bolt is relieved by a proportional amount. This action relieves some of the preload in the bolt. If the specimen is compressed enough, and the bolt is not torqued too much, eventually the load in the bolt will be entirely relieved. At this point the force in the bolt is given as:

$$F_b = 0 = (1514)T - \frac{E_b A_b}{l_1}(l_2 - l_3) \tag{19}$$

where

F_b = Force in bolt, given by equation 16 [N]
T = Bolt torque [N-m]
E_b = Modulus of Elasticity of bolt [207 GPa]
A_b = Cross-sectional area of bolt [2.7 x 10^{-5} m^2]
l_1 = Initial length of bolt [0.032 m]
l_2 = Length of bolt before clamping force is applied [m]
l_3 = Length of bolt after clamping force is applied [m]

or in English units as

$$F_b = 0 = (38.47)T - \frac{E_b A_b}{l_1}(l_2 - l_3) \tag{20}$$

where

F_b = Force in bolt, given by equation 17 [lbf]
T = Bolt torque [in-lbf]
E_b = Modulus of Elasticity of bolt [30 x 10^6 psi]
A_b = Cross-sectional area of bolt [0.0423 in^2]
l_1 = Initial length of bolt [1.25 in]
l_2 = Length of bolt before clamping force is applied [in]
l_3 = Length of bolt after clamping force is applied [in]

This equation can be written using as SI units as:

$$l_3 = l_2 - \frac{1514 \cdot T \cdot l_1}{E_b A_b} \tag{21}$$

or in English units as

$$l_3 = l_2 - \frac{38.47 \cdot T \cdot l_1}{E_b A_b} \tag{22}$$

Now, assuming the specimen obeys Hooke's Law, and neglecting Poissons effects, the through-the-thickness stress in the specimen under the wedge grips is given as:

$$\sigma_{ZZ} = E_{ZZ} \varepsilon_{ZZ} \tag{23}$$

Combining equations 19 and 23 and using the definition of strain results in:

$$\frac{0.595 \cdot P}{A_{ZZ}} + \frac{2F_b}{A_{ZZ}} = E_{ZZ}\left(\frac{t_3 - t_2}{t_1}\right) \tag{24}$$

where

P = Compressive force applied to test specimen [P_{max} = 33.3 kN (7500 lbf)]
A_{ZZ} = Area of specimen beneath the wedge grip [0.008 m^2 (1.25 in^2)]
E_{ZZ} = Through-the-thickness Modulus of Elasticity of specimen [8.96 GPa (1.3 x 10^6 psi]
t_1 = Initial thickness of specimen [0.0025 m (0.1 in)]
t_2 = Thickness of specimen before P is applied [m (in)]
tl_3 = Final thickness of specimen [m (in)]

Since the bolts are allowed to contract an amount equal to the compression of the test specimen,

$$\Delta t_{2-3} = -\Delta l_{2-3} \tag{25}$$

or

$$t_2 - t_3 = l_3 - l_2 \tag{26}$$

Now, setting the bolt force, F_b, equal to zero, the maximum torque that can be applied to the bolt can be calculated by combining equations 21, 24, and 26. This results in

$$\frac{0.595 \cdot P}{A_{zz}} = E_{zz} \frac{1514 \cdot T \cdot l_1}{t_1 E_b A_b} \tag{27}$$

In English units this can be accomplished by combining equations 22, 24, and 26 to obtain

$$\frac{0.595 \cdot P}{A_{zz}} = E_{zz} \frac{38.47 \cdot T \cdot l_1}{t_1 E_b A_b} \tag{28}$$

The average maximum load, P, that is applied to the specimen is 33.36 kN (7500 lbf). Using the appropriate value in equation 27 or 28 along with the appropriate values of the other variables,

the maximum bolt torque, *T*, that can be applied so that the bolt forces go to zero during the test is calculated to be 0.818 N-m (7.24 in-lbf).

The authors found that it was usually necessary to apply more torque than 0.818 N-m (7.24 in-lbf) to the wedge grip bolts; otherwise, the edge grips would slide off the specimen as the specimen/wedge grip assembly was place into the IITRI test fixture housings. Therefore, a bolt torque of 2.0 N-m (18 in-lbf) was used for most of the IITRI compression test specimens. This means that the force in the wedge grip bolts does not go to zero during the compression test. In order to examine the effect of this larger than optimum clamping force, a set of five specimens were tested in the IITRI test fixture using bolt torques of 0.40 N-m (3.5 in-lbf) and a second set of five specimens were tested using bolt torques of 2.0 N-m (18 in-lbf). The results of these tests are shown in table 10. The measured 0°-ply compressive strengths for the two sets of specimens are statistically equivalent. This indicates that the clamping force induced by bolt torques of 2.0 N-m (18.0 in-lbf) does not adversely affect the IITRI compression test. Using these results as a guide, the authors suggest that a clamping force of 2.0 N-m (18.0 in-lbf) be used to test specimens in the IITRI test fixture. This higher clamping force makes the specimen/wedge grip assembly much easier to handle during the installation of this assembly into the IITRI test fixture blocks, and also prevents errors caused by the specimen slipping in the wedge grips during the test.

TABLE 10. CROSS-PLY $[90/0]_{5s}$ AS4/3501-6 CARBON/EPOXY SPECIMENS TESTED IN THE IITRI TEST FIXTURE USING VARIABLE CLAMPING FORCES, PANEL PA05A (V_f-63.4%)

Specimen Number	Torque on Wedge Grip Bolts		0°-Ply Compressive Strength	
	[N-m]	[in-lbf]	[MPa]	[ksi]
IMCA01	0.40	3.5	1910	277
IMCA02	0.40	3.5	1910	277
IMCA03	0.40	3.5	1993	289
IMCA04	0.40	3.5	1951	283
IMCA05	0.40	3.5	1896	275
Average	0.40	3.5	1931	280
CV [%]			2.1	2.1
IMCA06	2.0	18	1917	278
IMCA07	2.0	18	2034	295
IMCA08	2.0	18	1910	277
IMCA09	2.0	18	1917	278
IMCA10	2.0	18	1937	281
Average	2.0	18	1944	282
CV [%]			2.7	2.7

Assuming the best case scenario, that the bolt forces go to zero during the IITRI compression test, the clamping force in the IITRI test fixture can easily be compared to the clamping force in the CLC test fixture. At an ultimate axial compressive stress in the test specimen of 989 MPa

(144 ksi), the force due to the clamping action of the IITRI wedge grips, f_{ZII}, is 19.0 kN (4272 lbf). This is larger than the force of 15.3 kN (3430 lbf) measured in the CLC-OR test fixture using the strain-gaged washers. Furthermore, as previously noted, equation 18 is very sensitive to the value chosen for μ, the coefficient of friction. In reality, the clamping force in the IITRI test fixture is probably even higher since graphite lubricant was used on the interface of the wedge grips and the mating wedge blocks. This lubricant reduces the coefficient of friction to a value less than 0.58, so less of the applied load has to be used to overcome friction between the two surfaces. Furthermore, if the bolt torque is higher than 0.818 N-m (7.24 in-lbf), the bolt forces do not become zero during the test, and the clamping force is even higher than the value given by equation 18.

In conclusion, the clamping forces in the IITRI test fixture are significantly higher than they are in the CLC test fixture. However, the exact amount of the difference is not known because the actual clamping forces in the IITRI test fixture were not directly measured in this study. The higher clamping force in the IITRI test fixture causes a larger stress concentration in the specimen gage section compared to the CLC test fixture. This should cause the 0°-ply compressive strengths obtained using the IITRI test fixture to be slightly lower than the comparable values obtained using the CLC test fixture.

5.2.3.3 Effect on Measured Compressive Strength of Varying Clamping Forces in CLC Test Fixture.

A postfailure visual inspection of the specimens tested in the CLC-OR test fixture and in the IITRI test fixture revealed a difference in the clamping pattern in the two fixtures. (The thermal-sprayed clamping surfaces on the test fixtures leave indentions on the faces of the test specimen.) It appeared that in the IITRI test fixture the clamping force was larger at the outer end of the specimen and that it diminished to zero at the start of the specimen gage section. In contrast, the CLC-OR test fixture appeared to have more clamping at the beginning of the gage section than it did at the outer end of the specimen. This difference in the test fixtures was purely fortuitous` and was due solely to the manner in which the test fixture components fit together. Section 5.2.4 discusses the effects of test fixture dimensional tolerances on the measured compressive properties.

This difference was proposed as an explanation for the difference in the measured strengths obtained in the two fixtures. It was thought that the CLC-OR test fixture was essentially pinching the specimen and creating a very high stress concentration at the beginning of the specimen gage section. In an attempt to duplicate the apparent clamping pattern in the IITRI test fixture, two sets of specimens were tested in the CLC-OR test fixture using a variable clamping force. One set of specimens was fabricated from Panel PA05A and the other set was fabricated from Panel PA07A. The two test fixture bolts at the top and the two fixture bolts at the bottom of the test fixture were torqued to a higher level than the four fixture bolts closest to the specimen gage section. The results of these tests are shown in table 11.

Varying the clamping force in the CLC-OR test fixture did appear to influence the measured 0°-ply compressive strength. When the total amount of clamping force from the test fixture bolts

TABLE 11. CROSS-PLY $[90/0]_{5s}$ AS4/3501-6 CARBON/EPOXY SPECIMENS TESTED IN THE CLC-OR TEST FIXTURE USING VARIABLE CLAMPING FORCES

Specimen Number	Torque on Specimen End Bolts		Torque on Specimen Gage Section Bolts		0°-Ply Compressive Strength	
	[N-m]	[in-lbf]	[N-m]	[in-lbf]	[MPa]	[ksi]
Panel PA05A						
VCA01	4.1	36	1.1	10	1751	254
VCA02	4.1	36	0.68	6	1869	271
VCA03	5.7	50	0.68	6	1729	251
VCA04	6.8	60	0	0	1702	249
VCA05	6.8	60	2.0	18	1609	233
Average					1732	251
CV [%]					4.8	4.8
Panel PA07A						
CVA01[1,2]	2.3	20	Finger	Finger	1650	239
CVA02[1,2]	2.9	26	1.1	10	1845	268
CVA03[1]	4.1	36	1.1	10	1883	273
Average					1793	260
CV [%]					7.0	7.0

[1]Specimen made from Panel PA07A
[2]Failed by end crushing

was not high enough, the specimen prematurely failed by end crushing. At the other extreme, when the clamping force was too high, the measured specimen strength dropped due to the increased stress concentration in the gage section, consistent with the results presented in section 5.2.3.1. The optimum clamping force, defined as the clamping force that resulted in the highest measured 0°-ply compressive strength, appeared to occur when the bolts at the end of the specimen were torqued to 4.1 N-m (36 in-lbf) and the bolts nearest the specimen gage section were torqued to 1.1 N-m (10 in-lbf). However, varying the clamping force failed to raise the 0°-ply compressive strengths measured in the CLC-OR test fixture to the level achieved in the IITRI test fixture. It will be recalled that the average 0°-ply compressive strength measured for specimens fabricated from Panel PA05A and tested in the IITRI test fixture was 2020 MPa (293 ksi) (see table 8).

The results presented in this section indicate that the distribution of the clamping force along the length of the test specimen has some effect on the measured 0°-ply compressive strength. It is unlikely that another IITRI test fixture would have the same clamping force distribution as the IITRI test fixture used in the present study. Therefore, it may be advantageous to fit the test fixture parts during fabrication so that the optimum clamping force distribution is achieved.

5.2.4 Effect of Dimensional Tolerances on 0°-Ply Compressive Strength.

At this point in the investigation of the difference in strengths measured by the two fixtures, it was proposed that the particular CLC-OR test fixture being used might have some inherent flaw

that caused the reduced strengths. This CLC test fixture had been fabricated within the CMRG by modifying an ELSS test fixture (Irion and Adams, 1981). The original ELSS test fixture had not been machined to close tolerances. Even though the inspection of the test fixture using the digital CMM, as discussed in section 5.1.4, did not reveal any significant errors in alignment of the loading surfaces, it was suspected that some part of the test fixture was out of alignment. So as to increase the stress concentration in the gage section of the test specimen. Two sources for errors in the test fixture were identified. The first source of error was the thermal-sprayed surface. It was very difficult to determine the uniformity of this surface because of its intentionally large surface roughness. It is possible that the surface was uneven enough to cause an increased stress concentration in the gage section.

The second source of error in the test fixture was identified as compounding dimensional tolerances. Although inspection of the CLC test fixture with the digital CMM revealed that each of the loading surfaces was flat and parallel to within 0.025 mm (0.001″), it was possible that when the test fixture was assembled and under full load, errors in the test fixture dimensions added together in a detrimental way.

In order to investigate the possibility that the reduced strengths in the CLC-OR test fixture were a characteristic of the specific CLC test fixture being used, three new CLC test fixtures were obtained from Wyoming Test Fixtures, Inc. Two of the test fixtures, Serial Numbers CU-EL-24 and CU-EL-25, were fabricated of AISI C1018 low-carbon steel the same as CLC-OR, and the third test fixture, WTF-EL-15, was fabricated of 17-4PH stainless steel. In the present report these test fixtures will be referred to as CLC-24, CLC-25, and CLC-15, respectively, with the original CLC test fixture fabricated by the CMRG and used to this point again being referred to as CLC-OR. Test specimens were fabricated from Panel PA07A, a $[90/0]_{5s}$, cross-ply laminate fabricated from AS4/3501-6 carbon/epoxy. This panel had a fiber volume content of 62.8%. Five ungaged specimens were tested in each of the three new CLC test fixtures and the results were compared to the values previously obtained using the IITRI and CLC-OR test fixtures. The results of these tests are shown in table 12.

TABLE 12. AVERAGE COMPRESSIVE STRENGTHS FOR AS4/3501-6 CARBON/ EPOXY $[90/0]_{5s}$ SPECIMENS FROM PANEL PA07A (V_f = 62.8%) TESTED IN VARIOUS FIXTURES

Fixture Number	Compressive Strength, σ^c_{11}		
	[GPa]	[ksi]	CV
CLC-OR	1.807	262	2.9
CLC-24	1.993	289	1.7
CLC-25	2.020	293	1.0
CLC-15	2.013	292	2.3
IITRI	1.944	282	2.6

A one-way ANOVA test at the 95% confidence level was used to compare these data. This test revealed that there was a statistically significant difference in the average 0°-ply compressive strengths measured in the different fixtures. A pair-wise multiple comparison, using

Bonferroni's Method (Christensen, 1996), revealed that there was not a statistically significant difference between the strengths measured in the IITRI, CLC-24, CLC-25, and CLC-15 test fixtures, but that the strengths measured in these fixtures were significantly higher than the strength measured in the original CLC test fixture, CLC-OR. This result indicates that there is some inherent problem with the original CLC test fixture. Further visual inspection did not reveal the source of the problem; however, it is suspected that the compounding dimensional tolerances and variations in the thermal-sprayed surface were combining in such a way as to be detrimental to the performance of this particular test fixture. It was significant that the average 0°-ply compressive strength measured in each of the three new CLC test fixtures was higher than the average 0°-ply compressive strength measured in the IITRI test fixture. This was the expected result since the analysis by Xie and Adams (1993) showed that the stress concentrations associated with pure shear loading is higher than for combined shear and end loading.

The effect that compounding dimensional tolerances can have on the measured 0°-ply compressive strength was then demonstrated using the IITRI test fixture. First, a piece of shim stock 0.217 mm (0.005″) thick was placed between one of the lower wedge grip spacers and the mating wedge block, as shown in figure 30. A set of five test specimens, fabricated from Panel PA08A, a $[90/0]_{5s}$ cross-ply laminate fabricated from AS4/3501-6 carbon/epoxy prepreg were tested in the IITRI test fixture in this configuration. Panel PA08A had a fiber volume content of 62.2%. Then, the 0.127-mm (0.005″) -thick shim was replaced by a 0.25-mm (0.010″) -thick shim and another set of five test specimens from Panel PA08A were tested. The results, shown in table 13, were very dramatic.

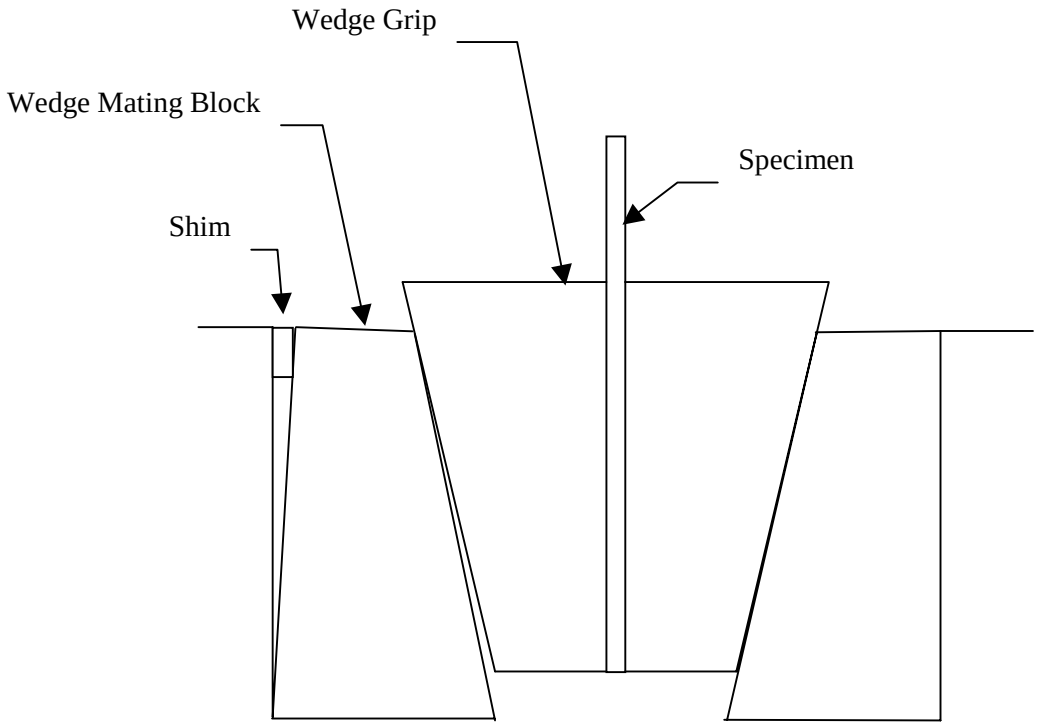

FIGURE 30. SHIM STOCK INSERTED BETWEEN IITRI WEDGE GRIPS AND MATING BLOCK

TABLE 13. AVERAGE COMPRESSIVE STRENGTHS FOR AS4/3501-6 CARBON/ EPOXY $[90/0]_{5s}$ SPECIMENS TESTED IN THE IITRI TEST FIXTURE WITH SHIM INSERTS, PANEL PA08A (V_f = 62.2%)

	Compressive Strength, σ^c_{11}		
Alignment Condition	[MPa]	[ksi]	CV
IITRI – no shim	1951	283	3.7
IITRI – 0.127-mm (0.005″) shim	1813	263	4.8
IITRI- 0.25-mm (0.010″) shim	1730	251	4.1

The induced error in the IITRI test fixture alignment of only 0.127 mm (0.005″) caused the measured 0°-ply compressive strength to drop to the level observed in the original CLC test fixture, CLC-OR. An error in the test fixture alignment of 0.25 mm (0.010″) caused the measured 0°-ply compressive strength to drop even further; a drop in the measured strength of more than 11% was observed for this case.

There are ten mating surfaces in each half of the IITRI test fixture that have to be machined. If the dimensional tolerances on these parts are ±0.025 mm (±0.001″), which is very conservative, then it is very possible to have an alignment error of more than 0.127 mm (0.005″) in the assembled fixture. This alignment error is independent of the specimen thickness tolerance, which is also on the order of ±0.025 mm (±0.001″). In comparison, there are only four loading surfaces in each half of the CLC test fixture. It is certainly possible that the small errors in the alignment of these surfaces could combine together with the variations in the thermal-sprayed surface and the specimen thickness to add up to an alignment error of more than 0.127 mm (0.005″). This could very well explain the low values obtained using the original CLC test fixture. Another item of evidence in support of this theory is that all of the new CLC test fixtures, CLC-24, CLC-25, and CLC-15, were fabricated by Wyoming Test Fixtures, Inc., which maintains a much higher level of care and quality control than could be attained by the CMRG shop, and the 0°-ply compressive strengths measured using these fixtures were higher than the IITRI average. The results of this study prompted the use of the 17-4PH stainless steel CLC test fixture, CLC-15, for the remainder of the CLC tests conducted in the present investigation.

The message here is that great care must be taken when manufacturing compression test fixtures. It is recognized that accumulation of tolerances is difficult to control, and specifying very small tolerances would drastically increase the cost and time associated with test fixture fabrication. Therefore, it may not be feasible to apply extreme quality control measures to the fabrication process. However, each fixture should be checked for proper alignment. The authors recommend that an aluminum test specimen with back-to-back strain gages be installed and loaded in the test fixture to check for induced bending. In addition, the clamping pattern left in the aluminum specimen by the thermal-sprayed surfaces of the test fixture gives some indication of the distribution of the clamping forces applied by the test fixture. If a problem exists in the alignment of the test fixture or in the distribution of clamping forces, it may be necessary to modify the test fixture parts to obtain an adequate fit.

5.2.5 Effect of Specimen Surface Finish on 0°-Ply Compressive Strength.

A small study was conducted to determine the effects of specimen surface finish on the measured 0°-ply compressive strength. This study was conducted using the specimens remaining from Panel PA03A, a $[90/0]_{5s}$ cross-ply AS4/3501-6 carbon/epoxy panel with a fiber volume content of 68.6%. Only a small number of specimens were remaining from Panel PA03A; consequently, there were not enough specimens to test a complete test matrix of surface finishes. However, this test matrix does indicate the effect of specimen surface finish on the measured 0°-ply compressive strength.

Specimens were tested with three surface finishes; as fabricated, hand lapped, and machine ground. A standard peel ply Northern 200 TFNP Teflon-coated, and porous glass scrim fabric had been used to fabricate Panel PA03A. This peel ply leaves the fabric pattern imbedded in the matrix material on the surface of the panel. Thus, the specimens with an as-fabricated surface finish had a fairly rough, but uniform surface finish. The hand-lapped specimens were lapped on a granite surface plate using 240 grit wet/dry emery paper followed by 320 grit wet/dry paper. These specimens were lapped dry. This procedure smoothed off the fabric pattern on the surface of the specimens and eliminated the gross thickness variations in the specimens. The machine-ground specimens were ground wet using a surface grinder with a 60 grit aluminum oxide grinding wheel. This left a very smooth finish on the specimens and it produced specimens with a very uniform thickness. Approximately 0.64 mm (0.0025″) of material was removed from each face of these specimens. This represented about one-half of the thickness of the outer 90° ply. The thickness of each machine-ground specimen varied by less than 0.0127 mm (0.0005″) over the entire 140 mm (5.50″) length of the specimen. The results of all these tests are given in table 14. These results indicated that the measured 0°-ply compressive strengths were not sensitive to the surface finish of the specimens. However, a visual inspection of the failed specimens revealed that removing the surface roughness by either the hand-lapping or the machine-grinding process improved the uniformity of the clamping force on the specimen. Consequently, the remainder of the specimens tested in this study were hand lapped. This process also reduced the amount of bending at specimen failure and decreased the variance in the measured strength data. Those benefits were well worth the small amount of effort required to lap these specimens by hand.

In this test matrix the 0°-ply compressive strengths obtained using the CLC-15 test fixture were statistically equivalent to the results obtained using the IITRI test fixture. The results obtained using the CLC-OR test fixture were significantly lower than the values obtained using the other two test fixtures. This lends further evidence that the initial concerns with the CLC test method were strictly related to the particular CLC-OR test fixture itself and were not inherent to the CLC test method.

5.3 COMPARATIVE EVALUATION OF THE CLC TEST METHOD AND THE IITRI TEST METHOD.

Using the new CLC test fixture, CLC-15, obtained from Wyoming Test Fixtures, Inc., a study was conducted to directly compare the behavior of the CLC Test Method to the IITRI Test Method.

TABLE 14. AVERAGE COMPRESSIVE STRENGTHS OF $[90/0]_{5s}$ AS4/3501-6 CARBON/EPOXY SPECIMENS WITH VARIOUS SURFACE FINISHES

Fixture Number and Specimen Finish	No. of Specimens	Compression Strength, σ^c_{11}		
		[MPa]	[ksi]	CV
CLC- OR				
Hand lapped	2	1917	278	5.4
Machine ground	4	1893	275	1.3
CLC-15				
Hand lapped	2	1997	290	1.1
Machine ground	3	2033	295	1.4
IITRI				
As-fabricated	4	1986	288	4.9
Machine ground	2	2015	293	1.71

The objectives of this testing were (1) to determine if there was a difference between the measured 0°-ply compressive strengths obtained by testing specimens in the two fixtures and; (2) to determine whether the 0°-ply compressive strength was independent of the laminate lay-up of the test specimens. Regarding the second objective, if the backed out 0°-ply compressive strength is truly the design strength of the material, then this value should be constant for any of the general or common structural laminates.

A number of factors were compared in order to gain a more in-depth understanding of these two test methods. These included the axial compressive modulus of the laminate, the specimen strain to failure, and the percent bending at failure. These factors were compared between test specimens of similar material and similar laminate orientation tested in the two different test fixtures. A simple t-test on the difference between two means, as described in section 4.5, was used to determine whether there was a statistical difference between the results obtained by the two test methods.

These comparative tests were performed using six different materials: (1) AS4/3501-6 carbon/ epoxy, (2) S2/SP381 glass/epoxy, (3) T300/3034 carbon/epoxy, (4) T50/2134A carbon/epoxy, (5) P75S/2034 carbon/epoxy, and (6) T800/2302-19 carbon/epoxy. Two laminate orientations were used: $[90/0]_{ns}$ cross-ply and $[45/0/-45/90]_{2s}$ quasi-isotropic. The last four materials were supplied by Boeing Space Systems Division in the form of fully cured 38.1- × 305-mm (1.5″ × 12.0″) test blanks. The first two materials were fabricated in-house using 305-mm (12.0″) -wide prepreg tape, as previously described in section 3.

The test results for these materials are shown in table 15. Five specimens were tested in each group; however, in a few instances, the mean values presented in the tables represent a smaller data set as indicated in the table. Only the specimens that had less than 10% bending at failure were retained in these data, the exception being the P75S/2034 carbon/epoxy specimens. The

TABLE 15. COMPRESSION STRENGTHS OF VARIOUS COMPOSITES AS MEASURED USING THE CLC-15 AND IITRI TEST FIXTURES

CLC-15 Test Fixture Results									
Material	No. of Replicates	E^c_x			σ^c_{11}			% Bending	
		[GPa]	[Msi]	CV	[MPa]	[ksi]	CV	Mean	CV
AS4/3501-6									
$[90/0]_{5s}$	5	n/a	n/a	n/a	1992	289	2.8	n/a	n/a
S2/SP381									
$[90/0]_{4s}$	5	30.3	4.4	1.8	1151	167	9.5	1.5	99
$[45/0/-45/90]_{2s}$	5	23.4	3.4	5.6	1060	154	6.3	1.1	64
T300/3034									
$[90/0]_{4s}$	5	63.4	9.2	1.6	1658	241	6.1	3.6	32
$[45/0/-45/90]_{2s}$	5	46.9	6.8	2.6	1629	236	7.3	2.6	43
T50/2134A									
$[90/0]_{4s}$	5	99.2	14.4	2.5	1018	148	5.0	5.9	57
$[45/0/-45/90]_{2s}$	5	62.0	9.0	2.9	923	134	3.1	3.7	61
P75S/2034									
$[90/0]_{4s}$	5	144.7	21.0	0.8	436	63.3	5.4	32	27
$[45/0/-45/90]_{2s}$	5	83.4	12.1	2.4	582	84.5	1.5	13	56
T800/2302-19									
$[90/0]_{4s}$	5	75.8	11.0	2.1	1709	248	3.2	2.3	71
$[45/0/-45/90]_{2s}$	4	52.4	7.6	0.2	1728	251	3.5	3.6	44
IITRI Test Fixture Results									
Material	No. of Replicates	E^c_x			σ^c_{11}			% Bending	
		[GPa]	[Msi]	CV	[MPa]	[ksi]	CV	Mean	CV
AS4/3501-6									
$[90/0]_{5s}$	5	n/a	n/a	n/a	1944	282	2.6	n/a	n/a
S2/SP381									
$[90/0]_{4s}$	5	28.9	4.2	1.9	915	131	4.0	5.4	61
$[45/0/-45/90]_{2s}$	5	22.7	3.3	3.6	921	134	5.0	1.9	68
T300/3034									
$[90/0]_{4s}$	5	63.4	9.2	1.8	1643	239	7	6.1	60
$[45/0/-45/90]_{2s}$	4	42.7	6.2	2.9	1577	229	4.5	2.8	71
T50/2134A									
$[90/0]_{4s}$	4	93.0	13.5	2.3	932	135	4.0	3.0	27
$[45/0/-45/90]_{2s}$	4	61.3	8.9	3.3	965	140	3.5	2.8	71
P75s/2034									
$[90/0]_{4s}$	3	116	16.9	1.6	416	60.3	6.6	36	52
$[45/0/-45/90]_{2s}$	4	81.3	11.8	2.9	567	82.3	4.6	7.5	51
T800/2302-19									
$[90/0]_{4s}$	5	77.2	11.2	7.2	1519	220	3.4	5.4	66
$[45/0/-45/90]_{2s}$	3	52.4	7.6	5.1	1705	248	3.3	2.4	7.3

n/a – not available

P75S/2034 carbon/epoxy specimens were very thin and almost all of the these specimens tested failed by gross Euler buckling. Consequently most of those specimens had more than 10% bending at failure. Therefore, all of the data points for the P75S/2034 carbon/epoxy specimens were retained. The plots of stress versus strain and percent bending versus average strain, along

with summary tables, can be found in appendix C for most of the specimens. The following exceptions apply; first, the results summarized in table 15 for AS4/3501-6 carbon/epoxy were obtained from ungaged test specimens, so stress versus strain and percent bending versus average strain plots were not available for these specimens. Second, a few of the strain gages mounted on the specimens listed in table 15 shorted out during the test, so there are no plots for these specimens. These details are noted in appendix C.

A two-sided t-test at the 95% confidence level was used to analyze the data shown in table 15. This test indicated that there was not a statistically significant difference between the two populations of test data. This means that the CLC and IITRI test methods can be considered equivalent test methods. It will be noted in table 15 that for the AS4/3501-6 carbon/epoxy specimens, the average values of σ^{c}_{11} obtained using the CLC-15 test fixture were slightly higher than those obtained using the IITRI test fixture. This general characteristic was repeated for the other materials also. This was the expected result since the theoretical analyses by Xie and Adams (1994) using a nonlinear finite element analysis procedure revealed that the stress concentrations at the end of the gage section were smaller for specimens loaded in combined shear and end loading than in shear loading. This result was also found in the finite element analysis conducted by Haeberle (1991). Accordingly, it was expected that the CLC-15 test fixture would produce slightly higher values than the IITRI test fixture for comparable test specimens.

A two-way ANOVA procedure was used to compare the backed out 0°-ply compressive strengths for the cross-ply and quasi-isotropic specimens tested in the CLC-15 and IITRI test fixtures. This procedure revealed that in general there was no statistically significant difference in the two test fixtures or between the two specimen laminate configurations. As for the AS4/3501-6 carbon/epoxy specimens discussed previously, this demonstrates that the CLC-15 and IITRI test fixtures yield statistically equivalent compressive property data. In addition, these results show that the 0°-ply compressive strength obtained from tests of cross-ply specimens is consistent with that value achieved in a commonly used structural laminate. Therefore, as hypothesized by Welsh and Adams (1994), a design value for the 0°-ply compressive strength can be obtained by applying a back-out factor to the measured compressive strength of a cross-ply laminate.

The largest discrepancy between test fixtures for the backed out 0°-ply compressive strength of the $[90/0]_{ns}$ composites was for the S2/SP381 glass/epoxy specimens. The 0°-ply compressive strengths measured using the IITRI test fixture were approximately 20% lower than the corresponding values obtained in the CLC-15 test fixture. The values obtained using the CLC-15 test fixture compare very well with those reported by 3M Corporation in MIL-HDBK-17 (1997). These data were generated using the Modified ASTM D 695 Test Method (SACMA SRM1-88, 1988). The low values obtained using the IITRI test fixture may be due to the high through-the-thickness clamping force generated in the IITRI test fixture. This high clamping force may cause local damage of the untabbed specimens, leading to premature specimen failures. Although a postfailure visual inspection did not reveal any difference between the failure modes of the specimens tested in the IITRI and the CLC test fixtures that would support this type of damage. Because of the explosive nature of the failures, much of the evidence was lost. It is typical of compression test specimen failures that their explosive nature

makes it nearly impossible to draw reasonable conclusions from inspections of the specimen failure modes.

There was some difference between the backed out 0°-ply strengths obtained using cross-ply and quasi-isotropic P75S/2034 carbon epoxy laminates. The average backed out 0°-ply compressive strength for the cross-ply laminates tested in the CLC-15 test fixture was 436 GPa (63.3 ksi) and the corresponding value for the IITRI test fixture was 415 GPa (60.3 ksi). For the quasi-isotropic laminates tested in the CLC-15 test fixture, the average 0°-ply compressive strength was 582 GPa (84.5 ksi) and for those specimens tested in the IITRI test fixture this value was 567 GPa (82.3 ksi). These differences indicate that there is a statistically significant difference between the 0°-ply compressive strengths obtained using the two laminates. However, these results are very suspect because the P75S/2034 carbon/epoxy specimens were relatively thin, nominally only 2.0 mm (0.077″), and none of the gaged cross-ply specimens tested exhibited less than 10% bending at failure. In fact, there were indications that all of the cross-ply specimens prematurely failed due to beam column buckling. The gage lengths for the $[90/0]_{4s}$ specimens were finally reduced to 2.54 mm (0.100″) to reduce the percent bending at failure. This reduction in gage length did decrease the amount of bending in the specimens at failure, but it did not have any statistically significant effect on the measured 0°-ply compressive strengths of these specimens. A discussion of the effect of specimen gage length on the measured 0°-ply compressive strength is included in section 5.4. When the conclusions drawn from these test data are weighed against the conclusions drawn from the other higher quality data, only minor importance can be given to these results. In any future compression testing of this high-modulus material, it would be desirable to increase the thickness of the laminates.

In conclusion, these data offer very strong evidence that the CLC test fixture is an acceptable test fixture for measuring the compressive properties of fibrous composite materials. In addition, the test results show that testing cross-ply laminates in the CLC test fixture generates valid design values for the 0°-ply compressive strength.

5.4 EFFECT OF SPECIMEN GAGE LENGTH ON MEASURED 0°-PLY COMPRESSIVE STRENGTH.

The test specimens used in the Modified ASTM D 695 Test Method (SACMA, 1988) have a gage length of 4.76 mm (0.188″). This gage length is significantly shorter than the 12.7 mm (0.500″) gage length recommended by ASTM D 3410 (1995). A number of researchers have noted that the Modified ASTM D 695 Test Method often produces erratically high values when compared to data obtained with the IITRI test fixture (Adams and Welsh, 1997). Earlier studies had indicated that the specimen gage length has very little affect on the measured compressive properties (Adams and Lewis, 1991; Smoot, 1982). However, these studies were conducted using unidirectional, tabbed test specimens. All of the problems associated with obtaining good compressive strength data from using unidirectional test specimens were not known at that time. Therefore, there are some doubts about the relevance of these past studies when assessing the influence of specimen gage length on the measured 0°-ply compressive strength of untabbed cross-ply and angle-ply compression test specimens.

These problems led the authors to conduct an independent study to investigate the influence of specimen gage length on the measured 0°-ply compressive strength of untabbed cross-ply specimens tested in the CLC test fixture. The test specimens were fabricated from Panel PA09A, an AS4/3501-6 carbon/epoxy $[90/0]_{5s}$ cross-ply laminate. This panel had a fiber volume content of 62.1%. Specimens of six different gage lengths were fabricated: 2.54 mm (0.100″), 3.81 mm (0.150″), 8.89 mm (0.350″), 12.7 mm (0.500″), 15.2 mm (0.600″), and 25.4 mm (1.000″). Back-to-back strain gages were used on the specimens with gage lengths of 8.89 mm (0.350″) and larger. The strain gages would not fit within the gage length of the shorter gage length specimens.

Five test specimens with each of the different gage lengths were tested. The results of these tests are summarized in table 16.

TABLE 16. COMPRESSION TEST RESULTS FOR AS4/3501-6 CARBON/ EPOXY $[90/0]_{5s}$ CROSS-PLY TEST SPECIMENS OF VARIOUS GAGE LENGTHS TESTED IN THE CLC TEST FIXTURE

Gage Length	Compressive Strength, σ^c_{11}			% Bending	
	[MPa]	[ksi]	CV	Mean	CV
3.81 mm (0.150″)	2052	298	2.4	n/a	n/a
8.89 mm (0.350″)	2102	305	3.6	6.2	27
12.7 mm (0.500″)	2049	297	1.0	24	57
15.2 mm (0.600″)	1812	263	4.9	17	58
25.4 mm (1.000″)	1382	201	3.5	81	17

n/a – not available; specimens were not gaged

However, the specimens with a gage length of 1.27 mm (0.100″) were not successfully tested. The average maximum strain of those other specimens that were tested with strain gages was 0.018. In a 139.7-mm (5.500″) -long specimen this means that the specimen is compressed nearly 2.54 mm (0.100″) from end to end. Thus, the 1.27-mm (0.100″) gage length specimen strained enough to allow the two halves of the test fixture blocks to come into contact before the specimen failed.

There was very good agreement between the specimens with gage lengths of 3.81 mm (0.150″), 8.89 mm (0.350″), and 12.7-mm (0.500″). The average 0°-ply compressive strengths for these three sets of specimens were 2052 GPa (298 ksi), 2102 GPa (305 ksi), and 2049 GPa (297 ksi), respectively. However, the specimens with gage lengths of 15.2 mm (0.600″) showed signs of buckling failure; the average measured 0°-ply compressive strength for these specimens was 1812 GPa (263 ksi), a 12% decrease.

The critical Euler buckling stress for a linearly elastic isotropic column with pinned-end conditions is given in equation 29. In this equation E_x is the modulus of elasticity, l is the

$$\sigma_{cr} = \frac{\pi^2 E_x I}{A l^2} \tag{29}$$

specimen gage length, and I and A are the cross-sectional moment of inertia and the cross-sectional area of the test specimen, respectively. Equation 29 can be altered to account for the effect of the layers in the composite laminate by replacing the quantity, E_xI, by the bending modulus as defined by Whitney (1987), as shown in equation 30. In this equation, the summation is carried out for each of the n plies in the laminate.

$$E_x^b I = \sum_{k=1}^{n} E_x^k I^k \tag{30}$$

Equation 1 of ASTM D 3410 (1995) alters the simple Euler buckling equation (equation 29) to account for the effects of shear forces acting in the column during buckling. This equation gives the relationship of specimen thickness, h, gage length, l, compressive modulus of the laminate, E_x, ultimate compressive strength, F^{cu}, and through-the-thickness shear modulus, G_{xz}, to the onset of Euler buckling, repeated here as equation 31.

$$h \geq \frac{l}{0.9069\sqrt{\left(1-\frac{1.2F^{cu}}{G_{xz}}\right)\left(\frac{E^c}{F^{cu}}\right)}} \tag{31}$$

This equation accounts for the effect of shearing stresses on the critical load; however, it assumes that the test specimen remains linearly elastic throughout the compression test. In reality the shear response, G_{xz}, of common composite laminates is very nonlinear. Even when based on the less conservative clamped-end conditions, inelastic buckling calculations may not always predict a higher buckling load than does equation 31. Therefore, it is possible in some cases that equation 31 is nonconservative and that it underpredicts the specimen thickness required to prevent Euler column buckling. For this reason it is important that back-to-back strain gages be used to monitor bending during the test.

Equation 31 can be rewritten in terms of the applied stress, as shown in equation 32 (Timoshenko and Gere, 1961):

$$\sigma_{cr} = \frac{\pi^2 E_x}{\frac{l^2 A}{I} + 1.2\pi^2 \frac{E_x}{G_{xz}}} \tag{32}$$

Equation 32 can also be modified to account for the plies in the laminate by using the bending modulus $E^b{}_xI$ as defined in equation 30. Equation 32 then becomes

$$\sigma_{cr} = \frac{\pi^2 E_x^b I}{l^2 A + 1.2\pi^2 \frac{E_x^b I}{G_{xz}}} \tag{33}$$

Equations 29, 30, 32, and 33 were used to predict the critical buckling stress for AS4/3501-6 carbon/epoxy $[90/0]_{5s}$ cross-ply specimens with gage lengths ranging from 2.54 mm (0.100″) to 38.1 mm (1.500″). The results of these calculations are shown in figure 31. The buckling stress shown is the laminate stress at which buckling occurs. It is not the 0°-ply stress at which buckling occurs. In other words, a back-out factor has not been applied to the critical buckling stress to calculate the stress in the 0° plies when buckling occurs.

Also shown in figure 31 is the average UCS of the AS4/3501-6 carbon/epoxy $[90/0]_{5s}$ specimens tested in the gage length study. In other words, this is the average *x*-direction compressive strength of the specimens shown in table 15 that had gage lengths of 3.81 mm (0.150″) through 12.7 mm (0.500″). The point where the buckling curve intersects this average strength curve is the critical gage length for the specimens. Those specimens with gage lengths below approximately 15 mm (0.60″) were predicted to reach the ultimate compressive strength of the material before they failed due to gross buckling since the critical buckling stress was higher than the ultimate compressive stress. However, those specimens that had longer gage lengths reached the critical buckling stress before they reached the ultimate compressive stress.

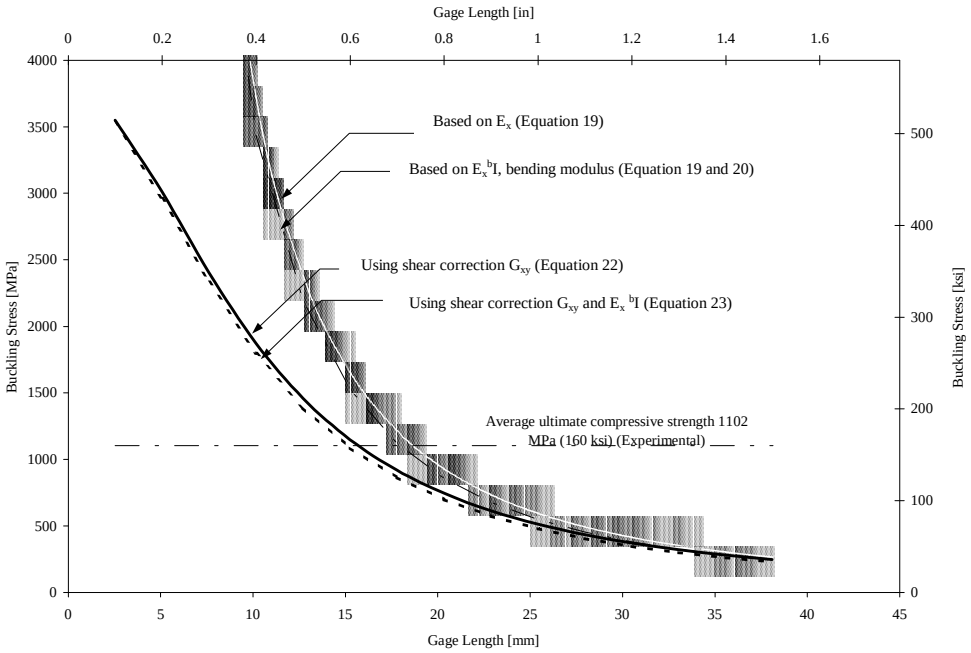

FIGURE 31. BUCKLING PREDICTIONS FOR AS4/3501-6 CARBON/EPOXY $[90/0]_{5s}$ TEST SPECIMENS

The test results for the six different groups of specimens tested can be added to this plot, as shown in figure 32. The specimens with gage lengths less than 15.2 mm (0.600″) failed at an average stress of 1102 GPa (160 ksi), but the maximum stress attained by the specimens with longer gage lengths tended to follow the buckling curves. The critical gage length predicted by equation 32 was 15.7 mm (0.620″) for the average axial direction laminate strength of 1102 GPa

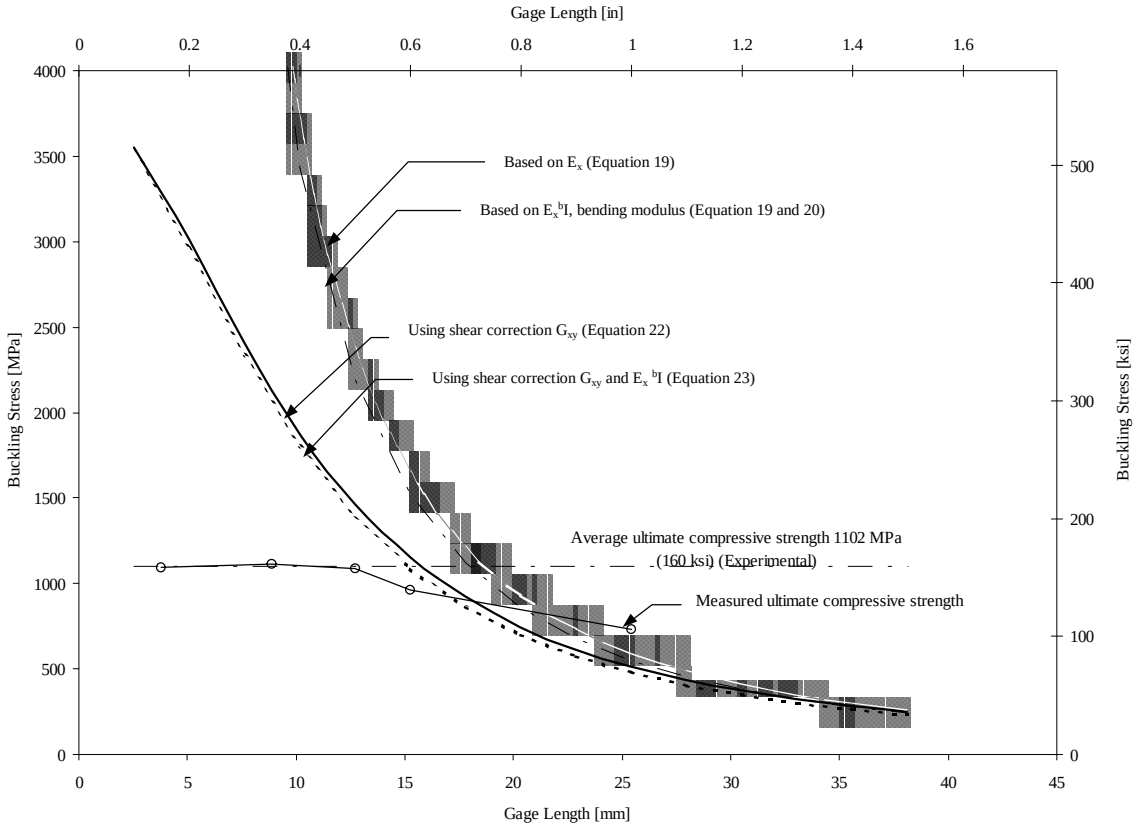

FIGURE 32. MEASURED COMPRESSIVE STRENGTH AND BUCKLING PREDICTIONS FOR AS4/3501-6 CARBON/EPOXY $[90/0]_{5s}$ CROSS-PLY SPECIMENS

(160 ksi). Therefore, it is not surprising that the 15.2-mm (0.600″) specimens showed signs of buckling when one considers the nonlinear shear modulus exhibited by this material. The specimens with gage lengths of 25.4 mm (1.000″) all buckled and thus failed at low stress levels. The average 0°-ply compressive strength for these specimens was only 1382 GPa (201 ksi) and the average percent bending at failure was nearly 82%.

In conclusion, the buckling behavior of the specimens was well predicted by equation 32, the equation used in ASTM D 3410 (1995) to guide the selection of the specimen thickness and gage length. In addition, the CLC test fixture was not sensitive to specimen gage length as long as the specimens did not buckle.

As a side note, the calculation of the critical buckling stress from equation 31 is not as straightforward as it may seem. This equation requires knowledge of the through-the-thickness shear modulus, G_{xz}. For a unidirectional composite this value is equivalent to the shear modulus, G_{12}, which is a commonly measured lamina property. However, for a cross-ply or angle-ply laminate the value of G_{xz} is not easy to measure. One way to measure this property is to stack up a number of plies such that the resulting laminate is roughly 19.1 mm (0.75″) thick. Then Iosipescu specimens, cut through-the-thickness of the thick panel, as shown in figure 33, can be tested.

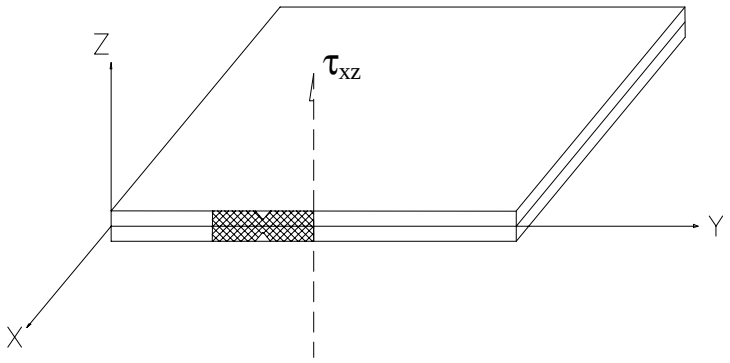

FIGURE 33. CUTTING OF IOSIPESCU SPECIMEN TO MEASURE G_{XZ}

A simple mechanics of materials model was thus developed to estimate the value of G_{xz}. This model is shown in figure 34. Since there is no shear coupling between the 90° and 0° plies, it can be assumed that the shear stresses in each ply are equal. Thus,

$$\tau_{90} = \tau_0 = \tau_c \tag{34}$$

The total shear deformation of the composite, Δ_c, is then equal to the sum of the shear deformations of all of the 90° (Δ_{90}), and 0° (Δ_0), plies, i.e.,

$$\Delta_c = \Delta_{90} + \Delta_0 \tag{35}$$

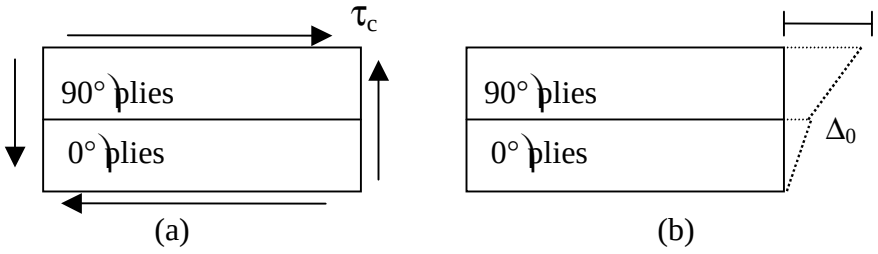

FIGURE 34. (a) MODEL OF CROSS-PLY LAMINATE FOR PREDICTION OF G_{XZ}
(b) SHEAR DEFORMATIONS

The shear deformation for each material can be written as the product of the corresponding shear strain and the material thickness, as shown in equation 36,

$$\begin{aligned} \Delta_c &= \gamma_c t_c \\ \Delta_{90} &= \gamma_{90} t_{90} \\ \Delta_0 &= \gamma_0 t_0 \end{aligned} \tag{36}$$

where t_c, t_{90}, and t_0 represent the total thickness of the composite, the 90° plies, and the 0° plies, respectively.

Then substituting equations 36 into 35 yields

$$\gamma_c t_c = \gamma_{90} t_{90} + \gamma_0 t_0 \tag{37}$$

Dividing through by t_c and recognizing that t_{90}/t_c and t_0/t_c are equivalent to the volume fractions γ_{90} and γ_0 of the 90° plies and the 0° plies, respectively, which are each equal to ½, yields

$$\gamma_c = \gamma_{90}\, t_{90}/t_c + \gamma_0\, t_0/t_c = \tfrac{1}{2}\gamma_{90} + \tfrac{1}{2}\gamma_0 \tag{38}$$

Assuming that the shear stress-shear strain relationship is linear, $\gamma = \tau/G$ can be substituted into equation 38, recognizing that for this loading condition $G_{90} = G_{23}$ and $G_0 = G_{12}$,

$$\tau_{xz}/G_{xz} = \tau_0/2G_{12} + \tau_{90}/2G_{23} \tag{39}$$

Now, substituting equation 34 into equation 39 simplifies this equation to the following relationship for the through-the-thickness shear modulus:

$$1/G_{xz} = \tfrac{1}{2}G_{12} + \tfrac{1}{2}G_{23} \tag{40}$$

or

$$G_{xz} = \frac{2}{\dfrac{1}{G_{12}} + \dfrac{1}{G_{23}}} \tag{41}$$

Using G_{12} = 6.10 GPa (0.885 Msi) and G_{23} = 3.60 GPa (0.522 Msi) in equation 41 results in G_{xz} = 4.53 GPa (0.657 Msi).

As a check of this analysis, a second estimate for G_{xz} can be obtained by calculating this property as a bulk modulus property using a simple rule of mixtures relation,

$$G_{xz} = G_{12}V_0 + G_{23}V_{90} \tag{42}$$

Using equation 42 and $V_0 = V_{90} = \tfrac{1}{2}$ results in G_{xz} = 4.85 GPa (0.703 Msi), which is fairly close to the value calculated using the previous model. However, the value calculated using this simple rule of mixtures analysis is known to overestimate the actual value of G_{xz}. The rule of mixtures analysis (the second model) assumes that the composite acts as a homogenous mixture so that the shear deformation of the 0° plies, the 90° plies, and the total composite are all equal, i.e., $\Delta_c = \Delta_{90} = \Delta_0$. In essence, the second model assumes the 90° plies act in parallel with the 0° plies, whereas the first model assumes the two types of plies act in series. The first model is a better representation of the actual material behavior, because in this model the 90° and 0° plies are allowed to deform different amounts depending on the relative values of G_{12} and G_{13}. For this reason it is recommended that equation 41 be used to calculate G_{xz}.

5.5 EFFECT OF PERCENT BENDING ON MEASURED 0°-PLY COMPRESSIVE STRENGTH.

As discussed in section 5.1.1, ASTM D 3410 (1995) requires that for compressive strength data to be considered valid, the amount of bending at failure must be less than 10%. However, the experimental data generated in this study indicate that this requirement may be too conservative.

Figure 35 shows a plot of percent bending at failure versus normalized 0°-ply compressive strength for all of the individual double-gaged specimens tested in this study for which valid results were obtained. This means that those specimens that exhibited buckling type failures were not included in this plot. In this plot, the 0°-ply compressive strength is normalized by the average 0°-ply compressive strength measured for that particular material. This average strength was determined using only the results from those specimens which exhibited less than 10% bending at failure. Figure 35 indicates that even when the bending at failure is as much as 50% there is not a significant drop in the measured 0°-ply compressive strength. When the percent bending at failure exceeds 50% there is a marked decline in the measured 0°-ply compressive strength. Examination of the percent bending versus average strain curves for these specimens reveals that the percent bending increased relatively quickly just before specimen failure. This characteristic indicates that these specimens failed due to gross Euler buckling; therefore, these data points were left off of figure 35. It appears, from examining figure 35, that the 0°-ply compressive strength is independent of the amount of bending in the specimen as long as the specimen does not fail prematurely by gross Euler buckling.

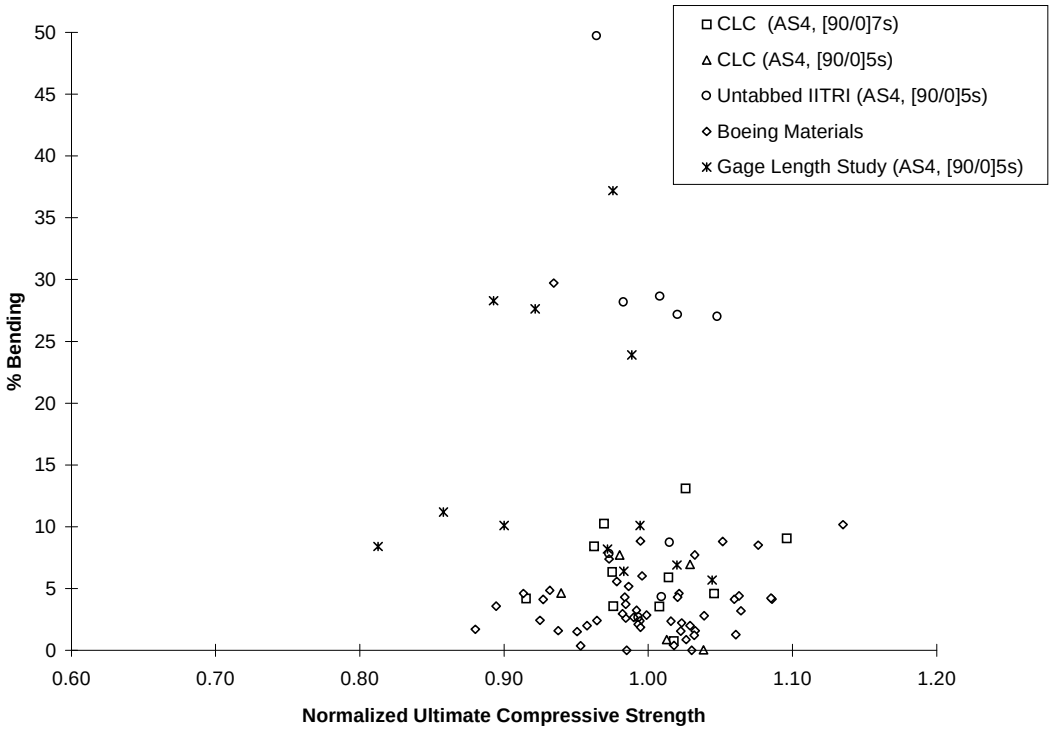

FIGURE 35. EFFECT OF BENDING ON MEASURED COMPRESSIVE STRENGTH

This finding is reinforced by the results generated early in the present study, as discussed in section 5.2. AS4/3501-6 carbon/epoxy $[90/0]_{5s}$ cross-ply specimens were tested in three configurations: (1) untabbed specimens tested in the CLC-OR test fixture, (2) untabbed specimens tested in the IITRI test fixture, and (3) tabbed specimens tested in the IITRI test fixture. The results were separated into two groups, the first group being those specimens with less than 10% bending at failure, and the second group being those specimens with more than 10% bending at failure. The first group is referred to as the acceptable group and the second group is referred to as the unacceptable group, in deference to the requirement given in ASTM D 3410. A two-sided t-test at the 95% confidence level was used to test the difference in the mean value of the measured 0°-ply compressive strength for these two groups. This test indicated that there was not a statistically significant difference between these two groups.

This finding, in conjunction with figure 35, indicates that the 10% bending limitation given in ASTM D 3410 (1995) may be unnecessary. Furthermore, figure 35 suggests that the percent bending in the test does not affect the measured strength results unless the critical Euler buckling stress is approached. A number of explanations have been given for this phenomenon, although none have been proven at this time. One explanation that appears to have some merit is described here.

Fiber microbuckling is generally considered to be the primary cause of compression failure in medium- to high-modulus fibrous composites (Haeberle, 1991). As the specimen is loaded in compression, a natural curvature develops in the specimen due to misalignment of the load or due to specimen irregularities. One would expect the fibers on the inside (concave) surface of the specimen curvature to microbuckle first because they are the most highly stressed. However, the plies adjacent to these fibers restrict them from buckling inward and the fibers do not buckle outward since the curvature of the specimen is already in the opposite direction. Thus, the fibers in the outermost 0° ply do not microbuckle, and the composite continues to take load. As the load on the composite is increased, the fibers in the next 0° ply approach their microbuckling limit. As before, the adjacent plies constrain the fibers from microbuckling. This process continues until the lateral support offered by the remaining adjacent plies is too small to constrain the critical 0° fibers from microbuckling. At that point, these 0° fibers microbuckle and the resulting instability causes the whole specimen to collapse. The interesting aspect of this theory is that as the amount of curvature in the specimen increases, the effectiveness of the lateral constraint against microbuckling increases. Thus, there is an offsetting effect between bending and microbuckling so that the measured compressive strength in the specimen appears to be independent of bending.

5.6 EFFECT OF MATERIAL NONLINEARITY ON BACKED OUT 0°-PLY STRENGTH.

One of the objections often voiced by opponents of the practice of using angle-ply and cross-ply laminates to determine the compressive properties of fibrous composite materials is that the 0°-ply compressive strength is not measured directly. A back-out factor must be used to determine this value, as discussed in section 4.4. The back-out factor depends on the properties of the composite material at failure, and it is well known that at these strain levels most composites exhibit at least some material nonlinearity. It is thought by some that this back-out factor must then be based on the properties of the composite at failure or else a large error in the

calculated 0°-ply compressive strength will result. This may be true for angle-ply laminates, since the back-out factor in this case depends on the lamina shear modulus, G_{12}, which is highly nonlinear. However, the back-out factor for cross-ply laminates is independent of G_{12}.

Table 17 shows material properties supplied by Boeing Space Systems Division for three of their materials tested in the present study. The back-out factors for $[90/0]_{ns}$ cross-ply specimens are calculated at each of the strain levels given. This table shows that the material nonlinearity has only a small effect on the calculated back-out factor for a cross-ply specimen. For example, the back-out factor for the cross-ply T800/2302-19 carbon/epoxy specimens changed by only 0.1% between 1000 με and 9000 με. The material properties were not given at the failure strains recorded, approximately 14,500 με. However, between zero and 9000 με the composite axial modulus, E_x, changed by roughly 31%, but between 9000 με and 14,500 με the axial modulus changed by only an additional 13%. Therefore, the back-out factor can be expected to change even less between 9000 με and 14,500 με than it did between 1000 με and 9000 με.

TABLE 17. SENSITIVITY OF BACK-OUT FACTORS TO MATERIAL NONLINEARITY BOEING $[90/0]_{4s}$ CROSS-PLY LAMINATES

Strain Level	$E_{11}^{c,chord}$	$E_{22}^{t,chord}$	G_{12}	υ_{12}^{chord}	Back-Out Factor
T50/2134A					
@ 1000 με)	30.6	1.15	0.80	0.359	1.928
@ 3000 με)	28.5	1.13	n/a	0.321	1.924
@ 6000 με)	26.5 (@5000)	1.09	n/a	n/a	1.922
P75S/2034					
@ 1000 με)	32.9	0.93	0.47	0.244	1.945
@ 3000 με)	21.3 (@2500)*	0.92	n/a	0.379	1.946
T800/2302-19					
@ 1000 με)	20.1	1.16	0.58	0.397	1.893
@ 3000 με)	19.3	1.14	n/a	0.397	1.890
@ 6000 με)	18.5	1.10	n/a	n/a	1.890
@ 9000 με)	17.7	1.04	n/a	n/a	1.891

n/a – not available
*Possibly anomalous data, but listed here as reported by Boeing.

The other two materials listed in table 17 exhibit similar characteristics. Therefore, since the error in neglecting the nonlinear properties of the materials is small, the back-out factor for cross-ply laminates can be calculated using the initial, linear elastic properties of the composite lamina. From this, one may conclude that the material nonlinearity has very little effect on the calculated back-out factor for cross-ply specimens.

6. CONCLUSIONS AND RECOMMENDATIONS FOR FUTURE WORK.

6.1 CONCLUSIONS.

A review of the compression testing literature revealed that there is still a great deal of confusion in the composites industry when it comes to measuring the compressive properties of fibrous composite materials. Different test methods have been standardized by various composite materials groups, such as the IITRI and Celanese Test Methods in ASTM D 3410-95 (ASTM, 1995) and the Boeing Modified ASTM D 695 Test Method in SACMA SRM 1-88 (SACMA, 1988). However, when the results from these test methods are compared to each other, or when the results generated in one testing laboratory are compared to the results obtained in another laboratory using the same test method, there is often a statistically significant difference in the measured compressive properties (Adsit, 19833). Therefore, a great deal of research has been conducted to develop an accurate and efficient compression test method. An attractive compression test method, the Wyoming CLC Test Method, has been described. In this test method, the lamina compression properties are obtained by testing untabbed, cross-ply specimens in the CLC test fixture. A back-out factor is then used to calculate the lamina compression properties from the measured laminate properties.

A large amount of effort was expended to investigate the important factors that influence the behavior of the Wyoming CLC Test Method. A parametric study revealed that specimen quality, dimensional tolerances of the test fixture, and alignment of the load train all had a significant impact on the measured compressive properties. Therefore, a large amount of time was spent to develop fabrication procedures and test methods that would minimize the variations in the measured laminate properties due to these factors.

This parametric study showed that the end-to-end thickness variation of the 140-mm (5.50″) -long test specimens should be less than 0.051 mm (0.002″) to prevent excessive bending in the test specimen at failure. It was also discovered that the 152-mm (6.0″) -diameter load platens should be parallel to within ±0.013 mm (±0.0005″) over the entire surface area.

Perhaps the most significant result of the parametric study was that compounding dimensional tolerances can have a very large effect on the measured compression strength. The original CLC test fixture used in this study, CLC-OR, was found to suffer from the effects of compounding dimensional tolerances. However, three new CLC test fixtures obtained from Wyoming Test Fixtures, Inc. did not suffer from this same problem. The CLC-OR test fixture was one of the first test fixtures fabricated by the CMRG at the University of Wyoming, and it was not fabricated to precise dimensional tolerances. Moreover, the process used to apply thermal-sprayed tungsten particles to the gripping surfaces was not very precise. It is important to note that the IITRI test fixture was also found to be very sensitive to compounding dimensional tolerances. There are roughly ten surfaces on each upper and lower half of the IITRI test fixture that must be machined. If the dimensional tolerances of these surfaces combine in such a way that the specimen is shifted out of alignment by even 0.127 mm (0.005″), the percent bending at failure and the measured compression strength are dramatically affected. It was concluded that the CLC-OR test fixture was an uncharacteristically bad test fixture and the IITRI test fixture that was used at the CMRG was probably a better than average IITRI test fixture.

The result of the careful attention paid to specimen fabrication, load train alignment, and test fixture dimensions was evident in the test results. The low coefficients of variation in the 0°-ply compression strengths generated in this study show that variations between laminates and between individual test specimens were reduced to a minimal amount. Second, the low amount of bending at failure in the test specimens indicated that the specimens were accurately fabricated, the test fixtures were well made, and the load train of the test machine was correctly aligned.

Following this parametric study of the CLC test method, a comparative study was conducted. In this study, the compression properties of $[90/0]_{ns}$ cross-ply specimens were measured using the new CLC test fixture obtained from Wyoming Test Fixtures, Inc. (Serial No. WTF-CLC-15) and the IITRI test fixture. This study showed that when properly used, the CLC test method generates compression property data statistically equivalent to the commonly used IITRI Test Method. In fact, the strengths measured in the CLC test fixture are slightly higher than the comparable strengths measured in the IITRI test fixture. This result is not surprising since finite element analysis indicates that the combined loading present in the CLC test fixture results in a smaller stress concentration in the gage section of the test specimen than does the pure shear loading present in the IITRI test fixture (Xie and Adams, 1993).

The comparative study revealed that the CLC test fixture is easier to use than the IITRI test fixture. In the IITRI test fixture the test specimen/wedge grip assembly often gets wedged into the housing block and must be knocked out of the cavity using a brass punch; the CLC test fixture does not suffer from this problem. In addition, the CLC test fixture has much less mass than the IITRI test fixture. The lighter mass of the CLC test fixture makes it easier to handle and achieve proper installation than the IITRI test fixture. This is also an important factor when testing at conditions other than ambient, as the amount of time required to reach a steady-state temperature is directly related to the mass of the test fixture. Furthermore, the CLC test fixture is much easier to fabricate and is therefore less expensive to purchase than the IITRI test fixture.

In the second portion of the comparative study, the 0°-ply compression strengths generated with cross-ply test specimens were compared to the 0°-ply compression strengths generated with quasi-isotropic test specimens. This study verified that the lamina compression properties for a fibrous composite material could be efficiently and accurately generated by testing cross-ply specimens. The ultimate compression strength of the cross-ply laminate, multiplied by a back-out factor, yielded the 0°-ply compression strength for the composite lamina. This value was statistically equivalent to the 0°-ply compression strength generated using the backed out strength values from the quasi-isotropic laminate. This verifies that a design value for the 0°-ply compression strength can be obtained by testing cross-ply specimens in the CLC test fixture.

There are two major advantages to testing cross-ply laminates to obtain lamina compression properties. First, cross-ply laminates can be successfully tested without the use of adhesively bonded end tabs; this saves a great deal of time when fabricating compression test specimens. Unidirectional test specimens require end tabs to be bonded to the specimen to prevent unacceptable failure modes, such as end crushing or failing within the specimen gage section. The use of adhesively bonded end tabs adds a great deal of time to specimen fabrication, and it also increases the chance for variability between the test specimens. A second advantage to

using cross-ply laminates, rather than angle-ply laminates, to generate lamina compression properties is that the back-out factor can be calculated using linear lamination theory. The errors associated with material nonlinearity are negligible for cross-ply laminates, but they are significant for angle-ply laminates.

In conclusion, the Wyoming CLC test method eliminates many of the problems associated with the IITRI compression test method, such as the mass of the test fixture, the large number of parts in the test fixture, the difficulty in machining the test fixture, and the increased stress concentrations associated with pure shear loading. Because of the above, the CLC test fixture is relatively easy to use and is less expensive to fabricate than the IITRI test fixture.

6.2 FUTURE WORK.

An improvement could possibly be made to the test fixture clamping mechanism. Currently eight ¼-28 UNF socket-head cap-head screws are used to apply the clamping pressure to the test specimen. This means that each of these eight screws must be torqued uniformly to prevent pinching the test specimen in a detrimental way. Currently, it is recommended that the bolts be torqued in increments of approximately 0.68 N-m (6 in-lbf) until a torque of 2.3 N-m (20 in-lbf) is reached. This means that each bolt must be torqued roughly four times for each specimen, so there are 32 torqueing operations required to install one test specimen in the CLC test fixture. It is suggested that the clamping mechanism could be changed to reduce this operation. It is possible that a single screw with a compression spring could be used to provide the required amount of clamping force. A stop could be used to prevent displacing the spring too far. In this way, a calibrated force could be applied to each specimen very quickly without the use of a torque wrench. This would speed up the specimen installation procedure considerably.

Several questions were prompted by the present study that justify further investigation. First, it would be interesting to see how the 0°-ply compression strength measured with the CLC test method compares with the 0°-ply compression strength at failure in a common structural component. If the CLC test method does indeed generate design values for the 0°-ply compression strength, then the stress at failure in the 0° plies of a common structural component should be similar to the values measured in the test specimens. It is suggested that two components be investigated, a sandwich beam in flexure and a cylindrical tube in axial compression. These two components have geometries and loading characteristics that are different than the test specimens used in the present study, but they are still simple enough so that they could be designed to fail in axial compression.

Another topic that deserves further investigation is the effect of bending in the test specimen on the measured 0°-ply compression strength. The data generated in the present study indicate that the amount of bending in the test specimen does not influence the measured 0°-ply compression strength. This is counter to the assumptions of simple mechanics of materials models. One theory that may explain this phenomena is based on specimen failure induced by microbuckling of the 0° plies. One would expect that if there was significant bending in the specimen, the fibers would microbuckle at a lower load. However, the plies adjacent to the critically loaded fibers may constrain the fibers from buckling outward, away from the specimen curvature, and the pre-existing curvature of the specimen prevents the fibers from microbuckling inward. Thus,

there would be an offsetting effect of microbuckling constraint and microbuckling load so that the ultimate 0°-ply compression strength remains constant. This effect may be present up to the point at which the bending in the specimen is so large that the 0° plies on the inside surface of the specimen, closest to the center of curvature of the specimen, begin to reach their ultimate compression strength. This theory could be checked by using a three-dimensional finite element model combined with a microbuckling failure criterion that accounts for the constraining effects of the adjacent plies.

7. BIBLIOGRAPHY.

Adams, D.F. and Finley, G.A., 1996, "Experimental Study of Thickness-Tapered Unidirectional Composite Compression Specimens," Experimental Mechanics, Vol. 36, No. 4, pp. 348-355.

Adams, D.F. and Finley, G.A., 1997, "Analysis of Thickness-Tapered Unidirectional Composite Compression Specimens," Journal of Composite Materials, Vol. 31, pp. 2283-2308.

Adams, D.F. and Lewis, E.Q., 1991, "Influence of Specimen Gage Length and Loading Method on the Axial Compressive Strength of a Unidirectional Composite Material," Experimental Mechanics, Vol. 31, No. 1, pp. 14-20.

Adams, D.F. and Odom, E.M., 1991, "Influence of Test Fixture Configuration on the Measured Compressive Strength of a Composite Material," Journal of Composites Technology & Research, JCTRER, Vol. 13, No. 1, pp. 36-40.

Adams, D.F. and Welsh, J.S., 1995, "Recommended Procedure for Generating Axial Compressive Strength Design Data for Composite Materials," presented at the MIL-HDBK-17 Polymer Matrix Composites Coordination Group Meeting, Clearwater, FL.

Adams, D.F. and Welsh, J.S., 1997, "The Wyoming Combined Loading Compression (CLC) Test Method," Journal of Composites Technology and Research, JCTRER, Vol. 19, No. 3, pp. 123-133.

Adsit, N.R., 1983, "Compression Testing of Graphite/Epoxy," Compression Testing of Homogeneous Materials and Composites, ASTM STP 808, R. Chait and R. Papirno, eds., American Society for Testing and Materials, Philadelphia, PA, pp. 175-186.

Agarwal, B.D. and Broutman, L.J., 1990, Analysis and Performance of Fiber Composites, Second Edition, Wiley and Sons, New York.

Airtech International, Inc., 2542 East Del Amo Boulevard, Carson, CA.

Anquez, L., 1994, "Experimental Investigations to Assess Typical Compressive Behavior of Composites," Proceedings of the 30th Polymer Matrix Composites Coordination Group Meeting (MIL-HDBK-17), New Orleans, LA, pp. 139-146.

ASTM D 792-66, 1992, “Specific Gravity and Density of Plastics by Displacement,” American Society for Testing and Materials, Philadelphia, PA.

ASTM D 3171-76, 1992, “Fiber Content of Resin-Matrix Composites by Matrix Digestion,” American Society for Testing and Materials, Philadelphia, PA.

ASTM D 3410, 1987, “Standard Test Method for Compressive Properties of Unidirectional or Crossply Fiber-Resin Composites,” American Society for Testing and Materials, Philadelphia, PA.

ASTM D 3410/D 3410M-95, 1995, “Standard Test Method for Compressive Properties of Polymer Matrix Composite Materials With Unsupported Gage Section by Shear Loading,” American Society for Testing and Materials, Philadelphia, PA.

ASTM D 5467-93, 1993, “Standard Test Method for Compressive Properties of Unidirectional Polymer Matrix Composites Using a Sandwich Beam,” American Society for Testing and Materials, Philadelphia, PA.

ASTM D 5687/D 5687M-95, 1995, “Guide for Preparation of Flat Composite Panels With Processing Guidelines for Specimen Preparation,” American Society for Testing and Materials, Philadelphia, PA.

Barker, A.J and Balasundaram, V., 1987, “Compression Testing of Carbon Fibre-Reinforced Plastics Exposed to Humid Environments,” Composites, Vol. 18, No. 3, pp. 217-226.

Berg, J.S. and Adams, D.F., 1988, An Evaluation of Composite Material Compression Test Methods, Report No. UW-CMRG-R-88-106, Composite Materials Research Group, University of Wyoming, Laramie, WY, June.

Boeing, 1988, “Advanced Composite Compression Tests,” Boeing Specification Support Standard BSS 7260, The Boeing Company, Seattle, WA.

Boeing, 1997, Boeing Space Systems Division, Private Correspondence with Jack Esposito.

Breivik, N.L., Gurdal, Z., and Griffin, O.H. Jr., 1992, “Compression of Laminate Composite Beams With Initial Damage,” Proceedings of the American Society for Composites Seventh Technical Conference, University Park, PA, October, pp. 972-981.

Cabot, Inc., P.O. Box 188, Tuscola, IL 61953, 800-253-3370.

Camponeschi, Jr., E.T., 1990, Compression Response of Thick Section Composite Materials, Report No. DTRC-SME-90/60, David Taylor Research Center, Annapolis, MD.

Camponeschi, E.T., Jr. and Hoynes, D., 1991, “Determination of Effective [0] Properties From [0/90] Laminate Testing,” ASTM D30.04 Spring 1991 Meeting, American Society for Testing and Materials, Philadelphia, PA.

Chaterjee, S., Adams, D.F., and Oplinger, D.W., 1993, Test Methods for Composites a Status Report Volume II: Compression Test Methods, Report No. DOT/FAA/CT-93/17-II, U.S. Department of Transportation, Federal Aviation Administration, Atlantic City, NJ.

Christensen, R., 1996, Analysis and Variance, Design and Regression, Chapman & Hall, New York, NY.

CMRG, 1992, "Typical Properties of Various Types of Polymer Matrix Unidirectional Composites," Composite Materials Research Group, University of Wyoming, Laramie, WY.

CMRG, 1996, "Tabbing Guide for Composite Test Specimens," Composite Materials Research Group, University of Wyoming, Laramie, WY.

Clark, R.K. and Lisagor, W.B., 1981, "Compression Testing of Graphite/Epoxy Composite Materials," Test Methods and Design Allowables for Fibrous Composites, ASTM STP 734, C.C. Chamis, Ed., American Society for Testing and Materials, Philadelphia, PA, pp. 34-53.

Colvin, G.E. and Swanson, S.R., 1990, "Mechanical Characterization of IM7/8551-7 Carbon/ Epoxy Under Biaxial Stress," Journal of Engineering Materials and Technology, Vol. 112, No. 1, January, pp. 61-67.

Crasto, A.S. and Kim, R.Y., 1991, "Compression Strengths of Advanced Composites From a Novel Mini-Sandwich Beam," SAMPE Quarterly, Vol. 22, No. 3, pp. 29-39.

DIN Standard 65 380, 1991, "Compression Test of Fiber-Reinforced Aerospace Plastics: Testing of Unidirectional Laminates and Woven-Fabric Laminates," Deutsches Institut for Normung, Koln, Germany.

Finley, G.A. and Adams, D.F., 1995, An Analytical and Experimenta1 Study of Unidirectional Thickness-Tapered Compression Specimens, Report No. UWCMRG-R-95-101, Composite Materials Research Group, University of Wyoming, Laramie, WY.

Gibson, R.F., 1994, Principles of Composite Material Mechanics, McGraw-Hill, New York, New York.

Haeberle, J.G., 1991, Strength and Failure Mechanisms of Unidirectional Carbon Fibre-Reinforced Plastics Under Axial Compression, Doctoral Dissertation, Dept. of Aeronautics, Imperial College of Science, Technology, and Medicine, London, UK.

Haeberle, J.G. and Matthews, F.L., 1993, "The Influence of Test Method on the Compressive Strength of Several Fiber-Reinforced Plastics," Journal of Advanced Materials, Vol. 25, No. 1, pp. 35-45.

Haeberle, J.G. and Matthews, F.L., 1994, "An Improved Technique for Compression Testing of Unidirectional Fiber-Reinforced Plastics; Development and Results," Composites, Vol. 25, No. 5, pp. 358-371.

Hart-Smith, L.J., 1991, "Generation of Higher Composite Materials Allowables Using Improved Test Coupons," Proceedings of the 36th International SAMPE Symposium, J. Stinson, Ed., pp. 1029-1044.

Hart-Smith, L.J., 1992, "Backing Out Equivalent Unidirectional Lamina Strengths From Tests on Cross-Plied Laminates," Proceedings of the 37th International SAMPE Symposium, G.C. Grimes, Ed., pp. 977-990.

Hercules, Inc., 1991, "Mechanical Test Cure Cycle for 3501-6 Epoxy," Magna, UT.

Hexcel TSB 124, 1992, "Bonded Honeycomb Sandwich Construction," Hexcel, 11555 Dublin Blvd., Dublin, CA 94568.

Hofer, J.R. and Rao, P.N., 1977, "A New Static Compression Fixture for Advanced Composite Materials," Journal of Testing and Evaluation, Vol. 5, No. 4, pp. 278-283.

Irion, M.N. and Adams, D.F., 1981, "Compression Creep Testing of Unidirectional Composite Materials," Composites, Vol. 12, No. 3, April, pp. 117-123.

Jones, R.M., 1999, Mechanics of Composite Materials, 2nd Edition, Taylor and Francis, Philadelphia, PA.

Kessler, J.A. and Adams, D.F., 1993, Standardization of Test Methods for Laminated Composites-Volume II: Experimental Effort, Technical Final Report No. MSC-TFR 3313/ 1706002, Composite Materials Research Group, University of Wyoming, Laramie, WY.

Marks Handbook, 1961, Baumeister, T., Ed., Seventh Edition, McGraw-Hill, New York, NY.

Measurements Group, Inc., 1979, "Strain Gage Installation With M-Bond 200 Adhesive," M-Line Accessories Instruction Bulletin B-127-13, Raleigh, NC.

Measurements Group, Inc., PO Box 27777, Raleigh, NC.

MIL-HDBK-17, 1996, "Comparison of 0° Compressive Strength for M55J/954-2A," Lockheed Martin Astronautics and Fiberite Inc., "Proceedings of the Polymer Matrix Composites Group Coordination Meeting," 34th Meeting, Shaumberg, IL.

MIL-HDBK-17, 1997, "Proceedings of the Polymer Matrix Composites Group Coordination Meeting," 35th Meeting, Tucson, AZ.

MIL-HDBK-17, 1998, "Proceedings of the Polymer Matrix Composites Group Coordination Meeting," 38th Meeting, New Orleans, LA.

Montgomery, D.C. and Runger, G.C., 1994, Applied Statistics and Probability for Engineers, John Wiley and Sons, Inc., New York, NY.

Newport Adhesives and Composites, Inc., 3121 West Central Ave., Santa Ana, CA.

Odom, E.M. and Adams, D.F., 1990, "Failure Modes of Unidirectional Carbon/Epoxy Composite Compression Specimens," Composites, Vol. 21, No. 4, pp. 189-296.

Park, I.K., 1971, "Tensile and Compressive Test Methods for High Modulus Graphite-Fibre Reinforced Composites," Paper No. 23, Proceedings of the International Conference on Carbon Fibers, Their Composites and Applications, The Plastics Institute, London.

Port, K.F., 1982, The Compressive Strength of Carbon Fiber Reinforced Plastics, Technical Report 82083, Royal Aircraft Establishment, Farnborough, U.K.

Popov, E.P, 1968, Introduction to Mechanics of Solids, Prentice Hall, Englewood Cliffs, NJ.

Purslow, D. and Collings, T.A., 1972, A Test Specimen for the Compressive Strength and Modulus of Unidirectional Carbon Fiber-Reinforced Plastic Laminates, RAE Technical Report 72096, Royal Aircraft Establishment, Farnborough, U.K.

Rawlinson, R., 1991, "The Use of Cross-Ply and Angle-Ply Composite Test Specimens to Generate Improved Material Property Data," Proceedings of the 36th International SAMPE Symposium, J. Stinson, Ed., pp. 1058-1068.

Regal Plastics, Inc., 3985 S. Kalamath, Englewood, CO.

SACMA, 1988, "Compressive Properties of Oriented Fiber-Resin Composites," SACMA Recommended Method SRM1-88, Suppliers of Advanced Composite Materials Association, Arlington, VA.

Shockey, P.D. and Waddoups, M.E., 1966, Strength and Modulus Determination of Composite Materials with Sandwich Beams, Report No. FZM4691, General Dynamics Corporation, Ft. Worth, TX.

Shigley, J.E. and Mischke, C.R., 1983, Mechanical Engineering Design, 4th Ed., McGraw-Hill, New York, NY.

Shuart, M.J., 1981, "An Evaluation of the Sandwich Beam Compression Test Method for Composites," Test Methods and Design Allowables for Fibrous Composites, ASTM STP 734, C.C. Chamis, Ed., American Society for Testing and Materials, Philadelphia, PA, pp. 152-165.

Smoot, M.A., 1982, "Compressive Response of Hercules AS1/3501-6 Graphite/Epoxy Composite," Report No. CCM-82-16, Center for Composite Materials, College of Engineering, University of Delaware, Newark, DE.

Spier, E.E. and Klouman, F.L., 1976, "Ultimate Compressive Strength and Nonlinear Stress-Strain Curves of Graphite/Epoxy Laminate," Proceedings of the 8th SAMPE Technical Conference, pp. 213-223.

Swanson, S.R. and Christoforou, A.P., 1986, "Response of Quasi-Isotropic Carbon/Epoxy Laminates to Biaxial Stress," Journal of Composite Materials, Vol. 20, No. 5, pp. 457-471.

Swanson, S.R. and Christoforou, A.P., 1987, "Progressive Failure in Carbon/Epoxy Laminates Under Biaxial Stress," Journal of Engineering Materials and Technology, Vol. 109, No. 1, pp. 12-16.

Swanson, S.R., Colvin, G.E., and Haslam, C.L., 1988, "Measurements of the Compression Behavior of AS4/3501-7 Carbon/Epoxy," 33rd International SAMPE Symposium, 1988.

Swanson, S.R. and Trask, B.C., 1989 "Strength of Quasi-Isotropic Laminates Under Off-Axis Loading," Composites Science and Technology, Vol. 34, No. 1, pp. 19-34.

Tan, S.C., 1992, "Stress Analysis and the Testing of Celanese and IITRI Compression Specimens," Composites Science and Technology, Vol. 44, pp. 57-70.

The Mathworks, Inc., 1998, Matlab Software Version 5.2.1, 24 Prime Park Way, Natick, MA, 10760-1500.

3M Aerospace, Inc., 1996, Structural Adhesive Film AF-111 Technical Data Sheet, Issue No. 2, March.

3M Corporation, Inc., 1997, Private Correspondence with Jerry Sundsrud, Aerospace Adhesives Division, 3M Center, Building 209-1C-22, St. Paul, MN 55144-1000.

Techkits, P.O. Box 105, Demarest, NJ 07627.

Timoshenko, S.P. and Gere, J.M., 1961, Theory of Elastic Stability, 2nd Edition, McGraw-Hill Book Co., New York, pp. 132-135.

TMI, Inc., 6122 South Strattler Ave., Salt Lake City, UT 84107.

Vinson, J.R. and Sierakowski, R.L., 1987, The Behavior of Structures Composed of Composite Materials, Martinus Nijhoff Publishers, Kluwer Academic Publishers, Hingham, MA.

Welsh, J.S. and Adams, D.F., 1995, Unidirectional Composite Compression Strengths Obtained by Testing Mini-Sandwich, Angle- and Cross-Ply Laminates, Report No. UW-CMRG-R-95-106, Composite Materials Research Group, University of Wyoming, Laramie, WY.

Welsh, J.S. and Adams, D.F., 1996, "Unidirectional Composite Compression Strengths Obtained by Testing Cross-Ply Laminates," Journal of Composites and Technology and Research, JCTRER, Vol. 18, No. 4, pp. 241-248.

Welsh, J.S. and Adams, D.F., 1997a, "An Experimental Investigation of the Mini-Sandwich Laminate as Used to Obtain Unidirectional Composite Compression Strengths," Journal of Composite Materials, Vol. 31, No. 3, pp. 293-314.

Welsh, J.S. and Adams, D.F., 1997, "Current Status of Compression Test Methods for Composite Materials," SAMPE Journal, Vol. 33, No. 1, pp. 35-43.

Westberg, R.W. and Abdallah, M.G., 1987, An Experimental and Analytical Evaluation of Three Compressive Test Methods for Unidirectional Graphite/Epoxy Composites, Report No. MISC-E524-10, Hercules Inc., Magna, UT.

Whitney, J.M, 1987, Structural Analysis of Laminated Anisotropic Plates, Technomic Publishing Co., Inc., Lancaster, PA, pp. 68-85.

Whitney, J.M., Crasto, A.S., and Kim, R.Y., 1992, "Failure Criteria for Laminated Composites Subjected to Compression Loading," Proceedings of the American Society for Composites, Seventh Technical Conference, University Park, PA, October, pp. 604-612.

Whitney, J.M. and Guihard, S.K., 1991, "Failure Modes in Compression Testing of Composite Materials," Proceedings of the 36th International SAMPE Symposium, J. Stinson, Ed., pp. 1069-1078.

Wilson, D.W., Altstadt, V., and Prandy, J., 1992, "On the Use of Laminate Test Methods to Characterize Lamina Compression Strength," Proceedings of the 37th International SAMPE Symposium, G.C. Grimes, Ed., pp. 606-619.

Woolstencroft, D.H., Curtis, A.R., and Harescaugh, R.I., 1981, "A Comparison of Test Techniques for the Evaluation of the Unidirectional Compressive Strength of Carbon Fiber-Reinforced Plastic," Composites, Vol. 12, No. 4, pp. 275-280.

Wyoming Test Fixtures Inc., 1996, Product Catalog No. 105, Laramie, WY.

Xie, M. and Adams, D.F., 1993, A Study of Various Compression and Shear Test Methods for Composite Materials Using an Elastic-Plastic Finite Element Analysis, Report No. UW-CMRG-R-93-103, Composite Materials Research Group, University of Wyoming, Laramie, WY.

Xie, M. and Adams, D.F., 1994, A Study of Compression and Shear Test Methods for Composite Materials Using a Nonlinear Finite Element Analysis, Report No. UW-CMRG-R-94-102, Composite Materials Research Group, University of Wyoming, Laramie, WY.

APPENDIX A—DERIVATION OF BACK-OUT FACTOR FOR 0°-PLY STRENGTH DETERMINATION

The following derivation extends the back-out factor calculation given by Camponeschi and Hoynes (1991) to any symmetric laminate. This back-out procedure was used to generate all of the back-out factors used in the present study. The notation used in this derivation is the standard laminate theory notation used by Agarwal and Broutman (1990).

For symmetric laminates

$$\{N\} = [A]\{\varepsilon^0\} \tag{A-1}$$

or

$$\begin{Bmatrix} N_x \\ N_y \\ N_{xy} \end{Bmatrix} = \begin{bmatrix} A_{11} A_{12} A_{16} \\ A_{12} A_{22} A_{26} \\ A_{16} A_{26} A_{66} \end{bmatrix} \begin{Bmatrix} \varepsilon^0_{x\,x} \\ \varepsilon^0_{yy} \\ \gamma^0_{xy} \end{Bmatrix} \tag{A-2}$$

Equation A-2 can be inverted to yield

$$\{\varepsilon^0\} = [A]^{-1}\{N\} \tag{A-3}$$

or

$$\begin{Bmatrix} \varepsilon^0_x \\ \varepsilon^0_y \\ \gamma^0_{xy} \end{Bmatrix} = \begin{bmatrix} A_{11} A_{12} A_{16} \\ A_{12} A_{22} A_{26} \\ A_{16} A_{26} A_{66} \end{bmatrix}^{-1} \begin{Bmatrix} N_x \\ N_y \\ N_{xy} \end{Bmatrix} \tag{A-4}$$

Assuming the lamina can be characterized by Hooke's Law and that they are under plane-stress conditions, the stresses in the k^{th} lamina can be written as

$$\{\sigma\}^k = [\overline{Q}]^k \{\varepsilon\}^k \tag{A-5}$$

where $[\overline{Q}]$ is the rotated plane stress stiffness matrix given as

$$[\overline{Q}] = [T]^{-1}[Q][T] \tag{A-6}$$

and

$$T = \begin{bmatrix} \cos^2\theta & \sin^2\theta & 2\sin\theta\cos\theta \\ \sin^2\theta & \cos^2\theta & -2\sin\theta\cos\theta \\ -\sin\theta\cos\theta & \sin\theta\cos\theta & \cos^2\theta - \sin^2\theta \end{bmatrix} \tag{A-7}$$

and

$$[Q] = \begin{bmatrix} \dfrac{E_{11}}{1-\nu_{12}\nu_{21}} & Sym & Sym \\ \dfrac{\nu_{12}E_{22}}{1-\nu_{12}\nu_{21}} & \dfrac{E_{11}}{1-\nu_{12}\nu_{21}} & Sym \\ 0 & 0 & G_{12} \end{bmatrix} \tag{A-8}$$

Using equations A-4 and A-5, the lamina stresses can be written as

$$\begin{Bmatrix} \sigma_x \\ \sigma_y \\ \tau_{xy} \end{Bmatrix}^k = \begin{bmatrix} \overline{Q}_{11} & \overline{Q}_{12} & \overline{Q_{16}} \\ & \overline{Q}_{22} & \overline{Q}_{26} \\ sym & & \overline{Q}_{66} \end{bmatrix} \begin{Bmatrix} A_{11}^{'}N_x \\ A_{12}^{'}N_x \\ A_{16}^{'}Nx \end{Bmatrix} \tag{A-9}$$

where

$$A_{11}^{'} = \frac{A_{22}A_{66} - A_{26}^2}{d} \qquad A_{12}^{'} = \frac{-A_{12}A_{66} + A_{16}A_{26}}{d} \qquad A_{16}^{'} = \frac{A_{12}A_{26} - A_{16}A_{22}}{d} \tag{A-10}$$

and

$$d = A_{11}A_{22}A_{66} - A_{11}A_{26}^2 - A_{12}^2A_{66} + 2A_{12}A_{16}A_{26} - A_{16}^2A_{22} \tag{A-11}$$

For the 0° lamina $[\overline{Q}] = [Q]$ and A'_{16} =0, so from equation A-9 the stress in the fiber direction, σ_x, is given as:

$$\sigma_x^0 = \overline{Q}_{11}A_{11}^{'}N_x + \overline{Q}_{12}A_{12}^{'}N_x \tag{A-12}$$

The back-out factor is then calculated as

$$BF = \left[Q_{11}A_{11}^{'} + Q_{12}A_{12}^{'}\right]N_x \cdot t \tag{A-13}$$

and the 0°-ply compressive stress is given as

$$\sigma_x^0 = BF \cdot \frac{P_{ult}}{A} \tag{A-14}$$

These calculations were programmed using Matlab Version 5.2.1 from The Mathworks, Inc. (1998). This code is listed on the following pages.

```
% File: bof.m
% Functions used: abd4.m; rotate.m; rot.m
clear;
clc;
echo on;

% This file calculates the back out factor used to determine the stress in
% the 0 degree ply of any general symmetric laminate.  This stress is
% determined by multiplying the back out factor by the compressive stress
% applied to the laminate.
%
%                          | P/A
%                          |
%                          V
%                 |----|----|----|----|
%                 |    |         |    |    |
%                 | 90 | 0  | 0  | 90 |
%                 |    |         |    |    |
%                 |____|____|____|____|
%
% Note: This solution is valid only for symmetric laminates
echo off;
z=0;
[layup,Qskin,A,total]=abd4(z);

d=A(1,1)*A(2,2)*A(3,3)-A(1,1)*A(2,3)^2-A(1,2)^2*A(3,3);
d=d+2*A(1,2)*A(1,3)*A(2,3)-A(2,2)*A(1,3)^2;
BF=(Qskin(1,1)*(A(2,2)*A(3,3)-A(2,3)^2)/d)*total;
BF=BF + (Qskin(1,2)*(A(1,3)*A(2,3)-A(1,2)*A(3,3))/d)*total;

fprintf('\nThe Back-Out Factor is.....\n');
BF

function [layup,Qskin,A,total]=abd4(z)
% file: abd4.m;

clear

echo on;
%
%   Program: ABD.m
%
%   This program calculates the ABD matrices of a composite sandwich plate
%   with any number of plies at angles specified by the user.  The program
%   determines the Q matrix for the core and composite face-sheets.
%
echo off;
A=zeros(3);
B=zeros(3);
D=zeros(3);
Qskin=zeros(3);
Qcore=zeros(3);
```

```
no_ply=input('How many plies are in the laminate?  ');
test2=input('Are all plies the same thickness?  yes=1 no=2 ');
total=0;

for i=1:no_ply
   if i==1 | test2==2
     fprintf(' \n Enter the ply thicknesses of ply %g....',i);
     t(i)=input(' ');
   else
     t(i)=t(i-1);
   end
   total=total+t(i);
end
h(1)=-total*0.5;
for i=2:no_ply+1
   h(i)=h(i-1)+t(i-1);
end

test=input('Are all layers of the same material? yes=1 no=2 ');

fprintf('\n What ply number is the core, starting with #1 on bottom?');
k_core=input('For no core enter zero (0):   ');

for i=1:no_ply
   if i==1 | test==2
     fprintf('*******************************************************\n');
     fprintf(' Enter Properties for ply #%g.  \n',i);
     fprintf(' Select the following materials \n');
     fprintf('      1.  AS4/3501-6 \n');
     fprintf('      2.  S2/5216 \n');
     fprintf('      3.  Other \n');
     test3=input('>');
     if test3 == 1
      E1=19.6e6
      E2=1.3e6
      G12=1.0e6
      Nu12=0.28
     elseif test3==2
      E1=8.62e6
      E2=2.63e6
      G12=1.07e6
      Nu12=0.27
     else
        E1=input('Enter the E11 Modulus  ');
        E2=input('Enter the E22 Modulus  ');
        G12=input('Enter the G12 Shear Modulus  ');
        Nu12=input('Enter the Poissions Ratio in the 1-2 Direction  ');
     end
    end

   % Calculate the Compliance Matrix S
   S=zeros(3);
   S(1,1)=1./E1;
   S(1,2)=-Nu12./E1;
   S(2,1)=S(1,2);
   S(2,2)=1./E2;
   S(3,3)=1./G12;

   Q=inv(S);
   if i == k_core
      Qcore=Q;
```

```
   end
   fprintf(' \n What is the angle of ply %g?  ',i);
   layup(i)=input(' Angle:  ');
   [Qbar] =rot(Q, layup(i));

   for j=1:3
      for k=1:3
      A(j,k)=Qbar(j,k)*(h(i+1)-h(i)) + A(j,k);
      B(j,k)=0.500*Qbar(j,k)*(h(i+1)^2-h(i)^2) + B(j,k);
      D(j,k)=0.333*Qbar(j,k)*(h(i+1)^3-h(i)^3) + D(j,k);
      end
   end
end
Qskin=Q;
fprintf('\nThe material matrices are.....\n');
A
B
D

function Qbar=rot(Q,angle)
%
%  file: rot.m
%  This function calculates the rotated plane stiffness matrix,C, given a
%  user specified rotation about the x3 axis.  Given the full 6x6 stiffness
%  matrix the function passes back the 3x3 plane stress stiffness matrix
%  in the rotated coordinate system.

% create copy of C matrix
% Input matrix of rotation angles
% angle=input('Angle:  ');
angle=angle*pi./180;
T=zeros(3);
T(1,1)=(cos(angle))^2;
T(1,2)=(sin(angle))^2;
T(1,3)=2*sin(angle)*cos(angle);
T(2,1)=(sin(angle))^2;
T(2,2)=(cos(angle))^2;
T(2,3)=-2*sin(angle)*cos(angle);
T(3,1)=-sin(angle)*cos(angle);
T(3,2)=sin(angle)*cos(angle);
T(3,3)=(cos(angle))^2-(sin(angle))^2;


% Multiply shear components of C matrix by 2
R=[1 0 0 ; 0 1 0 ; 0 0 2];

% transpose Q using Q'=inv(T)*Q*R*T*inv(R)
Qbar=inv(T)*Q*R*T*inv(R);
```

APPENDIX B—ANALYSIS OF CLAMPING FORCE ACTING ON SPECIMENS IN THE CLC AND IITRI TEST FIXTURES

In the IITRI test fixture the clamping force, f_z, consists of two parts. The first of these, f_{zI}, is the clamping force due to the preload in the fixture bolts. The second part, f_{zII}, is the clamping due to the action of the wedge grips against the test specimen. The clamping force in the specimen can be determined using a mechanics of materials analysis based on the model shown in figure B-1. The clamping force due to the preload in the fixture bolts, f_{zI}, is given as equation 5.1.7 (Shigley and Mischke, 1983).

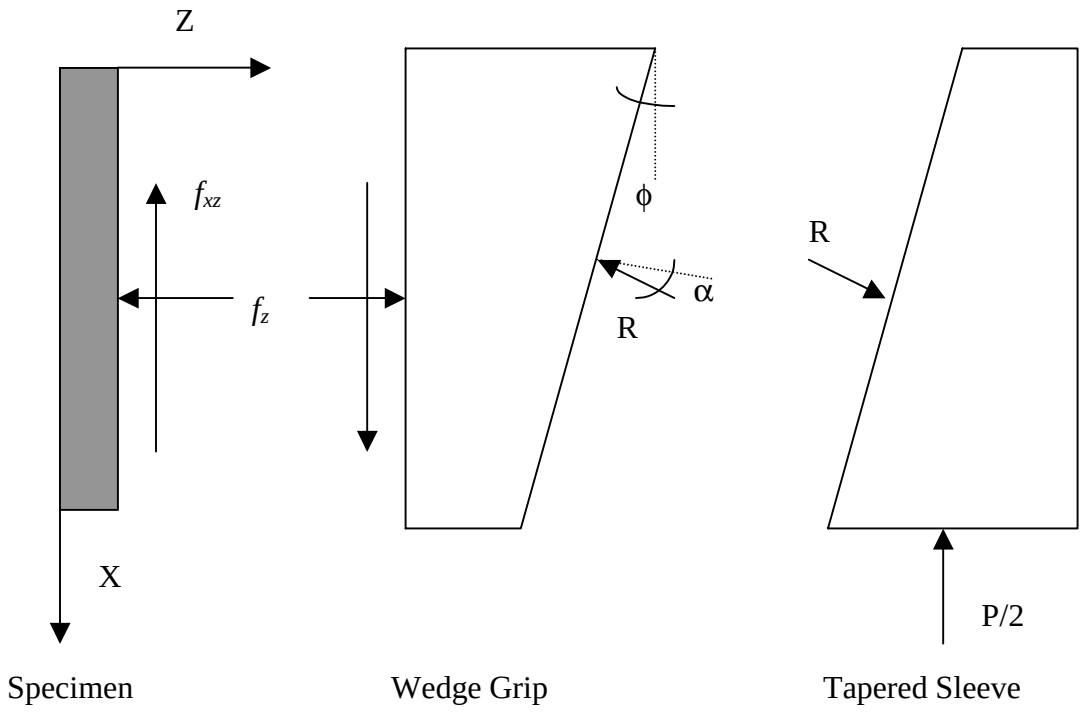

FIGURE B-1. FREE BODY DIAGRAM OF IITRI WEDGE GRIPS

The shear and normal forces in the gripped portion of the IITRI wedge grips are referred to as f_{xz} and f_z, respectively. The reaction force at the interface of the wedge grip and the tapered mating block of the test fixture is referred to as R. The coefficient of friction between the grip and the mating block of the fixture is referred to as μ. The angle of the reaction force with respect to the tapered sleeve and the wedge grip, α, depends on the taper angle of the wedge grip, ϕ.

The following relations can be obtained by considering equilibrium of the wedge grips:

$$R \cdot \cos(\alpha + \phi) = f_{zII} \tag{B-1}$$

and

$$R \cdot \sin(\alpha + \phi) = f_{xz} \tag{B-2}$$

where

f_{xII} = Normal force acting on specimen.

The frictional force that exists between the grip and the mating block is given as

$$(R \cdot \cos\alpha)\mu = R \sin\alpha \tag{B-3}$$

Then, combining equations B-1, B-2, and B-3 results in

$$\frac{f_{xz}}{f_{zII}} = \tan(\tan^{-1}\mu + \alpha) \tag{B-4}$$

where

μ = Coefficient of friction between wedge grips and mating block, 0.58 from Shigley and Mischke, 1983

φ = Taper angle of wedge grips, 10°

Substituting these values into equation B-4 results in

$$\frac{f_{xz}}{f_{zII}} = 0.84 \tag{B-5}$$

A force balance on the wedge grip gives the magnitude of the shear force applied to the specimen as a function of the applied axial compressive stress acting in the gage section of the test specimen:

$$f_{xz} = \tfrac{1}{2}\sigma \cdot A \tag{B-6}$$

where

A = Cross sectional area of the specimen
σ = Axial compressive stress existing in the gage section of the specimen

Now, substituting equation B-6 into B-5 results in an expression for the clamping force in the test specimen due to the shearing action of the wedge grips.

$$f_{zII} = \frac{\sigma \cdot A}{1.68} \tag{B-7}$$

The total clamping force on the test specimen in the IITRI test fixture is due to the combined action of the wedge grip bolts, f_{zI}, and the action of the wedge grips, f_{zII}. When the specimen is installed in the IITRI wedge grips, the bolts are torqued just enough so that the specimen does not slip in the grips during the initial stages of testing. Typically, 2.3 N-m (18 in-lbf) is enough to meet this requirement. The bolts are stretched a small amount due to the applied bolt torque. As the specimen is loaded in the IITRI test fixture, the wedge grips compress the specimen through-the-thickness. This allows the bolts to contract slightly and thus release some of the preload in the bolts. At some point during the test, if the bolts are not torqued an excessive amount, the preload in the bolts is reduced to zero, and the clamping force on the specimen is due only to the action of the wedge grips, f_{zII} (equation B-7). Conversely, if the test fixture bolts are torqued too tightly, the clamping force due to the test fixture bolts adds to the clamping force due to the wedge grips. In this case the total clamping force on the specimen is higher than needed to keep the specimen from slipping. This leads to a more severe stress concentration in the gage section of the specimen than is necessary.

APPENDIX C—SPECIMEN DATA FROM INITIAL COMPARATIVE TESTING

C.1 SPECIMEN IDENTIFICATION CODES.

A name was given to each test specimen to specify the fiber the specimen was made of, the test fixture used to test the specimen and the number of the individual specimen. This nomenclature is described, below.

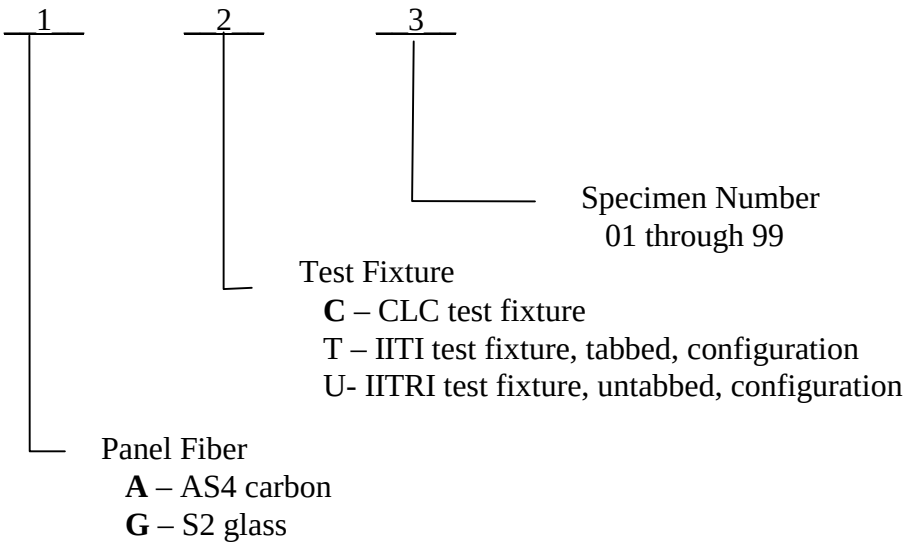

C.2 CONTENTS.

The tables listed on the following pages contain for each of the specimens tested in the Initial Comparative Study (see section 5.2) the measured *x*-direction modulus of the test specimen, the 0°-ply, compressive strength (calculated using the procedure described, in section 4.4) and the percent bending in the specimen at failure. Plus and minus signs are included on the values of percent bending at failure to indicate which direction the specimens bent during the test. This information is helpful in recognizing systematic errors in the test setup or load train alignment. Following these tables, the stress versus strain curve and the percent bending versus average strain curve is given for each specimen.

TABLE C-1. UNTABBED, CROSS-PLY $[90/0]_{5s}$ AS4/3501-6 CARBON/EPOXY SPECIMENS TESTED IN THE CLC-OR TEST FIXTURE, SPECIMENS FABRICATED FROM PANEL PA05A, V_f = 63.4%

Specimen Number	E^c_x		σ^c_{11}		Bending
	[GPa]	[Msi]	[MPa]	[ksi]	[%]
AC01	75.1	10.9	1943	282	-6.7
AC02	75.1	10.9	1964	285	0.1
AC03	73.0	10.6	1853	269	-7.7
AC04	75.1	10.9	1778	258	-4.6
AC05	74.4	10.8	1915	278	0.9
Mean	74.5	10.8	1891	274	
Std. Dev.	0.9	0.1	76	11	
CV [%]	1.2	1.2	4.0	4.0	

TABLE C-2. TABBED, CROSS-PLY $[90/0]_{5s}$ AS4/3501-6 CARBON/EPOXY SPECIMENS TESTED IN THE IITRI TEST FIXTURE, SPECIMENS FABRICATED FROM PANEL PA05A, V_f = 63.4%

Specimen Number	E^c_x		σ^c_{11}		Bending
	[GPa]	[Msi]	[MPa]	[ksi]	[%]
AT01	68.9	10.0	2060	299	-22.2
AT02	68.9	10.0	1881	273	44.1
AT03	68.2	9.9	1798	261	28.1
AT04	67.5	9.8	1950	283	17.7
AT05	69.6	10.1	1909	277	-28.0
Mean	68.6	10.0	1920	279	
Std. Dev.	0.8	0.1	96	14	
CV [%]	1.1	1.1	5.0	5.0	

TABLE C-3. UNTABBED, CROSS-PLY $[90/0]_{5s}$ AS4/3501-6 CARBON/EPOXY SPECIMENS TESTED IN THE IITRI TEST FIXTURE, SPECIMENS FABRICATED FROM PANEL PA05A, V_f = 63.4%

Specimen Number	E^c_x		σ^c_{11}		Bending
	[GPa]	[Msi]	[MPa]	[ksi]	[%]
AU01[1]	73.7	10.7	1950	283	-49.7
AU02	71.0	10.3	1991	289	-28.2
AU03	66.8	9.7	2039	296	28.7
AU04	82.7	12.0	2067	300	27.2
AU05	74.4	10.8	2122	308	27.0
AU06[2]	71.0	10.3	2012	292	2.7
AU07[2]	71.7	10.4	2053	298	-8.7
AU08[2]	68.2	9.9	2046	297	4.3
AU09[2]	71.0	10.3	1971	286	7.8
Mean	72.3	10.5	2028	294	
Std. Dev.	4.6	0.7	53	7.7	
CV [%]	6.3	6.3	2.6	2.6	

[1]A 1.52-mm (0.060″) shim was misplaced causing load misalignment, values are not included in averages

[2] 10.6-mm (0.416″) gage length

TABLE C-4. UNTABBED, CROSS-PLY $[90/0]_{7s}$ AS4/3501-6 CARBON/EPOXY SPECIMENS TESTED IN THE CLC-OR TEST FIXTURE, SPECIMENS FABRICATED FROM PANEL PA01B, V_f = 60.1%

Specimen Number	E^c_x		σ^c_{11}		Bending
	[GPa]	[Msi]	[MPa]	[ksi]	[%]
AC701[1]		n/a	1888	274	n/a
AC702	68.9	10.0	1798	261	4.6
AC703	64.1	9.3	1660	241	8.4
AC704	70.3	10.2	1736	252	3.5
AC705	71.0	10.3	1667	242	10.3
AC706	67.5	9.8	1578	229	4.2
Mean	68.2	9.9	1723	250	
Std. Dev.	2.8	0.4	111	16	
CV [%]	4.1	4.1	6.5	6.5	

[1]No plots available, gages shorted

TABLE C-5. UNTABBED, CROSS-PLY $[90/0]_{7s}$ AS4/3501-6 CARBON/EPOXY SPECIMENS TESTED IN THE IITRI TEST FIXTURE, SPECIMENS FABRICATED FROM PANEL PA01B, V_f = 60.1%

Specimen Number	E^c_x		σ^c_{11}		Bending
	[GPa]	[Msi]	[MPa]	[ksi]	[%]
AU701[1]	n/a	n/a	1790	260	n/a
AU702	67	9.7	1832	266	3.6
AU703	69	10.0	1904	276	5.9
AU704	65	9.4	1925	279	13.1
AU705	66	9.5	1830	266	-6.4
AU706	69	10.0	1911	277	-0.8
Mean	67	9.7	1865	271	
Std. Dev.	1.9	0.28	55	8.0	
CV [%]	2.9	2.9	2.9	2.9	

[1]Strain gages slipped

TABLE C-6. UNTABBED, CROSS-PLY $[90/0]_{7s}$ S2/301-NCT GLASS/EPOXY SPECIMENS TESTED IN THE CLC-OR TEST FIXTURE, SPECIMENS FABRICATED FROM PANEL PS04A, V_f = 56.1%

Specimen Number	E^c_x		σ^c_{x} [1]		Bending
	[GPa]	[Msi]	[MPa]	[ksi]	[%]
GC01	34	4.9	744	108	-5.1
GC02	39	5.6	765	111	18.8
GC03	34	4.9	675	98	17.9
GC04	32	4.7	716	104	20.0
GC05	32	4.7	710	103	9.0
GC06	35	5.0	730	106	-3.3
GC07	35	5.1	792	115	5.8
Mean	34	5.0	733	107	
Std. Dev.	2	0.3	38	6	
CV [%]	6.1	6.2	5.2	5.2	

[1]Ultimate *x*-direction compressive strength

TABLE C-7. UNTABBED, CROSS-PLY $[90/0]_{7s}$ S2/301-NCT GLASS/EPOXY SPECIMENS TESTED IN THE IITRI TEST FIXTURE, SPECIMENS FABRICATED FROM PANEL PS04A, V_f = 56.1%

Specimen Number	E^c_x		σ^c_x [1]		Bending
	[GPa]	[Msi]	[MPa]	[ksi]	[%]
GU01	32	4.6	641	93	46.1
GU02	32	4.7	696	101	32.5
GU03	33	4.8	861	125	7.5
GU04	37	5.3	634	92	50.0
GU05	32	4.7	717	104	12.5
GU06	35	5.1	792	115	4.4
GU07	32	4.7	813	118	9.1
Mean	33	4.8	736	107	
Std. Dev.	2	0.3	88	13	
CV [%]	5.2	5.2	11.7	11.7	

[1]Ultimate *x*-direction compressive strength

TABLE C-8. TABBED, CROSS-PLY $[90/0]_{7s}$ S2/301-NCT GLASS/EPOXY SPECIMENS TESTED IN THE IITRI TEST FIXTURE, SPECIMENS FABRICATED FROM PANEL PS04A, V_f = 56.1%

Specimen Number	E^c_x		σ^c_x [1]		Bending
	[GPa]	[Msi]	[MPa]	[ksi]	[%]
GT01	33	4.8	675	98	32.8
GT02	45	6.5	599	87	-77.5
GT03	37	5.3	634	92	-44.5
GT04	43	6.3	730	106	-14.8
Mean	39	5.7	660	96	
Std. Dev.	6	0.8	56	8.1	
CV [%]	13.6	13.6	8.5	8.5	

[1]Ultimate *x*-direction compressive strength

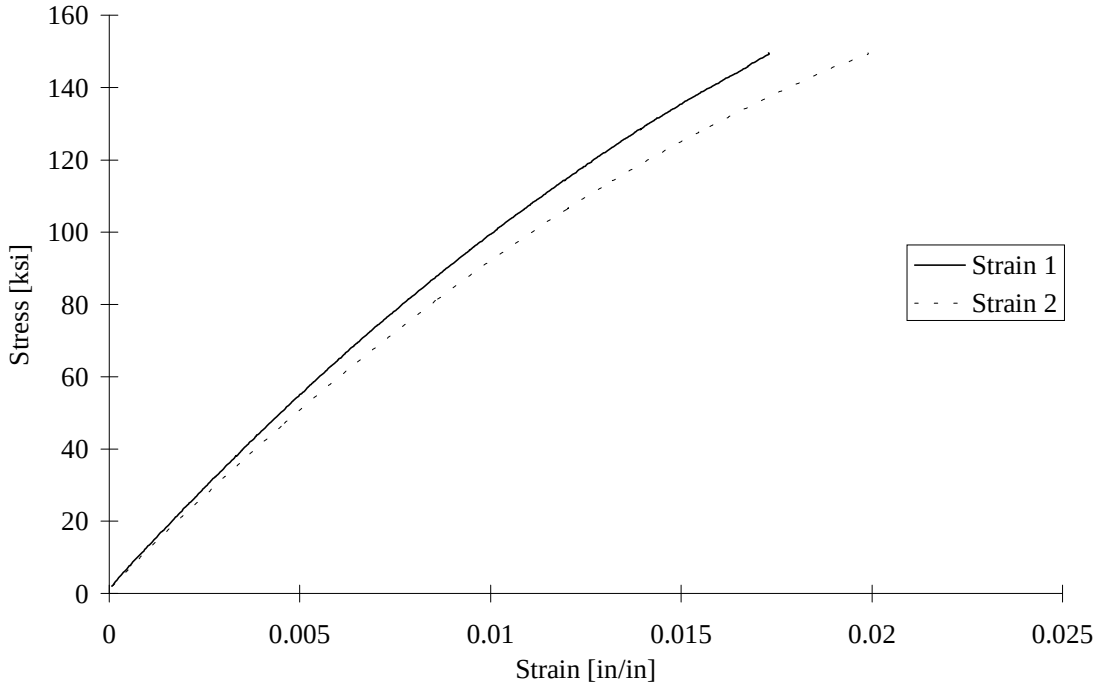

FIGURE C-1. TEST SPECIMEN AC01: AS4/3501-6 CARBON/EPOXY $[90/0]_{5s}$ CLC-OR TEST FIXTURE

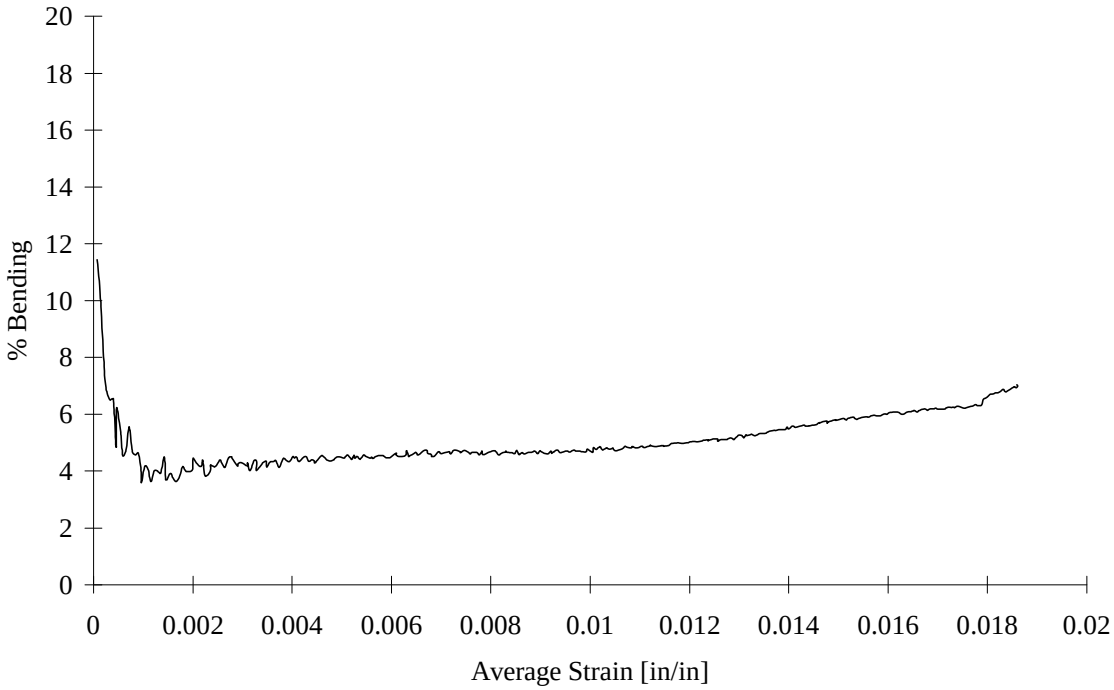

FIGURE C-2. TEST SPECIMEN AC01: AS4/3501-6 CARBON/EPOXY $[90/0]_{5s}$ CLC-OR TEST FIXTURE

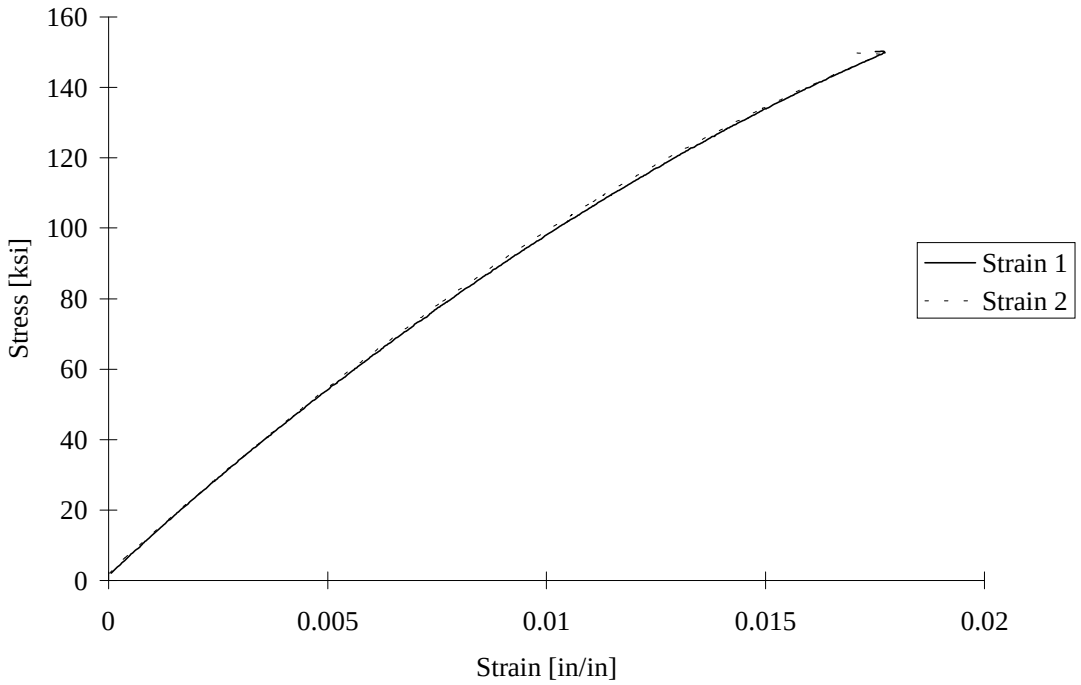

FIGURE C-3. TEST SPECIMEN AC02: AS4/3501-6 CARBON/EPOXY $[90/0]_{5s}$ CLC-OR TEST FIXTURE

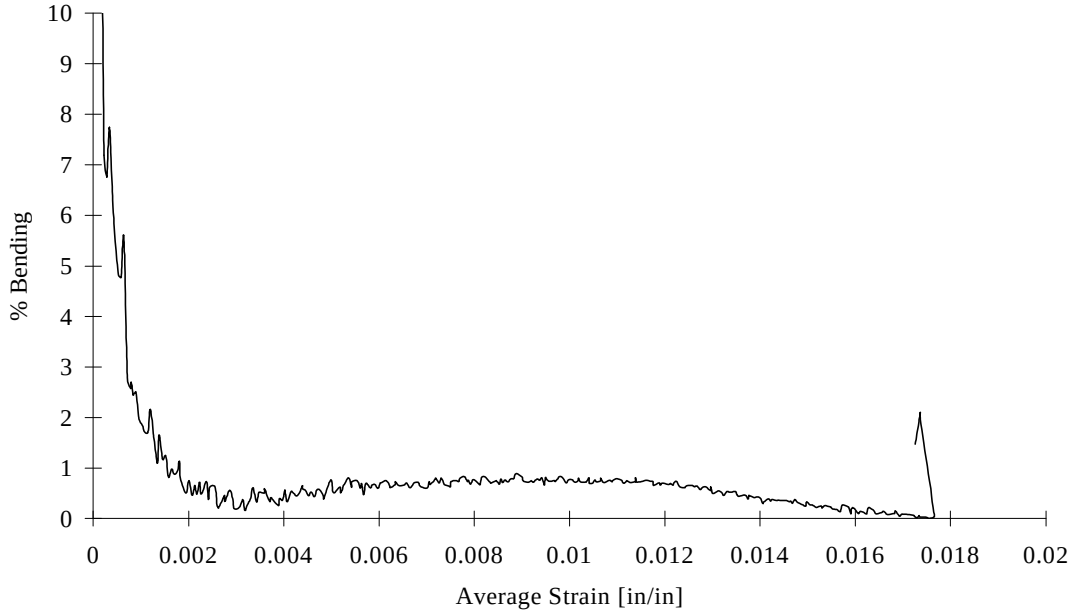

FIGURE C-4. TEST SPECIMEN AC02: AS4/3501-6 CARBON/EPOXY $[90/0]_{5s}$ CLC-OR TEST FIXTURE

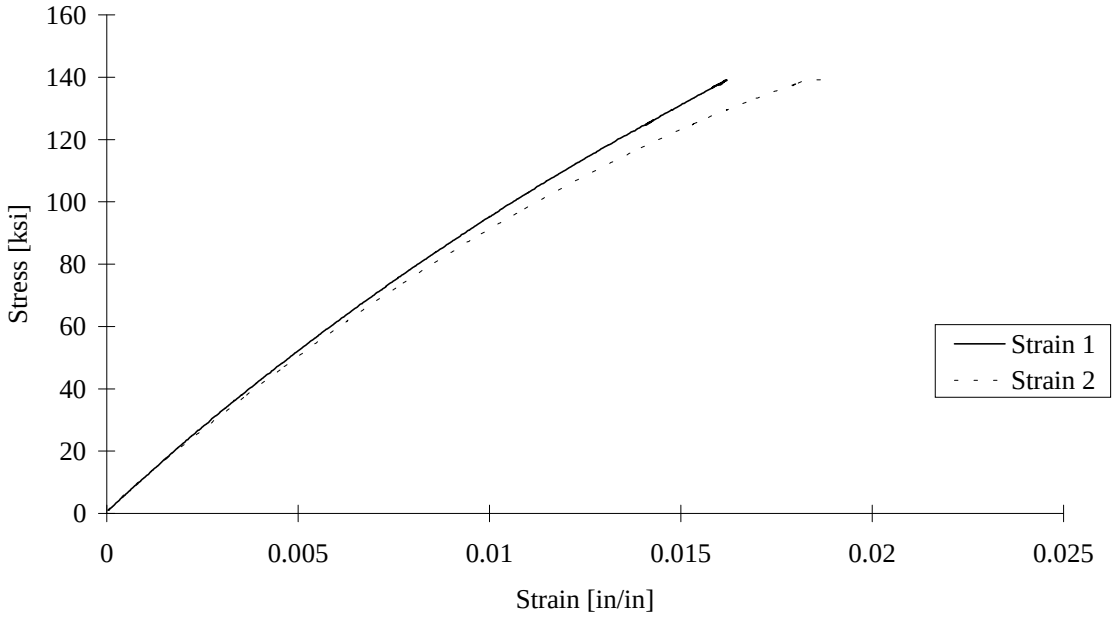

FIGURE C-5. TEST SPECIMEN AC03: AS4/3501-6 CARBON/EPOXY $[90/0]_{5s}$
CLC-OR TEST FIXTURE

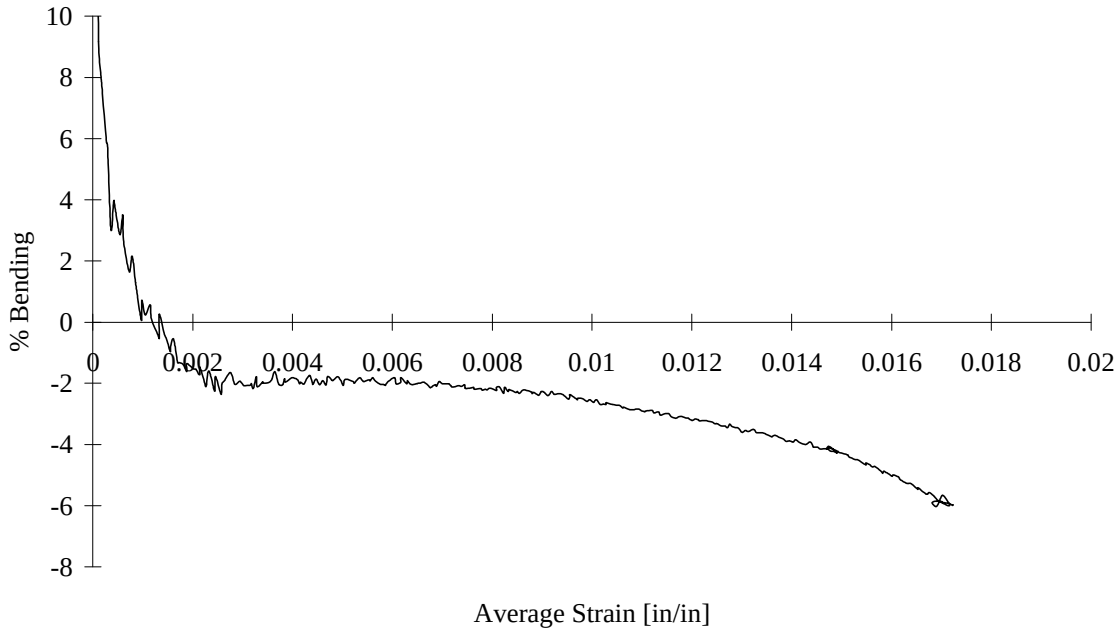

FIGURE C-6. TEST SPECIMEN AC03: AS4/3501-6 CARBON/EPOXY $[90/0]_{5s}$
CLC-OR TEST FIXTURE

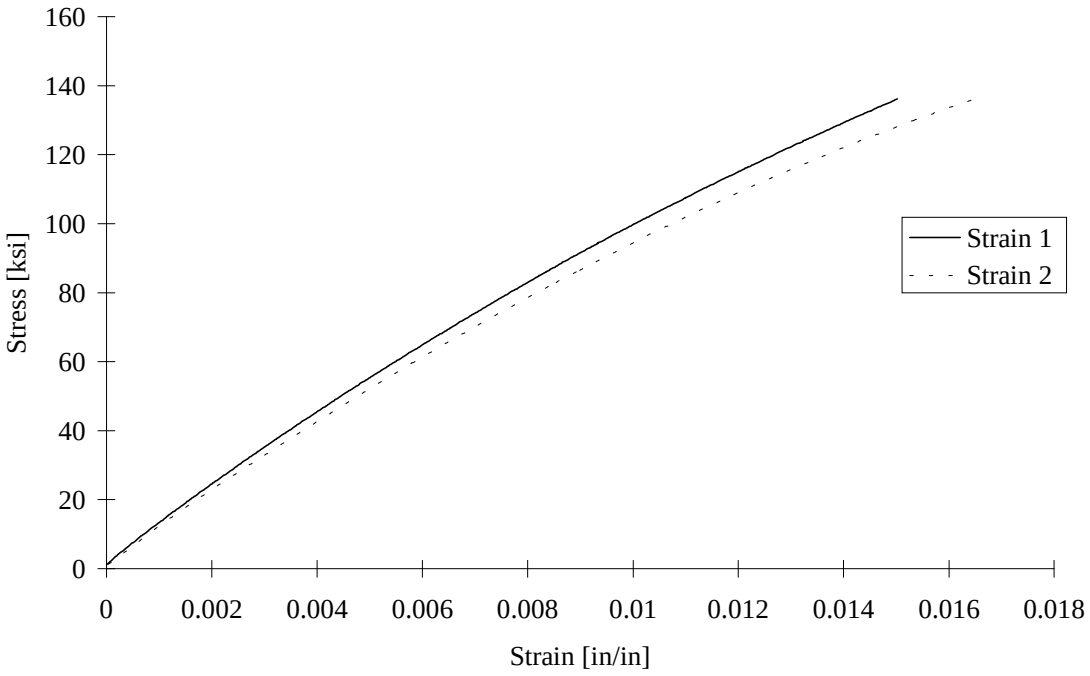

FIGURE C-7. TEST SPECIMEN AC04: AS4/3501-6 CARBON/EPOXY $[90/0]_{5s}$ CLC-OR TEST FIXTURE

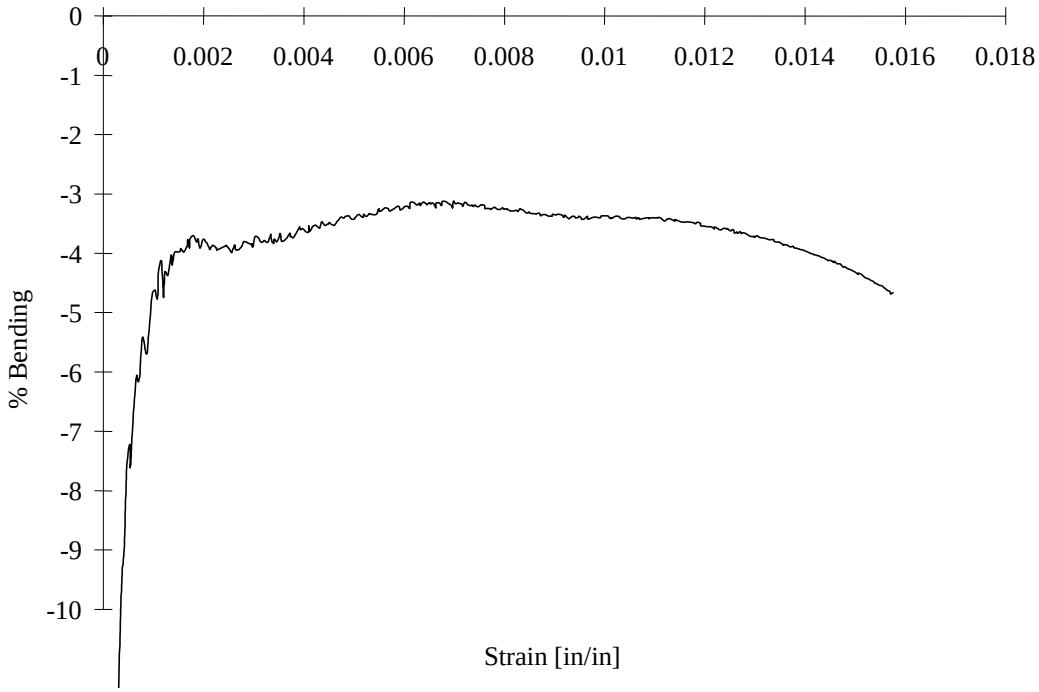

FIGURE C-8. TEST SPECIMEN AC04: AS4/3501-6 CARBON/EPOXY $[90/0]_{5s}$ CLC-OR TEST FIXTURE

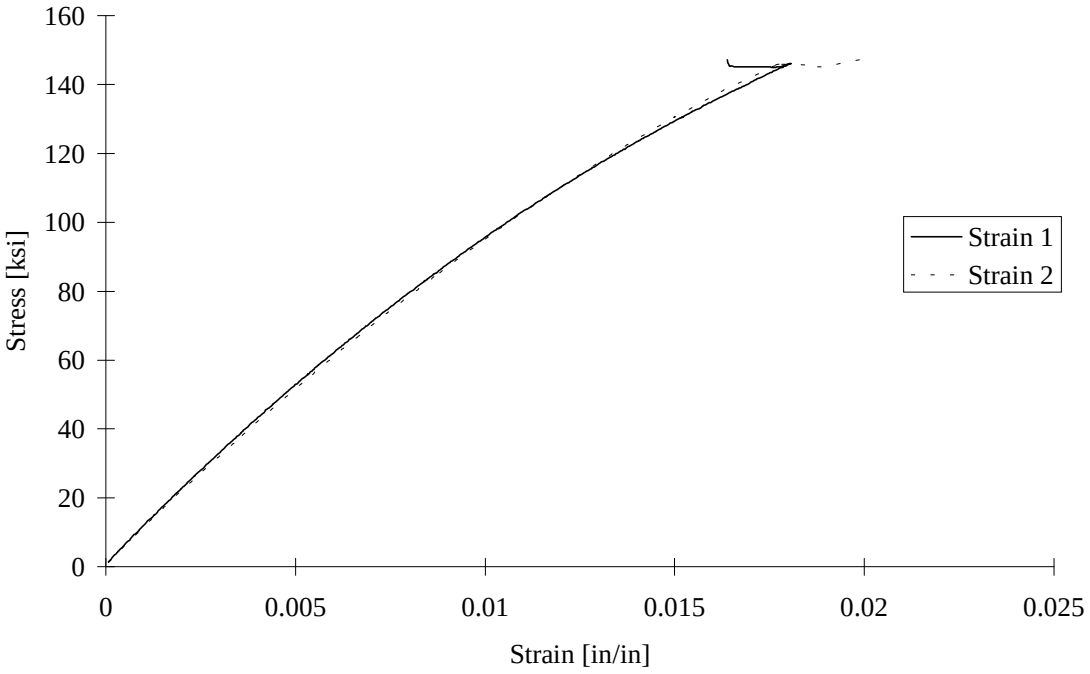

FIGURE C-9. TEST SPECIMEN AC05: AS4/3501-6 CARBON/EPOXY $[90/0]_{5s}$ CLC-OR TEST FIXTURE

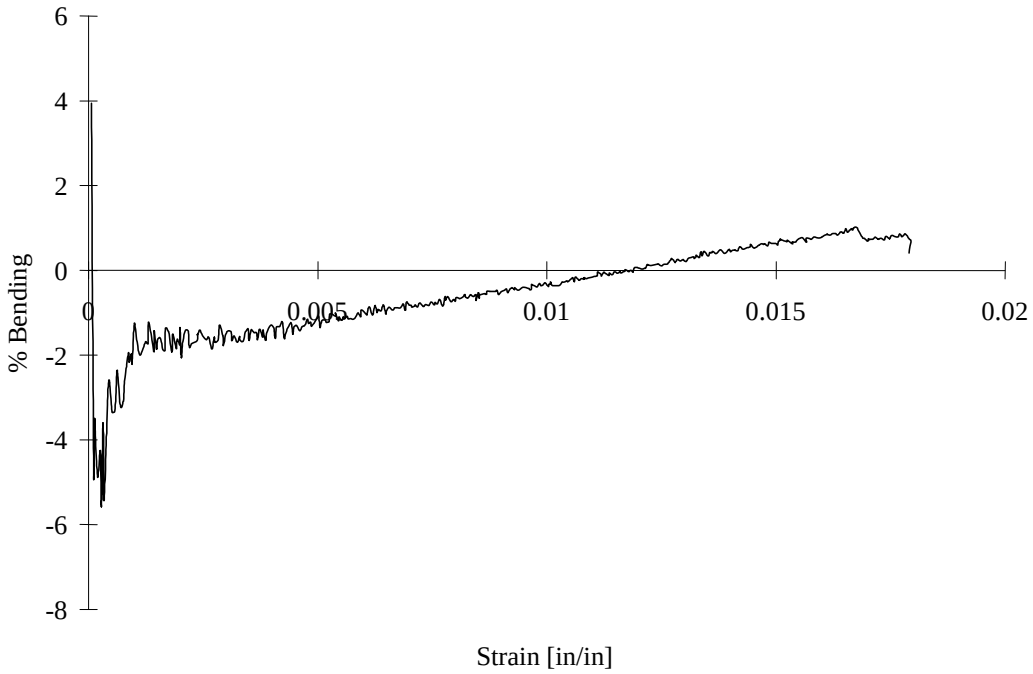

FIGURE C-10. TEST SPECIMEN AC05: AS4/3501-6 CARBON/EPOXY $[90/0]_{5s}$ CLC-OR TEST FIXTURE

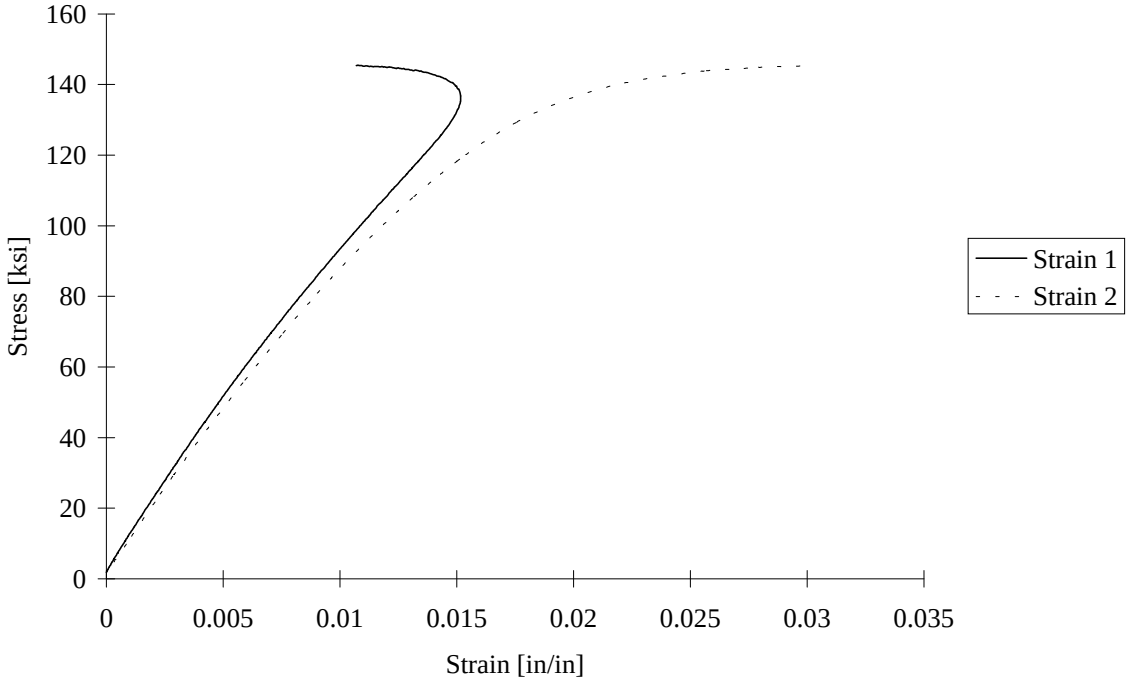

FIGURE C-11. TEST SPECIMEN AT01: TABBED, AS4/3501-6 CARBON/EPOXY $[90/0]_{5s}$
IITRI TEST FIXTURE

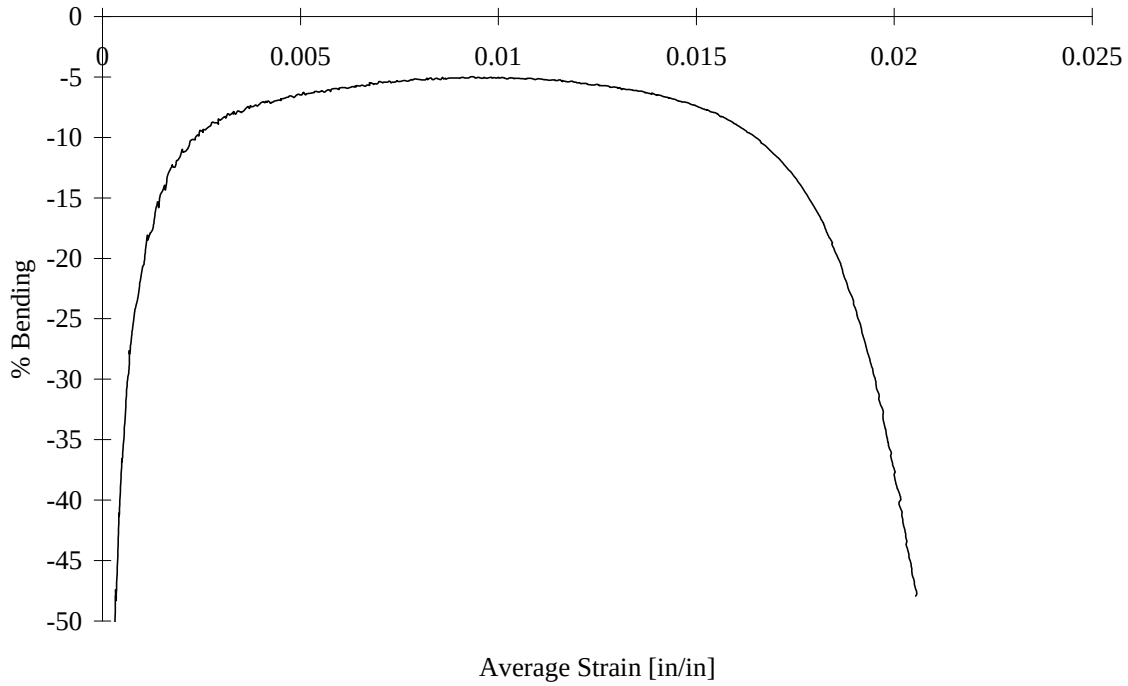

FIGURE C-12. TEST SPECIMEN AT01: TABBED, AS4/3501-6 CARBON/EPOXY $[90/0]_{5s}$
IITRI TEST FIXTURE

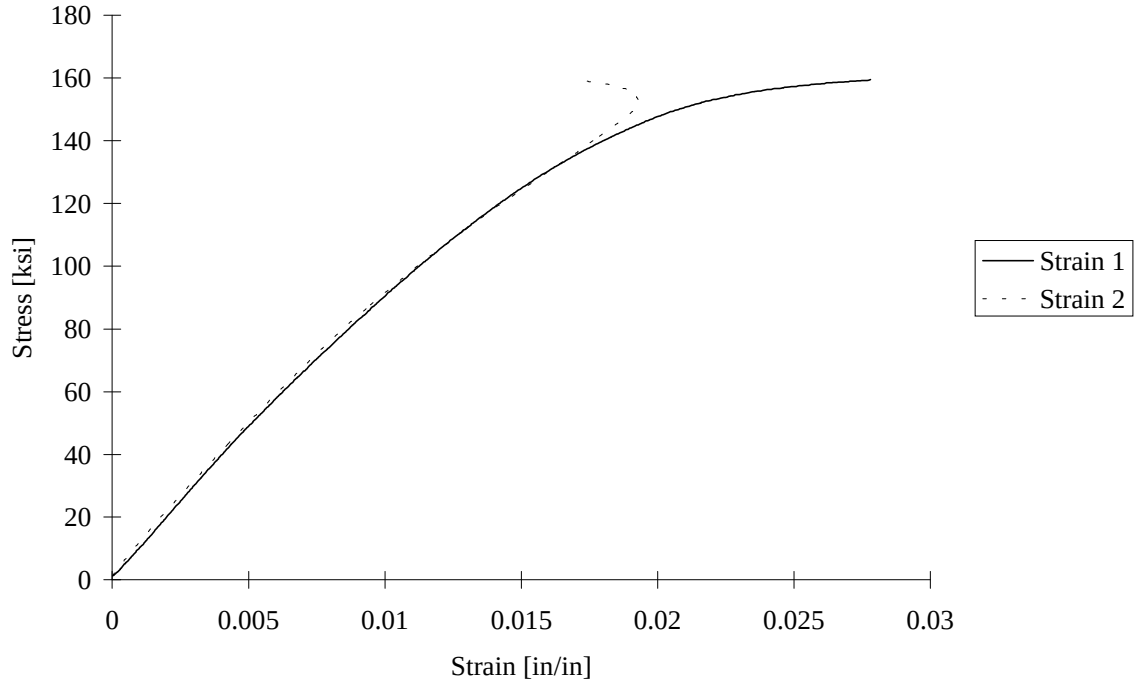

FIGURE C-13. TEST SPECIMEN AT02: TABBED, AS4/3501-6 CARBON/EPOXY $[90/0]_{5s}$
IITRI TEST FIXTURE

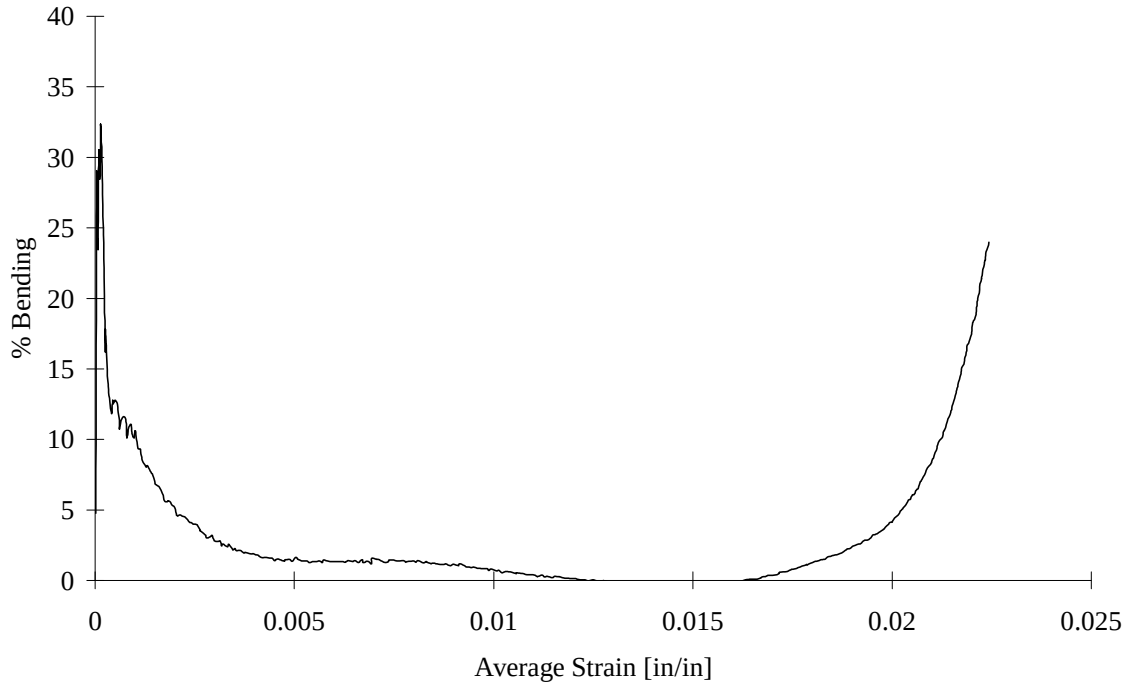

FIGURE C-14. TEST SPECIMEN AT02: TABBED, AS4/3501-6 CARBON/EPOXY $[90/0]_{5s}$
IITRI TEST FIXTURE

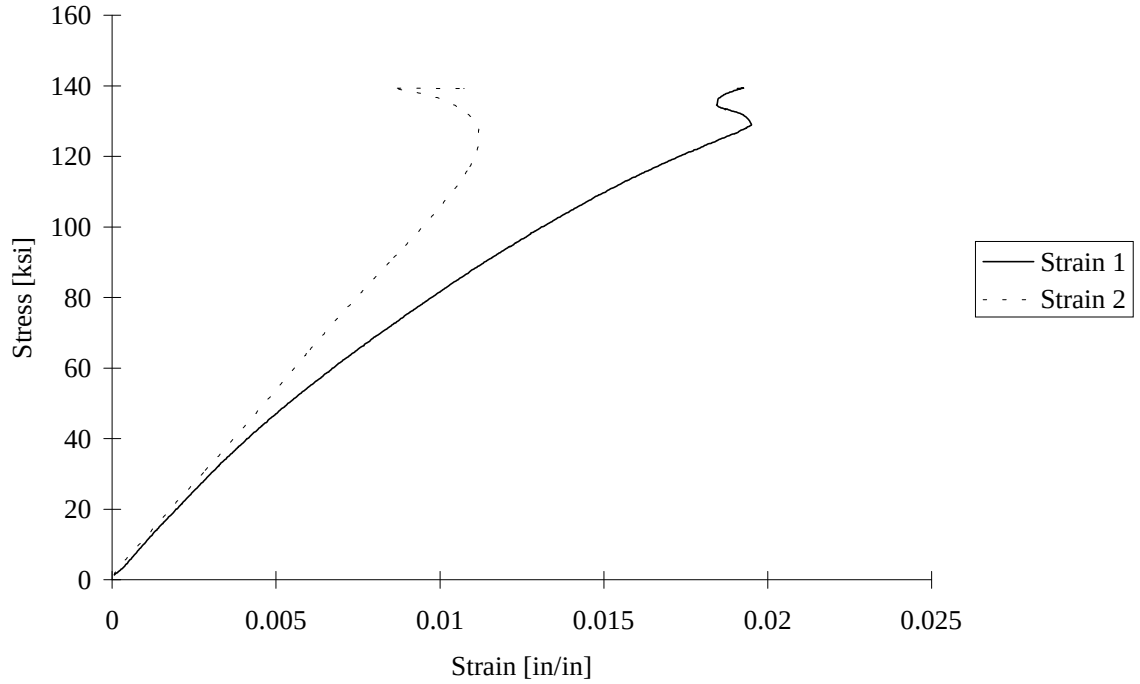

FIGURE C-15. TEST SPECIMEN AT03: TABBED, AS4/3501-6 CARBON/EPOXY $[90/0]_{5s}$
IITRI TEST FIXTURE

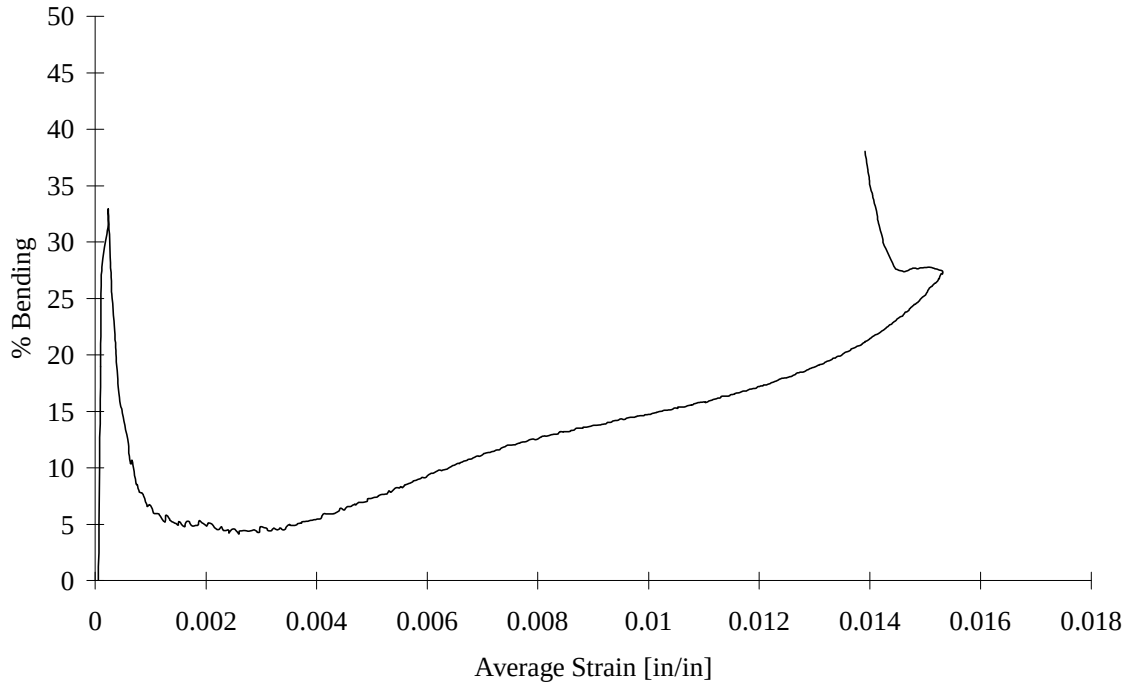

FIGURE C-16. TEST SPECIMEN AT03: TABBED, AS4/3501-6 CARBON/EPOXY $[90/0]_{5s}$
IITRI TEST FIXTURE

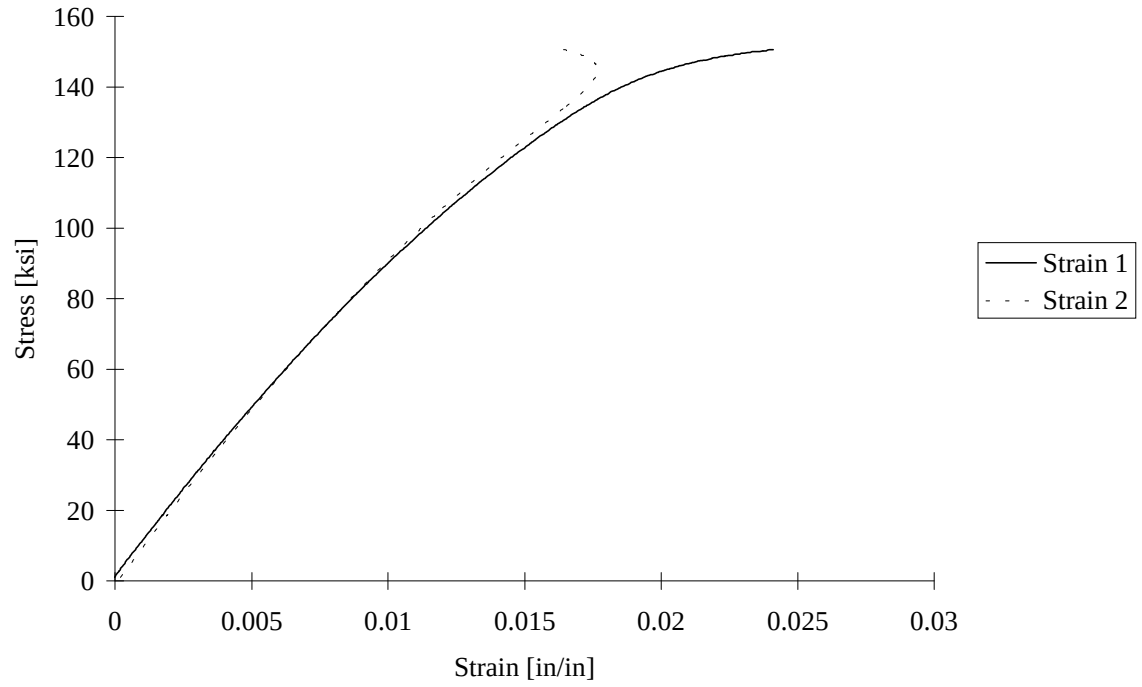

FIGURE C-17. TEST SPECIMEN AT04: TABBED, AS4/3501-6 CARBON/EPOXY $[90/0]_{5s}$
IITRI TEST FIXTURE

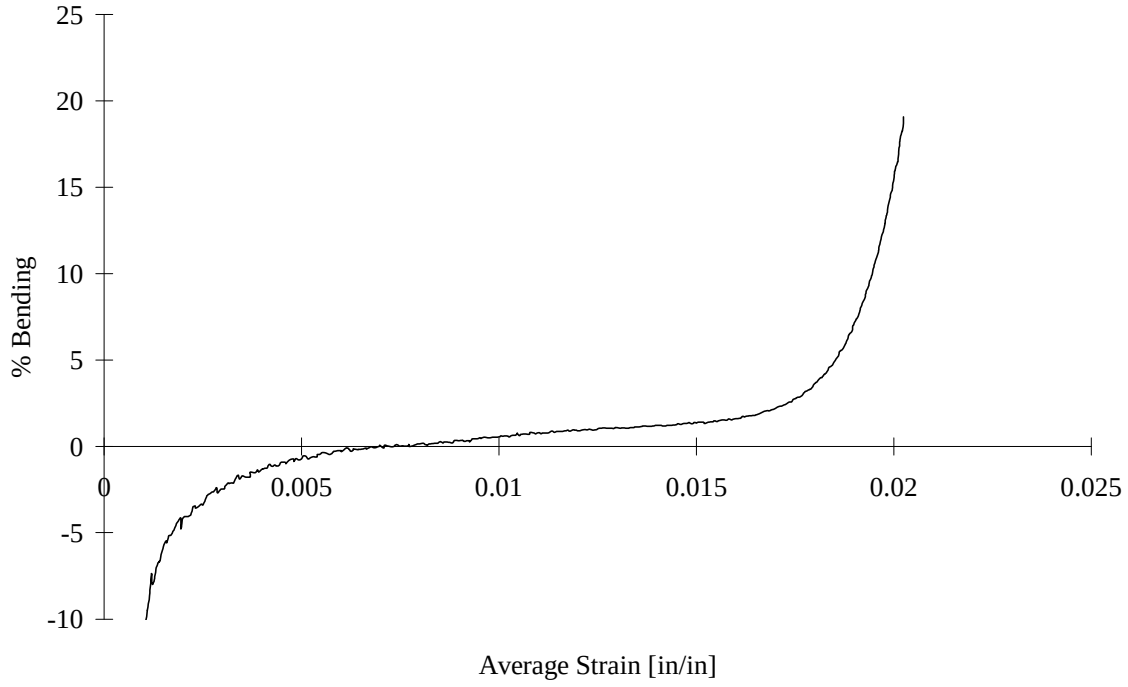

FIGURE C-18. TEST SPECIMEN AT04: TABBED, AS4/3501-6 CARBON/EPOXY $[90/0]_{5s}$
IITRI TEST FIXTURE

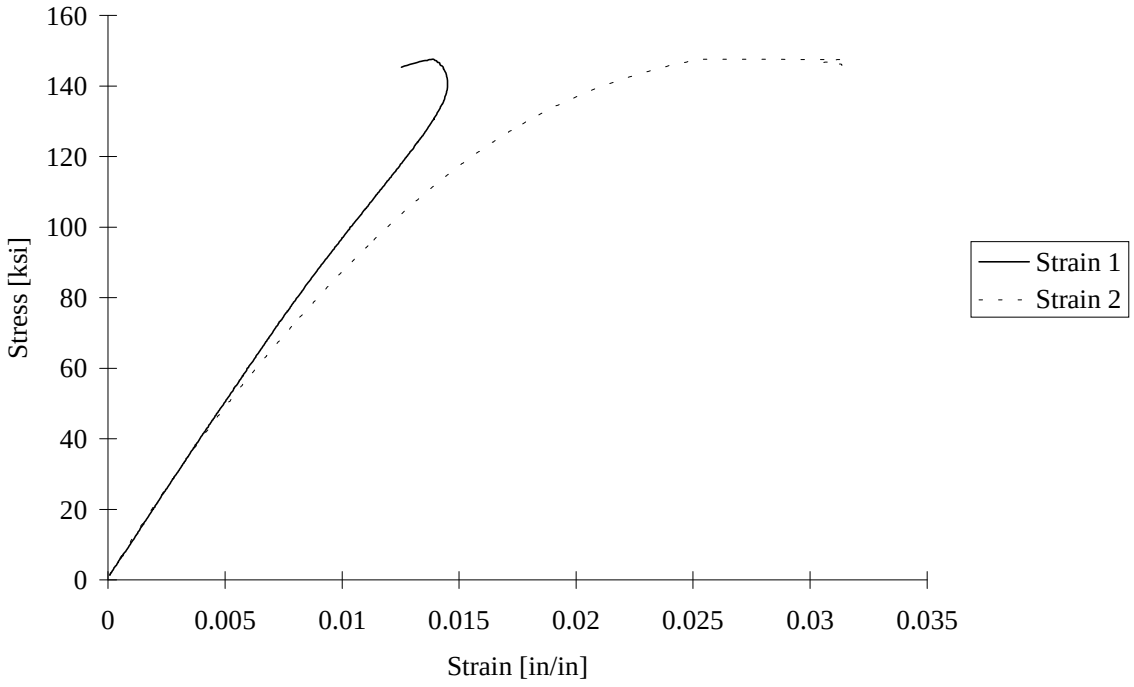

FIGURE C-19. TEST SPECIMEN AT05: TABBED, AS4/3501-6 CARBON/EPOXY $[90/0]_{5s}$
IITRI TEST FIXTURE

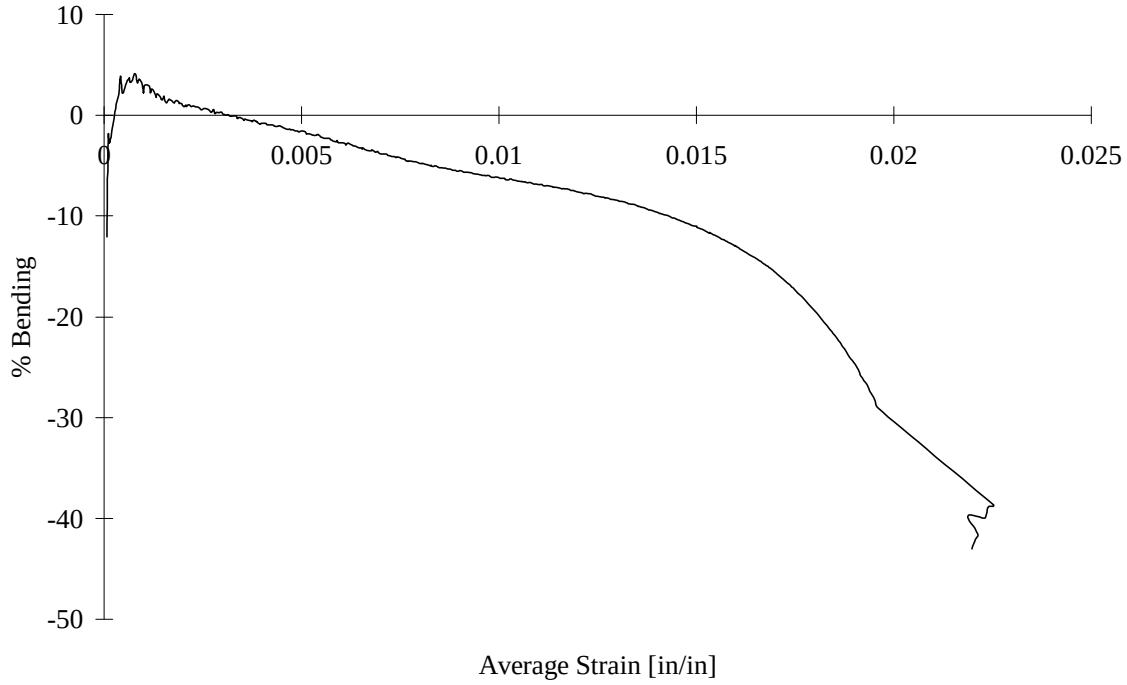

FIGURE C-20. TEST SPECIMEN AT05: TABBED, AS4/3501-6 CARBON/EPOXY $[90/0]_{5s}$
IITRI TEST FIXTURE

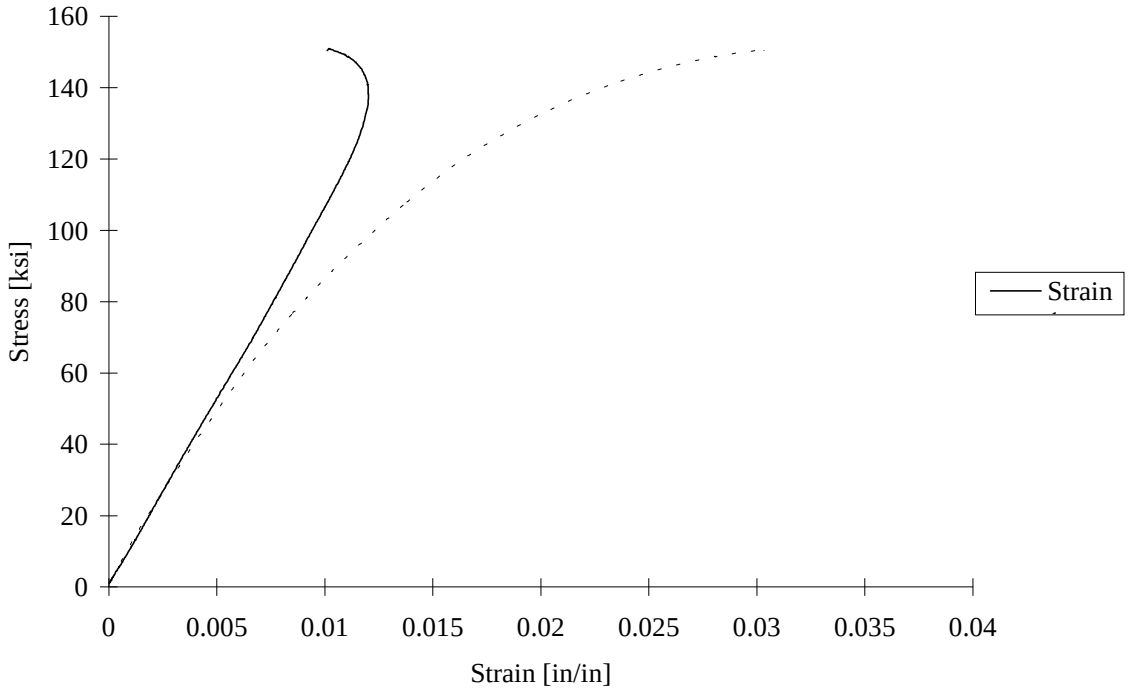

FIGURE C-21. TEST SPECIMEN AU01: UNTABBED, AS4/3501-6 CARBON/EPOXY $[90/0]_{5s}$ IITRI TEST FIXTURE

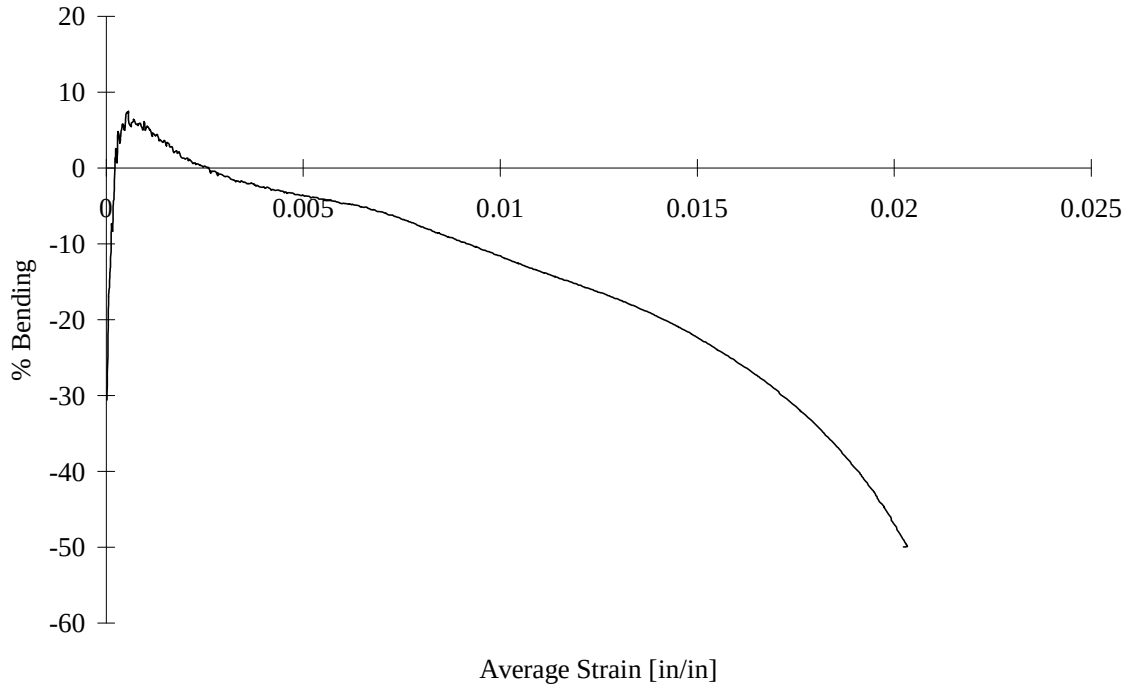

FIGURE C-22. TEST SPECIMEN AU01: UNTABBED, AS4/3501-6 CARBON/EPOXY $[90/0]_{5s}$ IITRI TEST FIXTURE

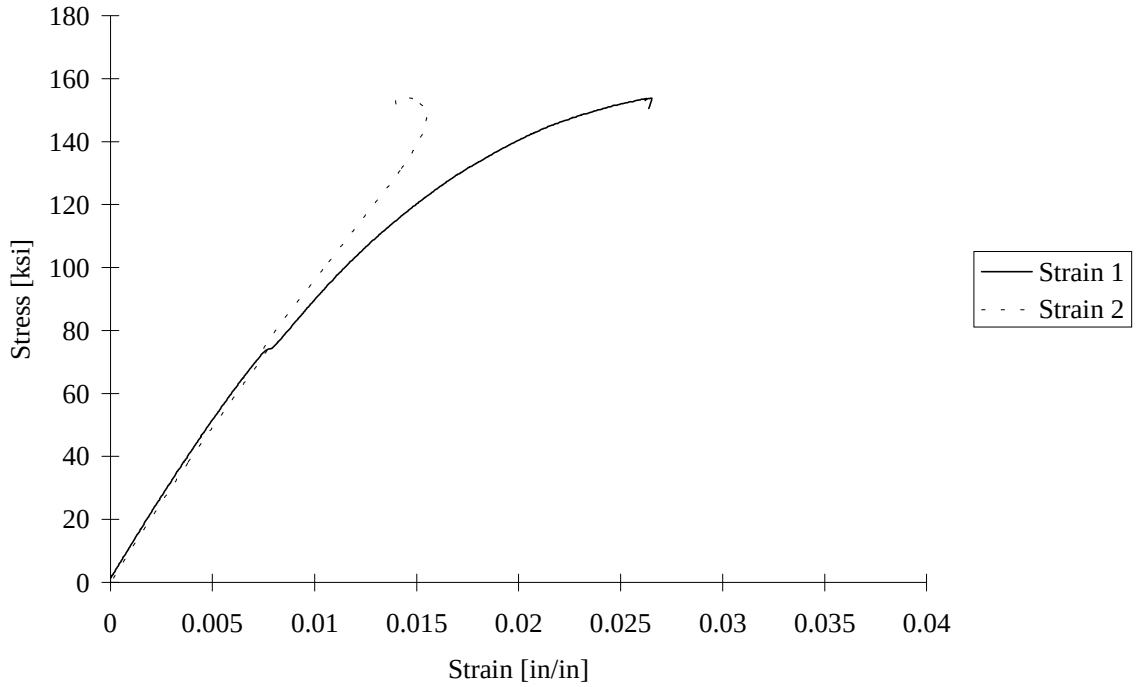

FIGURE C-23. TEST SPECIMEN AU02: UNTABBED, AS4/3501-6 CARBON/EPOXY $[90/0]_{5s}$ IITRI TEST FIXTURE

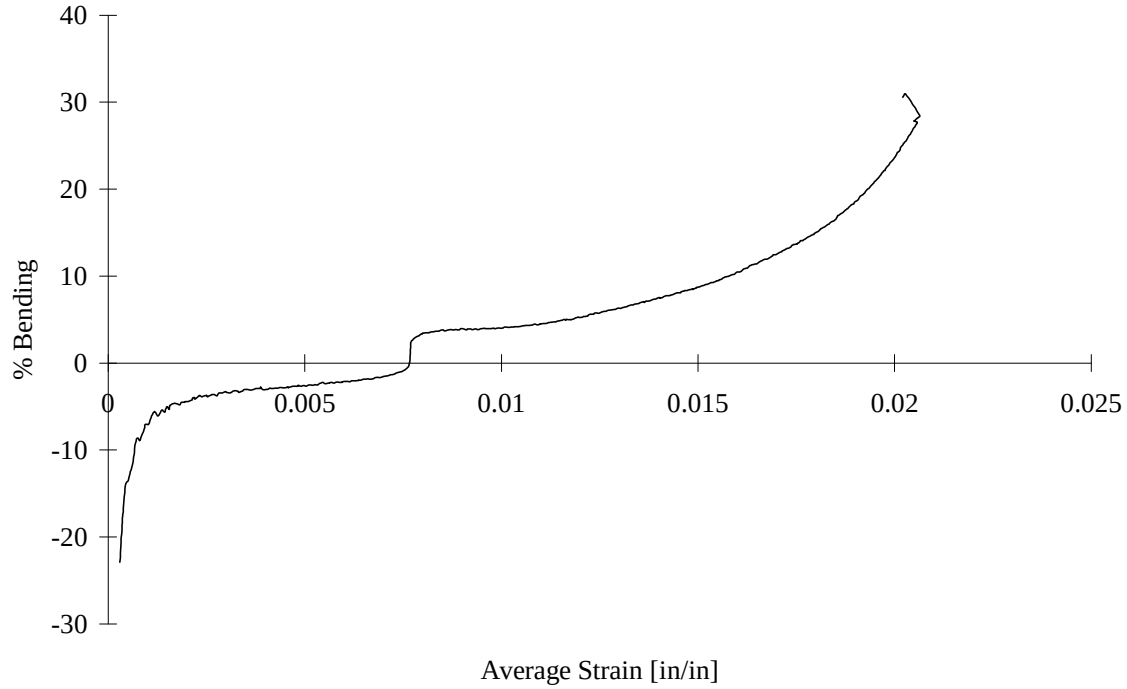

FIGURE C-24. TEST SPECIMEN AU02: UNTABBED, AS4/3501-6 CARBON/EPOXY $[90/0]_{5s}$ IITRI TEST FIXTURE

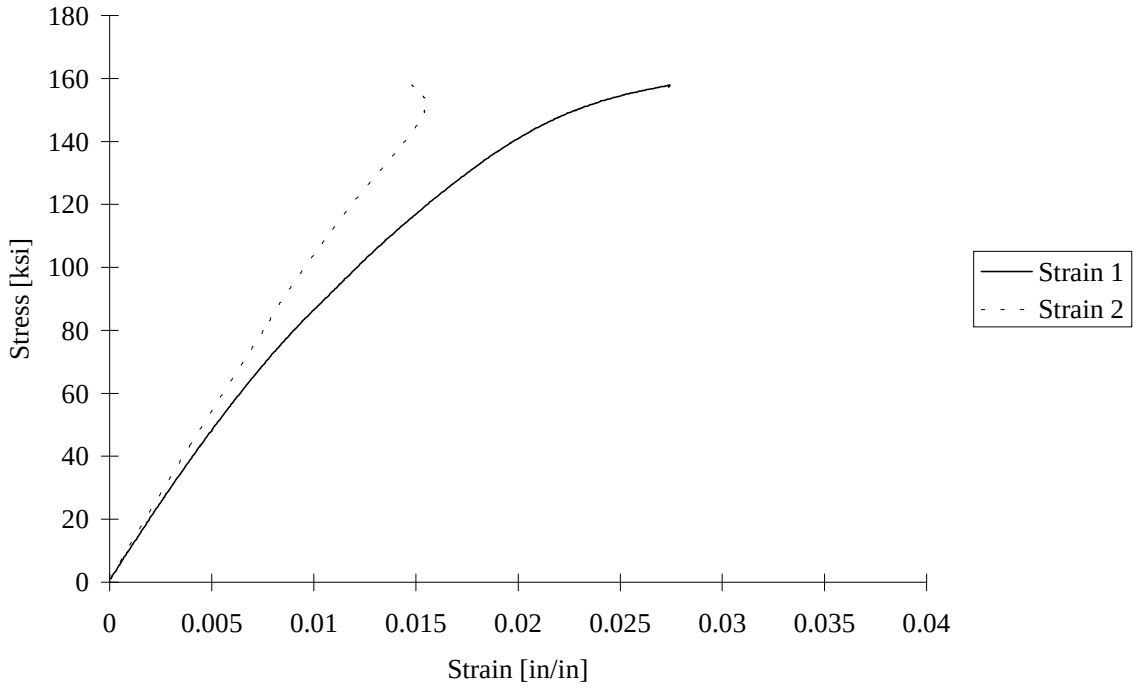

FIGURE C-25. TEST SPECIMEN AU03: UNTABBED, AS4/3501-6 CARBON/EPOXY $[90/0]_{5s}$ IITRI TEST FIXTURE

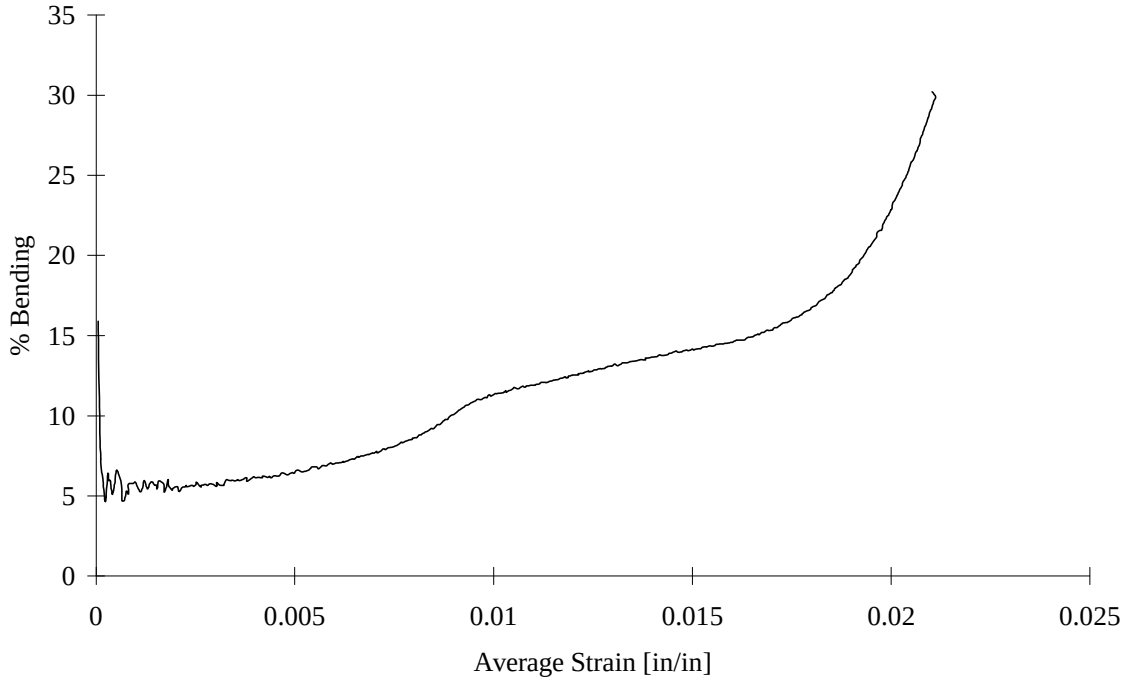

FIGURE C-26. TEST SPECIMEN AU03: UNTABBED, AS4/3501-6 CARBON/EPOXY $[90/0]_{5s}$ IITRI TEST FIXTURE

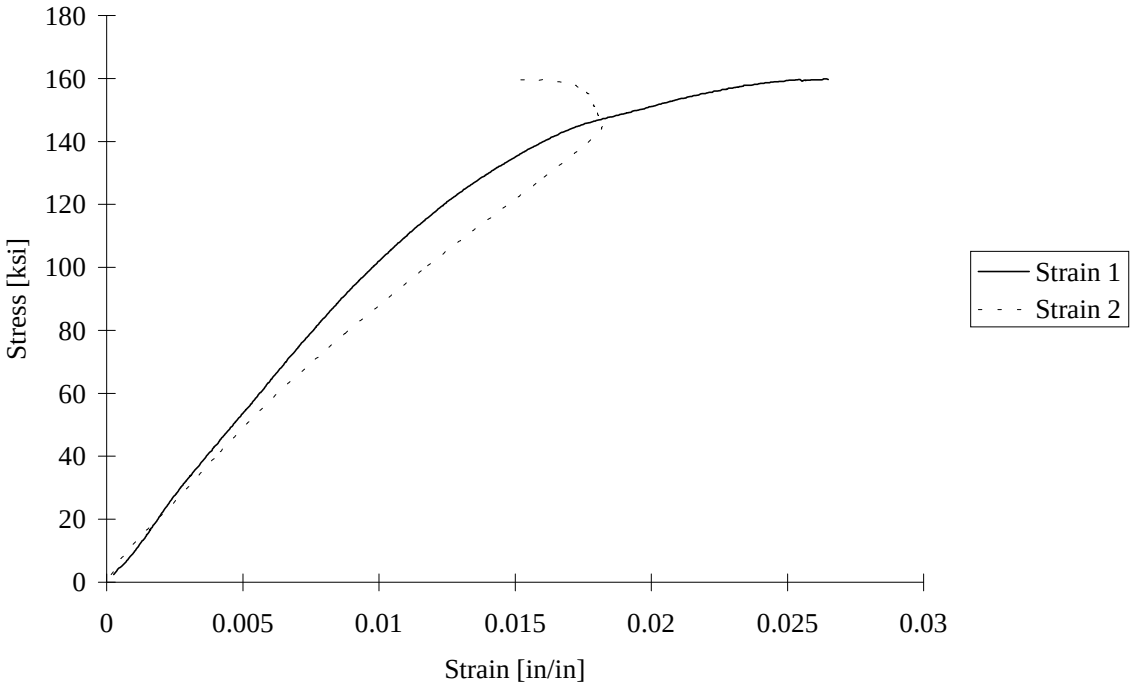

FIGURE C-27. TEST SPECIMEN AU04: UNTABBED, AS4/3501-6 CARBON/EPOXY $[90/0]_{5s}$ IITRI TEST FIXTURE

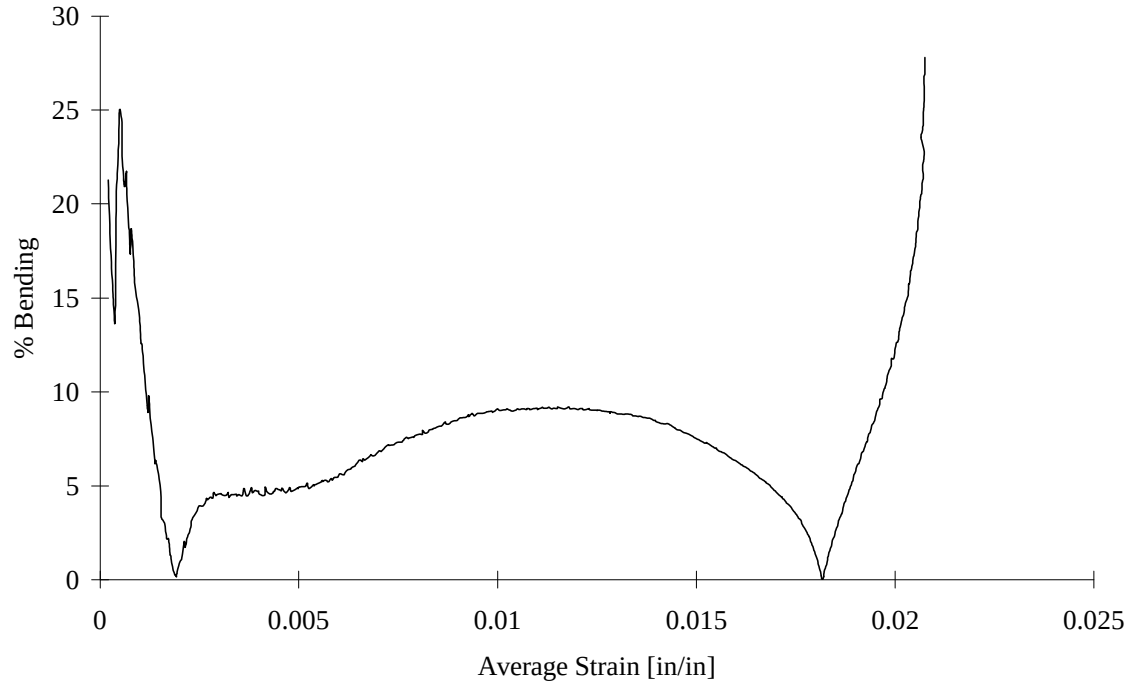

FIGURE C-28. TEST SPECIMEN AU04: UNTABBED, AS4/3501-6 CARBON/EPOXY $[90/0]_{5s}$ IITRI TEST FIXTURE

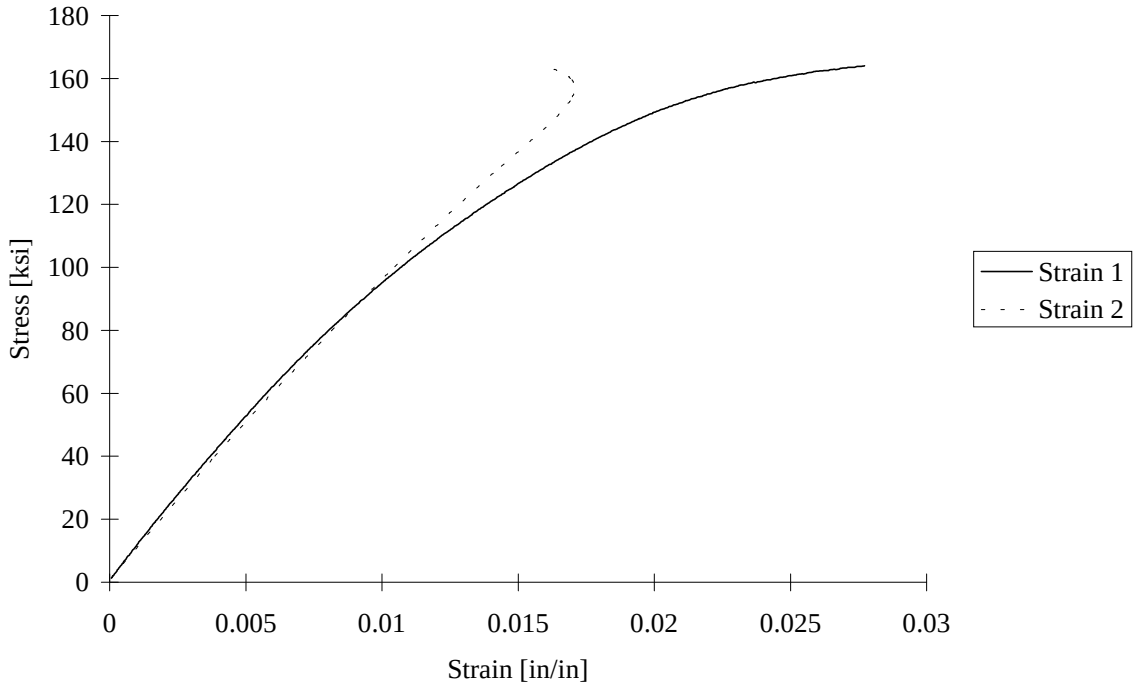

FIGURE C-29. TEST SPECIMEN AU05: UNTABBED, AS4/3501-6 CARBON/EPOXY $[90/0]_{5s}$ IITRI TEST FIXTURE

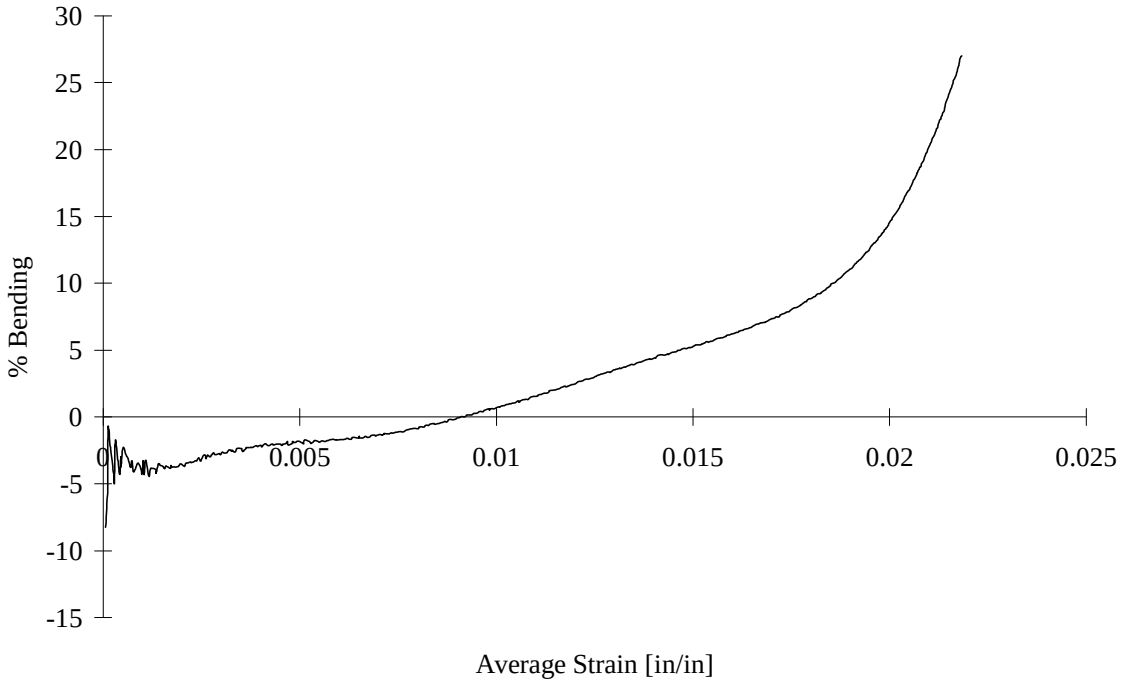

FIGURE C-30. TEST SPECIMEN AU05: UNTABBED, AS4/3501-6 CARBON/EPOXY $[90/0]_{5s}$ IITRI TEST FIXTURE

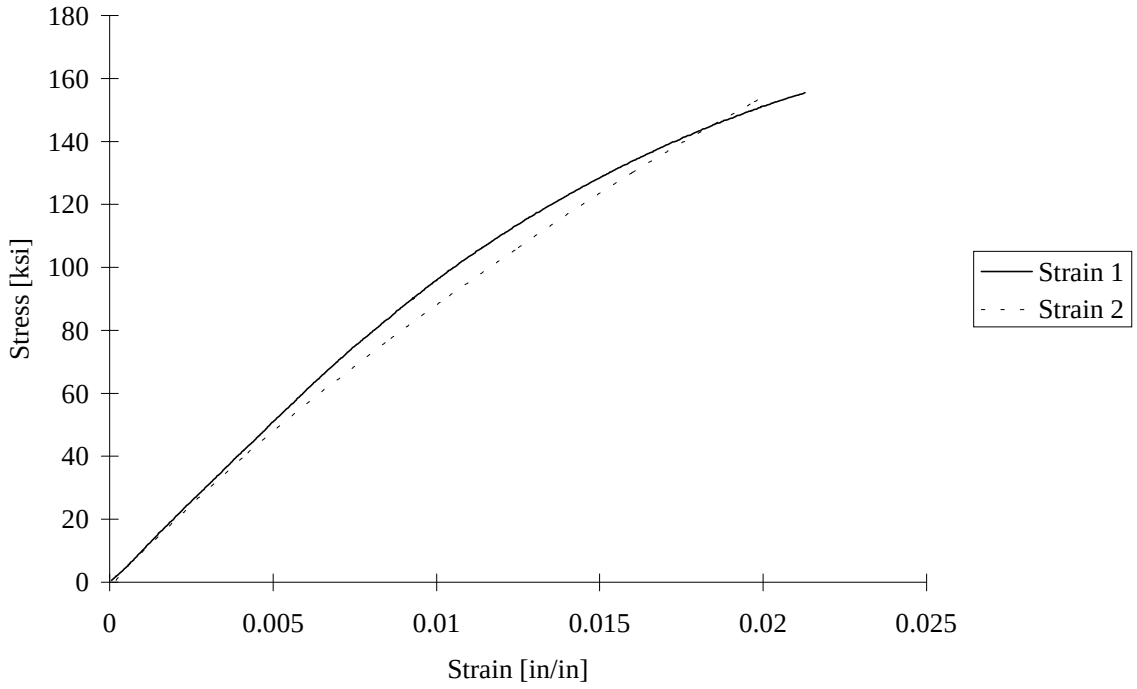

FIGURE C-31. TEST SPECIMEN AU06: UNTABBED, AS4/3501-6 CARBON/EPOXY $[90/0]_{5s}$ IITRI TEST FIXTURE

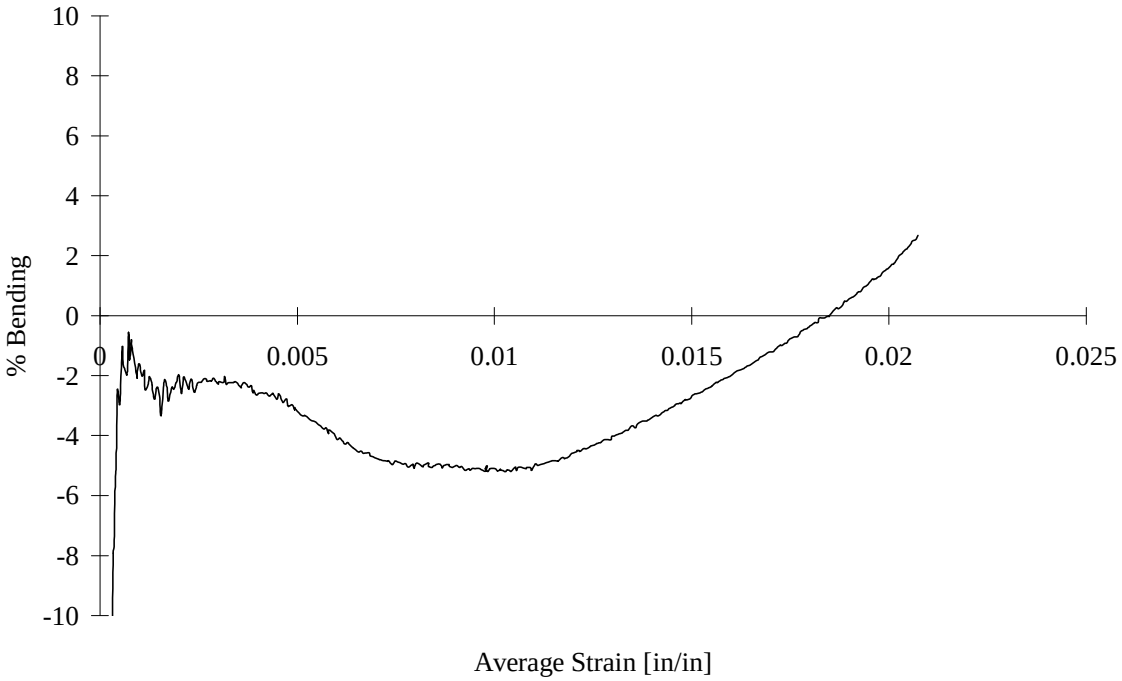

FIGURE C-32. TEST SPECIMEN AU06: UNTABBED, AS4/3501-6 CARBON/EPOXY $[90/0]_{5s}$ IITRI TEST FIXTURE

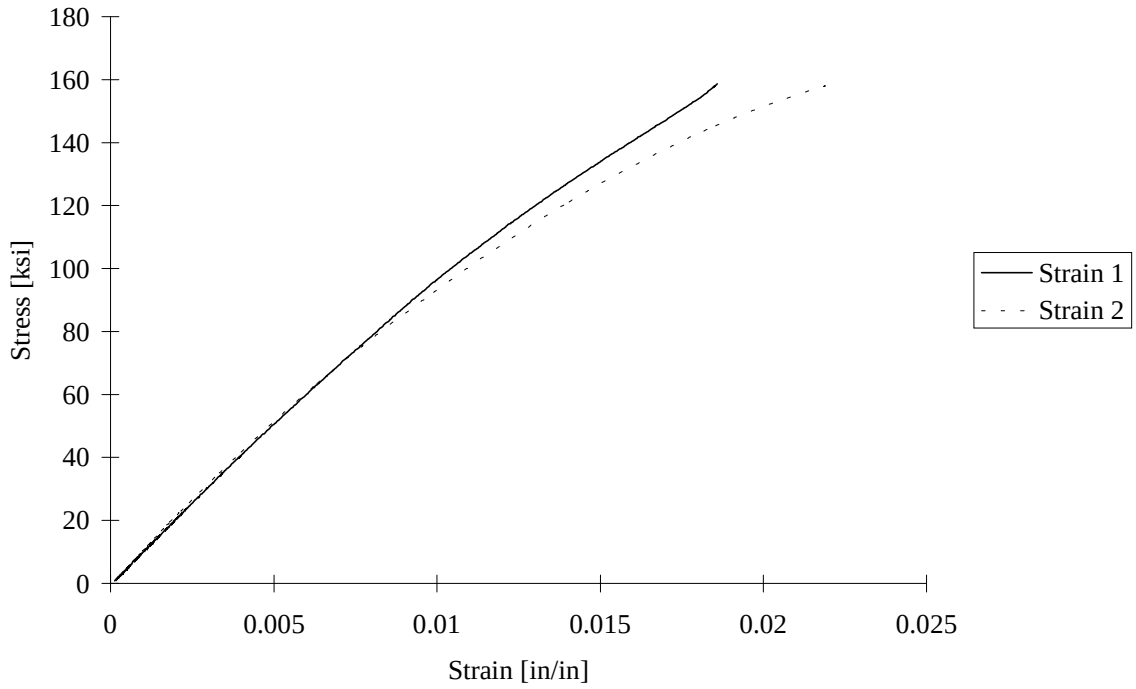

FIGURE C-33. TEST SPECIMEN AU07: UNTABBED, AS4/3501-6 CARBON/EPOXY $[90/0]_{5s}$ IITRI TEST FIXTURE

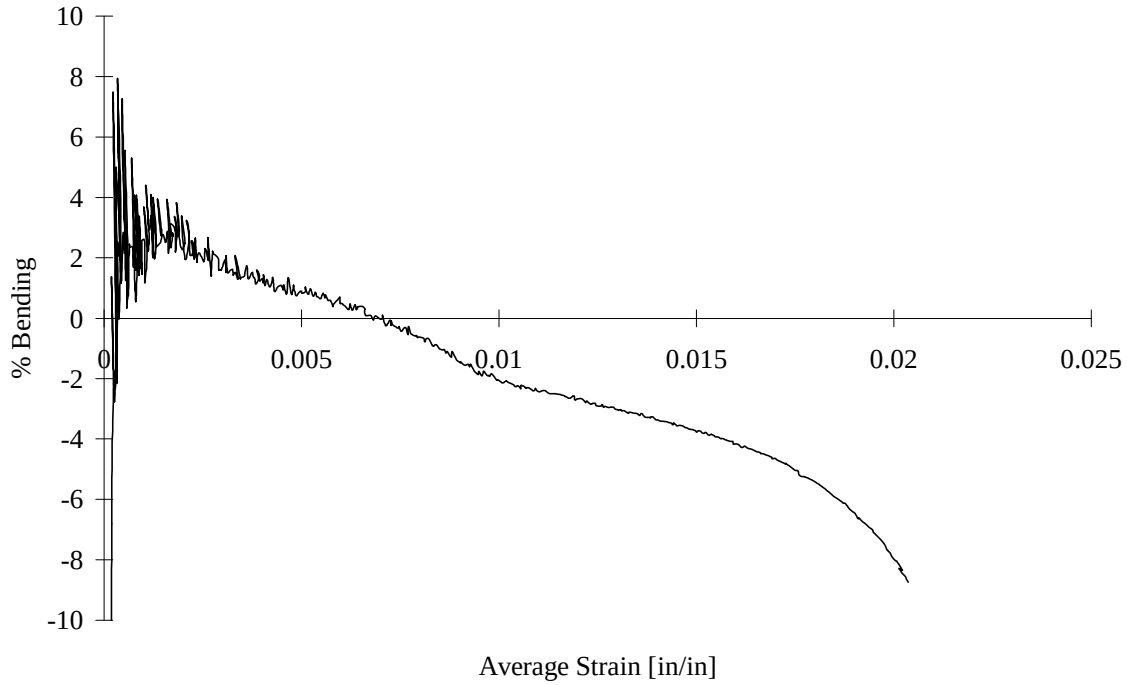

FIGURE C-34. TEST SPECIMEN AU07: UNTABBED, AS4/3501-6 CARBON/EPOXY $[90/0]_{5s}$ IITRI TEST FIXTURE

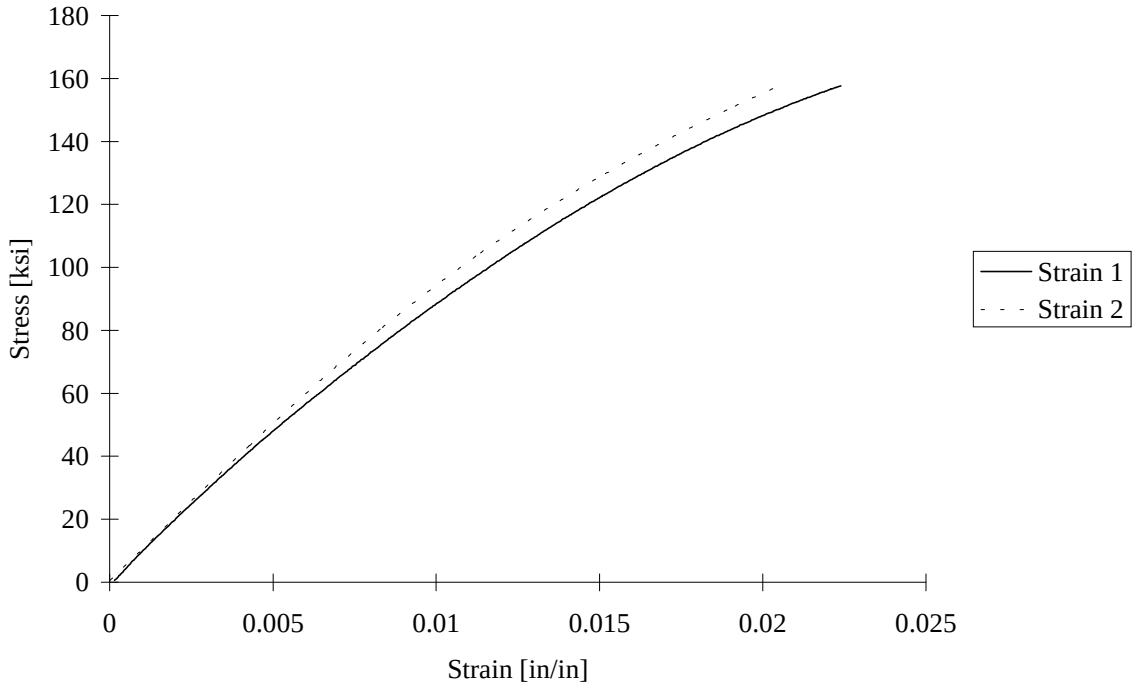

FIGURE C-35. TEST SPECIMEN AU08: UNTABBED, AS4/3501-6 CARBON/EPOXY $[90/0]_{5s}$ IITRI TEST FIXTURE

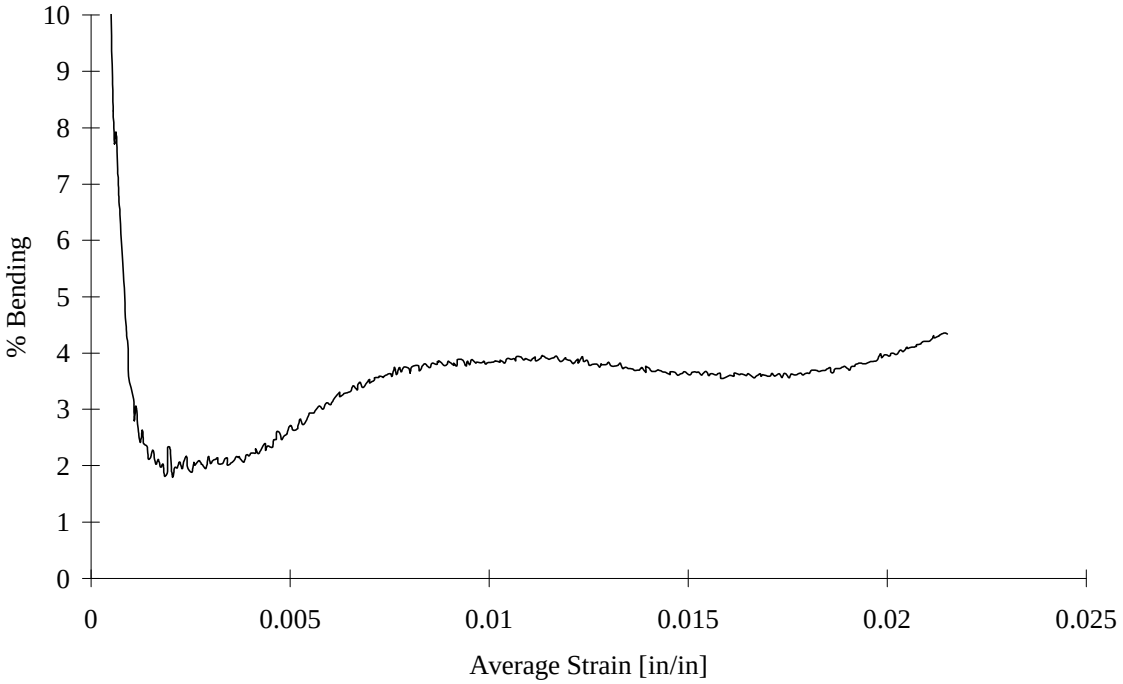

FIGURE C-36. TEST SPECIMEN AU08: UNTABBED, AS4/3501-6 CARBON/EPOXY $[90/0]_{5s}$ IITRI TEST FIXTURE

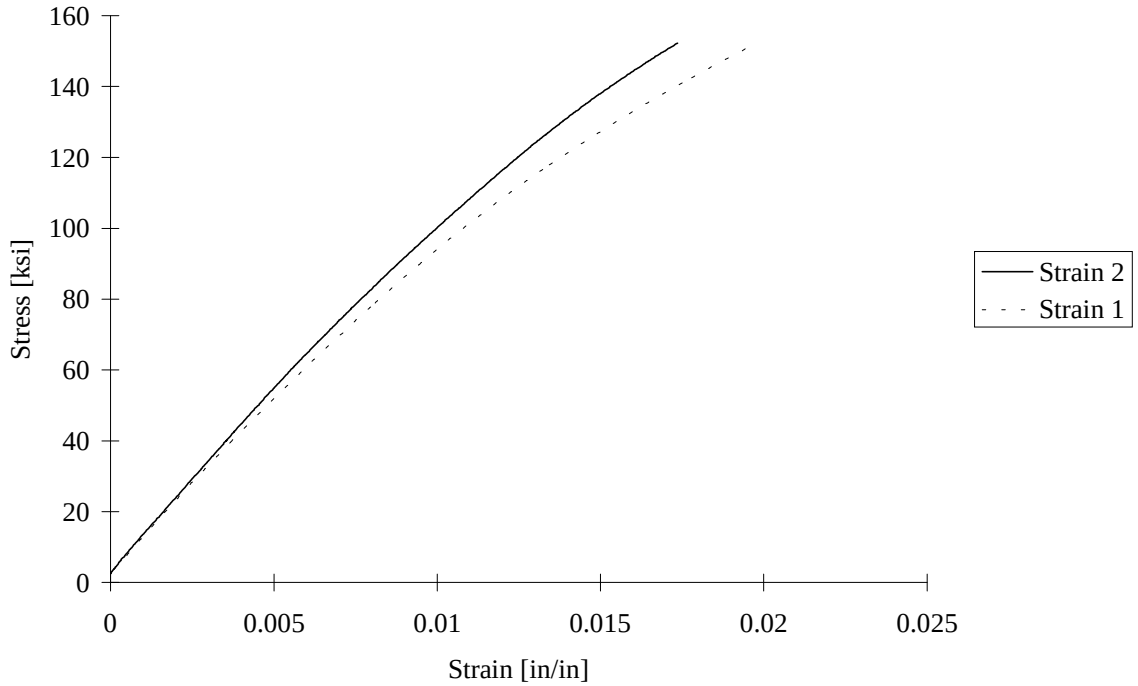

FIGURE C-37. TEST SPECIMEN AU09: UNTABBED, AS4/3501-6 CARBON/EPOXY $[90/0]_{5s}$ IITRI TEST FIXTURE

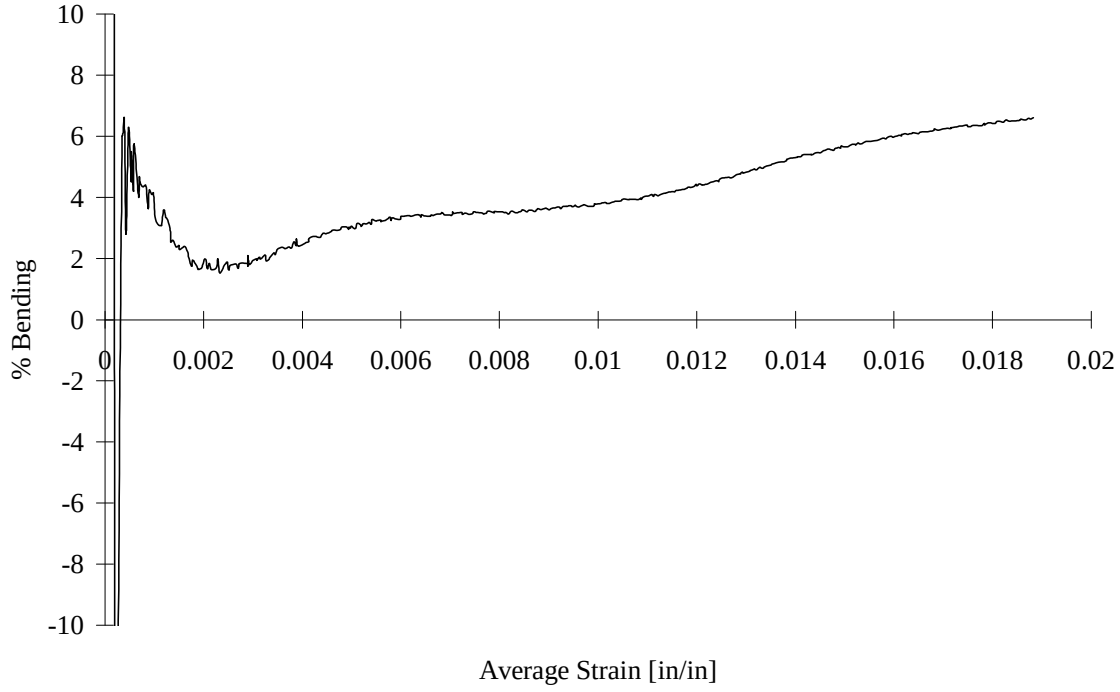

FIGURE C-38. TEST SPECIMEN AU09: UNTABBED, AS4/3501-6 CARBON/EPOXY $[90/0]_{5s}$ IITRI TEST FIXTURE

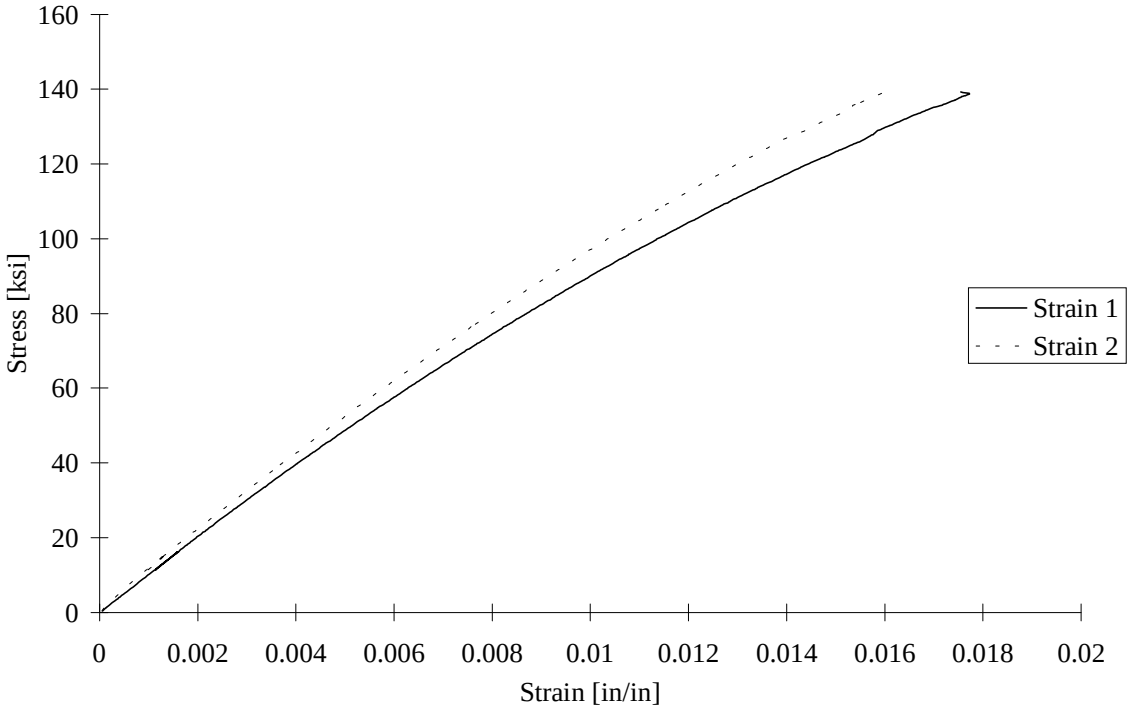

FIGURE C-39. TEST SPECIMEN AC702: AS4/3501-6 CARBON/EPOXY $[90/0]_{7s}$
CLC-OR TEST FIXTURE

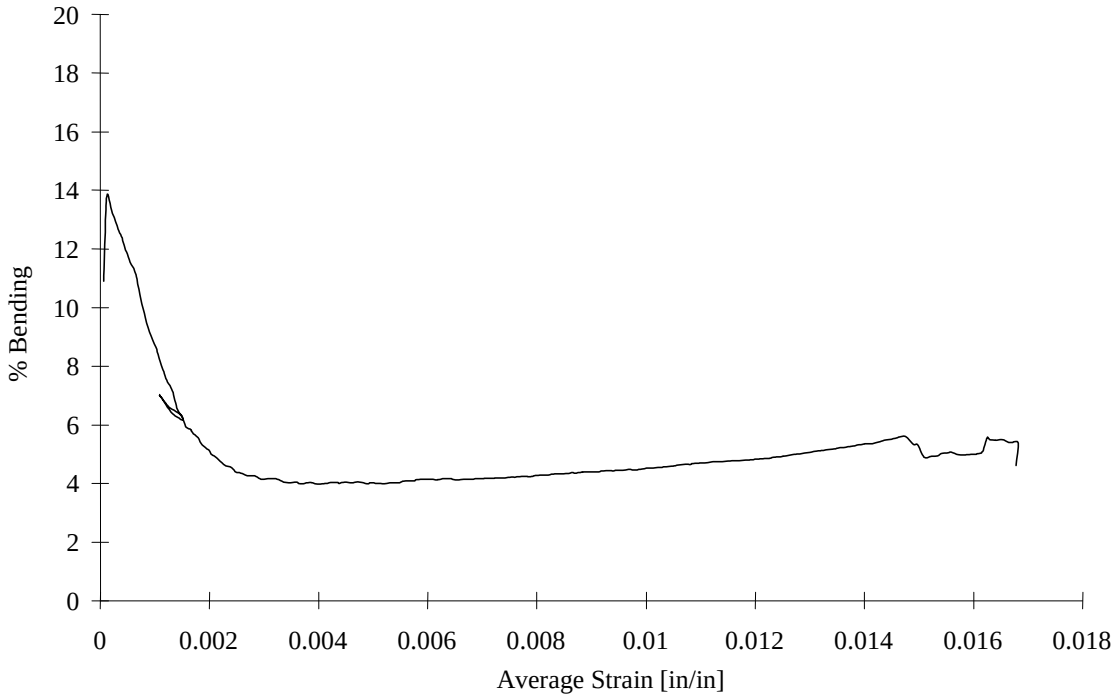

FIGURE C-40. TEST SPECIMEN AC702: AS4/3501-6 CARBON/EPOXY $[90/0]_{7s}$
CLC-OR TEST FIXTURE

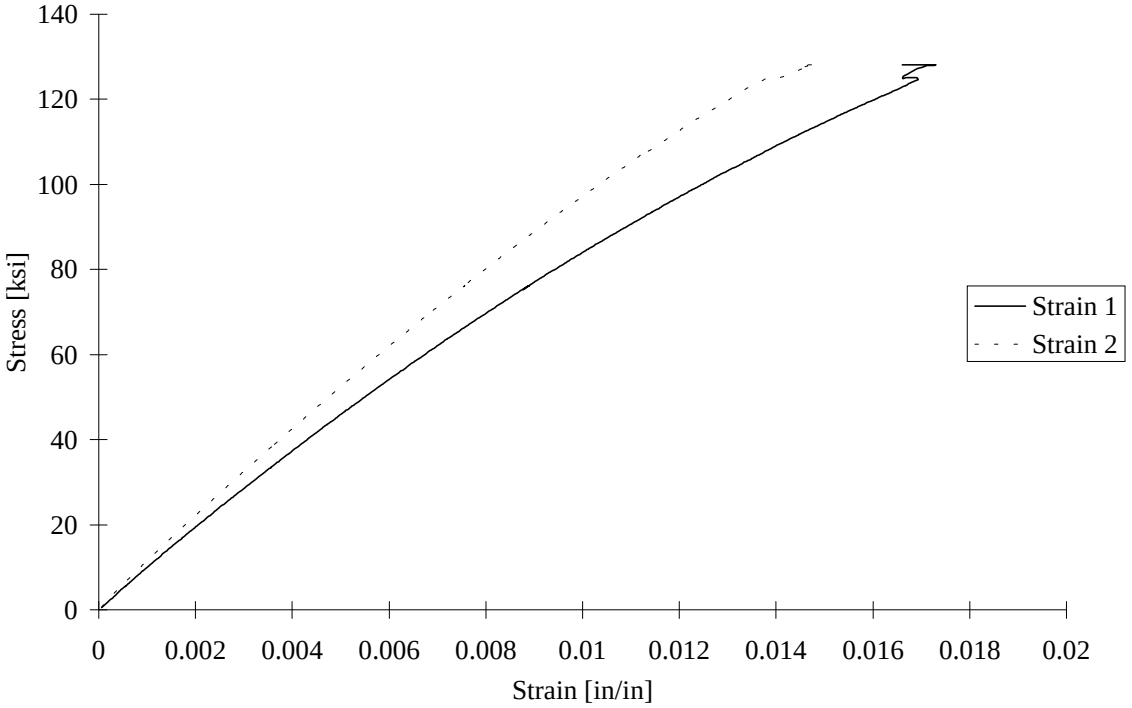

FIGURE C-41. TEST SPECIMEN AC703: AS4/3501-6 CARBON/EPOXY $[90/0]_{7s}$
CLC-OR TEST FIXTURE

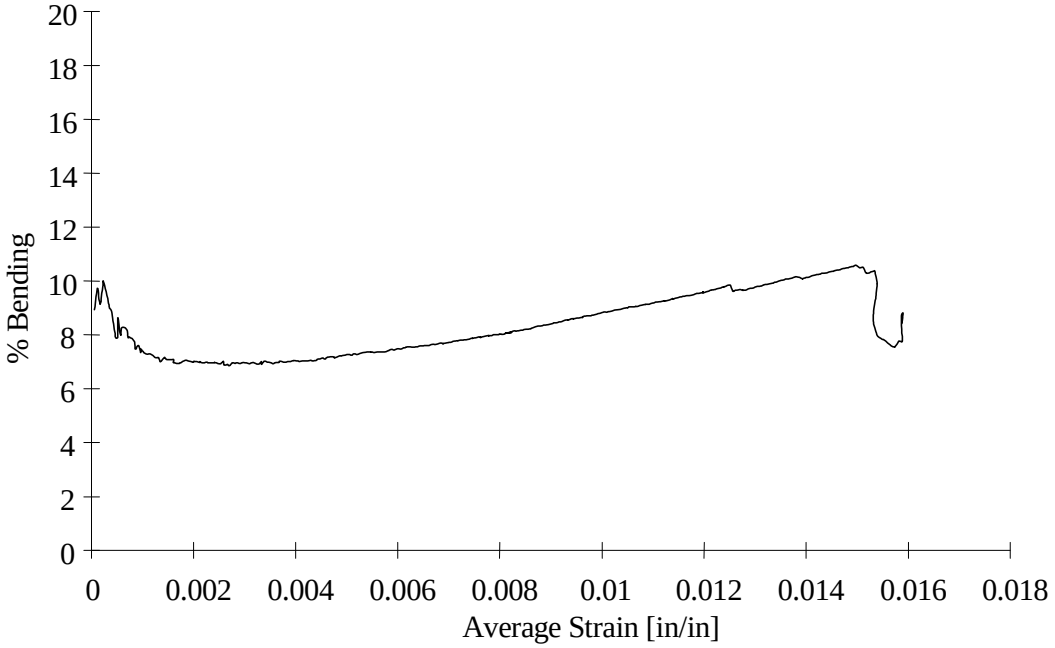

FIGURE C-42. TEST SPECIMEN AC703: AS4/3501-6 CARBON/EPOXY $[90/0]_{7s}$
CLC-OR TEST FIXTURE

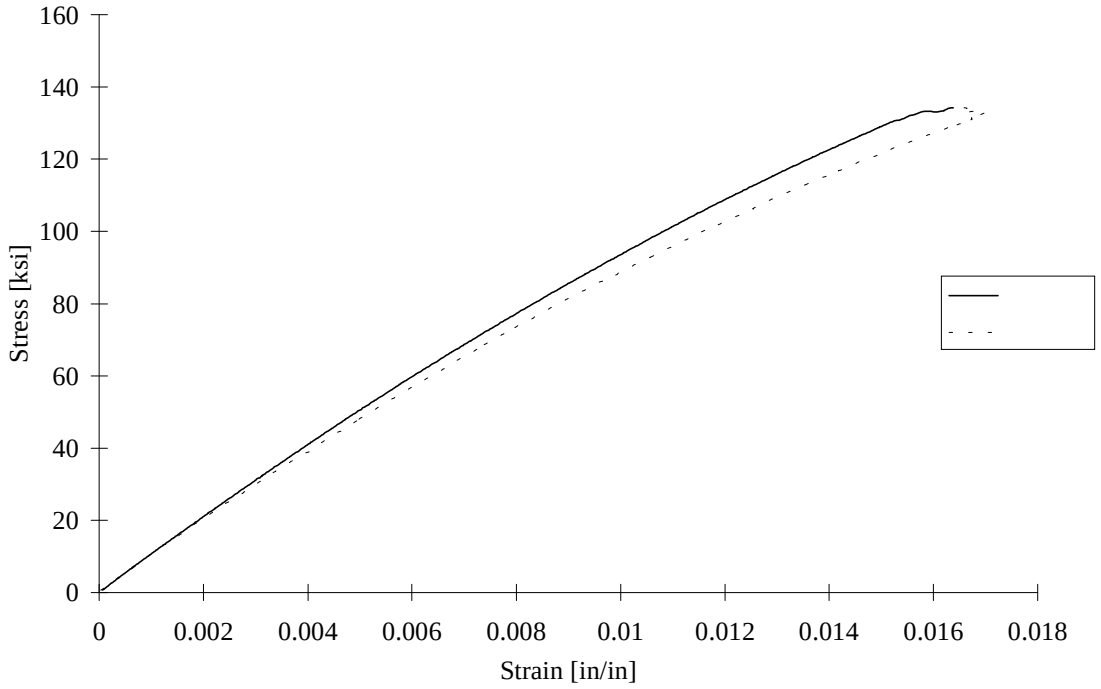

FIGURE C-43. TEST SPECIMEN AC704: AS4/3501-6 CARBON/EPOXY $[90/0]_{7s}$
CLC-OR TEST FIXTURE

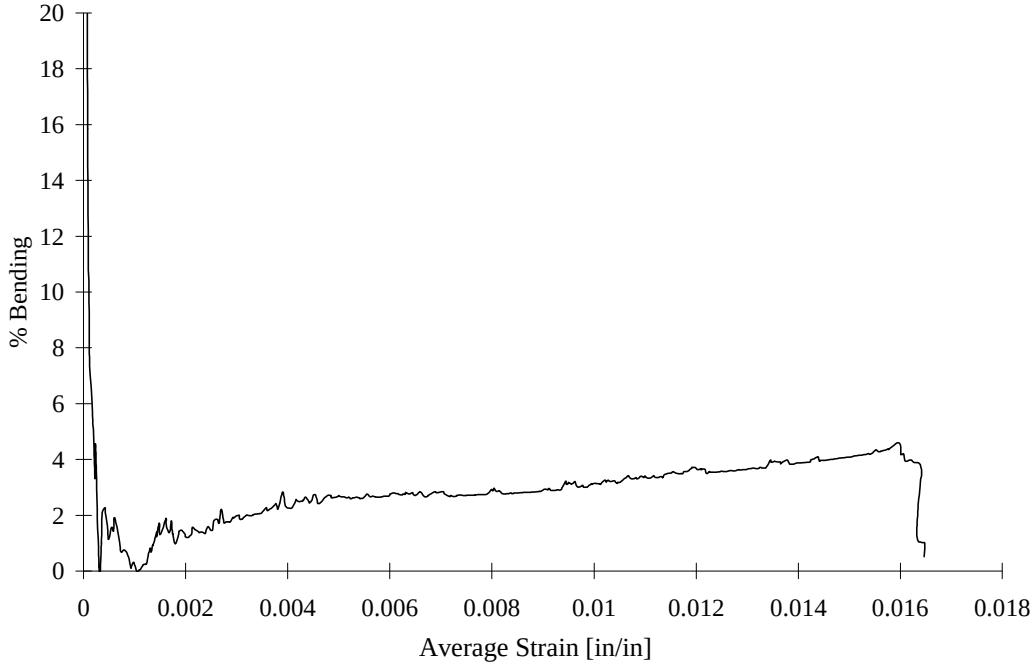

FIGURE C-44. TEST SPECIMEN AC704: AS4/3501-6 CARBON/EPOXY $[90/0]_{7s}$
CLC-OR TEST FIXTURE

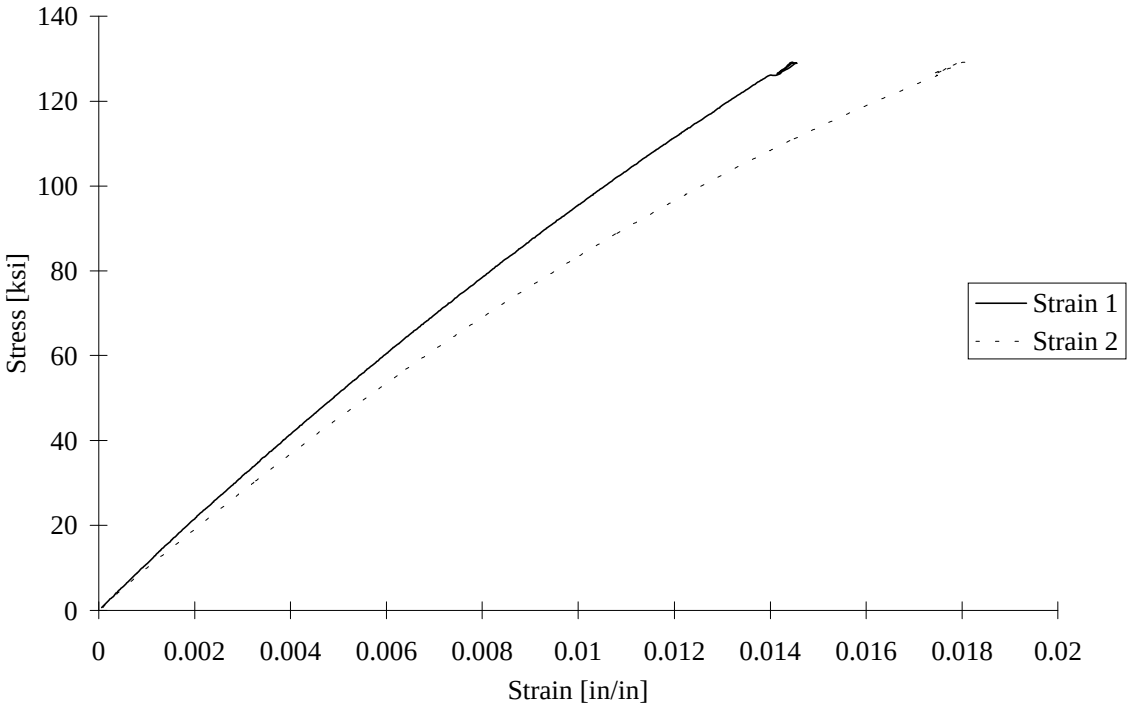

FIGURE C-45. TEST SPECIMEN AC705: AS4/3501-6 CARBON/EPOXY $[90/0]_{7s}$
CLC-OR TEST FIXTURE

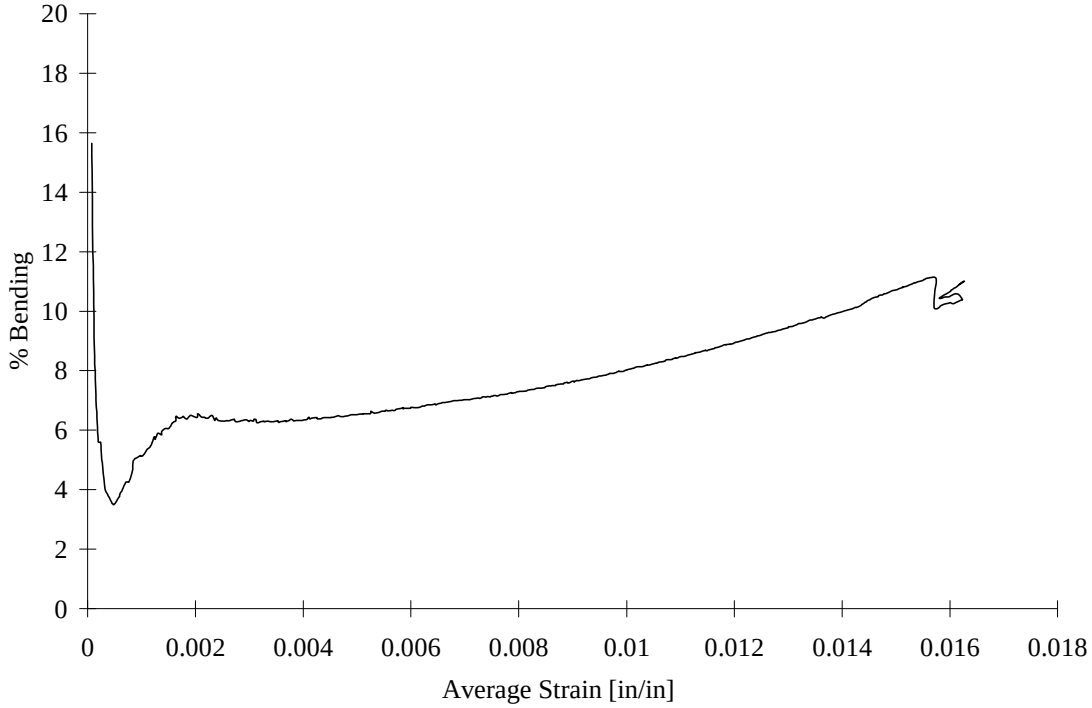

FIGURE C-46. TEST SPECIMEN AC705: AS4/3501-6 CARBON/EPOXY $[90/0]_{7s}$
CLC-OR TEST FIXTURE

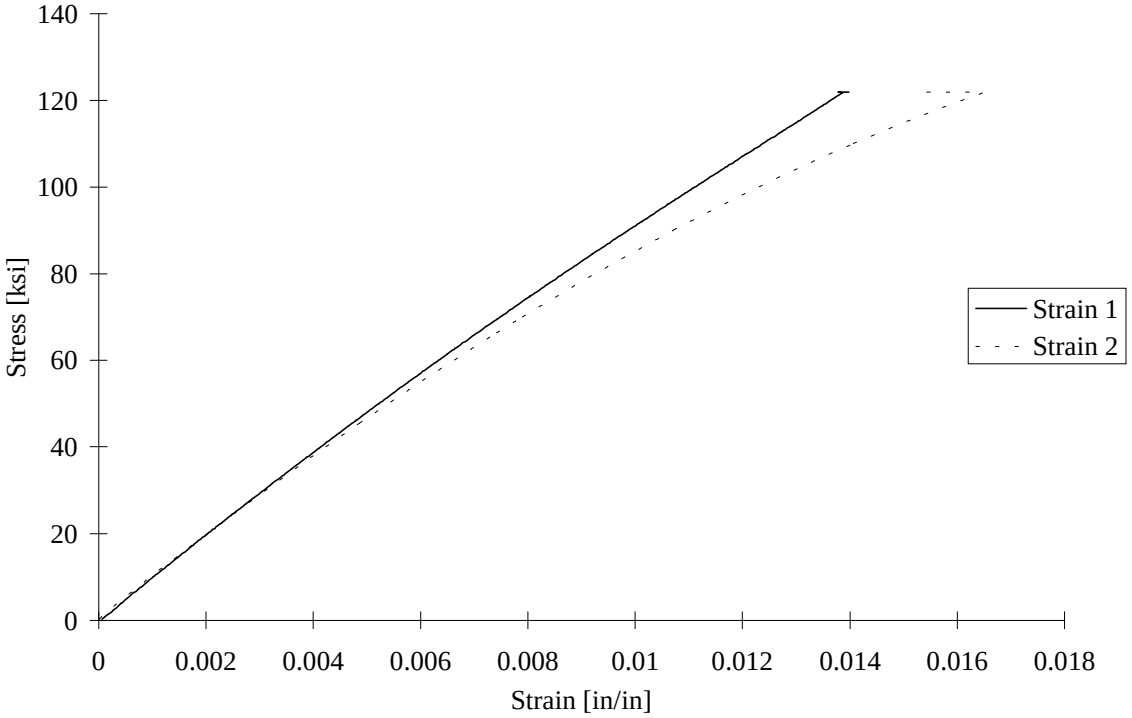

FIGURE C-47. TEST SPECIMEN AC706: AS4/3501-6 CARBON/EPOXY $[90/0]_{7s}$ CLC-OR TEST FIXTURE

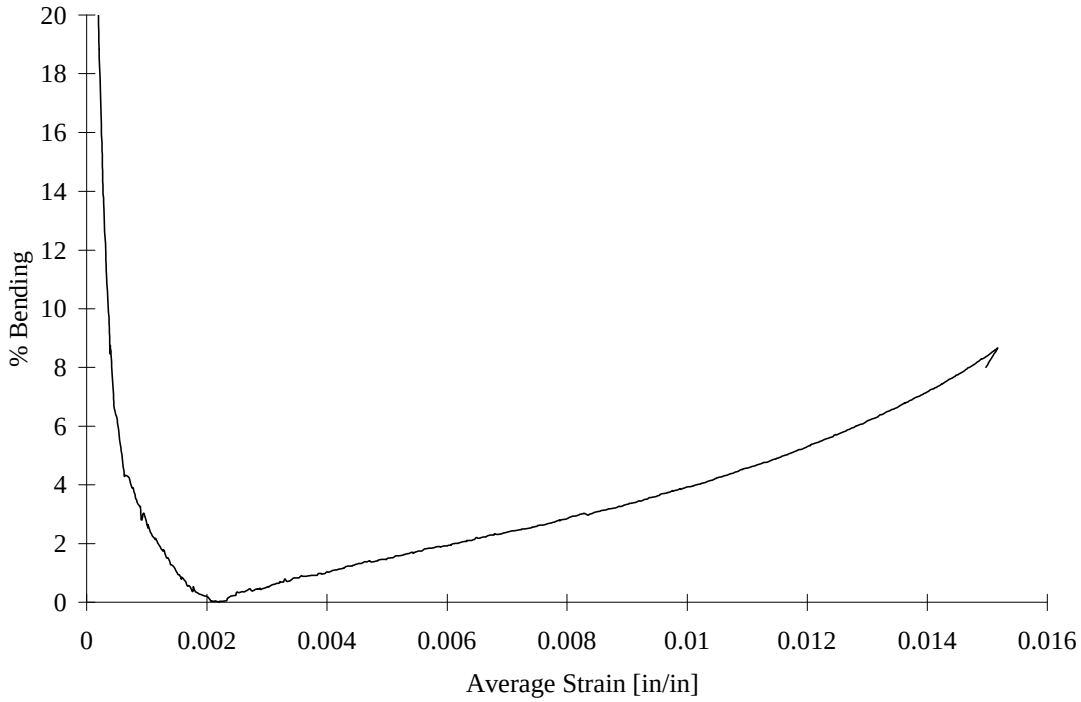

FIGURE C-48. TEST SPECIMEN AC706: AS4/3501-6 CARBON/EPOXY $[90/0]_{7s}$ CLC-OR TEST FIXTURE

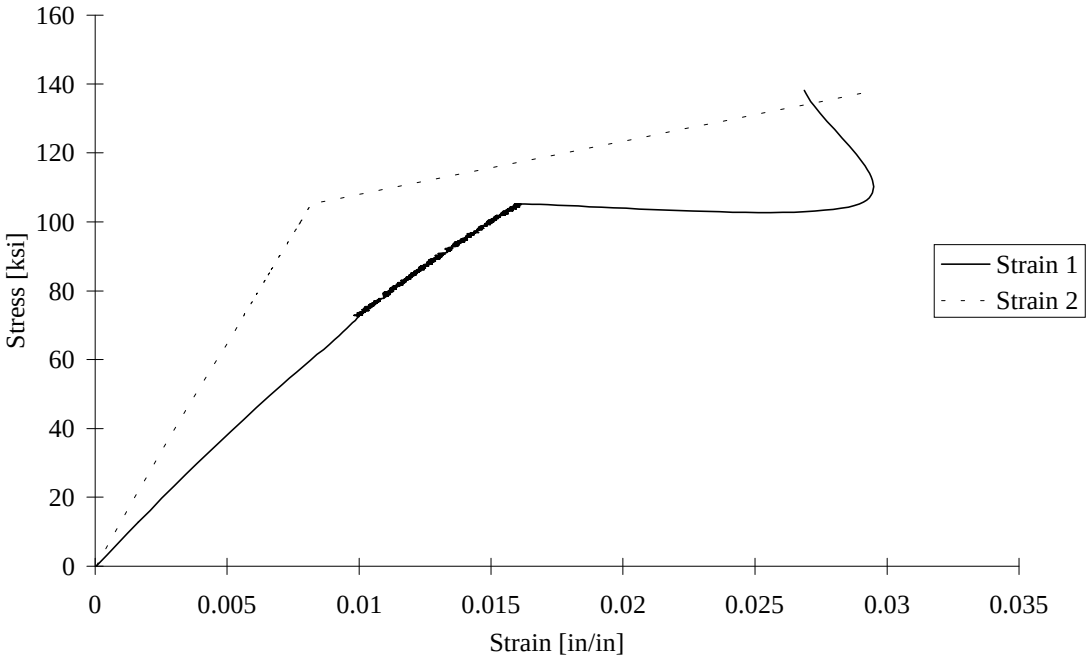

FIGURE C-49. TEST SPECIMEN AU701: UNTABBED, AS4/3501-6 CARBON/EPOXY $[90/0]_{7s}$ IITRI TEST FIXTURE

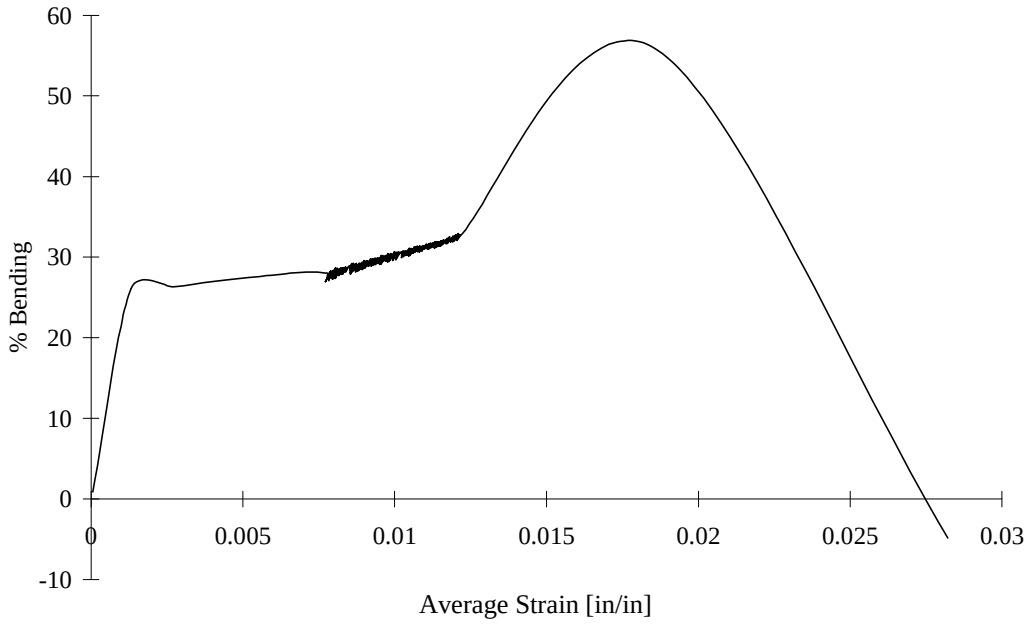

FIGURE C-50. TEST SPECIMEN AU701: UNTABBED, AS4/3501-6 CARBON/EPOXY $[90/0]_{7s}$ IITRI TEST FIXTURE

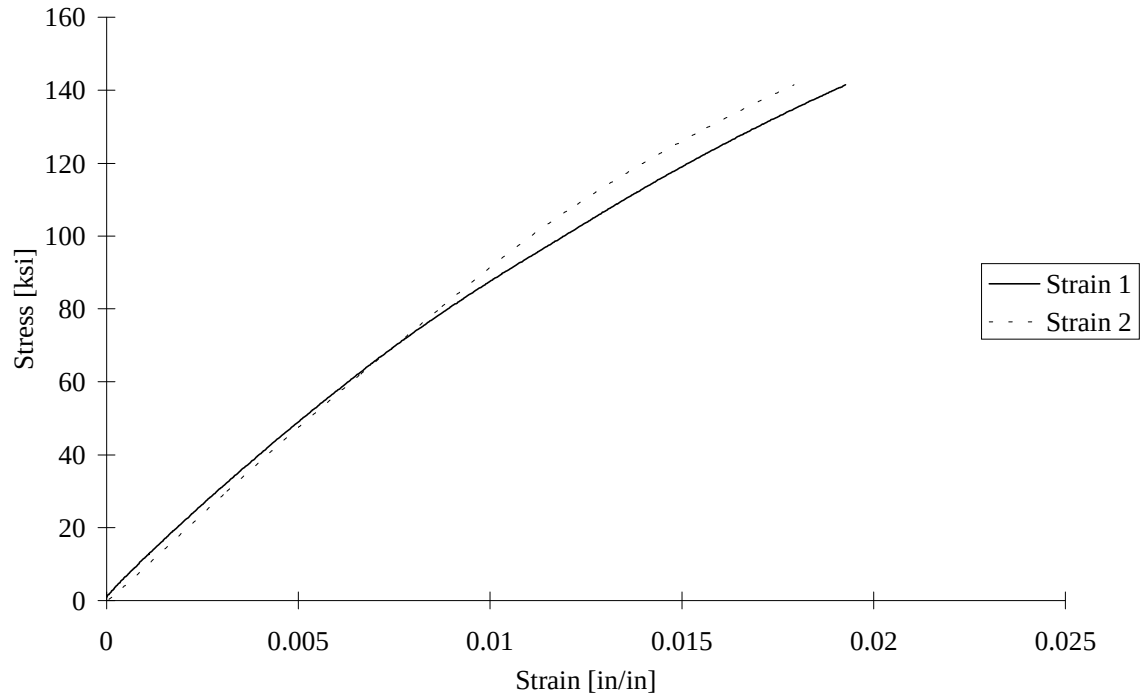

FIGURE C-51. TEST SPECIMEN AU702: UNTABBED, AS4/3501-6 CARBON/EPOXY $[90/0]_{7s}$ IITRI TEST FIXTURE

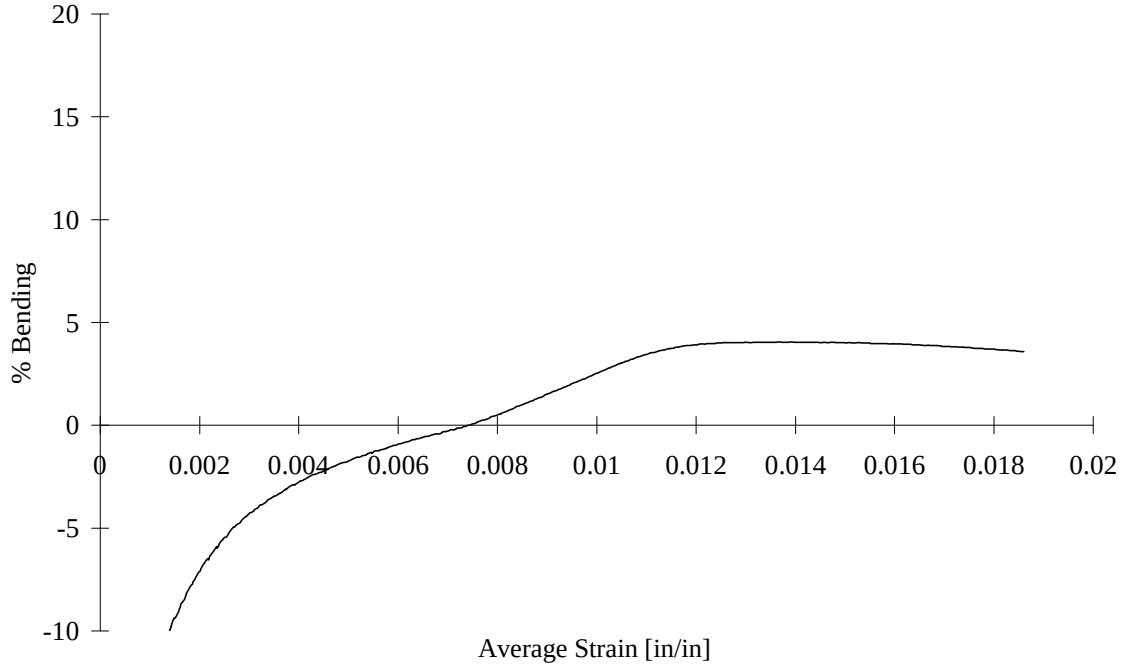

FIGURE C-52. TEST SPECIMEN AU702: UNTABBED, AS4/3501-6 CARBON/EPOXY $[90/0]_{7s}$ IITRI TEST FIXTURE

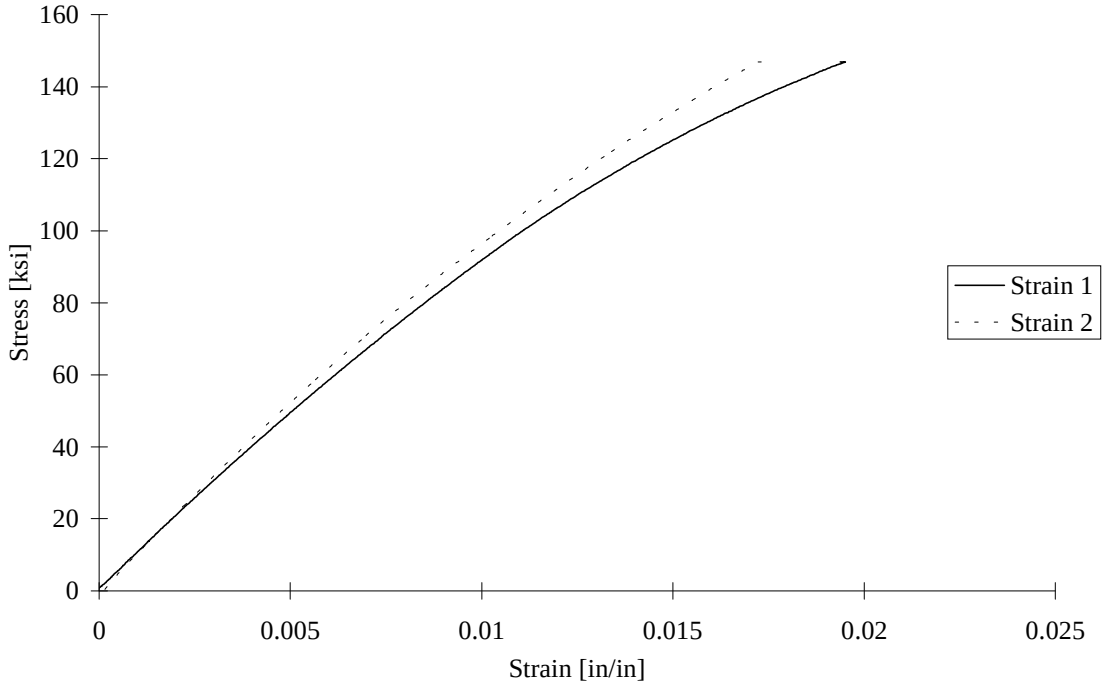

FIGURE C-53. TEST SPECIMEN AU703: UNTABBED, AS4/3501-6 CARBON/EPOXY $[90/0]_{7s}$ IITRI TEST FIXTURE

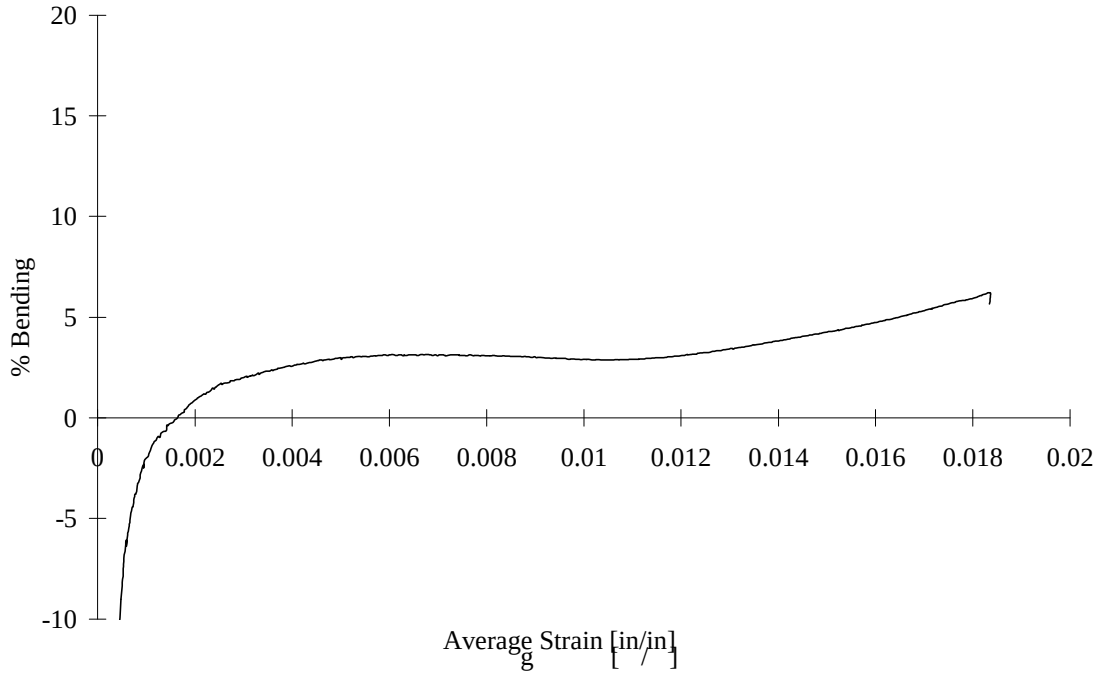

FIGURE C-54. TEST SPECIMEN AU703: UNTABBED, AS4/3501-6 CARBON/EPOXY $[90/0]_{7s}$ IITRI TEST FIXTURE

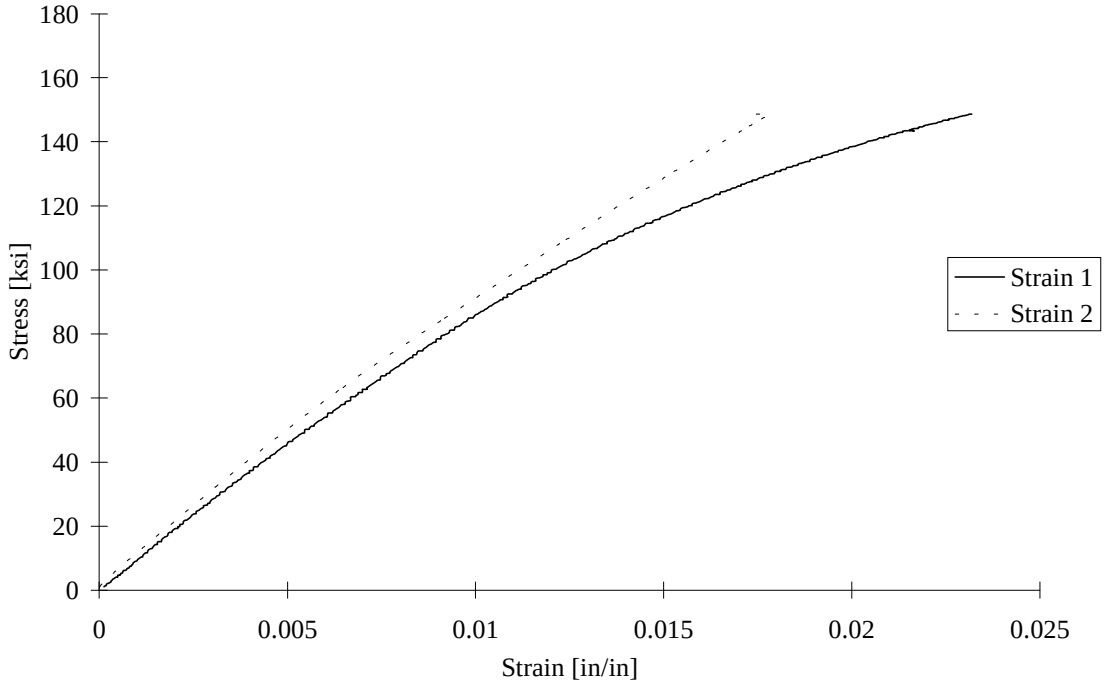

FIGURE C-55. TEST SPECIMEN AU704: UNTABBED, AS4/3501-6 CARBON/EPOXY $[90/0]_{7s}$ IITRI TEST FIXTURE

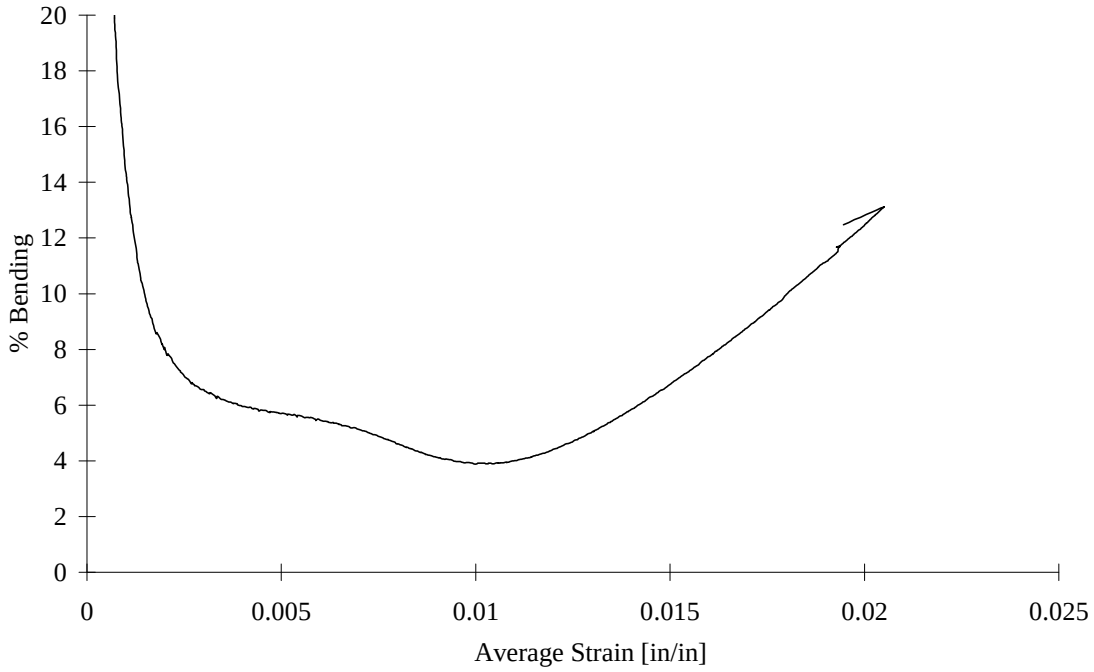

FIGURE C-56. TEST SPECIMEN AU704: UNTABBED, AS4/3501-6 CARBON/EPOXY $[90/0]_{7s}$ IITRI TEST FIXTURE

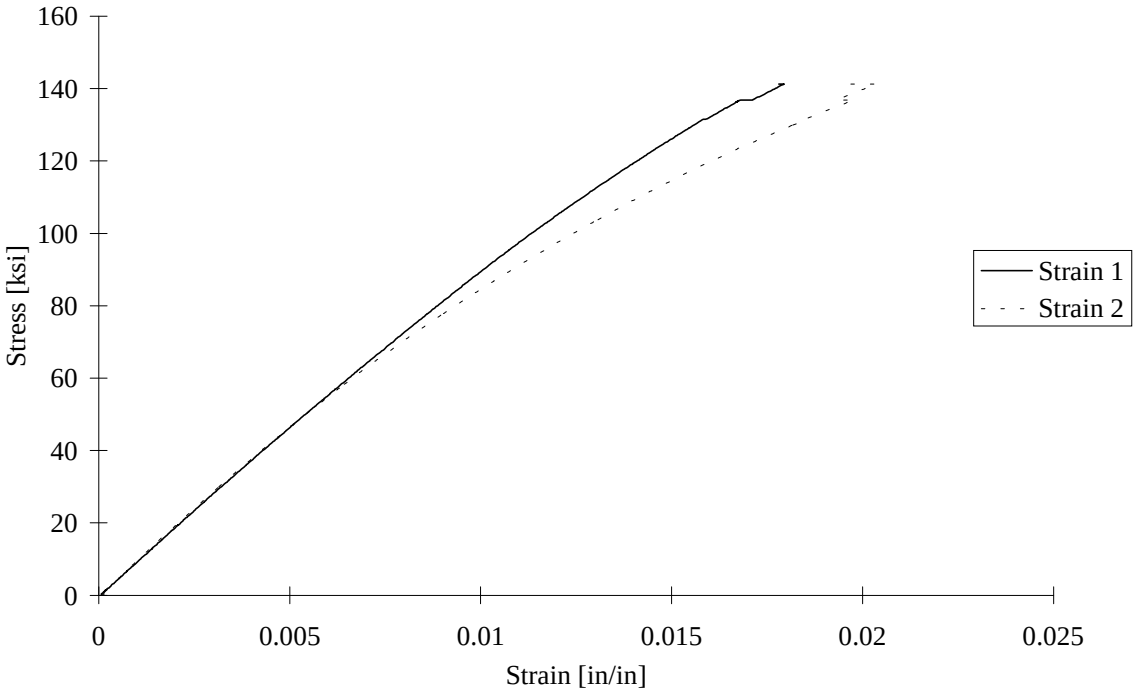

FIGURE C-57. TEST SPECIMEN AU705: UNTABBED, AS4/3501-6 CARBON/EPOXY $[90/0]_{7s}$ IITRI TEST FIXTURE

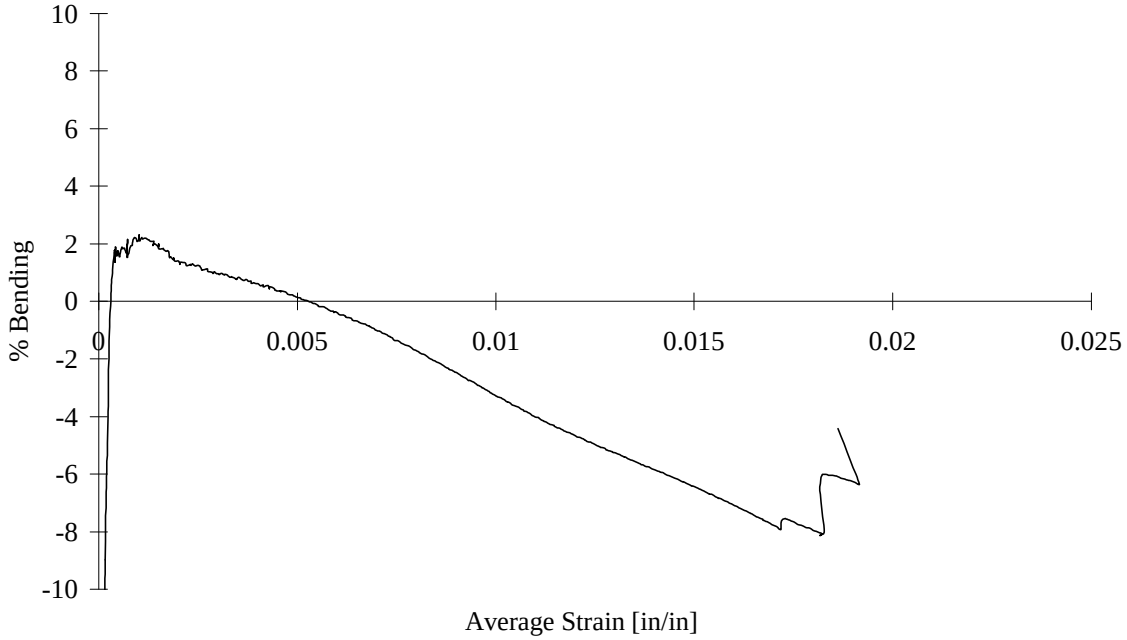

FIGURE C-58. TEST SPECIMEN AU705: UNTABBED, AS4/3501-6 CARBON/EPOXY $[90/0]_{7s}$ IITRI TEST FIXTURE

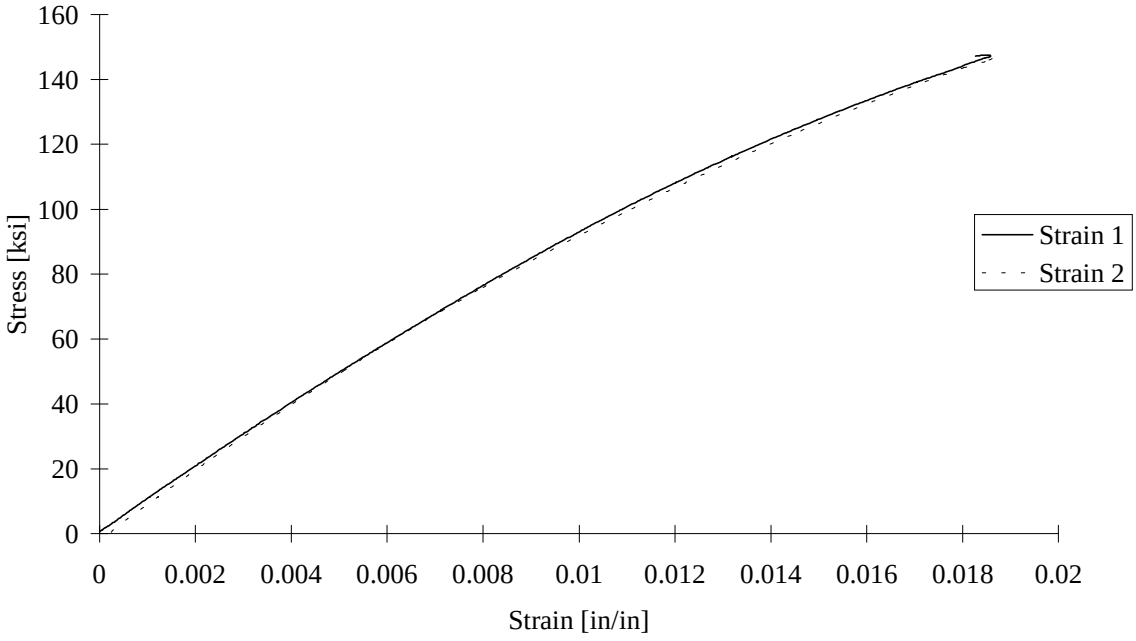

FIGURE C-59. TEST SPECIMEN AU706: UNTABBED, AS4/3501-6 CARBON/EPOXY $[90/0]_{7s}$ IITRI TEST FIXTURE

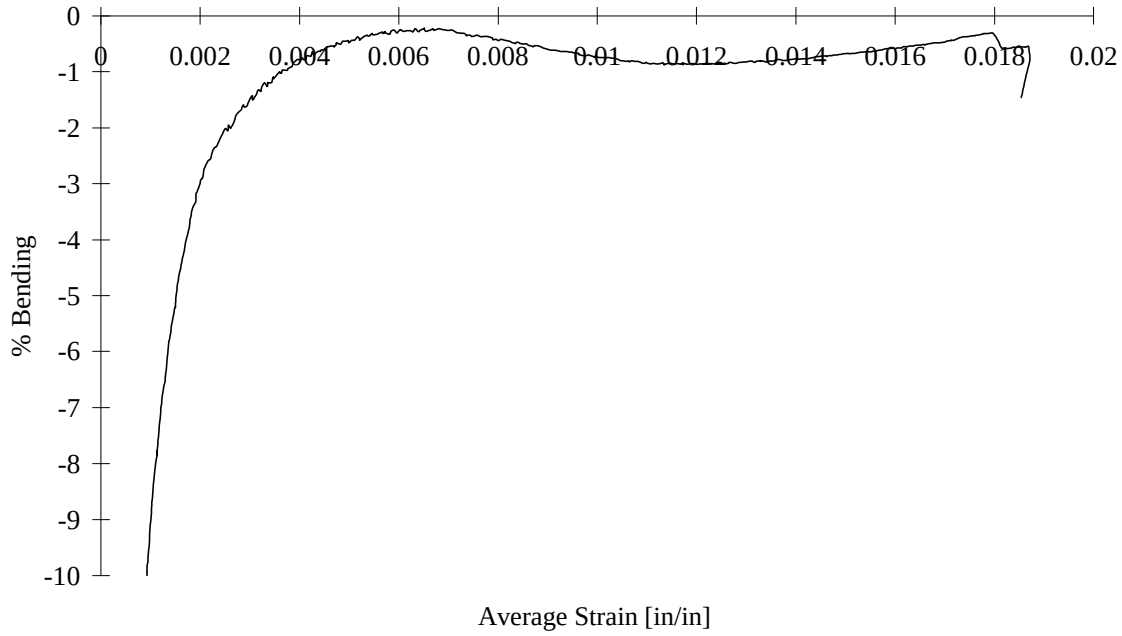

FIGURE C-60. TEST SPECIMEN AU706: UNTABBED, AS4/3501-6 CARBON/EPOXY $[90/0]_{7s}$ IITRI TEST FIXTURE

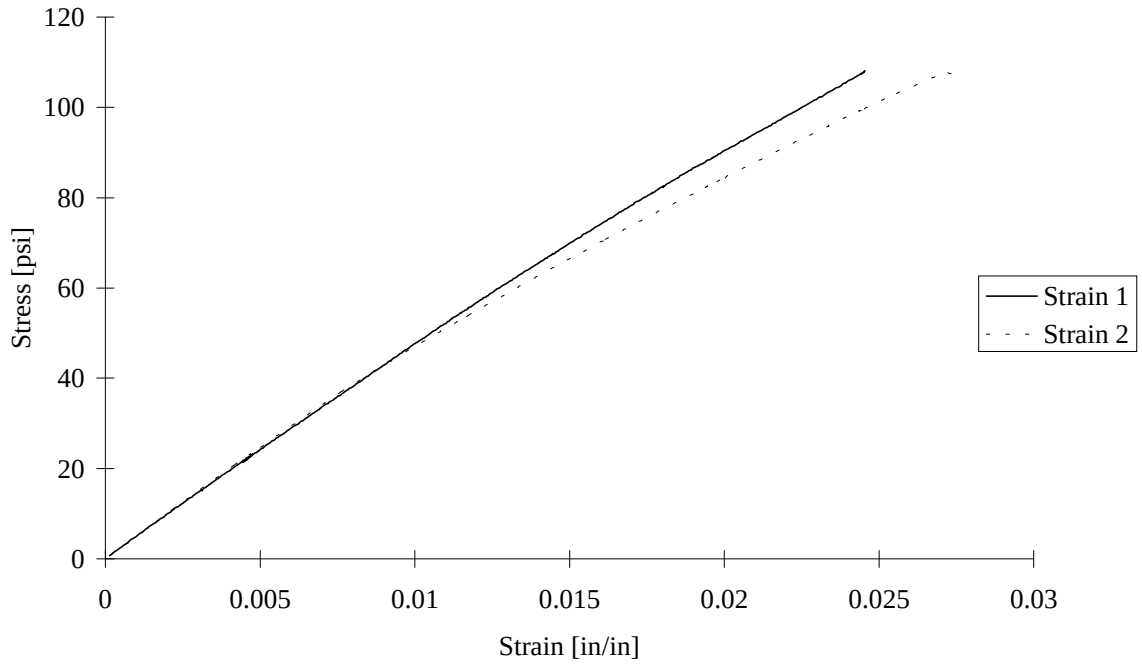

FIGURE C-61. TEST SPECIMEN GC01: S2/301-NCT GLASS/EPOXY $[90/0]_{5s}$ CLC-OR TEST FIXTURE

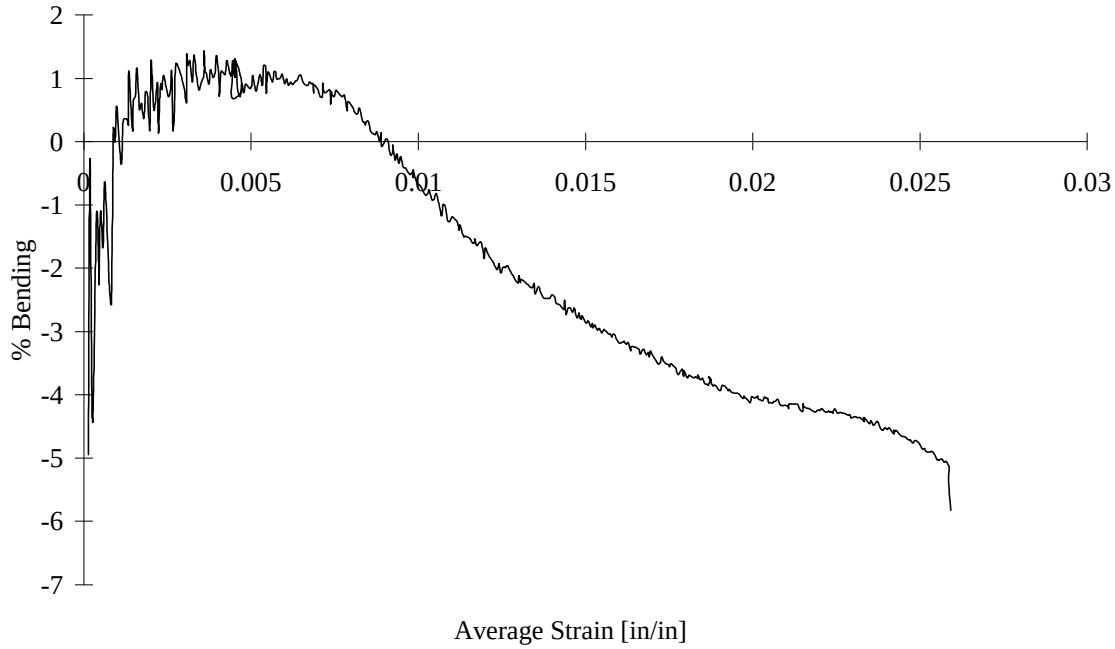

FIGURE C-62. TEST SPECIMEN GC01: S2/301-NCT GLASS/EPOXY $[90/0]_{5s}$ CLC-OR TEST FIXTURE

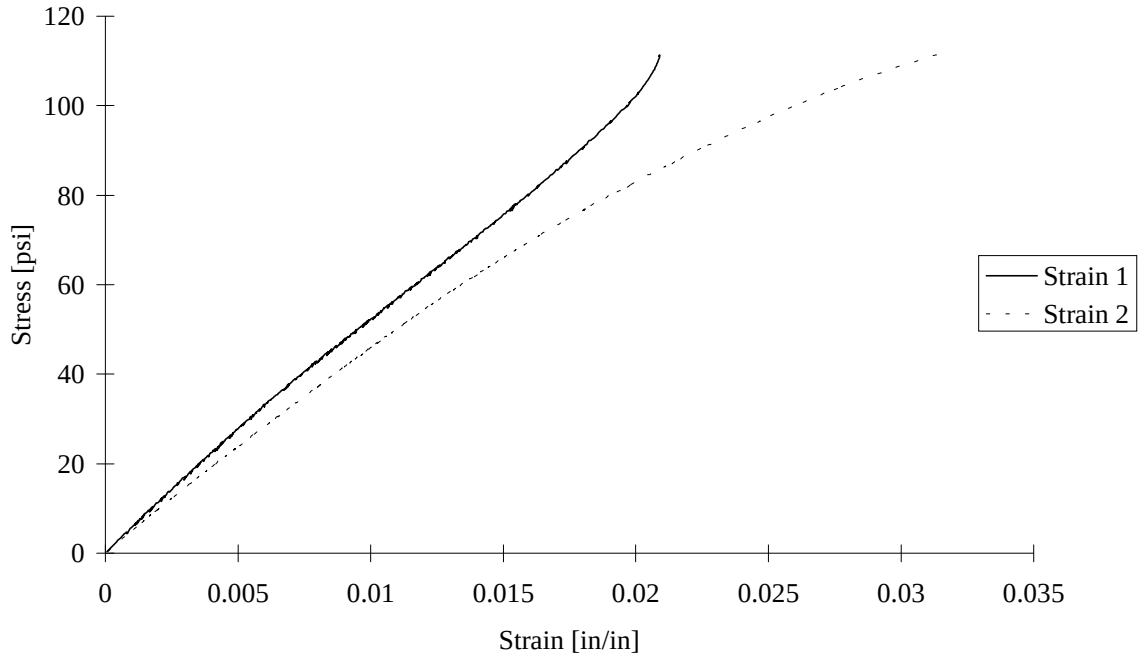

FIGURE C-63. TEST SPECIMEN GC02: S2/301-NCT GLASS/EPOXY $[90/0]_{5s}$ CLC-OR TEST FIXTURE

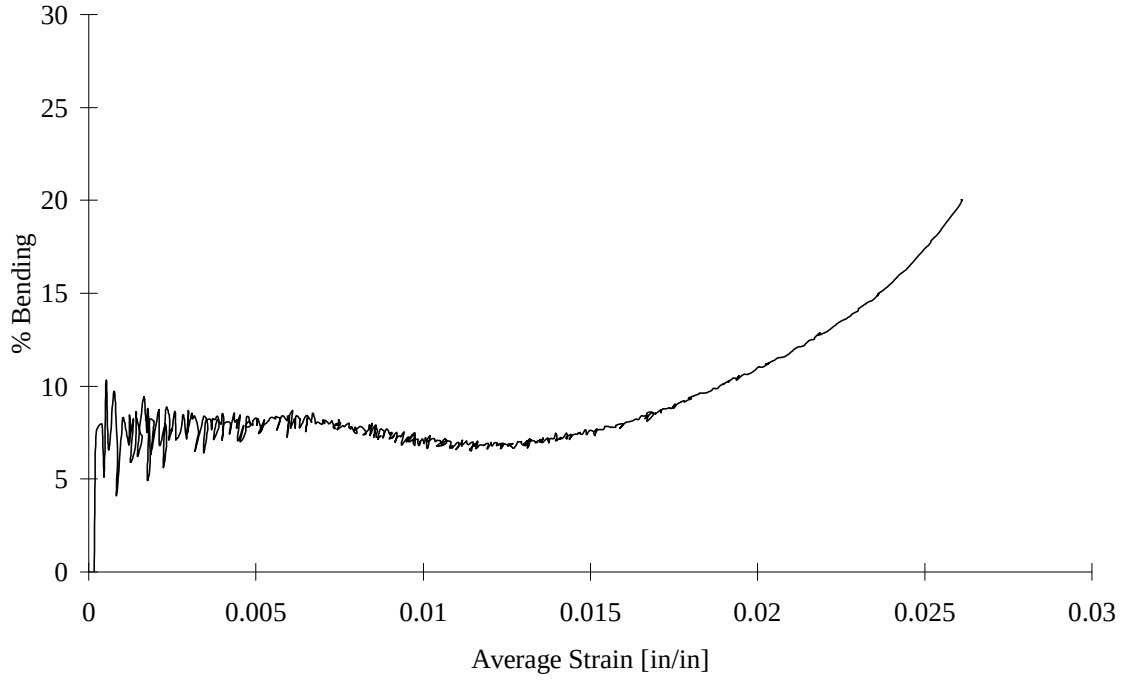

FIGURE C-64. TEST SPECIMEN GC02: S2/301-NCT GLASS/EPOXY $[90/0]_{5s}$ CLC-OR TEST FIXTURE

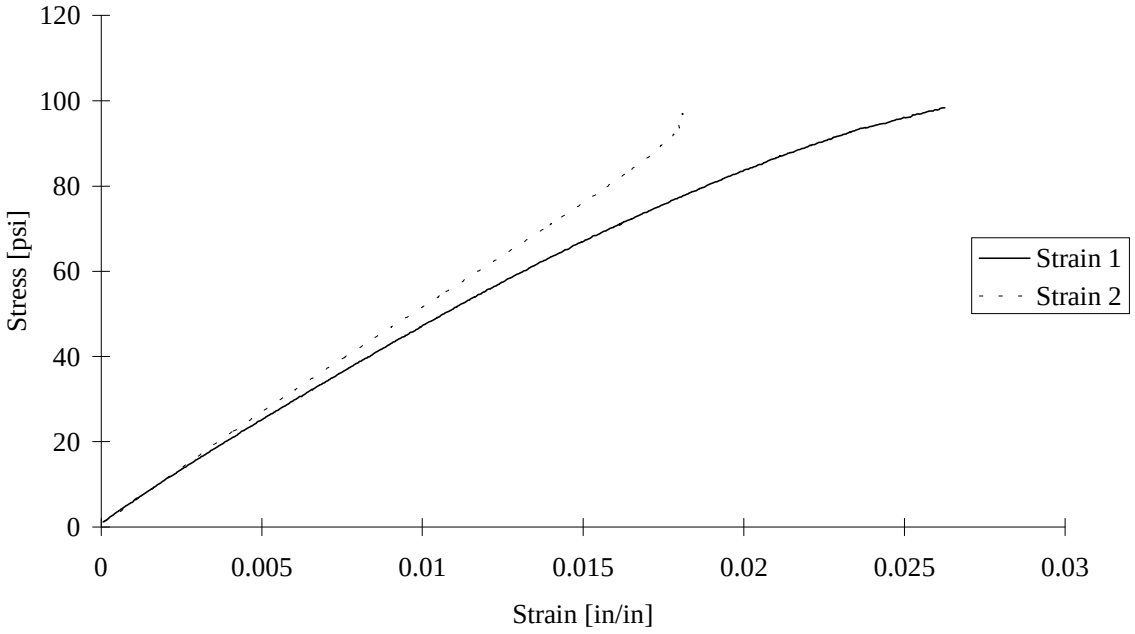

FIGURE C-65. TEST SPECIMEN GC03: S2/301-NCT GLASS/EPOXY $[90/0]_{5s}$
CLC-OR TEST FIXTURE

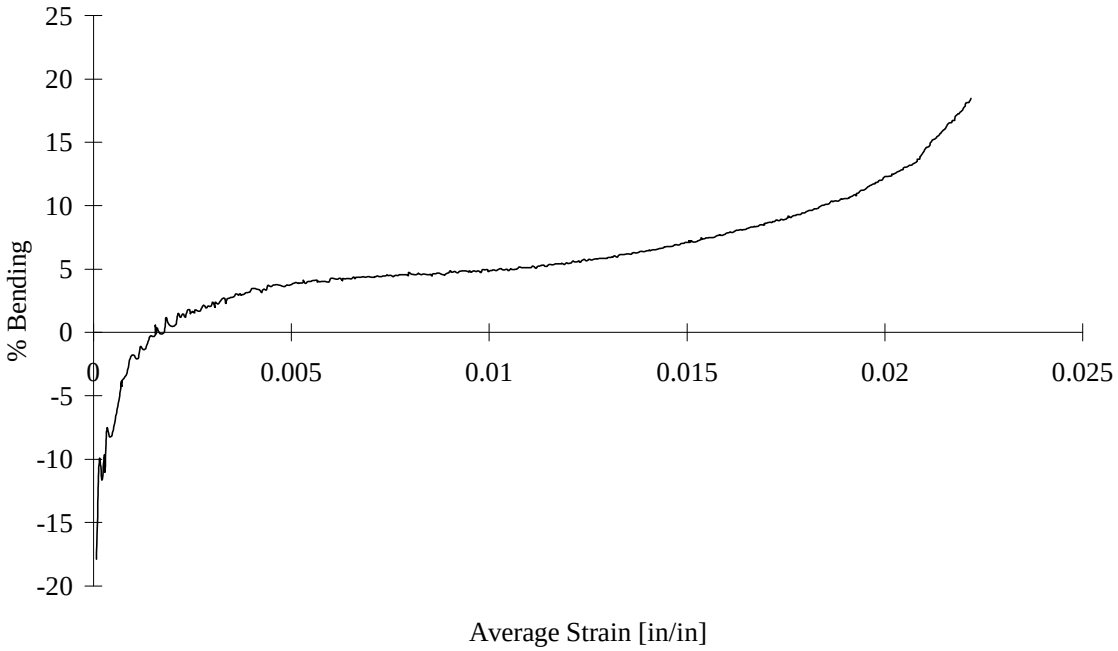

FIGURE C-66. TEST SPECIMEN GC03: S2/301-NCT GLASS/EPOXY $[90/0]_{5s}$
CLC-OR TEST FIXTURE

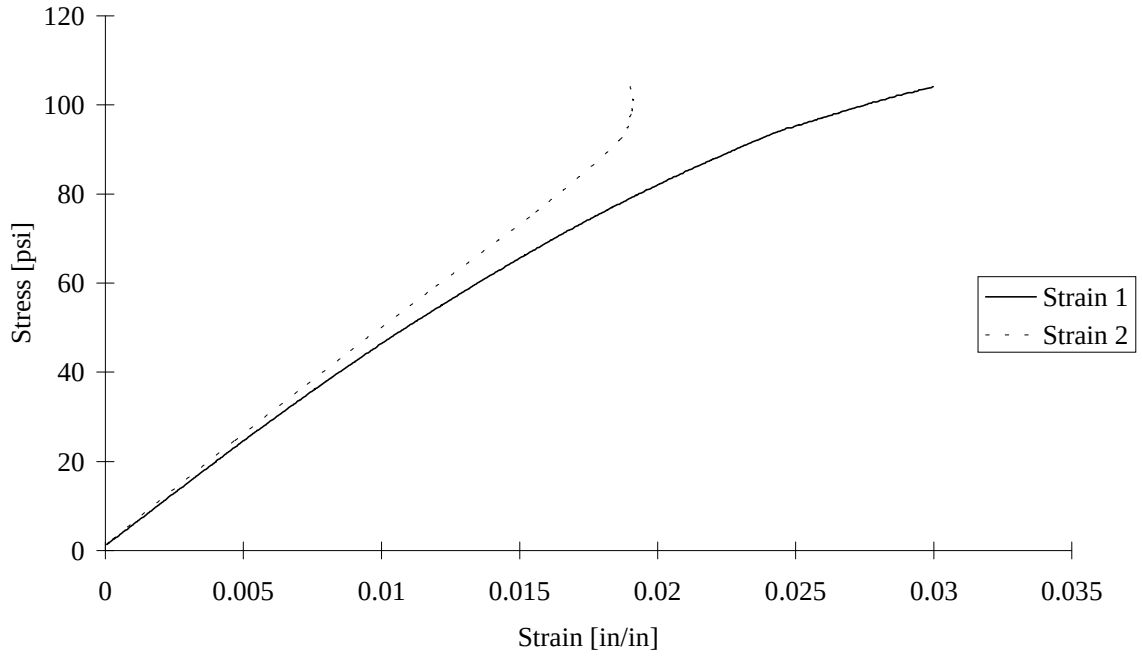

FIGURE C-67. TEST SPECIMEN GC04: S2/301-NCT GLASS/EPOXY $[90/0]_{5s}$
CLC-OR TEST FIXTURE

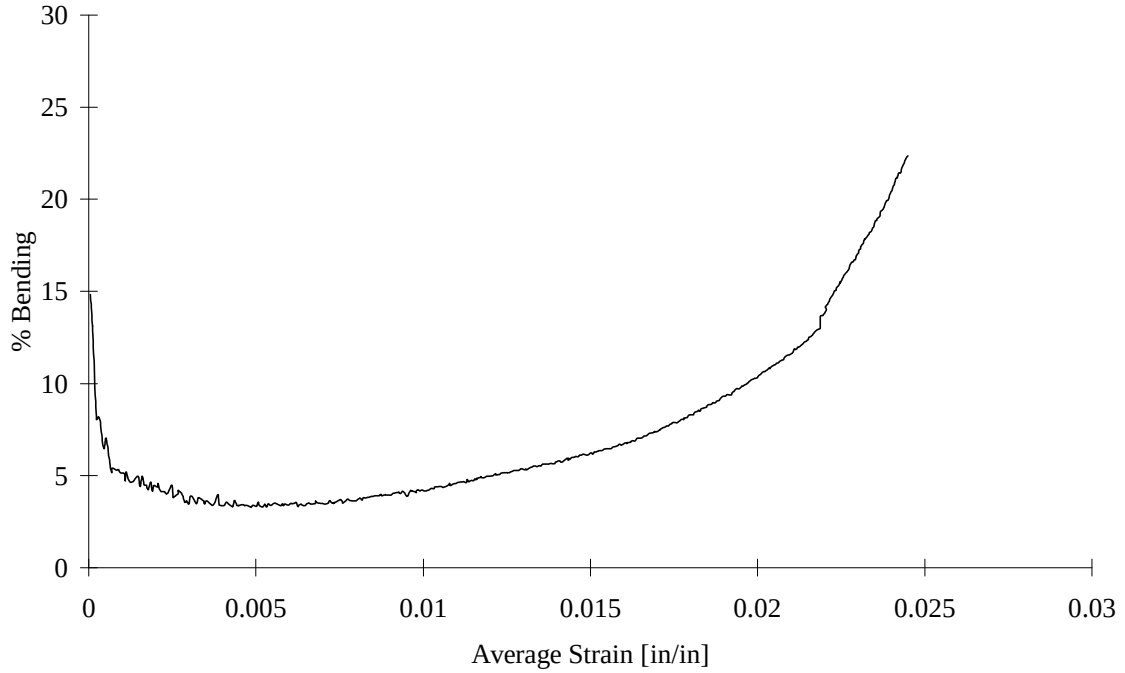

FIGURE C-68. TEST SPECIMEN GC04: S2/301-NCT GLASS/EPOXY $[90/0]_{5s}$
CLC-OR TEST FIXTURE

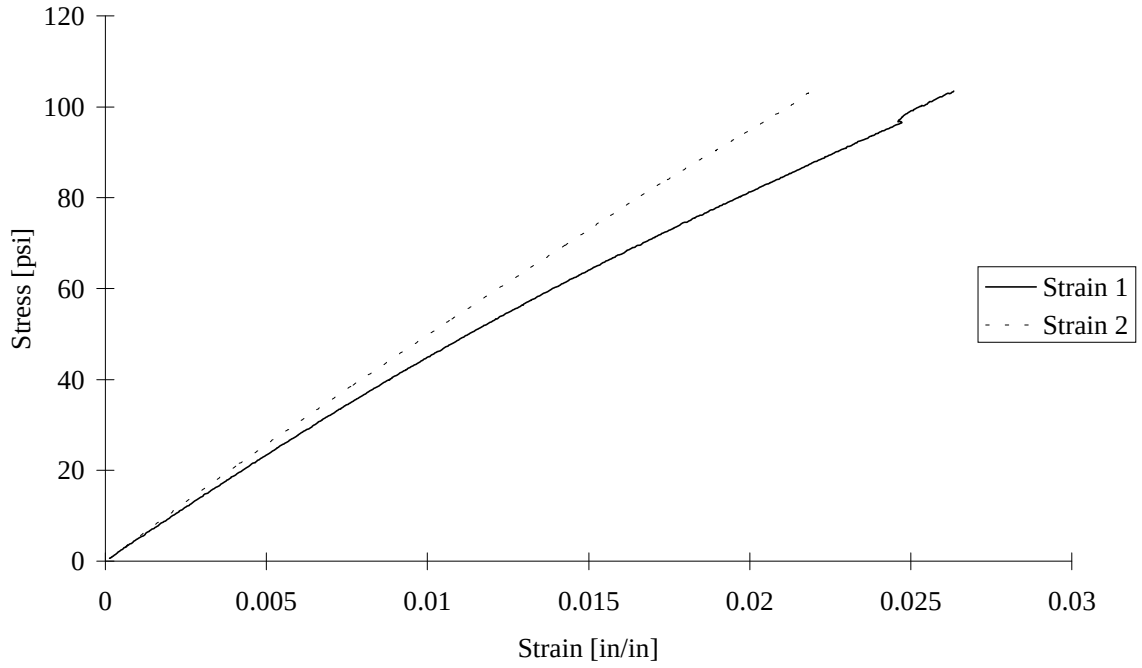

FIGURE C-69. TEST SPECIMEN GC05: S2/301-NCT GLASS/EPOXY $[90/0]_{5S}$
CLC-OR TEST FIXTURE

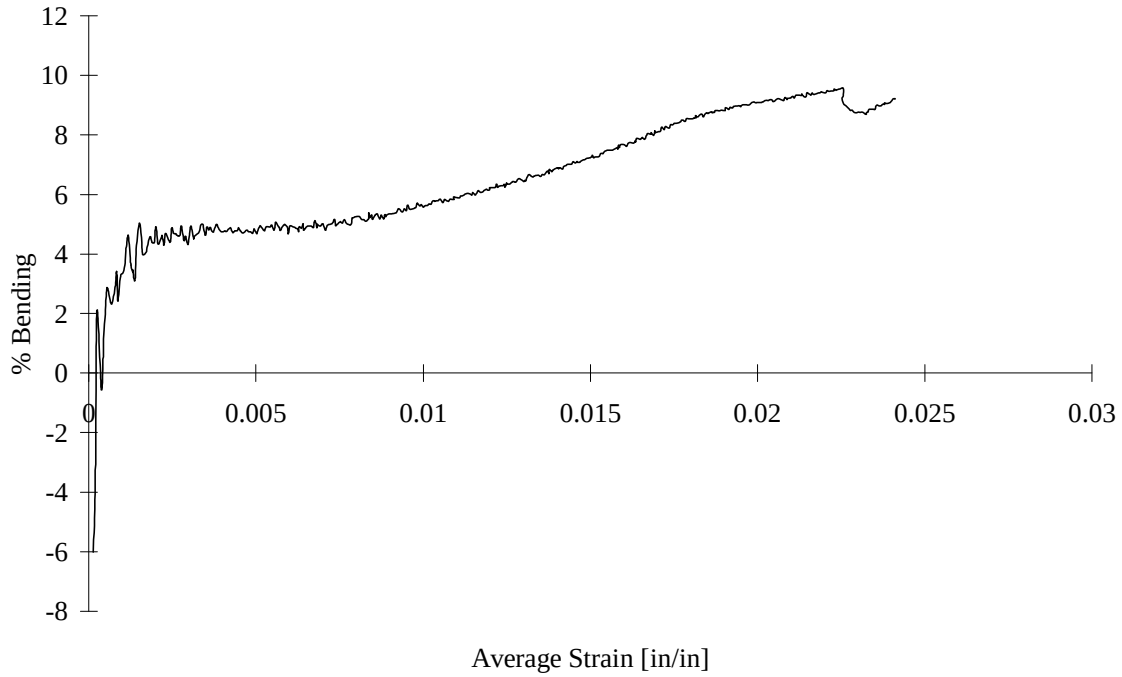

FIGURE C-70. TEST SPECIMEN GC05: S2/301-NCT GLASS/EPOXY $[90/0]_{5s}$
CLC-OR TEST FIXTURE

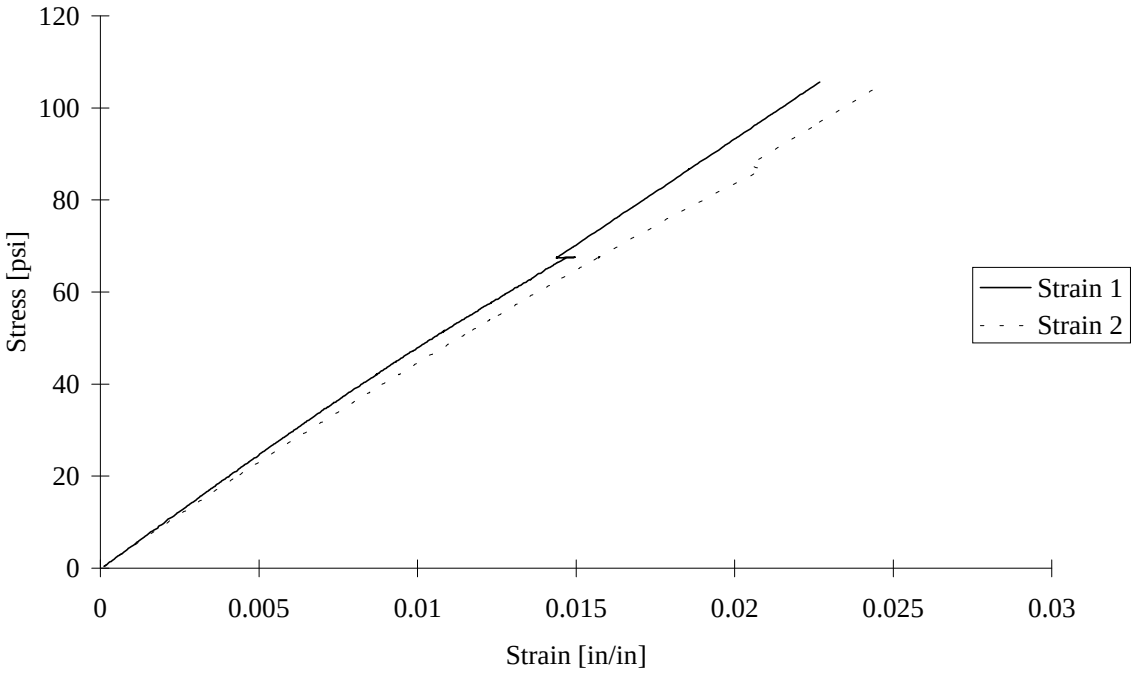

FIGURE C-71. TEST SPECIMEN GC06: S2/301-NCT GLASS/EPOXY $[90/0]_{5s}$ CLC-OR TEST FIXTURE

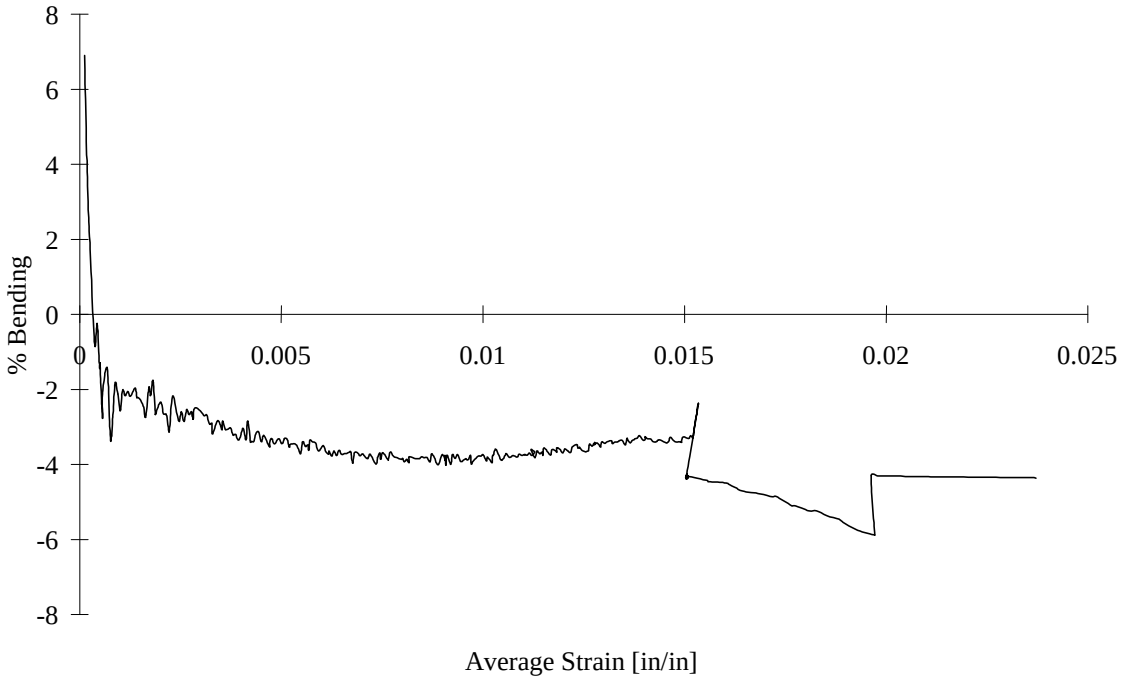

FIGURE C-72. TEST SPECIMEN GC06: S2/301-NCT GLASS/EPOXY $[90/0]_{5s}$ CLC-OR TEST FIXTURE

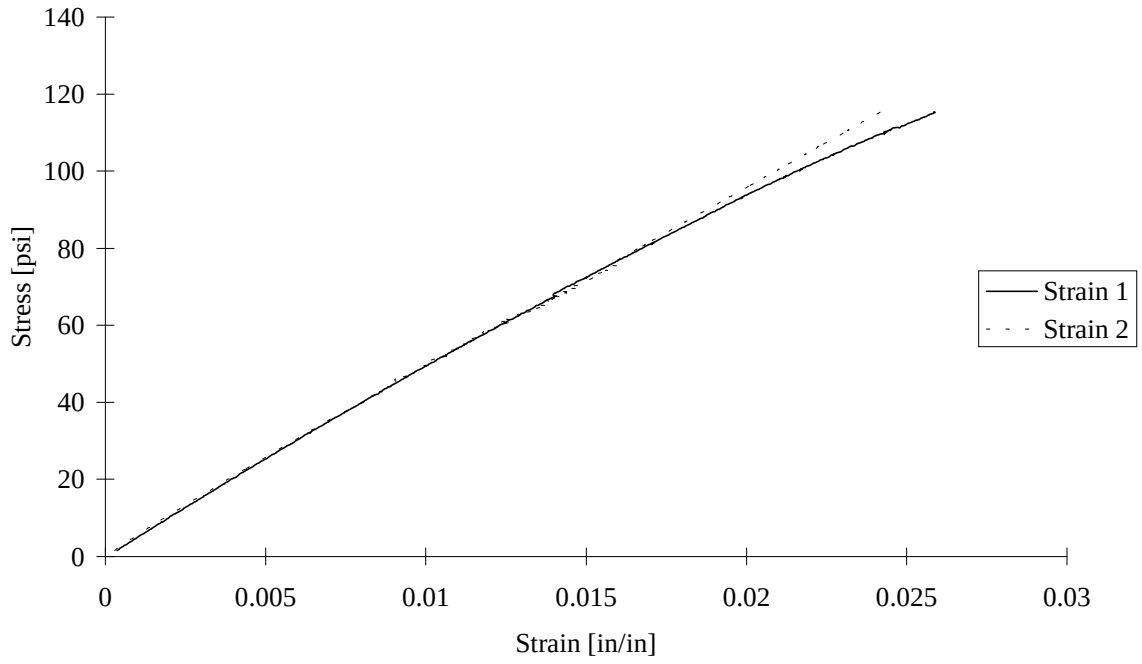

FIGURE C-73. TEST SPECIMEN GC07: S2/301-NCT GLASS/EPOXY $[90/0]_{5s}$ CLC-OR TEST FIXTURE

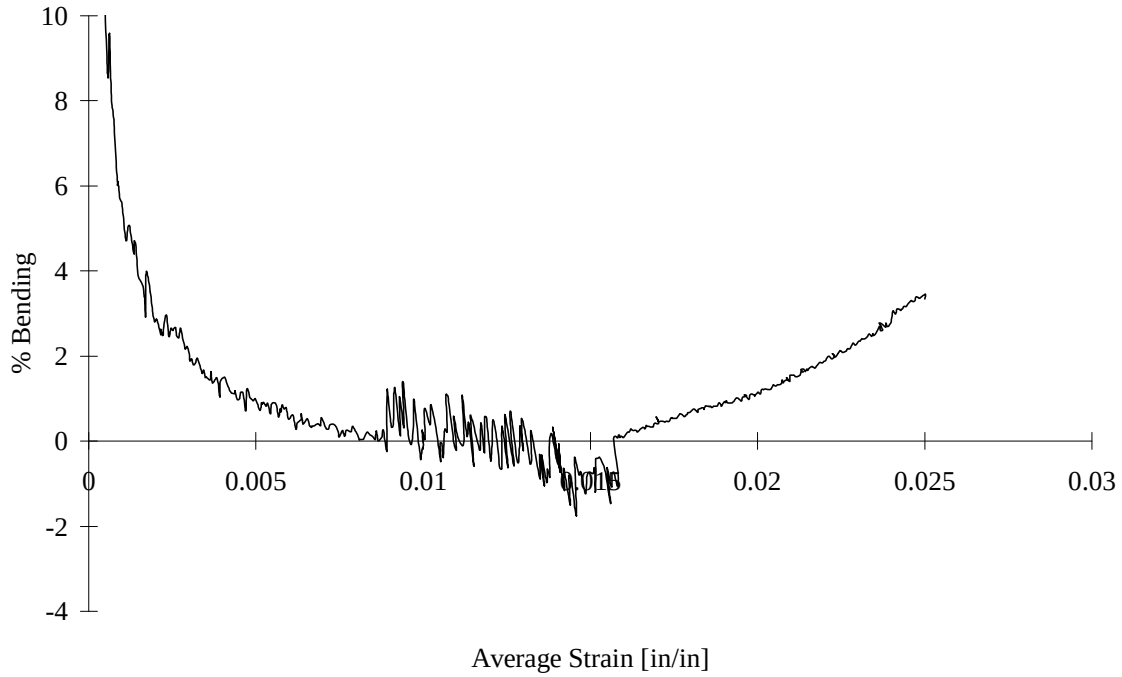

FIGURE C-74. TEST SPECIMEN GC07: S2/301-NCT GLASS/EPOXY $[90/0]_{5s}$ CLC-OR TEST FIXTURE

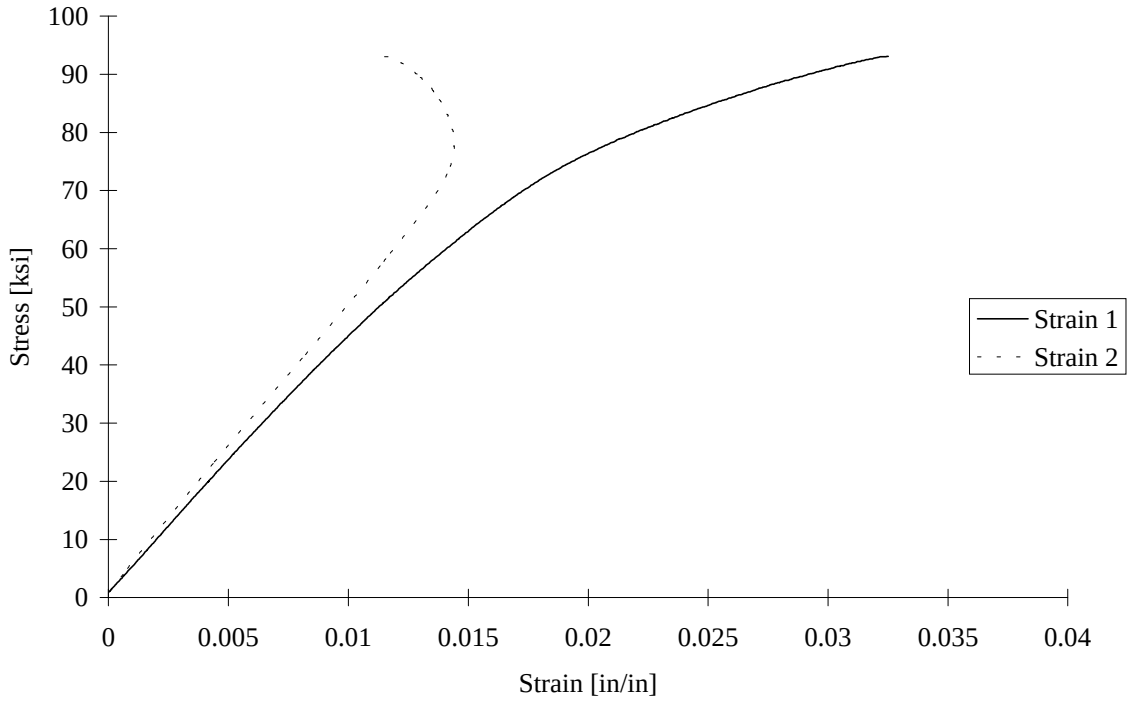

FIGURE C-75. TEST SPECIMEN GU01: UNTABBED, S2/301-NCT GLASS/EPOXY $[90/0]_{5s}$ IITRI TEST FIXTURE

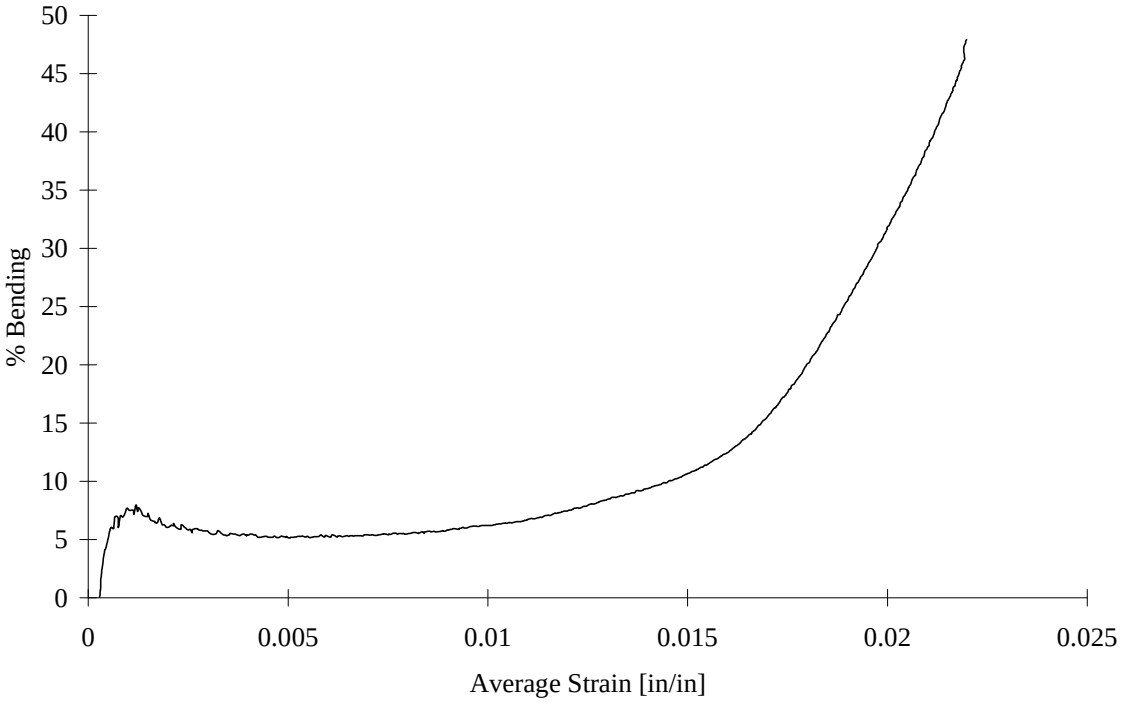

FIGURE C-76. TEST SPECIMEN GU01: UNTABBED, S2/301-NCT GLASS/EPOXY $[90/0]_{5s}$ IITRI TEST FIXTURE

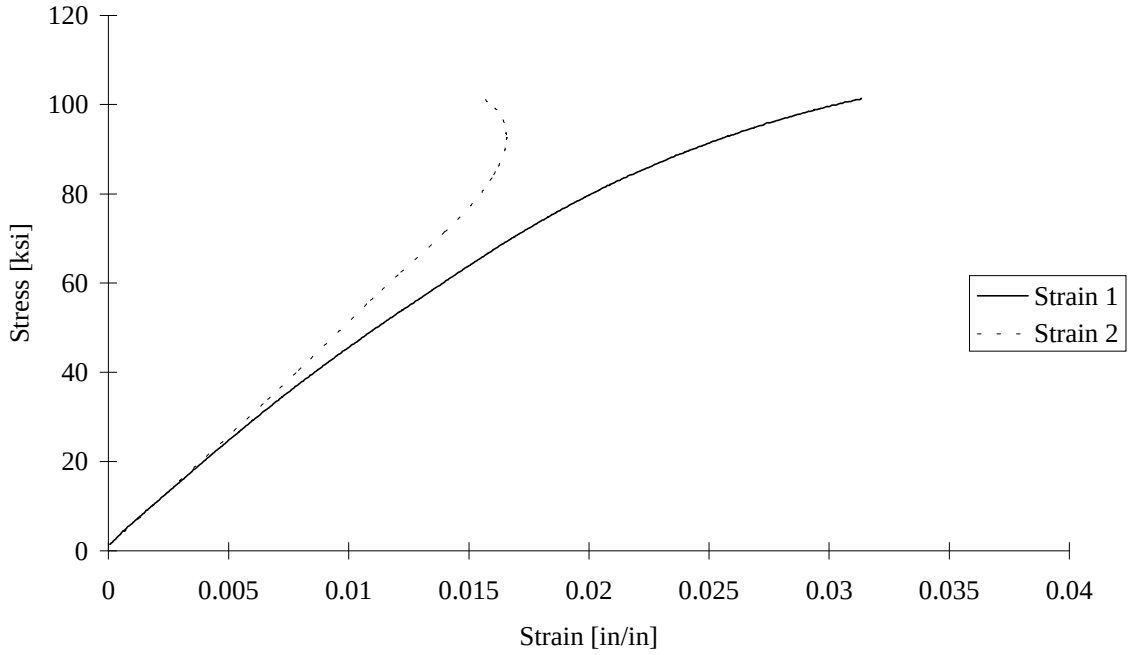

FIGURE C-77. TEST SPECIMEN GU02: UNTABBED, S2/301-NCT GLASS/EPOXY $[90/0]_{5s}$ IITRI TEST FIXTURE

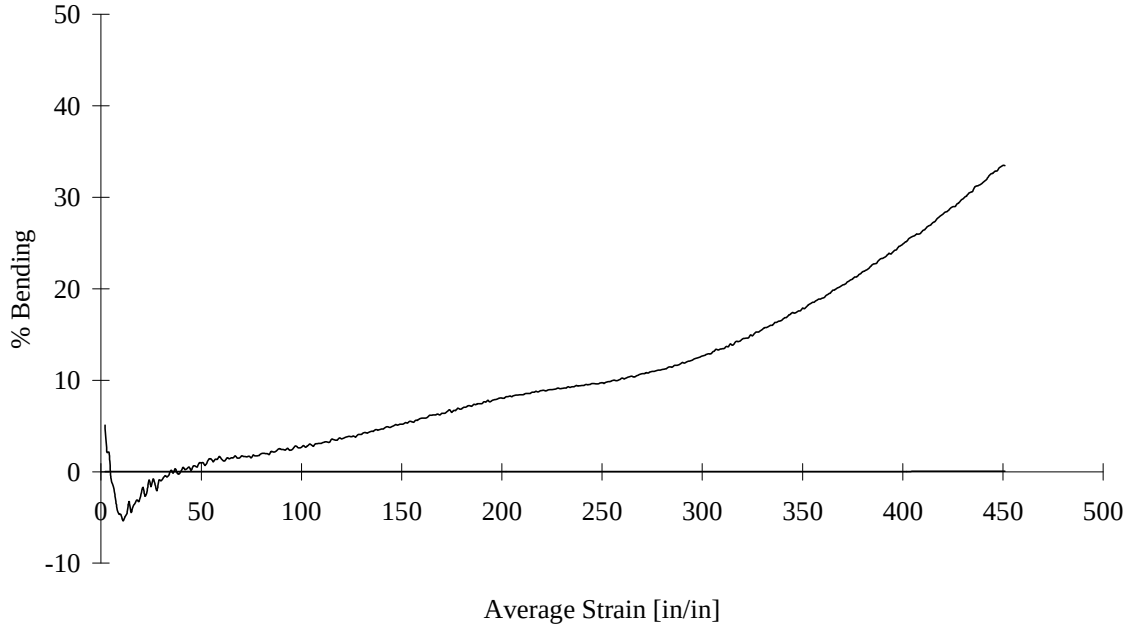

FIGURE C-78. TEST SPECIMEN GU02: UNTABBED, S2/301-NCT GLASS/EPOXY $[90/0]_{5s}$ IITRI TEST FIXTURE

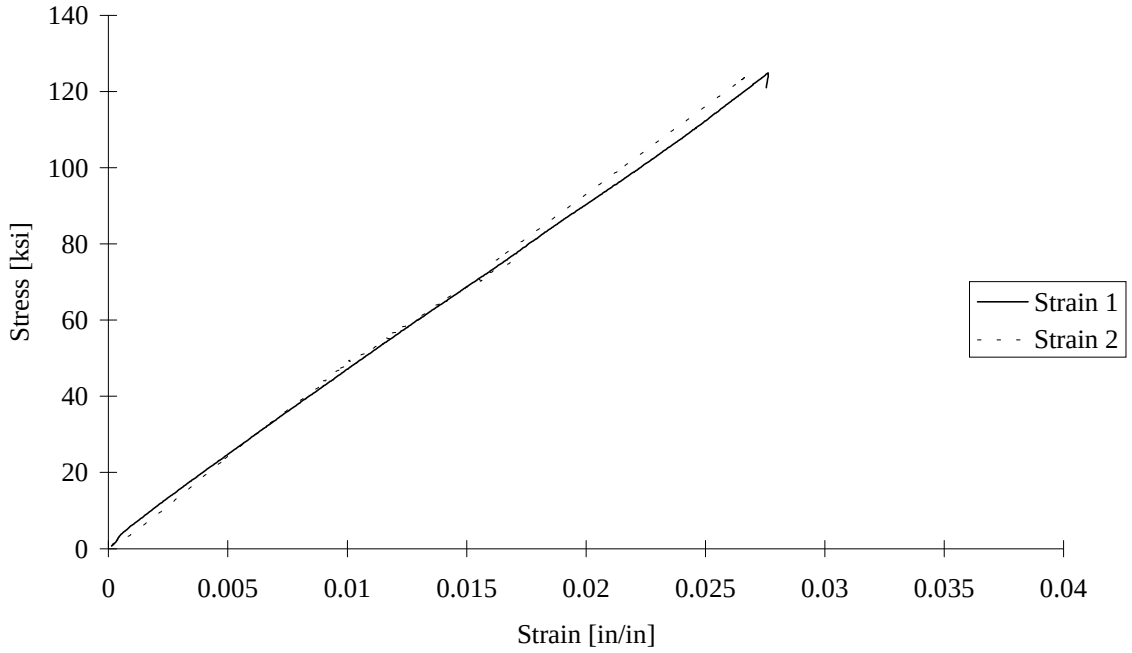

FIGURE C-79. TEST SPECIMEN GU03: UNTABBED, S2/301-NCT GLASS/EPOXY $[90/0]_{5s}$ IITRI TEST FIXTURE

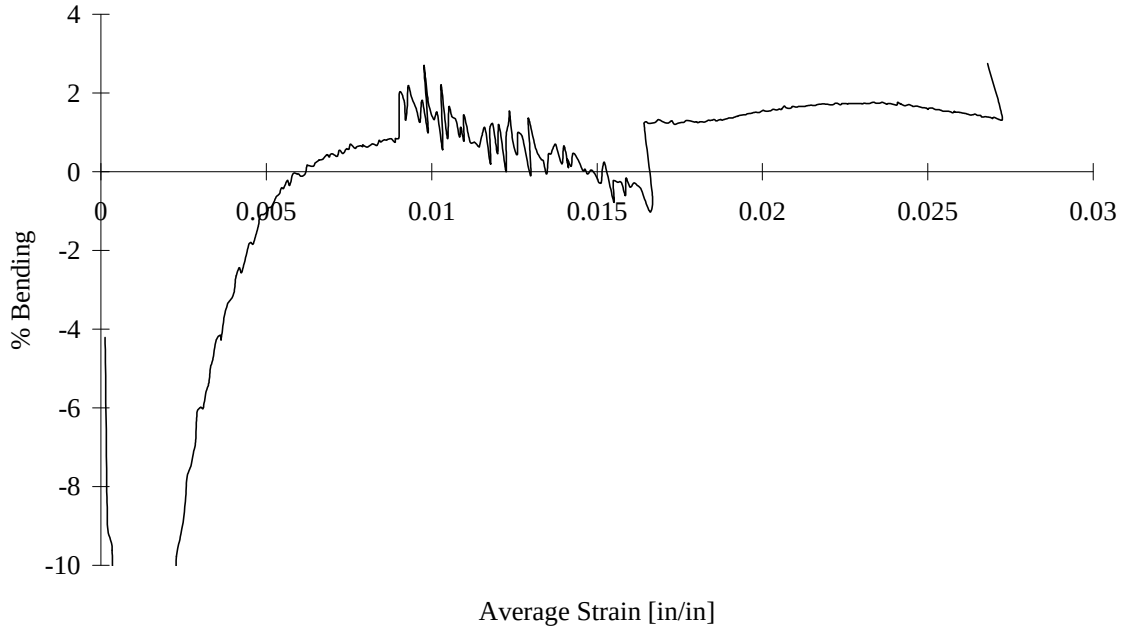

FIGURE C-80. TEST SPECIMEN GU03: UNTABBED, S2/301-NCT GLASS/EPOXY $[90/0]_{5s}$ IITRI TEST FIXTURE

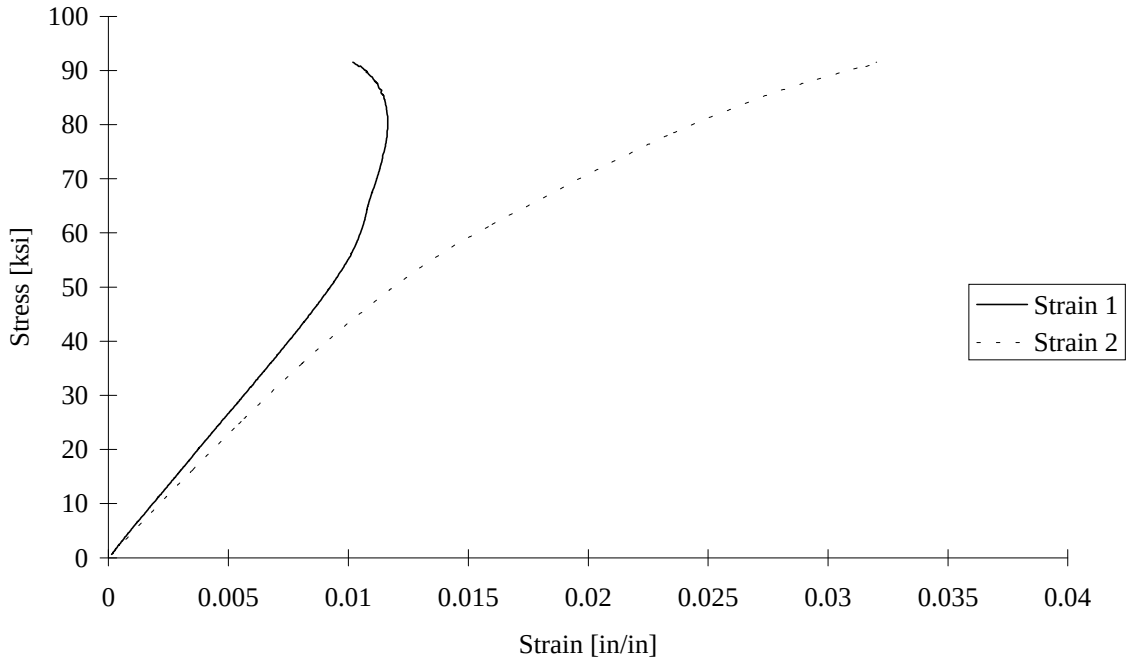

FIGURE C-81. TEST SPECIMEN GU04: UNTABBED, S2/301-NCT GLASS/EPOXY $[90/0]_{5s}$ IITRI TEST FIXTURE

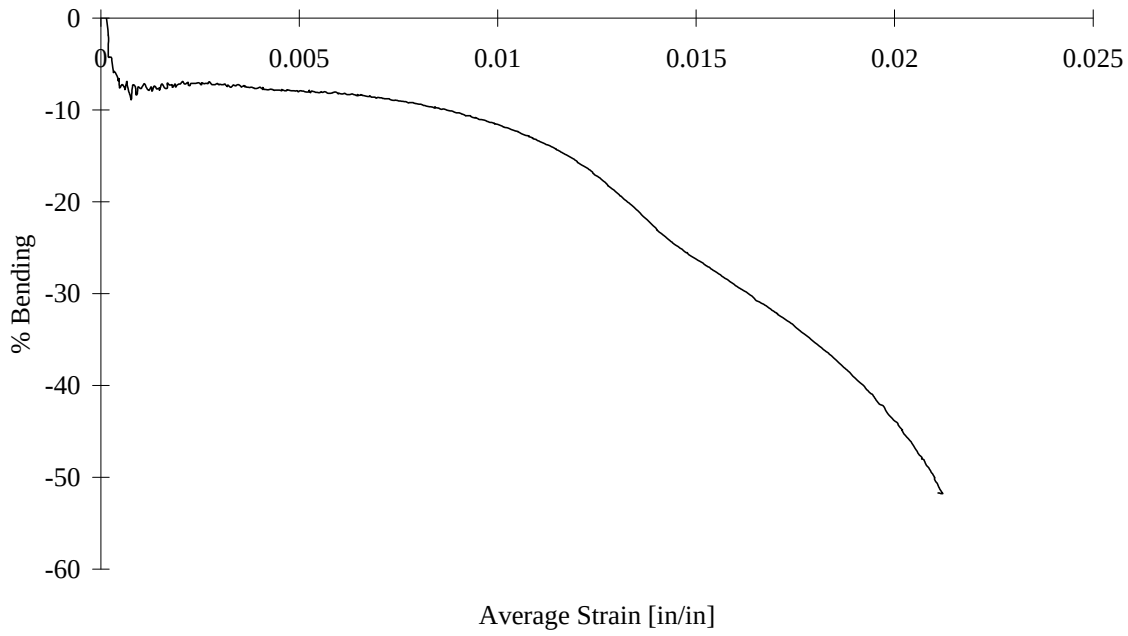

FIGURE C-82. TEST SPECIMEN GU04: UNTABBED, S2/301-NCT GLASS/EPOXY $[90/0]_{5s}$ IITRI TEST FIXTURE

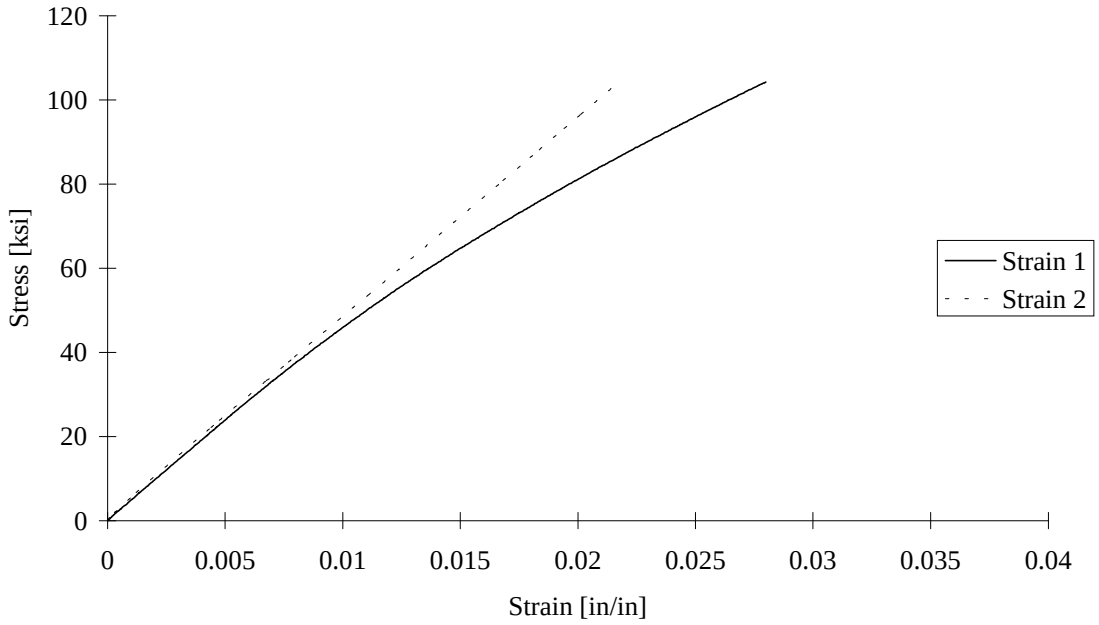

FIGURE C-83. TEST SPECIMEN GU05: UNTABBED, S2/301-NCT GLASS/EPOXY $[90/0]_{5s}$ IITRI TEST FIXTURE

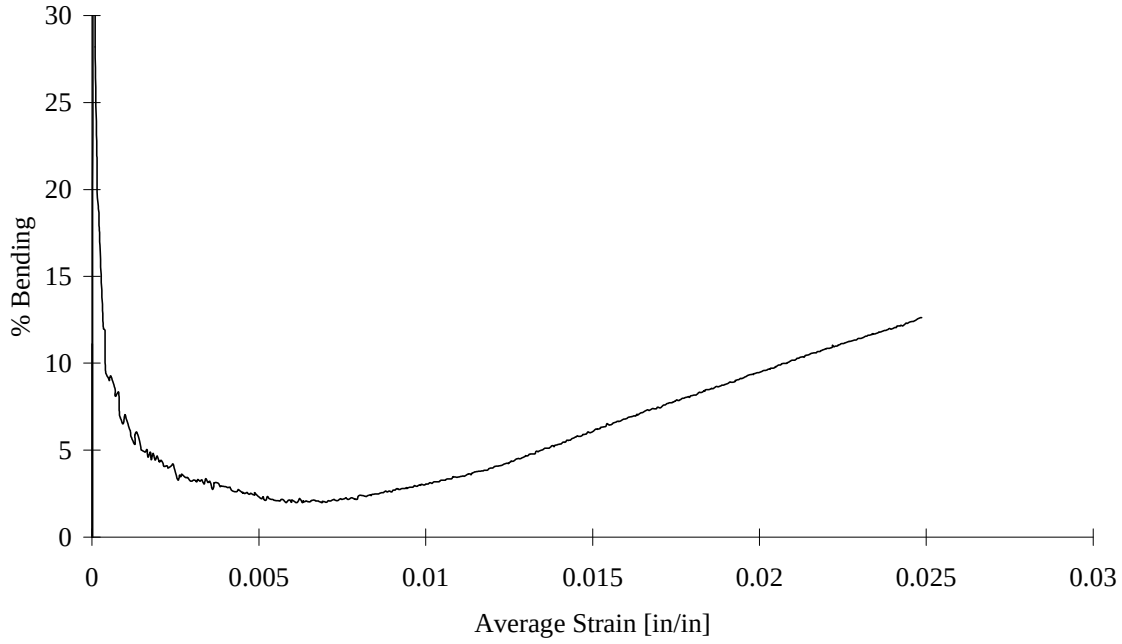

FIGURE C-84. TEST SPECIMEN GU05: UNTABBED, S2/301-NCT GLASS/EPOXY $[90/0]_{5s}$ IITRI TEST FIXTURE

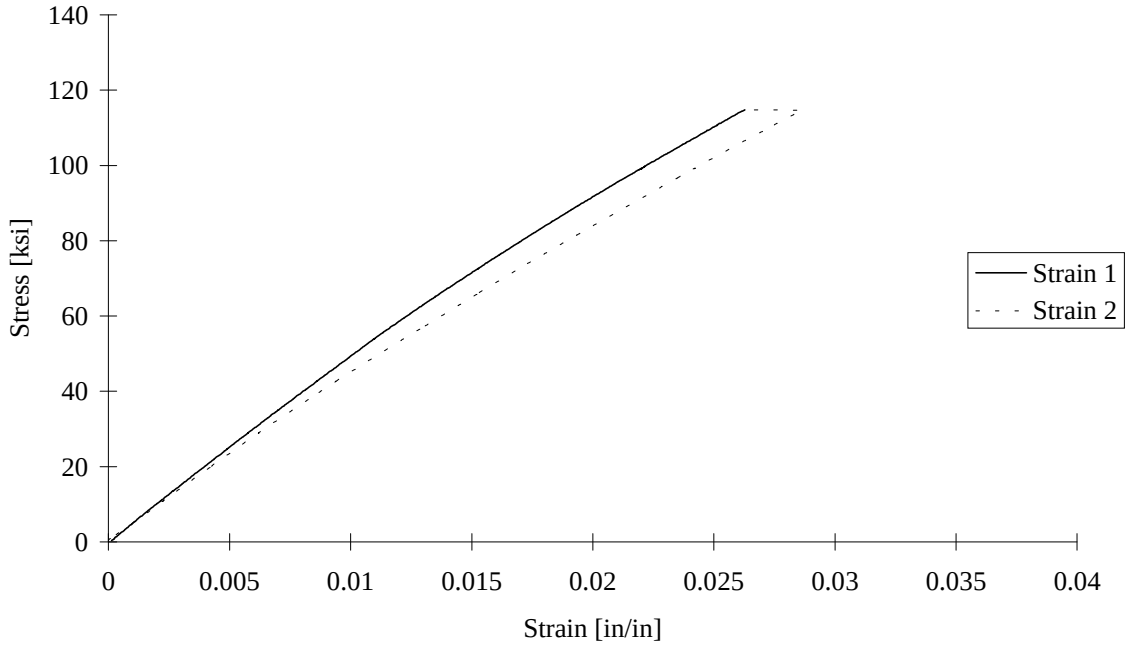

FIGURE C-85. TEST SPECIMEN GU06: UNTABBED, S2/301-NCT GLASS/EPOXY $[90/0]_{5s}$ IITRI TEST FIXTURE

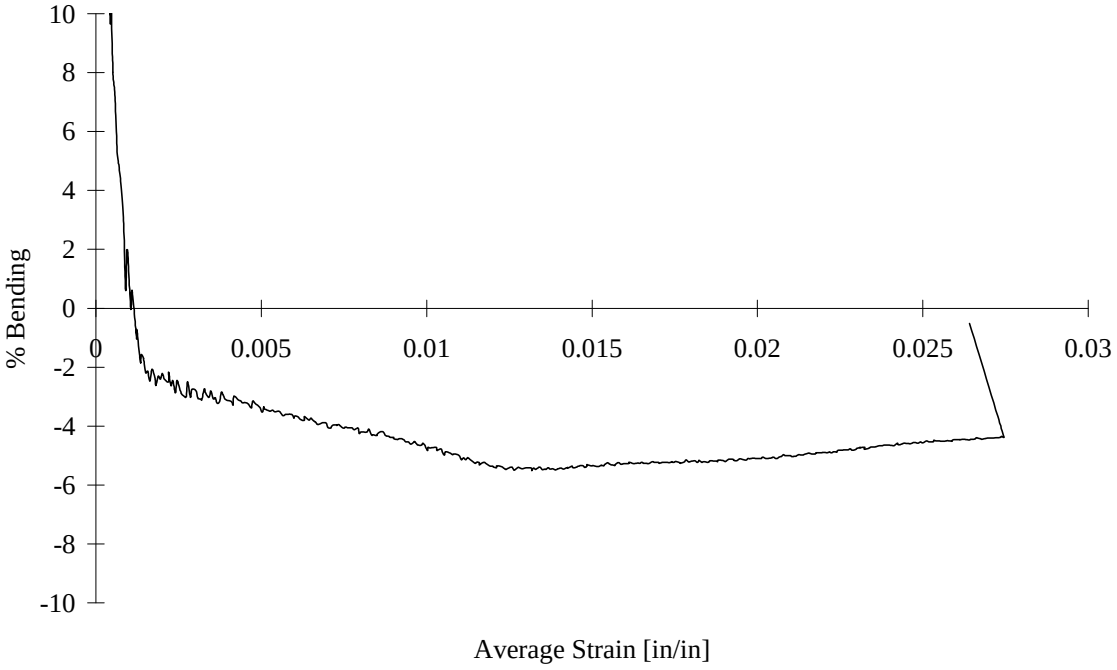

FIGURE C-86. TEST SPECIMEN GU06: UNTABBED, S2/301-NCT GLASS/EPOXY $[90/0]_{5s}$ IITRI TEST FIXTURE

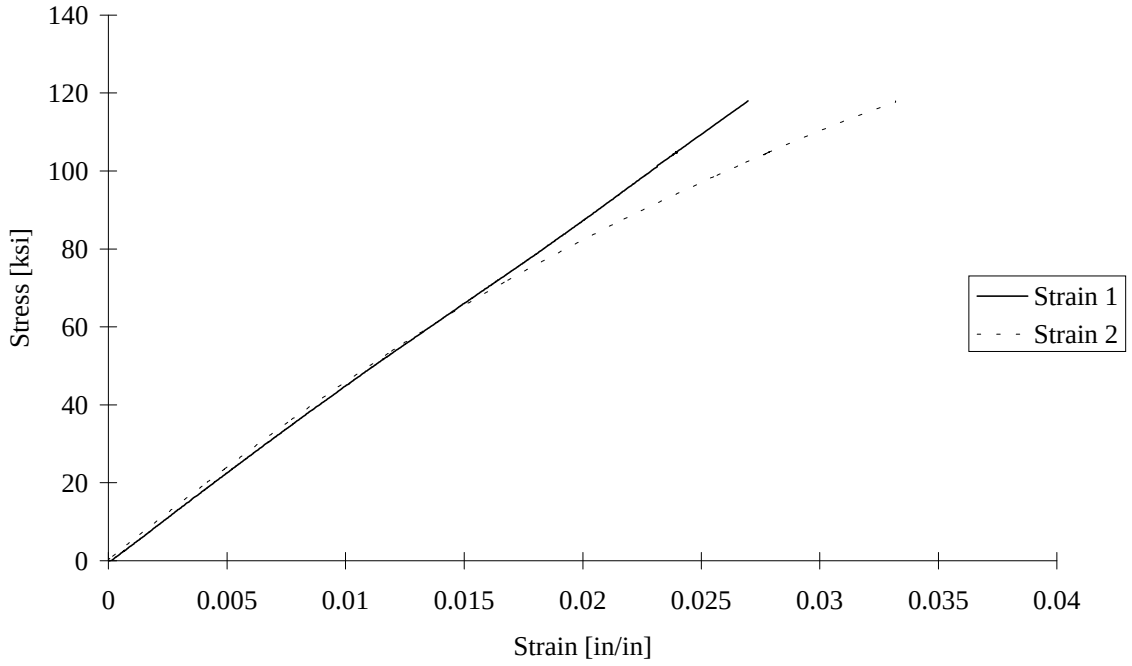

FIGURE C-87. TEST SPECIMEN GU07: UNTABBED, S2/301-NCT GLASS/EPOXY $[90/0]_{5s}$ IITRI TEST FIXTURE

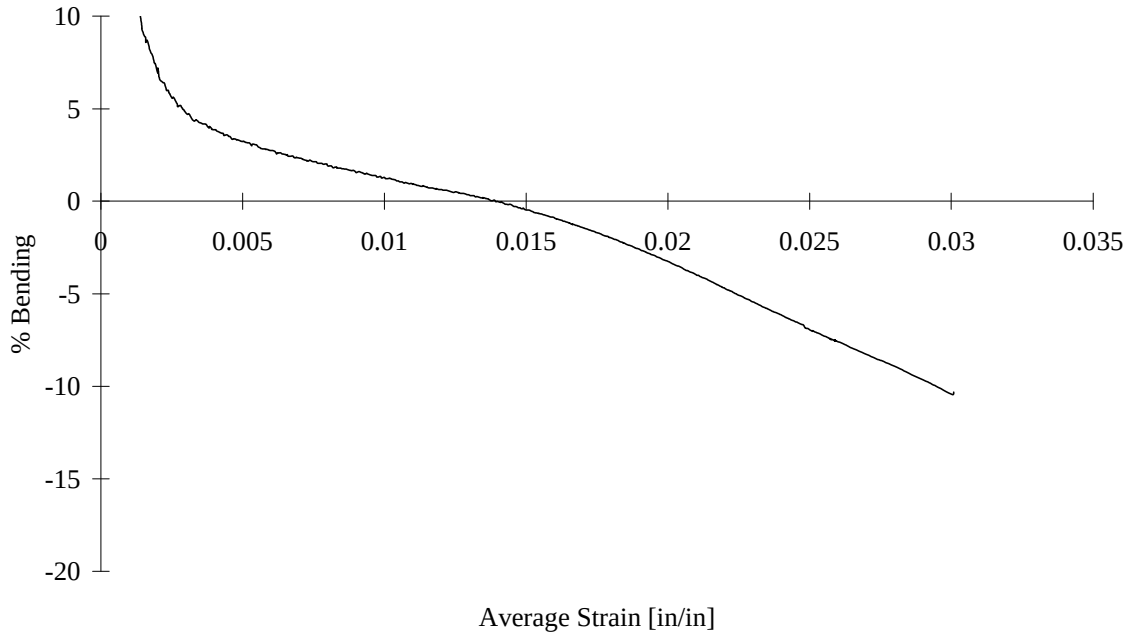

FIGURE C-88. TEST SPECIMEN GU07: UNTABBED, S2/301-NCT GLASS/EPOXY $[90/0]_{5s}$ IITRI TEST FIXTURE

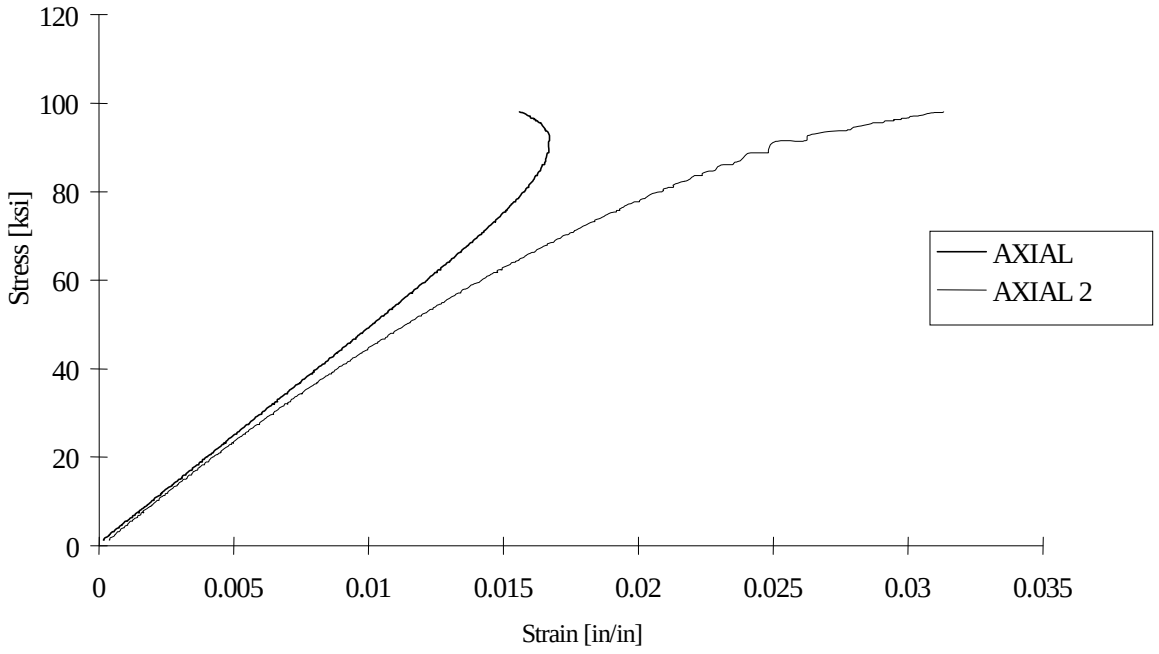

FIGURE C-89. TEST SPECIMEN GT01: TABBED, S2/301-NCT GLASS/EPOXY $[90/0]_{5s}$ IITRI TEST FIXTURE

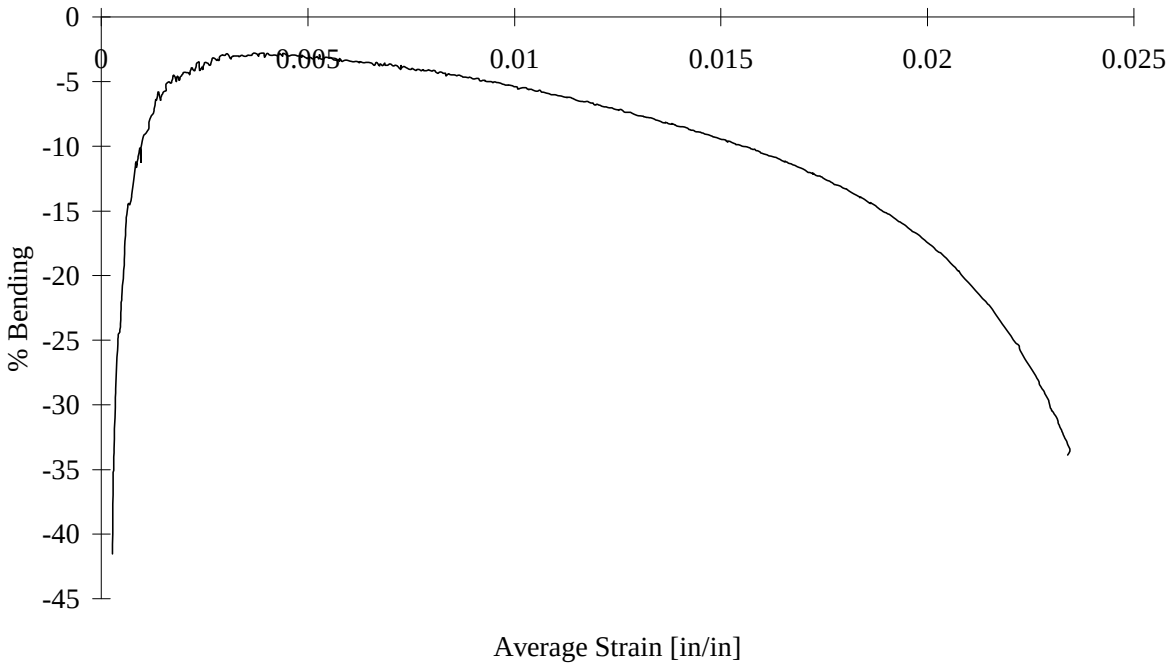

FIGURE C-90. TEST SPECIMEN GT01: TABBED, S2/301-NCT GLASS/EPOXY $[90/0]_{5s}$ IITRI TEST FIXTURE

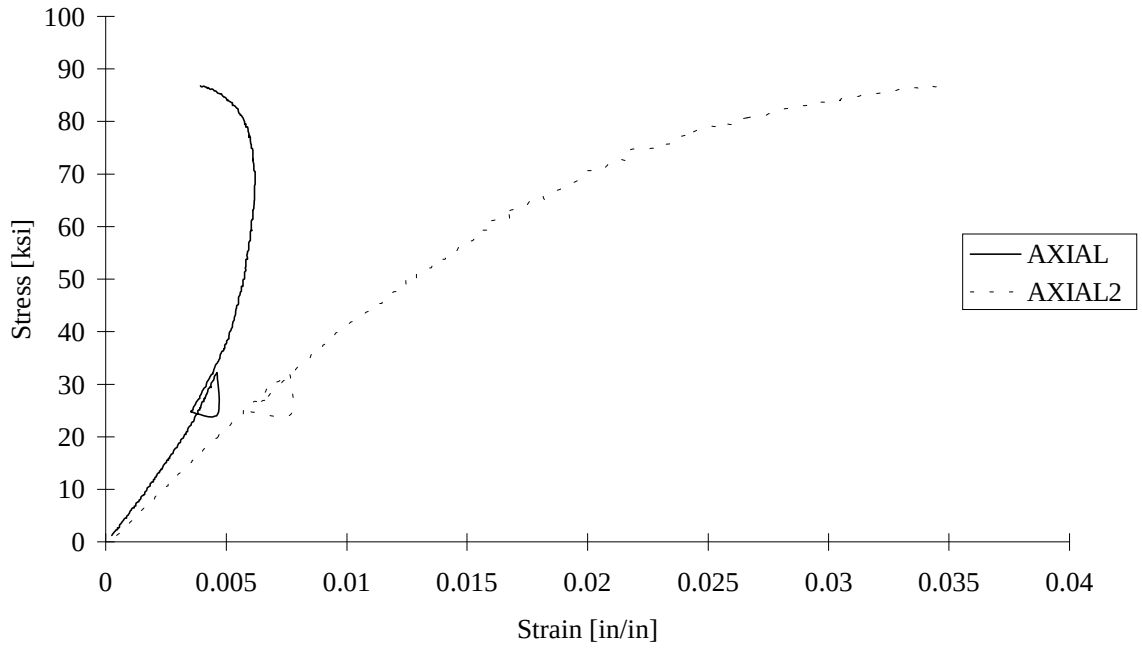

FIGURE C-91. TEST SPECIMEN GT02: TABBED, S2/301-NCT GLASS/EPOXY $[90/0]_{5s}$ IITRI TEST FIXTURE

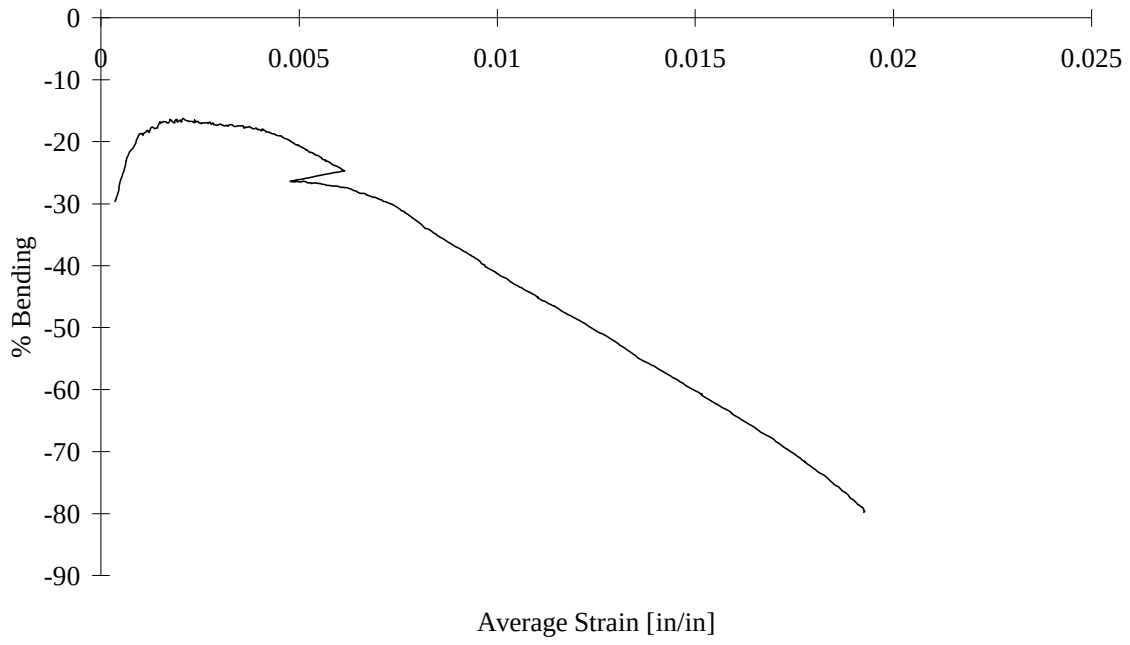

FIGURE C-92. TEST SPECIMEN GT02: TABBED, S2/301-NCT GLASS/EPOXY $[90/0]_{5s}$ IITRI TEST FIXTURE

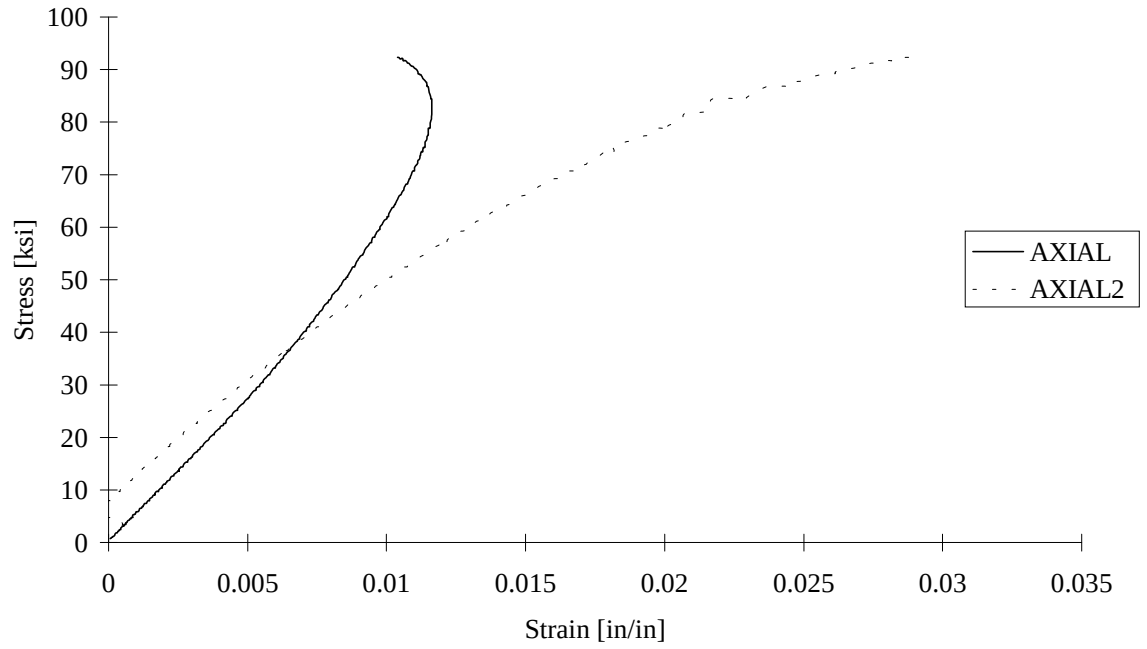

FIGURE C-93. TEST SPECIMEN GT03: TABBED, S2/301-NCT GLASS/EPOXY $[90/0]_{5s}$ IITRI TEST FIXTURE

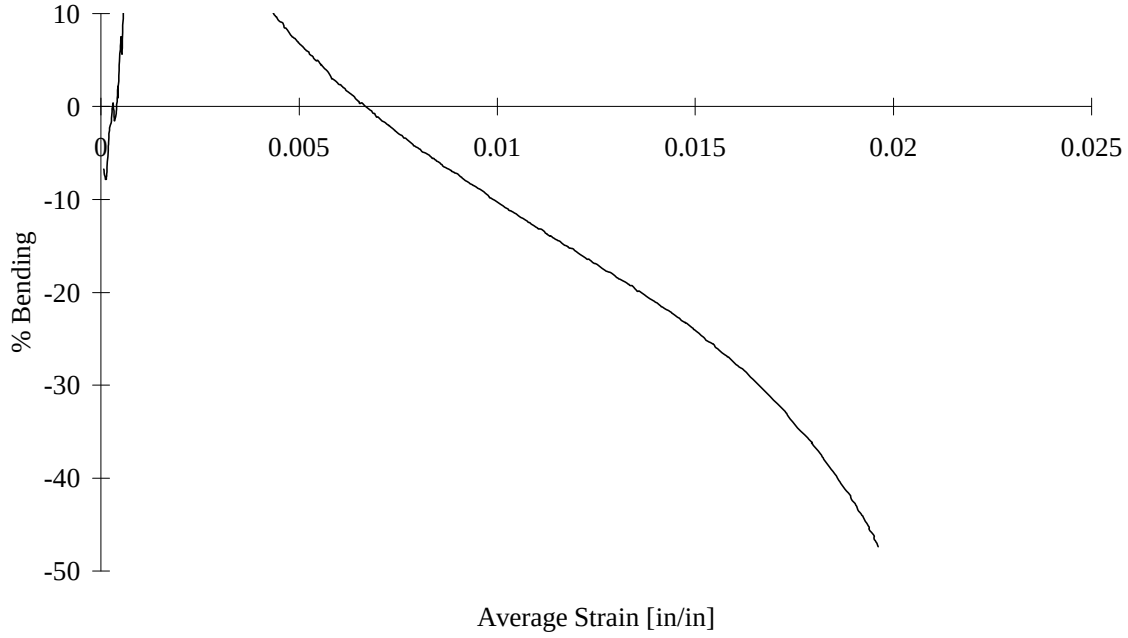

FIGURE C-94. TEST SPECIMEN GT03: TABBED, S2/301-NCT GLASS/EPOXY $[90/0]_{5s}$ IITRI TEST FIXTURE

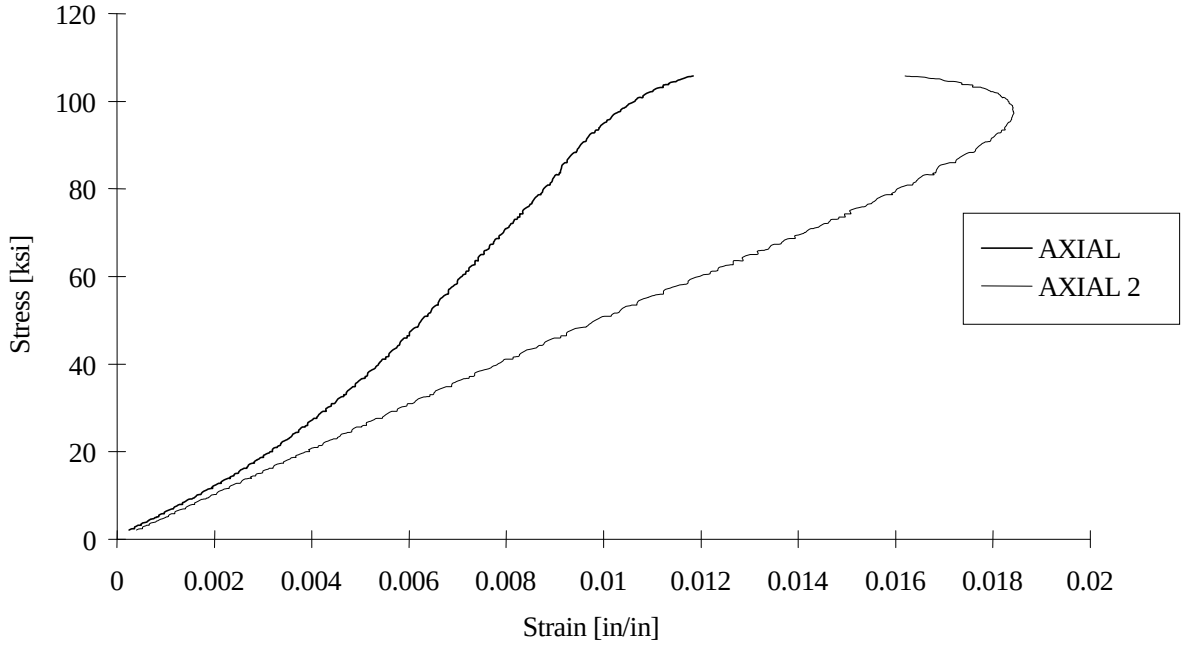

FIGURE C-95. TEST SPECIMEN GT04: TABBED, S2/301-NCT GLASS/EPOXY $[90/0]_{5s}$ IITRI TEST FIXTURE

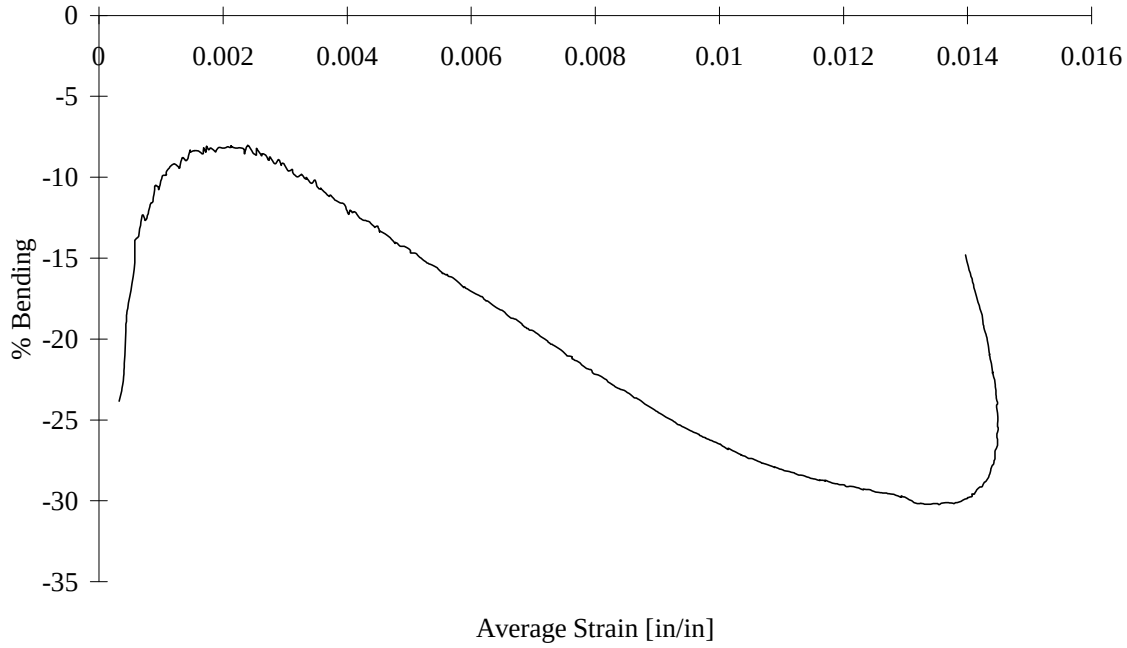

FIGURE C-96. TEST SPECIMEN GT04: TABBED, S2/301-NCT GLASS/EPOXY $[90/0]_{5s}$ IITRI TEST FIXTURE

APPENDIX D—SPECIMEN DATA FROM COMPARATIVE TESTING

D.1 SPECIMEN IDENTIFICATION CODES—BOEING SPECIMENS.

A name was given to each test specimen to specify the test fixture used to test the specimen, the fiber the specimen was made of, the laminate orientation, and the number of the individual specimen. This nomenclature is described, below. The test fixture designation is given first so that the specimen name will begin with a letter instead of a number. This was done to prevent problems when storing the specimen data on a DOS based computer.

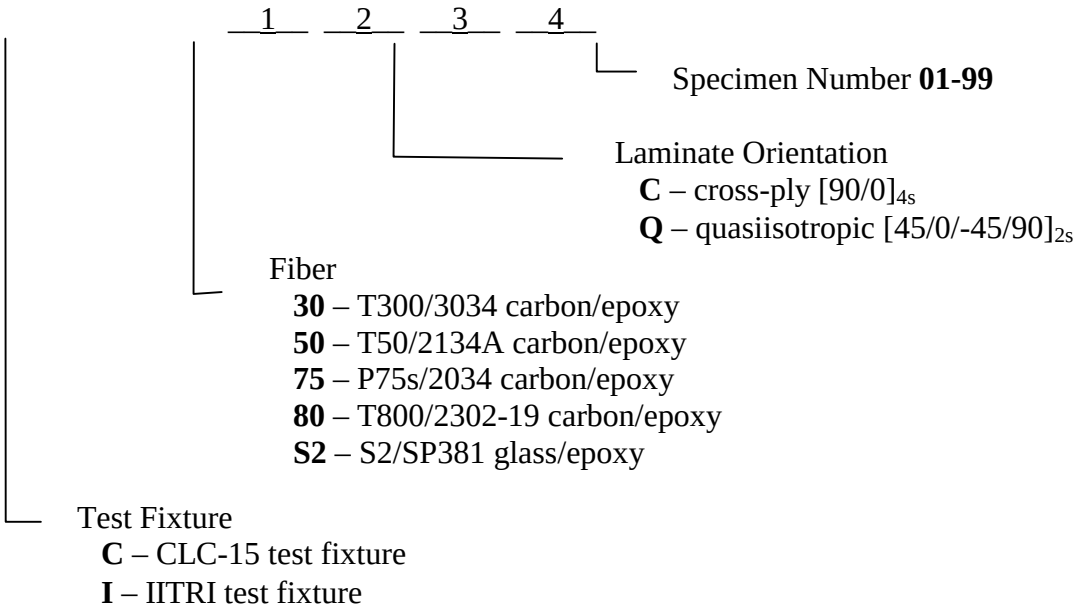

D.2 CONTENTS.

The tables listed on the following pages contain for each of the specimens tested in the Comparative Study (discussed in section 5.3) the measured x-direction modulus of the test specimen, the 0°-ply compressive strength (calculated using the procedure described, in section 4.4), and the percent bending in the specimen at failure. Plus and minus signs are included on the values of percent bending at failure to indicate which direction the specimens bent during the test. This information is helpful in recognizing systematic errors in the test setup or load train alignment. Following these tables, the stress versus strain curve and the percent bending versus average strain curve is given for each specimen (exceptions are noted in the following tables).

TABLE D-1. UNTABBED, CROSS-PLY $[90/0]_{4s}$ T300/3034 CARBON/EPOXY SPECIMENS TESTED IN THE CLC-15 TEST FIXTURE

Specimen Number	E^c_x		σ^c_{11}		Bending
	[GPa]	[Msi]	[MPa]	[ksi]	[%]
C30C01	64	9.3	1770	257	4.1
C30C02	64	9.3	1736	252	3.2
C30C03	62	9.0	1668	242	2.2
C30C04	62	9.0	1606	233	bad gage
C30C05	64	9.3	1519	220	-4.9
Mean	63	9.2	1660	241	
Std. Dev.	1	0.1	101	15	
CV [%]	1.6	1.6	6.1	6.1	

TABLE D-2. UNTABBED, CROSS-PLY $[90/0]_{4s}$ T300/3034 CARBON/EPOXY SPECIMENS TESTED IN THE IITRI TEST FIXTURE

Specimen Number	E^c_x		σ^c_{11}		Bending
	[GPa]	[Msi]	[MPa]	[ksi]	[%]
I30C01	63	9.2	1673	243	0.9
I30C02	62	9.1	1715	249	8.8
I30C03	65	9.4	1755	255	-8.5
I30C04	65	9.4	1622	235	-8.8
I30C05	63	9.1	1459	212	3.6
Mean	64	9.2	1645	239	
Std. Dev.	1	0.2	115	17	
CV [%]	1.8	1.8	7.0	7.0	

TABLE D-3. UNTABBED, QUASI-ISOTROPIC $[45/0/-45/90]_{2s}$ T300/3034 CARBON/EPOXY SPECIMENS TESTED IN THE CLC-15 TEST FIXTURE

Specimen Number	E^c_x		σ^c_{11}		Bending
	[GPa]	[Msi]	[MPa]	[ksi]	[%]
C30Q01	48	6.9	1694	246	-2.8
C30Q02	45	6.6	1605	233	-2.6
C30Q03	46	6.6	1435	208	-1.7
C30Q04	46	6.7	1684	244	1.6
C30Q05	48	6.9	1733	251	-4.4
Mean	47	6.8	1630	236	
Std. Dev.	1	0.2	119	17	
CV [%]	2.6	2.6	7.3	7.3	

TABLE D-4. UNTABBED, QUASI-ISOTROPIC $[45/0/-45/90]_{2s}$ T300/3034 CARBON/EPOXY SPECIMENS TESTED IN THE IITRI TEST FIXTURE

Specimen Number	E^c_x		σ^c_{11}		Bending
	[GPa]	[Msi]	[MPa]	[ksi]	[%]
I30Q01	43	6.3	1489	216	4.6
I30Q02	43	6.2	1604	233	4.3
I30Q03	41	6.0	1561	226	2.0
I30Q04	44	6.4	1660	241	0.4
Mean	43	6.2	1579	229	
Std. Dev.	1	0.2	72	10	
CV [%]	2.9	2.9	4.5	4.5	

Note: there only four specimens in this group.

TABLE D-5. UNTABBED, CROSS-PLY $[90/0]_{4s}$ T50/2134A CARBON/EPOXY SPECIMENS TESTED IN THE CLC-15 TEST FIXTURE

Specimen Number	E^c_x		σ^c_{11}		Bending
	[GPa]	[Msi]	[MPa]	[ksi]	[%]
C50C01	98	14.2	991	144	-7.7
C50C02	102	14.8	956	139	-6.0
C50C03	102	14.8	1090	158	-10.2
C50C04	97	14.1	1042	151	-4.2
C50C05	98	14.2	1018	148	-1.3
Mean	99	14.4	1019	148	
Std. Dev.	2	0.4	51	7	
CV [%]	2.5	2.5	5.0	5.0	

TABLE D-6. UNTABBED, CROSS-PLY $[90/0]_{4s}$ T50/2134A CARBON/EPOXY SPECIMENS TESTED IN THE IITRI TEST FIXTURE

Specimen Number	E^c_x		σ^c_{11}		Bending
	[GPa]	[Msi]	[MPa]	[ksi]	[%]
I50C01	93	13.5	897	130	29.7
I50C02	92	13.3	890	129	-4.1
I50C03	92	13.3	955	138	-2.4
I50C04	97	14.0	975	141	-2.4
I50C05	94	13.6	943	137	3.0
Mean	93	13.5	932	135	
Std. Dev.	2	0.3	37	5	
CV [%]	2.3	2.3	4.0	4.0	

TABLE D-7. UNTABBED, QUASI-ISOTROPIC $[45/0/-45/90]_{2s}$ T50/2134A CARBON/ EPOXY SPECIMENS TESTED IN THE CLC-15 TEST FIXTURE

Specimen Number	E^c_x		σ^c_{11}		Bending
	[GPa]	[Msi]	[MPa]	[ksi]	[%]
C50Q01	61	8.8	900	131	1.6
C50Q02	63	9.1	888	129	-2.4
C50Q03	60	8.7	945	137	-3.7
C50Q04	64	9.3	952	138	-3.3
C50Q05	61	8.8	934	135	-7.4
Mean	62	9.0	924	134	
Std. Dev.	2	0.3	28	4	
CV [%]	2.9	2.9	3.1	3.1	

TABLE D-8. UNTABBED, QUASI-ISOTROPIC $[45/0/-45/90]_{2s}$ T50/2134A CARBON/ EPOXY SPECIMENS TESTED IN THE IITRI TEST FIXTURE

Specimen Number	E^c_x		σ^c_{11}		Bending
	[GPa]	[MSi]	[MPa]	[ksi]	[%]
I50Q01	58	8.5	981	142	4.6
I50Q02	62	9.0	980	142	4.3
I50Q03	63	9.2	988	143	2.0
I50Q04	61	8.9	915	133	0.4
MEAN	61	8.9	966	140	
STD. DEV.	2	0.3	34	5	
CV [%]	3.3	3.3	3.5	3.5	

Note: there only four specimens in this group.

TABLE D-9. UNTABBED, CROSS-PLY $[90/0]_{4s}$ P75S/2034 CARBON/EPOXY SPECIMENS TESTED IN THE CLC-15 TEST FIXTURE

Specimen Number	E^c_x		σ^c_{11}		Bending
	[GPa]	[Msi]	[MPa]	[ksi]	[%]
C75C01	146	21.2	445	65	-26.1
C75C02[1]	144	20.9	471	68	-38.4
C75C03[1,3]	n/a	n/a	419	61	n/a
C75C04[2,3]	n/a	n/a	435	63	n/a
C75C05[2,3]	n/a	n/a	410	60	n/a
Mean	145	21.0	436	63	
Std. Dev.	1	0.2	24	3	
CV [%]	0.8	0.8	5.4	5.4	

[1]Gage length 9.53 mm (0.375″)
[2]Gage length 2.45 mm (0.097″)
[3]No plot available, gages shorted

TABLE D-10. UNTABBED, CROSS-PLY $[90/0]_{4s}$ P75S/2034 CARBON/EPOXY SPECIMENS TESTED IN THE IITRI TEST FIXTURE

Specimen Number	E^c_x		σ^c_{11}		Bending
	[GPa]	[Msi]	[MPa]	[ksi]	[%]
I75C01[3]	146	21.2	445	65	32.6
I75C02[1,3]	144	20.9	471	68	19.6
I75C03[1,3]	n/a	n/a	419	61	56.4
I75C04[2,3]	n/a	n/a	435	63	n/a
I75C05[2,3]	n/a	n/a	410	60	n/a
Mean	145	21.0	436	63	
Std. Dev.	1	0.2	24	3	
CV [%]	0.8	0.8	5.4	5.4	

[1]Gage length 9.53 mm (0.375″)
[2]Gage length 3.18 mm (0.125″)
[3]No plot available, gages shorted

TABLE D-11. UNTABBED, QUASI-ISOTROPIC $[45/0/-45/90]_{2s}$ P75S/2034 CARBON/ EPOXY SPECIMENS TESTED IN THE CLC-15 TEST FIXTURE

Specimen Number	E^c_x		σ^c_{11}		Bending
	[GPa]	[Msi]	[MPa]	[ksi]	[%]
C75Q01	80	11.6	568	82	11.1
C75Q02	83	12.0	589	85	-12.2
C75Q03	85	12.4	580	84	-26.7
C75Q04	85	12.3	589	85	-5.7
C75Q05	83	12.1	588	85	-10.4
Mean	83	12.1	583	85	
Std. Dev.	2	0.3	9	1	
CV [%]	2.4	2.4	1.5	1.5	

TABLE D-12. UNTABBED, QUASI-ISOTROPIC $[45/0/-45/90]_{2s}$ P75S/2034 CARBON/ EPOXY SPECIMENS TESTED IN THE IITRI TEST FIXTURE

Specimen Number	E^c_x		σ^c_{11}		Bending
	[GPa]	[Msi]	[MPa]	[ksi]	[%]
I75Q01	80	11.6	541	78	-10.6
I75Q02	83	12.0	597	87	5.9
I75Q03	84	12.2	581	84	10.7
I75Q04	79	11.5	551	80	-2.8
Mean	81	11.8	568	82	
StD- Dev.	2	0.3	26	4	
CV [%]	2.9	2.9	4.6	4.6	

Note: there only four specimens in this group.

TABLE D-13. UNTABBED, CROSS-PLY $[90/0]_{4s}$ T800/2302-19 CARBON/EPOXY SPECIMENS TESTED IN THE CLC-15 TEST FIXTURE

Specimen Number	E^c_x		σ^c_{11}		Bending
	[GPa]	[Msi]	[MPa]	[ksi]	[%]
C80C01	73	10.6	1703	247	2.1
C80C02	76	11.0	1631	236	1.5
C80C03	77	11.1	1692	245	-5.2
C80C04	76	11.1	1754	254	-1.6
C80C05	77	11.1	1770	257	-1.2
Mean	76	11.0	1710	248	
Std. Dev.	2	0.2	55	8	
CV [%]	2.1	2.1	3.2	3.2	

TABLE D-14. UNTABBED, CROSS-PLY $[90/0]_{4s}$ T800/2302-19 CARBON/EPOXY SPECIMENS TESTED IN THE IITRI TEST FIXTURE

Specimen Number	E^c_x		σ^c_{11}		Bending
	[GPa]	[Msi]	[MPa]	[ksi]	[%]
I80C01	82	11.9	1594	231	-9.8
I80C02	84	12.2	1517	220	-8.4
I80C03	74	10.8	1476	214	2.1
I80C04	72	10.4	1466	213	2.2
I80C05	74	10.7	1545	224	4.5
Mean	77	11.2	1520	220	
Std. Dev.	6	0.8	52	8	
CV [%]	7.2	7.2	3.4	3.4	

TABLE D-15. UNTABBED, QUASI-ISOTROPIC $[45/0/-45/90]_{2s}$ T800/2302-19 CARBON/EPOXY SPECIMENS TESTED IN THE CLC-15 TEST FIXTURE

Specimen Number	E^c_x		σ^c_{11}		Bending
	[GPa]	[Msi]	[MPa]	[ksi]	[%]
C80Q01	53	7.6	1706	247	-1.9
C80Q02	53	7.6	1678	243	-5.6
C80Q03	53	7.6	1714	249	-2.9
C80Q04	53	7.6	1818	264	4.1
C80Q05[1]	n/a	n/a	n/a	n/a	n/a
Mean	53	7.6	1729	251	
Std. Dev.	0	0.0	61	9	
CV [%]	0.2	0.2	3.5	3.5	

[1]No plot available, specimen was accidentally damaged

TABLE D-16. UNTABBED, QUASI-ISOTROPIC $[45/0/-45/90]_{2s}$ T800/2302-19 CARBON/ EPOXY SPECIMENS TESTED IN THE IITRI TEST FIXTURE

Specimen Number	E^c_x		σ^c_{11}		Bending
	[GPa]	[Msi]	[MPa]	[ksi]	[%]
I80Q01	51	7.4	1698	246	2.7
I80Q02	50	7.3	1654	240	2.4
I80Q03[1]	55	8.0	1767	256	bad gage
I80Q04[1]	n/a	n/a	n/a	n/a	
Mean	52	7.6	1707	247	
StD- Dev.	3	0.4	57	8	
CV [%]	5.1	5.1	3.3	3.3	

[1]No plot available, specimen was accidentally damaged
Note: there only four specimens in this group.

TABLE D-17. UNTABBED, CROSS-PLY $[90/0]_{7s}$ S2/SP381 CARBON/EPOXY SPECIMENS TESTED IN THE CLC-15 TEST FIXTURE

Specimen Number	E^c_x		σ^c_{11}		Bending
	[GPa]	[Msi]	[MPa]	[ksi]	[%]
CS2C01	31	4.5	1252	182	-1.2
CS2C02	31	4.5	1063	154	1.8
CS2C03	30	4.3	1250	181	3.9
CS2C04	31	4.4	1012	147	-0.4
CS2C05	30	4.4	1179	171	0.2
Mean	31	4.4	1151	167	
Std. Dev.	1	0.1	109	16	
CV [%]	1.8	1.8	9.5	9.5	

TABLE D-18. UNTABBED, CROSS-PLY $[90/0]_{7s}$ S2/SP381 CARBON/EPOXY SPECIMENS TESTED IN THE IITRI TEST FIXTURE

Specimen Number	E^c_x		σ^c_{11}		Bending
	[GPa]	[Msi]	[MPa]	[ksi]	[%]
IS2C01	29	4.2	935	136	-9.8
IS2C02	30	4.3	897	130	-8.4
IS2C03	29	4.1	972	141	2.1
IS2C04	29	4.3	889	129	2.2
IS2C05	29	4.3	886	128	4.5
Mean	29	4.2	916	133	
Std. Dev.	1	0.1	37	5	
CV [%]	1.9	1.9	4.0	4.0	

TABLE D-19. UNTABBED, QUASI-ISOTROPIC $[45/0/-45/90]_{2s}$ CARBON/EPOXY SPECIMENS TESTED IN THE CLC TEST FIXTURE

Specimen Number	E^c_x		σ^c_{11}		Bending
	[GPa]	[Msi]	[MPa]	[ksi]	[%]
CS2Q01	n/a	n/a	1066	155	2.0
CS2Q02	25	3.6	1089	158	0.9
CS2Q03	23	3.4	1151	167	0.4
CS2Q04	22	3.2	1024	149	n/a
CS2Q05	24	3.5	975	141	0.9
Mean	24	3.4	1061	154	
Std. Dev.	1	0.2	67	10	
CV [%]	5.6	5.6	6.3	6.3	

TABLE D-20. UNTABBED, QUASI-ISOTROPIC $[45/0/-45/90]_{2s}$ CARBON/EPOXY SPECIMENS TESTED IN THE IITRI TEST FIXTURE

Specimen Number	E^c_x		σ^c_{11}		Bending
	[GPa]	[Msi]	[MPa]	[ksi]	[%]
IS2Q01	22	3.2	984	143	0.1
IS2Q02	24	3.5	878	127	-1.9
IS2Q03	22	3.2	875	127	-3.1
IS2Q04	23	3.3	933	135	n/a
IS2Q05	22	3.2	938	136	2.4
Mean	23	3.3	922	134	
Std. Dev.	1	0.1	46	7	
CV [%]	3.6	3.6	5.0	5.0	

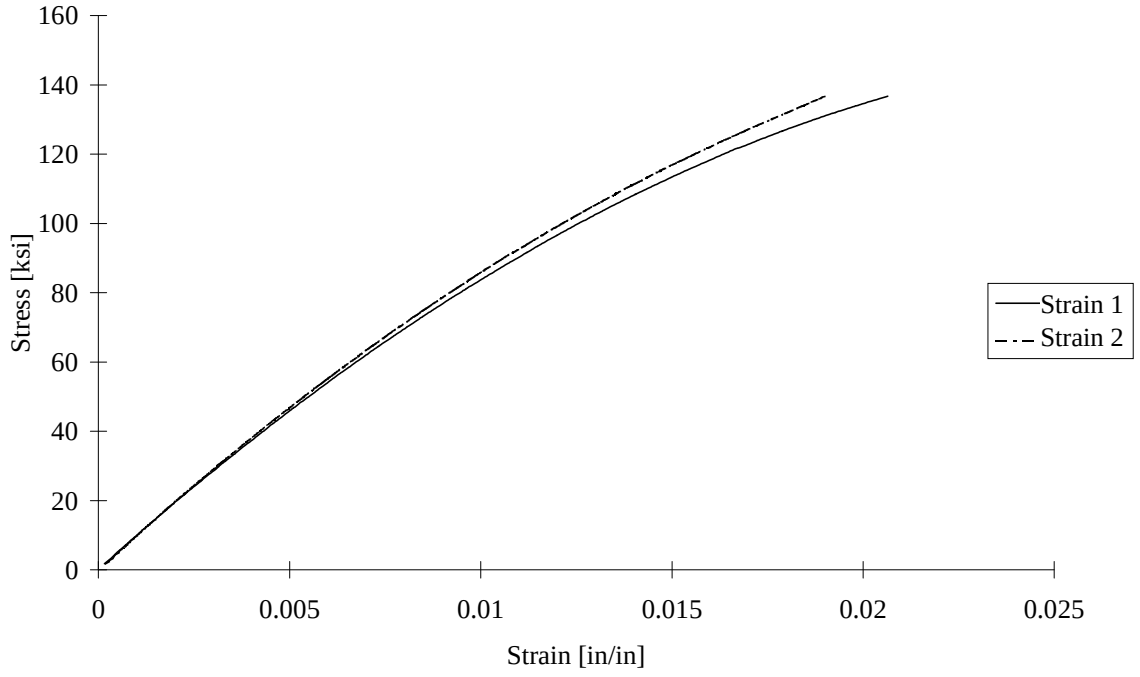

FIGURE D-1. TEST SPECIMEN C30C01: T300/3034 CARBON/EPOXY $[90/0]_{4s}$
CLC-15 TEST FIXTURE

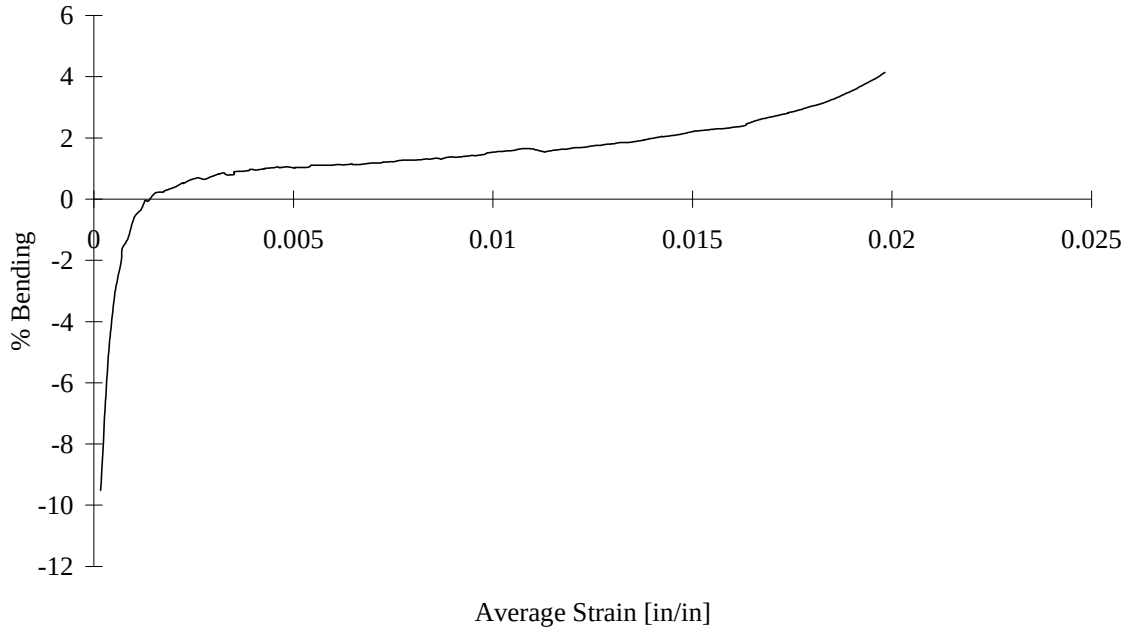

FIGURE D-2. TEST SPECIMEN C30C01: T300/3034 CARBON/EPOXY $[90/0]_{4s}$
CLC-15 TEST FIXTURE

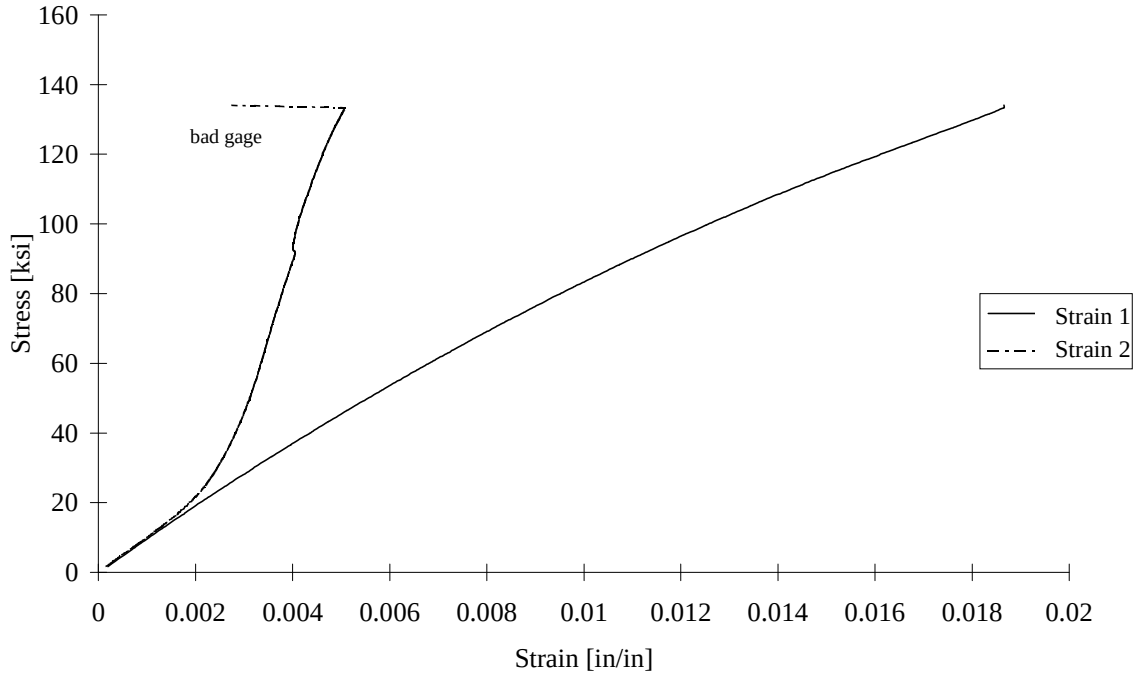

FIGURE D-3. TEST SPECIMEN C30C02: T300/3034 CARBON/EPOXY $[90/0]_{4s}$
CLC-15 TEST FIXTURE

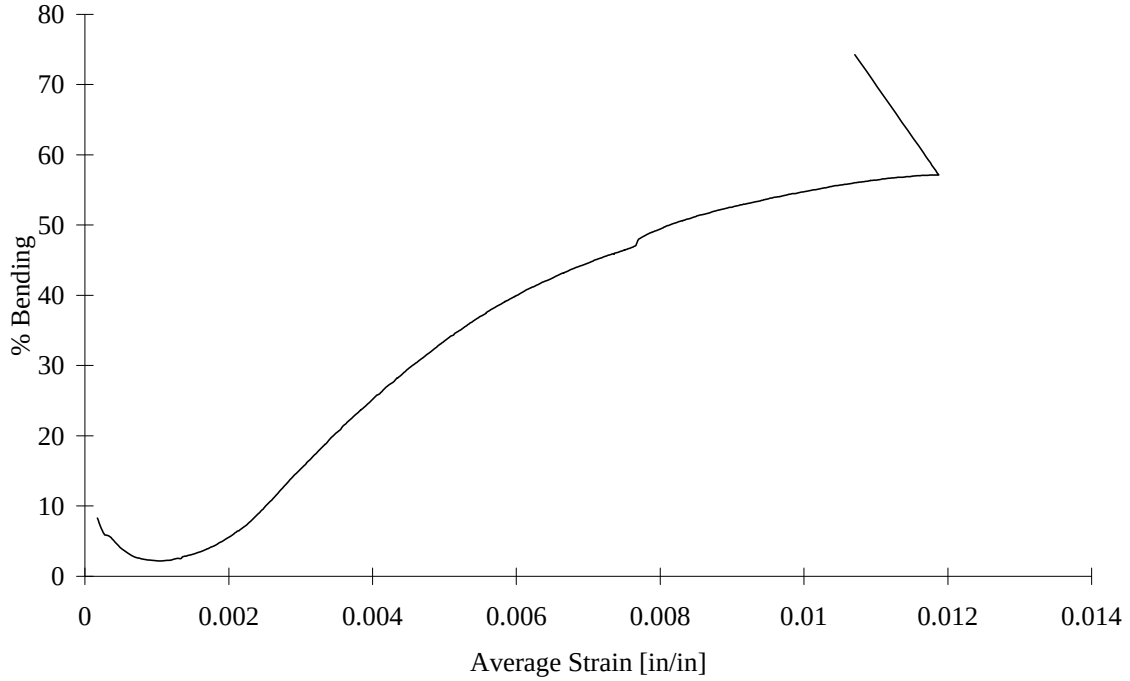

FIGURE D-4. TEST SPECIMEN C30C02: T300/3034 CARBON/EPOXY $[90/0]_{4s}$
CLC-15 TEST FIXTURE

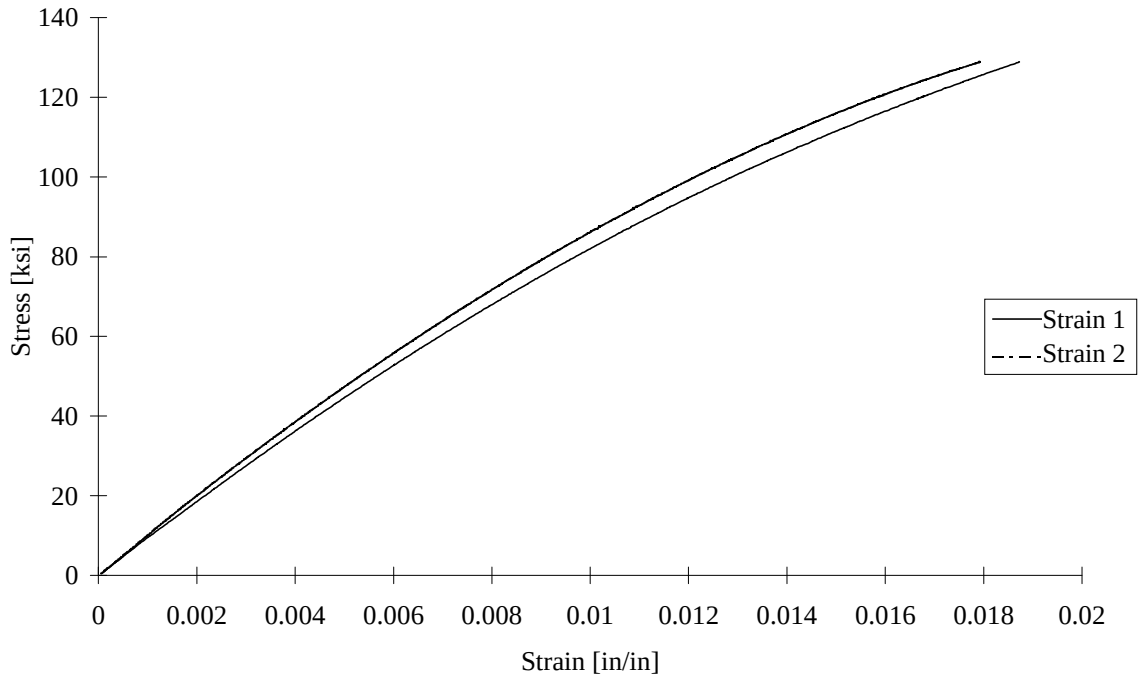

FIGURE D-5. TEST SPECIMEN C30C03: T300/3034 CARBON/EPOXY $[90/0]_{4s}$
CLC-15 TEST FIXTURE

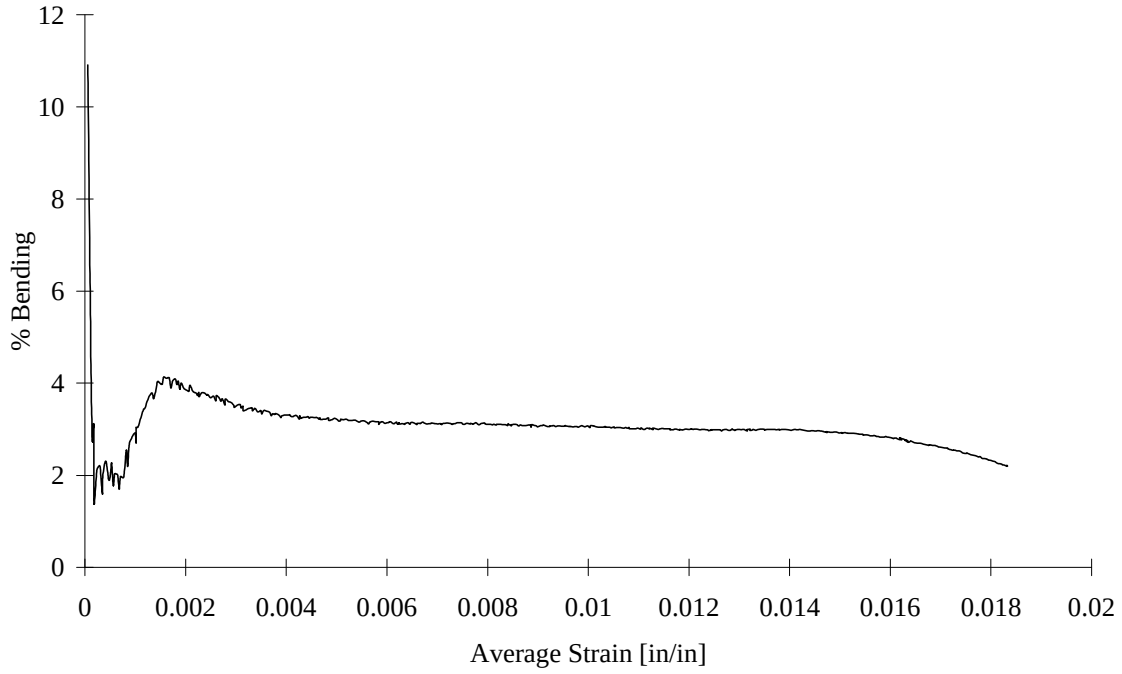

FIGURE D-6. TEST SPECIMEN C30C03: T300/3034 CARBON/EPOXY $[90/0]_{4s}$
CLC-15 TEST FIXTURE

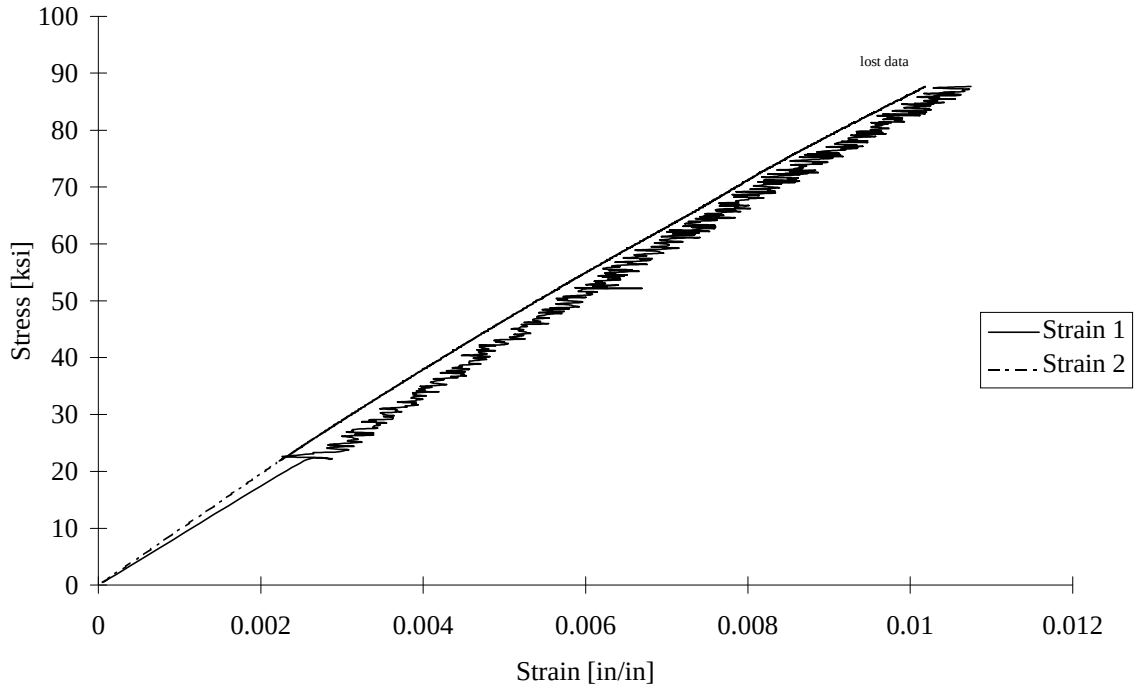

FIGURE D-7. TEST SPECIMEN C30C04: T300/3034 CARBON/EPOXY $[90/0]_{4s}$
CLC-15 TEST FIXTURE

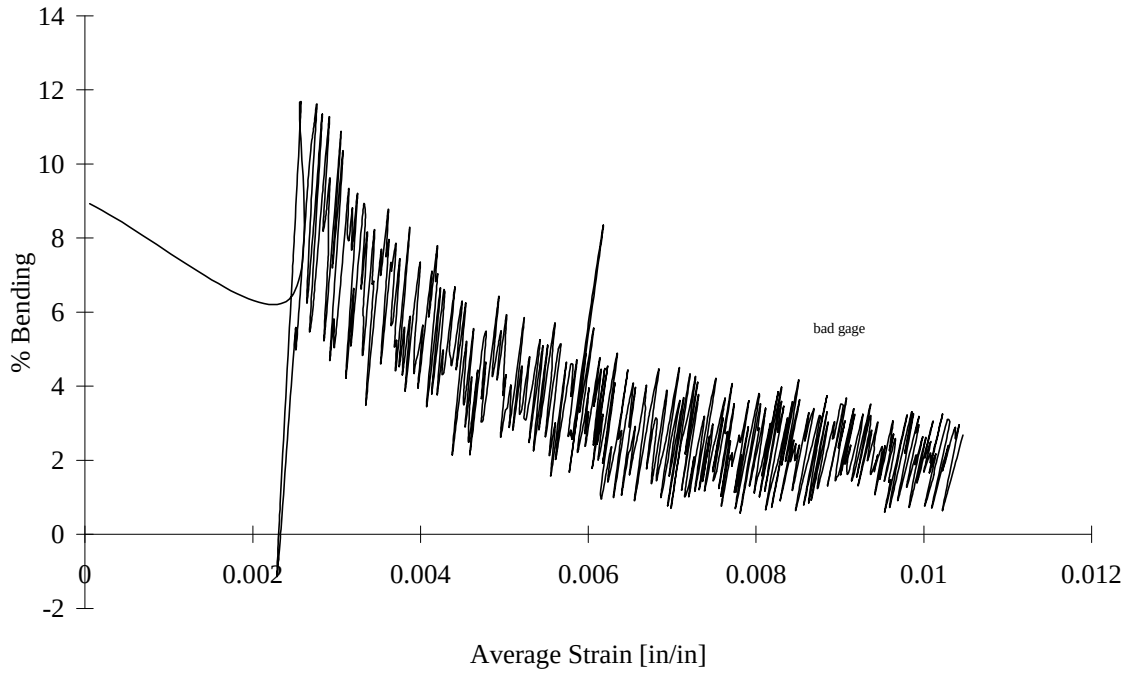

FIGURE D-8. TEST SPECIMEN C30C04: T300/3034 CARBON/EPOXY $[90/0]_{4s}$
CLC-15 TEST FIXTURE

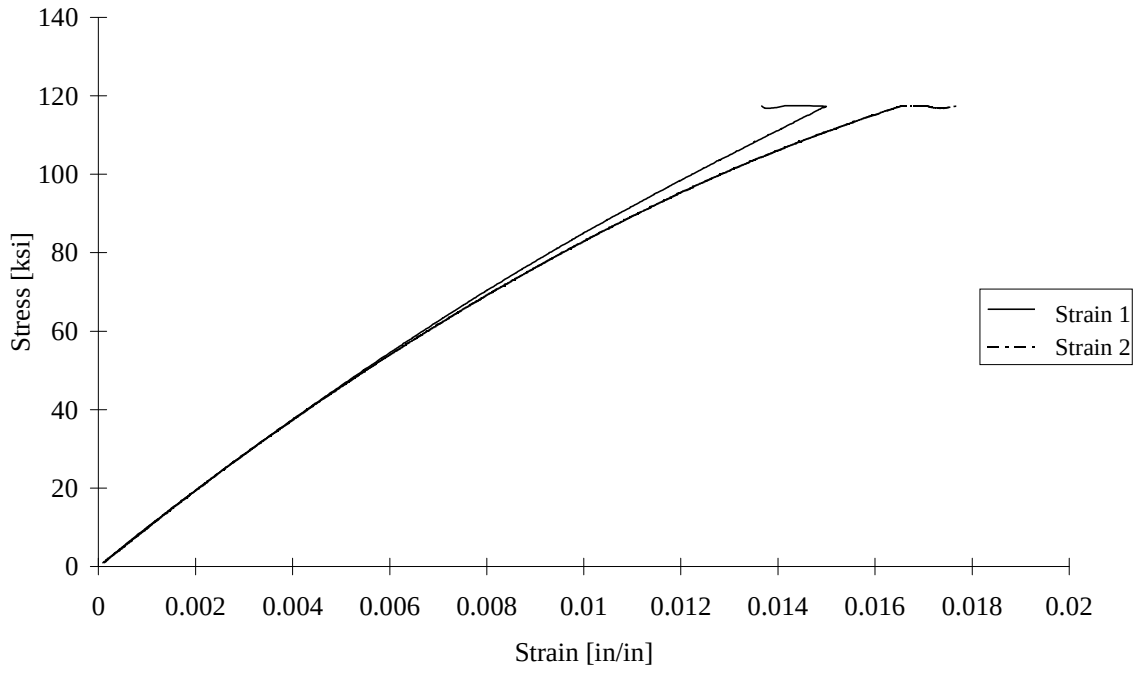

FIGURE D-9. TEST SPECIMEN C30C05: T300/3034 CARBON/EPOXY $[90/0]_{4s}$
CLC-15 TEST FIXTURE

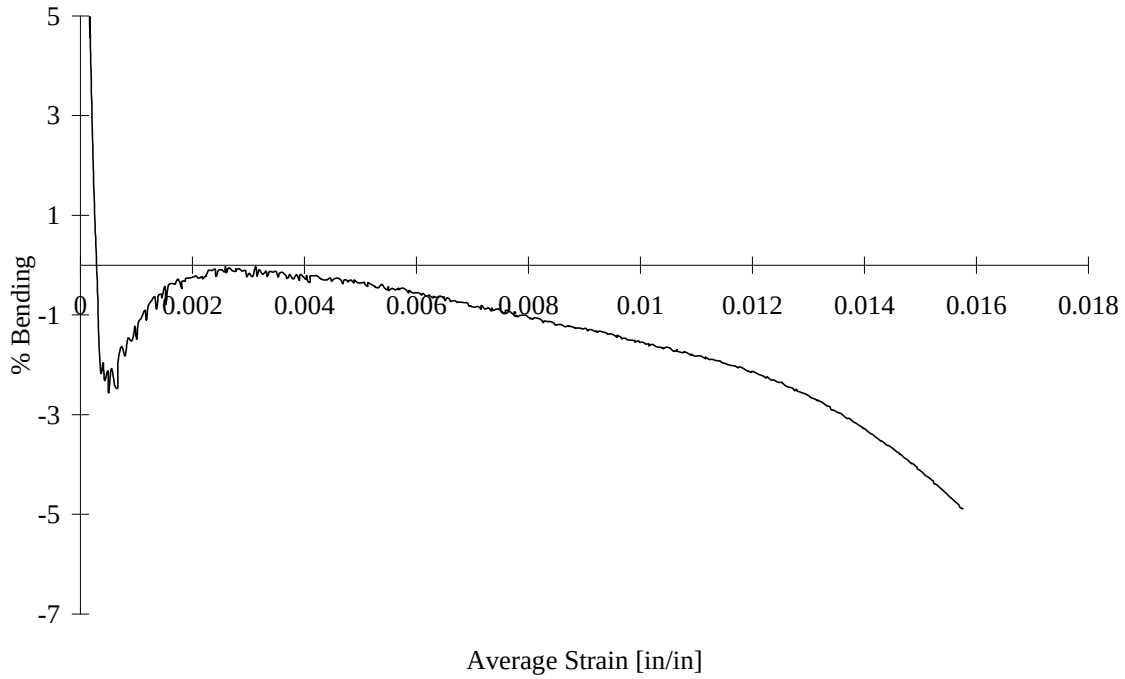

FIGURE D-10. TEST SPECIMEN C30C05: T300/3034 CARBON/EPOXY $[90/0]_{4s}$
CLC-15 TEST FIXTURE

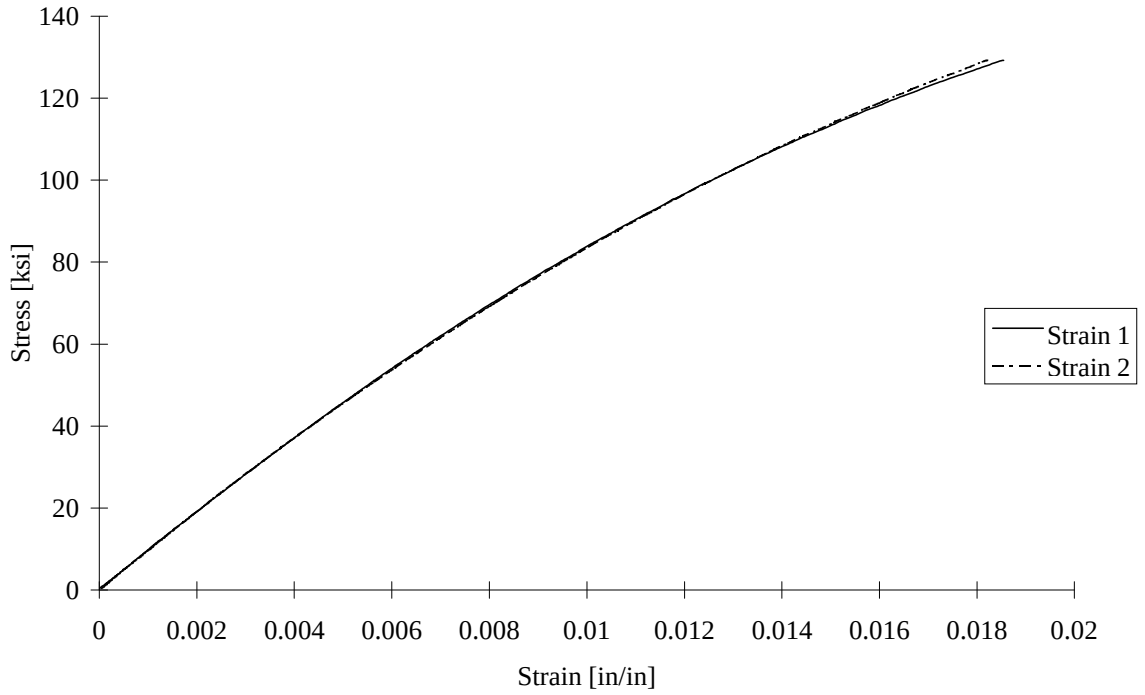

FIGURE D-11. TEST SPECIMEN I30C01: T300/3034 CARBON/EPOXY $[90/0]_{4s}$
IITRI TEST FIXTURE

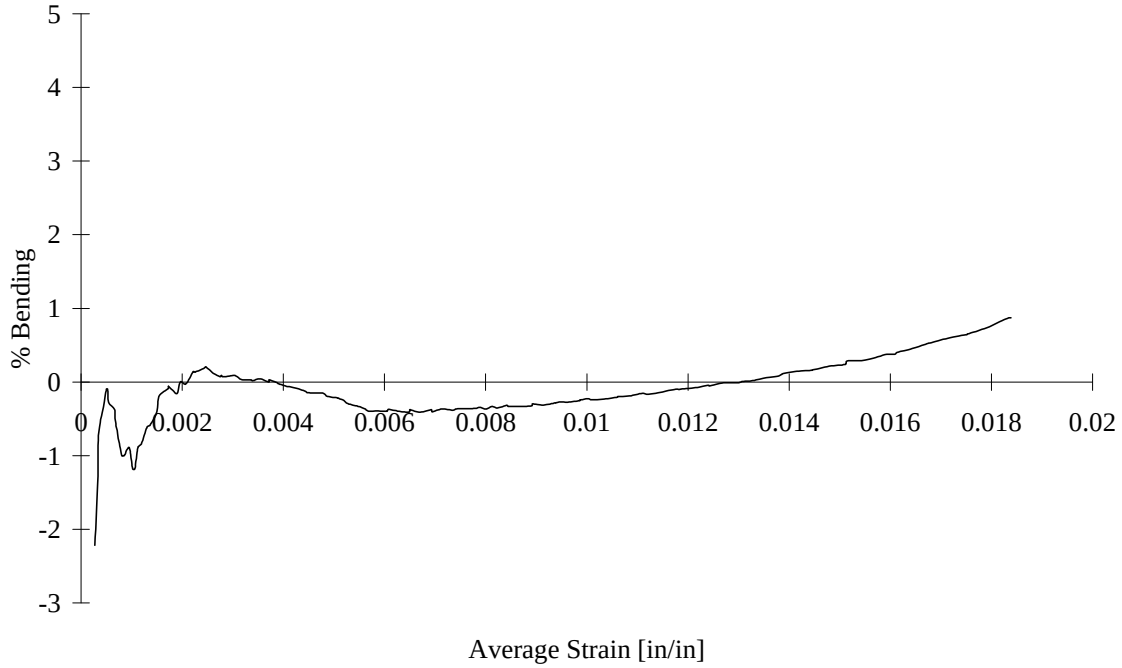

FIGURE D-12. TEST SPECIMEN I30C01: T300/3034 CARBON/EPOXY $[90/0]_{4s}$
IITRI TEST FIXTURE

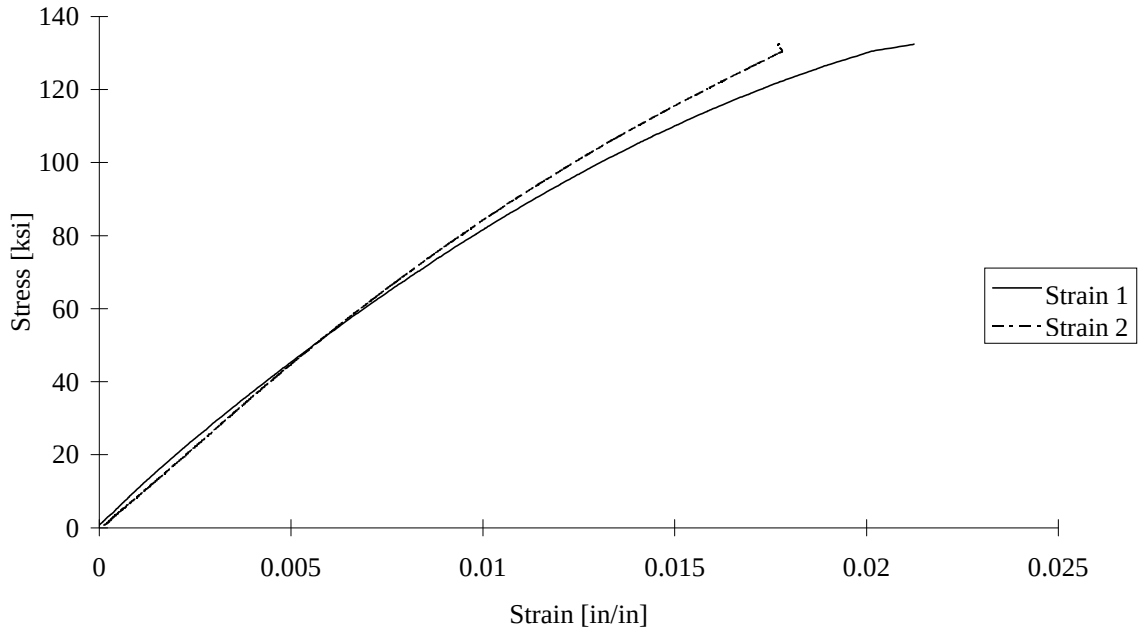

FIGURE D-13. TEST SPECIMEN I30C02: T300/3034 CARBON/EPOXY $[90/0]_{4s}$
IITRI TEST FIXTURE

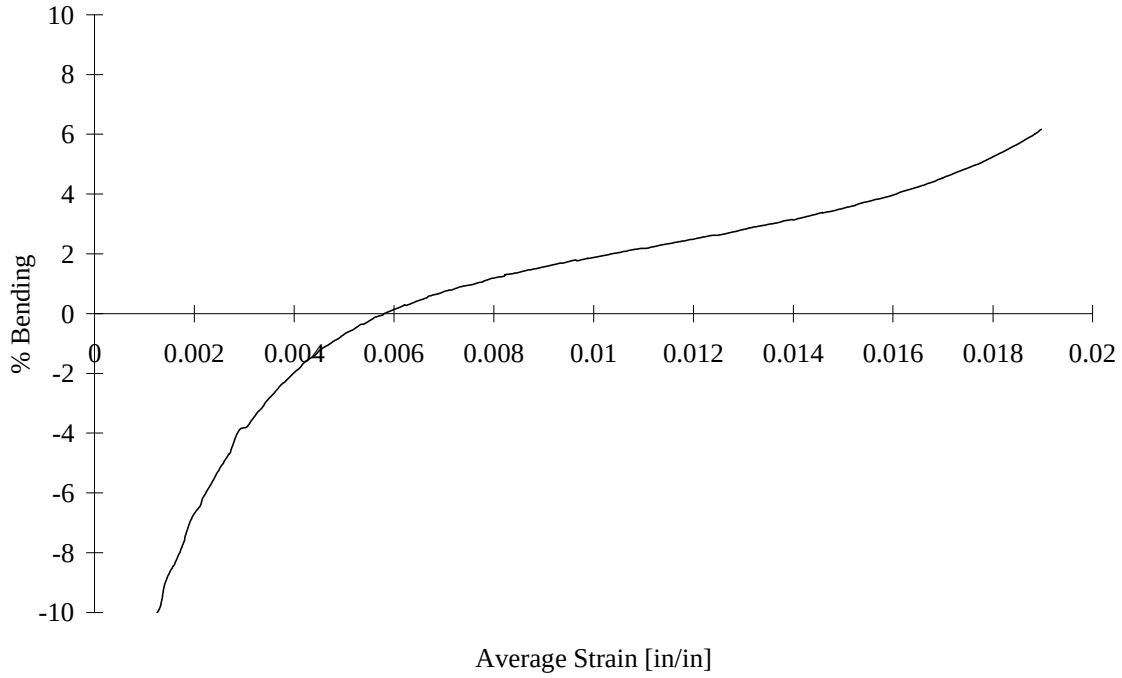

FIGURE D-14. TEST SPECIMEN I30C02: T300/3034 CARBON/EPOXY $[90/0]_{4s}$
IITRI TEST FIXTURE

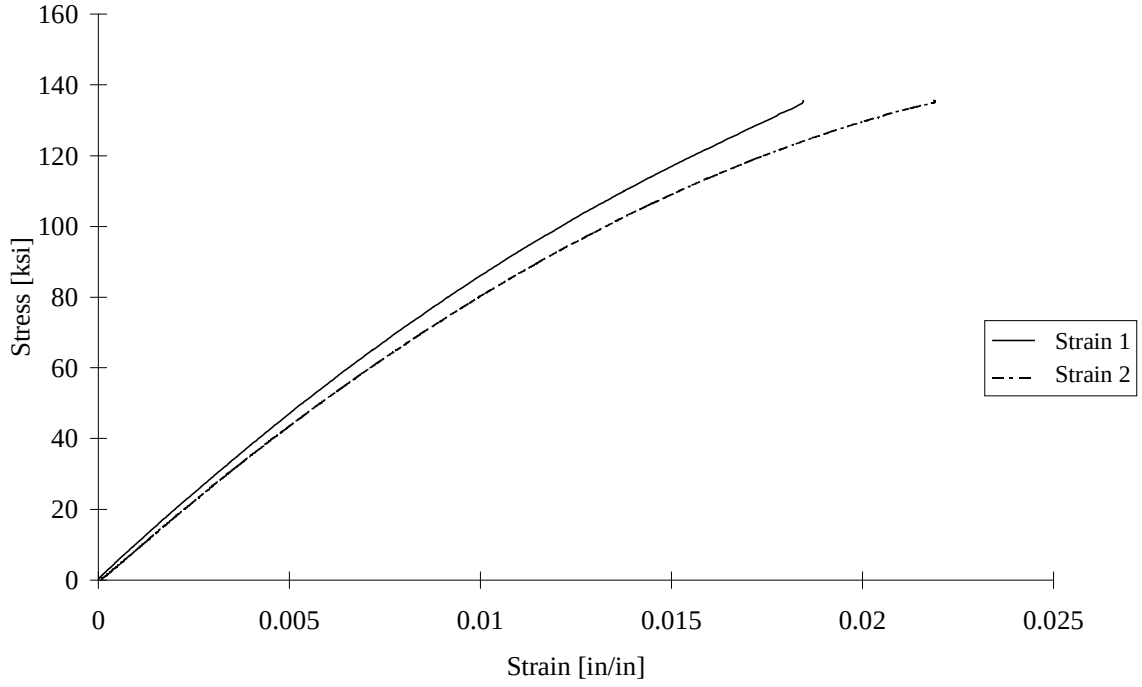

FIGURE D-15. TEST SPECIMEN I30C03: T300/3034 CARBON/EPOXY $[90/0]_{4s}$
IITRI TEST FIXTURE

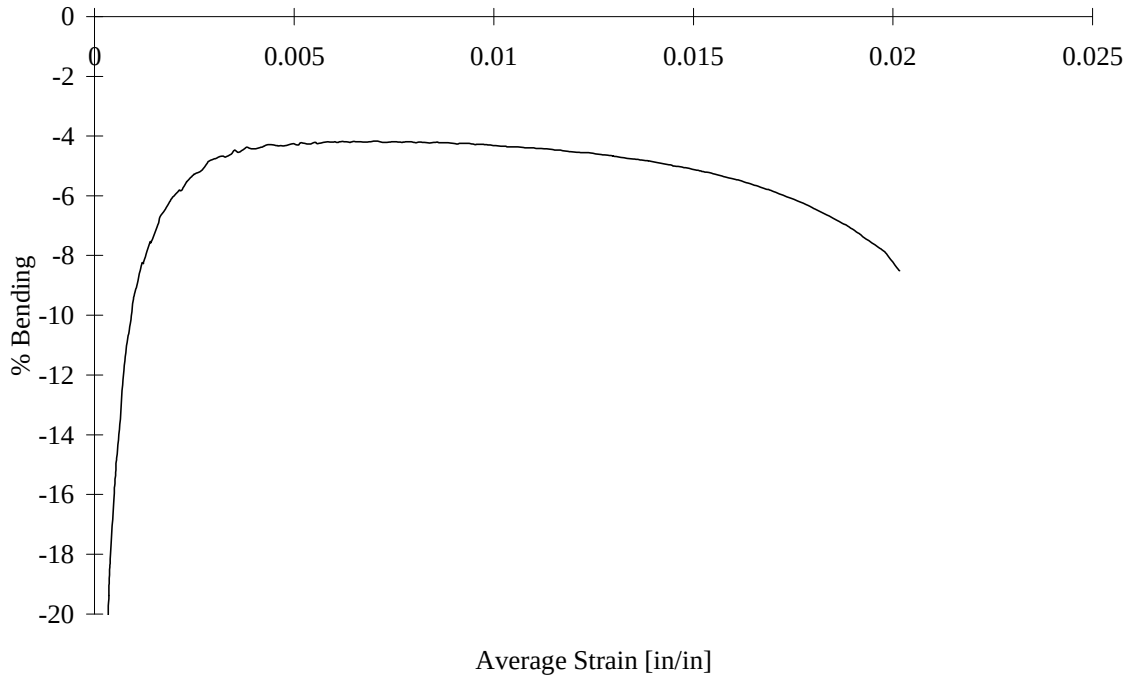

FIGURE D-16. TEST SPECIMEN I30C03: T300/3034 CARBON/EPOXY $[90/0]_{4s}$
IITRI TEST FIXTURE

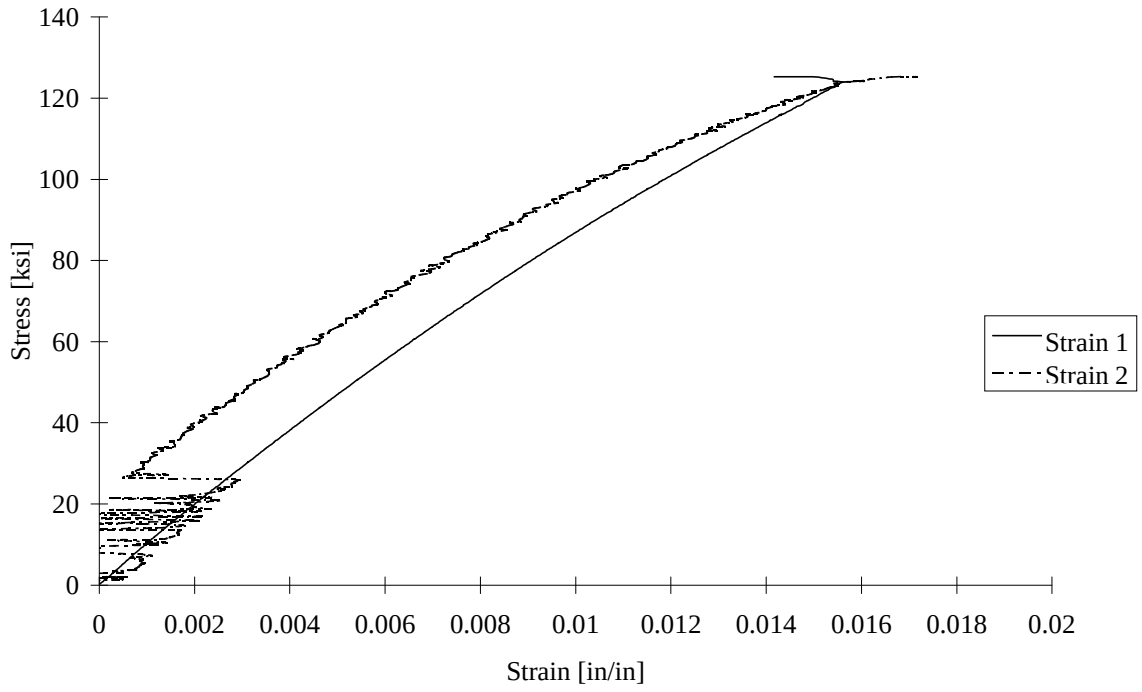

FIGURE D-17. TEST SPECIMEN I30C04: T300/3034 CARBON/EPOXY $[90/0]_{4s}$
IITRI TEST FIXTURE

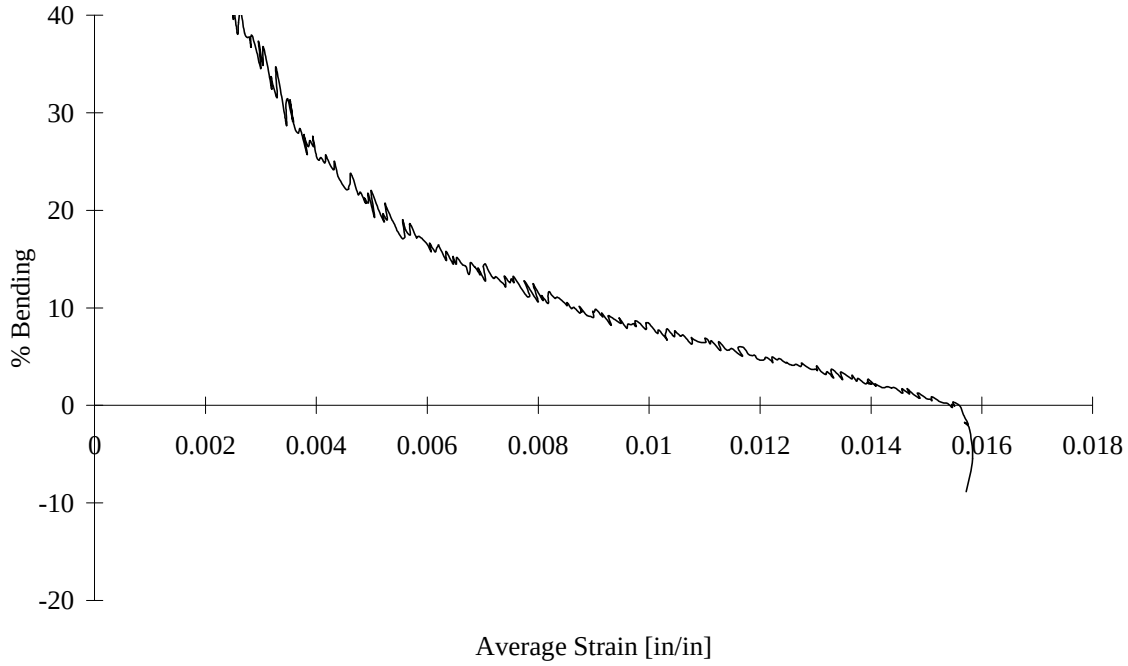

FIGURE D-18. TEST SPECIMEN I30C04: T300/3034 CARBON/EPOXY $[90/0]_{4s}$
IITRI TEST FIXTURE

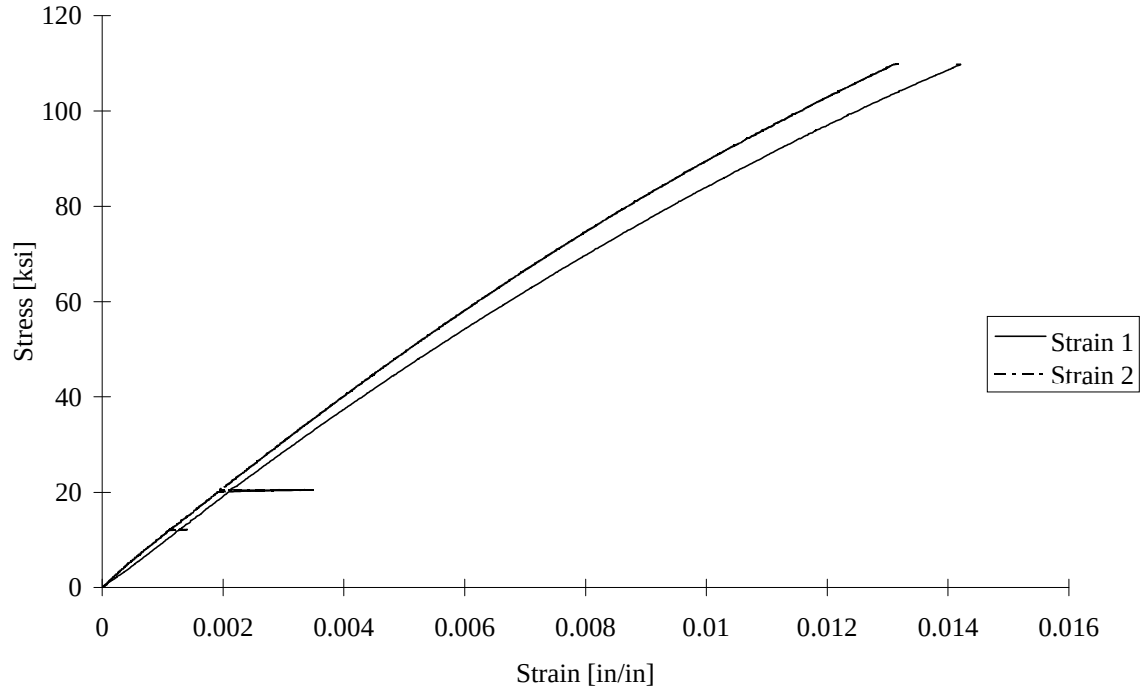

FIGURE D-19. TEST SPECIMEN I30C05: T300/3034 CARBON/EPOXY $[90/0]_{4s}$
IITRI TEST FIXTURE

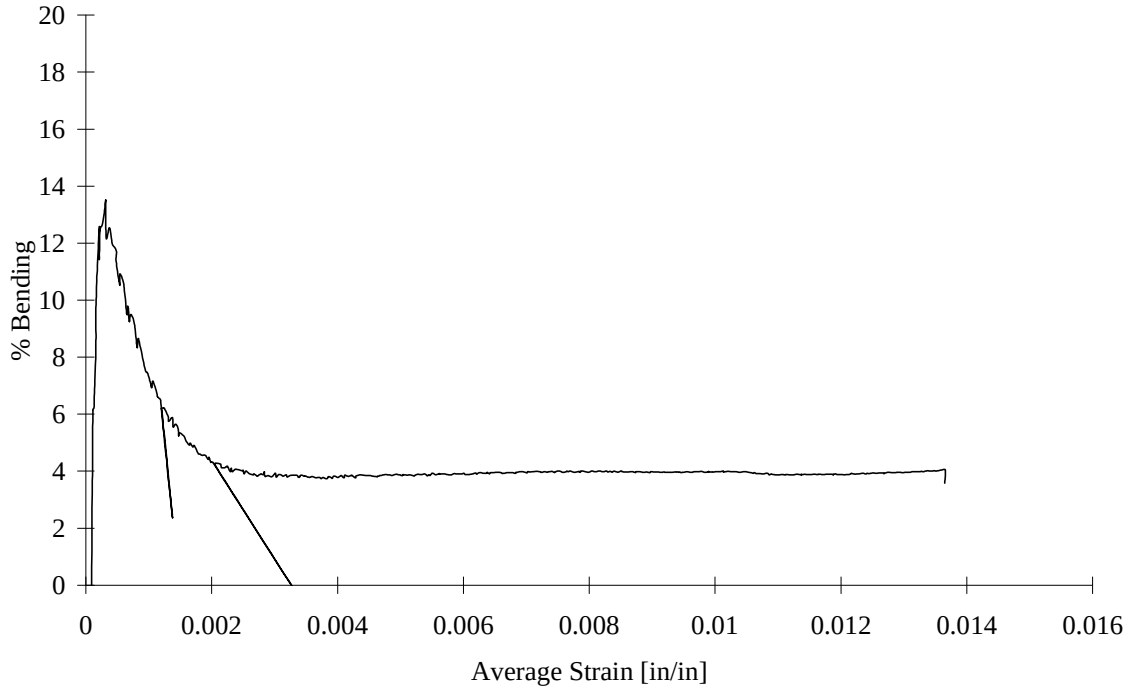

FIGURE D-20. TEST SPECIMEN I30C05: T300/3034 CARBON/EPOXY $[90/0]_{4s}$
IITRI TEST FIXTURE

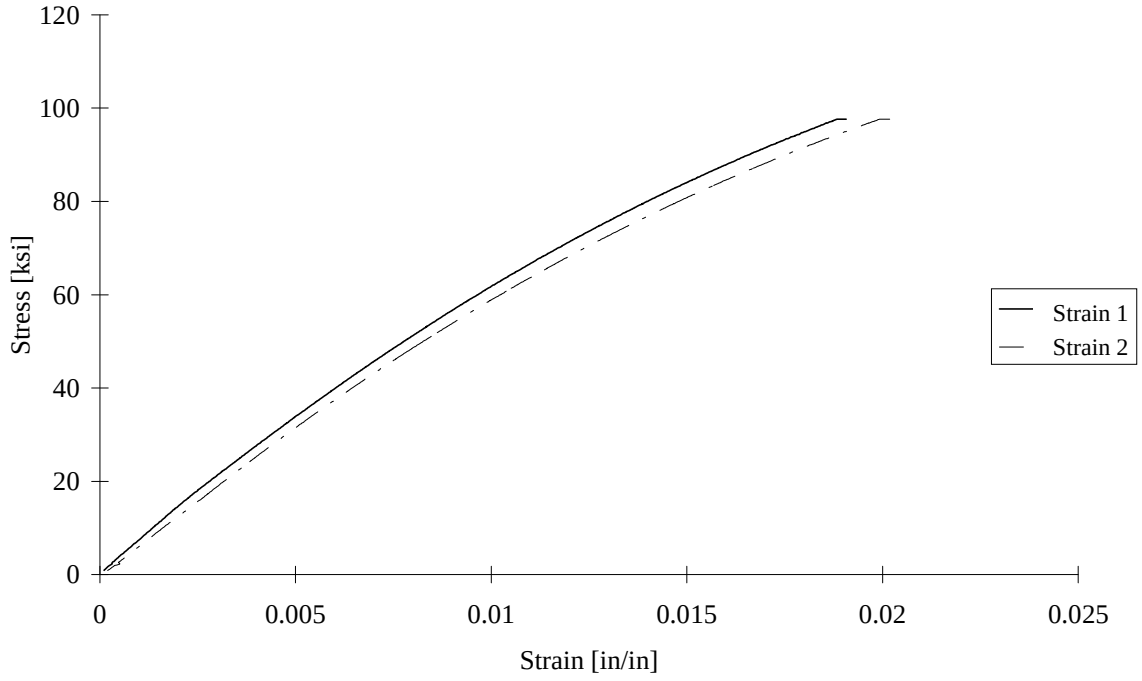

FIGURE D-21. TEST SPECIMEN C30Q01: T300/3034 CARBON/EPOXY $[45/0/-45/90]_{2s}$
CLC-15 TEST FIXTURE

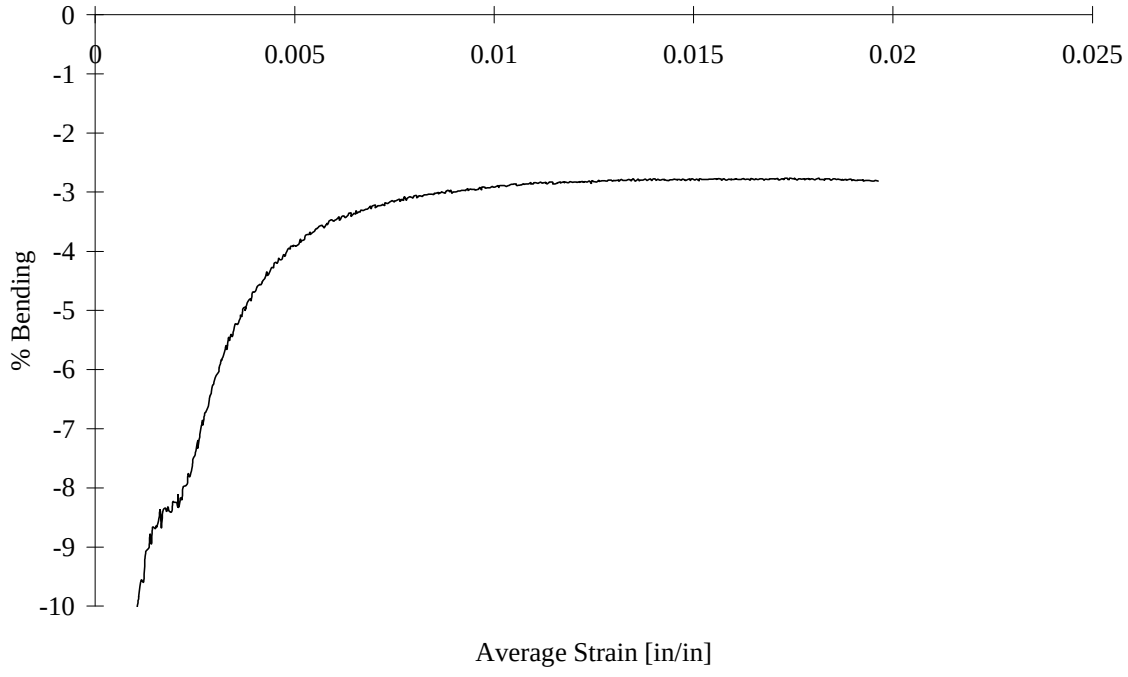

FIGURE D-22. TEST SPECIMEN C30Q01: T300/3034 CARBON/EPOXY $[45/0/-45/90]_{2s}$
CLC-15 TEST FIXTURE

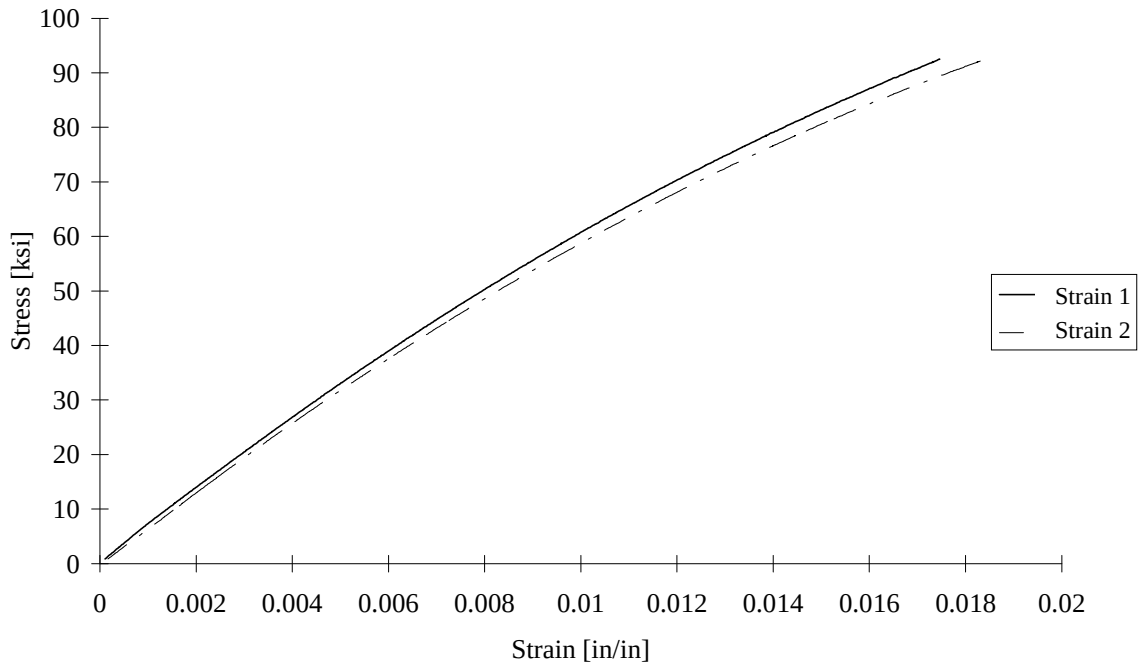

FIGURE D-23. TEST SPECIMEN C30Q02: T300/3034 CARBON/EPOXY $[45/0/-45/90]_{2s}$
CLC-15 TEST FIXTURE

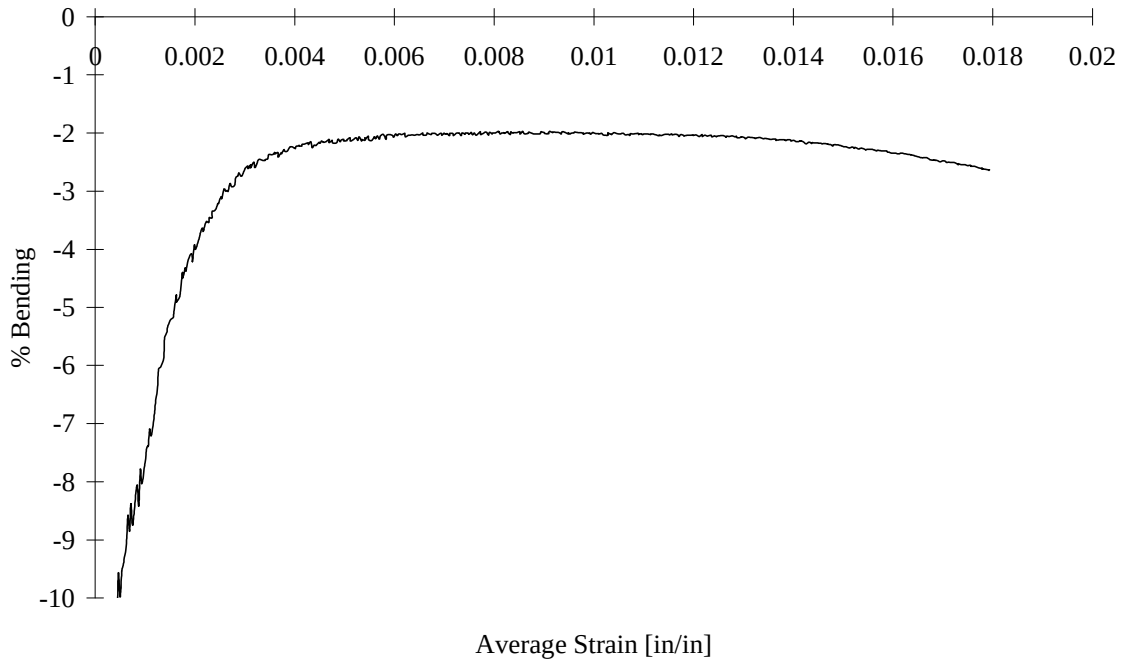

FIGURE D-24. TEST SPECIMEN C30Q02: T300/3034 CARBON/EPOXY $[45/0/-45/90]_{2s}$
CLC-15 TEST FIXTURE

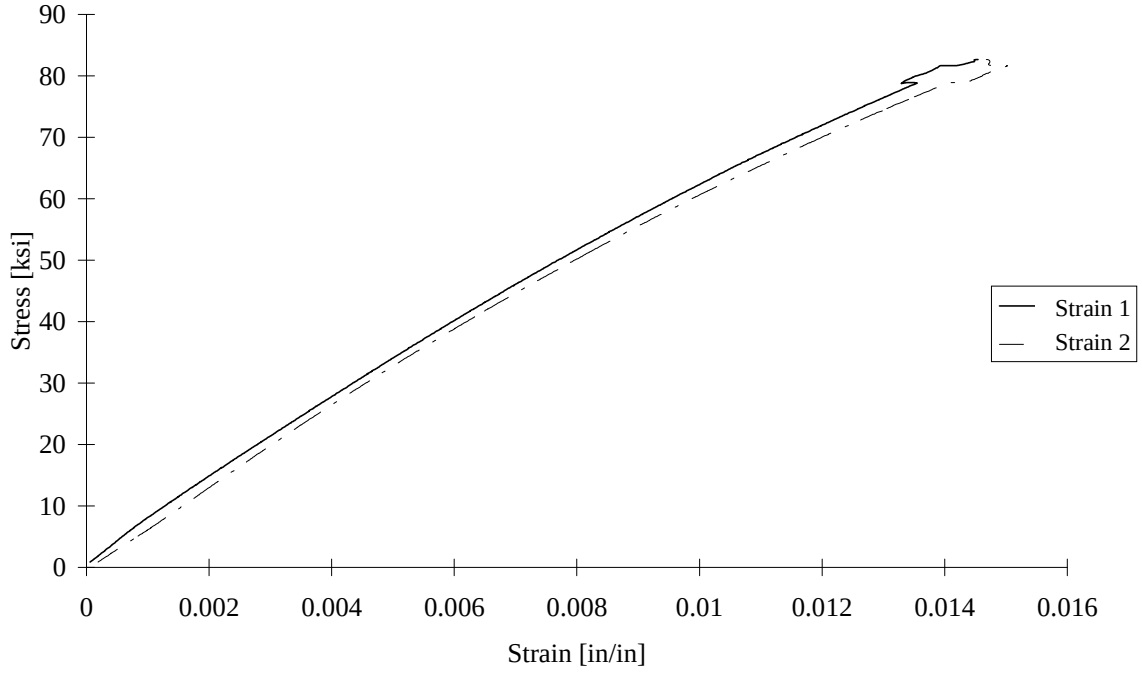

FIGURE D-25 TEST SPECIMEN C30Q03: T300/3034 CARBON/EPOXY $[45/0/-45/90]_{2s}$
CLC-15 TEST FIXTURE

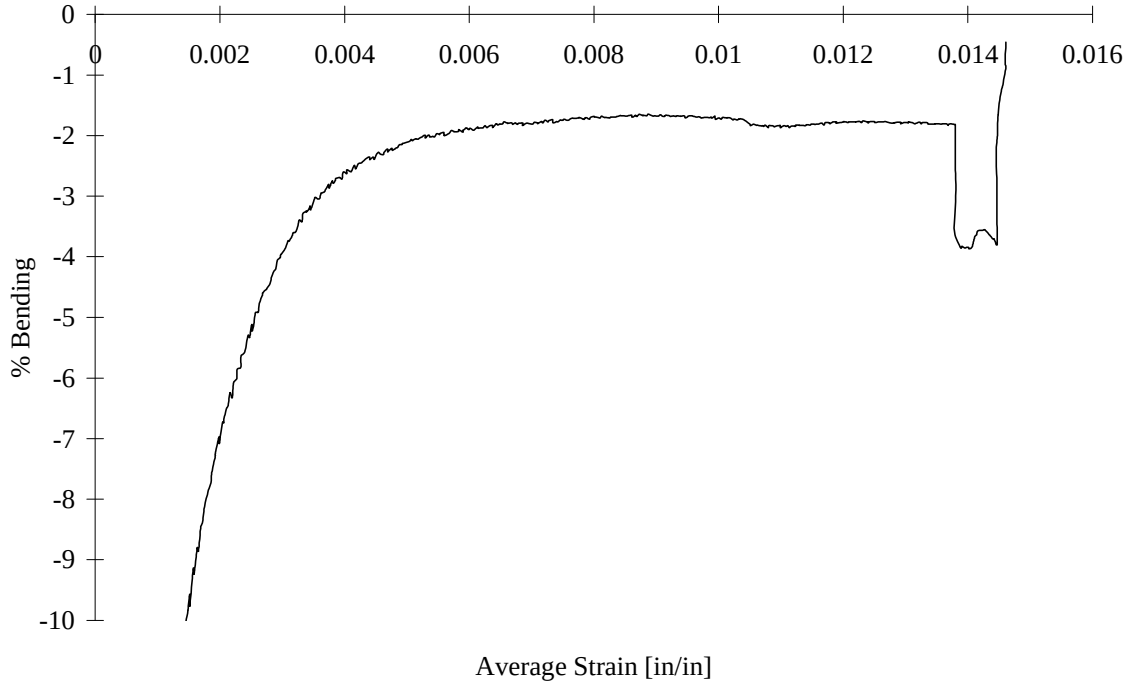

FIGURE D-26 TEST SPECIMEN C30Q03: T300/3034 CARBON/EPOXY $[45/0/-45/90]_{2s}$
CLC-15 TEST FIXTURE

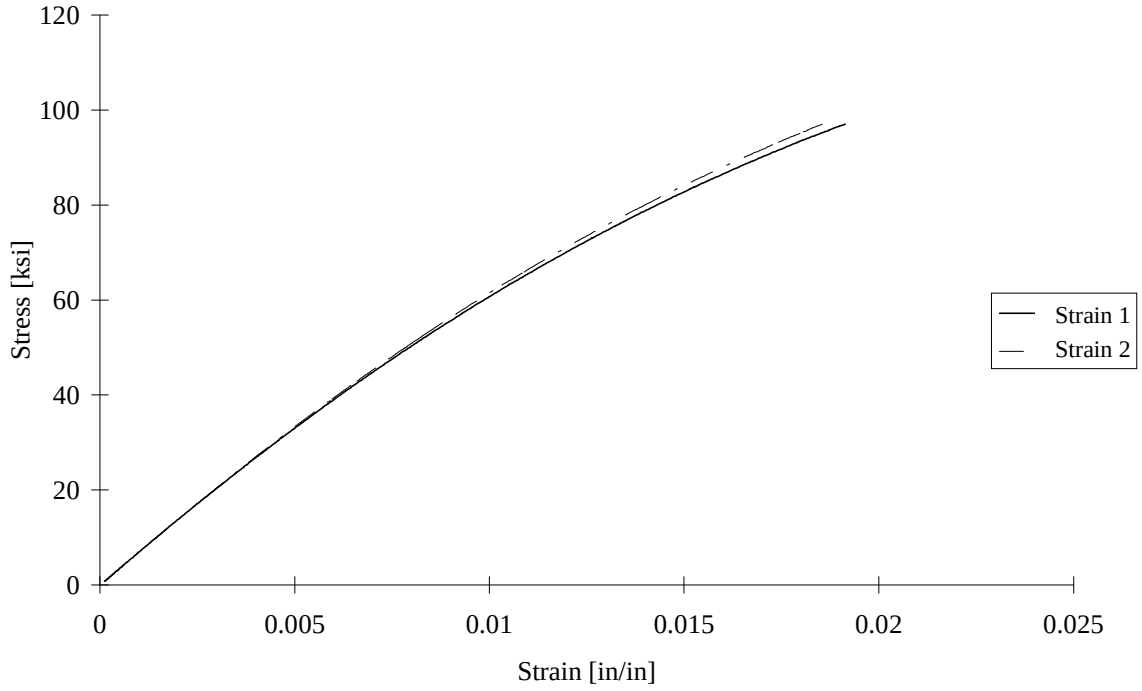

FIGURE D-27 TEST SPECIMEN C30Q04: T300/3034 CARBON/EPOXY $[45/0/-45/90]_{2s}$
CLC-15 TEST FIXTURE

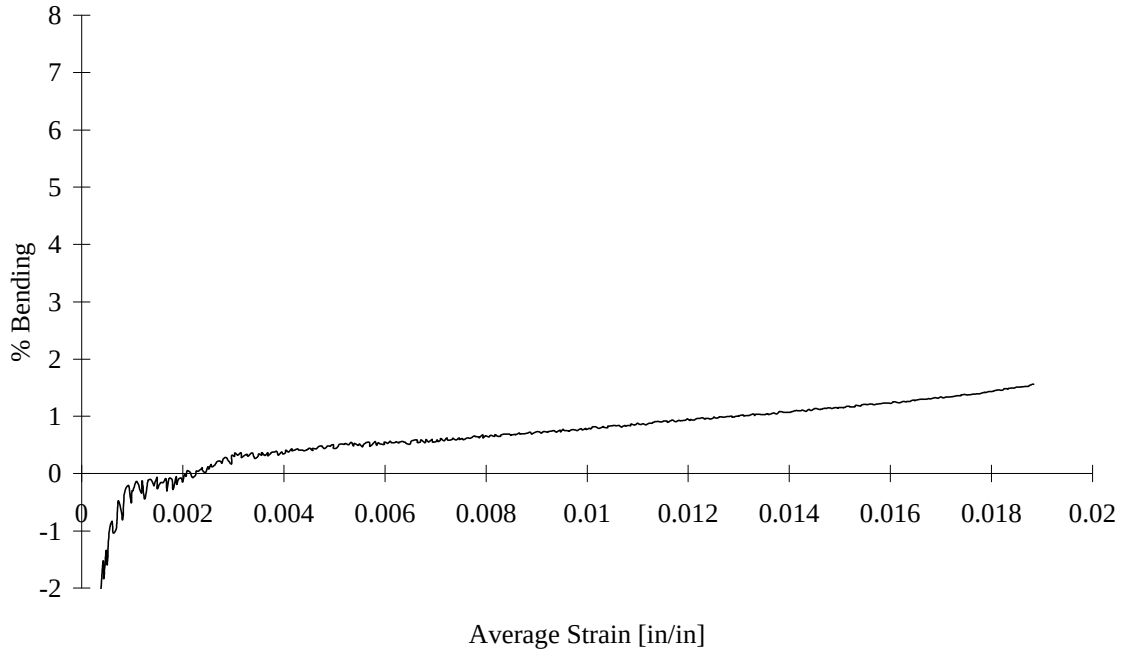

FIGURE D-28 TEST SPECIMEN C30Q04: T300/3034 CARBON/EPOXY $[45/0/-45/90]_{2s}$
CLC-15 TEST FIXTURE

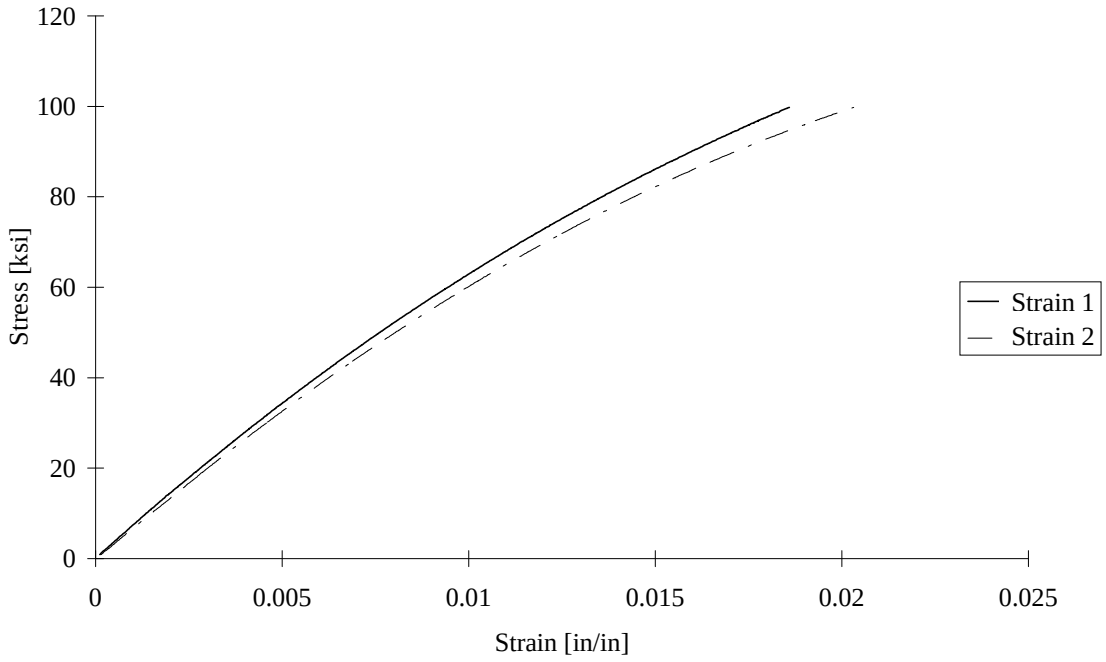

FIGURE D-29 TEST SPECIMEN C30Q05: T300/3034 CARBON/EPOXY $[45/0/-45/90]_{2s}$
CLC-15 TEST FIXTURE

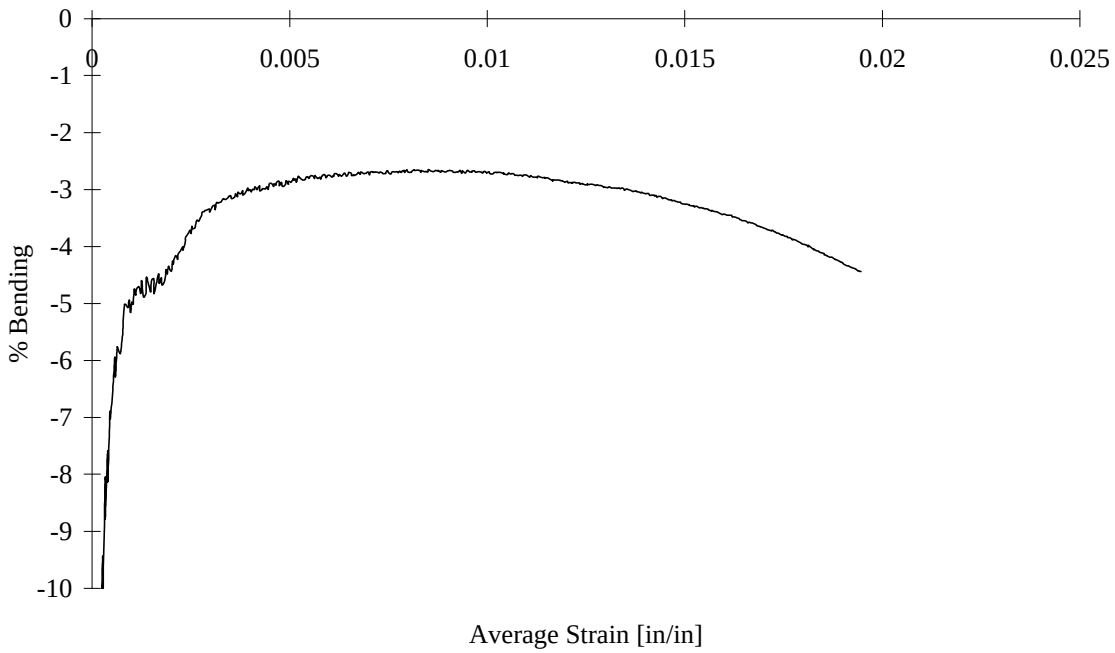

FIGURE D-30. TEST SPECIMEN C30Q05: T300/3034 CARBON/EPOXY $[45/0/-45/90]_{2s}$
CLC-15 TEST FIXTURE

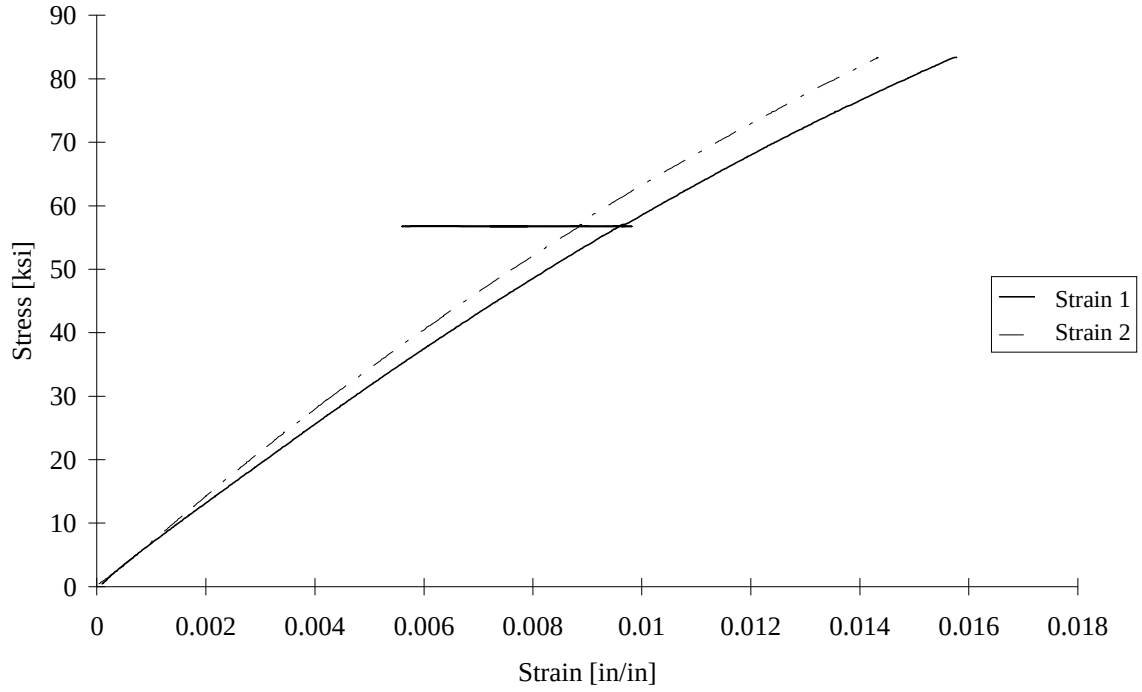

FIGURE D-31. TEST SPECIMEN I30Q01: T300/3034 CARBON/EPOXY $[45/0/-45/90]_{2s}$
IITRI TEST FIXTURE

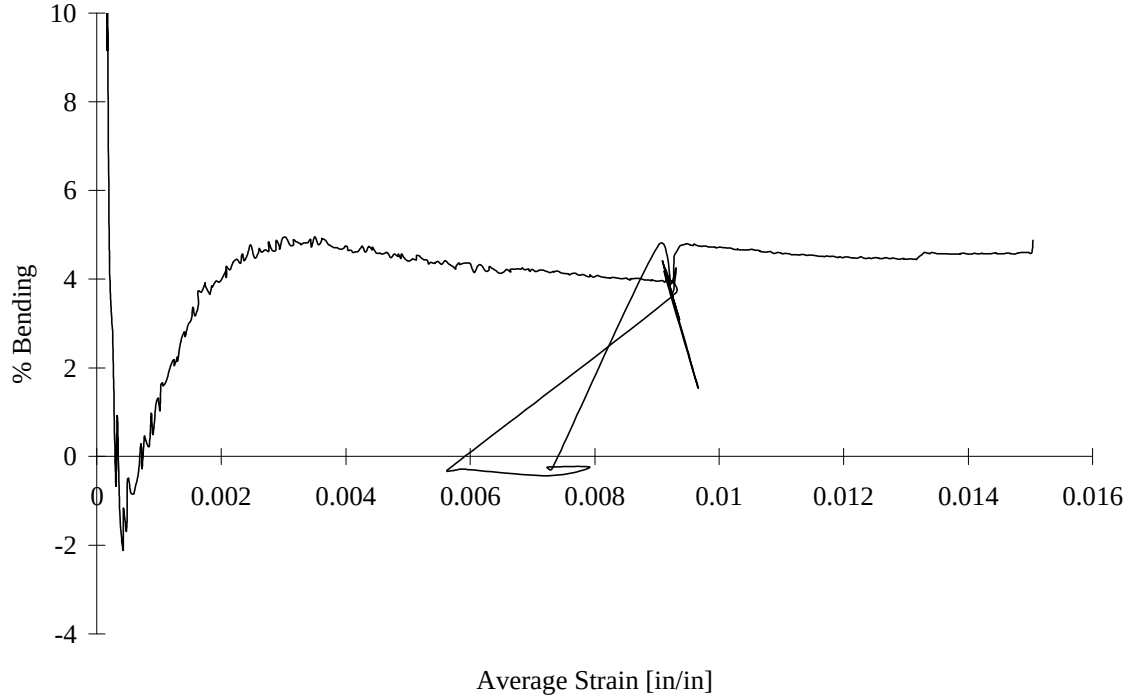

FIGURE D-32. TEST SPECIMEN I30Q01: T300/3034 CARBON/EPOXY $[45/0/-45/90]_{2s}$
IITRI TEST FIXTURE

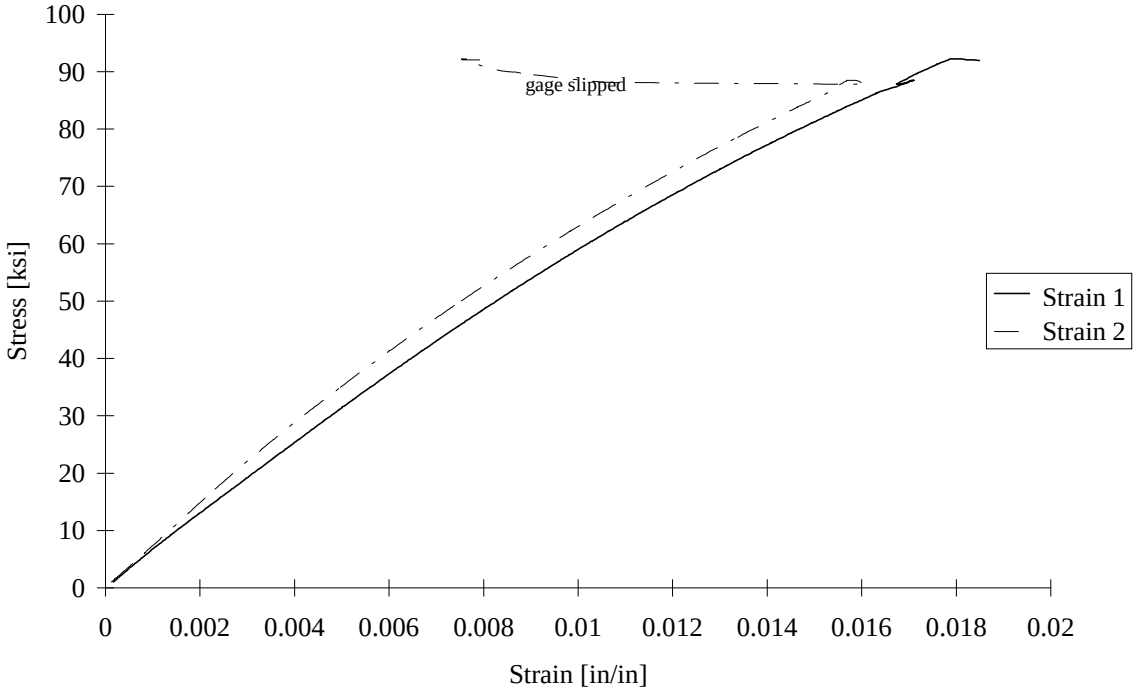

FIGURE D-33. TEST SPECIMEN I30Q02: T300/3034 CARBON/EPOXY $[45/0/-45/90]_{2s}$
IITRI TEST FIXTURE

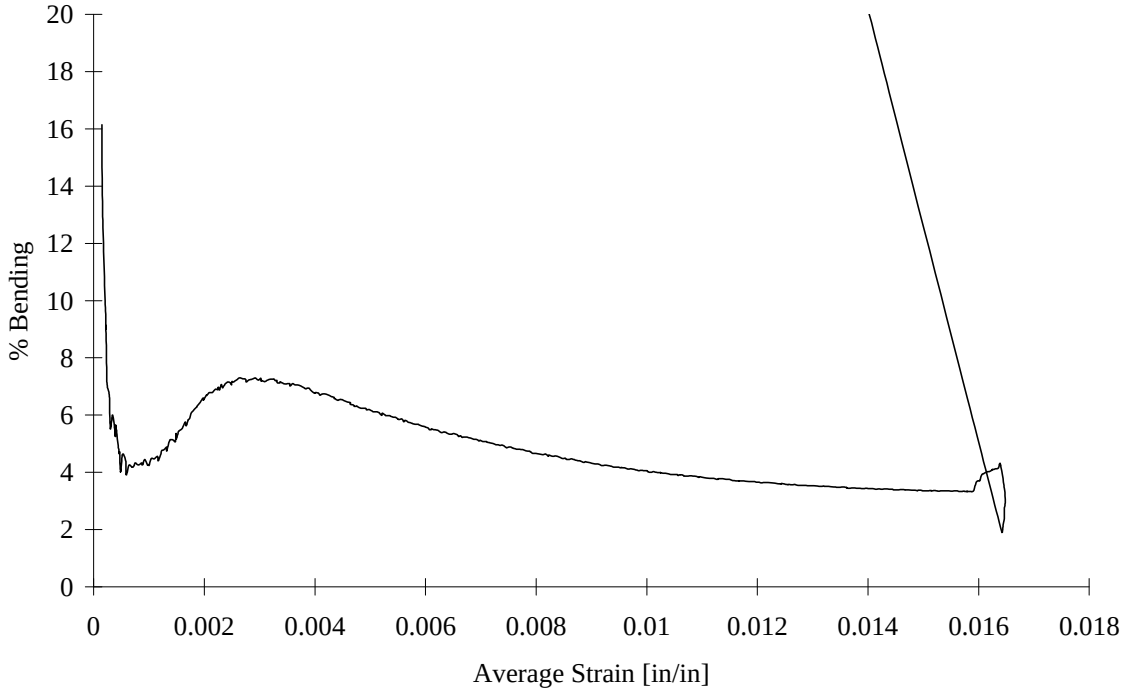

FIGURE D-34. TEST SPECIMEN I30Q02: T300/3034 CARBON/EPOXY $[45/0/-45/90]_{2s}$
IITRI TEST FIXTURE

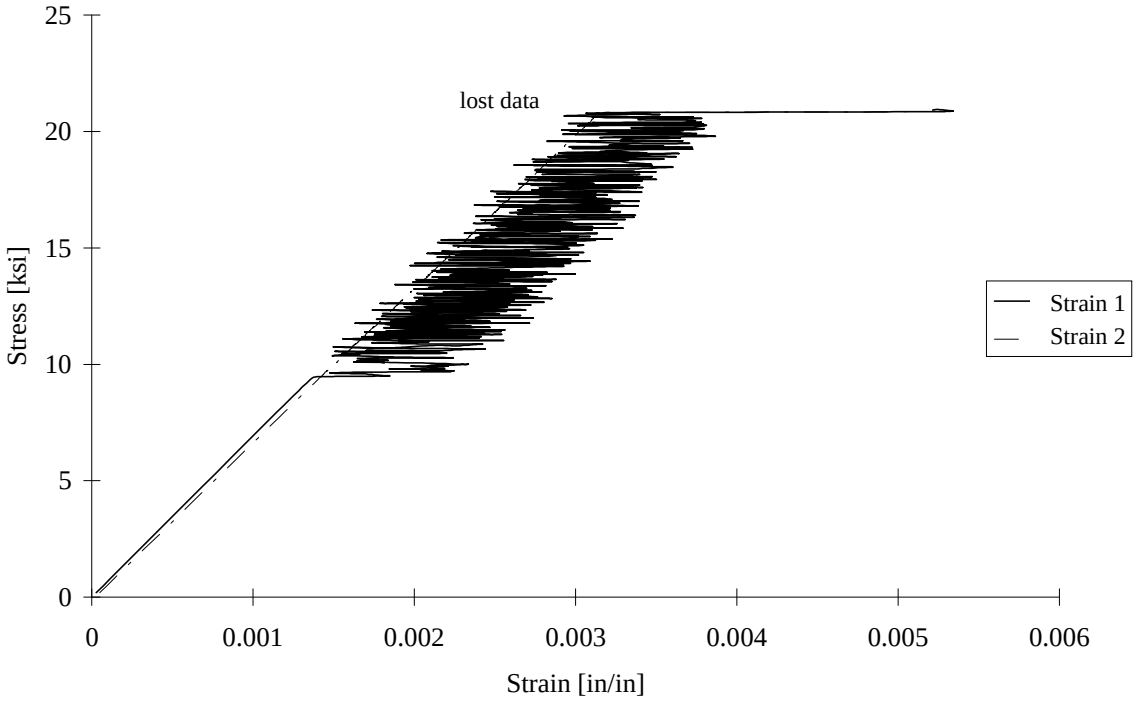

FIGURE D-35. TEST SPECIMEN I30Q03: T300/3034 CARBON/EPOXY $[45/0/-45/90]_{2s}$
IITRI TEST FIXTURE

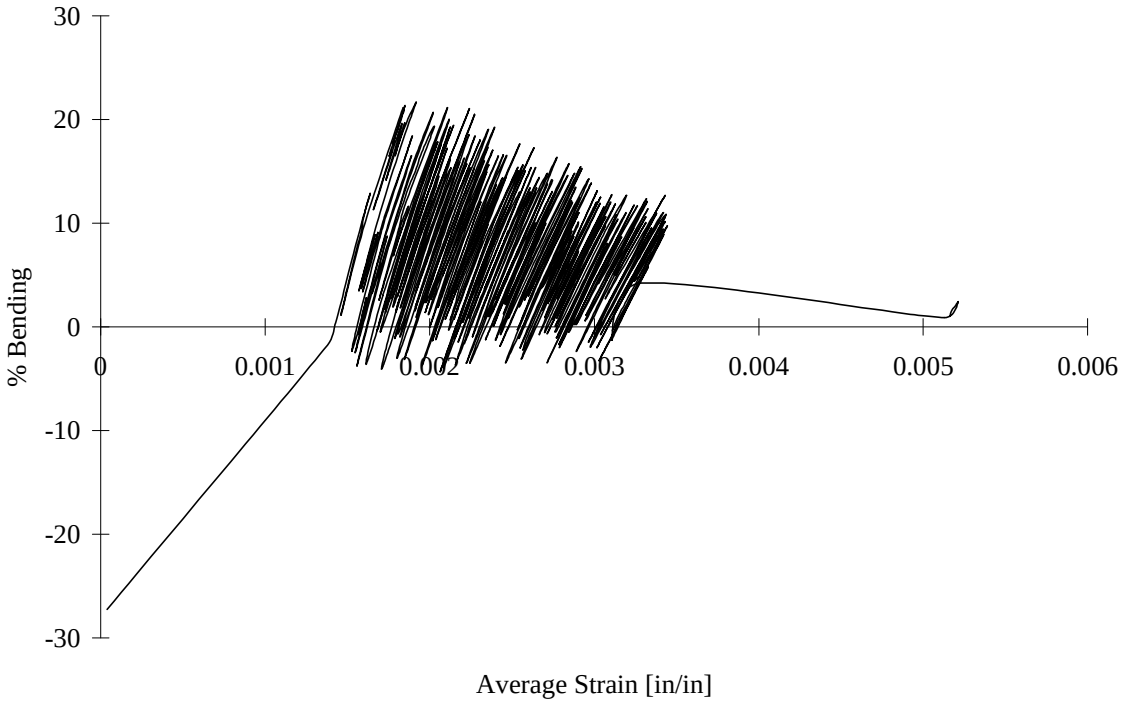

FIGURE D-36. TEST SPECIMEN I30Q03: T300/3034 CARBON/EPOXY $[45/0/-45/90]_{2s}$
IITRI TEST FIXTURE

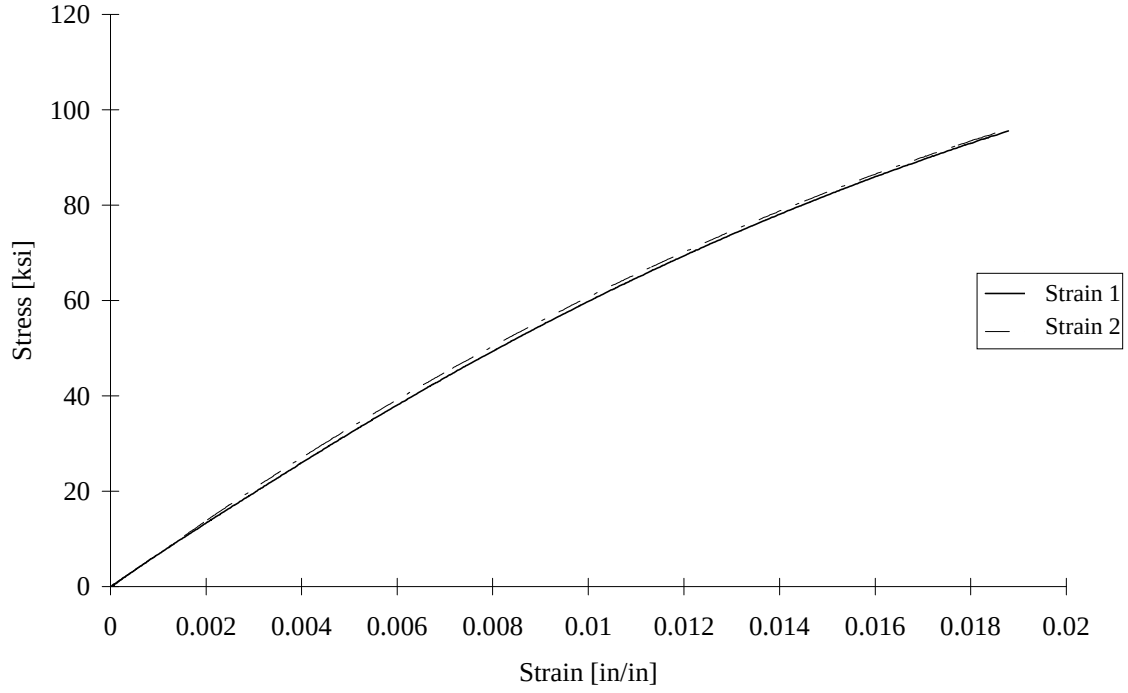

FIGURE D-37. TEST SPECIMEN I30Q04: T300/3034 CARBON/EPOXY $[45/0/-45/90]_{2s}$
IITRI TEST FIXTURE

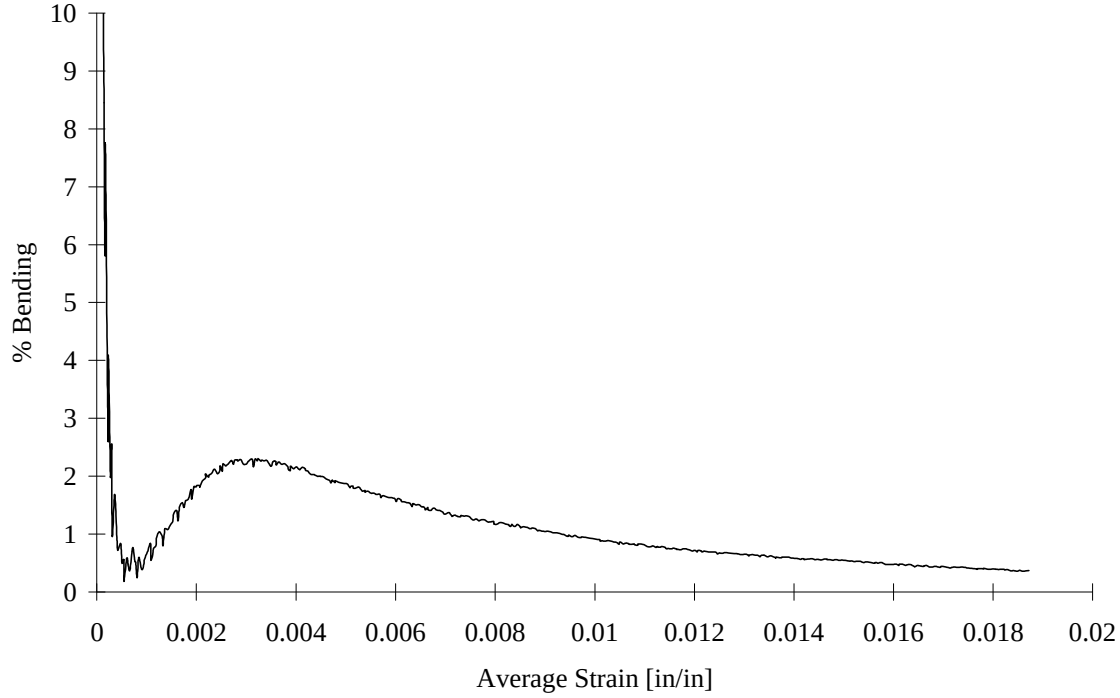

FIGURE D-38. TEST SPECIMEN I30Q04: T300/3034 CARBON/EPOXY $[45/0/-45/90]_{2s}$
IITRI TEST FIXTURE

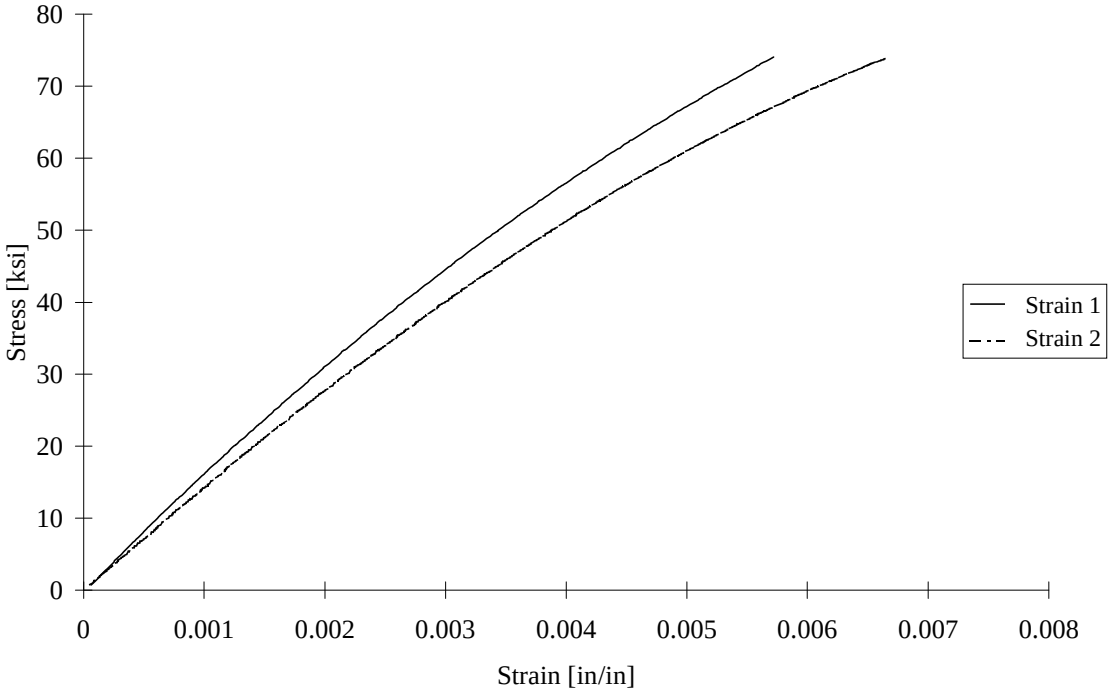

FIGURE D-39. TEST SPECIMEN C50C01: T50/2134A CARBON/EPOXY $[90/0]_{4s}$
CLC-15 TEST FIXTURE

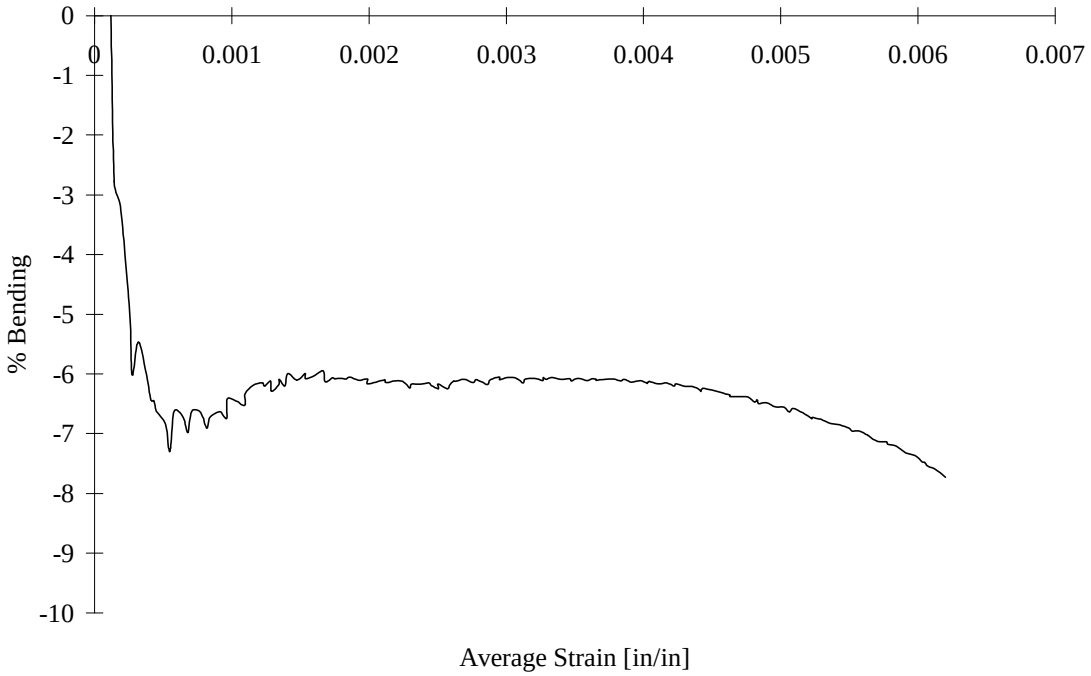

FIGURE D-40. TEST SPECIMEN C50C01: T50/2134A CARBON/EPOXY $[90/0]_{4s}$
CLC-15 TEST FIXTURE

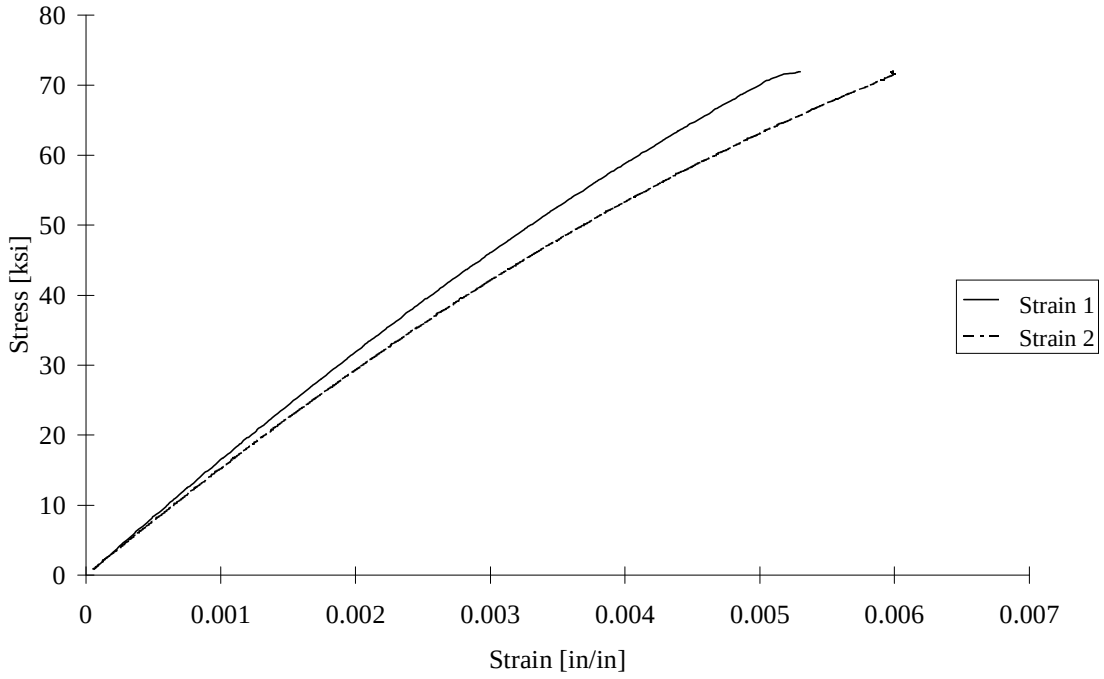

FIGURE D-41. TEST SPECIMEN C50C02: T50/2134A CARBON/EPOXY $[90/0]_{4s}$
CLC-15 TEST FIXTURE

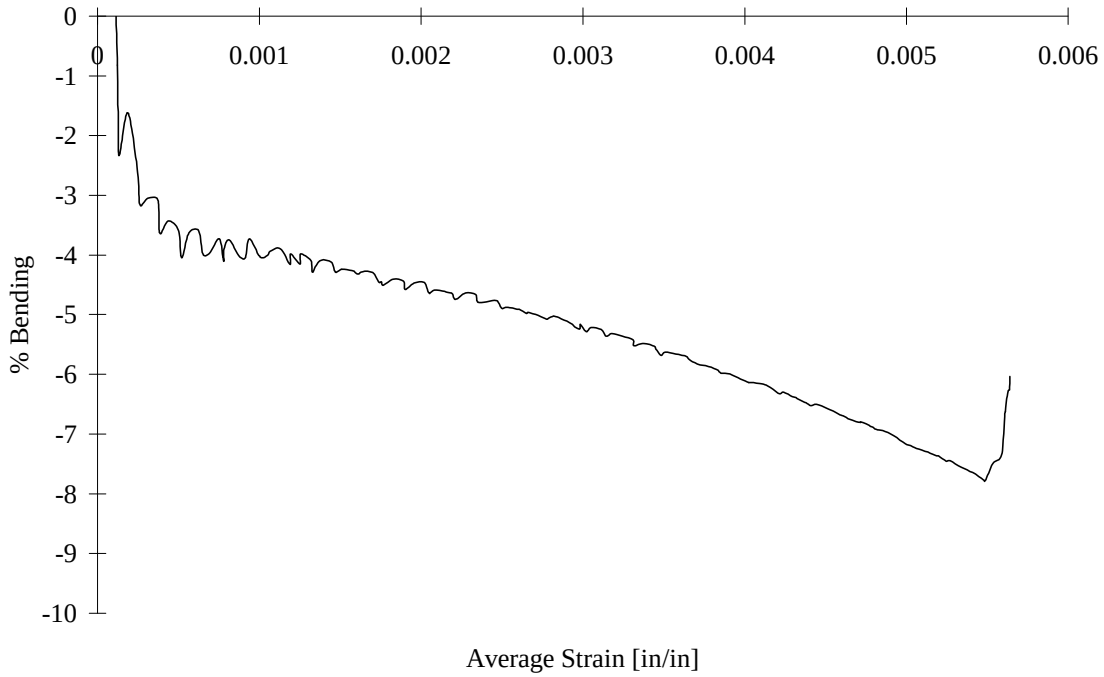

FIGURE D-42. TEST SPECIMEN C50C02: T50/2134A CARBON/EPOXY $[90/0]_{4s}$
CLC-15 TEST FIXTURE

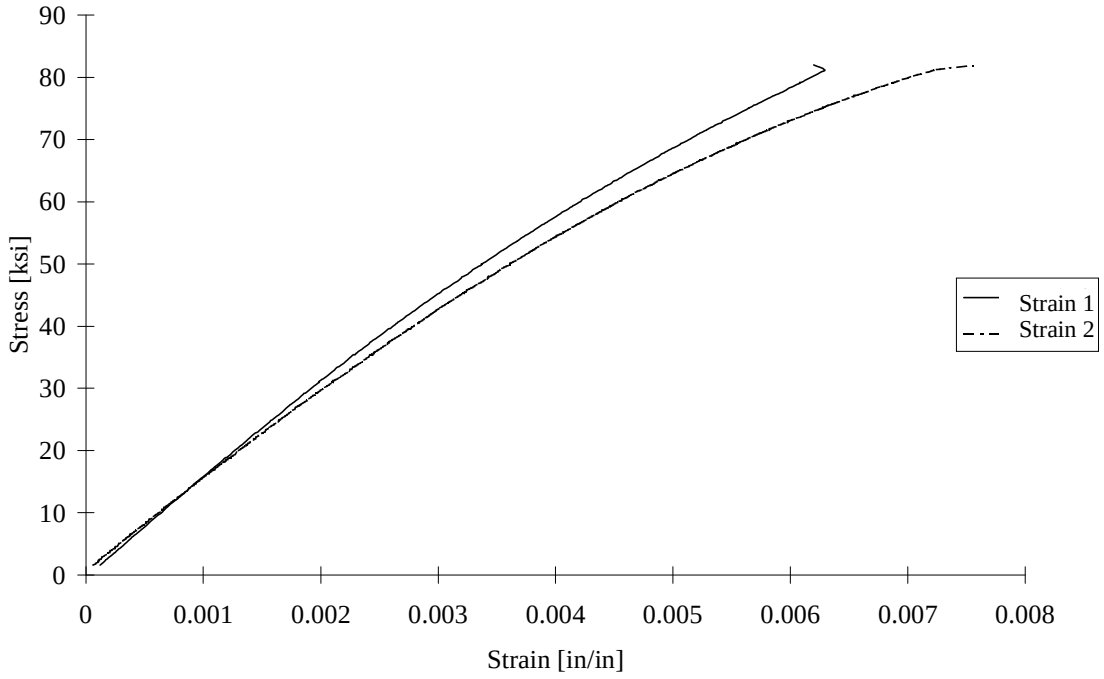

FIGURE D-43. TEST SPECIMEN C50C03: T50/2134A CARBON/EPOXY $[90/0]_{4s}$
CLC-15 TEST FIXTURE

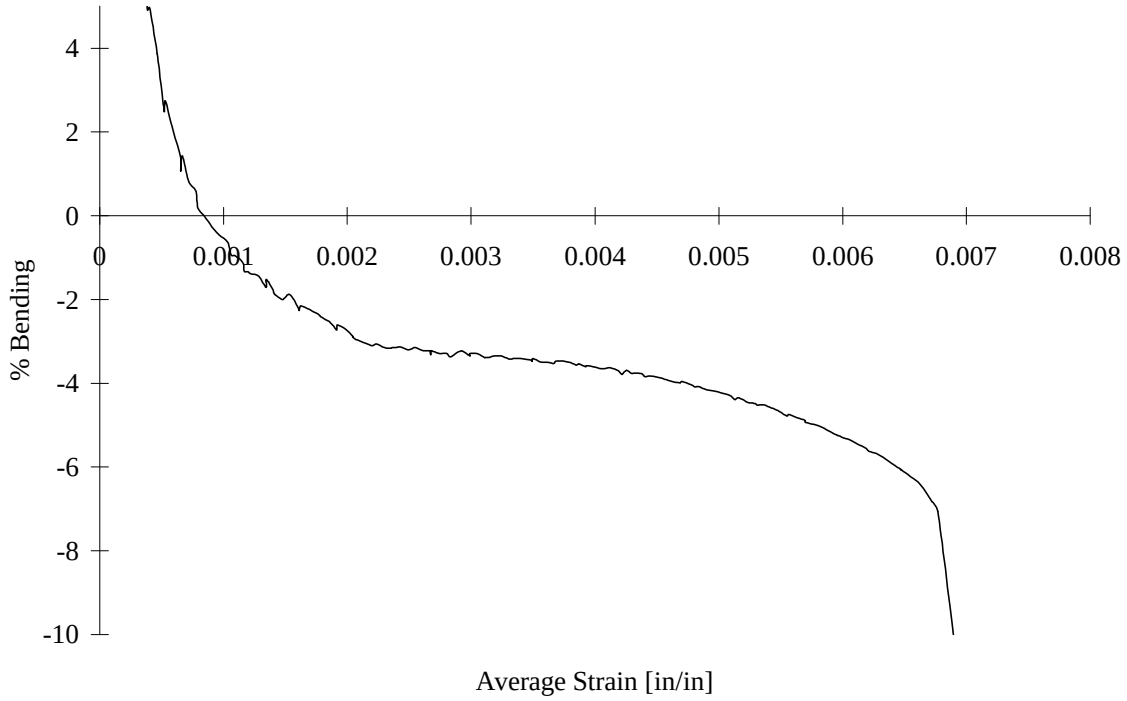

FIGURE D-44. TEST SPECIMEN C50C03: T50/2134A CARBON/EPOXY $[90/0]_{4s}$
CLC-15 TEST FIXTURE

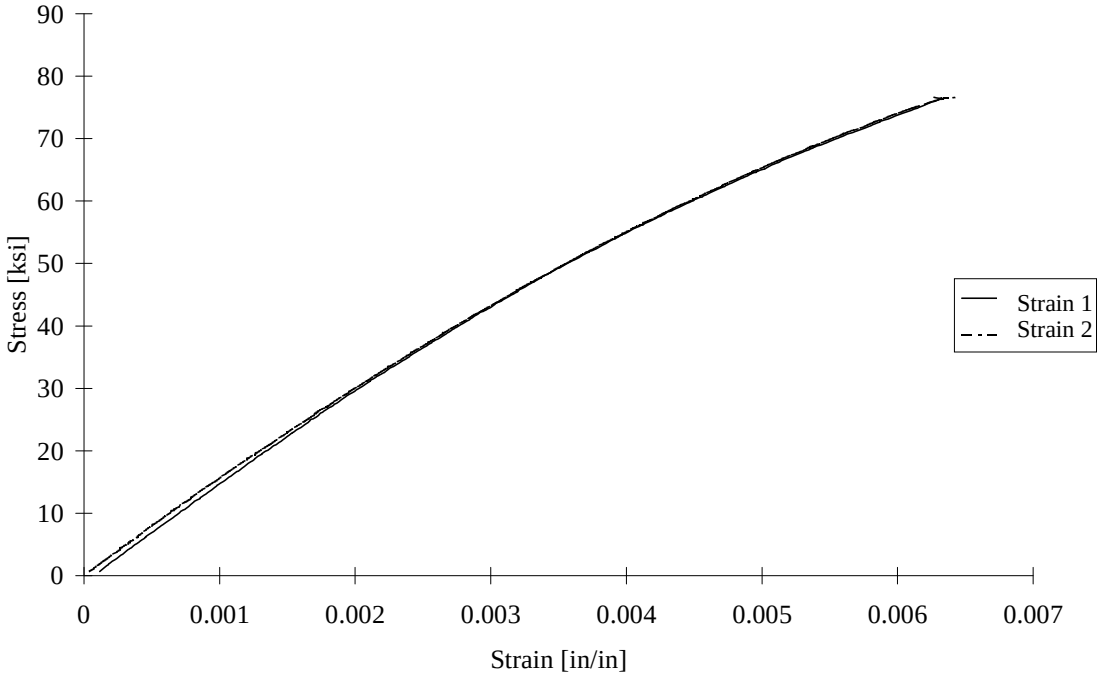

FIGURE D-45. TEST SPECIMEN C50C04: T50/2134A CARBON/EPOXY $[90/0]_{4s}$
CLC-15 TEST FIXTURE

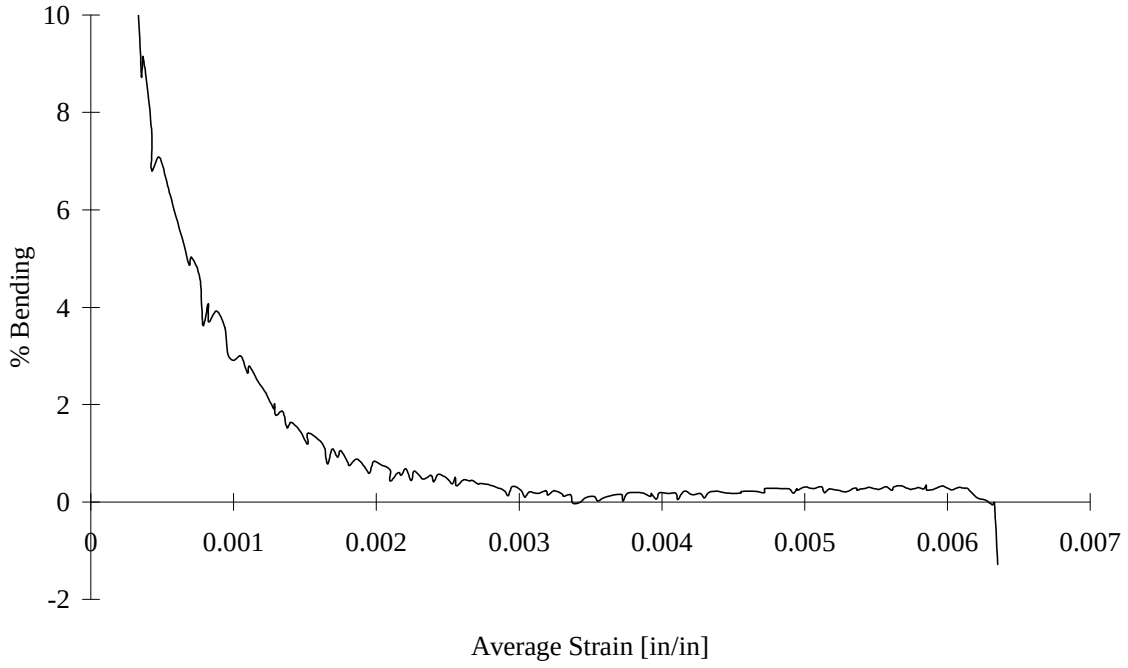

FIGURE D-46. TEST SPECIMEN C50C04: T50/2134A CARBON/EPOXY $[90/0]_{4s}$
CLC-15 TEST FIXTURE

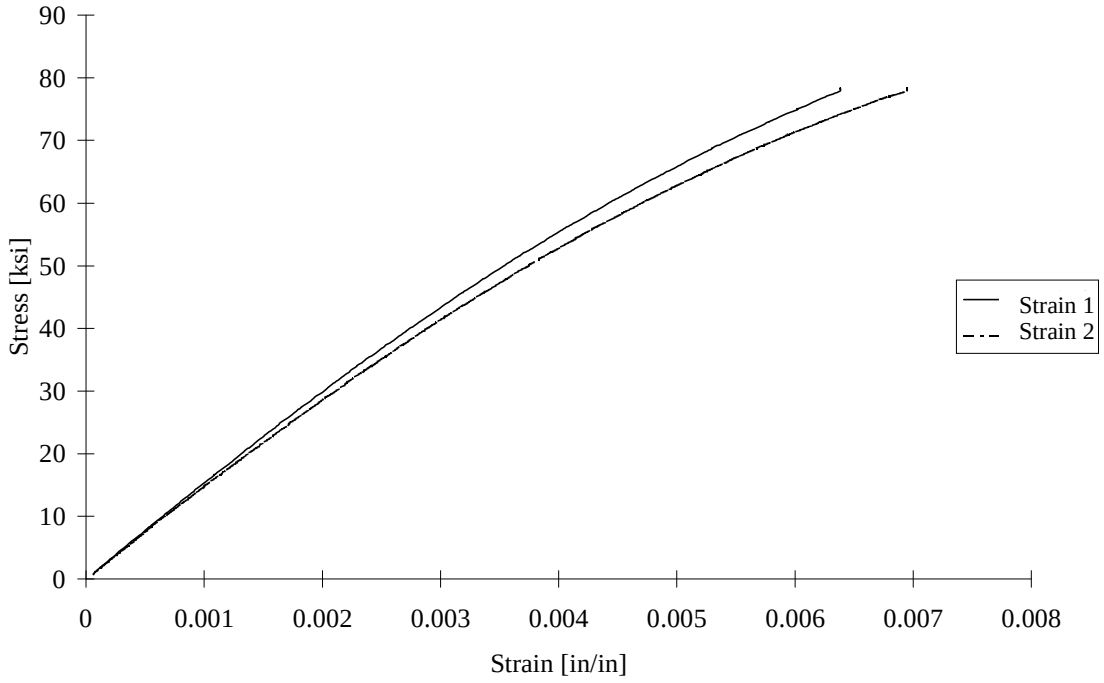

FIGURE D-47. TEST SPECIMEN C50C05: T50/2134A CARBON/EPOXY $[90/0]_{4s}$
CLC-15 TEST FIXTURE

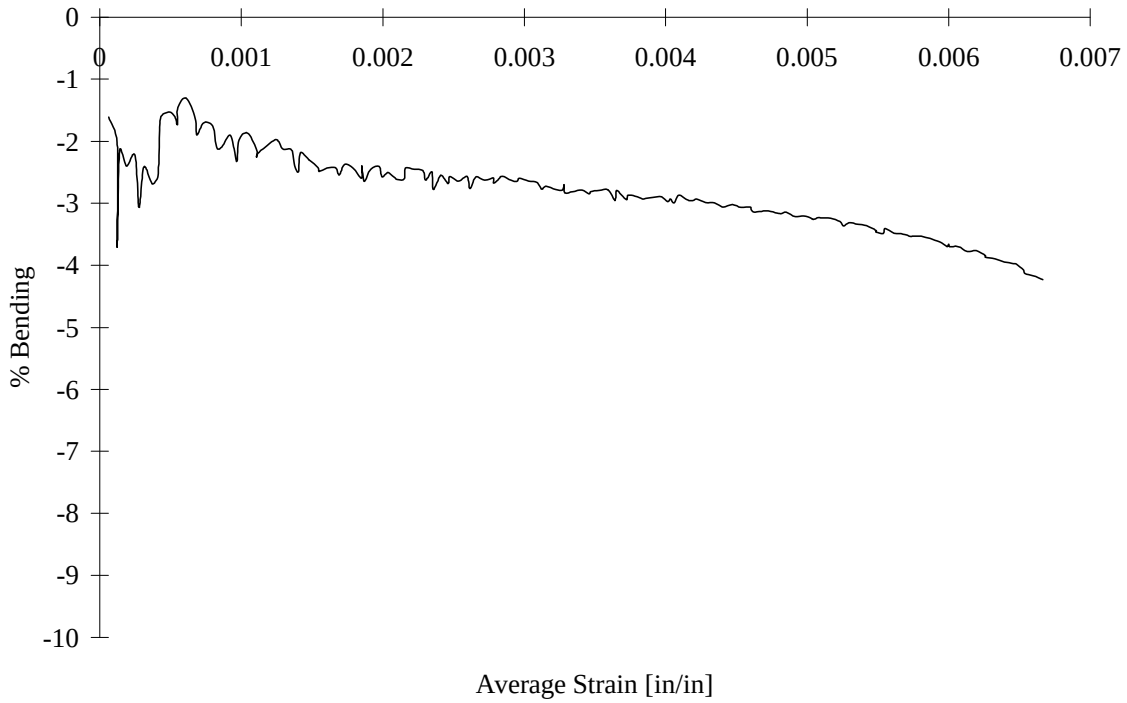

FIGURE D-48. TEST SPECIMEN C50C05: T50/2134A CARBON/EPOXY $[90/0]_{4s}$
CLC-15 TEST FIXTURE

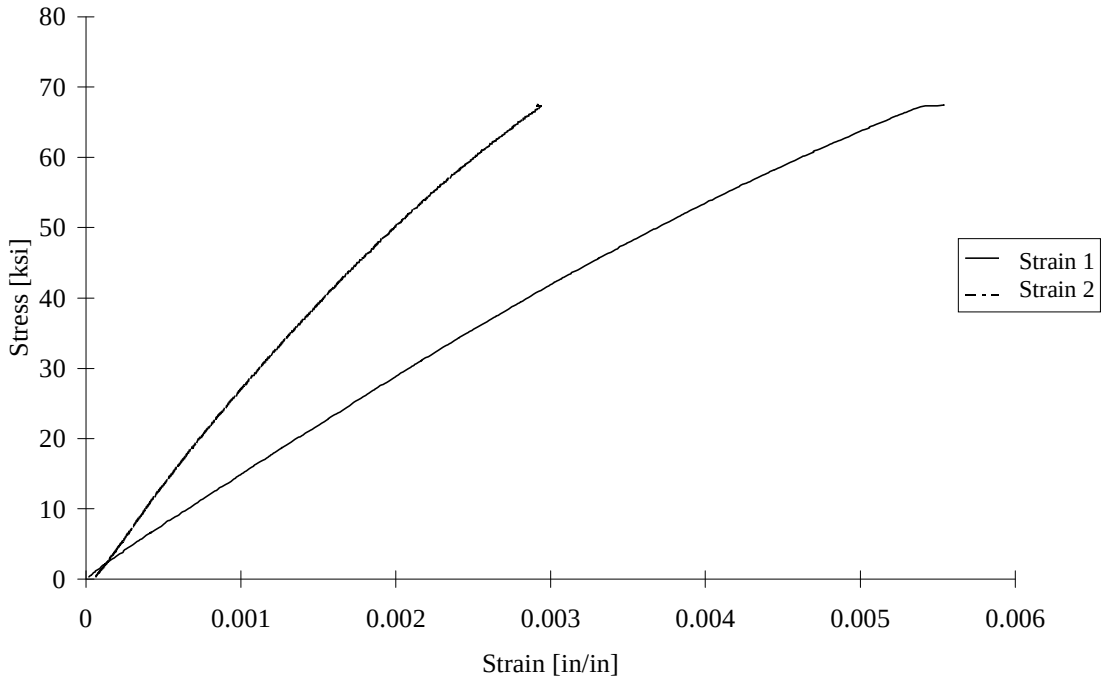

FIGURE D-49. TEST SPECIMEN I50C01: T50/2134A CARBON/EPOXY $[90/0]_{4s}$
IITRI TEST FIXTURE

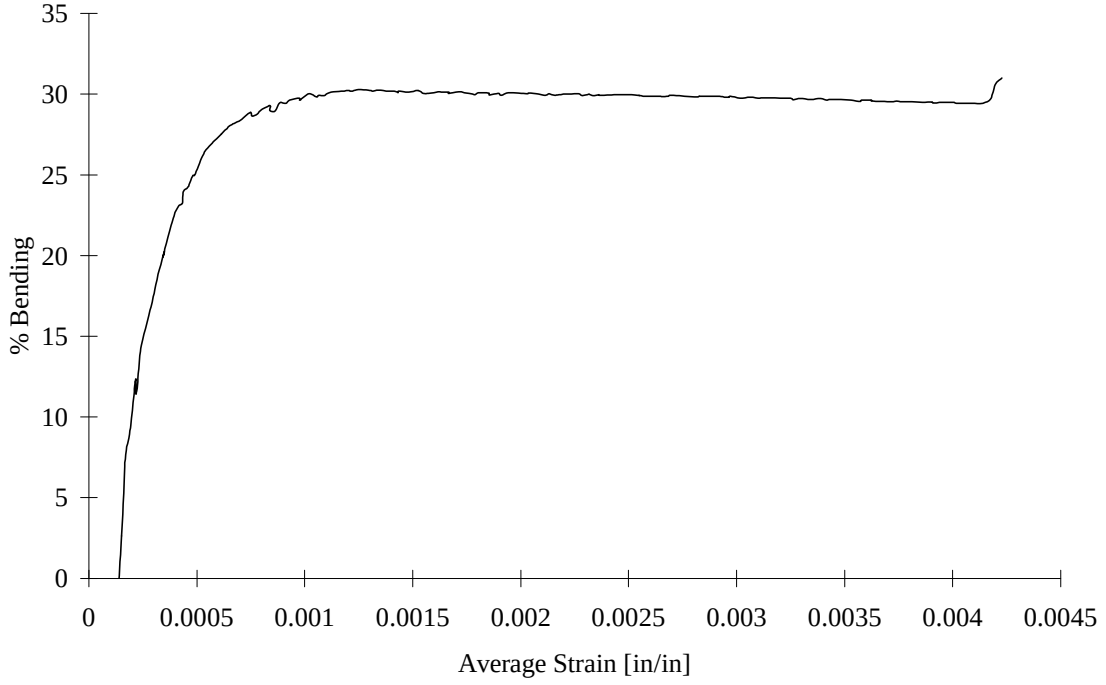

FIGURE D-50. TEST SPECIMEN I50C01: T50/2134A CARBON/EPOXY $[90/0]_{4s}$
IITRI TEST FIXTURE

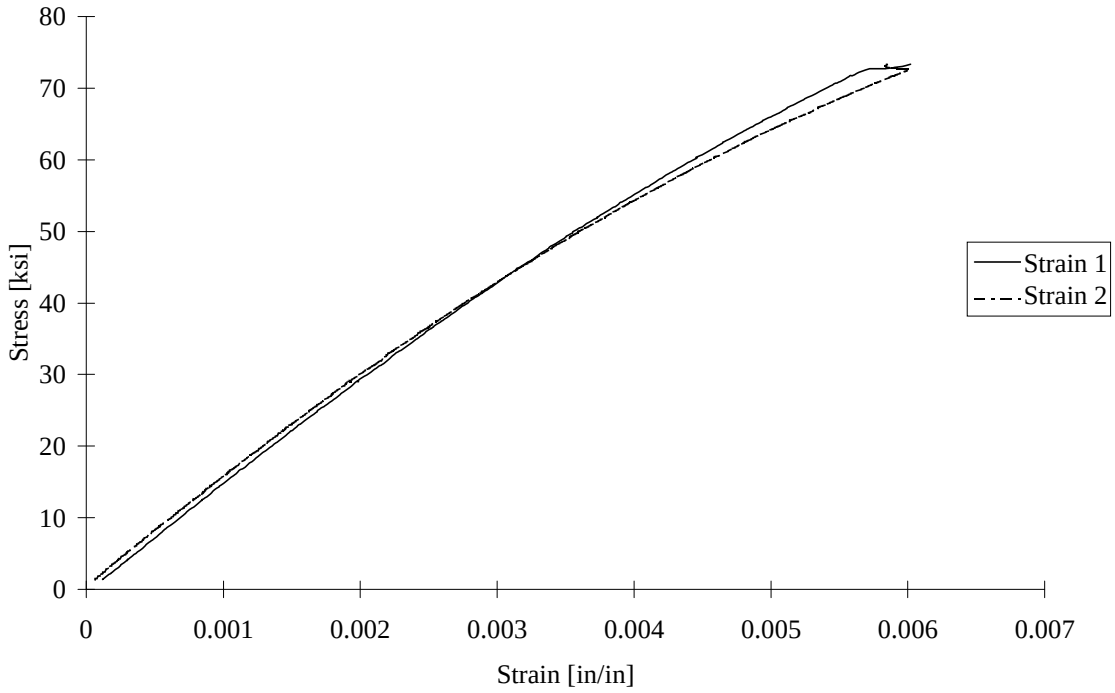

FIGURE D-51. TEST SPECIMEN I50C02: T50/2134A CARBON/EPOXY $[90/0]_{4s}$
IITRI TEST FIXTURE

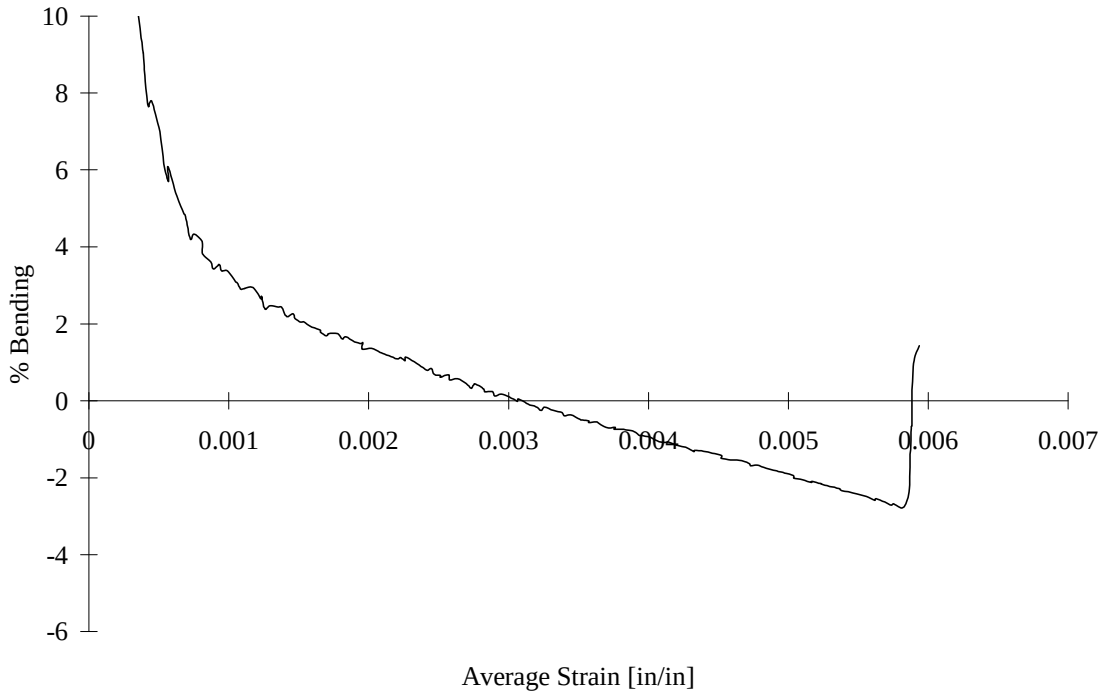

FIGURE D-52. TEST SPECIMEN I50C02: T50/2134A CARBON/EPOXY $[90/0]_{4s}$
IITRI TEST FIXTURE

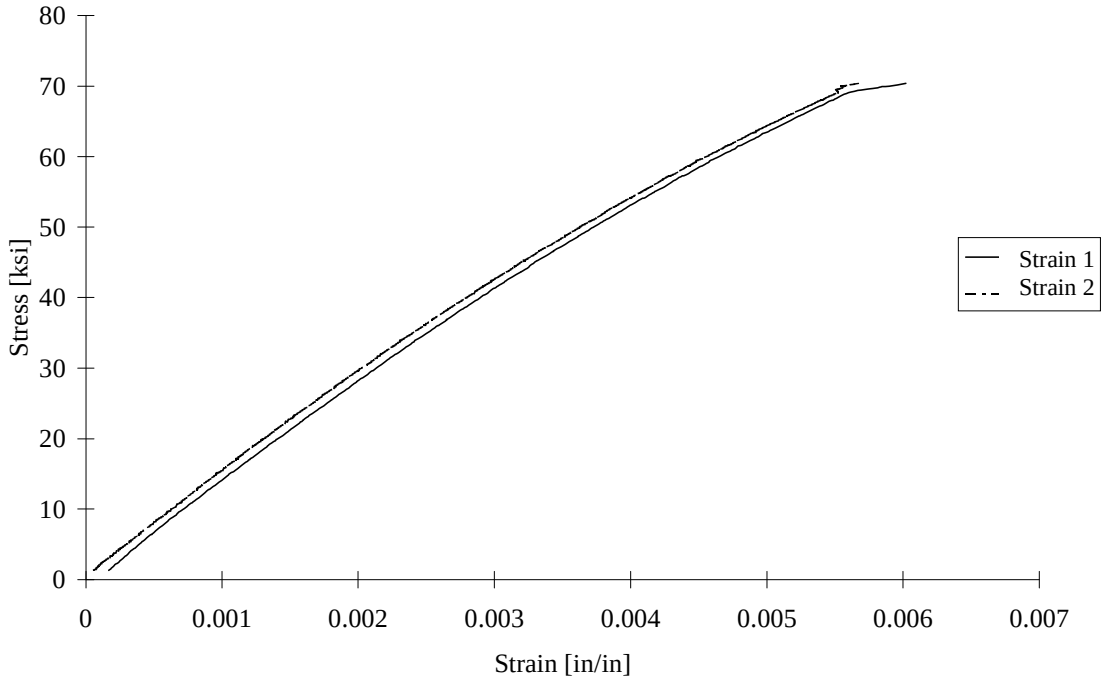

FIGURE D-53. TEST SPECIMEN I50C03: T50/2134A CARBON/EPOXY $[90/0]_{4s}$
IITRI TEST FIXTURE

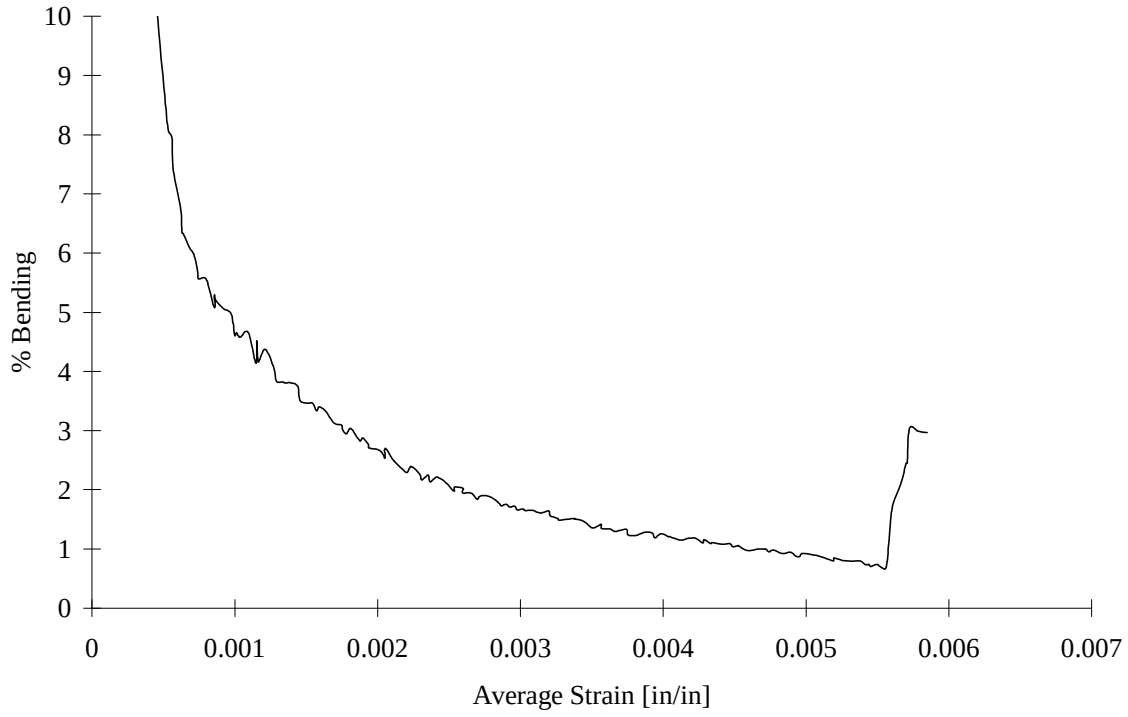

FIGURE D-54. TEST SPECIMEN I50C03: T50/2134A CARBON/EPOXY $[90/0]_{4s}$
IITRI TEST FIXTURE

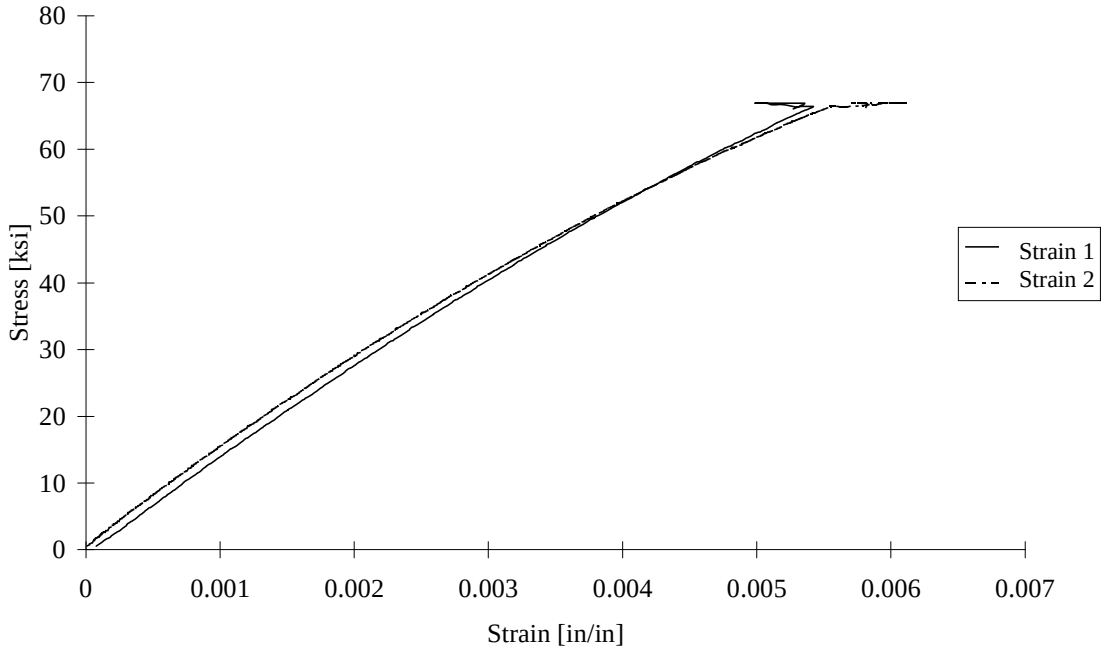

FIGURE D-55. TEST SPECIMEN I50C04: T50/2134A CARBON/EPOXY $[90/0]_{4s}$
IITRI TEST FIXTURE

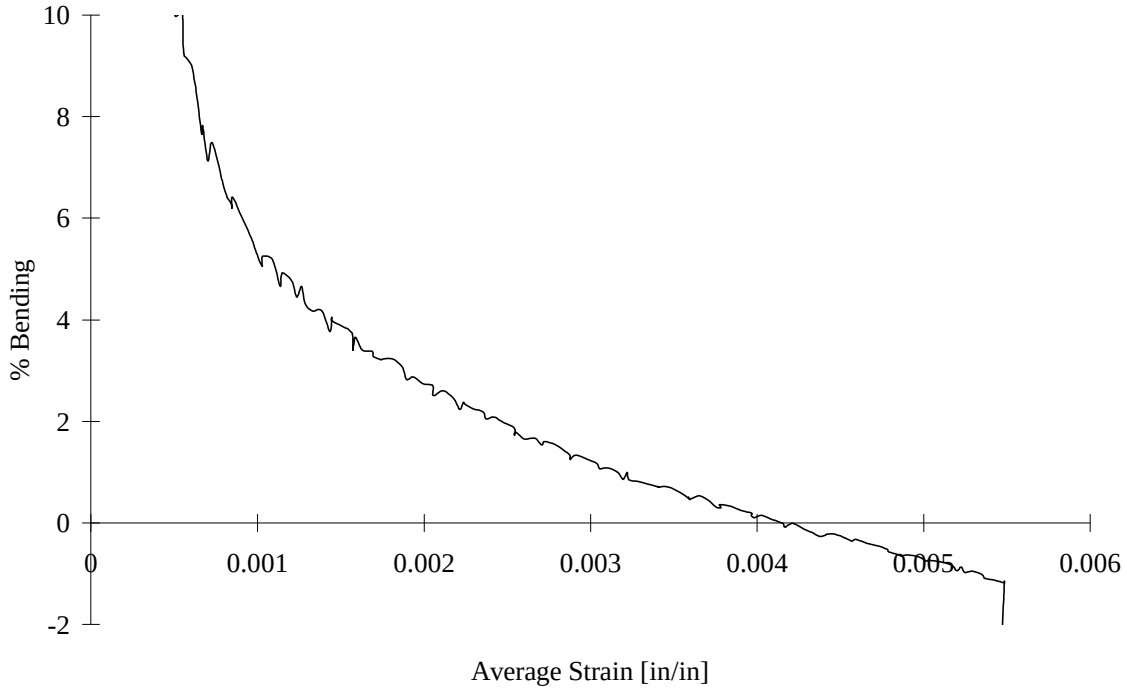

FIGURE D-56. TEST SPECIMEN I50C04: T50/2134A CARBON/EPOXY $[90/0]_{4s}$
IITRI TEST FIXTURE

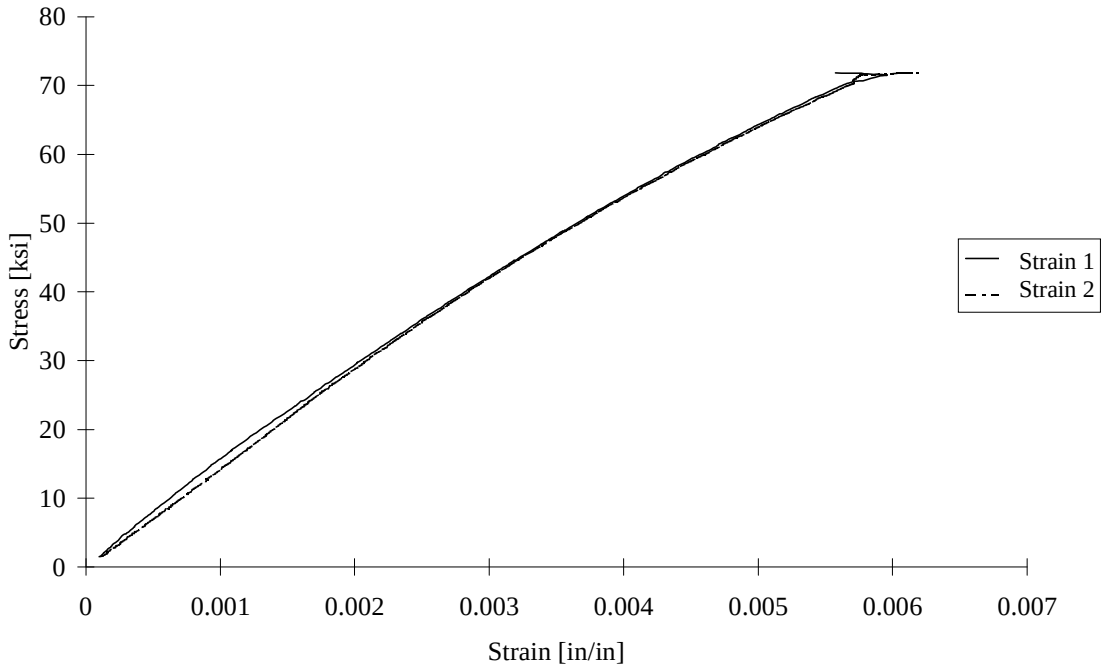

FIGURE D-57. TEST SPECIMEN I50C05: T50/2134A CARBON/EPOXY $[90/0]_{4s}$
IITRI TEST FIXTURE

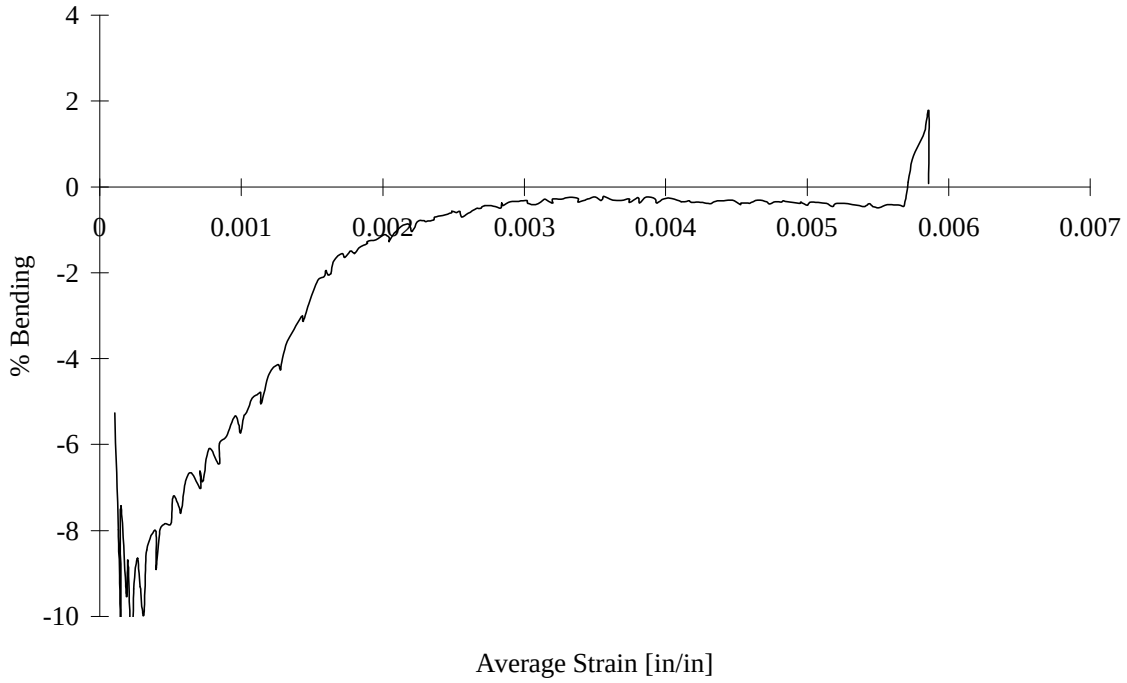

FIGURE D-58. TEST SPECIMEN I50C05: T50/2134A CARBON/EPOXY $[90/0]_{4s}$
IITRI TEST FIXTURE

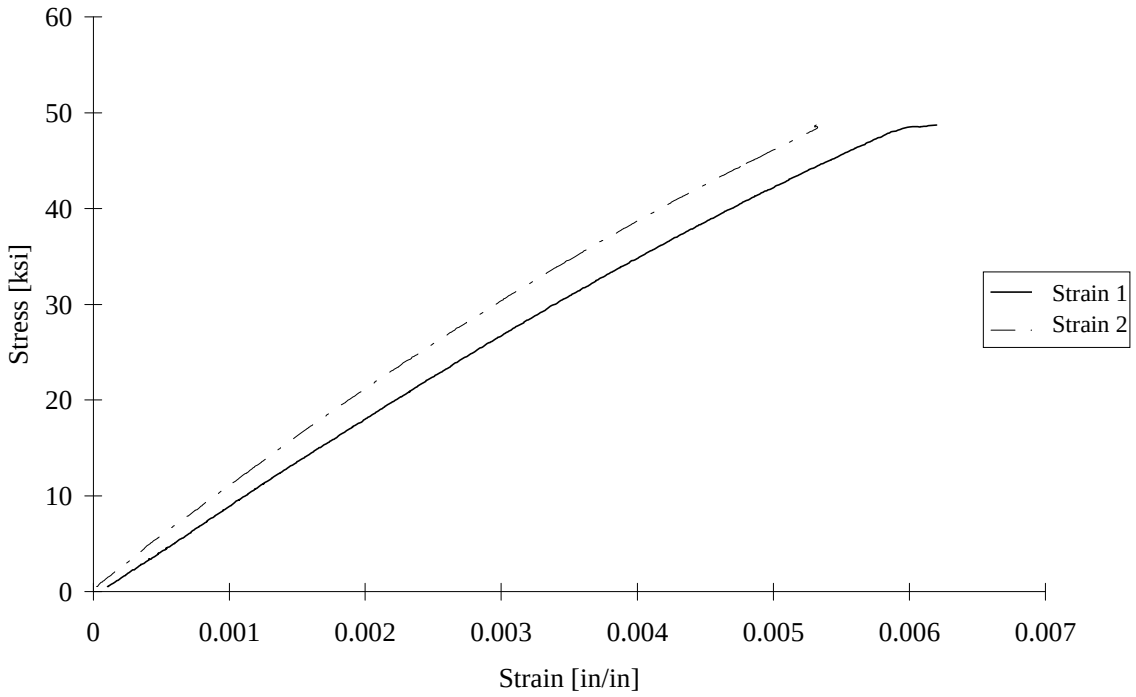

FIGURE D-59. TEST SPECIMEN C50Q01: T50/2134A CARBON/EPOXY $[45/0/-45/90]_{2s}$
CLC-15 TEST FIXTURE

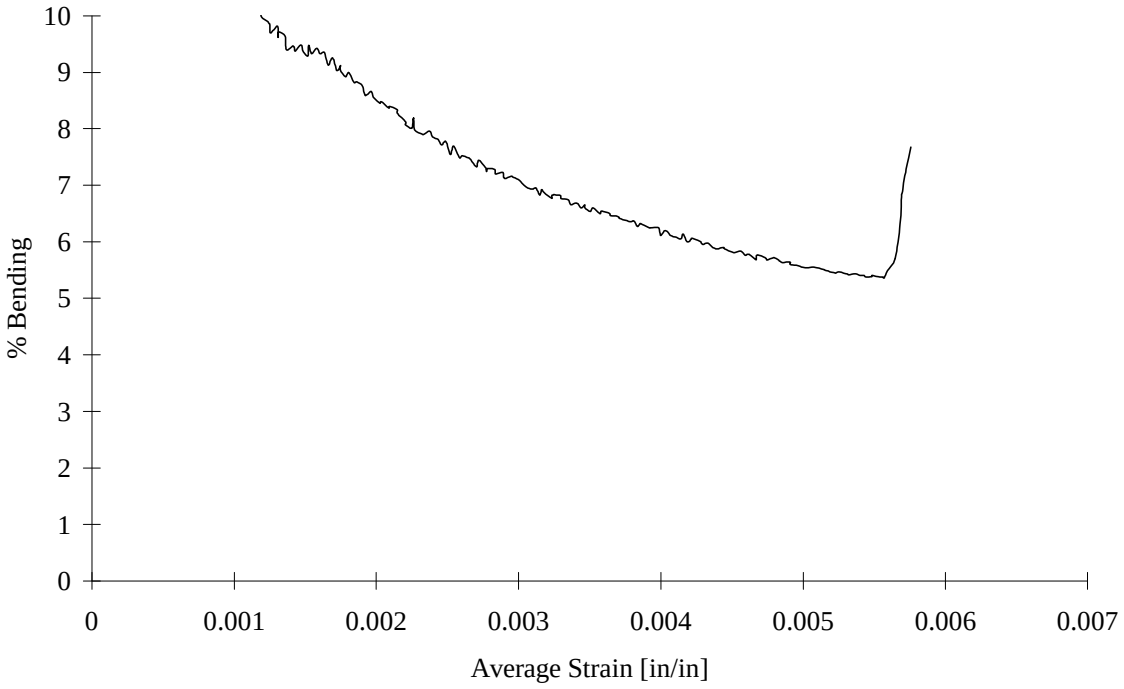

FIGURE D-60. TEST SPECIMEN C50Q01: T50/2134A CARBON/EPOXY $[45/0/-45/90]_{2s}$
CLC-15 TEST FIXTURE

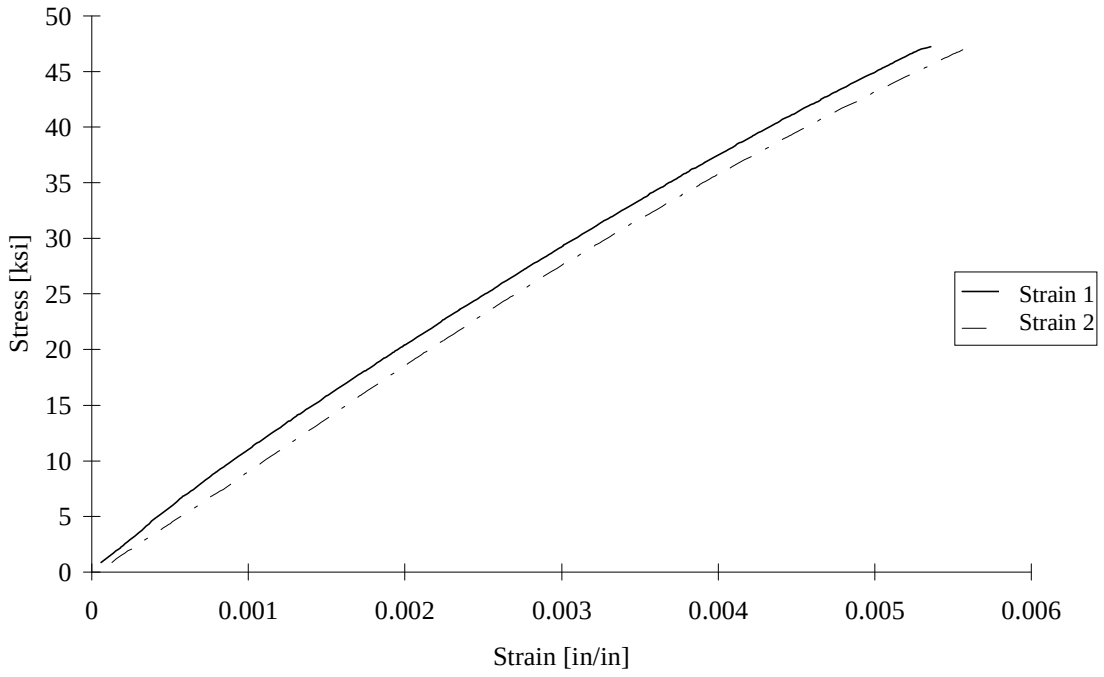

FIGURE D-61. TEST SPECIMEN C50Q02: T50/2134A CARBON/EPOXY $[45/0/-45/90]_{2s}$
CLC-15 TEST FIXTURE

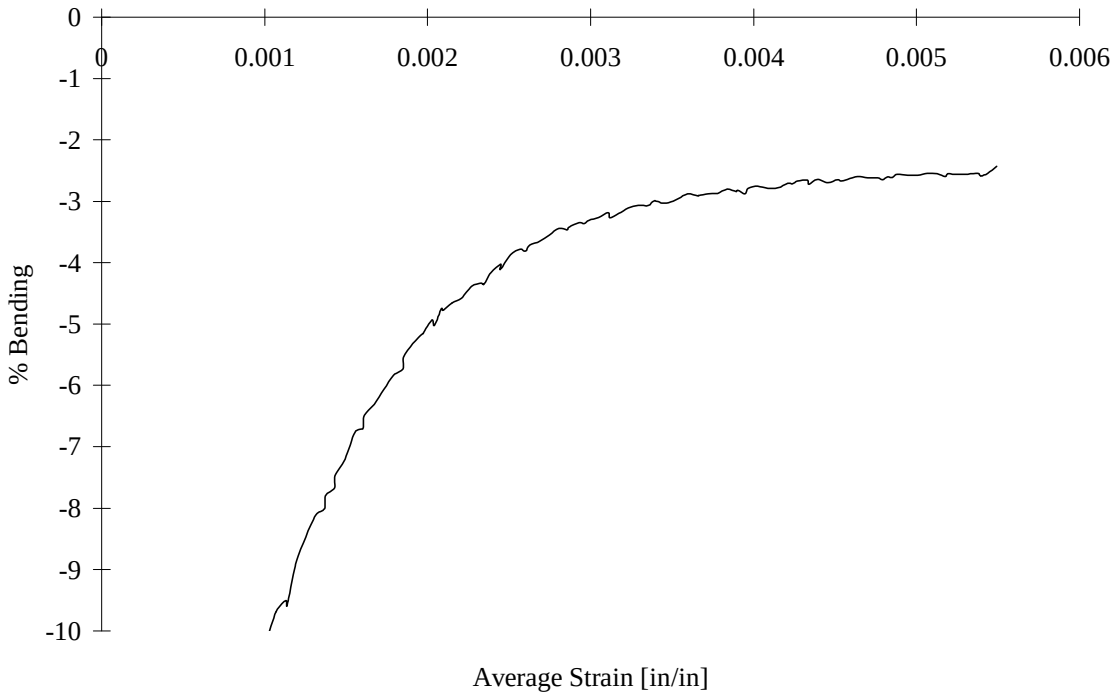

FIGURE D-62. TEST SPECIMEN C50Q02: T50/2134A CARBON/EPOXY $[45/0/-45/90]_{2s}$
CLC-15 TEST FIXTURE

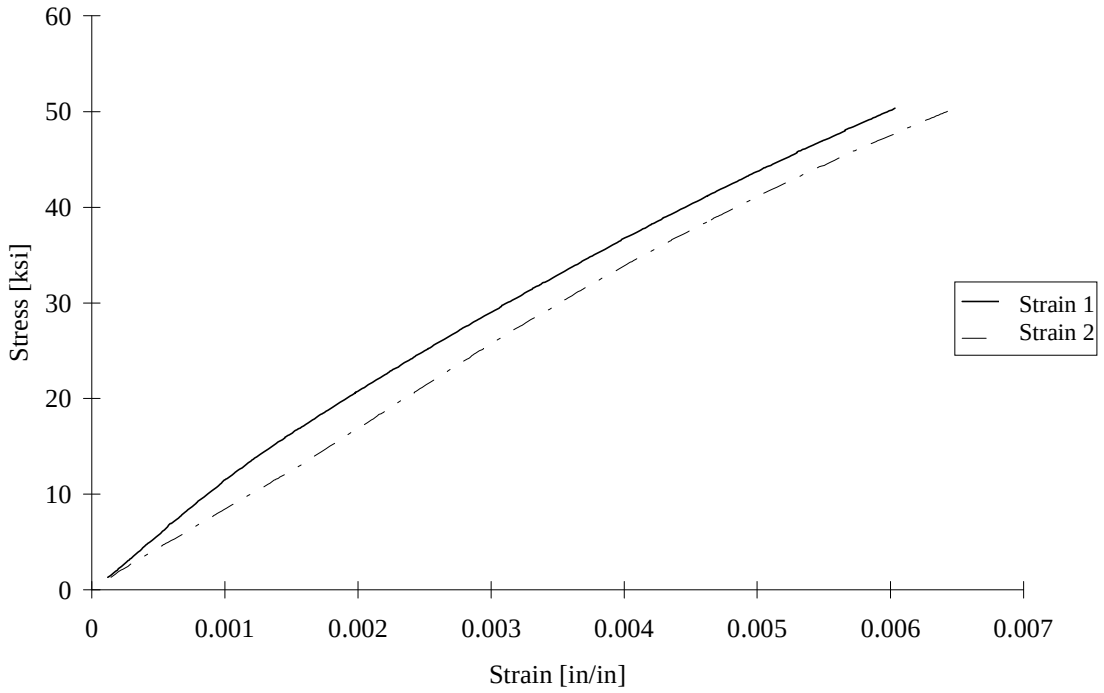

FIGURE D-63. TEST SPECIMEN C50Q03: T50/2134A CARBON/EPOXY $[45/0/-45/90]_{2s}$
CLC-15 TEST FIXTURE

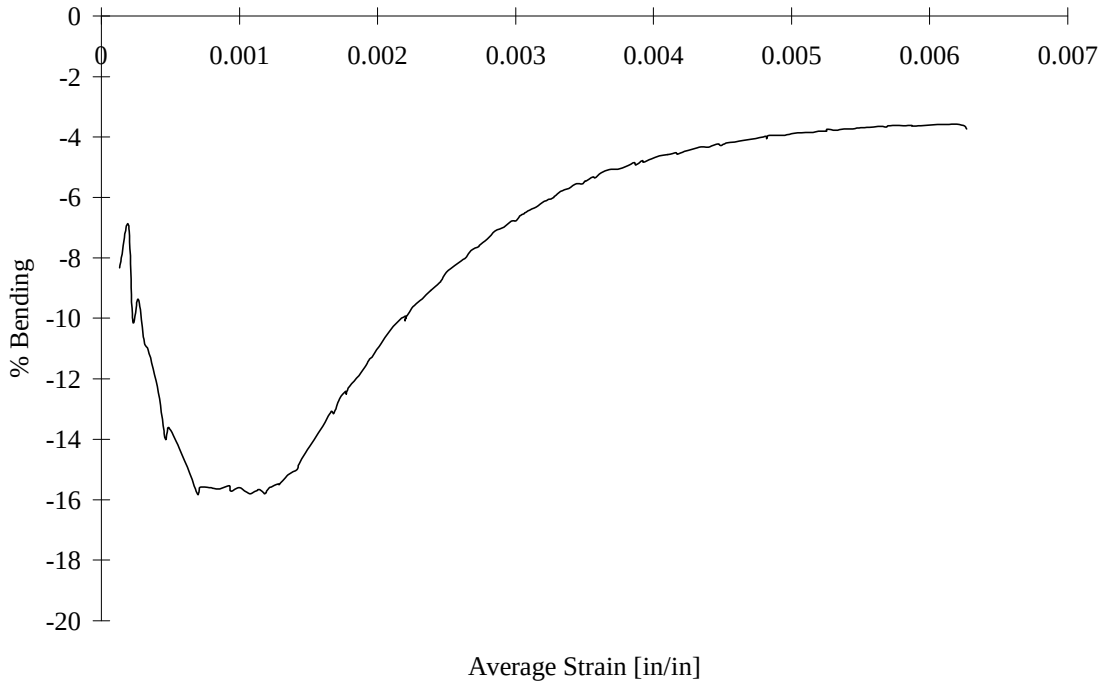

FIGURE D-64. TEST SPECIMEN C50Q03: T50/2134A CARBON/EPOXY $[45/0/-45/90]_{2s}$
CLC-15 TEST FIXTURE

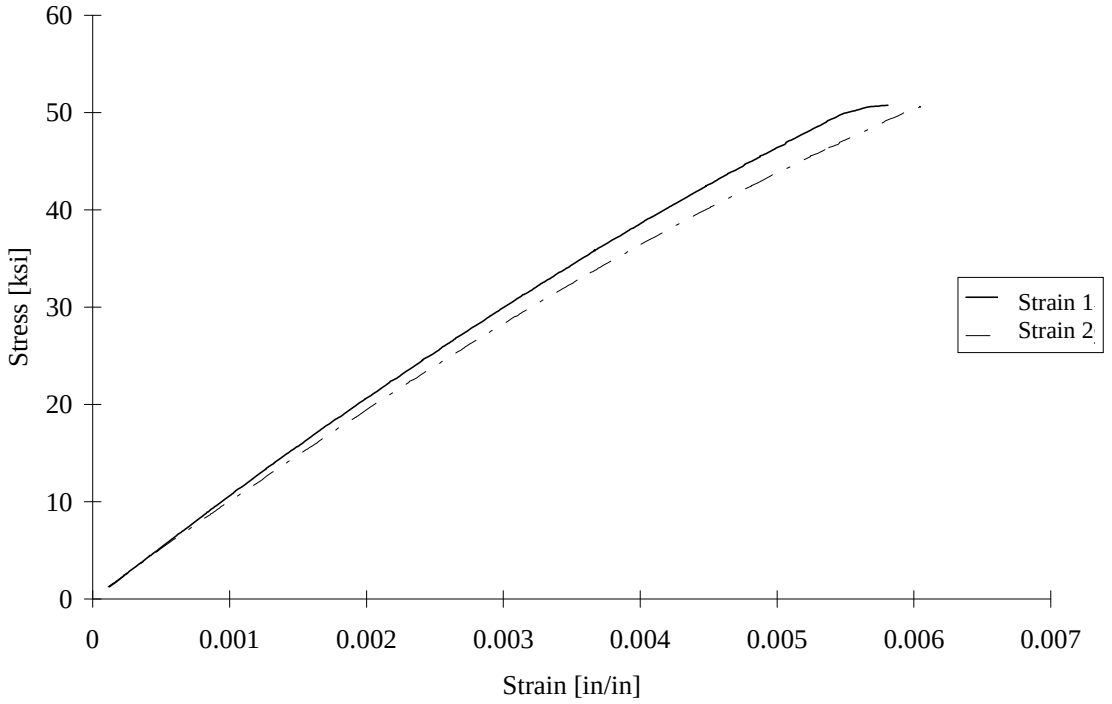

FIGURE D-65. TEST SPECIMEN C50Q04: T50/2134A CARBON/EPOXY $[45/0/-45/90]_{2s}$
CLC-15 TEST FIXTURE

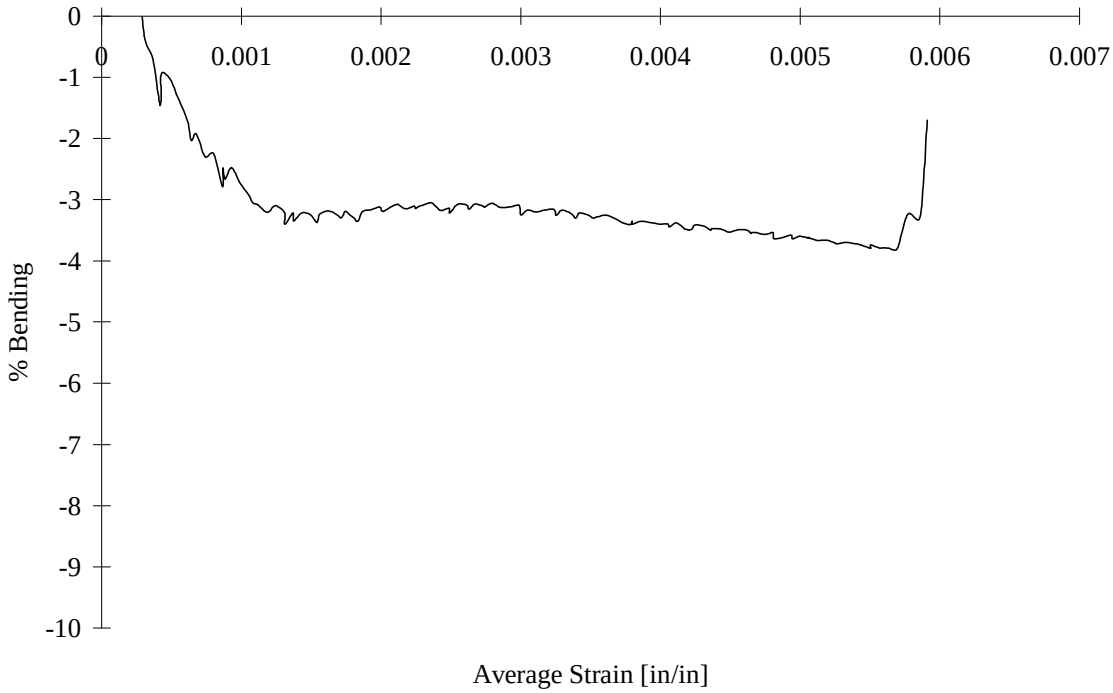

FIGURE D-66. TEST SPECIMEN C50Q04: T50/2134A CARBON/EPOXY $[45/0/-45/90]_{2s}$
CLC-15 TEST FIXTURE

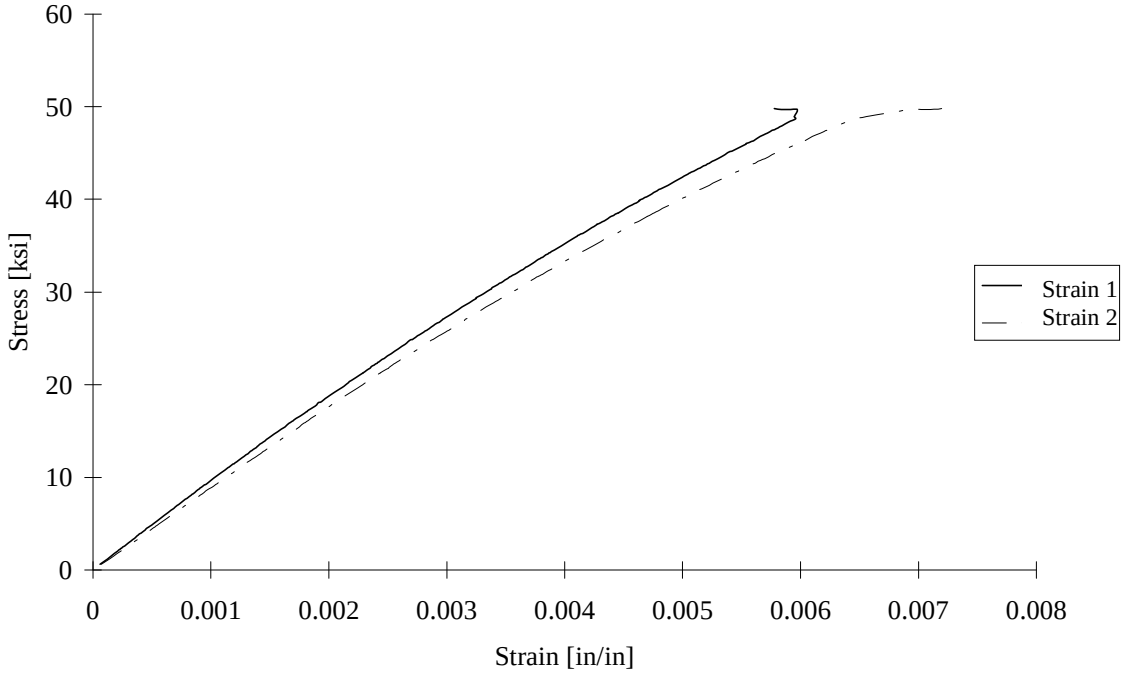

FIGURE D-67. TEST SPECIMEN C50Q05: T50/2134A CARBON/EPOXY $[45/0/-45/90]_{2s}$
CLC-15 TEST FIXTURE

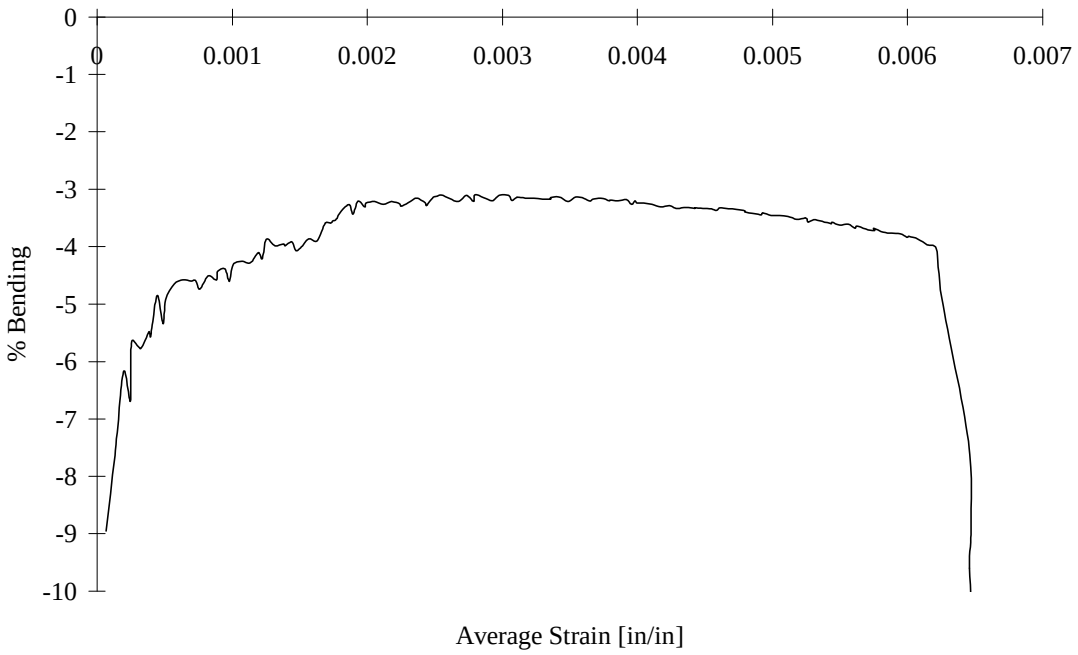

FIGURE D-68. TEST SPECIMEN C50Q05: T50/2134A CARBON/EPOXY $[45/0/-45/90]_{2s}$
CLC-15 TEST FIXTURE

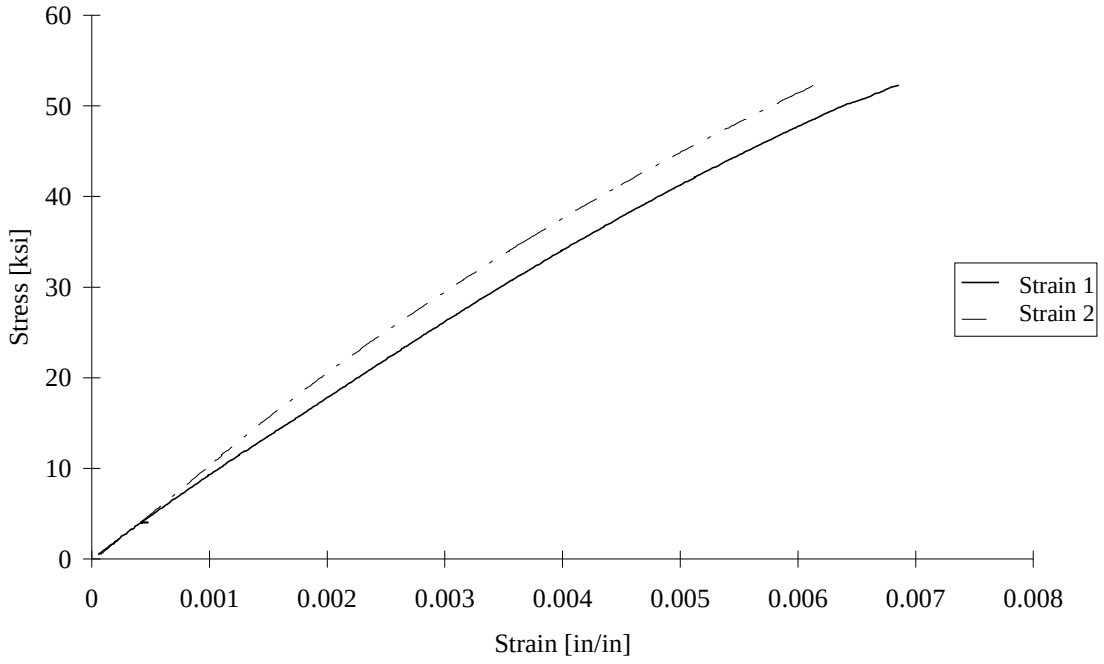

FIGURE D-69. TEST SPECIMEN I50Q01: T50/2134A CARBON/EPOXY $[45/0/-45/90]_{2s}$
IITRI TEST FIXTURE

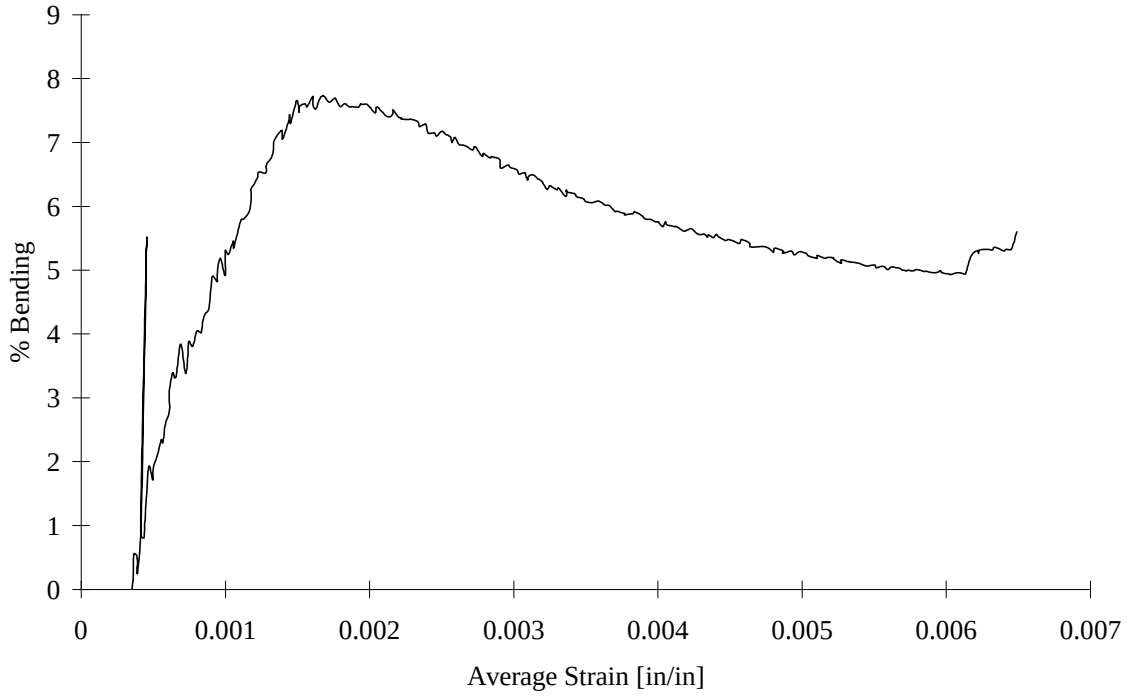

FIGURE D-70. TEST SPECIMEN I50Q01: T50/2134A CARBON/EPOXY $[45/0/-45/90]_{2s}$
IITRI TEST FIXTURE

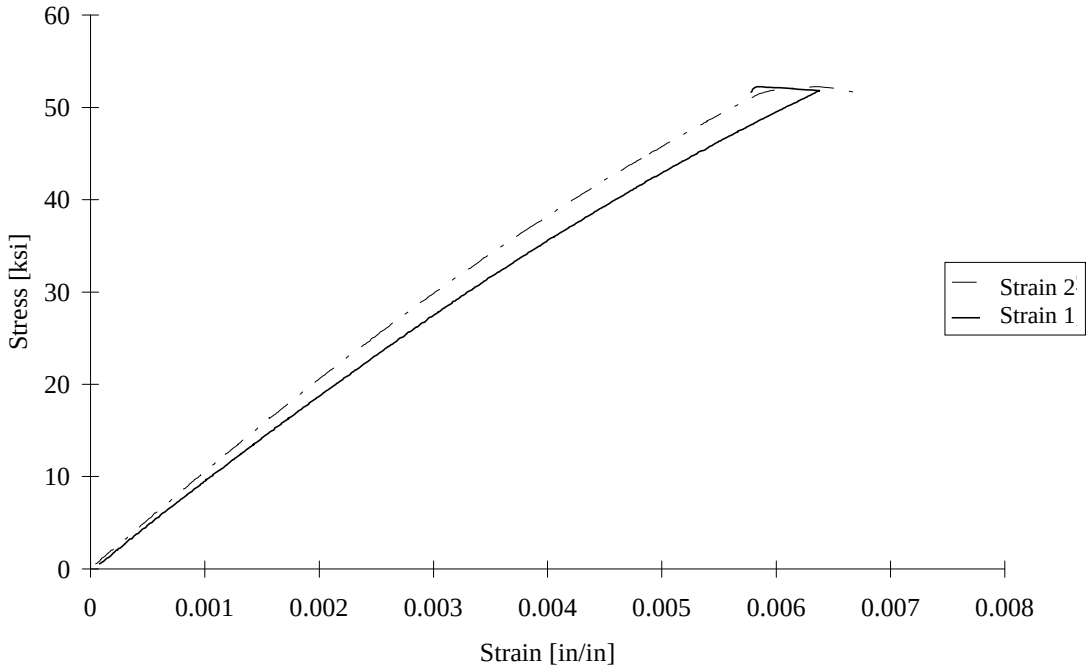

FIGURE D-71. TEST SPECIMEN I50Q02: T50/2134A CARBON/EPOXY $[45/0/-45/90]_{2s}$
IITRI TEST FIXTURE

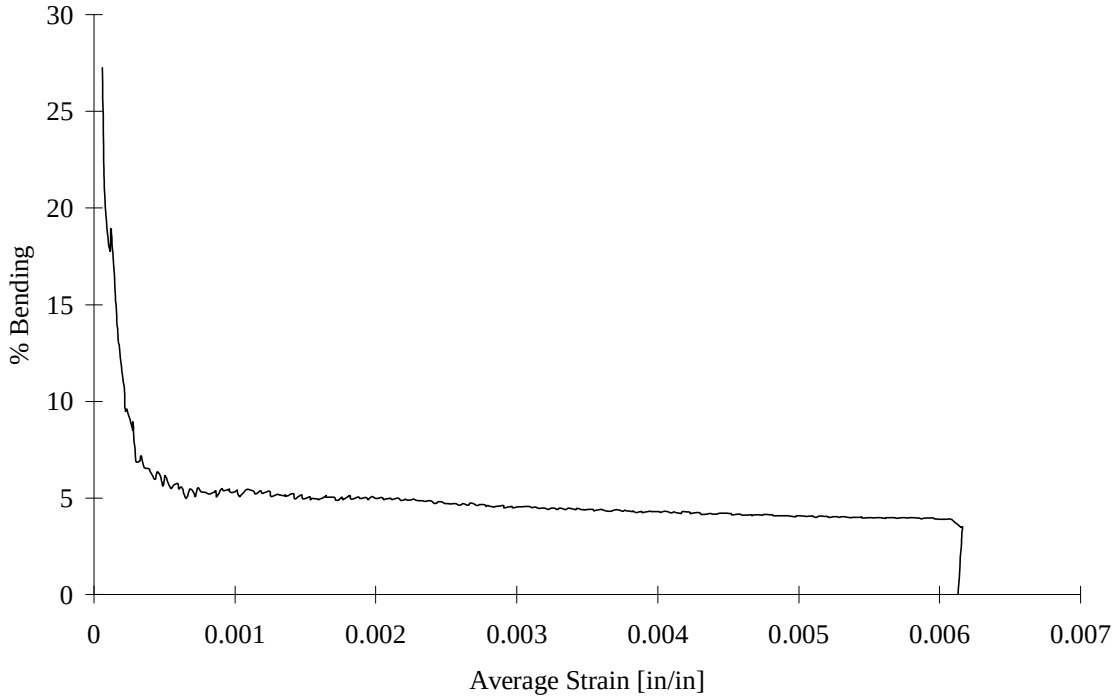

FIGURE D-72. TEST SPECIMEN I50Q02: T50/2134A CARBON/EPOXY $[45/0/-45/90]_{2s}$
IITRI TEST FIXTURE

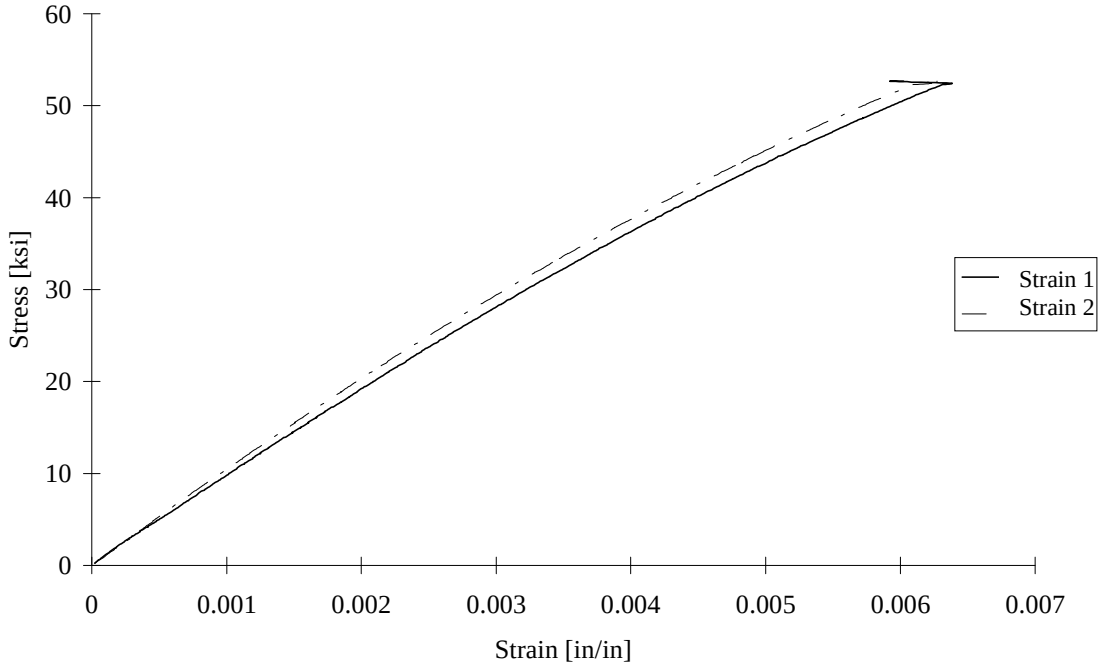

FIGURE D-73. TEST SPECIMEN I50Q03: T50/2134A CARBON/EPOXY $[45/0/-45/90]_{2s}$
IITRI TEST FIXTURE

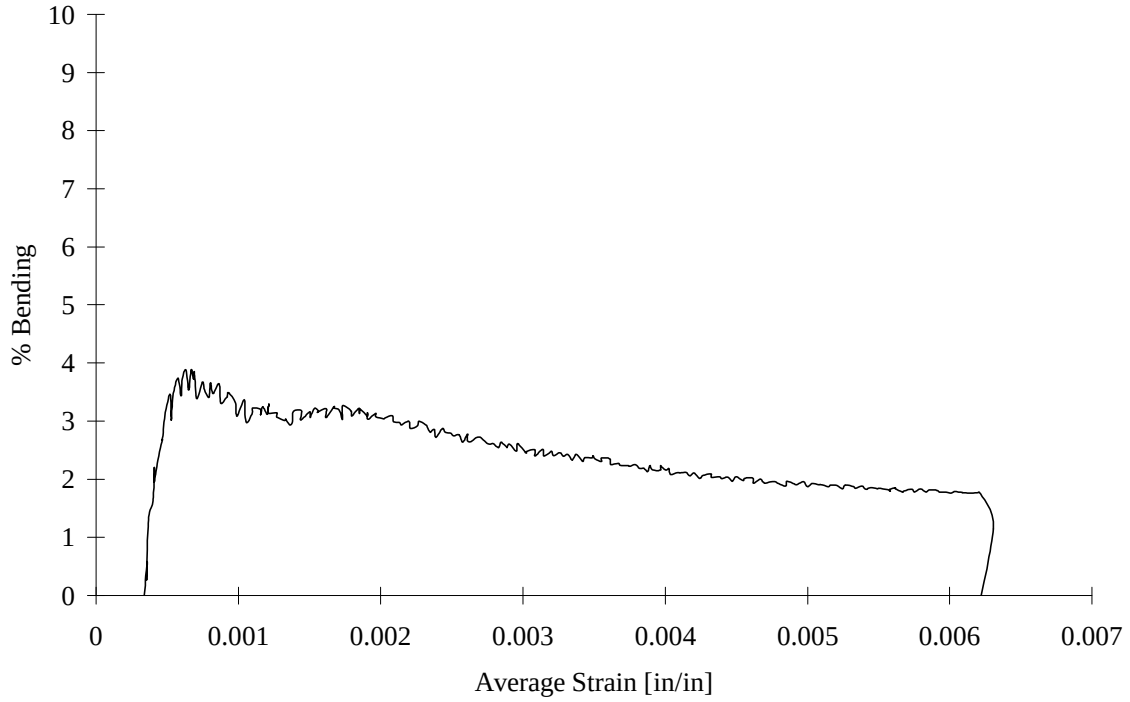

FIGURE D-74. TEST SPECIMEN I50Q03: T50/2134A CARBON/EPOXY $[45/0/-45/90]_{2s}$
IITRI TEST FIXTURE

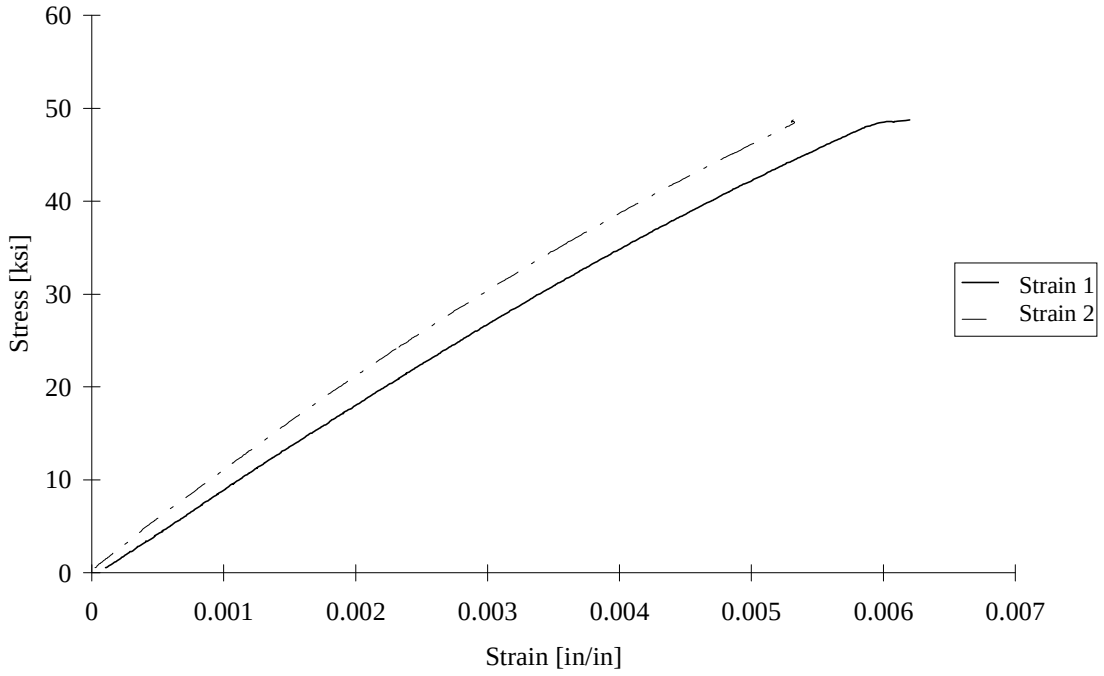

FIGURE D-75. TEST SPECIMEN I50Q04: T50/2134A CARBON/EPOXY $[45/0/-45/90]_{2s}$
IITRI TEST FIXTURE

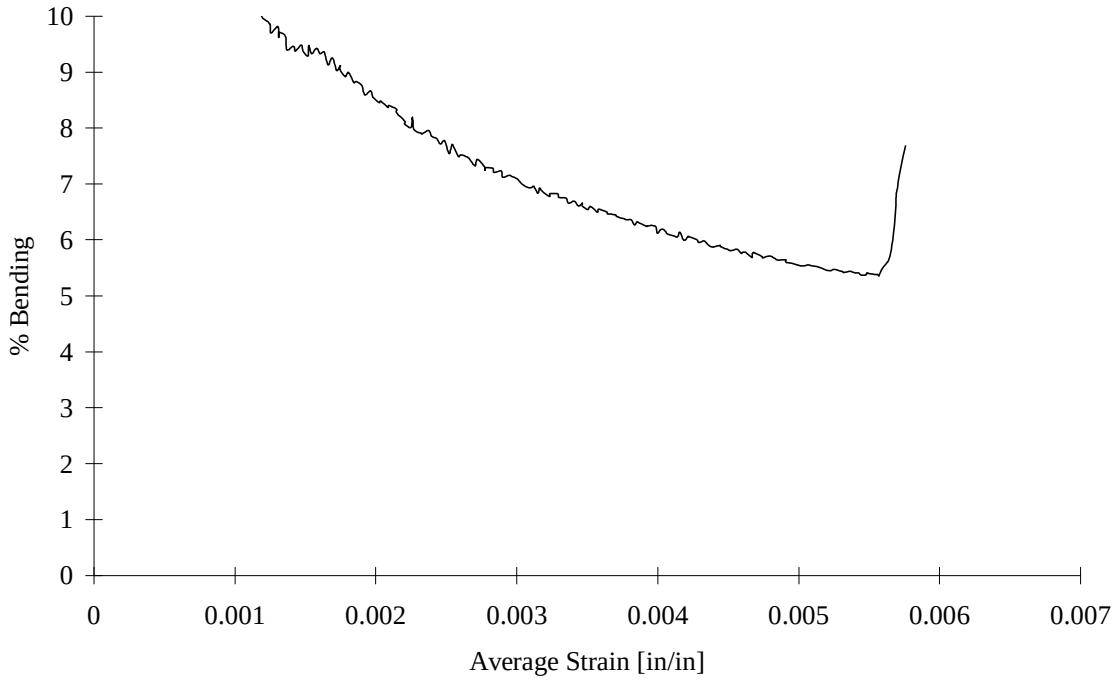

FIGURE D-76. TEST SPECIMEN I50Q04: T50/2134A CARBON/EPOXY $[45/0/-45/90]_{2s}$
IITRI TEST FIXTURE

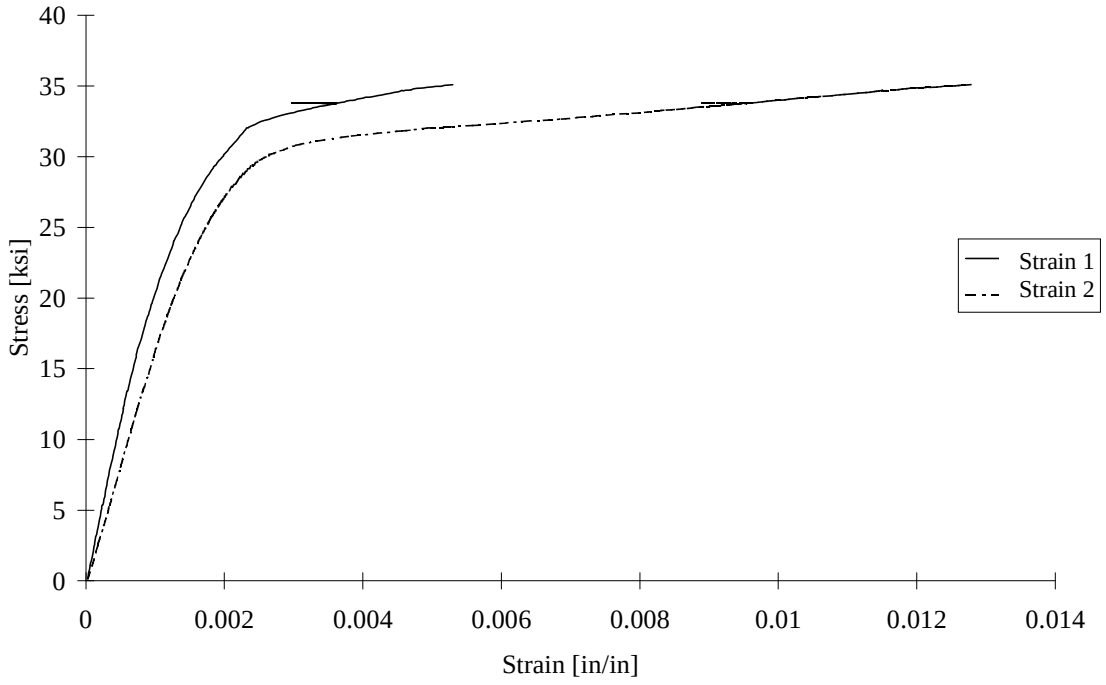

FIGURE D-77. TEST SPECIMEN C75C01: P75S/2034 CARBON/EPOXY $[90/0]_{4s}$
CLC-15 TEST FIXTURE

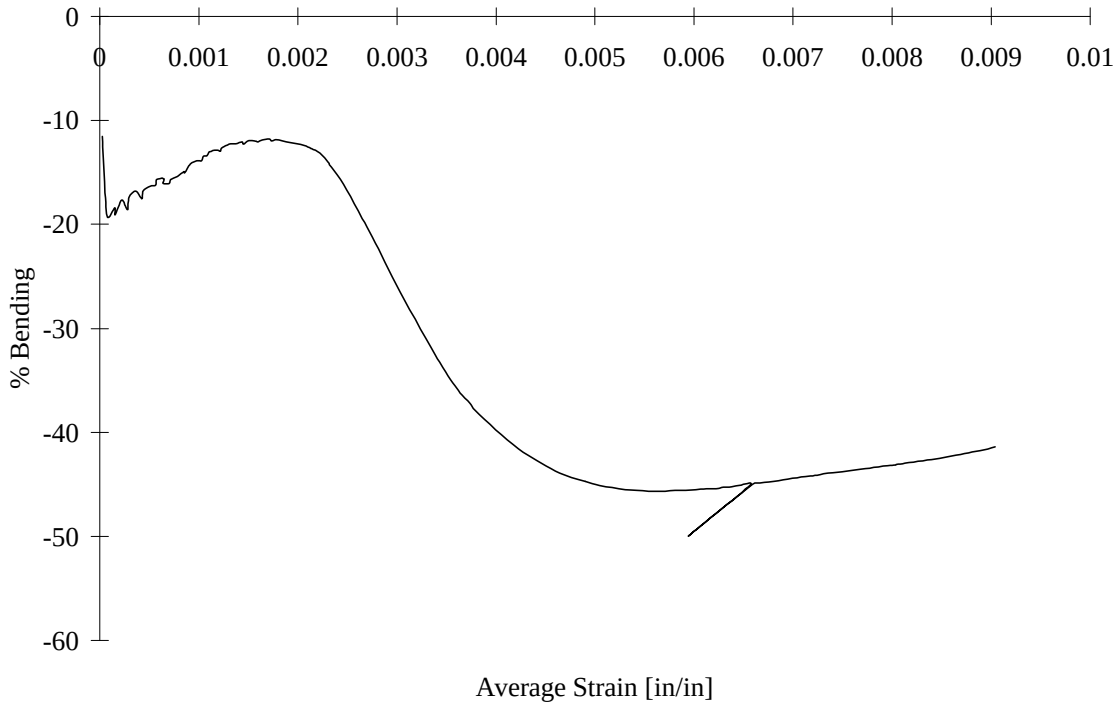

FIGURE D-78. TEST SPECIMEN C75C01: P75S/2034 CARBON/EPOXY $[90/0]_{4s}$
CLC-15 TEST FIXTURE

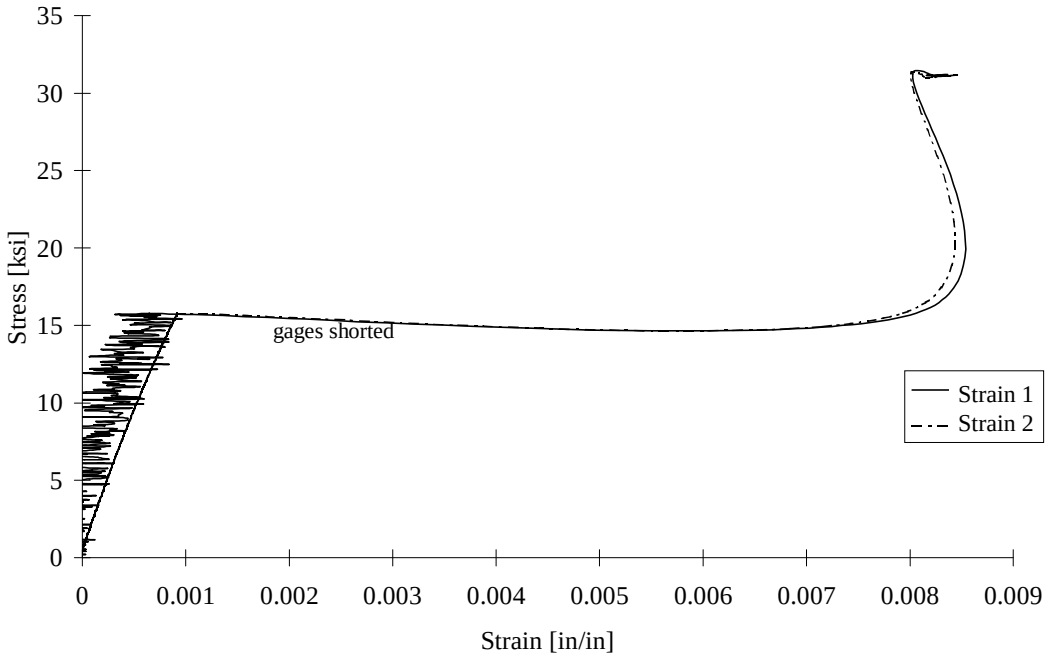

FIGURE D-79. TEST SPECIMEN C75C02: P75S/2034 CARBON/EPOXY $[90/0]_{4s}$ CLC-15 TEST FIXTURE

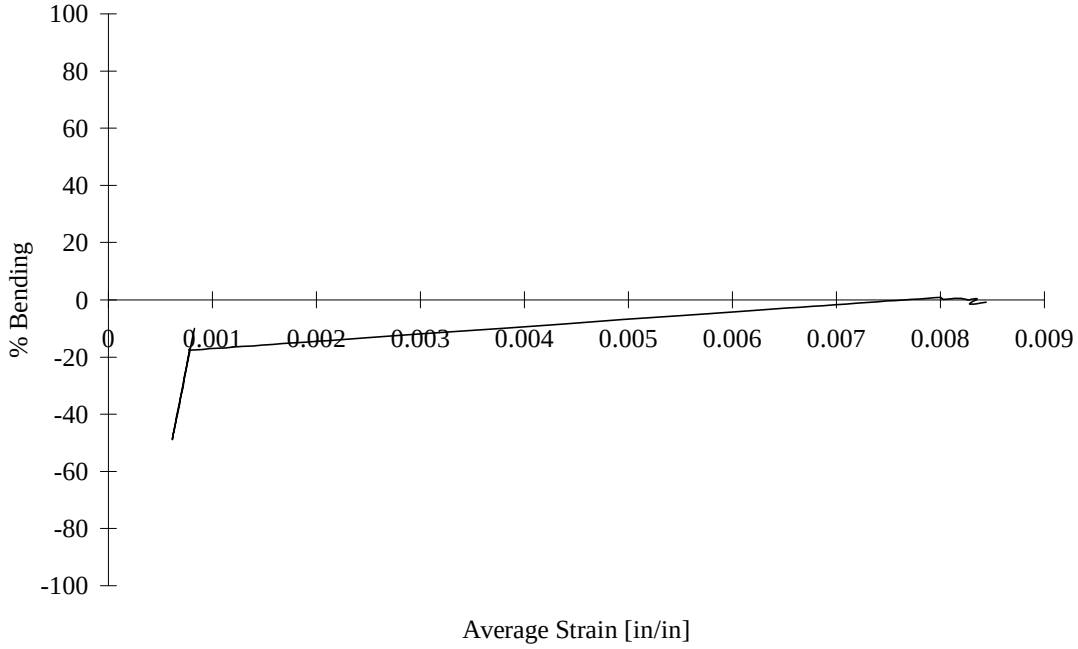

FIGURE D-80. TEST SPECIMEN C75C02: P75S/2034 CARBON/EPOXY $[90/0]_{4s}$ CLC-15 TEST FIXTURE

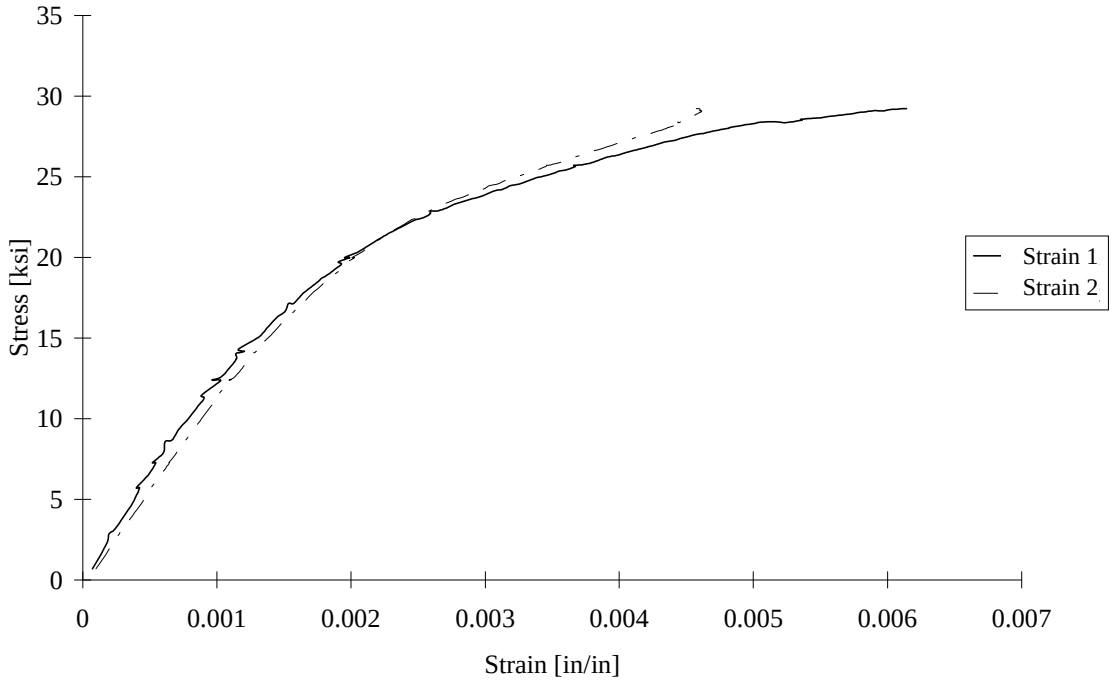

FIGURE D-81. TEST SPECIMEN C75Q01: P75S/2034 CARBON/EPOXY $[45/0/-45/90]_{2s}$
CLC-15 TEST FIXTURE

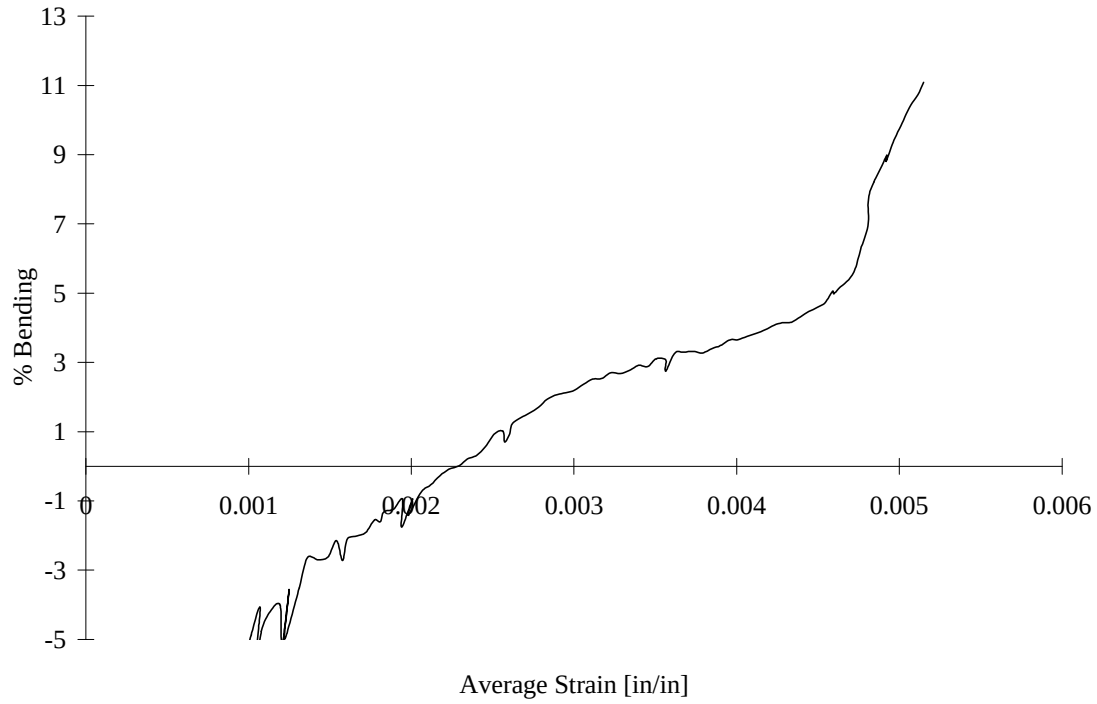

FIGURE D-82. TEST SPECIMEN C75Q01: P75S/2034 CARBON/EPOXY $[45/0/-45/90]_{2s}$
CLC-15 TEST FIXTURE

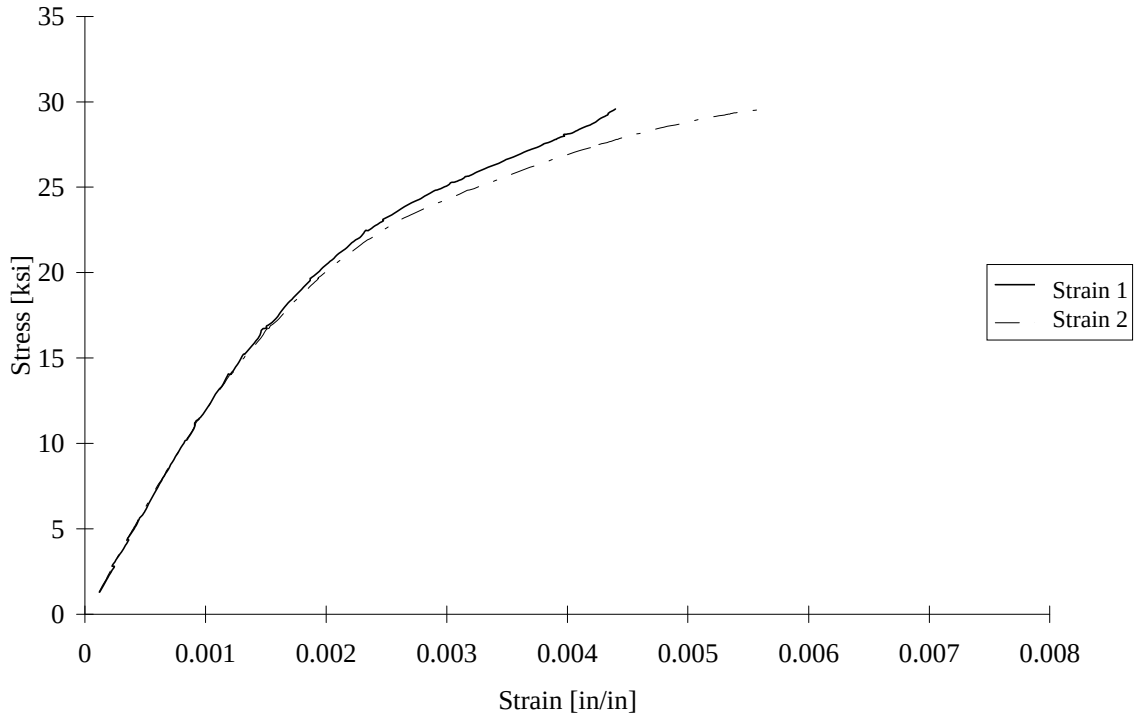

FIGURE D-83. TEST SPECIMEN C75Q02: P75S/2034 CARBON/EPOXY $[45/0/-45/90]_{2s}$
CLC-15 TEST FIXTURE

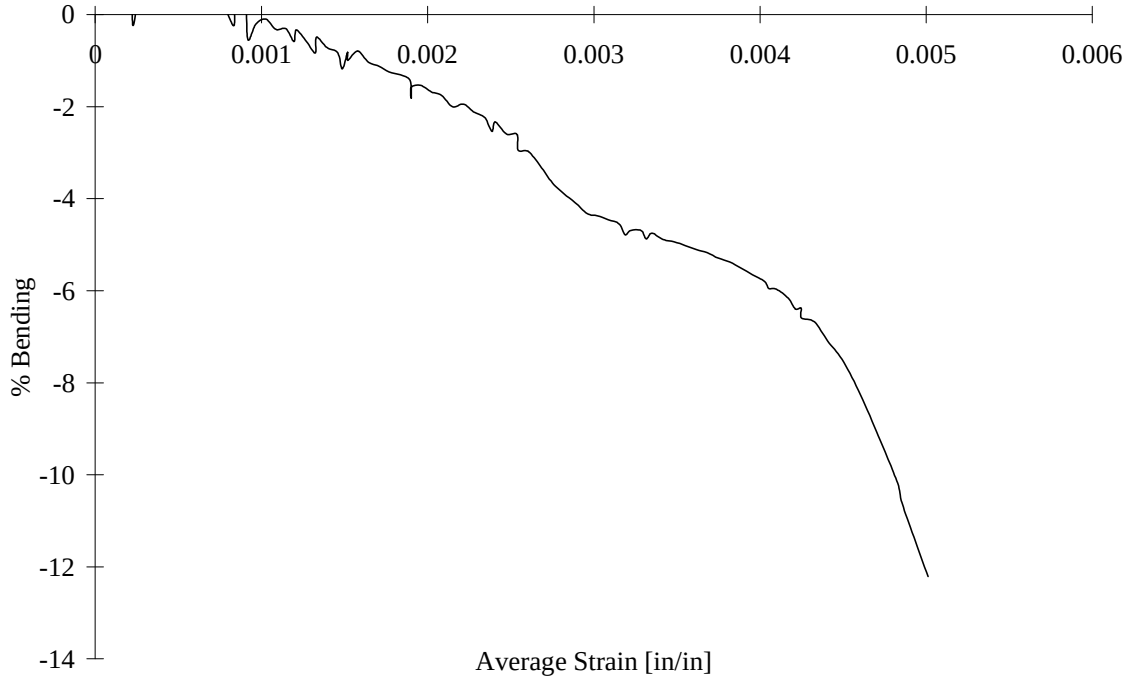

FIGURE D-84. TEST SPECIMEN C75Q02: P75S/2034 CARBON/EPOXY $[45/0/-45/90]_{2s}$
CLC-15 TEST FIXTURE

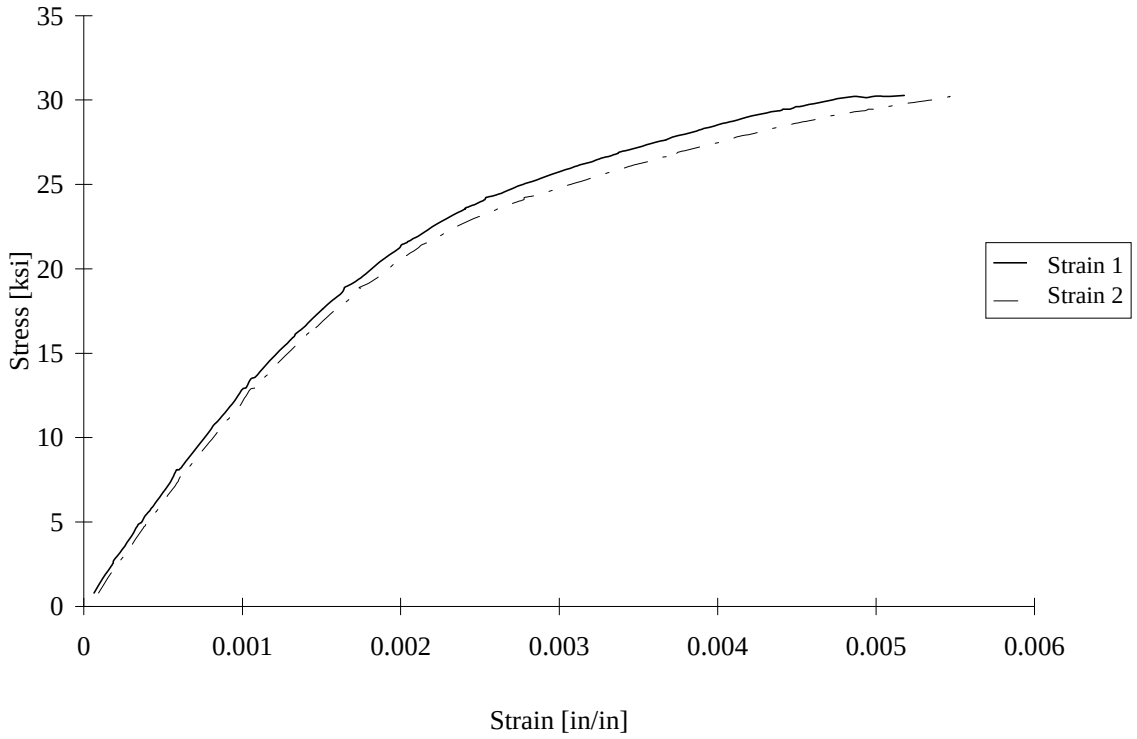

FIGURE D-85. TEST SPECIMEN C75Q04: P75S/2034 CARBON/EPOXY $[45/0/-45/90]_{2s}$
CLC-15 TEST FIXTURE

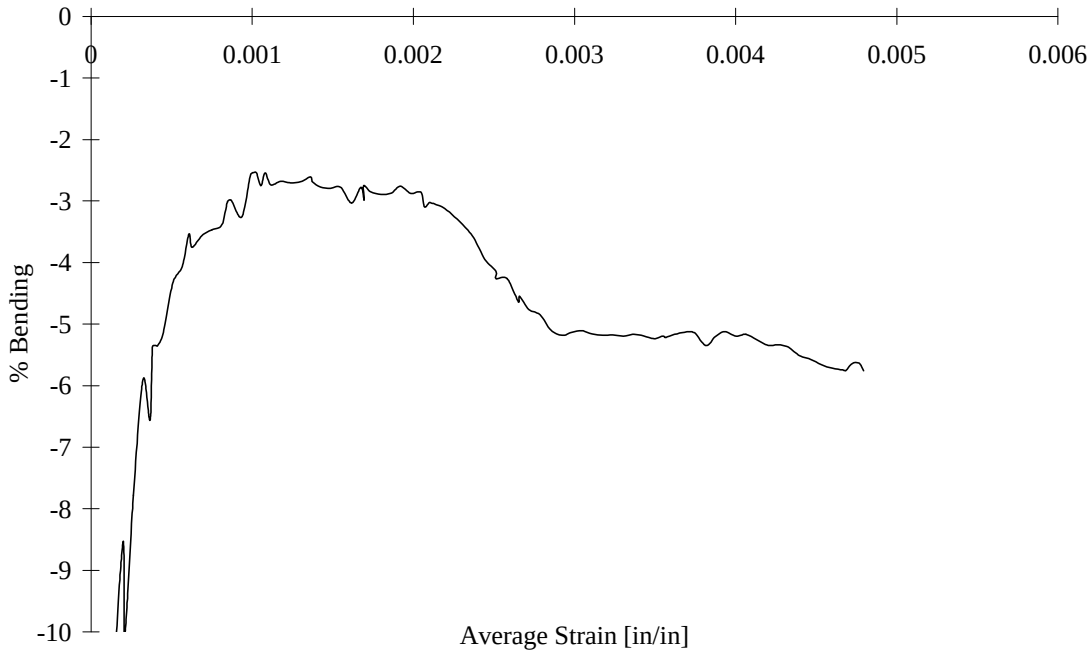

FIGURE D-86. TEST SPECIMEN C75Q04: P75S/2034 CARBON/EPOXY $[45/0/-45/90]_{2s}$
CLC-15 TEST FIXTURE

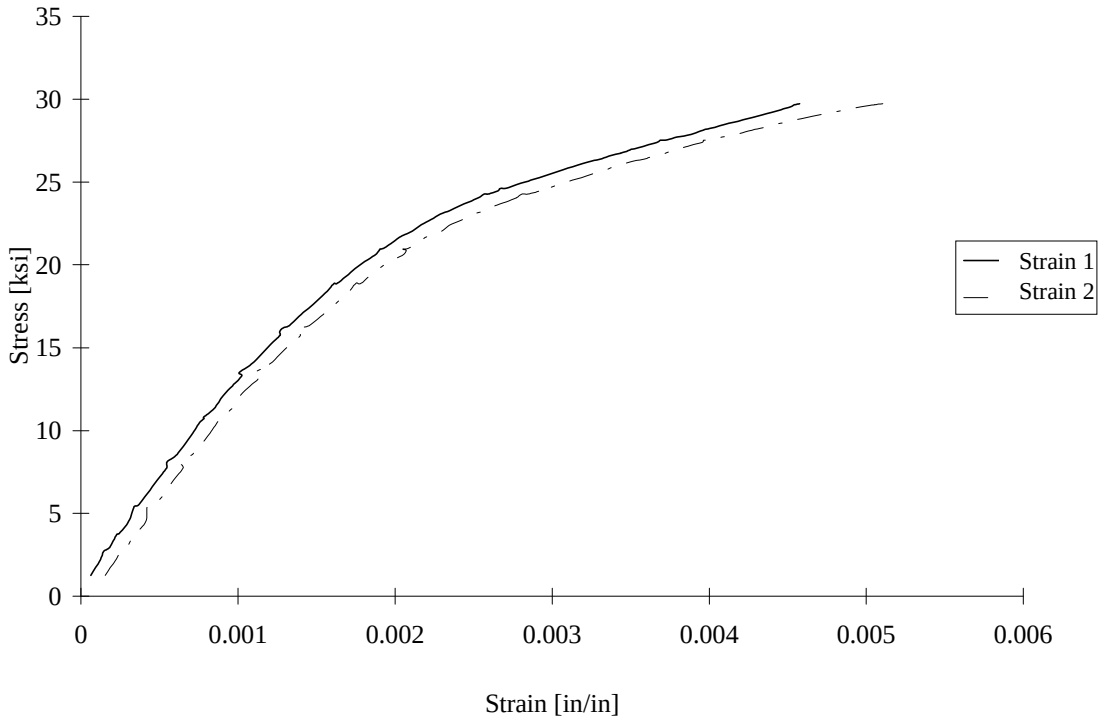

FIGURE D-87. TEST SPECIMEN C75Q05: P75S/2034 CARBON/EPOXY $[45/0/-45/90]_{2s}$
CLC-15 TEST FIXTURE

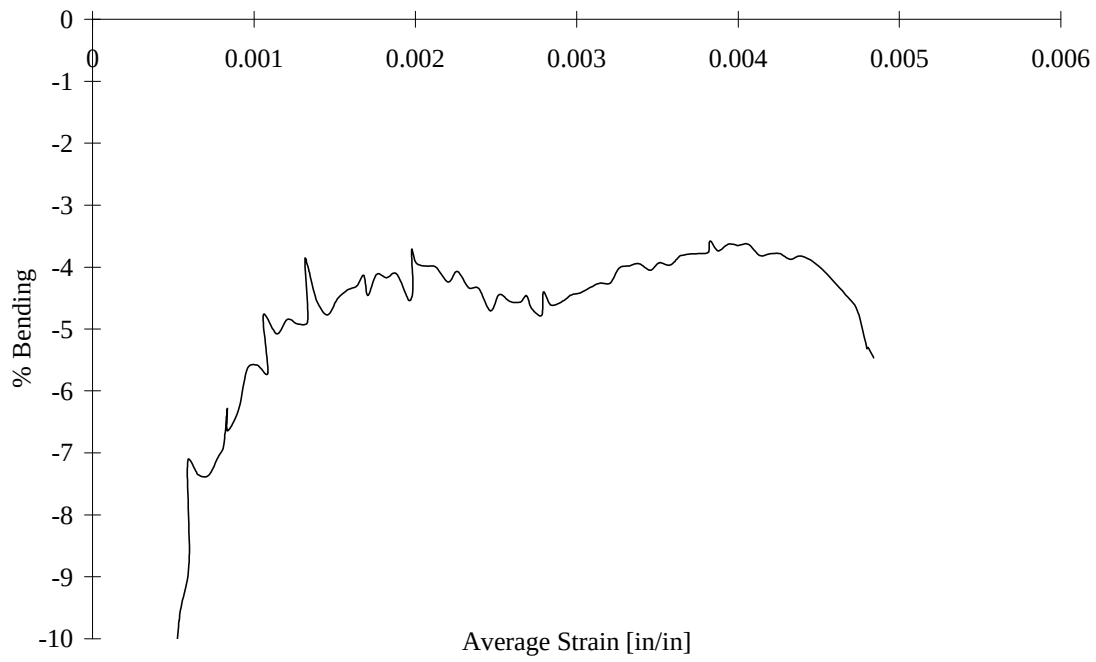

FIGURE D-88. TEST SPECIMEN C75Q05: P75S/2034 CARBON/EPOXY $[45/0/-45/90]_{2s}$
CLC-15 TEST FIXTURE

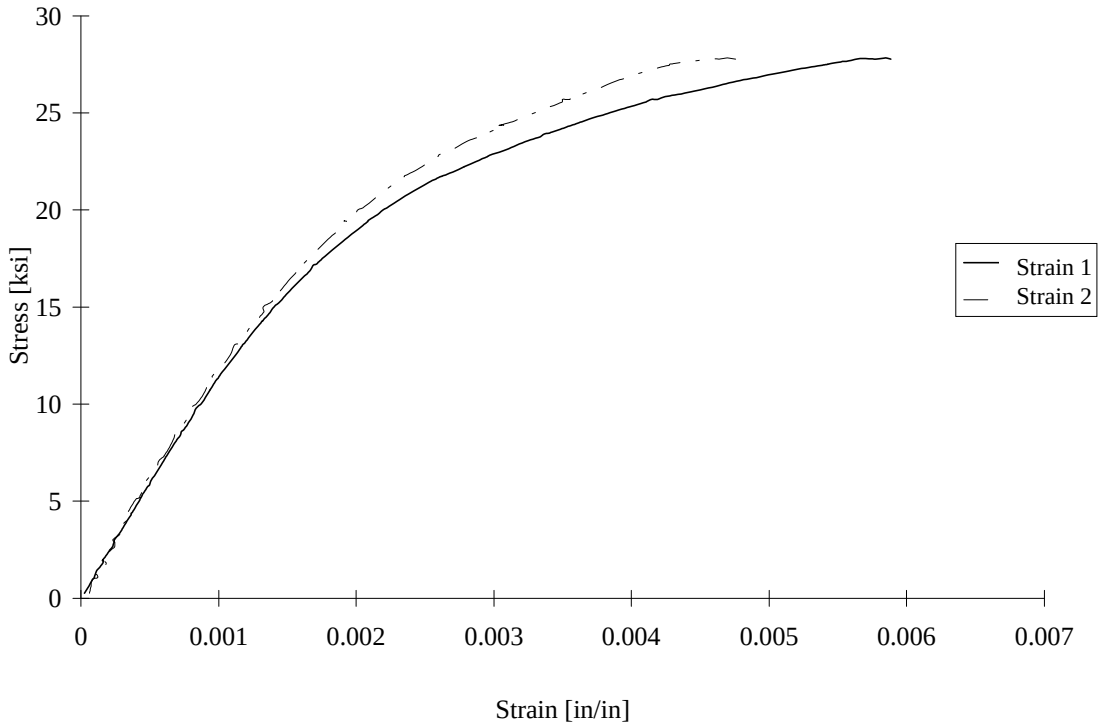

FIGURE D-89. TEST SPECIMEN I75Q01: P75S/2034 CARBON/EPOXY $[45/0/-45/90]_{2s}$
IITRI TEST FIXTURE

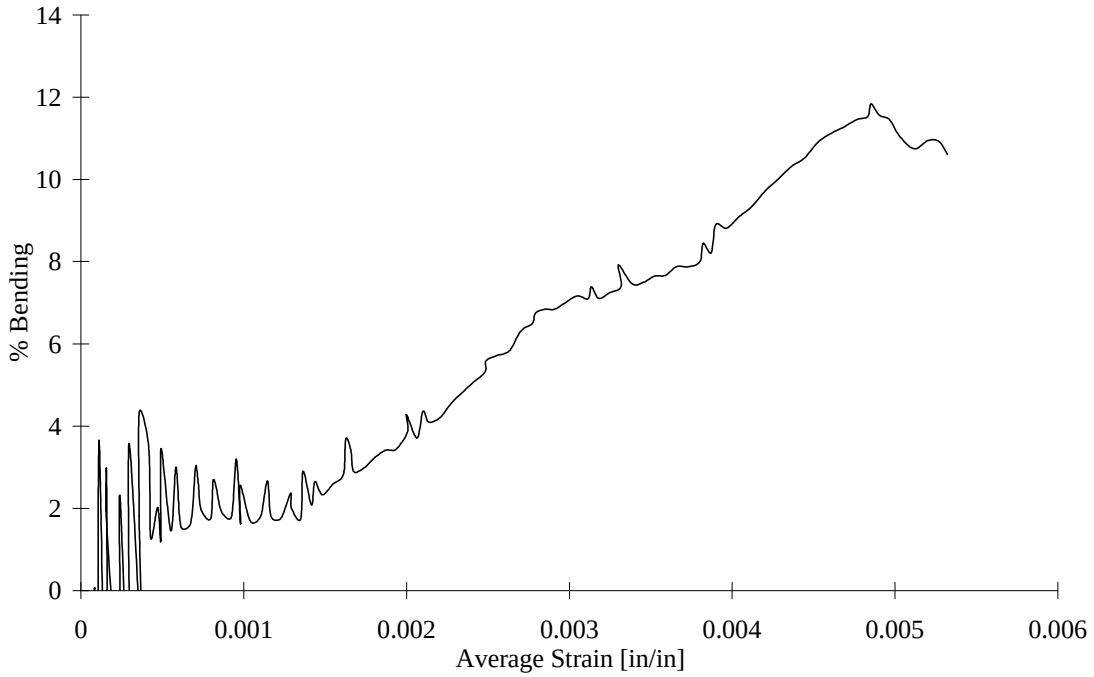

FIGURE D-90. TEST SPECIMEN I75Q01: P75S/2034 CARBON/EPOXY $[45/0/-45/90]_{2s}$
IITRI TEST FIXTURE

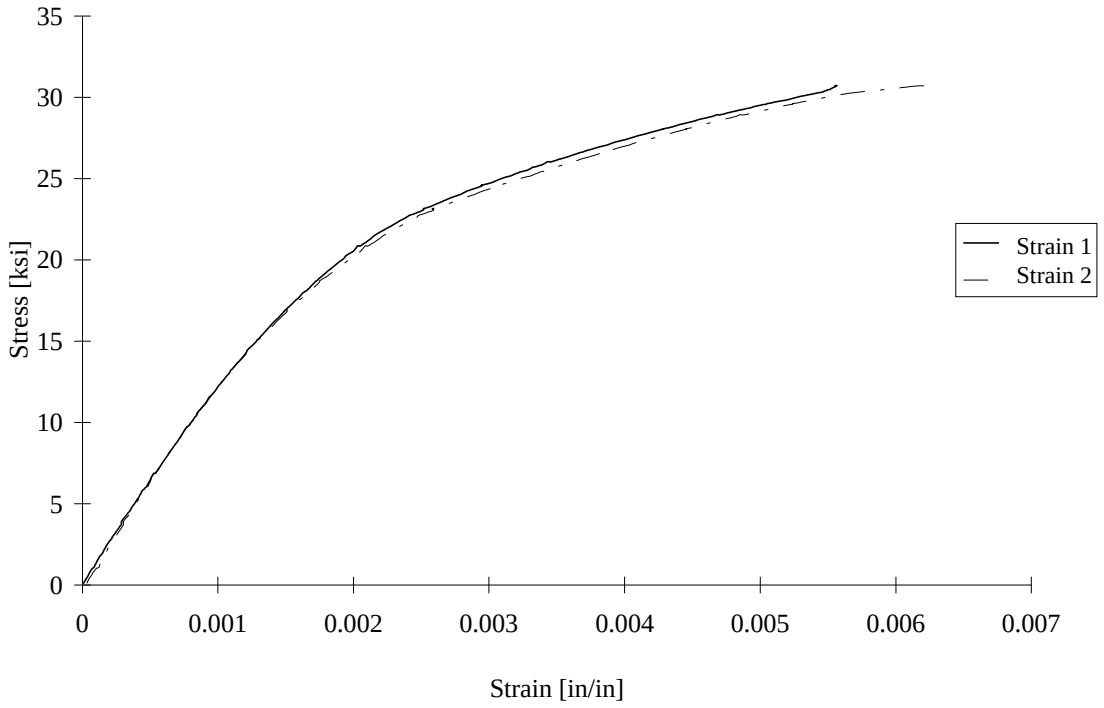

FIGURE D-91. TEST SPECIMEN I75Q02: P75S/2034 CARBON/EPOXY $[45/0/-45/90]_{2s}$ IITRI TEST FIXTURE

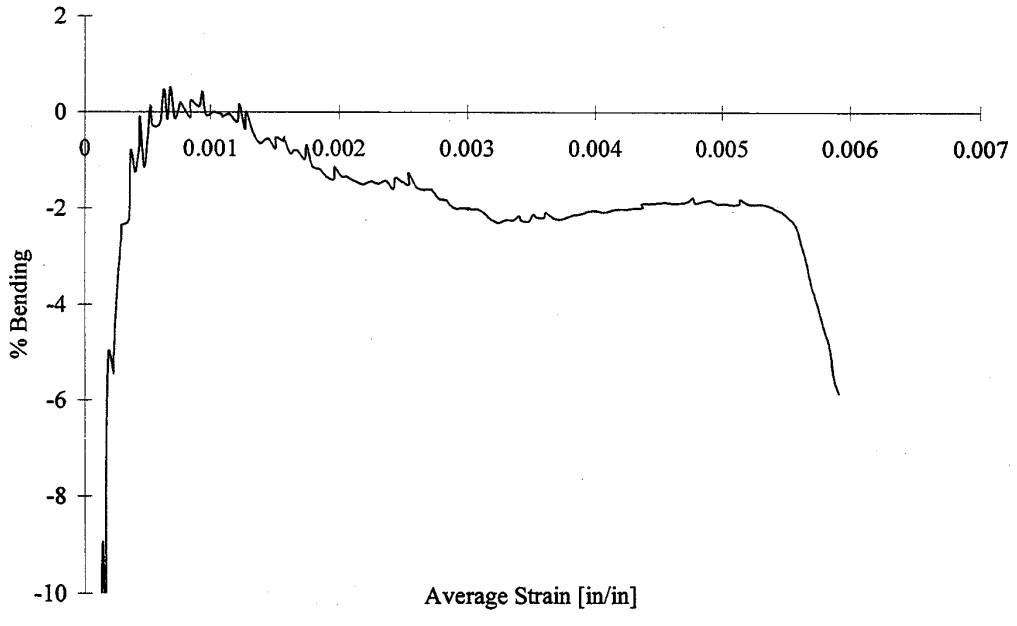

FIGURE D-92. TEST SPECIMEN I75Q02: P75S/2034 CARBON/EPOXY $[45/0/-45/90]_{2s}$ IITRI TEST FIXTURE

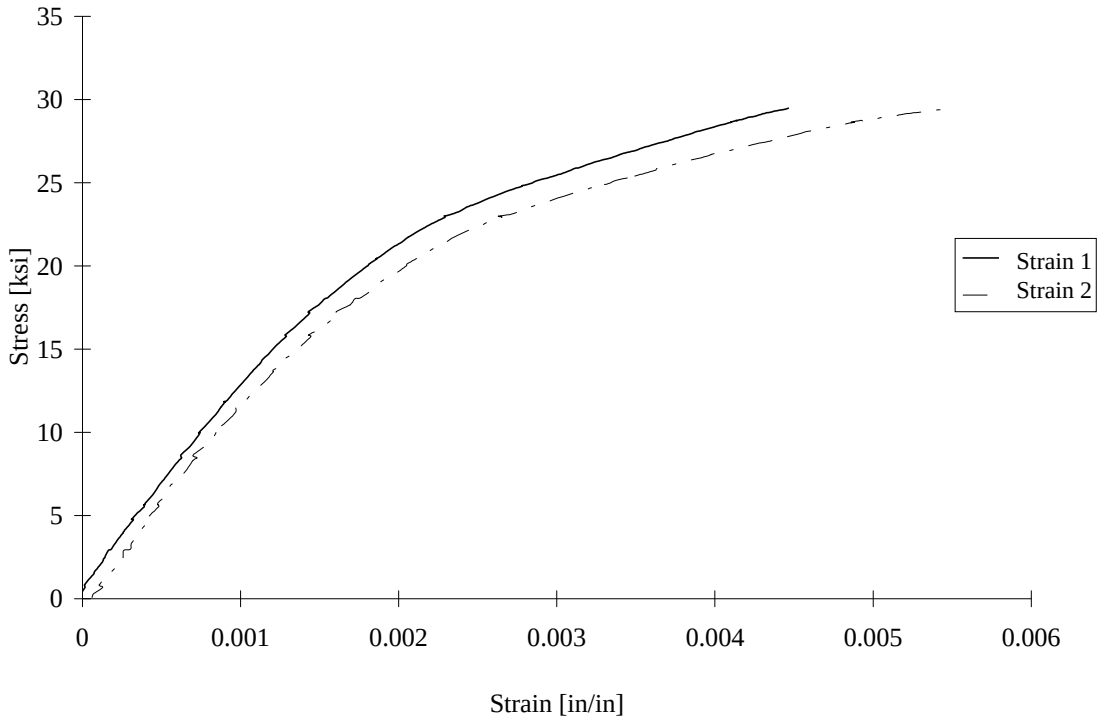

FIGURE D-93. TEST SPECIMEN I75Q03: P75S/2034 CARBON/EPOXY $[45/0/-45/90]_{2s}$
IITRI TEST FIXTURE

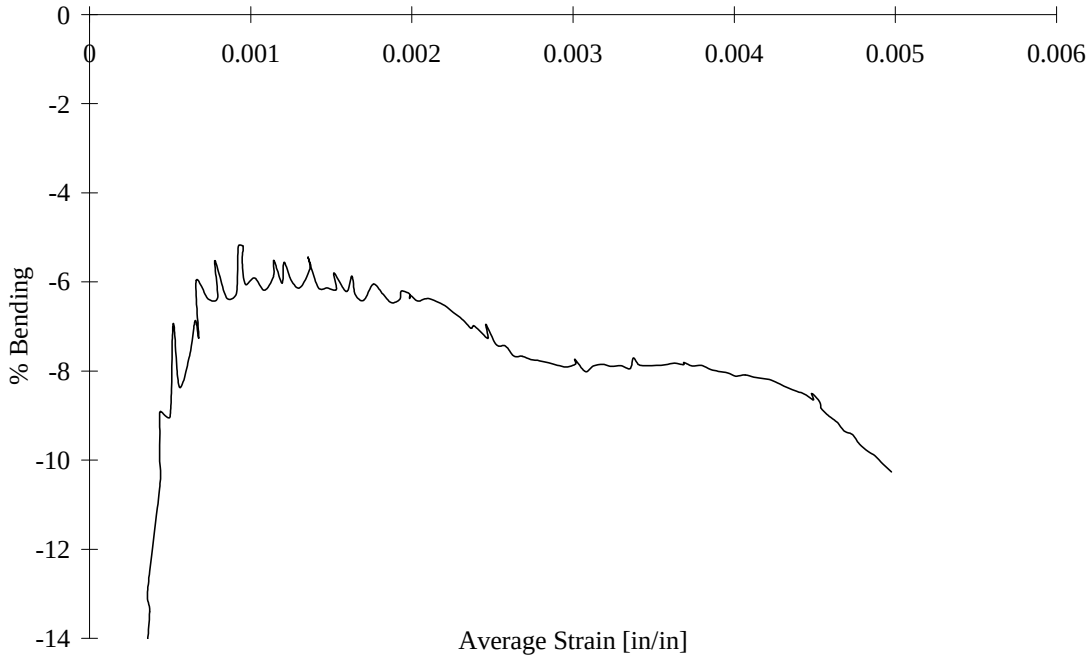

FIGURE D-94. TEST SPECIMEN I75Q03: P75S/2034 CARBON/EPOXY $[45/0/-45/90]_{2s}$
IITRI TEST FIXTURE

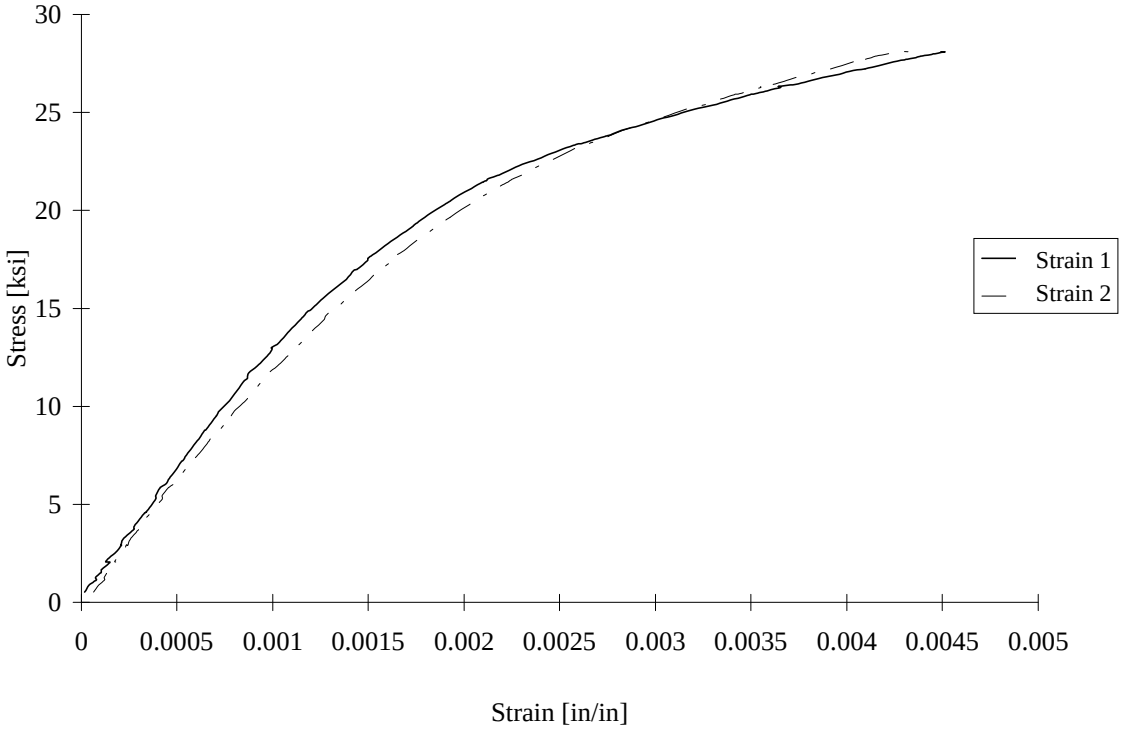

FIGURE D-95. TEST SPECIMEN I75Q04: P75S/2034 CARBON/EPOXY $[45/0/-45/90]_{2s}$ IITRI TEST FIXTURE

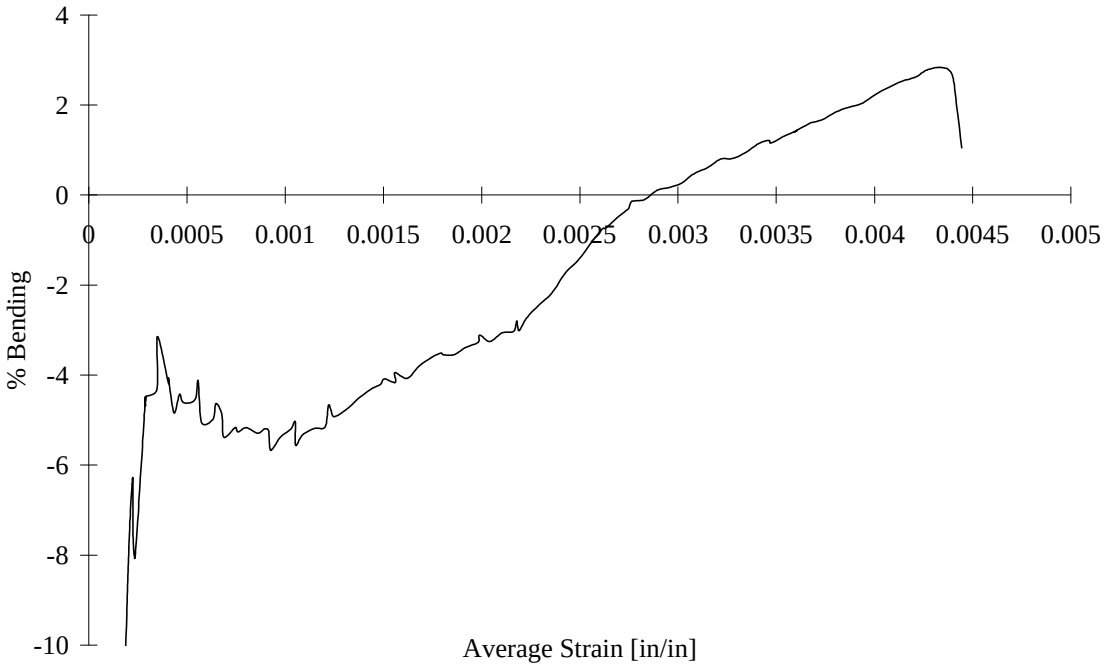

FIGURE D-96. TEST SPECIMEN I75Q04: P75S/2034 CARBON/EPOXY $[45/0/-45/90]_{2s}$ IITRI TEST FIXTURE

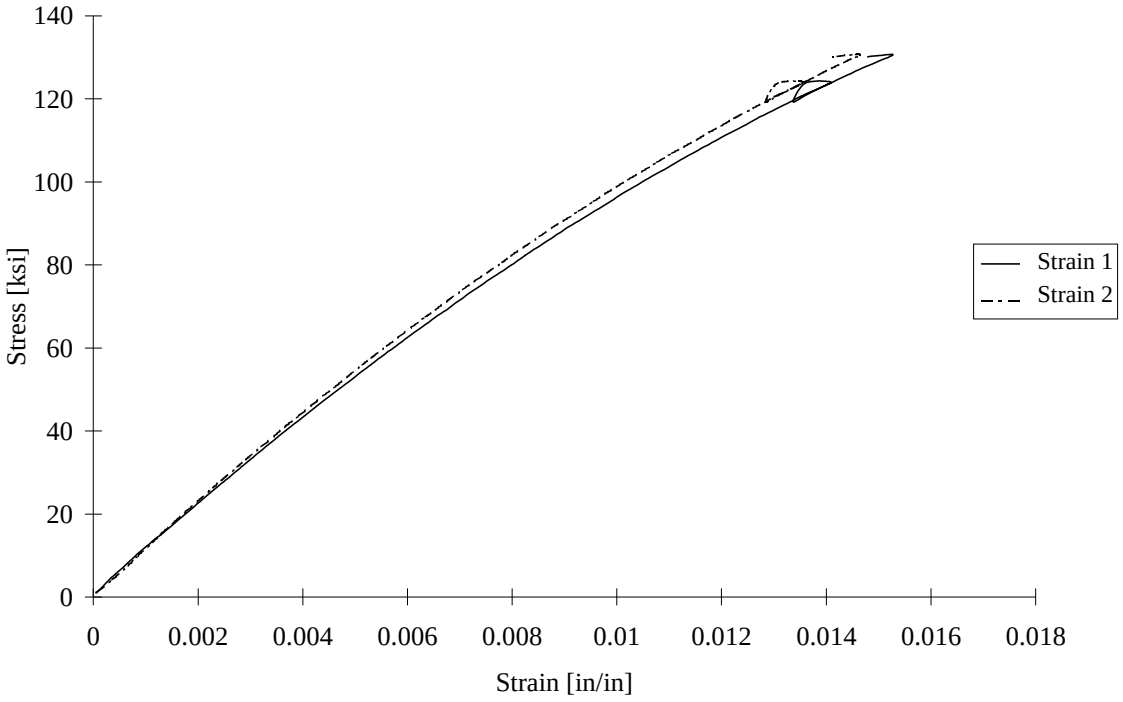

FIGURE D-97. TEST SPECIMEN C80C01: T800/2302-19 CARBON/EPOXY $[90/0]_{4s}$
CLC-15 TEST FIXTURE

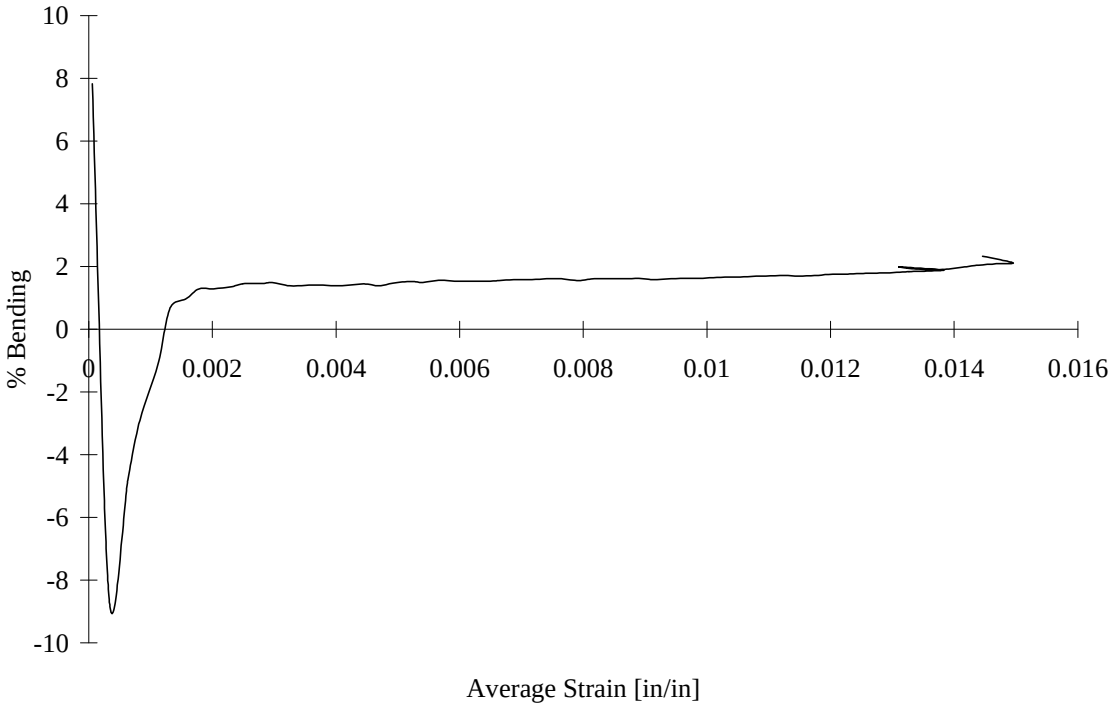

FIGURE D-98. TEST SPECIMEN C80C01: T800/2302-19 CARBON/EPOXY $[90/0]_{4s}$
CLC-15 TEST FIXTURE

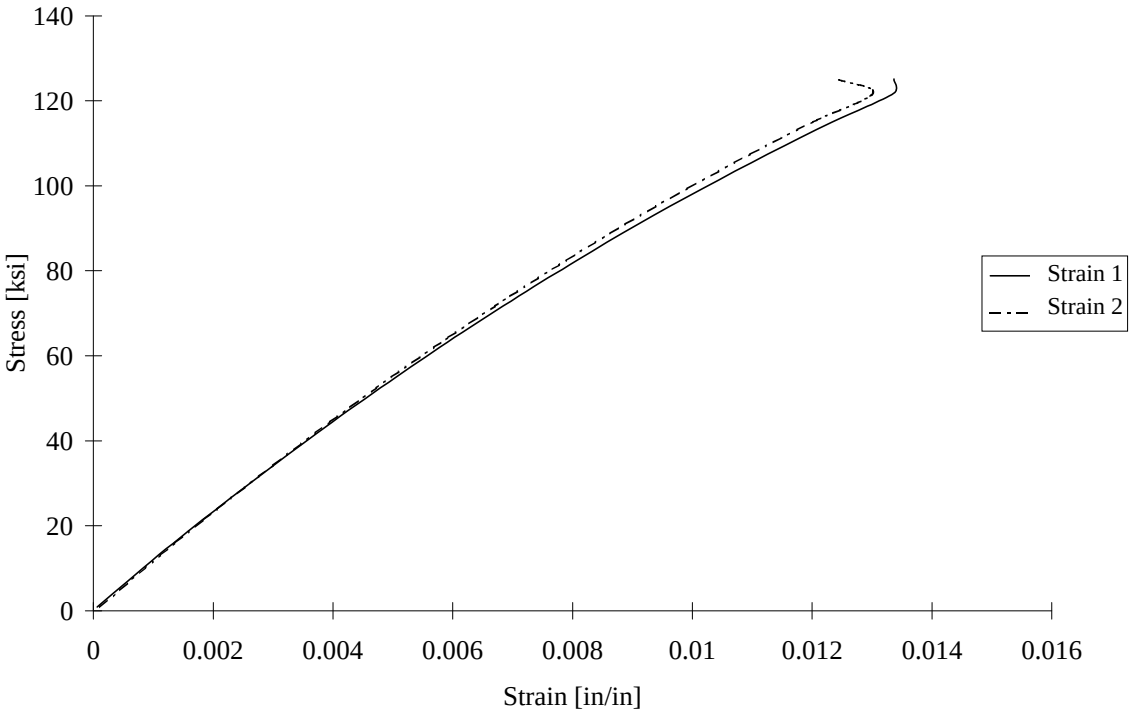

FIGURE D-99. TEST SPECIMEN C80C02: T800/2302-19 CARBON/EPOXY $[90/0]_{4s}$
CLC-15 TEST FIXTURE

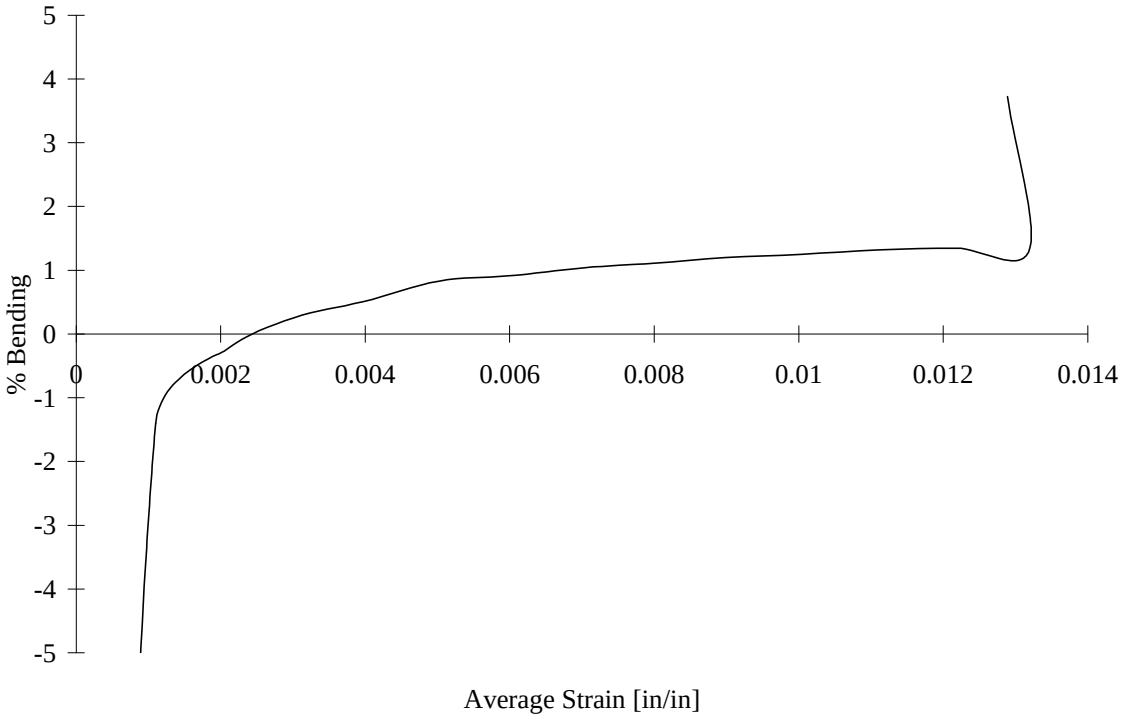

FIGURE D-100. TEST SPECIMEN C80C02: T800/2302-19 CARBON/EPOXY $[90/0]_{4s}$
CLC-15 TEST FIXTURE

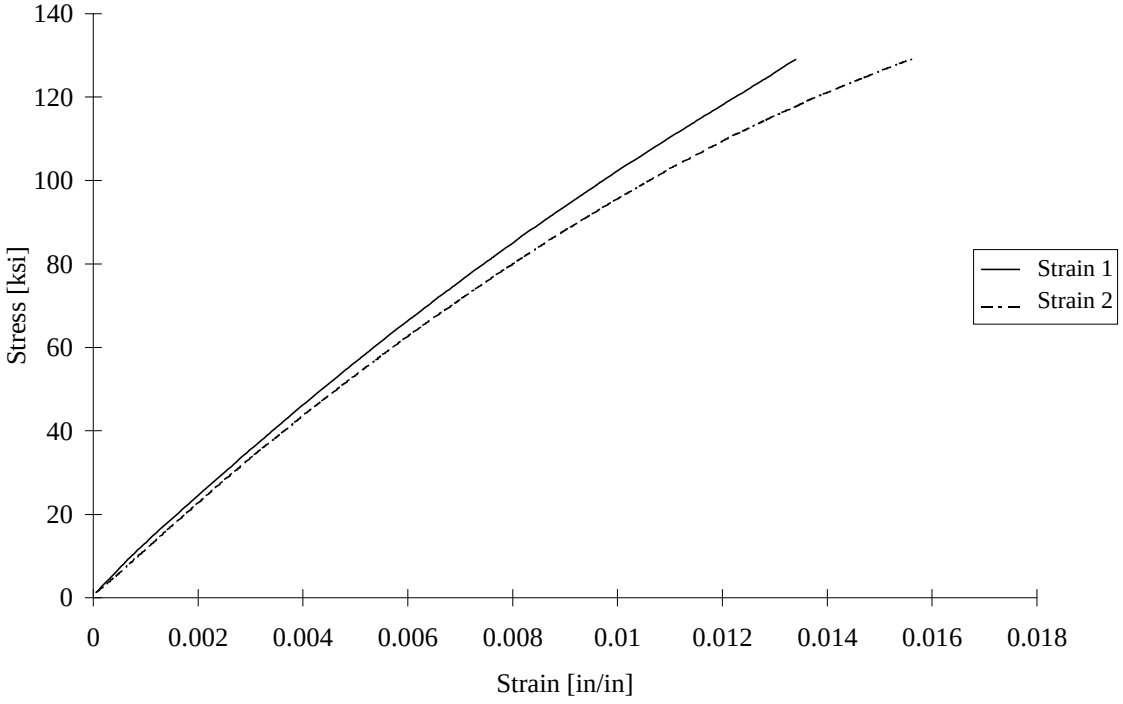

FIGURE D-101. TEST SPECIMEN C80C03: T800/2302-19 CARBON/EPOXY $[90/0]_{4s}$
CLC-15 TEST FIXTURE

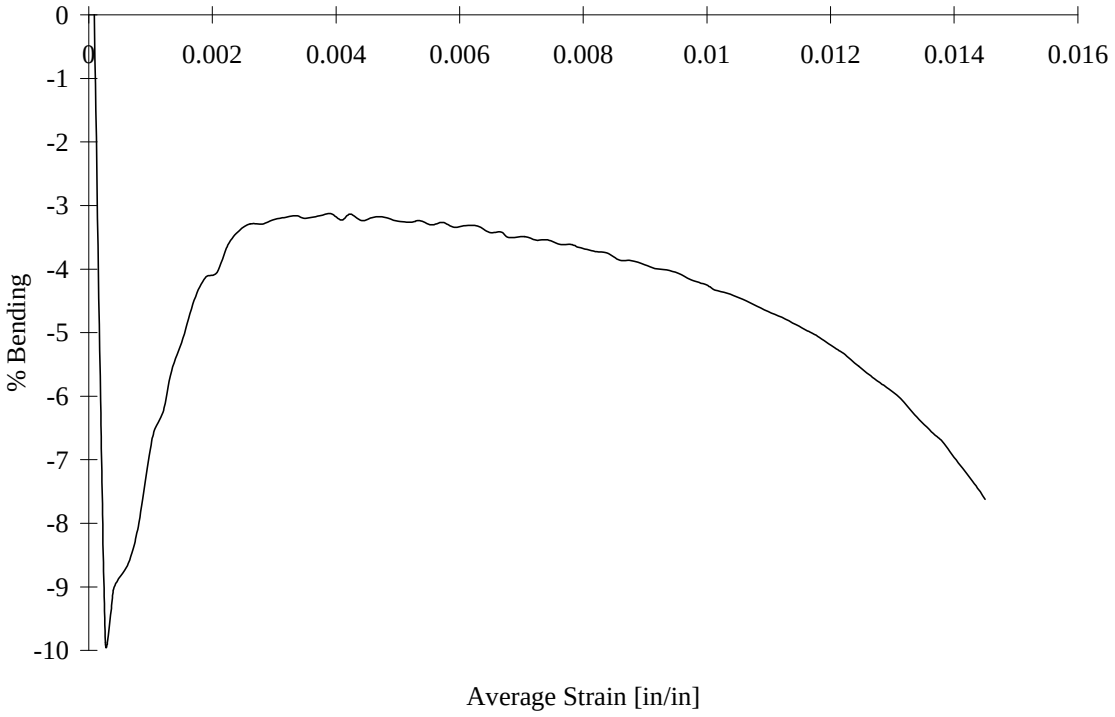

FIGURE D-102. TEST SPECIMEN C80C03: T800/2302-19 CARBON/EPOXY $[90/0]_{4s}$
CLC-15 TEST FIXTURE

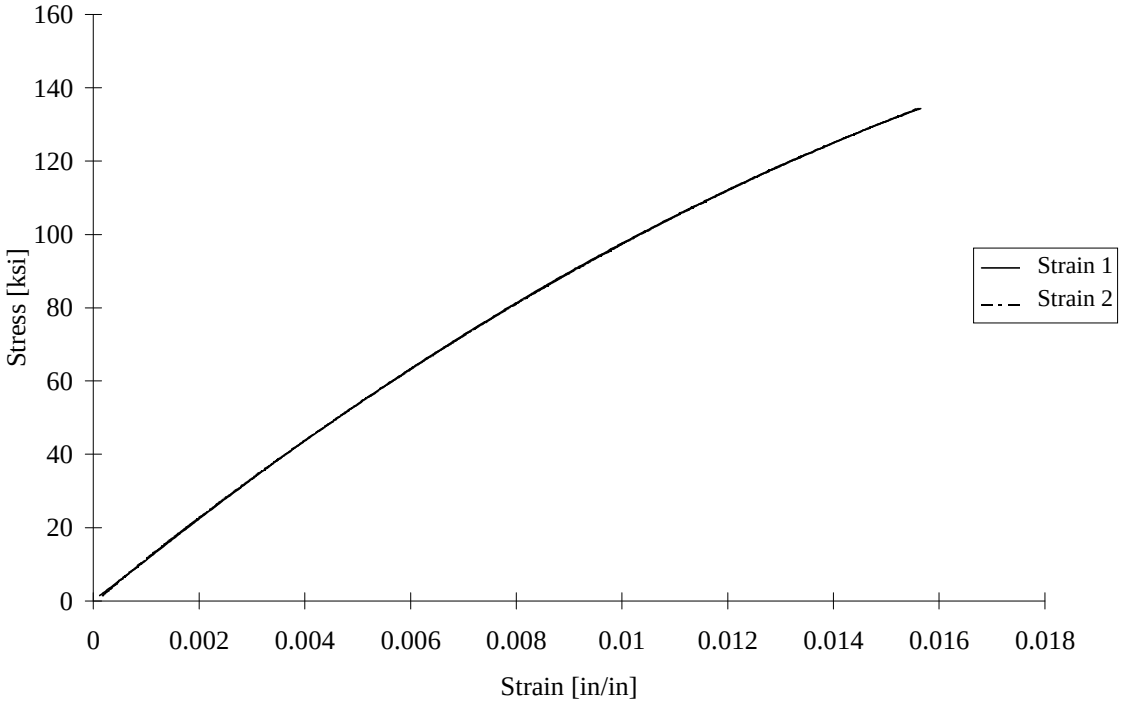

FIGURE D-103. TEST SPECIMEN C80C04: T800/2302-19 CARBON/EPOXY $[90/0]_{4s}$
CLC-15 TEST FIXTURE

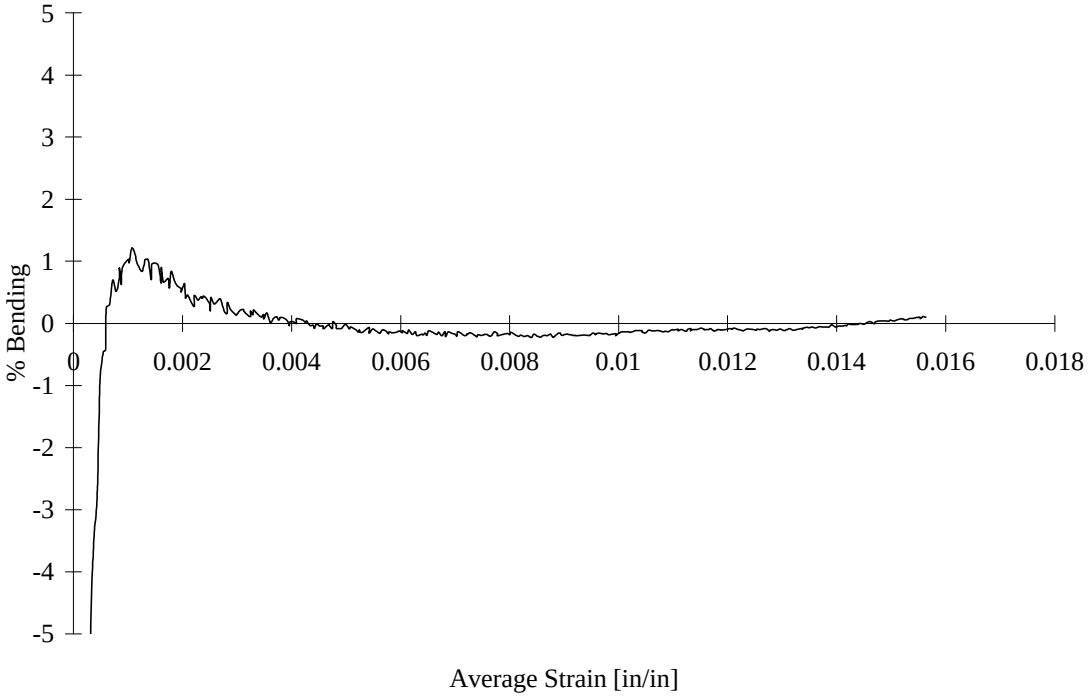

FIGURE D-104. TEST SPECIMEN C80C04: T800/2302-19 CARBON/EPOXY $[90/0]_{4s}$
CLC-15 TEST FIXTURE

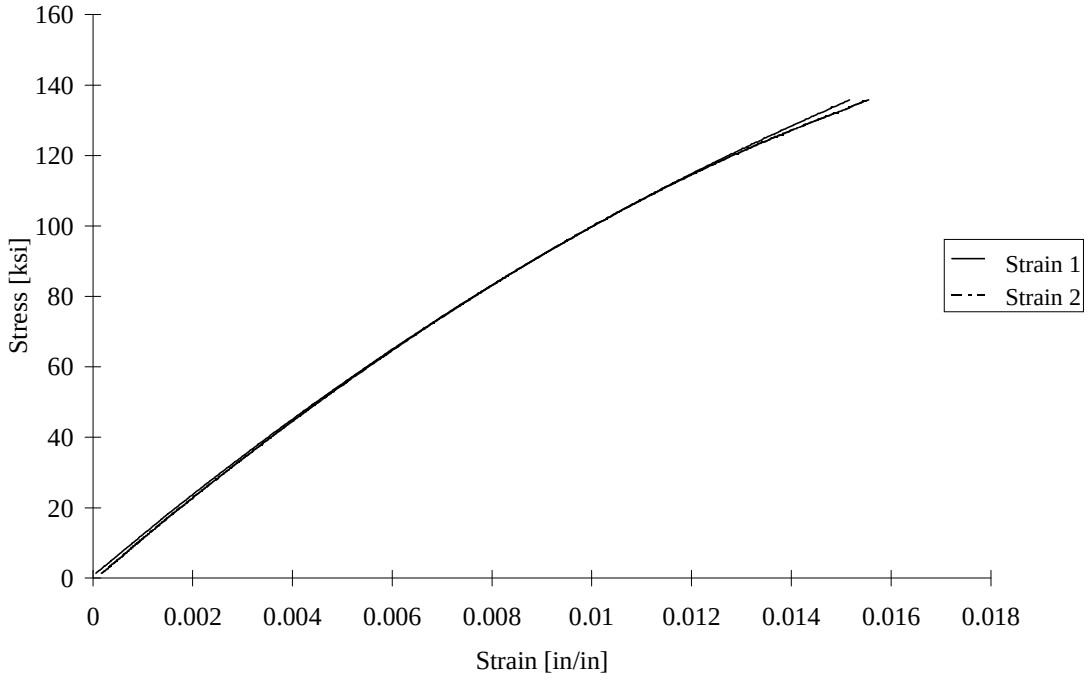

FIGURE D-105. TEST SPECIMEN C80C05: T800/2302-19 CARBON/EPOXY $[90/0]_{4s}$
CLC-15 TEST FIXTURE

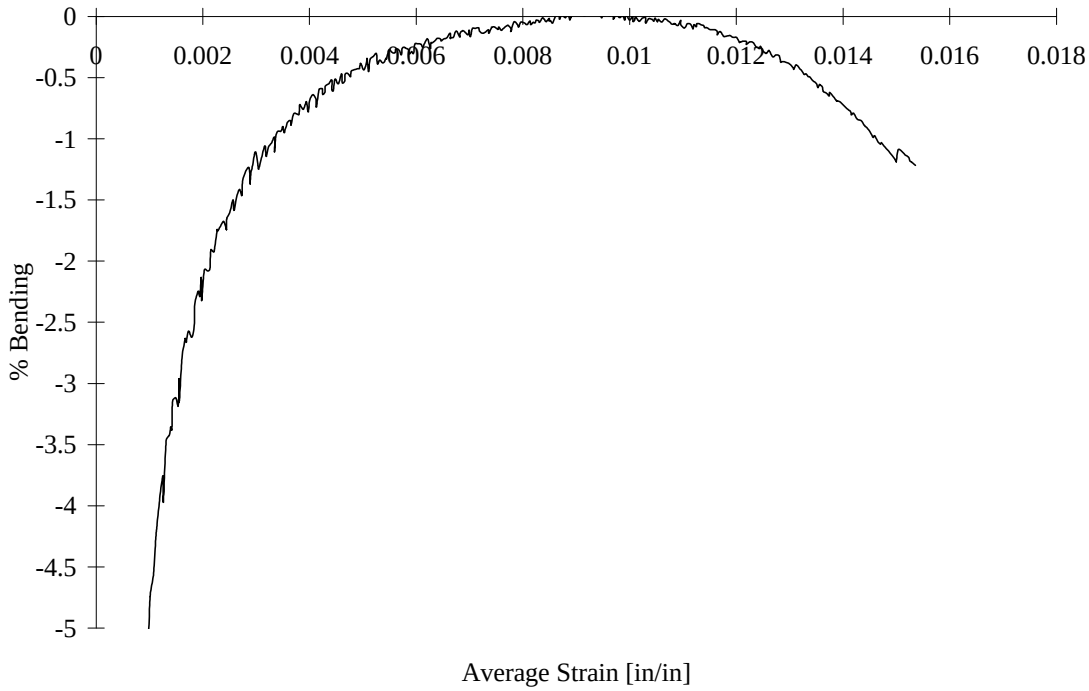

FIGURE D-106. TEST SPECIMEN C80C05: T800/2302-19 CARBON/EPOXY $[90/0]_{4s}$
CLC-15 TEST FIXTURE

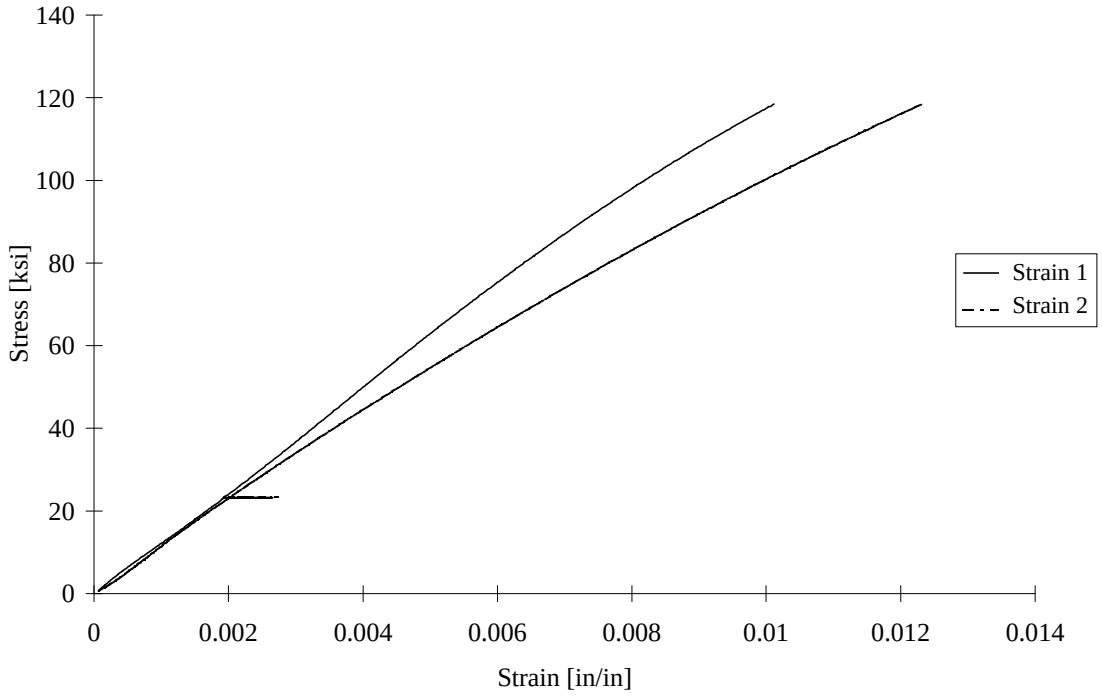

FIGURE D-107. TEST SPECIMEN I80C01: T800/2302-19 CARBON/EPOXY $[90/0]_{4s}$
IITRI TEST FIXTURE

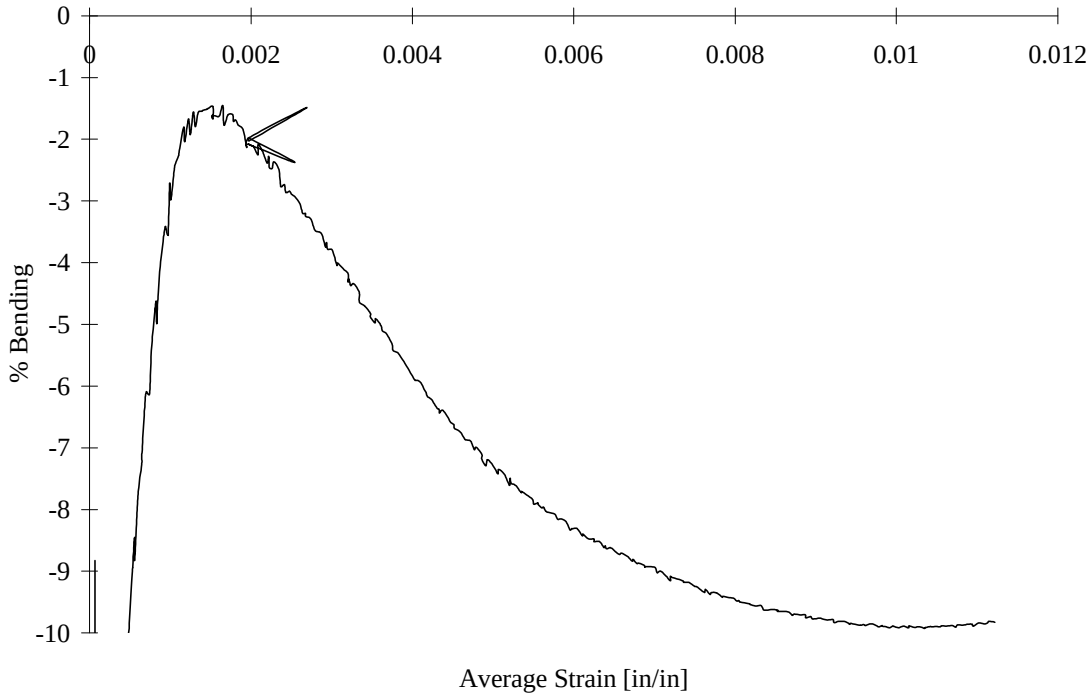

FIGURE D-108. TEST SPECIMEN I80C01: T800/2302-19 CARBON/EPOXY $[90/0]_{4s}$
IITRI TEST FIXTURE

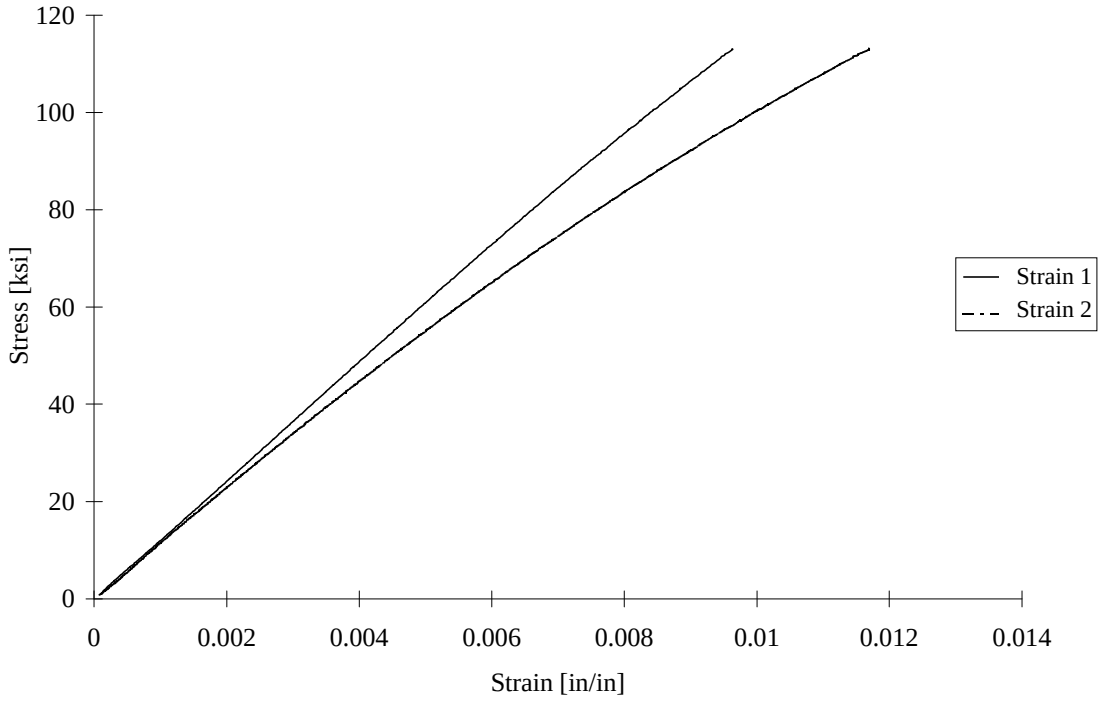

FIGURE D-109. TEST SPECIMEN I80C02: T800/2302-19 CARBON/EPOXY $[90/0]_{4s}$
IITRI TEST FIXTURE

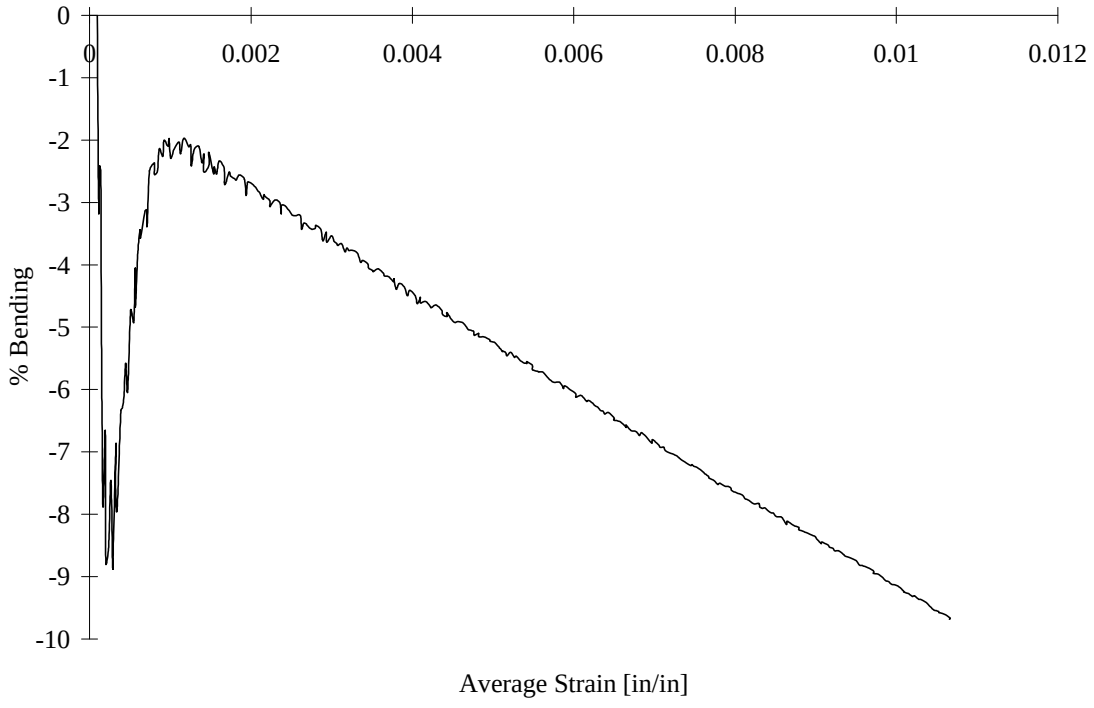

FIGURE D-110. TEST SPECIMEN I80C02: T800/2302-19 CARBON/EPOXY $[90/0]_{4s}$
IITRI TEST FIXTURE

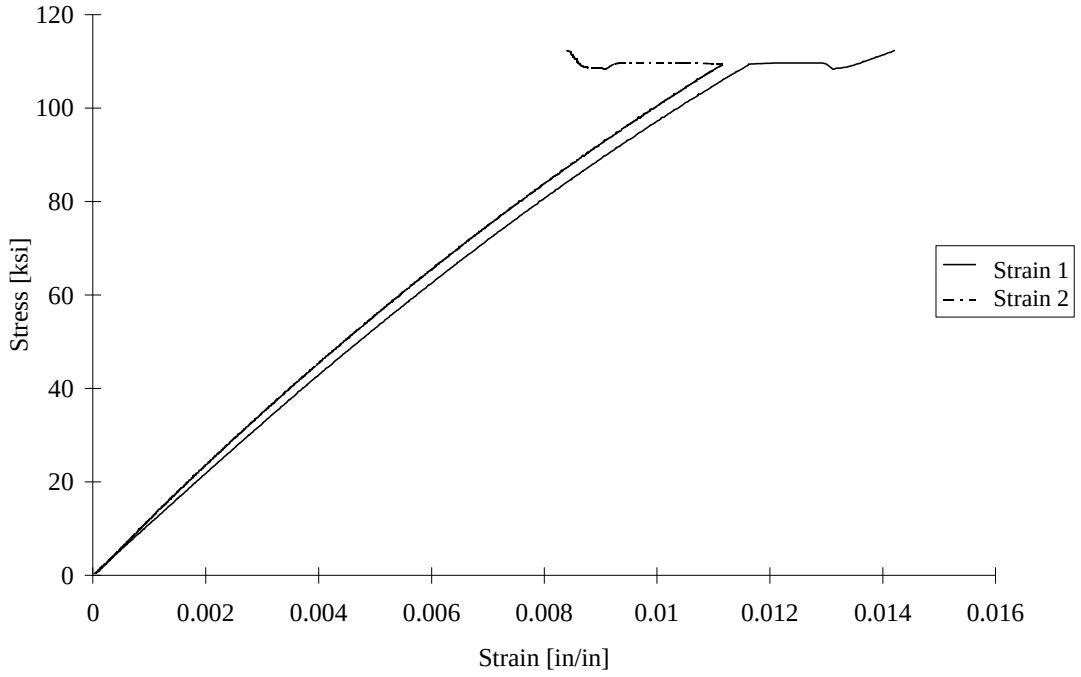

FIGURE D-111. TEST SPECIMEN I80C03: T800/2302-19 CARBON/EPOXY $[90/0]_{4s}$
IITRI TEST FIXTURE

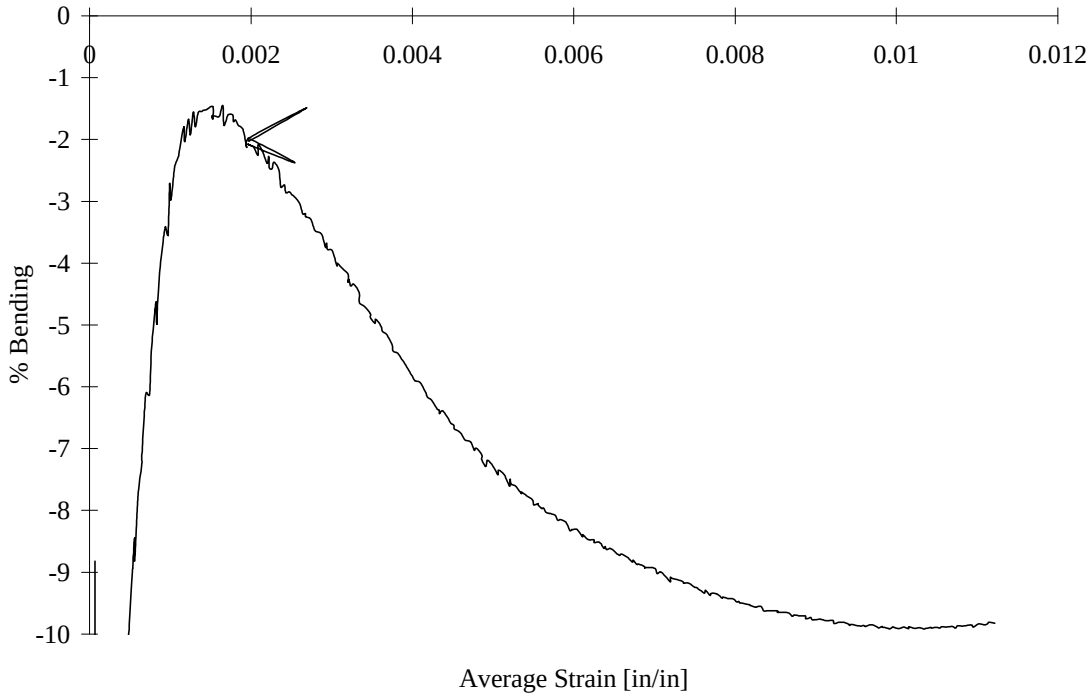

FIGURE D-112. TEST SPECIMEN I80C03: T800/2302-19 CARBON/EPOXY $[90/0]_{4s}$
IITRI TEST FIXTURE

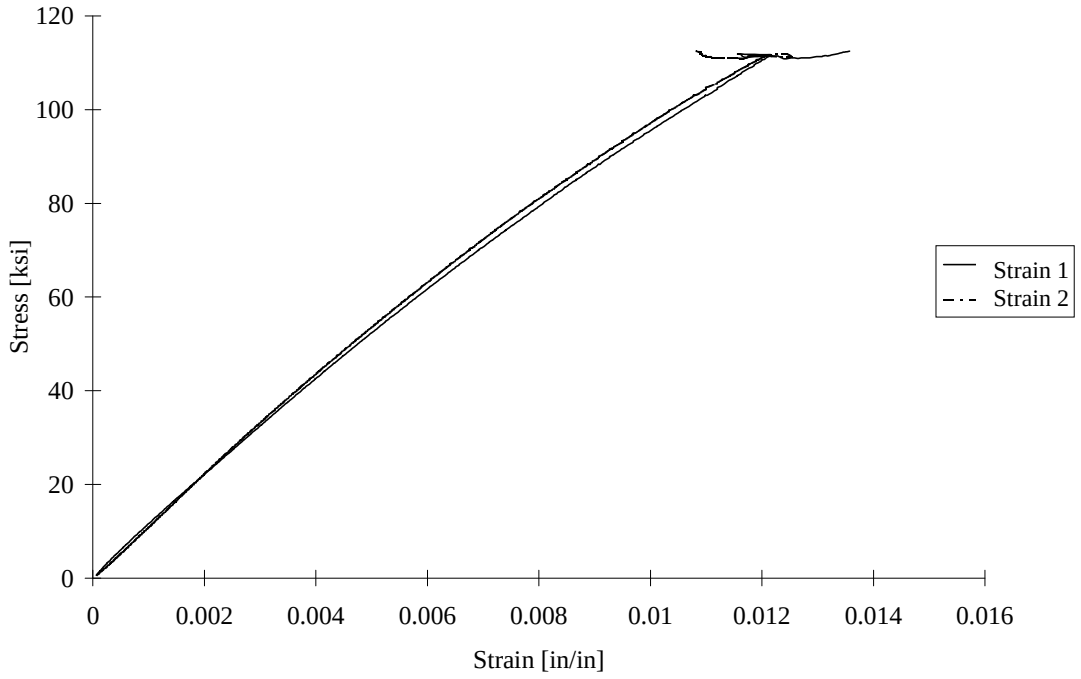

FIGURE D-113. TEST SPECIMEN I80C04: T800/2302-19 CARBON/EPOXY $[90/0]_{4s}$
IITRI TEST FIXTURE

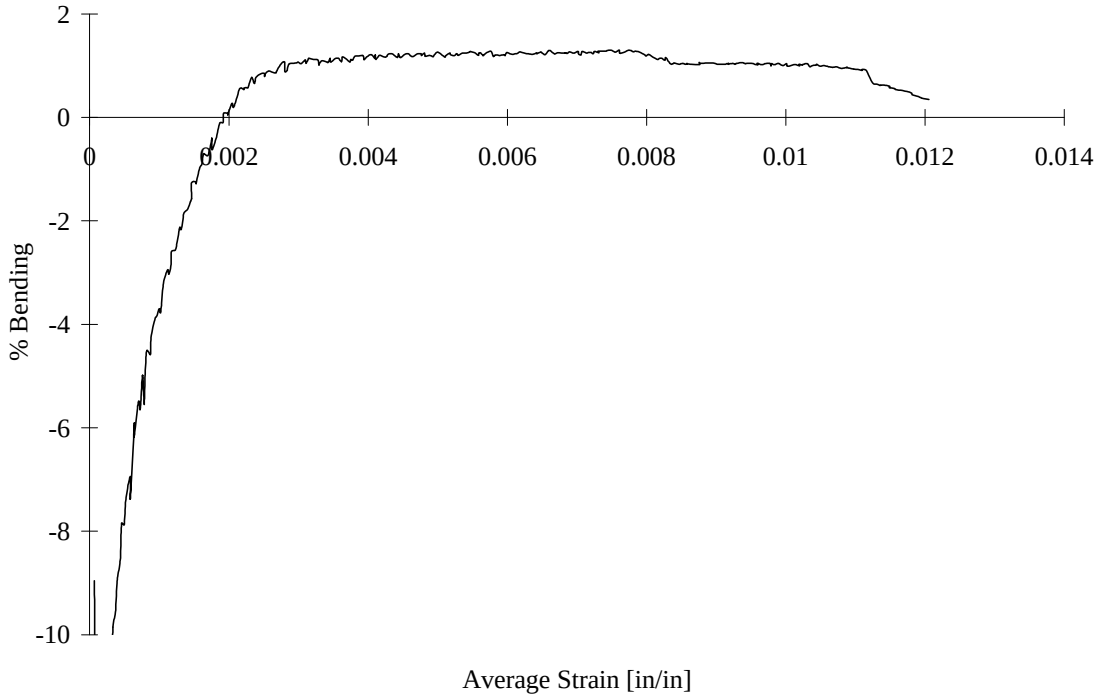

FIGURE D-114. TEST SPECIMEN I80C04: T800/2302-19 CARBON/EPOXY $[90/0]_{4s}$
ITRI TEST FIXTURE

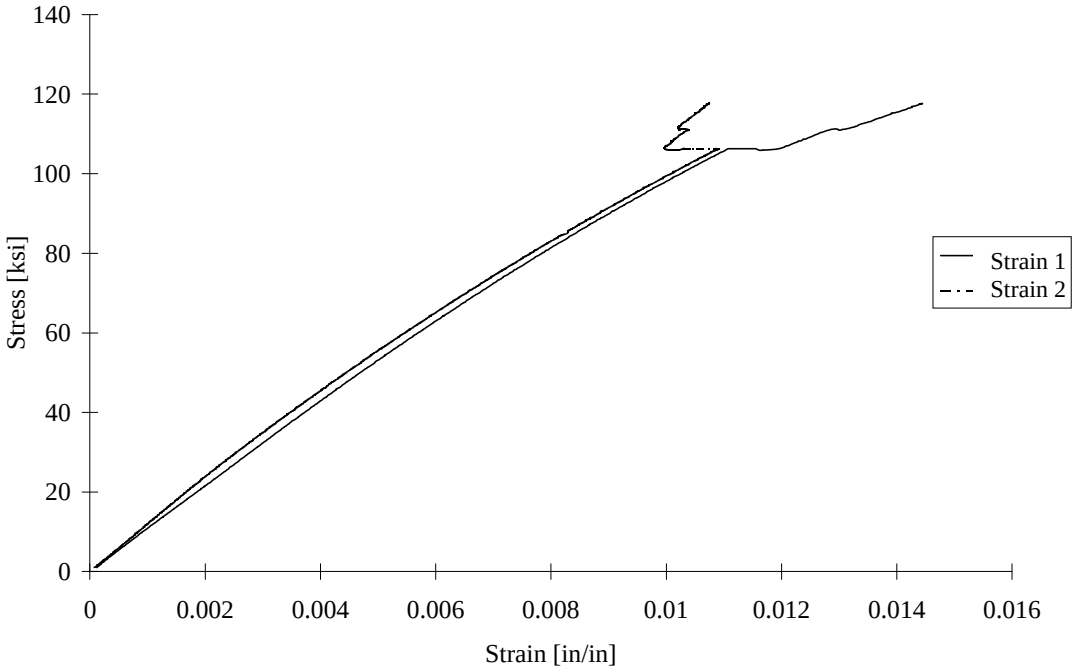

FIGURE D-115. TEST SPECIMEN I80C05: T800/2302-19 CARBON/EPOXY $[90/0]_{4s}$ IITRI TEST FIXTURE

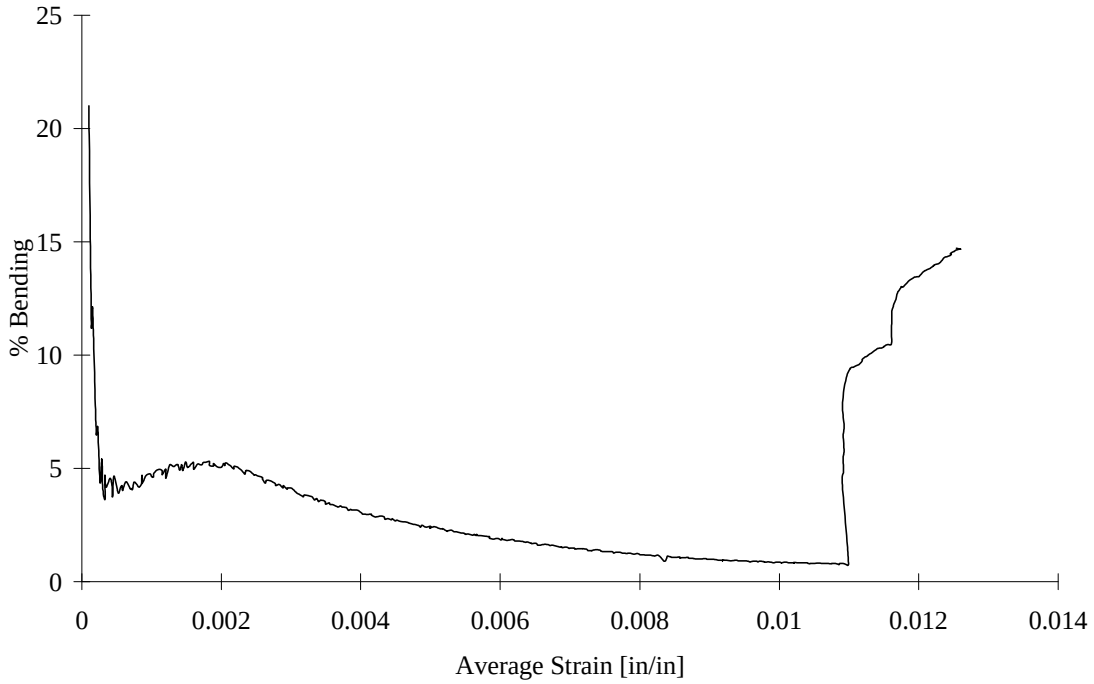

FIGURE D-116. TEST SPECIMEN I80C05: T800/2302-19 CARBON/EPOXY $[90/0]_{4s}$ IITRI TEST FIXTURE

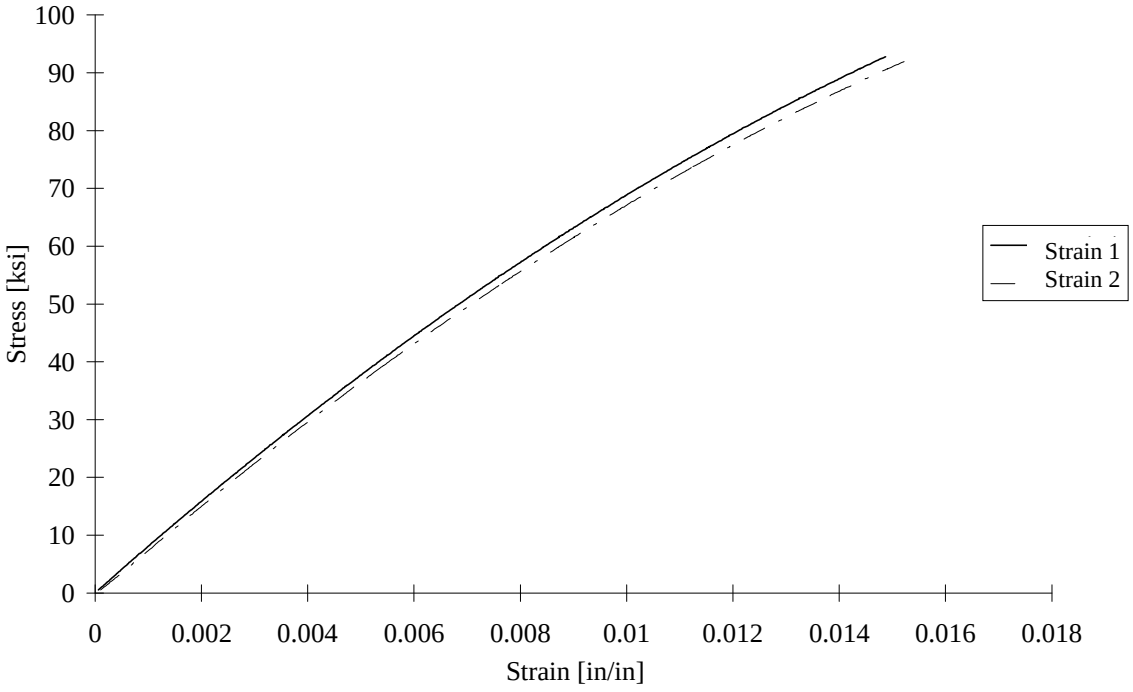

FIGURE D-117. TEST SPECIMEN C80Q01: T800/2302-19 CARBON/EPOXY $[45/0/-45/90]_{2s}$ CLC-15 TEST FIXTURE

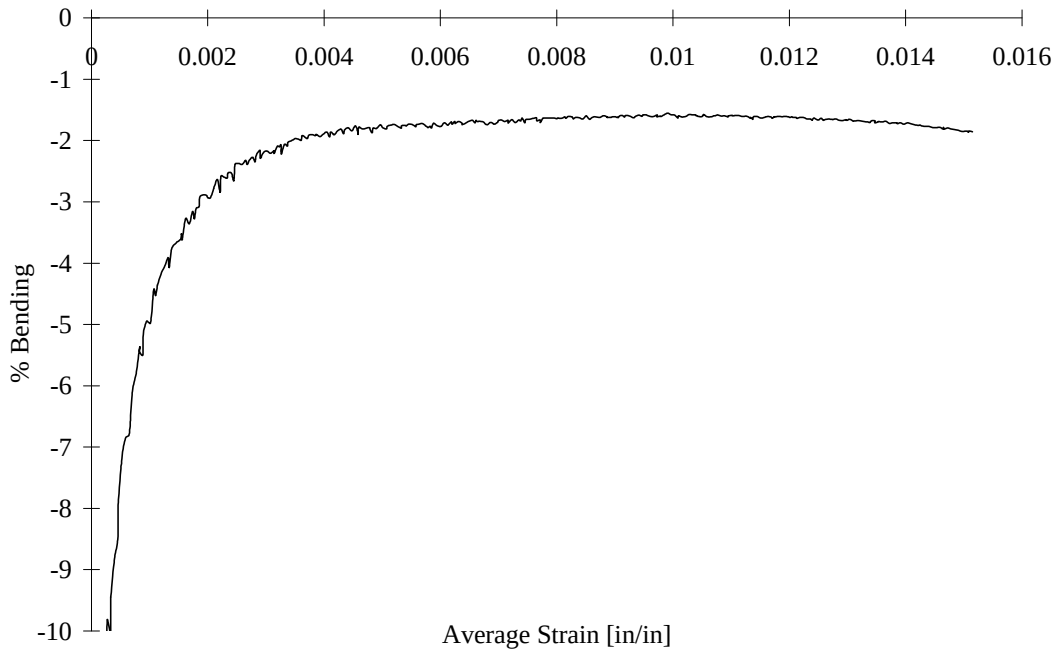

FIGURE D-118. TEST SPECIMEN C80Q01: T800/2302-19 CARBON/EPOXY $[45/0/-45/90]_{2s}$ CLC-15 TEST FIXTURE

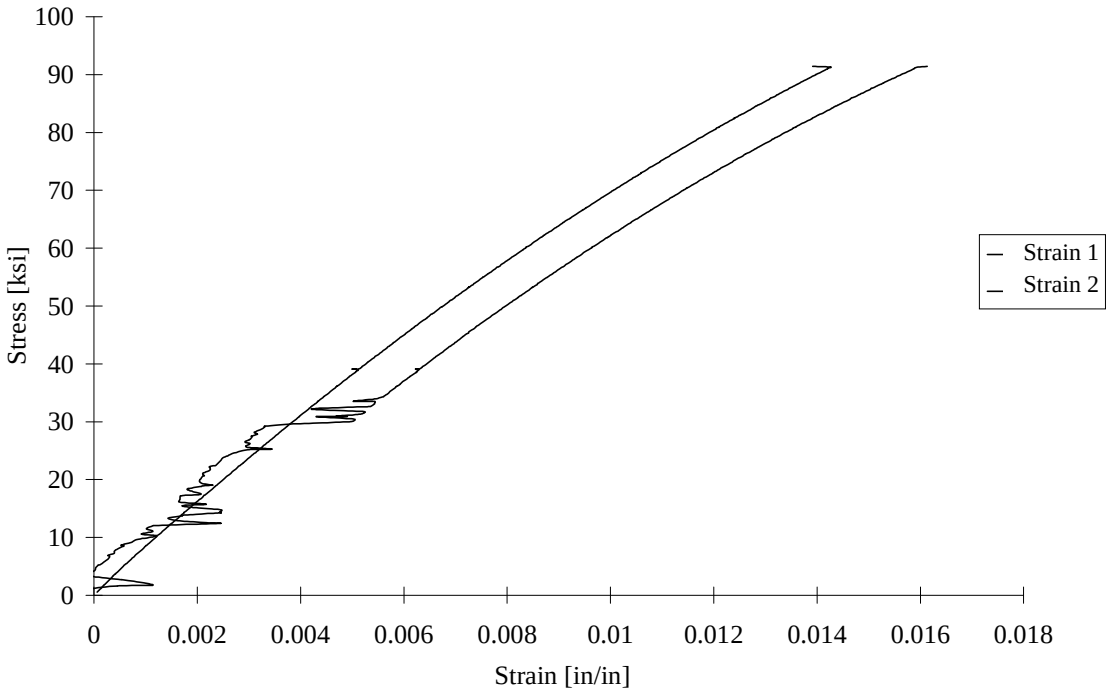

FIGURE D-119. TEST SPECIMEN C80Q02: T800/2302-19 CARBON/EPOXY $[45/0/-45/90]_{2s}$ CLC-15 TEST FIXTURE

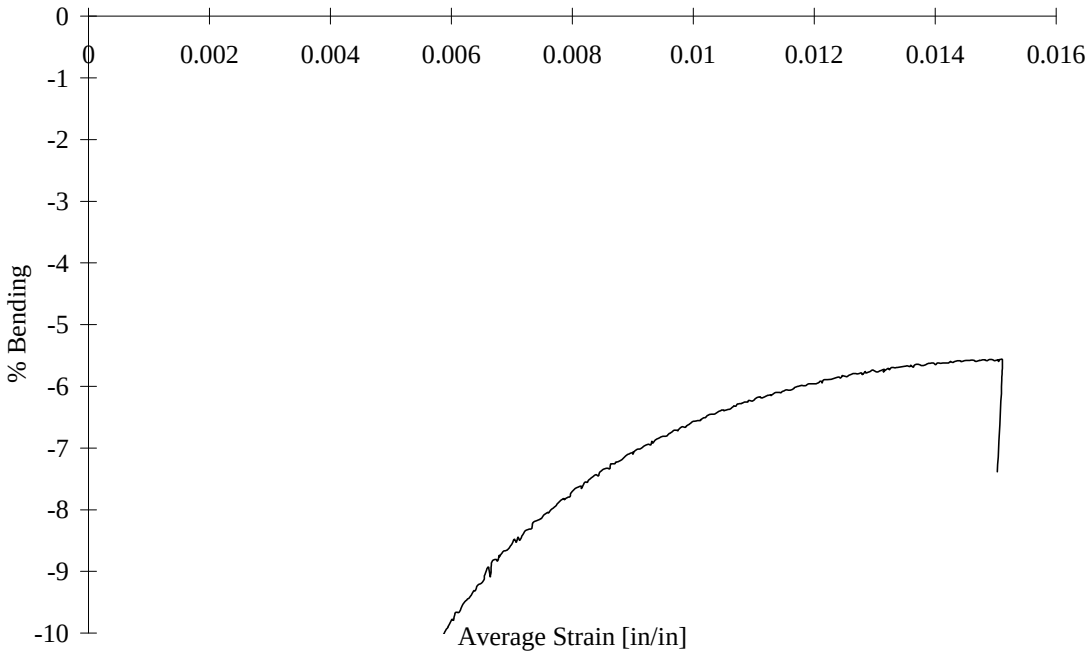

FIGURE D-120. TEST SPECIMEN C80Q02: T800/2302-19 CARBON/EPOXY $[45/0/-45/90]_{2s}$ CLC-15 TEST FIXTURE

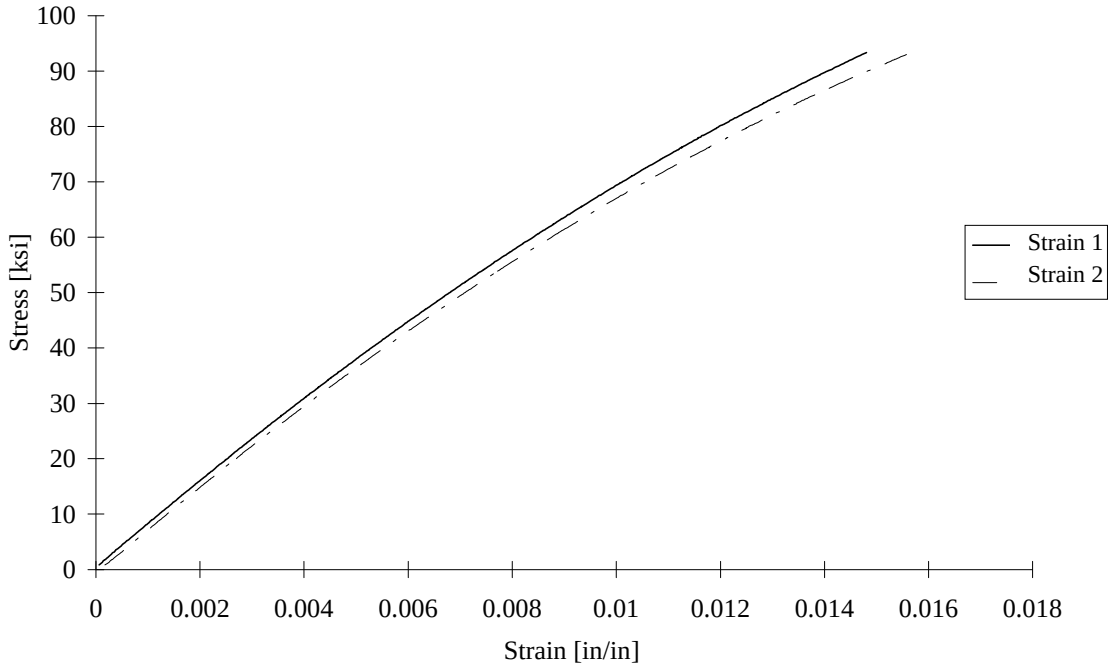

FIGURE D-121. TEST SPECIMEN C80Q03: T800/2302-19 CARBON/EPOXY $[45/0/-45/90]_{2s}$ CLC-15 TEST FIXTURE

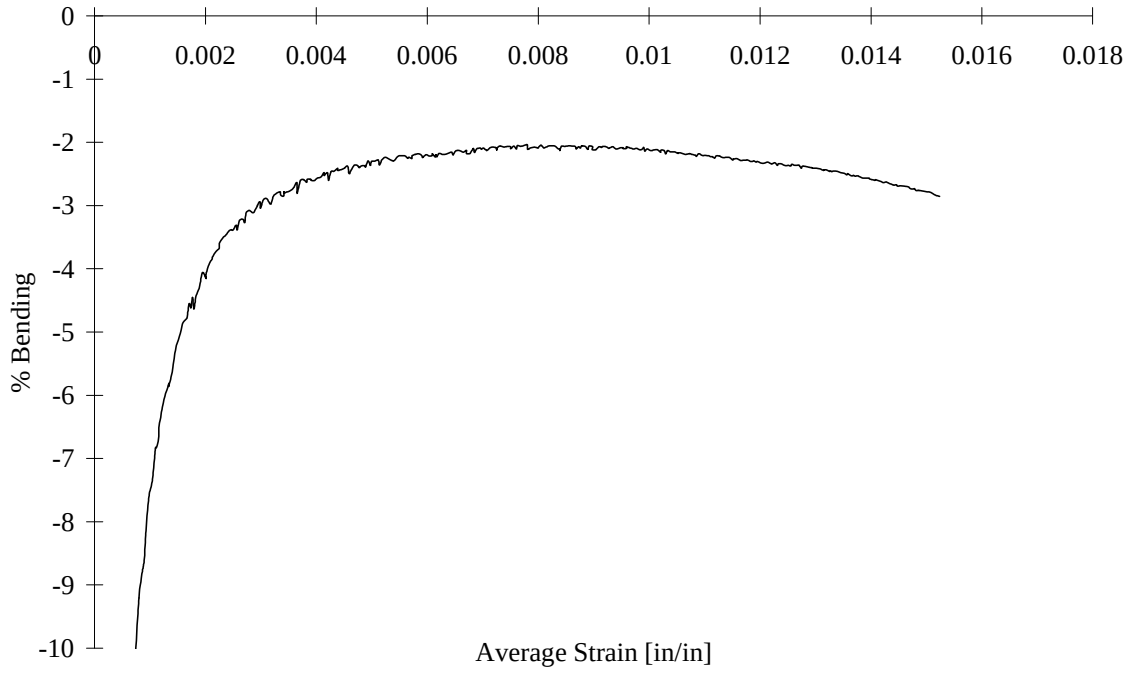

FIGURE D-122. TEST SPECIMEN C80Q03: T800/2302-19 CARBON/EPOXY $[45/0/-45/90]_{2s}$ CLC-15 TEST FIXTURE

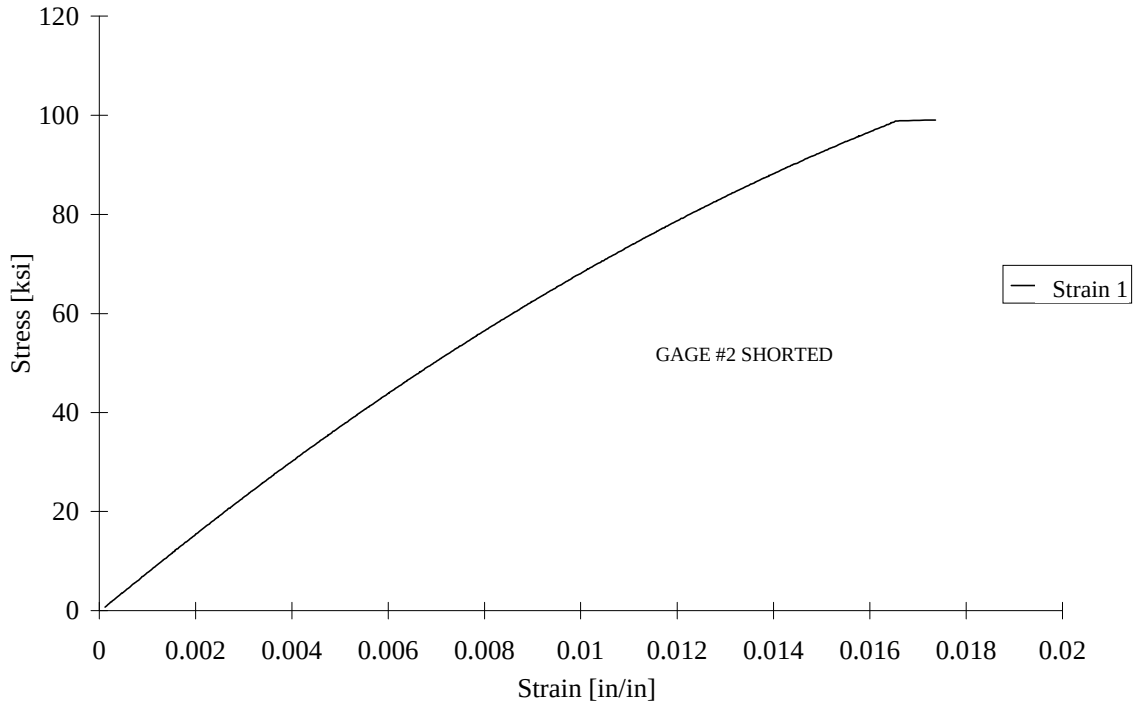

FIGURE D-123. TEST SPECIMEN C80Q04: T800/2302-19 CARBON/EPOXY $[45/0/-45/90]_{2s}$ CLC-15 TEST FIXTURE

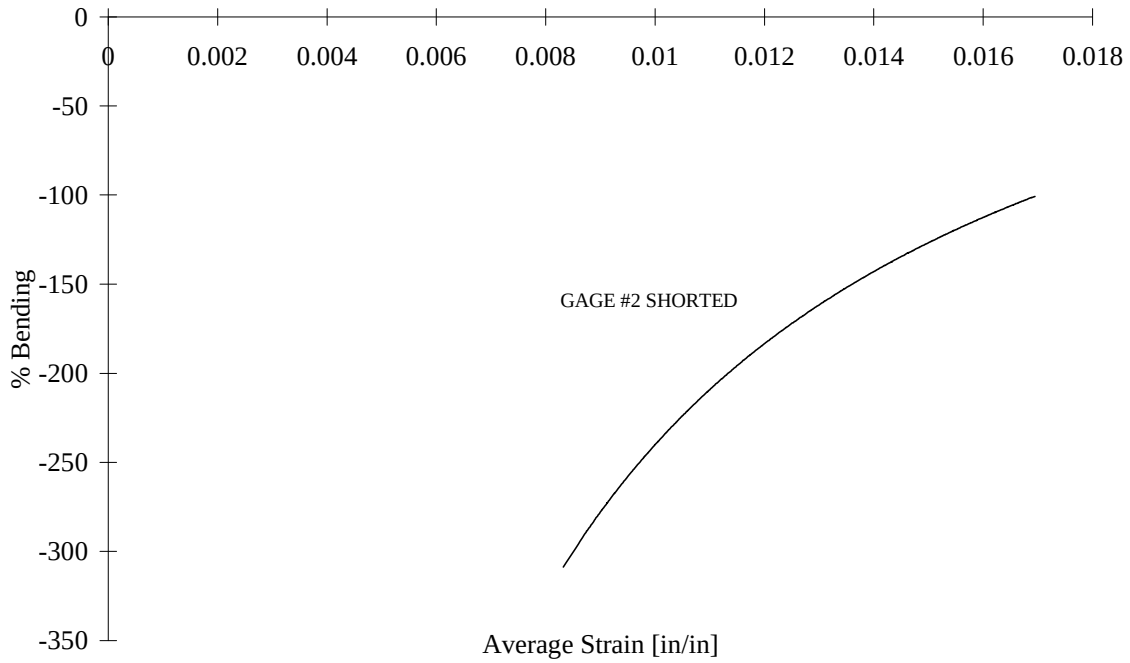

FIGURE D-124. TEST SPECIMEN C80Q04: T800/2302-19 CARBON/EPOXY $[45/0/-45/90]_{2s}$ CLC-15 TEST FIXTURE

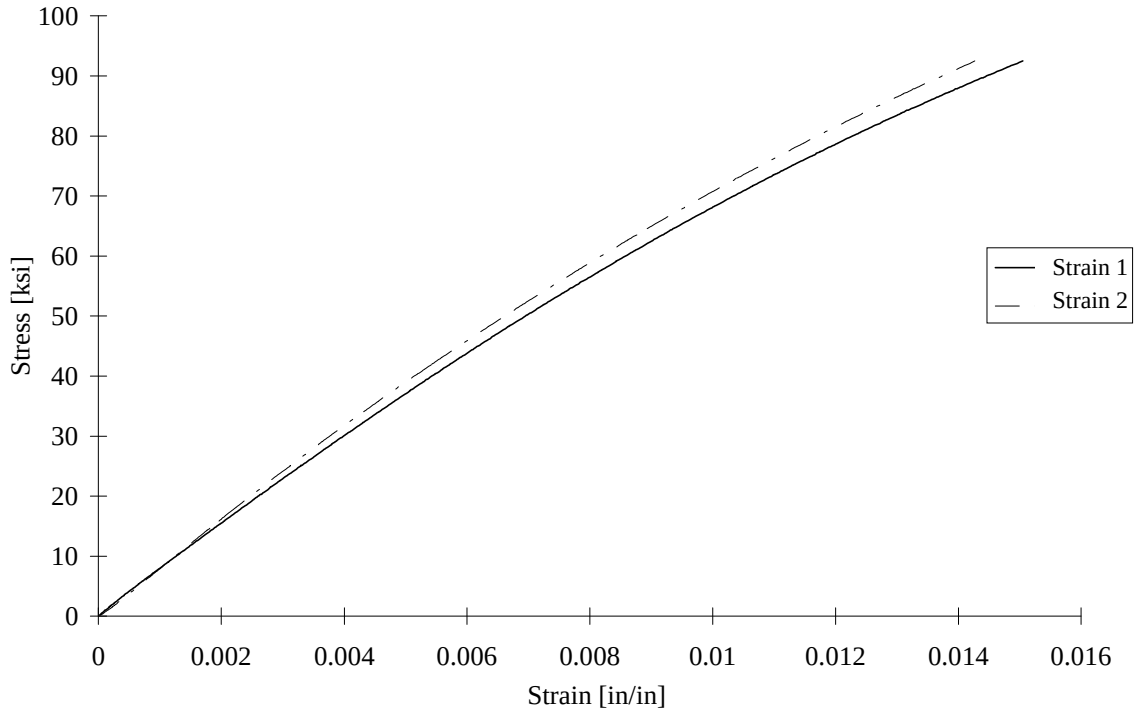

FIGURE D-125. TEST SPECIMEN I80Q01: T800/2302-19 CARBON/EPOXY $[45/0/-45/90]_{2s}$
IITRI TEST FIXTURE

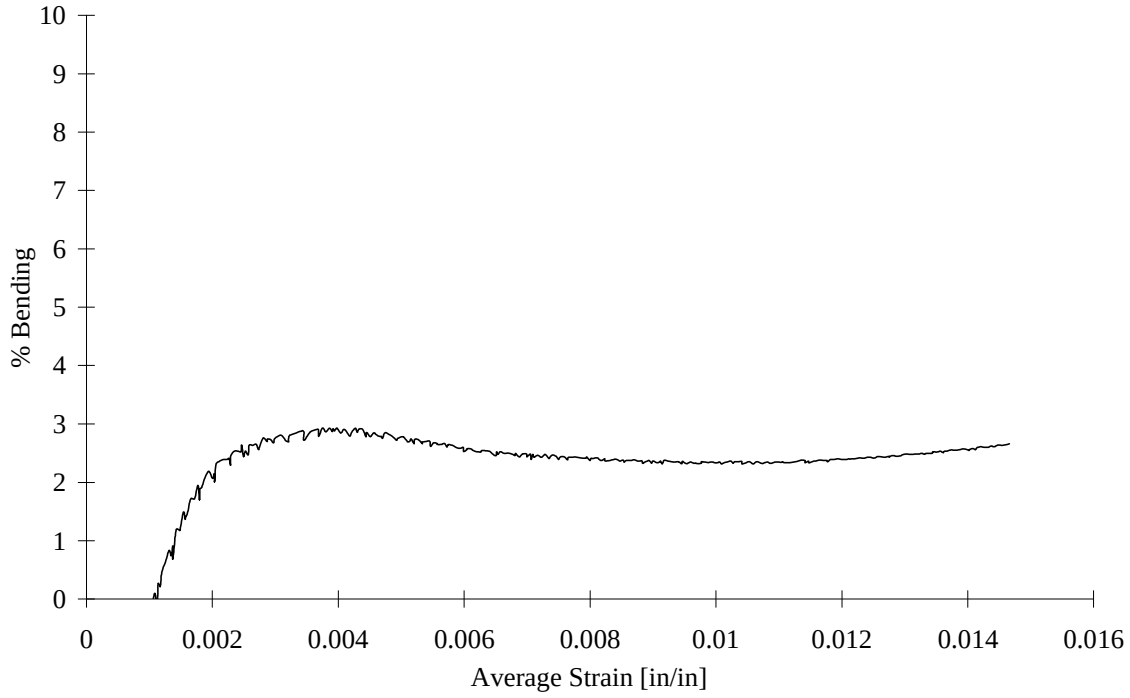

FIGURE D-126. TEST SPECIMEN I80Q01: T800/2302-19 CARBON/EPOXY $[45/0/-45/90]_{2s}$
IITRI TEST FIXTURE

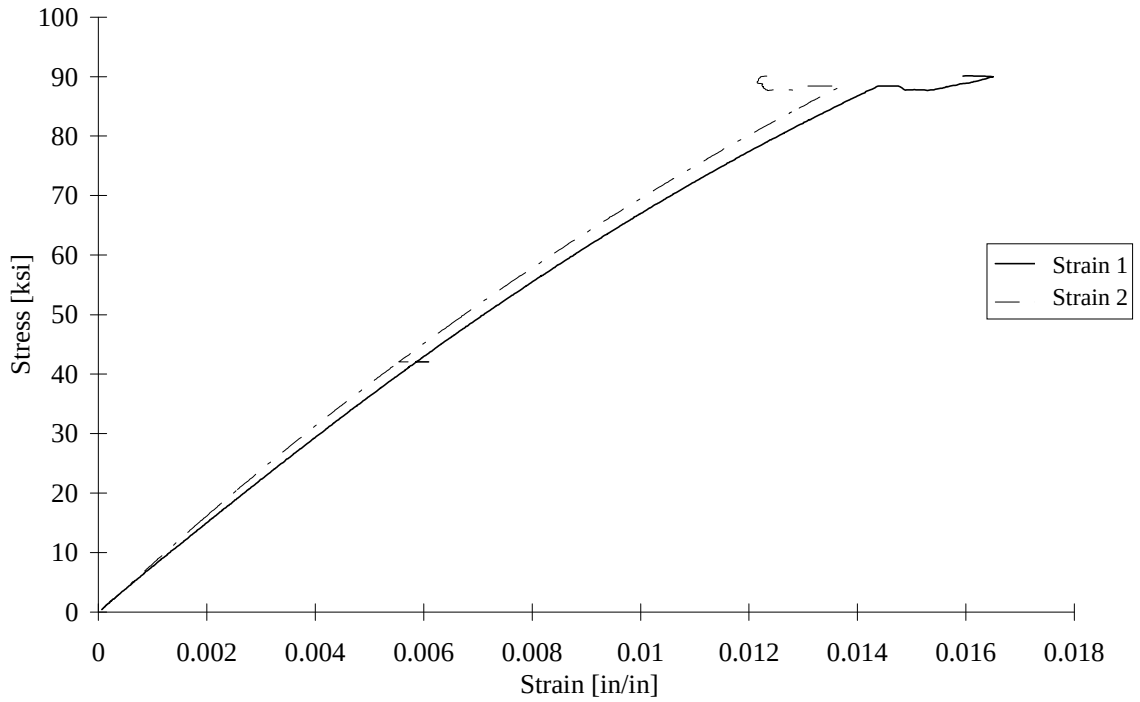

FIGURE D-127. TEST SPECIMEN I80Q02: T800/2302-19 CARBON/EPOXY $[45/0/-45/90]_{2s}$
IITRI TEST FIXTURE

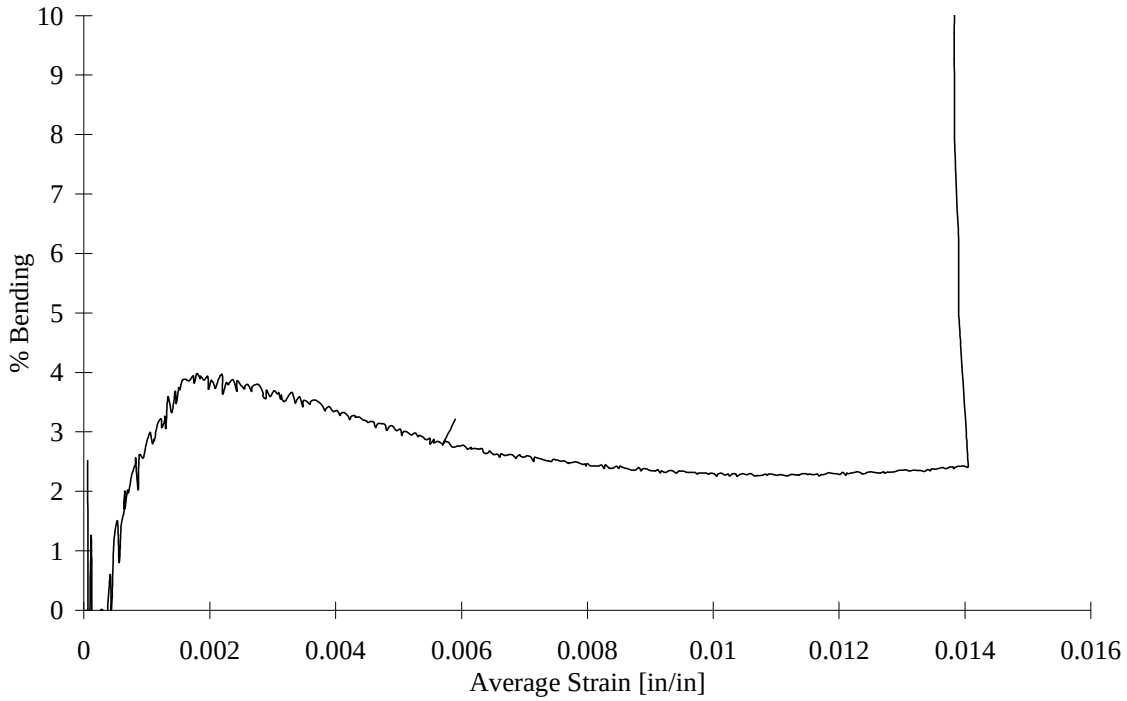

FIGURE D-128. TEST SPECIMEN I80Q02: T800/2302-19 CARBON/EPOXY $[45/0/-45/90]_{2s}$
IITRI TEST FIXTURE

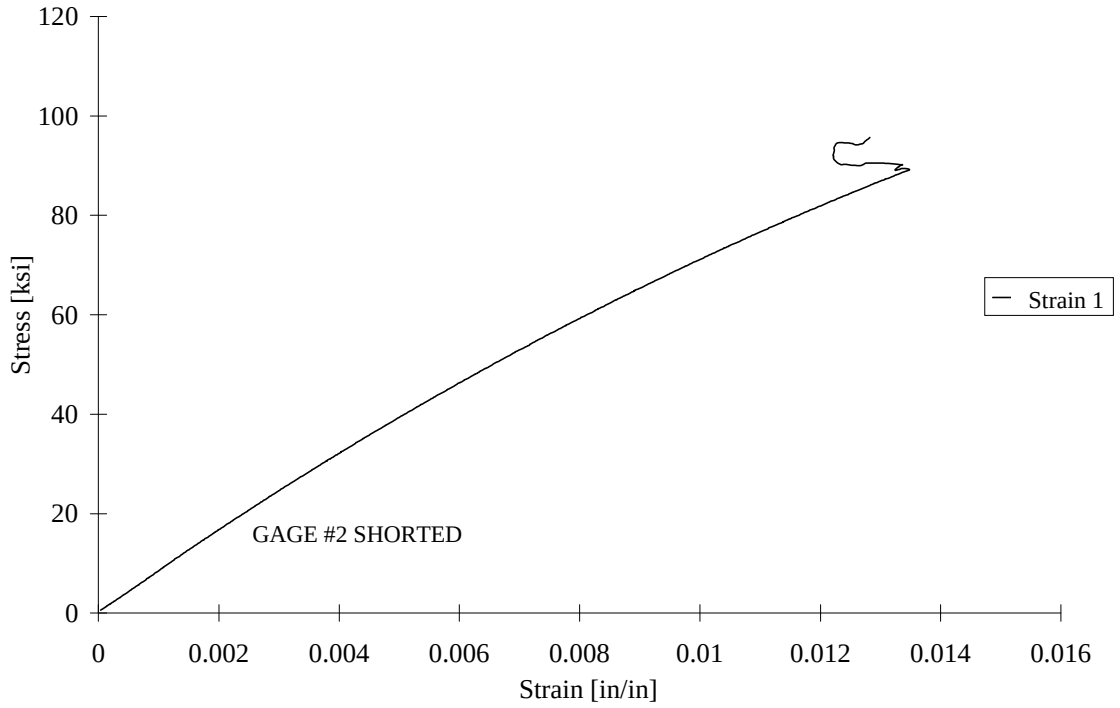

FIGURE D-129. TEST SPECIMEN I80Q03: T800/2302-19 CARBON/EPOXY $[45/0/-45/90]_{2s}$
IITRI TEST FIXTURE

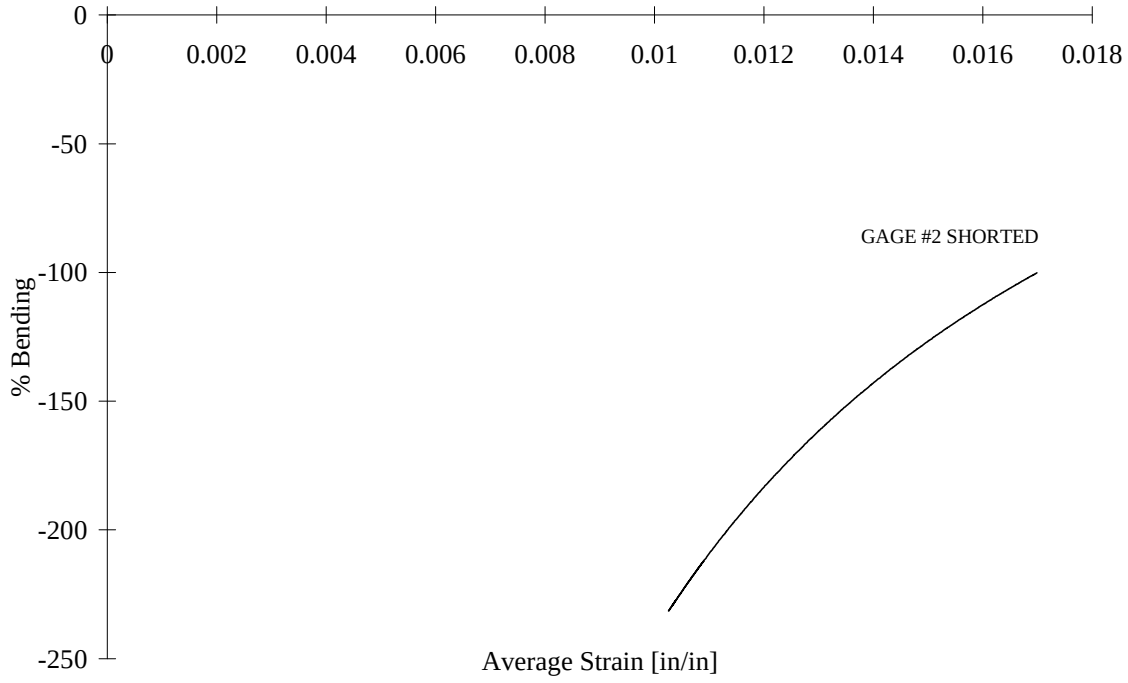

FIGURE D-130. TEST SPECIMEN I80Q03: T800/2302-19 CARBON/EPOXY $[45/0/-45/90]_{2s}$
IITRI TEST FIXTURE

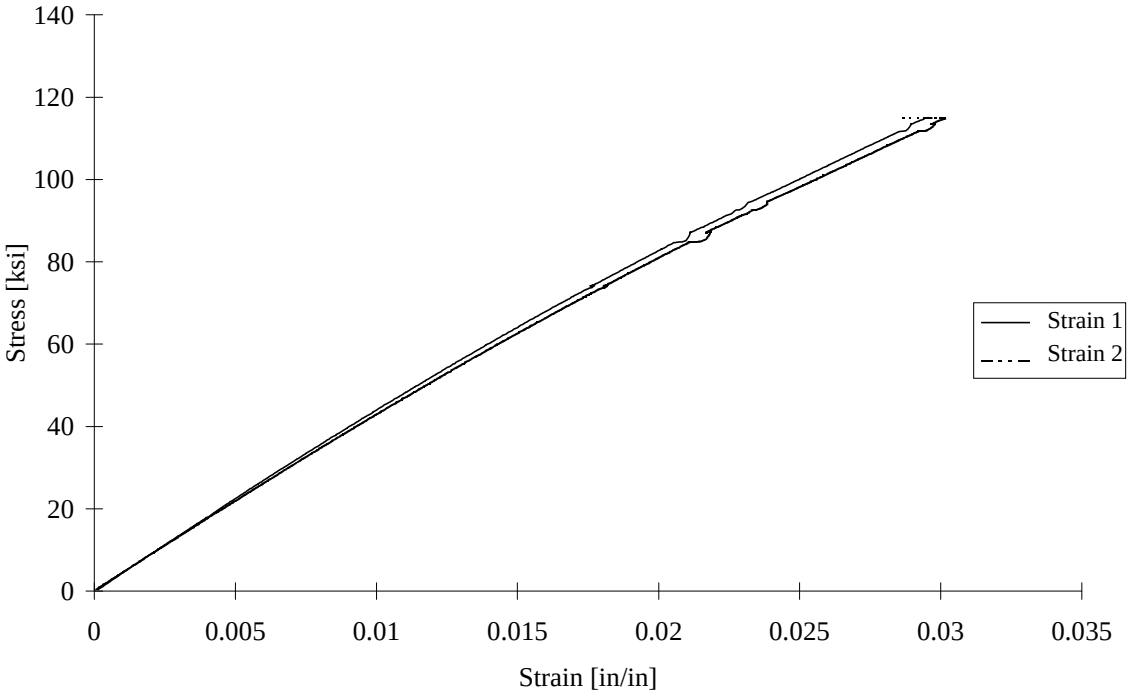

FIGURE D-131. TEST SPECIMEN CS2C01: S2/SP381 GLASS/EPOXY $[90/0]_{7s}$
CLC-15 TEST FIXTURE

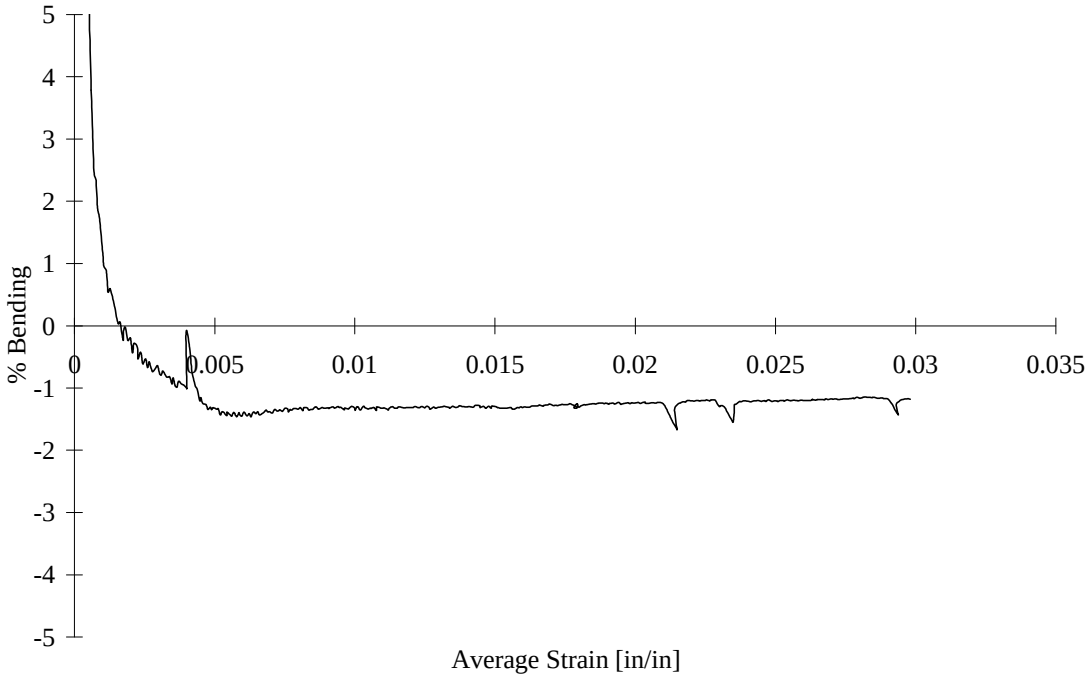

FIGURE D-132. TEST SPECIMEN CS2C01: S2/SP381 GLASS/EPOXY $[90/0]_{7s}$
CLC-15 TEST FIXTURE

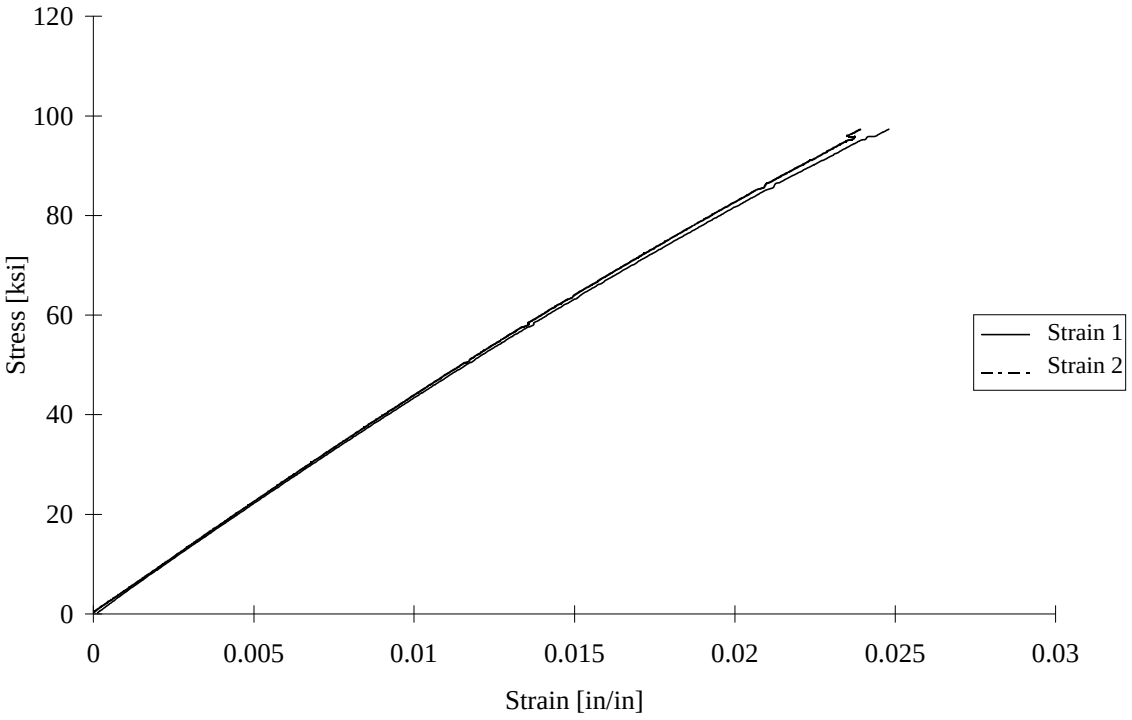

FIGURE D-133. TEST SPECIMEN CS2C02: S2/SP381 GLASS/EPOXY $[90/0]_{7s}$
CLC-15 TEST FIXTURE

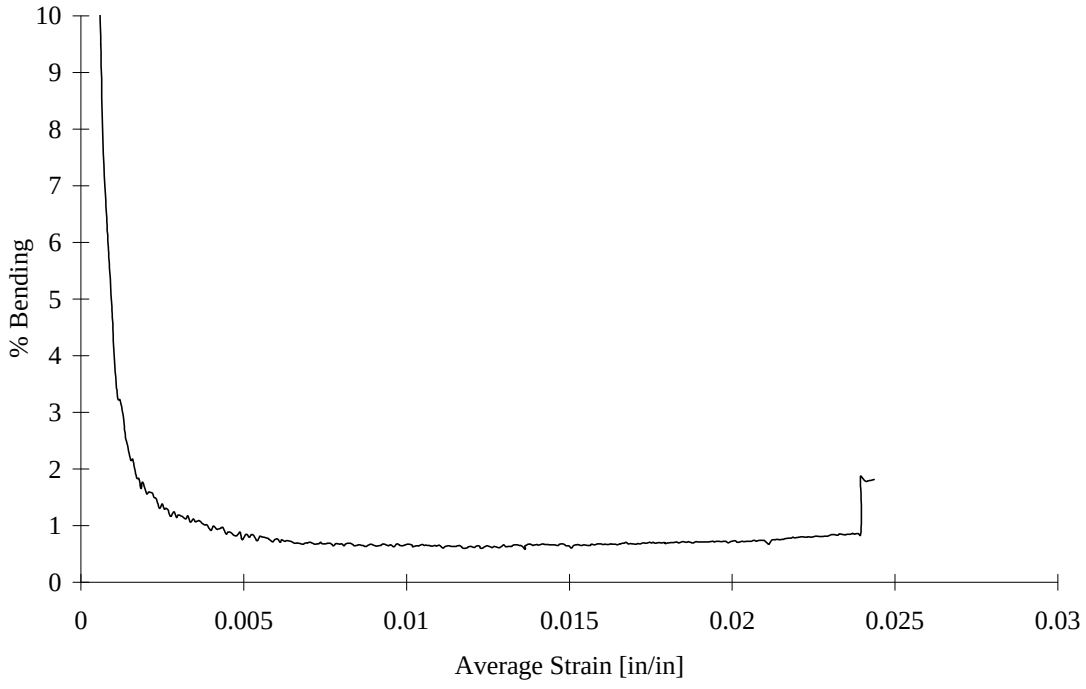

FIGURE D-134. TEST SPECIMEN CS2C02: S2/SP381 GLASS/EPOXY $[90/0]_{7s}$
CLC-15 TEST FIXTURE

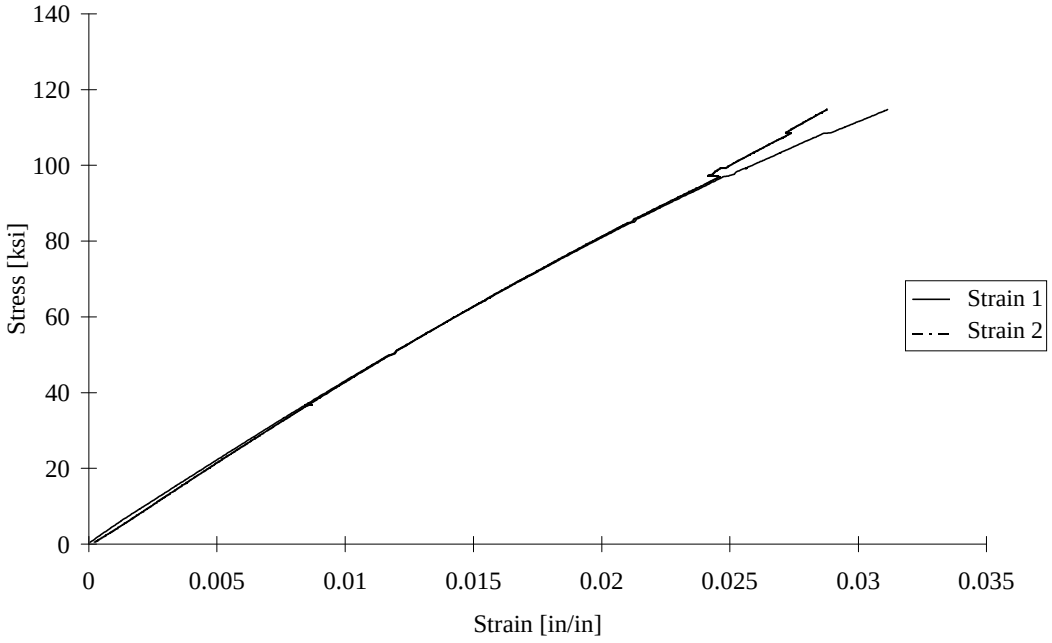

FIGURE D-135. TEST SPECIMEN CS2C03: S2/SP381 GLASS/EPOXY $[90/0]_{7s}$
CLC-15 TEST FIXTURE

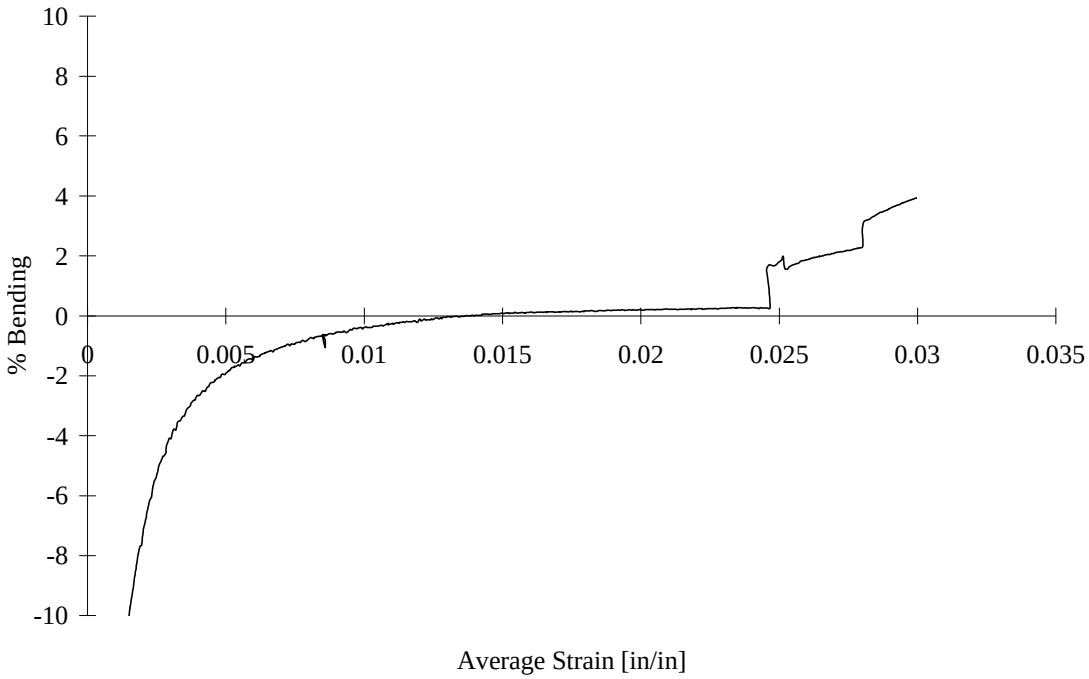

FIGURE D-136. TEST SPECIMEN CS2C03: S2/SP381 GLASS/EPOXY $[90/0]_{7s}$
CLC-15 TEST FIXTURE

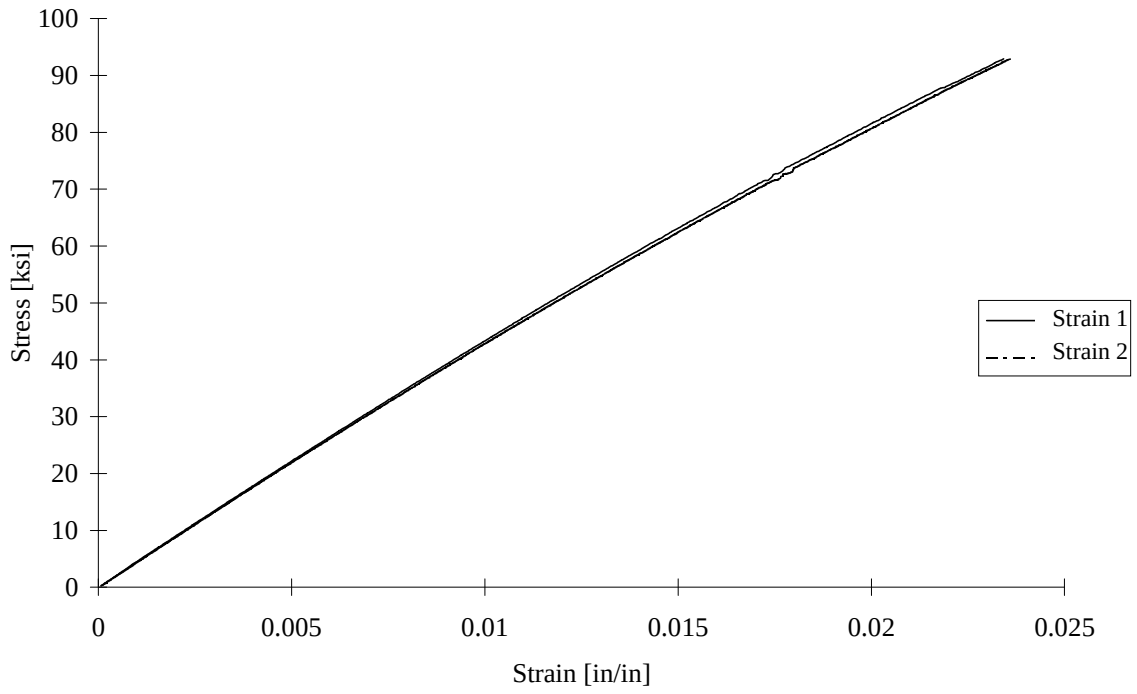

FIGURE D-137. TEST SPECIMEN CS2C04: S2/SP381 GLASS/EPOXY $[90/0]_{7s}$
CLC-15 TEST FIXTURE

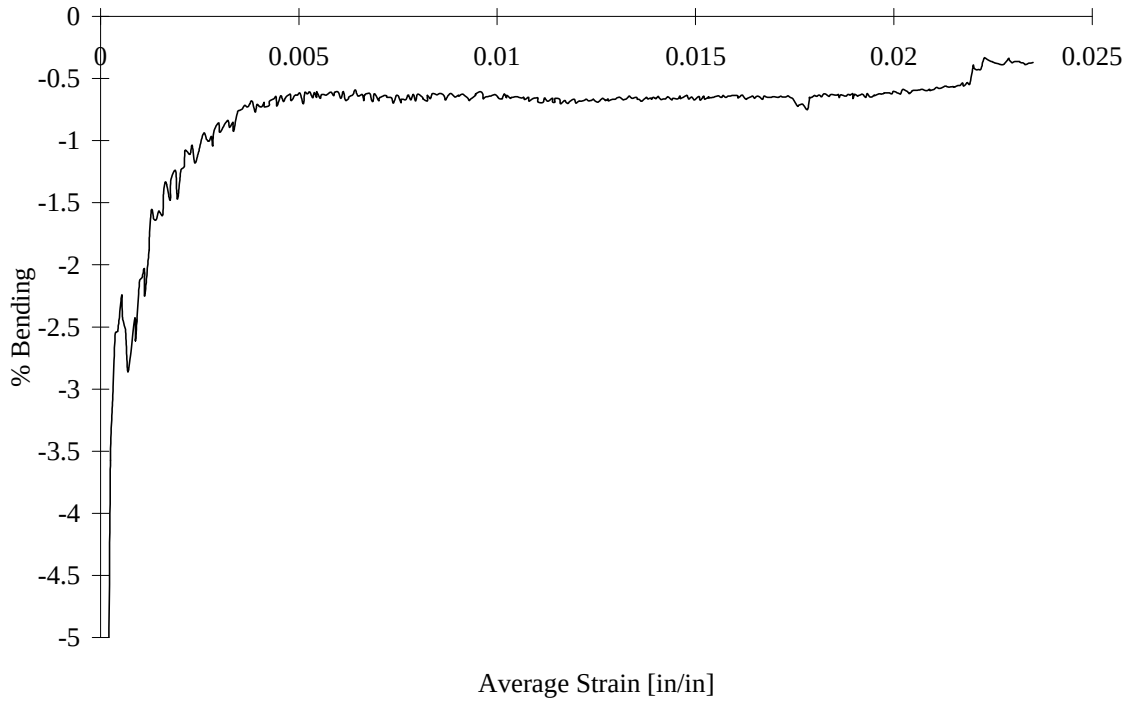

FIGURE D-138. TEST SPECIMEN CS2C04: S2/SP381 GLASS/EPOXY $[90/0]_{7s}$
CLC-15 TEST FIXTURE

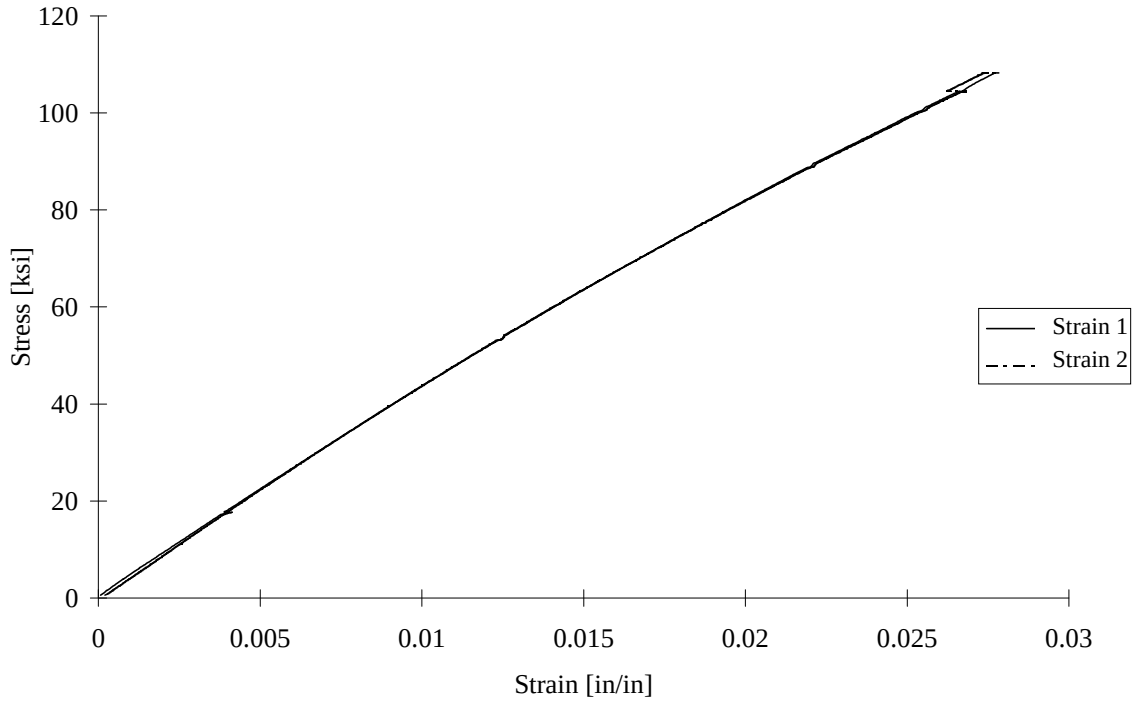

FIGURE D-139. TEST SPECIMEN CS2C05: S2/SP381 GLASS/EPOXY $[90/0]_{7s}$
CLC-15 TEST FIXTURE

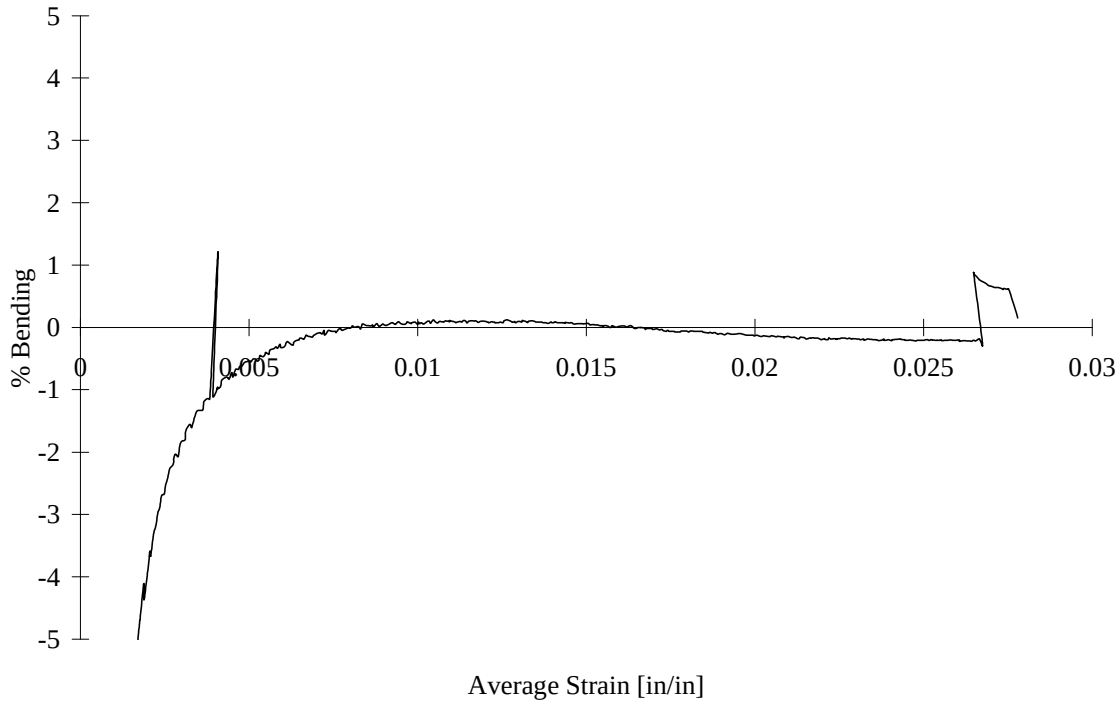

FIGURE D-140. TEST SPECIMEN CS2C05: S2/SP381 GLASS/EPOXY $[90/0]_{7s}$
CLC-15 TEST FIXTURE

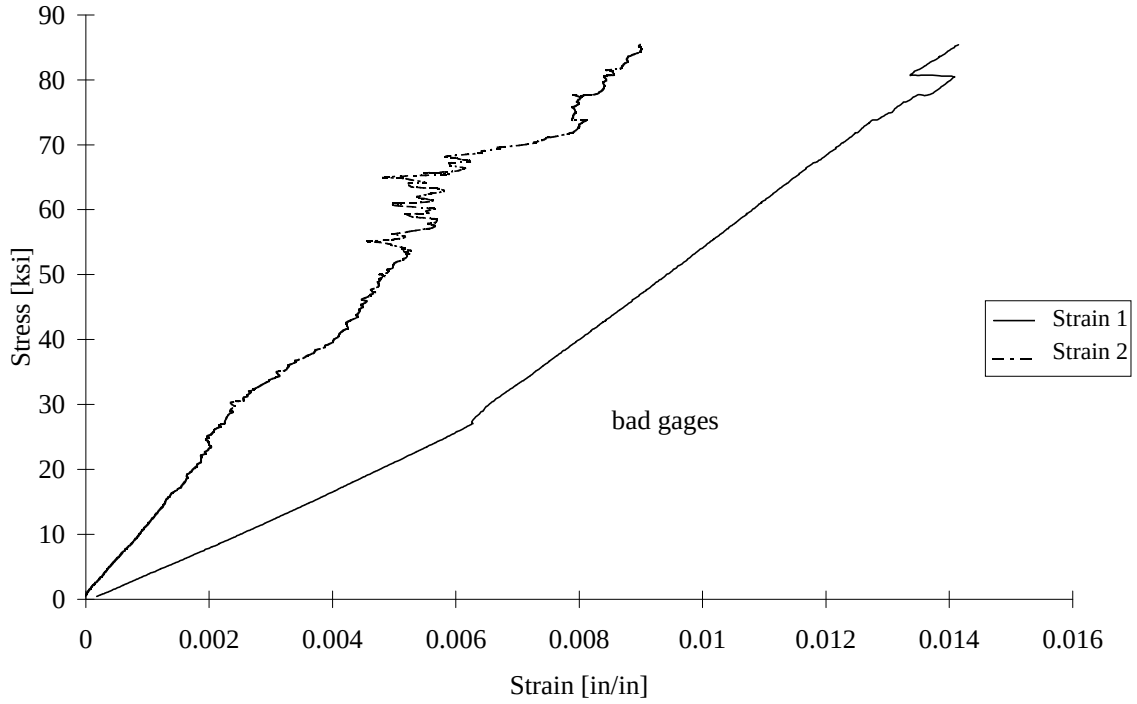

FIGURE D-141. TEST SPECIMEN IS2C01: S2/SP381 GLASS/EPOXY $[90/0]_{7s}$
IITRI TEST FIXTURE

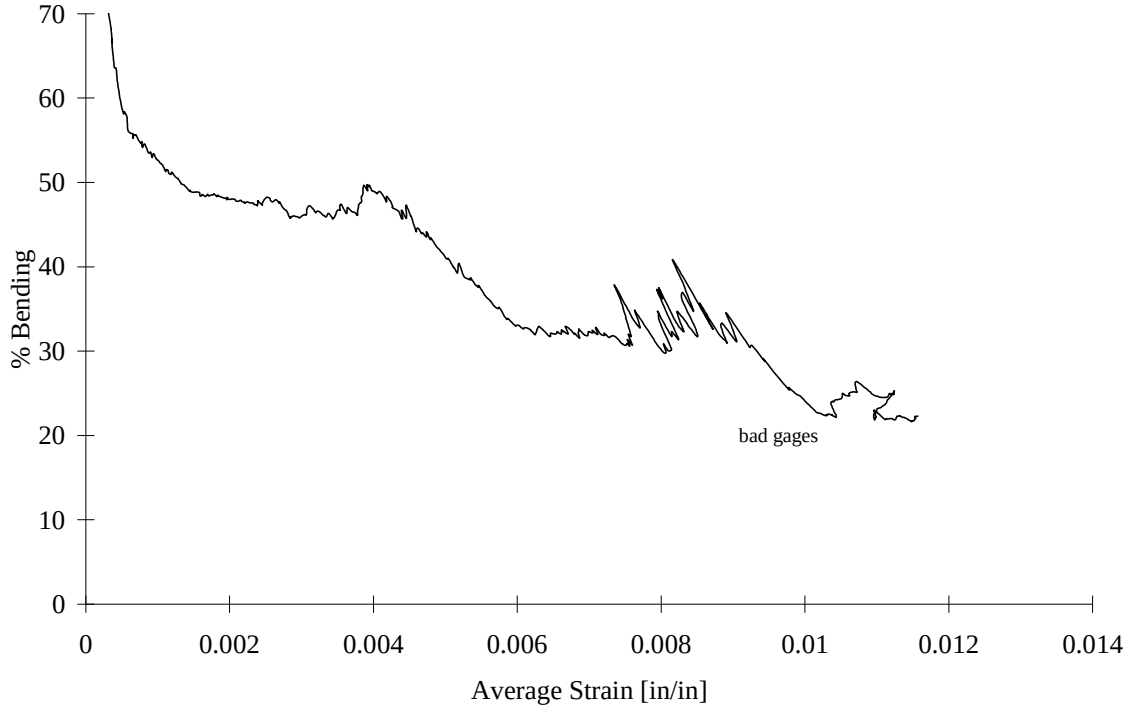

FIGURE D-142. TEST SPECIMEN IS2C01: S2/SP381 GLASS/EPOXY $[90/0]_{7s}$
IITRI TEST FIXTURE

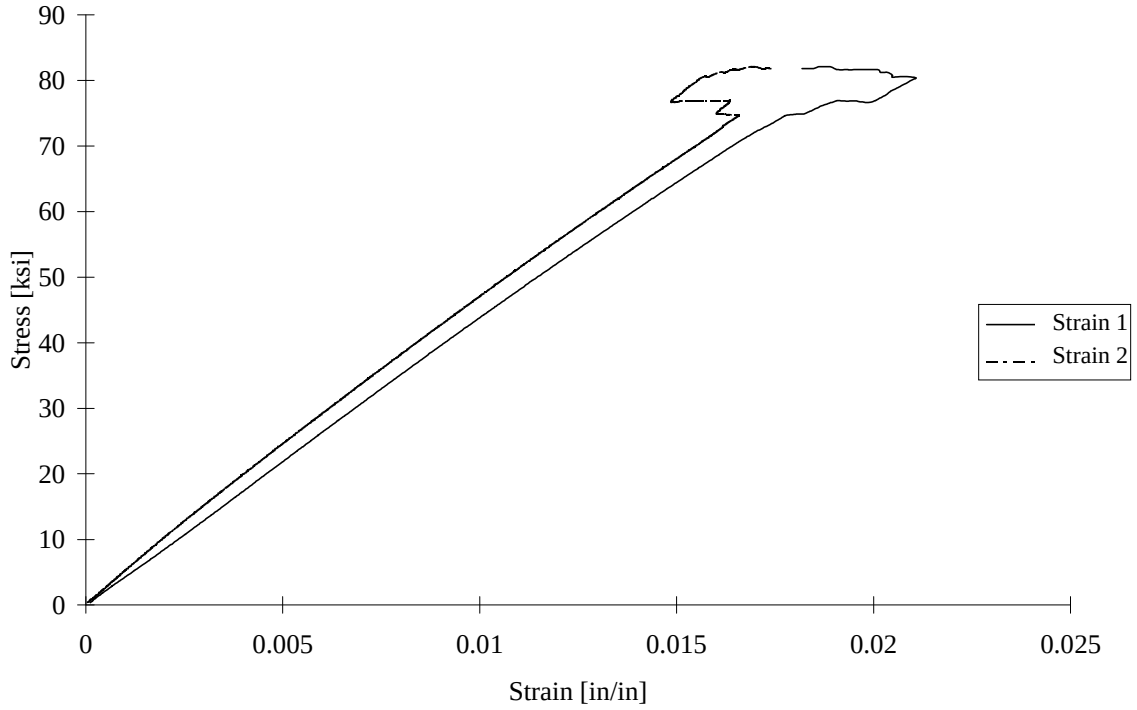

FIGURE D-143. TEST SPECIMEN IS2C02: S2/SP381 GLASS/EPOXY $[90/0]_{7s}$
IITRI TEST FIXTURE

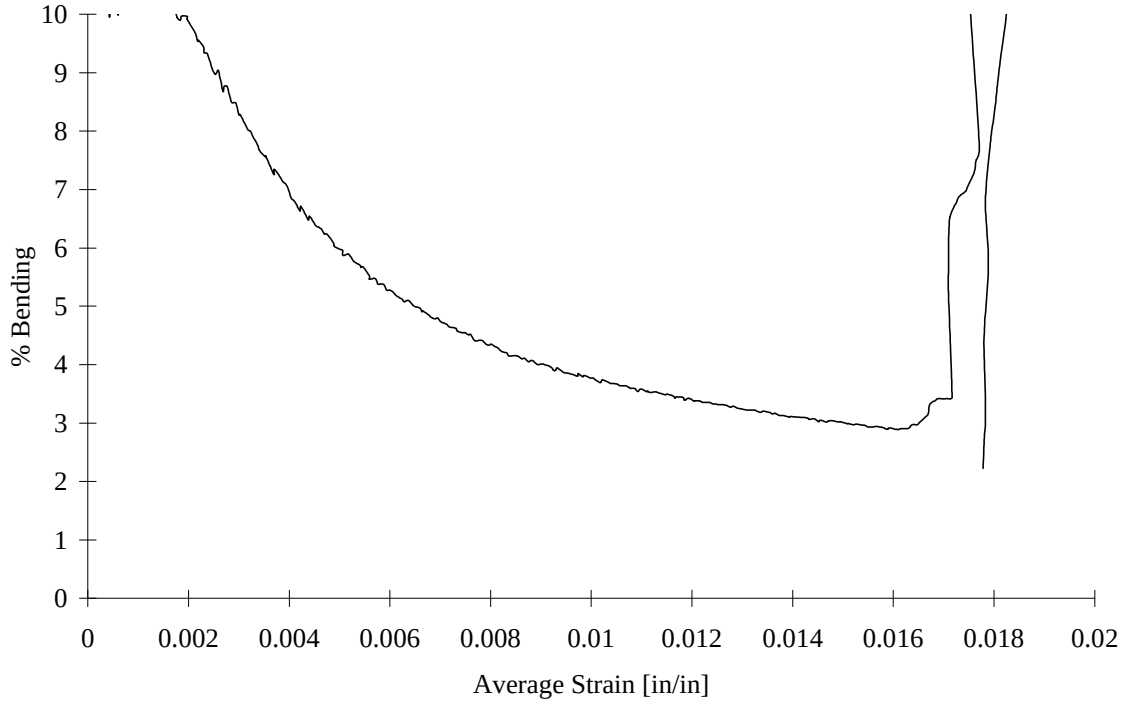

FIGURE D-144. TEST SPECIMEN IS2C02: S2/SP381 GLASS/EPOXY $[90/0]_{7s}$
IITRI TEST FIXTURE

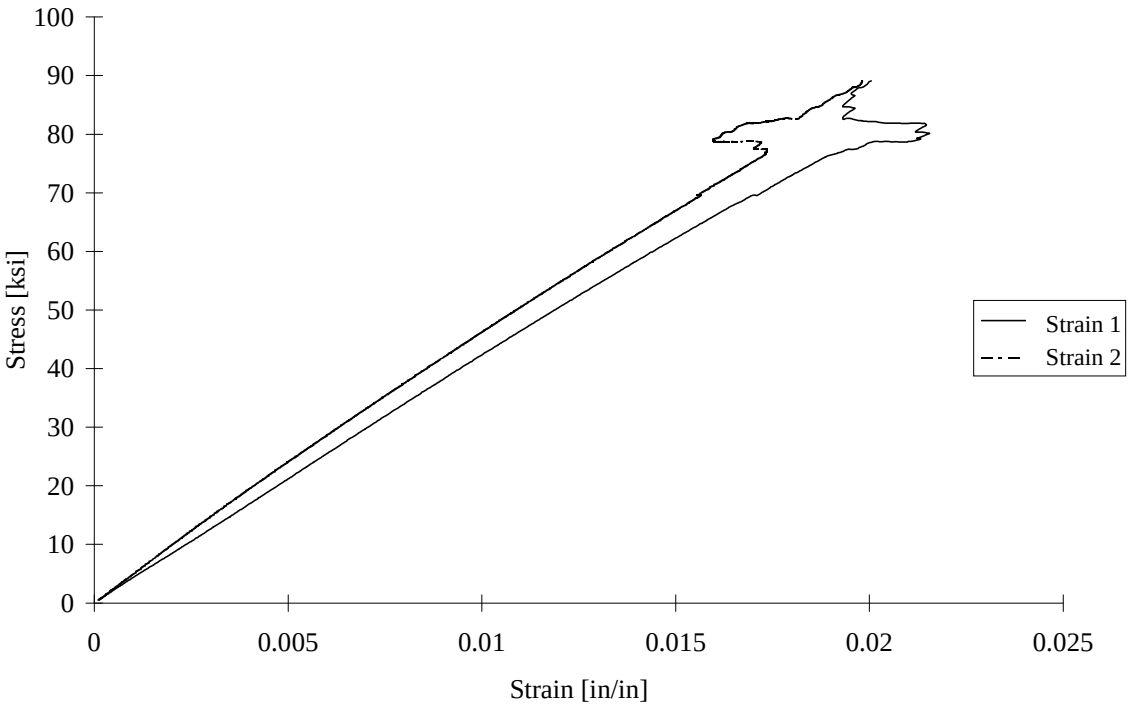

FIGURE D-145. TEST SPECIMEN IS2C03: S2/SP381 GLASS/EPOXY $[90/0]_{7s}$
IITRI TEST FIXTURE

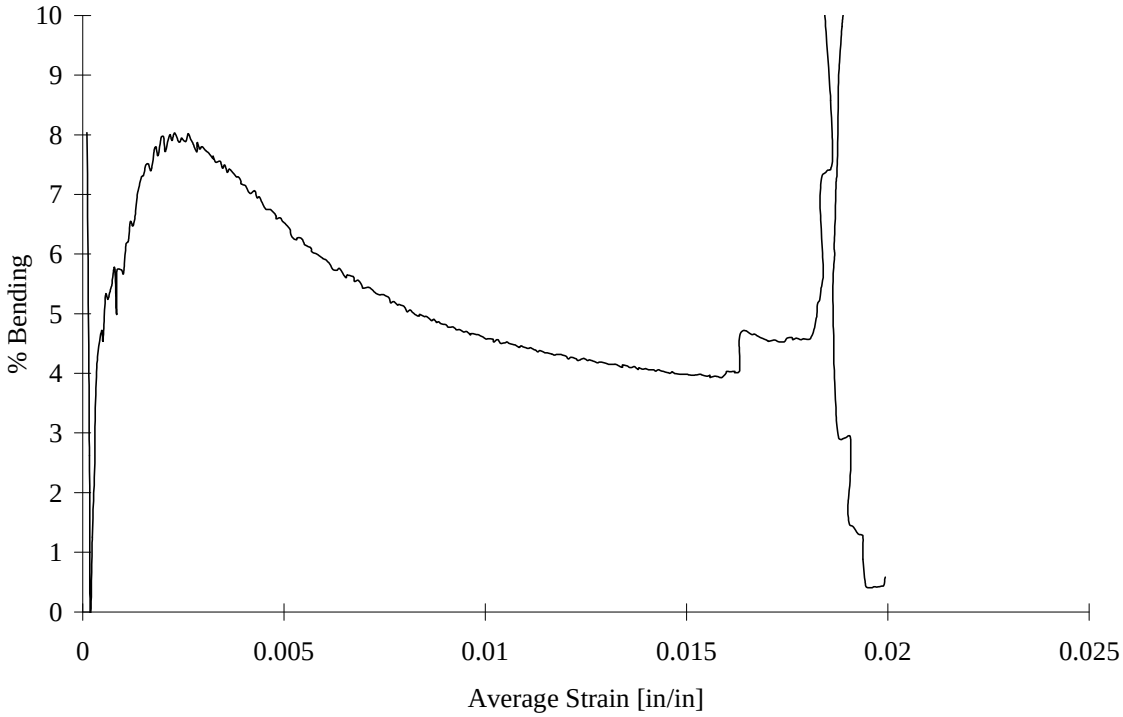

FIGURE D-146. TEST SPECIMEN IS2C03: S2/SP381 GLASS/EPOXY $[90/0]_{7s}$
IITRI TEST FIXTURE

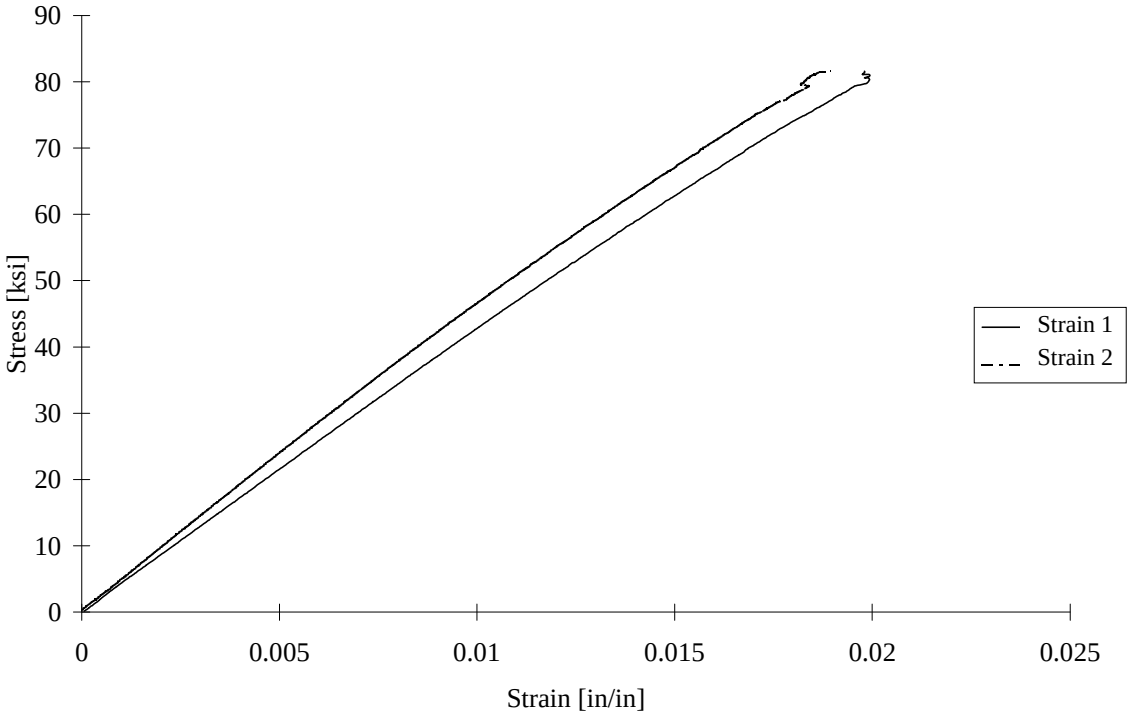

FIGURE D-147. TEST SPECIMEN IS2C04: S2/SP381 GLASS/EPOXY $[90/0]_{7s}$
IITRI TEST FIXTURE

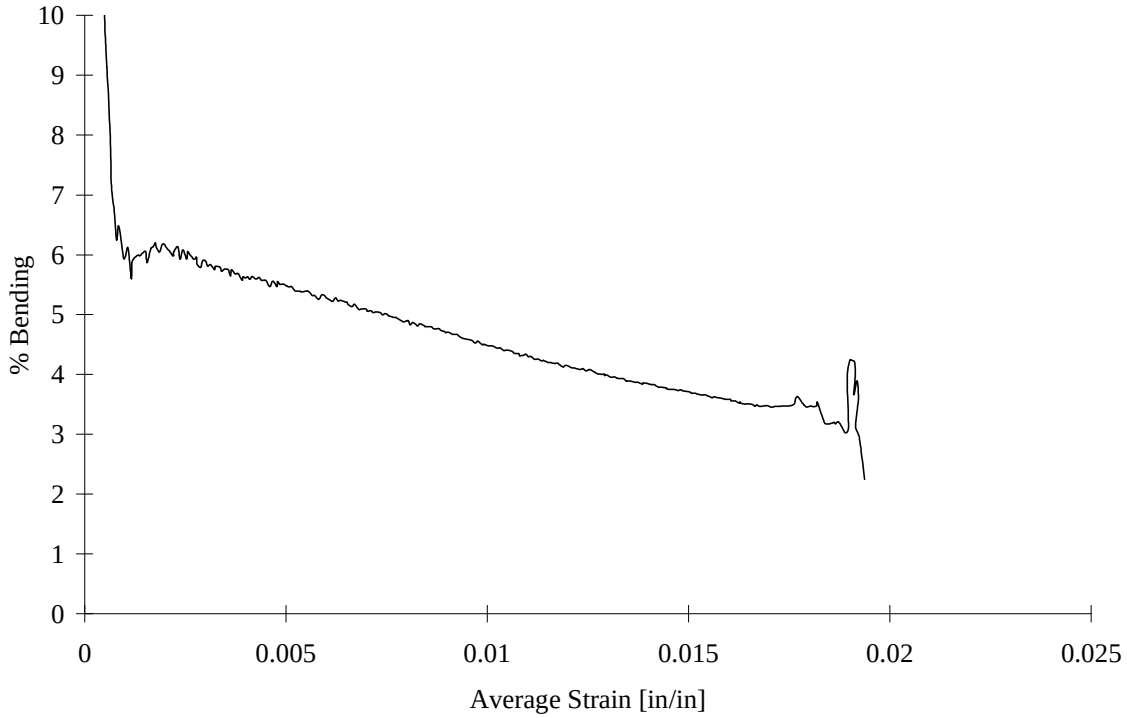

FIGURE D-148. TEST SPECIMEN IS2C04: S2/SP381 GLASS/EPOXY $[90/0]_{7s}$
IITRI TEST FIXTURE

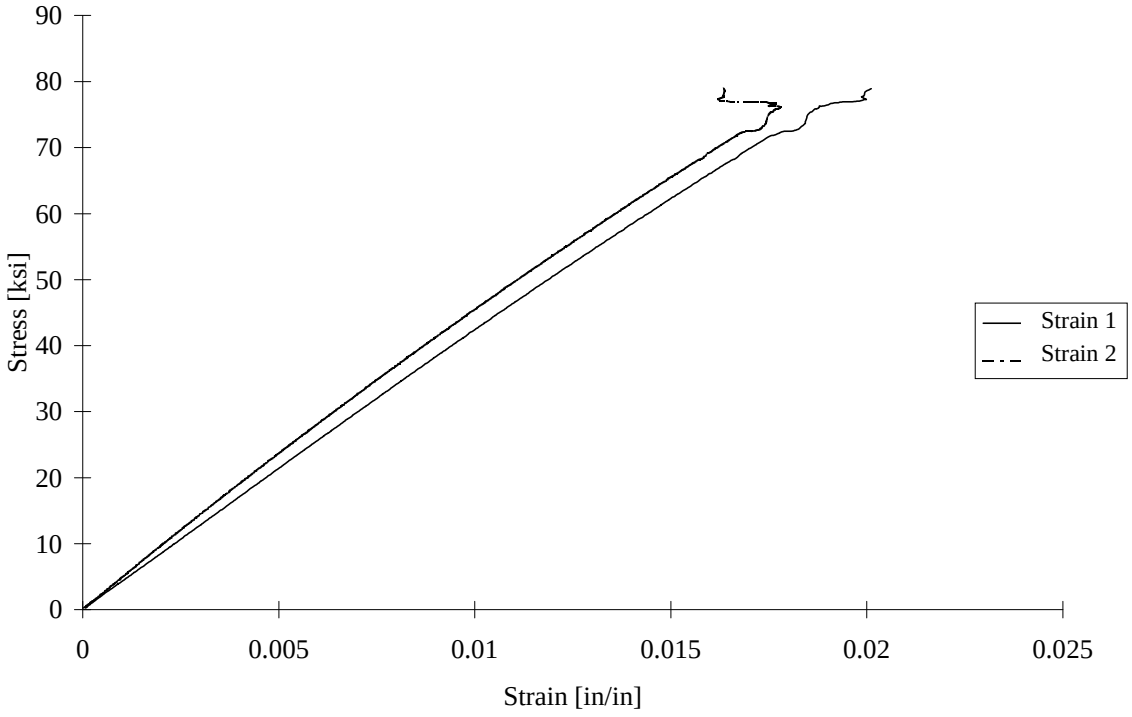

FIGURE D-149. TEST SPECIMEN IS2C05: S2/SP381 GLASS/EPOXY $[90/0]_{7s}$
IITRI TEST FIXTURE

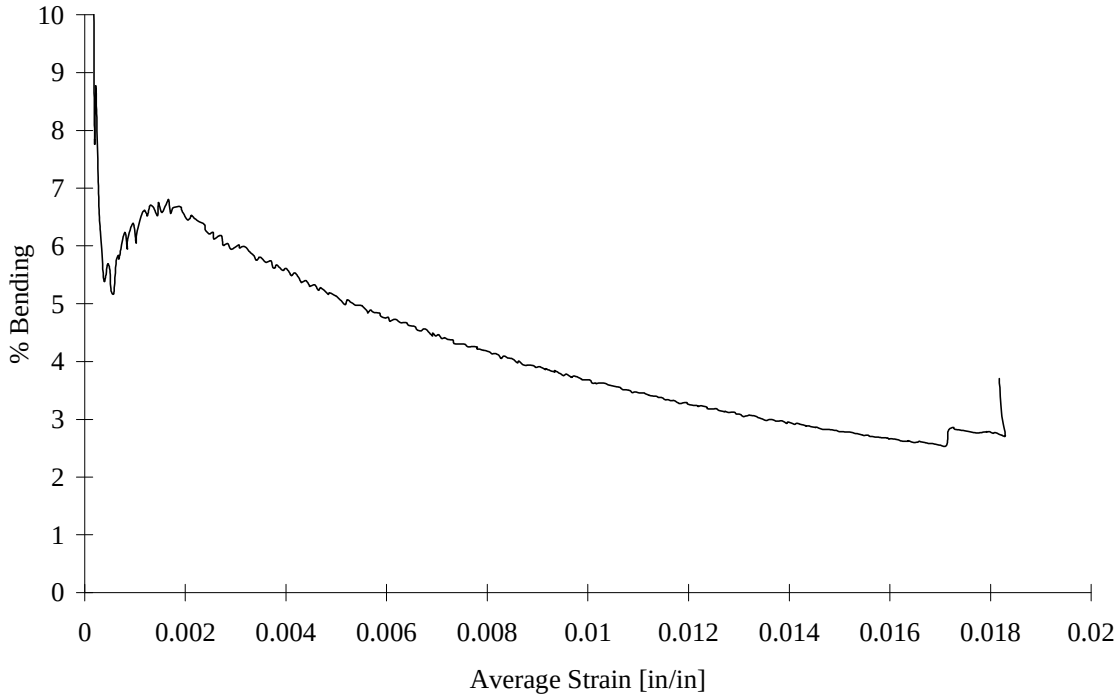

FIGURE D-150. TEST SPECIMEN IS2C05: S2/SP381 GLASS/EPOXY $[90/0]_{7s}$
IITRI TEST FIXTURE

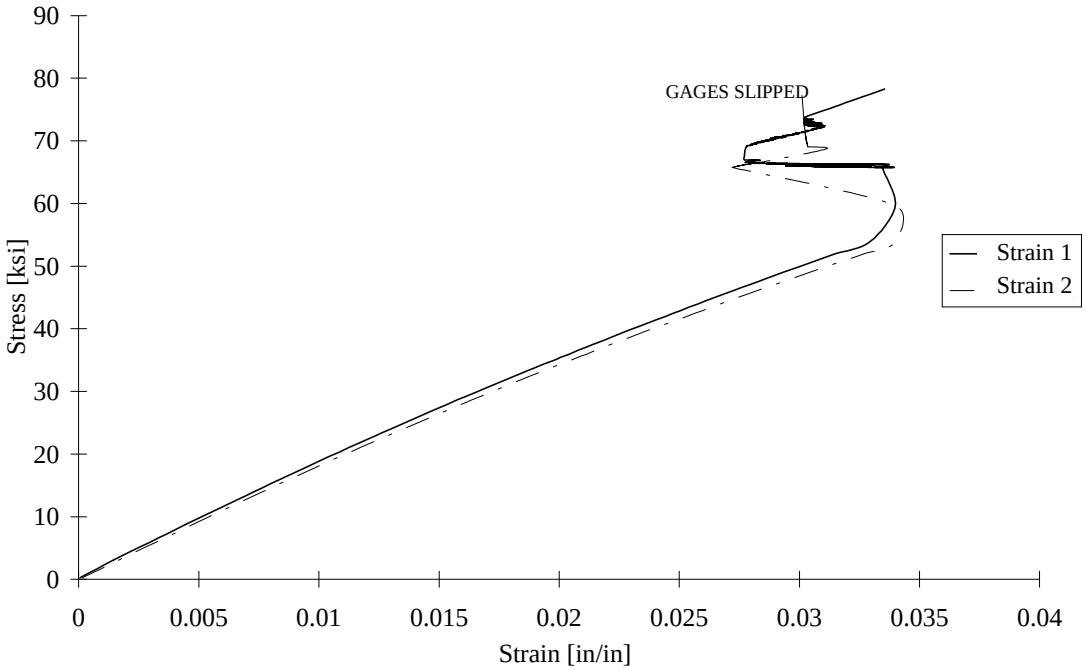

FIGURE D-151. TEST SPECIMEN CS2Q01: S2/SP381 GLASS/EPOXY $[45/0/-45/90]_{2s}$
CLC-15 TEST FIXTURE

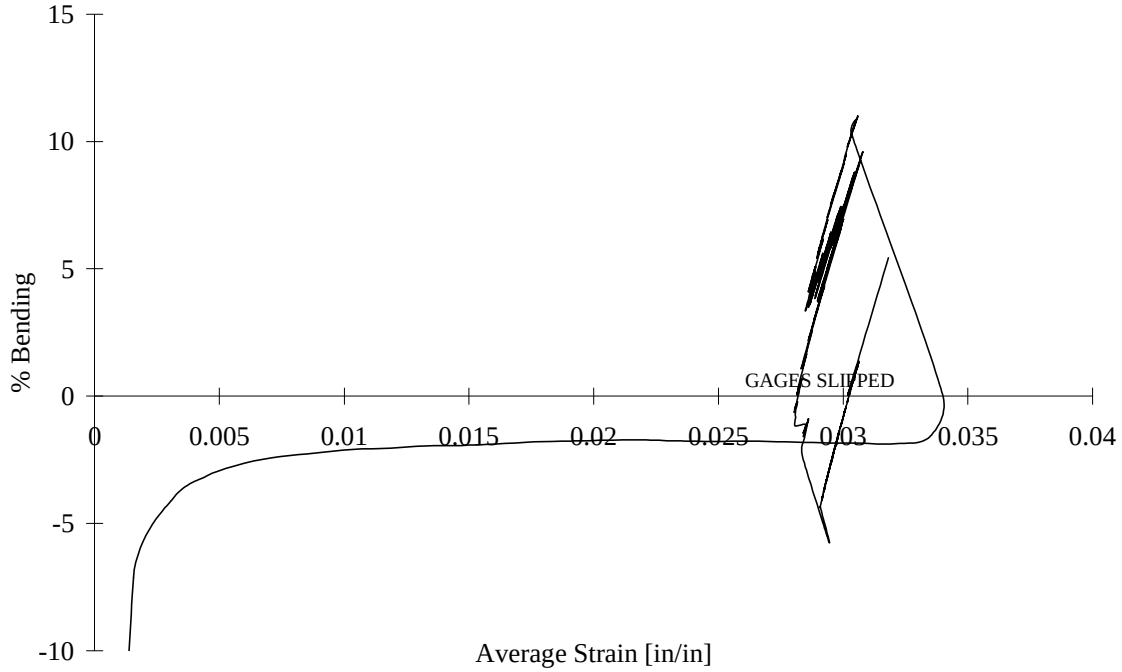

FIGURE D-152. TEST SPECIMEN CS2Q01: S2/SP381 GLASS/EPOXY $[45/0/-45/90]_{2s}$
CLC-15 TEST FIXTURE

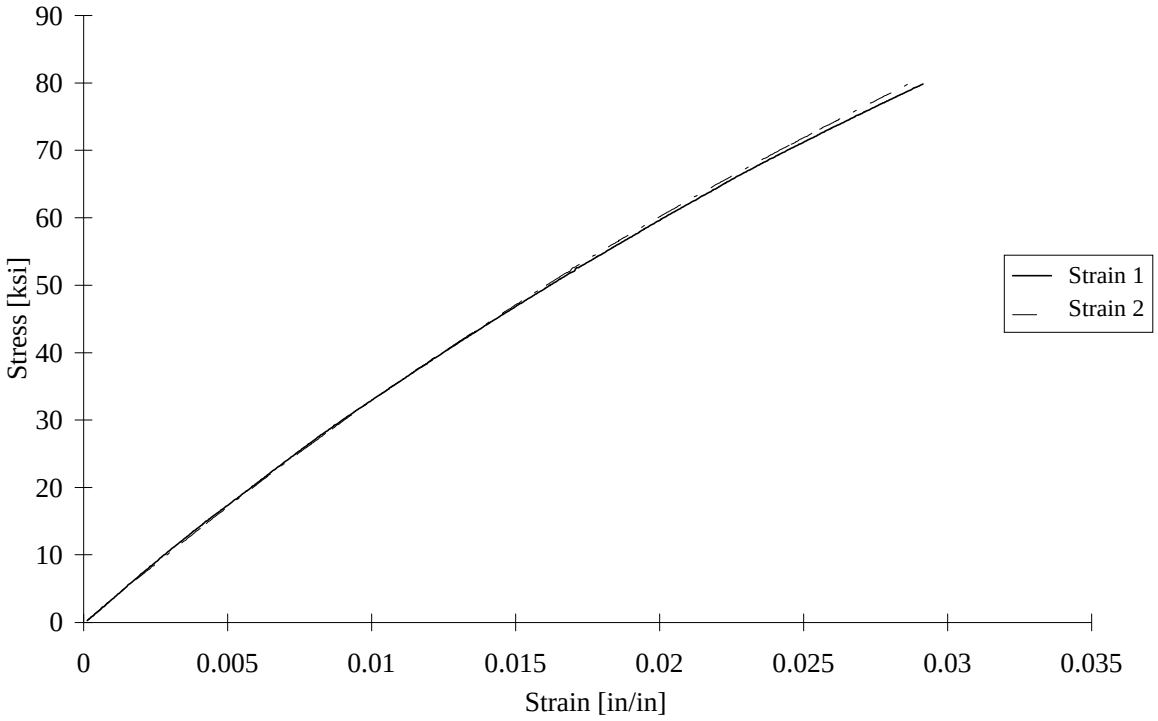

FIGURE D-153. TEST SPECIMEN CS2Q02: S2/SP381 GLASS/EPOXY $[45/0/-45/90]_{2s}$
CLC-15 TEST FIXTURE

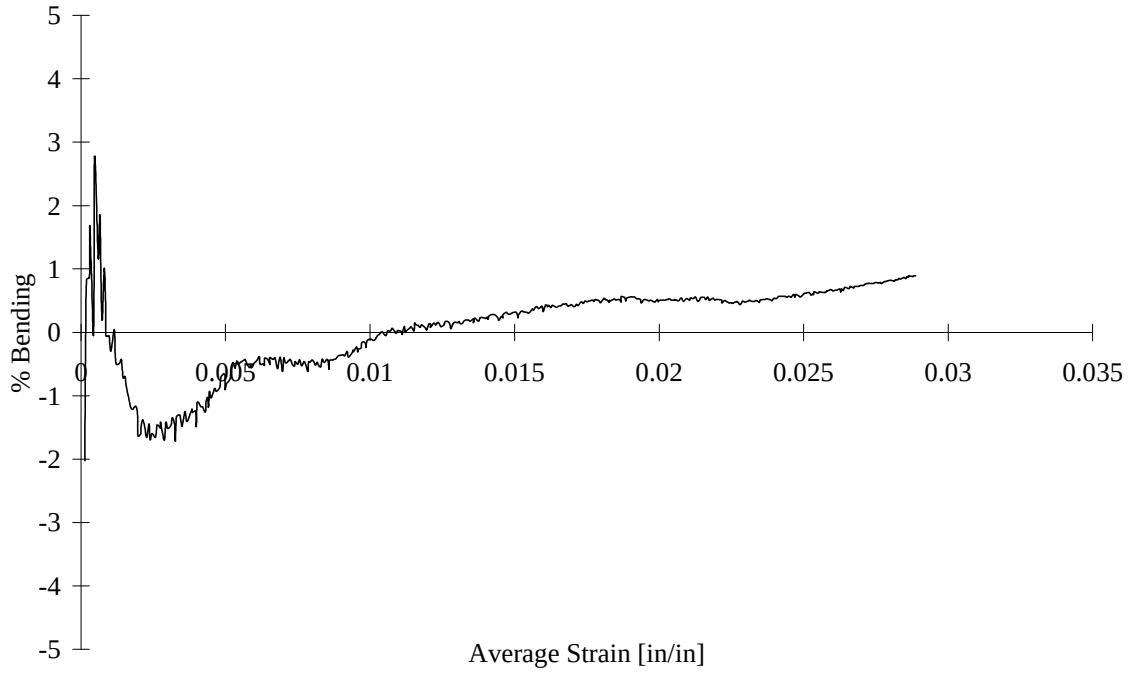

FIGURE D-154. TEST SPECIMEN CS2Q02: S2/SP381 GLASS/EPOXY $[45/0/-45/90]_{2s}$
CLC-15 TEST FIXTURE

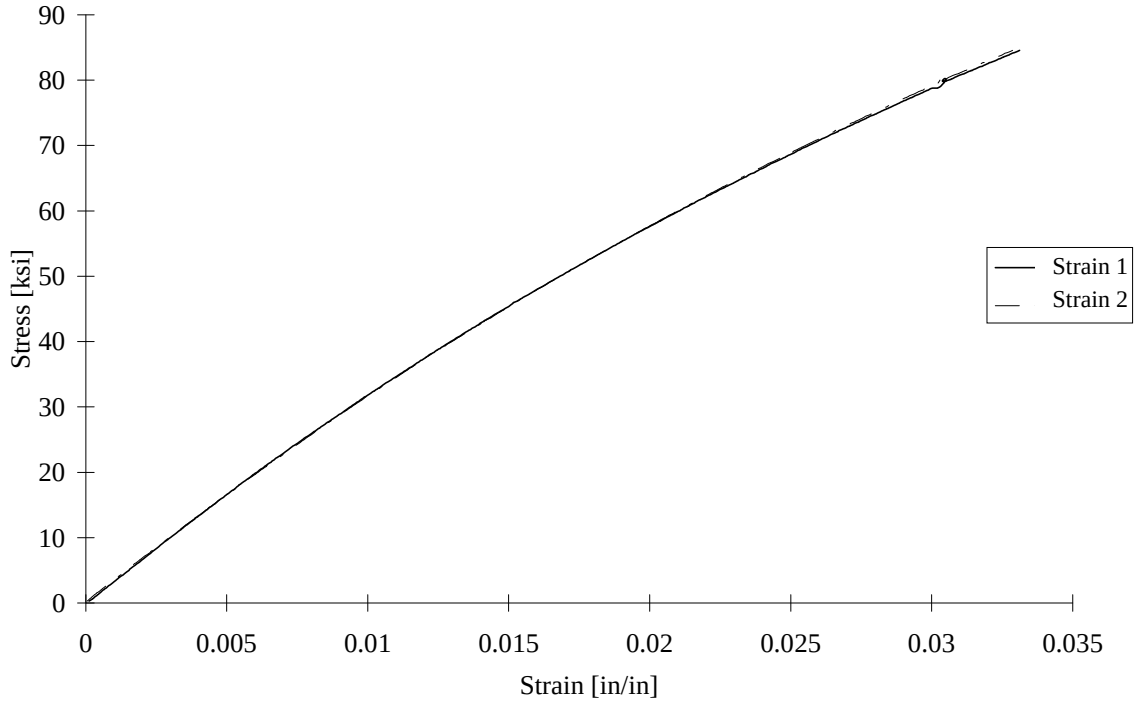

FIGURE D-155. TEST SPECIMEN CS2Q03: S2/SP381 GLASS/EPOXY $[45/0/-45/90]_{2s}$
CLC-15 TEST FIXTURE

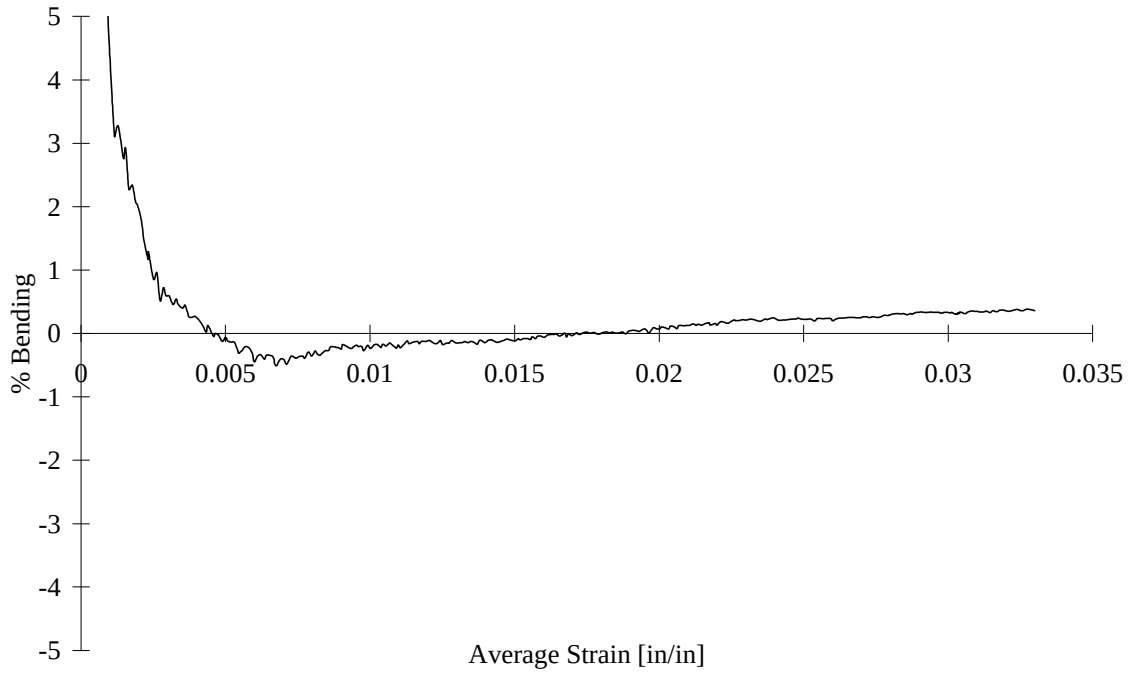

FIGURE D-156. TEST SPECIMEN CS2Q03: S2/SP381 GLASS/EPOXY $[45/0/-45/90]_{2s}$
CLC-15 TEST FIXTURE

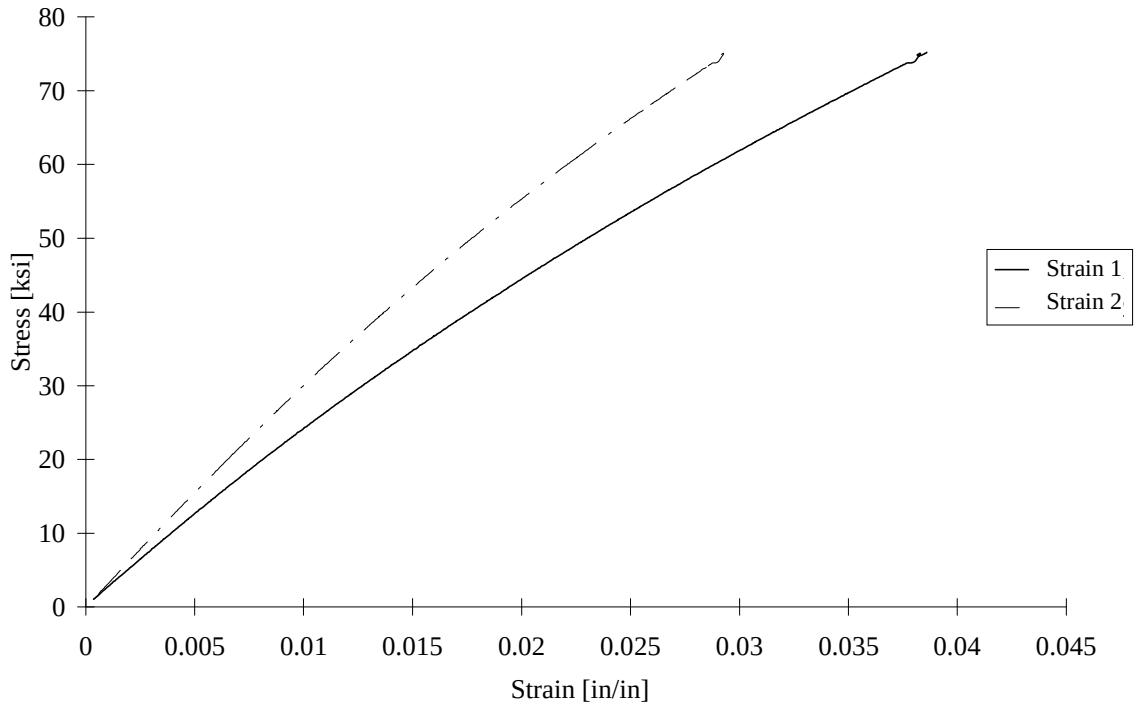

FIGURE D-157. TEST SPECIMEN CS2Q04: S2/SP381 GLASS/EPOXY $[45/0/-45/90]_{2s}$
CLC-15 TEST FIXTURE

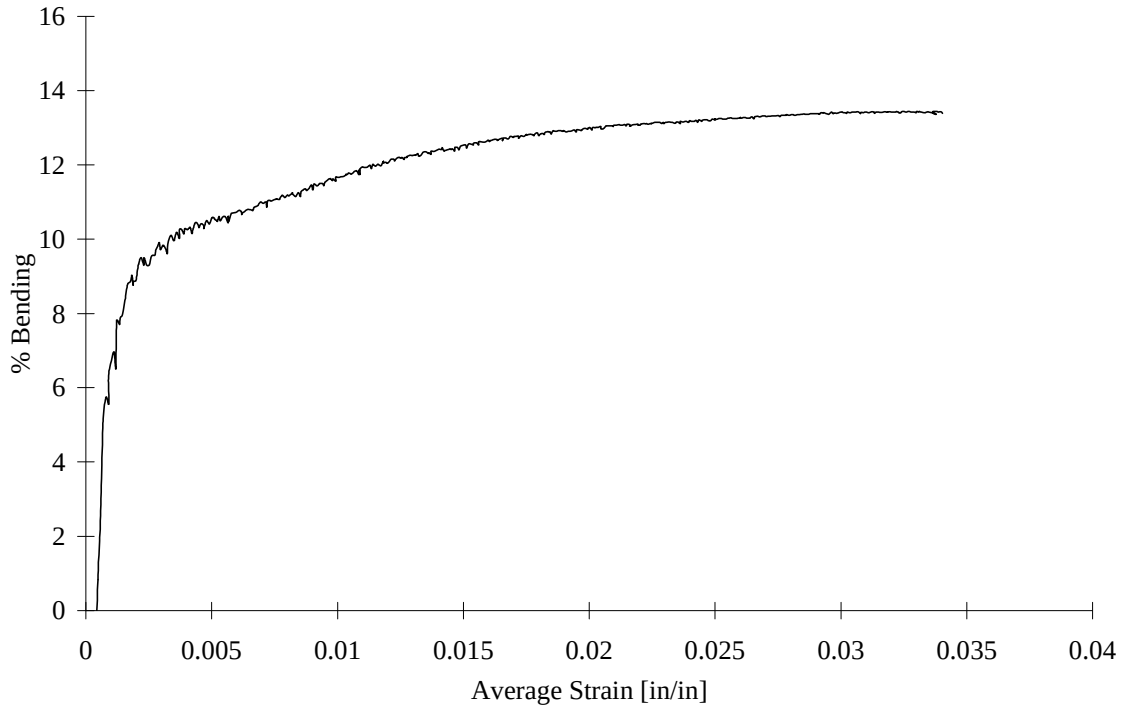

FIGURE D-158. TEST SPECIMEN CS2Q04: S2/SP381 GLASS/EPOXY $[45/0/-45/90]_{2s}$
CLC-15 TEST FIXTURE

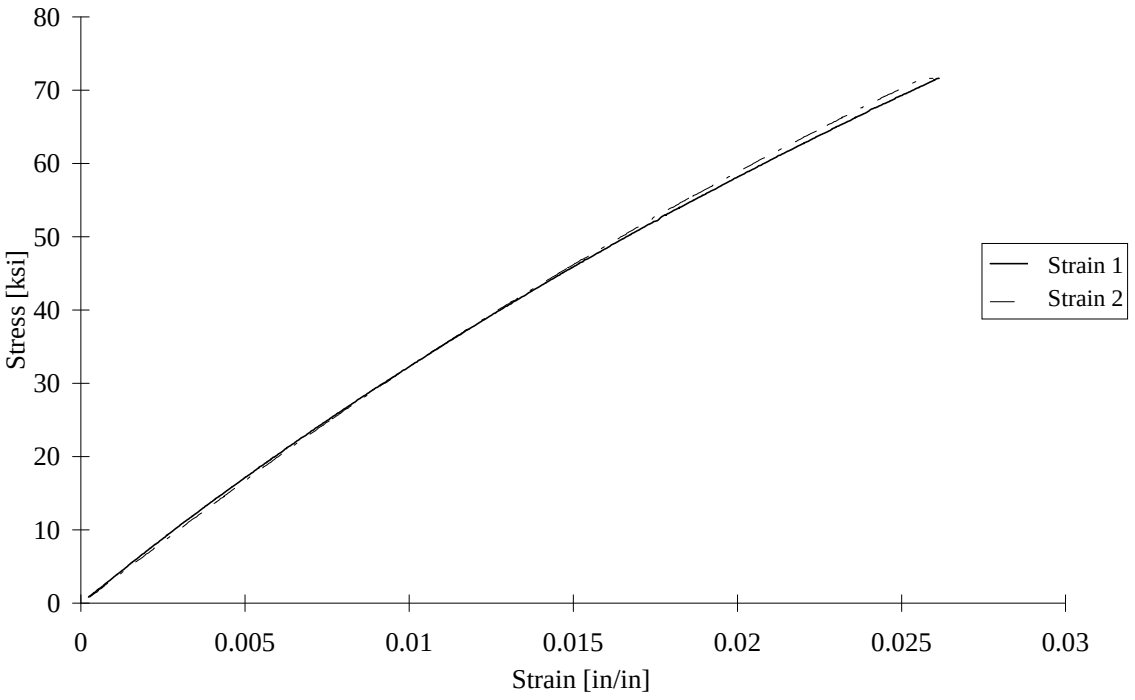

FIGURE D-159. TEST SPECIMEN CS2Q05: S2/SP381 GLASS/EPOXY $[45/0/-45/90]_{2s}$
CLC-15 TEST FIXTURE

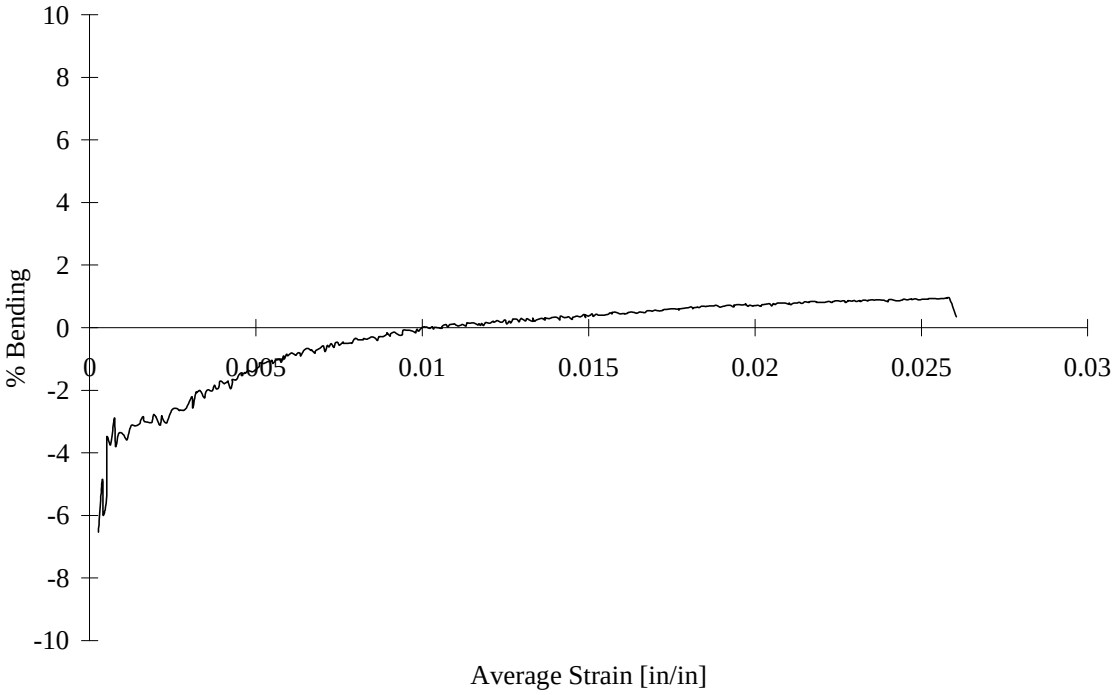

FIGURE D-160. TEST SPECIMEN CS2Q05: S2/SP381 GLASS/EPOXY $[45/0/-45/90]_{2s}$
CLC-15 TEST FIXTURE

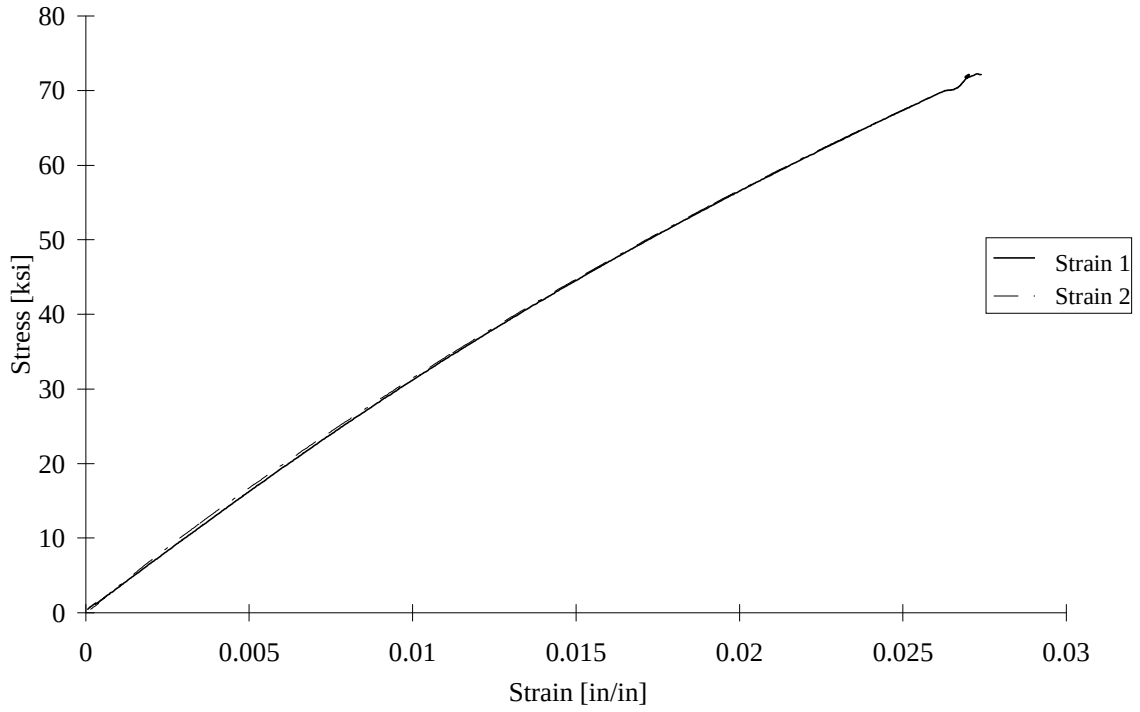

FIGURE D-161. TEST SPECIMEN IS2Q01: S2/SP381 GLASS/EPOXY $[45/0/-45/90]_{2s}$
IITRI TEST FIXTURE

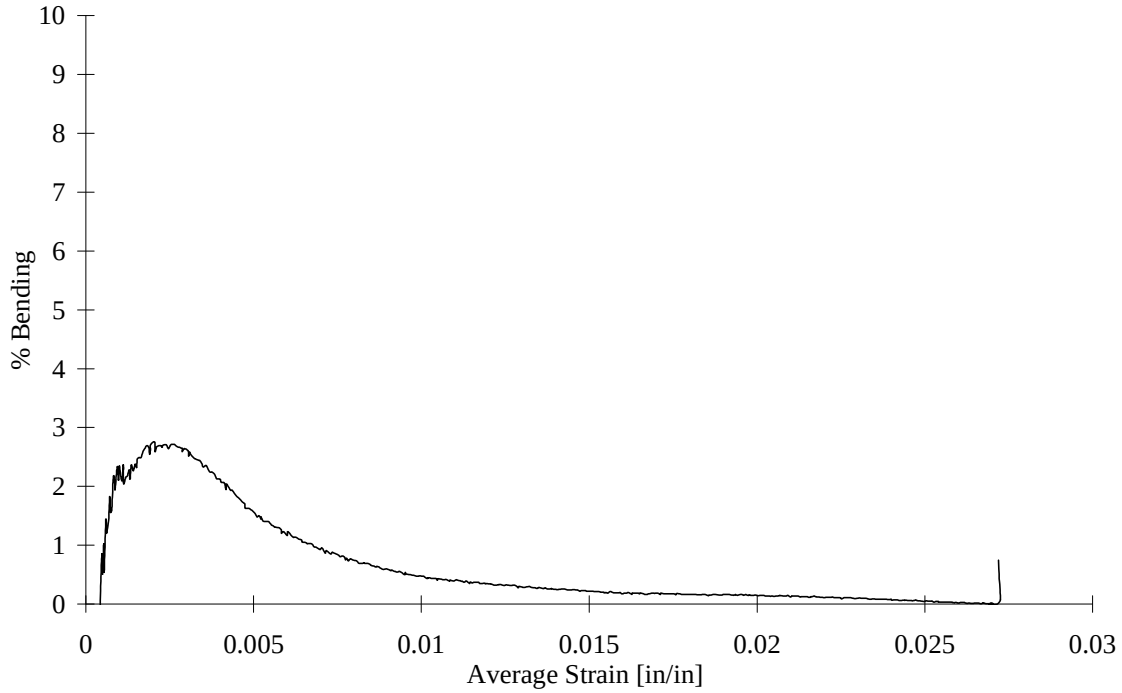

FIGURE D-162. TEST SPECIMEN IS2Q01: S2/SP381 GLASS/EPOXY $[45/0/-45/90]_{2s}$
IITRI TEST FIXTURE

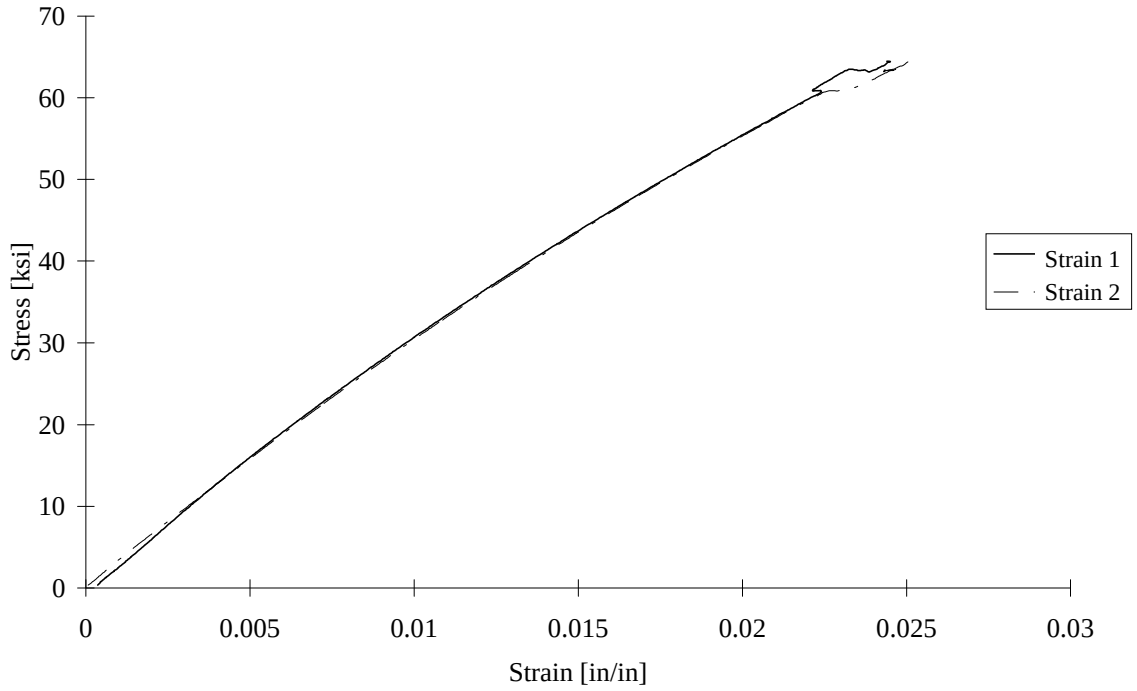

FIGURE D-163. TEST SPECIMEN IS2Q02: S2/SP381 GLASS/EPOXY $[45/0/-45/90]_{2s}$
IITRI TEST FIXTURE

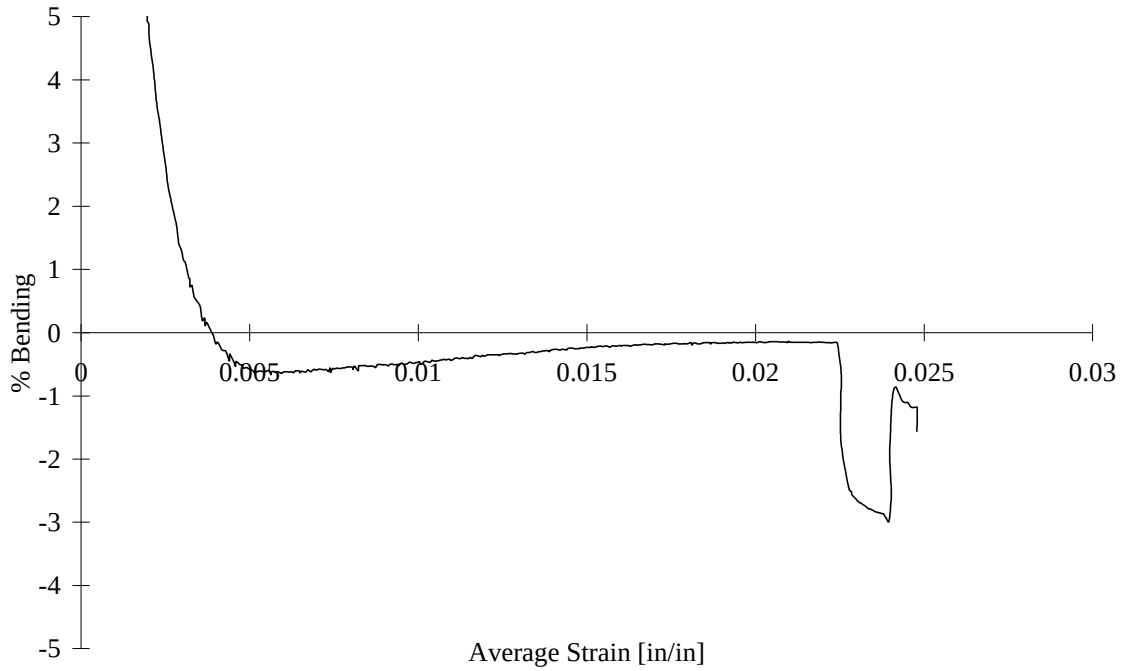

FIGURE D-164. TEST SPECIMEN IS2Q02: S2/SP381 GLASS/EPOXY $[45/0/-45/90]_{2s}$
IITRI TEST FIXTURE

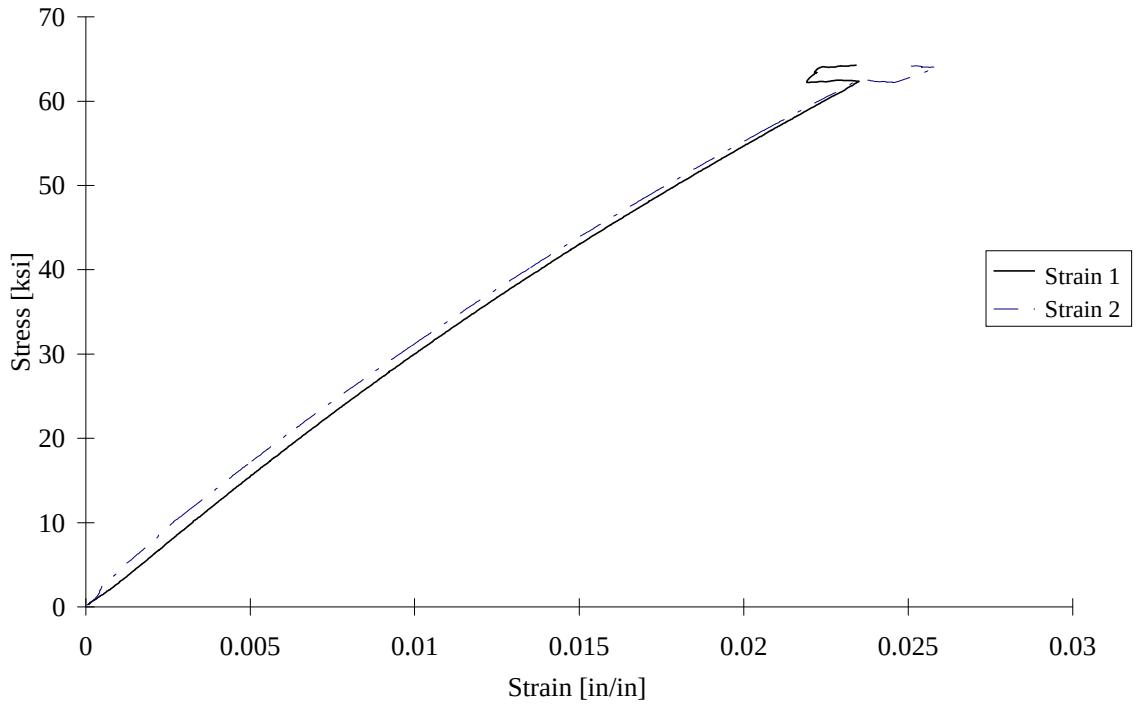

FIGURE D-165. TEST SPECIMEN IS2Q03: S2/SP381 GLASS/EPOXY $[45/0/-45/90]_{2s}$
IITRI TEST FIXTURE

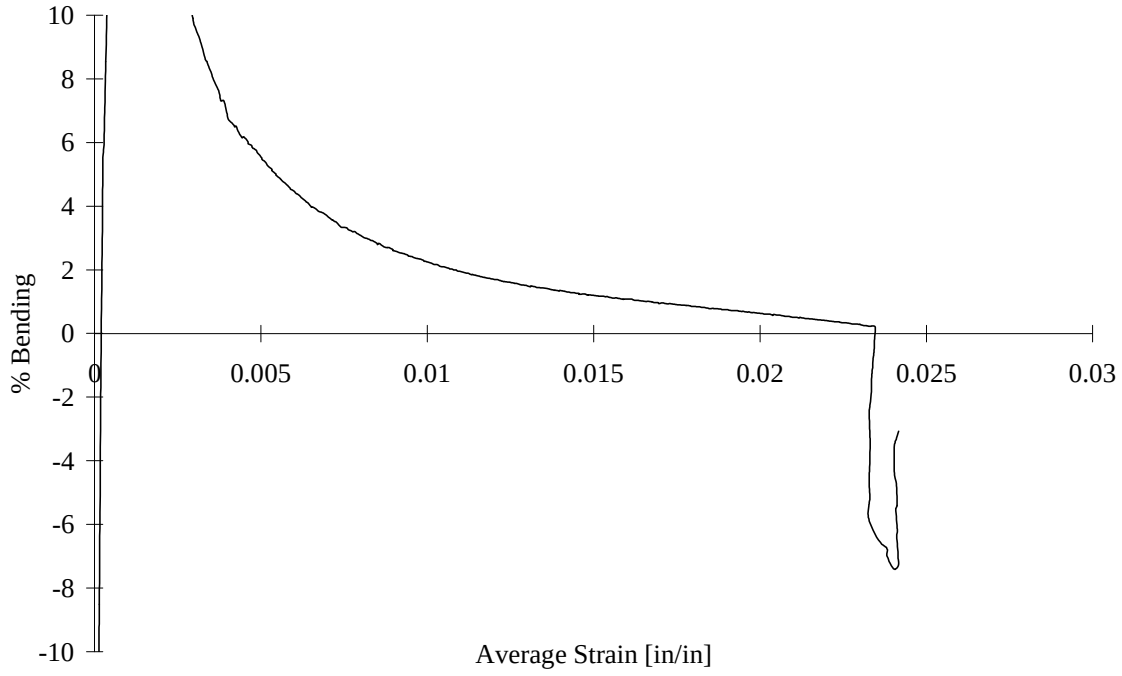

FIGURE D-166. TEST SPECIMEN IS2Q03: S2/SP381 GLASS/EPOXY $[45/0/-45/90]_{2s}$
IITRI TEST FIXTURE

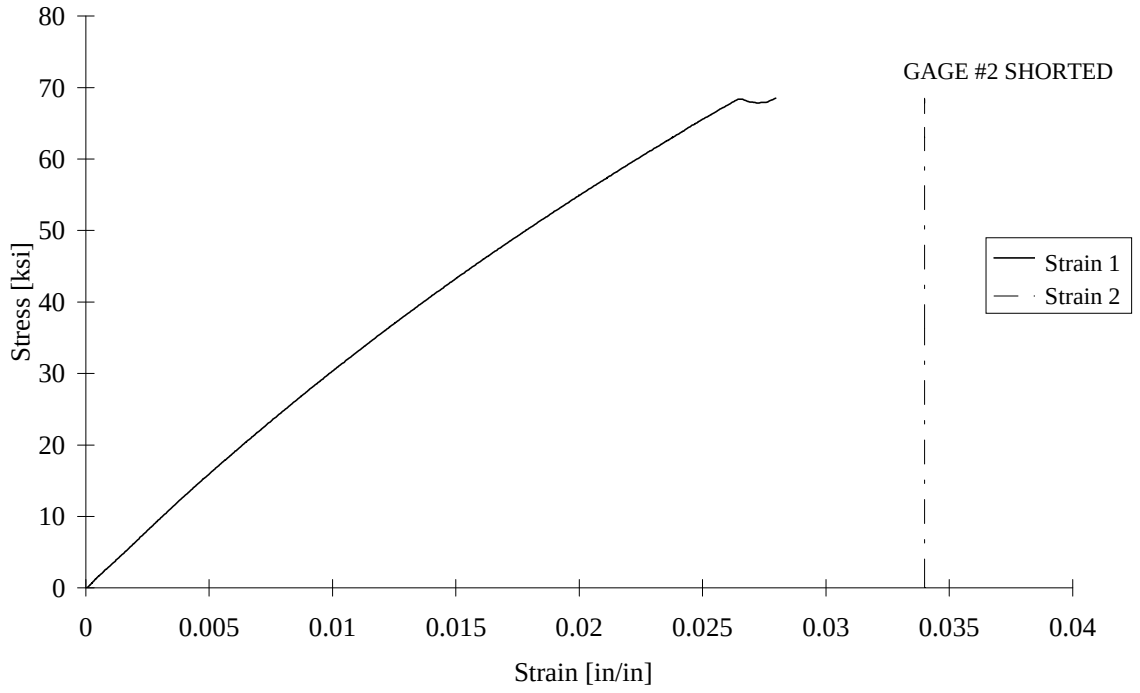

FIGURE D-167. TEST SPECIMEN IS2Q04: S2/SP381 GLASS/EPOXY $[45/0/-45/90]_{2s}$
IITRI TEST FIXTURE

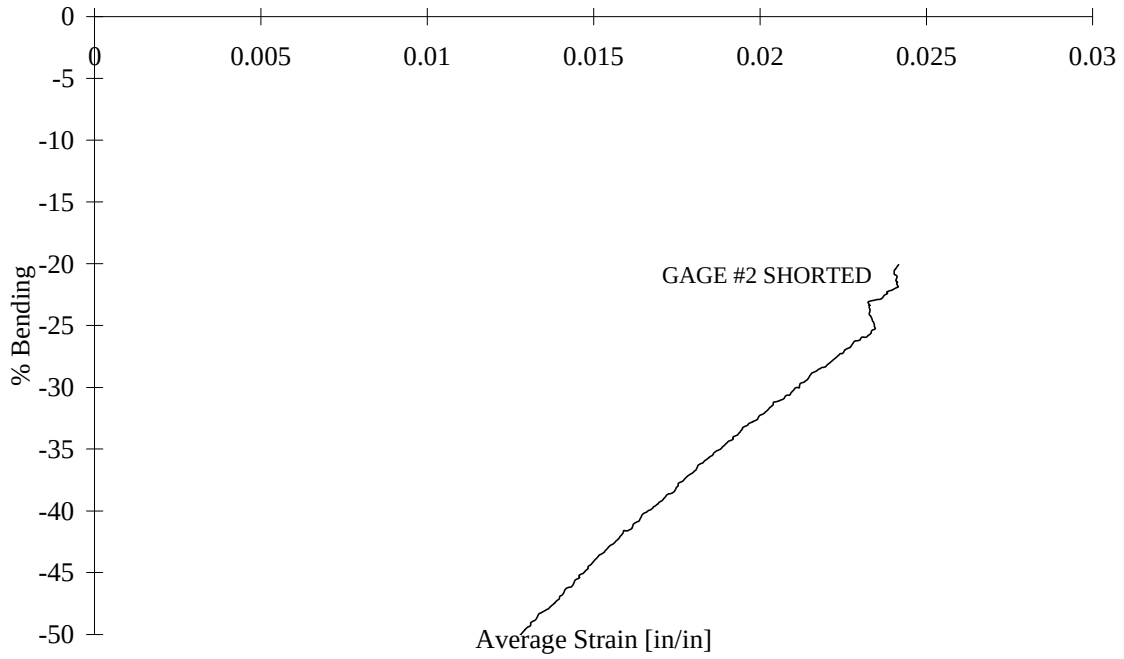

FIGURE D-168. TEST SPECIMEN IS2Q04: S2/SP381 GLASS/EPOXY $[45/0/-45/90]_{2s}$
IITRI TEST FIXTURE

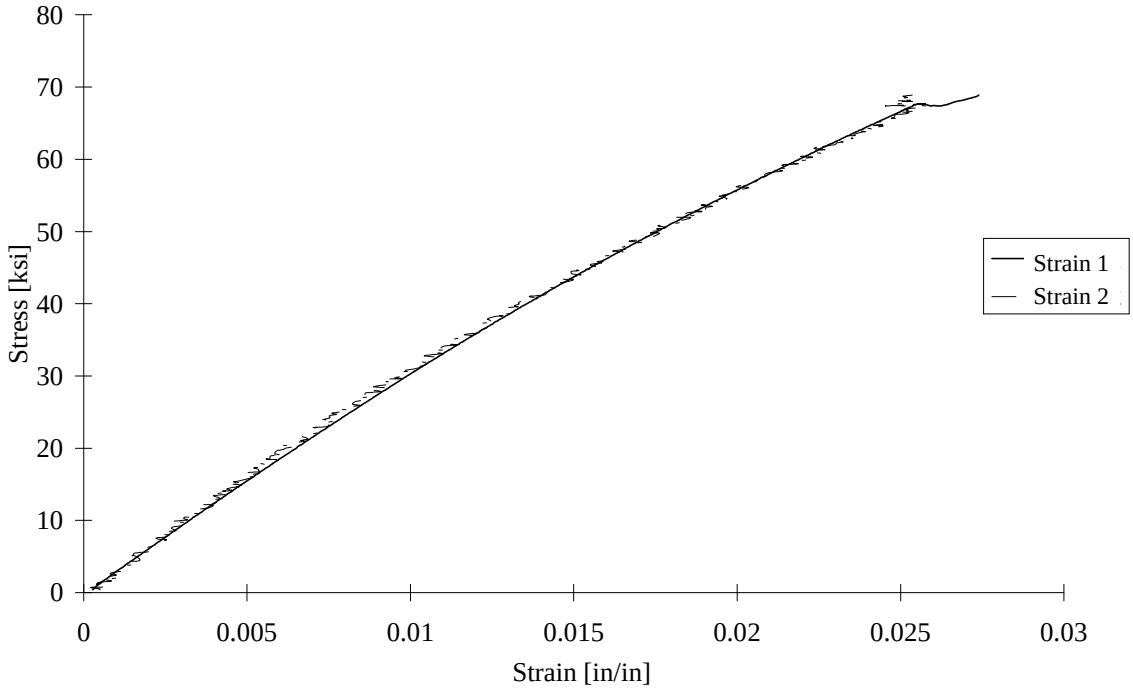

FIGURE D-169. TEST SPECIMEN IS2Q05: S2/SP381 GLASS/EPOXY $[45/0/-45/90]_{2s}$
IITRI TEST FIXTURE

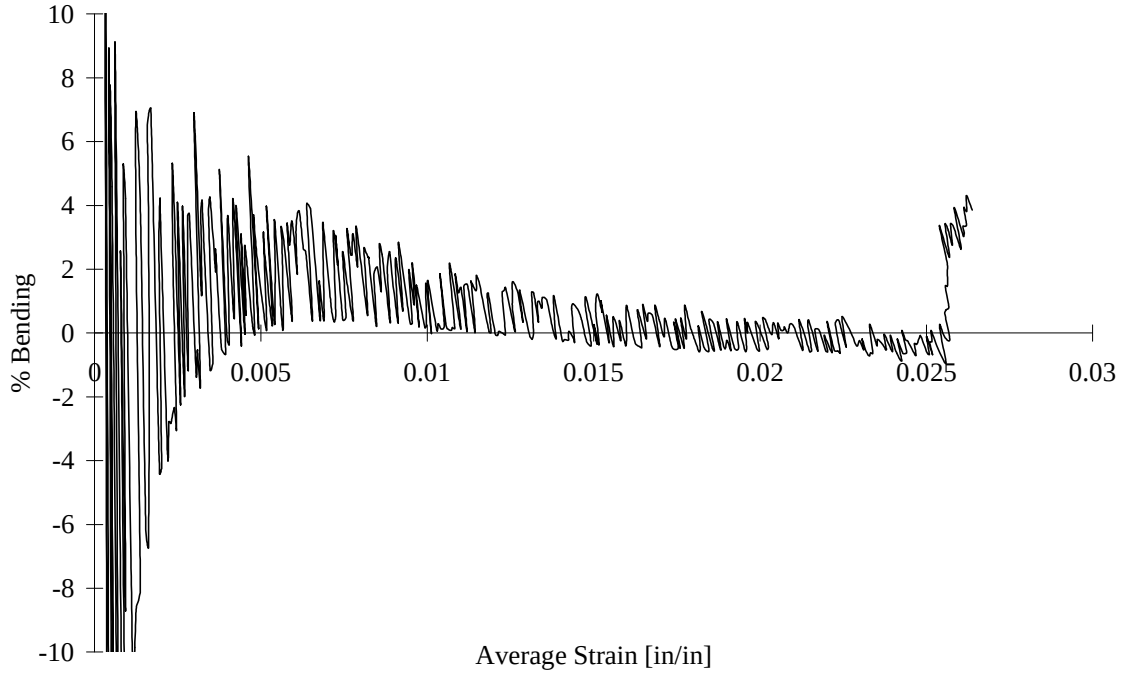

FIGURE D-170. TEST SPECIMEN IS2Q05: S2/SP381 GLASS/EPOXY $[45/0/-45/90]_{2s}$
IITRI TEST FIXTURE